Chapter 1

Introduction

Visible light is a ubiquitous phenomenon, the true nature of which has always been studied by mankind. From a physical point of view it represents a small fraction of the electromagnetic spectrum that can be perceived by the human eye. Visible light is usually defined as having wavelengths between the ultraviolet with 400 nm wavelength and the infrared with 700 nm wavelength, which corresponds to a frequency range of about 430–750 THz, see Fig. 1.1. In physics, the term 'light' sometimes refers more generally to electromagnetic radiation of any wavelength, whether it is visible or not. In this sense, also X-rays and gamma rays at shorter wavelengths as well as microwaves and radio waves at longer wavelengths are called light.

Like all types of electromagnetic radiation, visible light propagates as waves, which are characterized by certain primary properties. Apart from being characterized by a frequency or a wavelength they have an amplitude, a polarization, an intensity, and a direction of propagation. Furthermore, they propagate in vacuum with a speed of 299 792 458 m/s, which is one of the fundamental constants of nature. The seminal Michelson-Morley experiment even showed that this light speed turns out to be identical in all inertial systems.

However, the energy imparted by the waves is absorbed at single locations the way particles are absorbed. The absorbed energy of electromagnetic waves is called a 'photon' and represents the quantum of light. When a wave of light is absorbed as a photon, its energy instantly collapses to a single location, what is called the wave function collapse. This dual wave-like and particle-like nature of light is known as the wave-particle duality.

Quantum optics studies the nature and effects of light as quantized photons and represents an important research area in modern physics. The first major development leading to that understanding was the correct modeling of the black-body radiation spectrum by Max Planck in 1900 under the hypothesis of light being emitted in discrete units of energy. Further evidence for the corpuscular nature of light was revealed by Albert Einstein and his explanation in 1905 of the photoelectric effect, which deals with electromagnetic radiation hitting a material and, as a consequence, electrons being emitted. And then in 1913 Niels Bohr showed that the hypothesis of optical radiation being quantized corresponded to his theory of the quantized

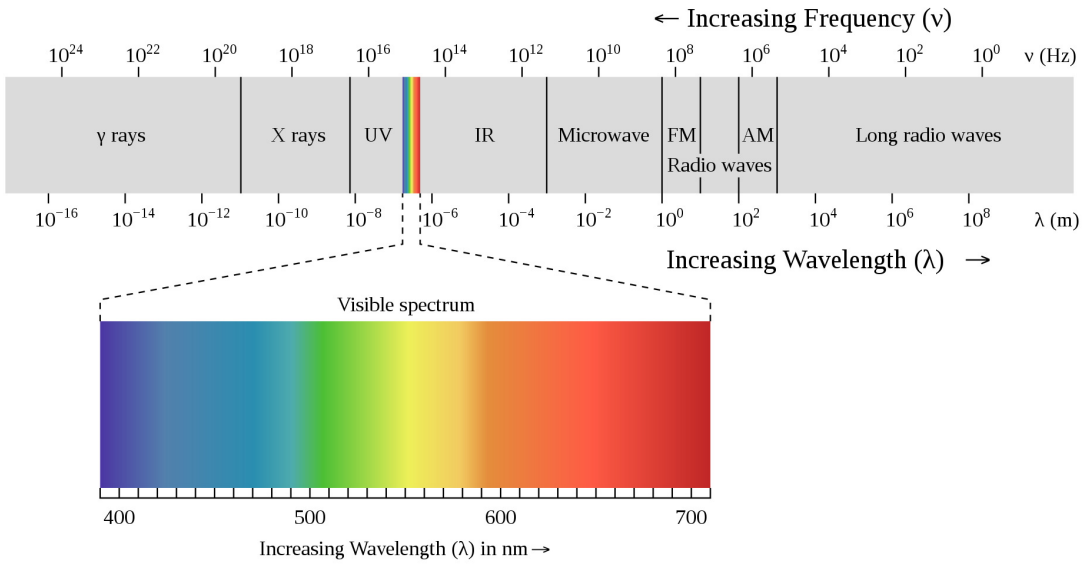

Figure 1.1: The electromagnetic spectrum with the visible light being highlighted.

energy levels of atoms. The understanding of the interaction between light and matter following these developments was crucial for the development of quantum mechanics as a whole. However, the subfields of quantum mechanics dealing with matter-light interaction were regarded for decades as a research of matter rather than of light and one spoke, hence, of atomic physics.

This only changed in 1960 when the first laser was built by Theodore Maiman at Hughes Research Laboratories based on theoretical work by Charles Townes and Arthur Schawlow. This represents a device that emits light through a process of light amplification based on the stimulated emission of electromagnetic radiation. Since then laser science, i.e. the research into the principles, the design and the application of these devices, became an important field. For instance, over the decades one managed to develop different laser types like gas lasers, solid-state lasers, fiber lasers, photonic crystal lasers, semiconductor lasers, dye lasers, and free-electron lasers, which operate at different wavelengths, see Fig. 1.2a). Furthermore, the quantum mechanics underlying the laser principles was studied now with more emphasis on the properties of light, and the name quantum optics became more and more customary.

The development of laser science was accompanied and triggered by the exploration of the theoretical foundations of quantum optics. This followed the basic work of Paul Dirac on quantum field theory in 1927 and the birth of quantum electrodynamics around the Second World War as the relativistic treatment of the light and matter interaction by Freeman Dyson, Richard Feynman, Julian Schwinger, and Shinichiro Tomonaga. Namely, the quantum theory was applied to the electromagnetic field in the 1950s and 1960s by Roy Glauber, John Klauder, Leonard Mandel, George Sudarshan, and many others in order to gain a more detailed understanding of the statistics of light, which quantifies its degree of coherence. In particular, this led to the introduction and the manipulation of different states of light, such as thermal states, coherent

a) 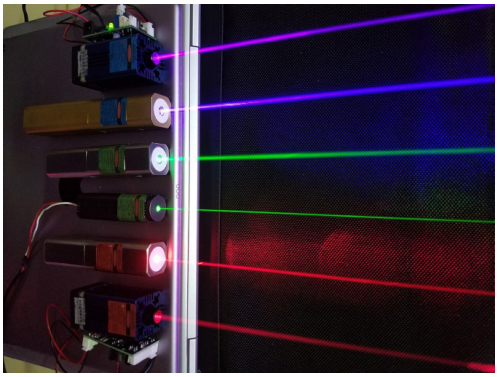 b) 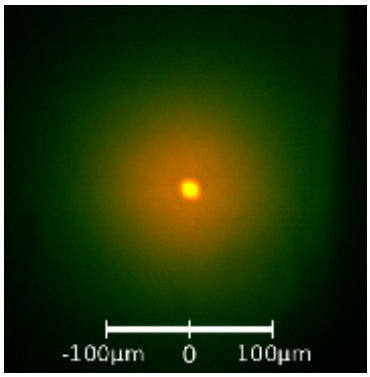

Figure 1.2: Different light sources: a) Red (660 and 635 nm), green (532 and 520 nm), and blue-violet (445 and 405 nm) laser light; b) Orange (585 nm) light of a photon Bose-Einstein condensate in the center and thermal wings in green according to Ref. [18].

states or the more exotic squeezed states. As a consequence it became clear that light cannot be fully described by just referring to the electromagnetic waves in the classical picture as also its quantum or thermal fluctuations have to be taken into account as well.

On the application side many intriguing phenomena were discovered, some of which we mention here. One of them was the development of mode-locked oscillators, which generate ultrashort laser pulses with a time duration of the order of a picosecond. They have a broadband optical spectrum and are characterized by a high peak intensity, that usually leads to nonlinear interactions in various materials including air and are, thus, studied in the field of nonlinear optics. Another line of research deals with applications in the realm of molecular or solid-state physics. For instance, Raman spectroscopy is used to determine vibrational modes of molecules, which provide a structural fingerprint by which molecules can be identified. Further remarkable results were obtained by demonstrating quantum entanglement and quantum teleportation, quantum cryptography as well as by realizing quantum logic gates. This led to the emergence of quantum information technology, which represents a subfield of quantum optics and is devoted, for instance, to build a quantum computer.

Another breakthrough was to apply the mechanical forces of light on matter in order to levitate and to position an atomic cloud in a magneto-optical trap. Combined with the laser cooling and the evaporative cooling this led, finally, to the experimental realization of a Bose-Einstein condensate, which is a macroscopic quantum phenomenon predicted by Albert Einstein in 1925 on the basis of a work of Satyendranath Bose. Namely, in 1995 Wolfgang Ketterle, Eric Cornell, and Carl Wieman managed to realize a macroscopic occupation of the ground state for a sample of alkali atoms, which has the diluteness of a millionth of the density of air at temperatures in the nanoKelvin regime. This discovery led to a new sub-field of quantum optics, which analyzes these days the properties of ultracold atomic or molecular quantum gases.

The generic black-body radiation, i.e. an electromagnetic radiation in thermal equilibrium with the cavity walls, does not show the phenomenon of Bose-Einstein condensation. In such systems

photons have a vanishing chemical potential, meaning that their number is not conserved when the temperature of the photon gas is varied. Thus, at low temperatures, photons disappear in the cavity walls instead of occupying the cavity ground state. Nevertheless, the group of Martin Weitz at the University of Bonn achieved in 2010 a Bose-Einstein condensate of photons in this system. The cavity mirrors provide both a confining potential and a non-vanishing effective photon mass, making the system formally equivalent to a two-dimensional gas of trapped, bosons with a mass, which is about 10 orders of magnitude lower than the mass of a single rubidium atom. Due to multiple scattering processes with dye molecules the photons thermalize at the temperature of the dye solution, which is room temperature. Upon increasing the photon density, the photon energies have a Bose-Einstein distribution with a massively populated ground-state mode as the Bose-Einstein condensate, which corresponds to the bright spot in the center, on top of a broad thermal wing, see Fig. 1.2b). Thus, in conclusion, Bose-Einstein condensation, which demonstrates the wave nature of material particles, now offers further illumination of wave-particle duality: it has been observed in light itself [19]. The intriguing properties of photon Bose-Einstein condensates are investigated experimentally in Bonn, London, Twente, Utrecht and, quite soon, also in Kaiserslautern, where a new set-up is currently being built up.

This lecture provides an introduction into the intriguing field of quantum optics from a theoretical point of view, although partially also experimental set-ups and results are discussed. In Chapter 2 we start with performing the formal quantization of the Maxwell field by applying the canonical field quantization method. Furthermore, as concrete applications, we calculate several quantum fluctuation effects like the electric field vacuum correlations, the Casimir effect, and the Lamb shift. Afterwards, in Chapter 3 we discuss for a single electromagnetic mode the properties of different quantum states of the radiation field together with both their density matrices and their quasi-probability distributions in phase space as well as possible experimental realizations. Subsequently Chapter 4 is devoted to explore the emission and absorption of light by matter, where the latter is treated non-relativistically. A perturbative treatment leads to the three elementary Einstein processes. Restricting ourselves approximately to two atomic states we can treat their interaction with the electromagnetic field exactly. In the case of a classical or a quantum mechanical description of light this leads to the Rabi or the Jaynes-Cummings model, respectively. A full quantum mechanical treatment of light field and atoms is worked out in Chapter 5 both without and with a coupling to an environment, which provides losses or pumping. As a prime example we deal here with the semiclassical and the quantum mechanical laser theory. And, finally, Chapter 6 works out a theory of photon Bose-Einstein condensation on the basis of a paraxial approximation in the microcavity. In particular, we discuss consequences of the two sources of an effective photon-photon interaction, which is the local and instantaneous Kerr interaction and the thermo-optic interaction being non-local in both space and time. Thus, in summary, apart from a general overview about quantum optics, this lecture strives for comparing specifically the properties of the two light sources shown in Fig. 1.2, namely a laser and a photon Bose-Einstein condensate.

Chapter 2

Quantization of Maxwell Field

All electrodynamic processes are described by the Maxwell equations. Surprisingly they represent the equations of motion of a first-quantized theory, although the Planck constant $\hbar$ does not appear explicitly. This apparent contradiction is resolved by the following consideration. If the quanta of the Maxwell field, i.e. the photons, had a finite rest mass M, then it would appear due to dimensional reasons together with spatio-temporal derivatives as a mass term in the equations of motion in form of the inverse Compton wavelength. This length scale $1/\lambda_C = Mc/2\pi\hbar$ emerges from combining the Heisenberg uncertainty principle of quantum mechanics with the principle of special relativity that the largest possible velocity is provided by the light velocity. Thus, performing the limit of a vanishing rest mass, i.e. $M \to 0$, also the Planck constant $\hbar$ vanishes automatically from the respective equations of motion.

In this chapter we start with reviewing this first-quantized Maxwell theory. Afterwards, we provide its field-theoretical formulation in the sense of Lagrange and Hamilton. On the basis of this we then invoke the canonical field quantization formalism and work out systematically the second quantization of the Maxwell theory. In particular, we have to deal with the intricate consequences of the underlying local gauge symmetry, which is due to the vanishing rest mass of the quanta of the Maxwell field. In this way we derive from first principles step by step the respective properties of a single photon as, for instance, its energy.

Furthermore, we present three examples of quantum fluctuation effects of the second-quantized Maxwell theory. At first we determine the vacuum correlation function of the electric field, which cannot be measured directly with an intensity detector and was only recently proven experimentally. Therefore, historically, it was important to provide an indirect evidence for the existence of vacuum fluctuations of the electromagnetic field. To this end we calculate the Casimir effect, that two plane-parallel metal plates with a vacuum in between turn out to attract each other due to vacuum energy fluctuations. And, finally, we discuss the Lamb shift that the degeneracy of the two hydrogen energy levels $2^2\mathrm{s}_{1/2}$ and $2^2\mathrm{p}_{1/2}$, which is an immediate consequence of the Dirac equation, is lifted due to interaction of the vacuum energy fluctuations with the hydrogen electron. Thus, we conclude that in physics the vacuum is not nothing [20].

2.1 Maxwell Equations

Forces of an electromagnetic field upon electric charges, which are at rest or move, are mediated by both the electric field strength $\mathbf{E}$ and the magnetic induction $\mathbf{B}$. Physically both vector fields are generated by the charge density ρ and the current density $\mathbf{j}$. Mathematically they are determined by partial differential equations, which were first formulated by James Clerk Maxwell. The general structure of the Maxwell equations is prescribed by the Helmholtz vector decomposition theorem, which states that any vector field is uniquely determined by its respective divergence and rotation in combination with appropriate boundary conditions. With this the electric field strength $\mathbf{E}$ follows from

$$\begin{aligned} \operatorname{div} \mathbf{E} &= \frac{\rho}{\varepsilon_0}\,, && (2.1)\\ \operatorname{rot} \mathbf{E} &= -\frac{\partial \mathbf{B}}{\partial t}\,, && (2.2) \end{aligned}$$

whereas the magnetic induction $\mathbf{B}$ is defined by

$$\begin{aligned} \operatorname{div} \mathbf{B} &= 0\,, && (2.3)\\ \operatorname{rot} \mathbf{B} &= \mu_0 \mathbf{j} + \frac{1}{c^2}\frac{\partial \mathbf{E}}{\partial t}\,. && (2.4) \end{aligned}$$

Here the vacuum dielectric constant ϵ_0, the vacuum permeability μ_0, and the vacuum light velocity c are related via

$$c = \frac{1}{\sqrt{\varepsilon_0 \mu_0}}\,. \tag{2.5}$$

We remark that (2.1), (2.4) and (2.2), (2.3) are denoted as the inhomogeneous and homogeneous Maxwell equations, respectively. Furthermore, we read off from the inhomogeneous Maxwell equations (2.1) and (2.4) the consistency equation that charge density ρ and current density $\mathbf{j}$ are not independent from each other but must fulfill the continuity equation

$$\frac{\partial \rho}{\partial t} + \operatorname{div} \mathbf{j} = 0\,, \tag{2.6}$$

which implies the charge conservation. Namely, considering the time derivative of the charge

$$Q = \int d^3x\, \rho(\mathbf{x}, t)\,, \tag{2.7}$$

we obtain from (2.6) and applying the theorem of Gauß

$$\frac{\partial Q}{\partial t} = -\oint d\mathbf{f} \cdot \mathbf{j}(\mathbf{x}, t)\,. \tag{2.8}$$

Here the surface integral at infinity vanishes as the current density $\mathbf{j}(\mathbf{x}, t)$ is assumed to vanish fast enough at infinity, yielding

$$\frac{\partial Q}{\partial t} = 0\,. \tag{2.9}$$

Note that we formulate the Maxwell equations (2.1)–(2.4) according to the International System of Units, which is abbreviated by SI from the French Système international d'unités. Instead, in quantum field theory quite often the rational Lorentz-Heaviside unit system is used, where one assumes $\varepsilon_0 = \mu_0 = c = 1$ in order to simplify the notation. But we stick consistently to the SI unit system, although this might be considered to be more cumbersome, as this has the advantage that at each stage of the calculation one obtains results, which are, at least in principle, directly accessible in an experiment.

2.2 Local Gauge Symmetry

From the homogeneous Maxwell equations (2.2) and (2.3) we conclude straight-forwardly that both the electric field strength $\mathbf{E}$ and the magnetic induction $\mathbf{B}$ follow from differentiation of a scalar potential φ and a vector potential $\mathbf{A}$:

$$\mathbf{B} = \operatorname{rot} \mathbf{A}\,, \tag{2.10}$$

$$\mathbf{E} = -\operatorname{grad} \varphi - \frac{\partial \mathbf{A}}{\partial t}\,. \tag{2.11}$$

From the inhomogeneous Maxwell equations (2.1) and (2.4) as well as from (2.10) and (2.11) we then determine coupled partial differential equations for the scalar potential φ and the vector potential $\mathbf{A}$:

$$-\Delta \varphi - \frac{\partial}{\partial t} \operatorname{div} \mathbf{A} = \frac{\rho}{\varepsilon_0}\,, \tag{2.12}$$

$$\frac{1}{c^2}\frac{\partial^2 \mathbf{A}}{\partial t^2} - \Delta \mathbf{A} + \operatorname{grad}\left(\frac{1}{c^2}\frac{\partial \varphi}{\partial t} + \operatorname{div} \mathbf{A}\right) = \mu_0 \mathbf{j}\,. \tag{2.13}$$

The equations (2.10)–(2.13) turn out to be invariant with respect to a local gauge transformation with an arbitrary gauge function Λ:

$$\varphi' = \varphi + \frac{\partial \Lambda}{\partial t} \tag{2.14}$$

$$\mathbf{A}' = \mathbf{A} - \operatorname{grad} \Lambda\,. \tag{2.15}$$

Thus, a local gauge transformation does not have any physical consequences, but it changes the mathematical description of the electromagnetic field. For instance, choosing a particular gauge allows to decouple the coupled equations of motion (2.12) and (2.13). In the following we briefly discuss the two most prominent gauges.

The *Coulomb gauge* assumes that the longitudinal part of the vector potential $\mathbf{A}$ vanishes, i.e.

$$\operatorname{div} \mathbf{A} = 0\,. \tag{2.16}$$

With this (2.12) and (2.13) reduce to

$$\Delta \varphi = -\frac{\rho}{\varepsilon_0}\,, \tag{2.17}$$

$$\frac{1}{c^2}\frac{\partial^2 \mathbf{A}}{\partial t^2} - \Delta \mathbf{A} = \mu_0 \mathbf{j} - \frac{1}{c^2}\frac{\partial}{\partial t} \operatorname{grad} \varphi\,. \tag{2.18}$$

As the scalar potential $\varphi(\mathbf{x},t)$ obeys the Poisson equation (2.17), it is determined instantly at each time t by the corresponding value of the charge density $\rho(\mathbf{x},t)$ according to

$$\varphi(\mathbf{x},t) = \int d^3x' \, \frac{\rho(\mathbf{x}',t)}{4\pi\varepsilon_0|\mathbf{x}-\mathbf{x}'|} \,. \tag{2.19}$$

Due to (2.16) and (2.19) we conclude that from the original four fields φ and $\mathbf{A}$ only two of them represent dynamical degrees of freedom. As a consequence, the quantization of the electromagnetic field thus yields later on two types of photons. The advantage of the Coulomb gauge is that the remaining two dynamical degrees of freedom of the electromagnetic field can be physically identified with the two transversal degrees of freedom of the vector potential $\mathbf{A}$. The disadvantage of the Coulomb gauge is that it is not manifestly Lorentz invariant. Thus, the Coulomb gauge is only valid in a particular inertial system.

The *Lorentz gauge* is defined via

$$\frac{1}{c^2}\frac{\partial\varphi}{\partial t} + \operatorname{div}\mathbf{A} = 0 \,. \tag{2.20}$$

With this the coupled equations of motions (2.12) and (2.13) yield uncoupled inhomogeneous wave equations:

$$\frac{1}{c^2}\frac{\partial^2\varphi}{\partial t^2} - \Delta\,\varphi \;=\; \frac{\rho}{\varepsilon_0} \,, \tag{2.21}$$

$$\frac{1}{c^2}\frac{\partial^2\mathbf{A}}{\partial t^2} - \Delta\,\mathbf{A} \;=\; \mu_0\,\mathbf{j} \,. \tag{2.22}$$

The advantage is here that the Lorentz gauge (2.20) as well as the decoupled equations of motion (2.21), (2.22) are Lorentz invariant. On the other hand, the quantization of the electromagnetic field on the basis of the Lorentz gauge, as worked out by Suraj Gupta and Konrad Bleuler, turns out to have an essential disadvantage. Namely, apart from the two physical transversal degrees of freedom also an unphysical longitudinal degree of freedom of the electromagnetic field emerges, which has to be eliminated afterwards with some effort.

In the following we restrict us for simplicity to the free electrodynamic field, where neither electric charges nor currents are present:

$$\rho(\mathbf{x},t) = 0 \,, \qquad \mathbf{j}(\mathbf{x},t) = \mathbf{0} \,. \tag{2.23}$$

Furthermore, we assume from now on the Coulomb gauge (2.16) as it represents the basis of the standard formulation for the second quantization of the Maxwell theory and is commonly used in quantum optics. From (2.16), (2.19), and (2.23) we then conclude that the scalar potential vanishes:

$$\varphi(\mathbf{x},t) = 0 \,. \tag{2.24}$$

Note that (2.16) and (2.24) together is also known as the radiation gauge. From (2.17), (2.23), and (2.24) we then read off that the vector potential obeys the homogeneous wave equation:

$$\frac{1}{c^2}\frac{\partial^2\mathbf{A}(\mathbf{x},t)}{\partial t^2} - \Delta\mathbf{A}(\mathbf{x},t) = \mathbf{0} \,. \tag{2.25}$$

Thus, in radiation gauge the vector potential $\mathbf{A}(\mathbf{x},t)$ is determined from solving the homogeneous wave equation (2.25) by taking into account the Coulomb gauge (2.16). Once the vector potential is known, one obtains from (2.10) the magnetic induction, whereas the electric field (2.11) reduces due to the radiation gauge (2.16) and (2.24) to

$$\mathbf{E}(\mathbf{x},t) = -\frac{\partial \mathbf{A}(\mathbf{x},t)}{\partial t}\,. \tag{2.26}$$

2.3 Lagrange Formulation

Now we work out a field-theoretic formulation of the Maxwell theory by setting up a variational principle, whose Euler-Lagrange equations are equivalent to the Maxwell equations for the free electrodynamic field. Thus, the action $\mathcal{A}$ represents a functional of the vector potential $\mathbf{A}$ alone and is defined as a spatio-temporal integral of a Lagrange density $\mathcal{L}$:

$$\mathcal{A}\left[\mathbf{A}(\bullet,\bullet)\right] = \int dt \int d^3x\, \mathcal{L}\,. \tag{2.27}$$

As the underlying equation of motion in form of the homogeneous wave equation (2.25) is of second order in the spatio-temporal derivatives of the vector potential, the Lagrange density can only contain derivatives up to first order:

$$\mathcal{L} = \mathcal{L}\left(A_k(\mathbf{x},t), \frac{\partial A_k(\mathbf{x},t)}{\partial t}, \partial_j A_k(\mathbf{x},t)\right)\,. \tag{2.28}$$

Then the corresponding Hamilton principle states that the functional derivative of the action with respect to the components of the vector potential vanishes:

$$\frac{\delta \mathcal{A}}{\delta A_k(\mathbf{x},t)} = 0\,. \tag{2.29}$$

An introduction into the technique of functional derivatives is found, for instance, in the Refs. [21, Section 4.2] and [22, Section 2.3]. The resulting Euler-Lagrange equations of this classical field theory then read

$$\frac{\partial \mathcal{L}}{\partial A_k(\mathbf{x},t)} - \partial_j \frac{\partial \mathcal{L}}{\partial\, \partial_j A_k(\mathbf{x},t)} - \frac{\partial}{\partial t} \frac{\partial \mathcal{L}}{\partial\, \frac{\partial A_k(\mathbf{x},t)}{\partial t}} = 0\,. \tag{2.30}$$

Note that we use here the Einstein summation convention that one has to sum over all indices, which appear twice. The underlying Lagrange density turns out to be the difference of the electric and the magnetic energy density

$$\mathcal{L} = \frac{\varepsilon_0}{2}\,\mathbf{E}^2 - \frac{1}{2\mu_0}\,\mathbf{B}^2\,, \tag{2.31}$$

Then, using (2.10) and (2.26), the Lagrange density (2.31) reads in terms of the vector potential as follows:

$$\mathcal{L} = \frac{\varepsilon_0}{2}\left(\frac{\partial \mathbf{A}(\mathbf{x},t)}{\partial t}\right)^2 - \frac{1}{2\mu_0}\left[\boldsymbol{\nabla} \times \mathbf{A}(\mathbf{x},t)\right]^2\,. \tag{2.32}$$

With an additional calculation the Lagrange density (2.32) can be simplified. To this end we consider

$$(\boldsymbol{\nabla} \times \mathbf{A})^2 = \epsilon_{jkl}\, \partial_k A_l\, \epsilon_{jmn}\, \partial_m A_n\,, \tag{2.33}$$

which reduces due to the contraction rule of the three-dimensional Levi-Cività symbol ϵ_{ijk}

$$\epsilon_{ijk}\epsilon_{lmk} = \delta_{il}\delta_{jm} - \delta_{im}\delta_{jl} \tag{2.34}$$

to the expression

$$(\boldsymbol{\nabla} \times \mathbf{A})^2 = \partial_k A_l \partial_k A_l - \partial_k \left(A_l \partial_l A_k\right) + A_l \partial_l \partial_k A_k\,. \tag{2.35}$$

Inserting (2.35) into (2.32), the second term does not contribute to the action (2.27) due to applying the Gauß theorem and can thus be neglected in the Lagrange density. Furthermore, the third term in (2.35) is zero in the Coulomb gauge (2.16), so we end up with

$$\mathcal{L} = \frac{\varepsilon_0}{2} \frac{\partial A_k(\mathbf{x},t)}{\partial t} \frac{\partial A_k(\mathbf{x},t)}{\partial t} - \frac{1}{2\mu_0}\, \partial_j A_k(\mathbf{x},t) \partial_j A_k(\mathbf{x},t)\,. \tag{2.36}$$

Thus, we obtain the following partial derivatives from the Lagrange density (2.36)

$$\frac{\partial \mathcal{L}}{\partial A_k(\mathbf{x},t)} = 0\,, \qquad \frac{\partial \mathcal{L}}{\partial\, \partial_j A_k(\mathbf{x},t)} = -\frac{1}{\mu_0}\, \partial_j A_k(\mathbf{x},t)\,, \qquad \frac{\partial \mathcal{L}}{\partial\, \frac{\partial A_k(\mathbf{x},t)}{\partial t}} = \varepsilon_0 \frac{\partial A_k(\mathbf{x},t)}{\partial t}\,, \tag{2.37}$$

so the corresponding Euler-Lagrange equations (2.30) reduce, indeed, to the homogeneous wave equation (2.25).

2.4 Hamilton Formulation

In order to proceed from the Lagrange to the Hamilton formulation, we have to determine the momentum field $\boldsymbol{\pi}$, which is canonically conjugated to the vector potential $\mathbf{A}$. Taking into account (2.37) it follows as

$$\boldsymbol{\pi}(\mathbf{x},t) = \frac{\delta \mathcal{A}}{\delta\, \frac{\partial \mathbf{A}(\mathbf{x},t)}{\partial t}} = \frac{\partial \mathcal{L}}{\partial\, \frac{\partial \mathbf{A}(\mathbf{x},t)}{\partial t}} = \varepsilon_0 \frac{\partial \mathbf{A}(\mathbf{x},t)}{\partial t}\,. \tag{2.38}$$

This corresponds to the classical expression for the momentum $\mathbf{p} = m\dot{\mathbf{x}}$, provided we identify the coordinate $\mathbf{x}$ with the vector potential $\mathbf{A}$ and the mass m with the vacuum dielectric constant ε_0. A subsequent Legendre transformation

$$\mathcal{H} = \boldsymbol{\pi}(\mathbf{x},\mathbf{t}) \frac{\partial \mathbf{A}(\mathbf{x},t)}{\partial t} - \mathcal{L} \tag{2.39}$$

converts then the Lagrange density (2.36) to the Hamilton density

$$\mathcal{H} = \frac{1}{2\epsilon_0}\, \pi_k(\mathbf{x},t)\pi_k(\mathbf{x},t) + \frac{1}{2\mu_0}\, \partial_k A_l(\mathbf{x},t) \partial_k A_l(\mathbf{x},t)\,. \tag{2.40}$$

Due to (2.10), (2.26), and (2.38) this turns out to coincide with the well-known energy density of the free electromagnetic field in SI units:

$$\mathcal{H} = \frac{\varepsilon_0}{2}\,\mathbf{E}^2 + \frac{1}{2\mu_0}\,\mathbf{B}^2\,, \tag{2.41}$$

which is the sum of the electric and the magnetic energy density. Furthermore, a spatial integral over the Hamilton density yields the Hamilton function

$$H = \int d^3x\,\mathcal{H}\,, \tag{2.42}$$

which follows from (2.40) to be

$$H = \frac{1}{2}\int d^3x \left\{ \frac{1}{\epsilon_0}\,\pi_k(\mathbf{x},t)\pi_k(\mathbf{x},t) + \frac{1}{\mu_0}\,\partial_k A_l(\mathbf{x},t)\partial_k A_l(\mathbf{x},t) \right\}. \tag{2.43}$$

Note that the first (second) term represents the kinetic (potential) energy of the electromagnetic field.

2.5 Canonical Field Quantization

The electrodynamic field is now quantized in the Heisenberg picture by exchanging the fields $A_j(\mathbf{x},t)$ and $\pi_j(\mathbf{x},t)$ with their corresponding field operators $\hat{A}_j(\mathbf{x},t)$ and $\hat{\pi}_j(\mathbf{x},t)$. To this end we perform a bosonic field quantization and demand equal-time commutation relations. At first, we demand that the field operators $\hat{A}_j(\mathbf{x},t)$ and $\hat{\pi}_j(\mathbf{x},t)$ commute, as usual, among themselves, respectively:

$$\left[\hat{A}_k(\mathbf{x},t), \hat{A}_l(\mathbf{x}',t)\right]_- = 0, \tag{2.44}$$

$$\left[\hat{\pi}_k(\mathbf{x},t), \hat{\pi}_l(\mathbf{x}',t)\right]_- = 0. \tag{2.45}$$

But when it comes to the equal-time commutation relations between the field operators $\hat{A}_j(\mathbf{x},t)$ and $\hat{\pi}_j(\mathbf{x},t)$, the situation turns out to be more intriguing. Let us investigate tentatively whether naive equal-time commutation relations of the form

$$\left[\hat{A}_k(\mathbf{x},t), \hat{\pi}_l(\mathbf{x}',t)\right]_- = i\hbar\,\delta_{kl}\delta(\mathbf{x}-\mathbf{x}') \tag{2.46}$$

are possible. On the one hand, a derivative with respect to x_k then yields at the left-hand side of (2.46) to

$$\partial_k \left[\hat{A}_k(\mathbf{x},t), \hat{\pi}_l(\mathbf{x}',t)\right]_- = \left[\partial_k \hat{A}_k(\mathbf{x},t), \hat{\pi}_l(\mathbf{x}',t)\right]_- = 0\,, \tag{2.47}$$

as we have to demand the quantized version of the Coulomb gauge (2.16):

$$\partial_j \hat{A}_j(\mathbf{x},t) = 0\,. \tag{2.48}$$

On the other, a derivative with respect to x_k at the right-hand side of (2.46) leads to

$$i\hbar\,\delta_{kl}\partial_k\delta(\mathbf{x}-\mathbf{x}') = i\hbar\,\partial_l\delta(\mathbf{x}-\mathbf{x}') \neq 0\,, \tag{2.49}$$

i.e. to an expression, which is non-zero in obvious contradiction to (2.47). Therefore, we are forced to modify the naive equal-time commutation relations (2.46) in such a way that it becomes compatible with the quantized version of the Coulomb gauge (2.48). To this end we consider the Fourier transformed of the right-hand side of (2.46)

$$i\hbar\,\delta_{kl}\delta(\mathbf{x}-\mathbf{x}') = i\hbar\int\frac{d^3k}{(2\pi)^3}\,\delta_{kl}\,e^{i\mathbf{k}(\mathbf{x}-\mathbf{x}')} \tag{2.50}$$

and substitute this expression by a yet to be determined transversal delta function

$$i\hbar\,\delta^T_{kl}(\mathbf{x}-\mathbf{x}') = i\hbar\int\frac{d^3k}{(2\pi)^3}\,\delta^T_{kl}(\mathbf{k})\,e^{i\mathbf{k}(\mathbf{x}-\mathbf{x}')}\,. \tag{2.51}$$

The Fourier transformed of the transversal delta function is then fixed from demanding that the derivative of (2.51) with respect to x_k vanishes, i.e.

$$i\hbar\,\partial_k\delta^T_{kl}(\mathbf{x}-\mathbf{x}') = i\hbar\int\frac{d^3k}{(2\pi)^3}\,ik_k\,\delta^T_{kl}(\mathbf{k})\,e^{i\mathbf{k}(\mathbf{x}-\mathbf{x}')} = 0\,. \tag{2.52}$$

For this to be valid it is sufficient that the transversality condition

$$k_k\,\delta^T_{kl}(\mathbf{k}) = 0 \tag{2.53}$$

is fulfilled. By comparing (2.50) and (2.51) a suitable ansatz for the Fourier transformed of the transversal delta function reads

$$\delta^T_{kl}(\mathbf{k}) = \delta_{kl} + k_k k_l\,f(\mathbf{k})\,. \tag{2.54}$$

The yet unknown function $f(\mathbf{k})$ follows then from inserting (2.54) into (2.53):

$$f(\mathbf{k}) = -\frac{1}{\mathbf{k}^2}\,. \tag{2.55}$$

Thus, from (2.51), (2.54), and (2.55) we then conclude for the transversal delta function

$$\delta^T_{kl}(\mathbf{x}-\mathbf{x}') = \delta_{kl}\delta(\mathbf{x}-\mathbf{x}') + \partial'_k\partial'_l\int\frac{d^3k}{(2\pi)^3}\,\frac{1}{\mathbf{k}^2}\,e^{i\mathbf{k}(\mathbf{x}-\mathbf{x}')}\,. \tag{2.56}$$

The remaining integral is known, for instance, within the realm of electrostatics from determining the Green function of the Poisson equation and yields the Coulomb potential. Thus, we obtain for the transversal delta function

$$\delta^T_{kl}(\mathbf{x}-\mathbf{x}') = \delta_{kl}\,\delta(\mathbf{x}-\mathbf{x}') + \frac{1}{4\pi}\,\partial'_k\partial'_l\,\frac{1}{|\mathbf{x}-\mathbf{x}'|}\,. \tag{2.57}$$

And, finally, we summarize our derivation by stating that the naive equal-time commutation relations (2.46) have to be modified by

$$\Big[\hat{A}_k(\mathbf{x},t),\hat{\pi}_l(\mathbf{x}',t)\Big]_- \;=\; i\hbar\,\delta^T_{kl}(\mathbf{x}-\mathbf{x}') \tag{2.58}$$

in order to be compatible with the quantized version of the Coulomb gauge (2.48).

However, one should be aware that a derivation of commutation relations always has an essential caveat. As hard as one tries to consistently determine such basic principles, they are always attached with heuristic elements. Whether commutation relations are at the end correct or not can only be verified by checking any prediction following from them against experimental measurements. In this spirit we will show later on that demanding the bosonic equal-time commutation relations (2.44), (2.45), and (2.58) leads, indeed, to a consistent description of the electromagnetic field with the help of usual annihilation and creation operators for photons, i.e. the quanta of light.

2.6 Heisenberg Equations

Furthermore, proceeding with the second-quantized formalism, we obtain from the Hamilton function (2.43) the Hamilton operator

$$\hat{H} = \frac{1}{2} \int d^3x' \left\{ \frac{1}{\epsilon_0} \hat{\pi}_k(\mathbf{x}', t) \hat{\pi}_k(\mathbf{x}', t) + \frac{1}{\mu_0} \partial'_k \hat{A}_l(\mathbf{x}', t) \partial'_k \hat{A}_l(\mathbf{x}', t) \right\} . \tag{2.59}$$

Note that the order of the operators in (2.59) does not play a role due to the commutation relations (2.44) and (2.45). Let us now evaluate the Heisenberg equation for the field operator

$$i\hbar \frac{\partial \hat{A}_j(\mathbf{x}, t)}{\partial t} = \left[\hat{A}_j(\mathbf{x}, t), \hat{H} \right]_- \tag{2.60}$$

by inserting therein the Hamilton operator (2.59). In order to calculate (2.60) the following ABC-rule for commutators turns out to be useful

$$\left[\hat{A}\hat{B}, \hat{C} \right]_- = \hat{A} \left[\hat{B}, \hat{C} \right]_- + \left[\hat{A}, \hat{C} \right]_- \hat{B} \, , \tag{2.61}$$

which follows immediately from the definition of the commutator. After applying (2.61) as well as the equal-time commutation relations (2.44), (2.45), and (2.58) we get at first

$$i\hbar \frac{\partial \hat{A}_j(\mathbf{x}, t)}{\partial t} = \frac{i\hbar}{\epsilon_0} \int d^3x' \, \delta^T_{jk}(\mathbf{x} - \mathbf{x}') \, \hat{\pi}_k(\mathbf{x}', t) \, . \tag{2.62}$$

Taking into account the transversal delta function (2.57), a partial integration yields

$$i\hbar \frac{\partial \hat{A}_j(\mathbf{x}, t)}{\partial t} = \frac{i\hbar}{\epsilon_0} \left\{ \hat{\pi}_j(\mathbf{x}, t) - \frac{1}{4\pi} \int d^3x' \left(\partial'_j \frac{1}{|\mathbf{x} - \mathbf{x}'|} \right) \partial'_k \hat{\pi}_k(\mathbf{x}', t) \right\} . \tag{2.63}$$

With this we reproduce the quantized version of (2.38), as the last term in (2.63) vanishes due to the quantized version of the Coulomb gauge (2.48):

$$\frac{\partial \hat{A}_j(\mathbf{x}, t)}{\partial t} = \frac{1}{\epsilon_0} \hat{\pi}_j(\mathbf{x}, t) \, . \tag{2.64}$$

Correspondingly, the Heisenberg equation for the momentum field operator reads

$$i\hbar\frac{\partial\hat{\pi}_j(\mathbf{x},t)}{\partial t} = \left[\hat{\pi}_j(\mathbf{x},t),\hat{H}\right]_- . \tag{2.65}$$

Using (2.61) as well as the equal-time commutation relations (2.44), (2.45), and (2.58) we get at first

$$i\hbar\,\frac{\partial\hat{\pi}_j(\mathbf{x},t)}{\partial t} = \frac{-i\hbar}{\mu_0}\int d^3x'\,\partial'_k\delta^T_{jl}(\mathbf{x}-\mathbf{x}')\,\partial'_k\hat{A}_l(\mathbf{x}',t)\,, \tag{2.66}$$

so a partial integration yields

$$i\hbar\,\frac{\partial\hat{\pi}_j(\mathbf{x},t)}{\partial t} = \frac{i\hbar}{\mu_0}\int d^3x'\,\delta^T_{jl}(\mathbf{x}-\mathbf{x}')\,\Delta'\hat{A}_l(\mathbf{x}',t)\,, \tag{2.67}$$

Due to the explicit form of the transversal delta function (2.57) and a partial integration we then get

$$i\hbar\,\frac{\partial\hat{\pi}_j(\mathbf{x},t)}{\partial t} = \frac{i\hbar}{\mu_0}\left\{\partial_k\partial_k\hat{A}_j(\mathbf{x},t) - \frac{1}{4\pi}\int d^3x'\,\left(\partial'_j\,\frac{1}{|\mathbf{x}-\mathbf{x}'|}\right)\,\Delta'\,\partial'_l\hat{A}_l(\mathbf{x}',t)\right\}. \tag{2.68}$$

With the quantized version of the Coulomb gauge (2.48) this reduces finally to

$$\frac{\partial\hat{\pi}_j(\mathbf{x},t)}{\partial t} = \frac{1}{\mu_0}\,\Delta\hat{A}_j(\mathbf{x},t)\,. \tag{2.69}$$

Thus, we conclude from (2.5), (2.64), and (2.69) that the field operator $\hat{\mathbf{A}}(\mathbf{x},t)$ obeys like the classical field $\mathbf{A}(\mathbf{x},t)$ in (2.25) the homogeneous wave equation:

$$\frac{1}{c^2}\,\frac{\partial^2\hat{\mathbf{A}}(\mathbf{x},t)}{\partial t^2} - \Delta\hat{\mathbf{A}}(\mathbf{x},t) = \mathbf{0}\,. \tag{2.70}$$

2.7 Solution of Wave Equation

We start with solving the operator-valued wave equation (2.70) by a Fourier decomposition into plane waves:

$$\hat{\mathbf{A}}(\mathbf{x},t) = \int d^3k\,\hat{\mathbf{A}}(\mathbf{k},t)\,e^{i\mathbf{k}\mathbf{x}}\,. \tag{2.71}$$

Inserting (2.71) into (2.70) one obtains for the expansion operators $\hat{\mathbf{A}}(\mathbf{k},t)$ the differential equation

$$\frac{\partial^2\hat{\mathbf{A}}(\mathbf{k},t)}{\partial t^2} + \omega^2_{\mathbf{k}}\,\hat{\mathbf{A}}(\mathbf{k},t) = \mathbf{0}\,, \tag{2.72}$$

where the dispersion relation turns out to be linear:

$$\omega_{\mathbf{k}} = c|\mathbf{k}|\,. \tag{2.73}$$

Thus, according to (2.72), the expansion operators $\hat{\mathbf{A}}(\mathbf{k},t)$ follow for each wave vector $\mathbf{k}$ the dynamics of a harmonic oscillator:

$$\hat{\mathbf{A}}(\mathbf{k},t) = \hat{\mathbf{A}}^{(1)}(\mathbf{k})\, e^{-i\omega_{\mathbf{k}}t} + \hat{\mathbf{A}}^{(2)}(\mathbf{k})\, e^{i\omega_{\mathbf{k}}t}\,, \tag{2.74}$$

so that the field operator (2.71) results in

$$\hat{\mathbf{A}}(\mathbf{x},t) = \int d^3k \left\{ \hat{\mathbf{A}}^{(1)}(\mathbf{k}) e^{i(\mathbf{kx}-\omega_{\mathbf{k}}t)} + \hat{\mathbf{A}}^{(2)}(\mathbf{k}) e^{i(\mathbf{kx}+\omega_{\mathbf{k}}t)} \right\}. \tag{2.75}$$

Performing in the second integral the substitution $\mathbf{k} \to -\mathbf{k}$ and taking into account the symmetry of the dispersion relation (2.73), i.e.

$$\omega_{\mathbf{k}} = \omega_{-\mathbf{k}}\,, \tag{2.76}$$

the Fourier decomposition (2.75) is converted into

$$\hat{\mathbf{A}}(\mathbf{x},t) = \int d^3k \left\{ \hat{\mathbf{A}}^{(1)}(\mathbf{k}) e^{i(\mathbf{kx}-\omega_{\mathbf{k}}t)} + \hat{\mathbf{A}}^{(2)}(-\mathbf{k}) e^{-i(\mathbf{kx}-\omega_{\mathbf{k}}t)} \right\}. \tag{2.77}$$

Thus, the adjoint field operator reads

$$\hat{\mathbf{A}}^{\dagger}(\mathbf{x},t) = \int d^3k \left\{ \hat{\mathbf{A}}^{(1)\dagger}(\mathbf{k}) e^{-i(\mathbf{kx}-\omega_{\mathbf{k}}t)} + \hat{\mathbf{A}}^{(2)\dagger}(-\mathbf{k}) e^{i(\mathbf{kx}-\omega_{\mathbf{k}}t)} \right\}. \tag{2.78}$$

As the vector potential of electrodynamics is real, we demand that the field operator as its second-quantized counterpart is self-adjoint, i.e.

$$\hat{\mathbf{A}}(\mathbf{x},t) = \hat{\mathbf{A}}^{\dagger}(\mathbf{x},t)\,. \tag{2.79}$$

Due to the completeness of the plane waves we then conclude from (2.77) and (2.78):

$$\hat{\mathbf{A}}^{(1)}(\mathbf{k}) = \hat{\mathbf{A}}^{(2)\dagger}(-\mathbf{k})\,, \qquad \hat{\mathbf{A}}^{(2)}(-\mathbf{k}) = \hat{\mathbf{A}}^{(1)\dagger}(\mathbf{k})\,, \tag{2.80}$$

where the second condition follows from the first one and, thus, does not contain any new information. Therefore, we deduce from (2.80)

$$\hat{\mathbf{A}}^{(1)}(\mathbf{k}) = \hat{\mathbf{A}}(\mathbf{k})\,, \qquad \hat{\mathbf{A}}^{(2)}(\mathbf{k}) = \hat{\mathbf{A}}^{\dagger}(-\mathbf{k})\,. \tag{2.81}$$

Inserting the finding (2.81) into the Fourier decomposition (2.77), we finally obtain

$$\hat{\mathbf{A}}(\mathbf{x},t) = \int d^3k \left\{ \hat{\mathbf{A}}(\mathbf{k}) e^{i(\mathbf{kx}-\omega_{\mathbf{k}}t)} + \hat{\mathbf{A}}^{\dagger}(\mathbf{k}) e^{-i(\mathbf{kx}-\omega_{\mathbf{k}}t)} \right\}. \tag{2.82}$$

2.8 Polarization Vectors

Now we acquire a more detailed understanding of the description of plane waves. To this end we define two linearly polarized plane waves with the wave vector $\mathbf{k}$ and the dispersion (2.73) via

$$\mathbf{A}_1(\mathbf{x},t) = A_1 \boldsymbol{\epsilon}_1 e^{i(\mathbf{kx}-\omega_{\mathbf{k}}t)}\,, \qquad \mathbf{A}_2(\mathbf{x},t) = A_2 \boldsymbol{\epsilon}_2 e^{i(\mathbf{kx}-\omega_{\mathbf{k}}t)}\,. \tag{2.83}$$

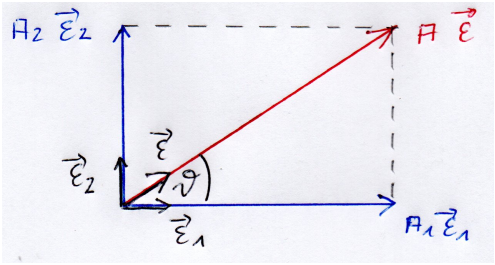

Figure 2.1: Adding two linearly polarized plane waves according to (2.85) with complex amplitudes A_1 and A_2, which have the same phase.

Here A_1, A_2 represent the respective complex-valued amplitudes and $\boldsymbol{\epsilon}_1$, $\boldsymbol{\epsilon}_2$ denote two complex-valued polarization vectors, which are orthonormalized according to

$$\boldsymbol{\epsilon}_i^* \boldsymbol{\epsilon}_j = \delta_{ij} \,. \tag{2.84}$$

Let us consider now the sum of those two linearly polarized plane waves:

$$\mathbf{A}(\mathbf{x},t) = \mathbf{A}_1(\mathbf{x},t) + \mathbf{A}_2(\mathbf{x},t) = (A_1\boldsymbol{\epsilon}_1 + A_2\boldsymbol{\epsilon}_2)\, e^{i(\mathbf{kx}-\omega_\mathbf{k} t)} \,. \tag{2.85}$$

Provided that both complex amplitudes $A_1 = |A_1|e^{i\varphi}$ and $A_2 = |A_2|e^{i\varphi}$ have the same phase φ, also their sum (2.85) is linearly polarized and we get

$$\mathbf{A}(\mathbf{x},t) = A\boldsymbol{\epsilon} e^{i(\mathbf{kx}-\omega_\mathbf{k} t)} \,. \tag{2.86}$$

Here the resulting amplitude A is given by

$$A = \sqrt{|A_1|^2 + |A_2|^2}\, e^{i\varphi} \tag{2.87}$$

and the resulting polarization vector $\boldsymbol{\epsilon}$ has the angle

$$\vartheta = \arctan \frac{|A_2|}{|A_1|} \tag{2.88}$$

with respect to $\boldsymbol{\epsilon}_1$, see Fig. 2.1. However, in the more general case that both complex amplitudes $A_1 = |A_1|e^{i\varphi_1}$ and $A_2 = |A_2|e^{i\varphi_2}$ have different phases $\varphi_1 \neq \varphi_2$, the sum (2.85) represents an elliptically polarized plane wave. Let us illustrate this for the simpler situation of a circularly polarized plane wave, which occurs provided that both complex amplitudes A_1 and A_2 have the same absolute value and their phases differ by 90°:

$$A_1 = \frac{A_0}{\sqrt{2}} \,, \qquad A_2 = \pm i \frac{A_0}{\sqrt{2}} \,. \tag{2.89}$$

Inserting (2.89) into (2.85) we obtain for the sum of the two linearly polarized plane waves

$$\mathbf{A}(\mathbf{x},t) = \frac{A_0}{\sqrt{2}}\, (\boldsymbol{\epsilon}_1 \pm i\boldsymbol{\epsilon}_2)\, e^{i(\mathbf{kx}-\omega_\mathbf{k} t)} \,. \tag{2.90}$$

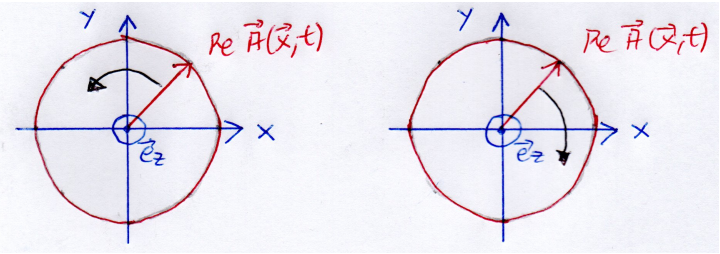

Figure 2.2: Adding two linearly polarized plane waves according to (2.85) with complex amplitudes A_1 and A_2 with the same absolute value and phases, which differ by 90°.

In order to be concrete we choose now the coordinate axes in such a way that the plane wave propagates in z-direction, whereas the two polarization vectors $\boldsymbol{\epsilon}_1$ and $\boldsymbol{\epsilon}_2$, which are normalized according to (2.84), point in x- and y-direction:

$$\mathbf{k} = k \begin{pmatrix} 0 \\ 0 \\ 1 \end{pmatrix}, \qquad \boldsymbol{\epsilon}_1 = \begin{pmatrix} 1 \\ 0 \\ 0 \end{pmatrix}, \qquad \boldsymbol{\epsilon}_2 = \begin{pmatrix} 0 \\ 1 \\ 0 \end{pmatrix}. \tag{2.91}$$

With this Eq. (2.90) reduces to

$$\mathbf{A}(\mathbf{x},t) = \frac{A_0}{\sqrt{2}} \begin{pmatrix} 1 \\ \pm i \\ 0 \end{pmatrix} e^{i(k\mathbf{e}_z\mathbf{x} - \omega_{k\mathbf{e}_z} t)}. \tag{2.92}$$

Considering the real part of the vector potential $\mathbf{A}(\mathbf{x},t)$ at a fixed space point $\mathbf{x}$, it represents a vector in the xy-plane with constant absolute value A_0, which rotates on a circle with the frequency $\omega_{k\mathbf{e}_z}$:

$$\mathrm{Re}\, A_x(\mathbf{x},t) = \frac{A_0}{\sqrt{2}} \cos k(z-ct), \quad \mathrm{Re}\, A_y(\mathbf{x},t) = \mp \frac{A_0}{\sqrt{2}} \sin k(z-ct), \quad \mathrm{Re}\, A_z(\mathbf{x},t) = 0. \tag{2.93}$$

For the upper (lower) sign the rotation is performed anti-clockwise (clockwise) for an observer looking in the direction of the oncoming light beam. Such a plane wave is called in optics left-(right-) circularly polarized light, whereas in elementary particle physics one says that such a plane wave has positive (negative) helicity, see Fig. 2.2.

2.9 Construction of Polarization Vectors

Let us discuss the helicity of an electromagnetic wave in more detail. To this end one has to take into account the two characteristic properties of the photon as the quantum of light. Like any other elementary particle it has an internal angular momentum called spin $\mathbf{S}$, which corresponds to its intrinsic rotation. Furthermore, the photon turns out to have a rest mass, which vanishes. This implies that the spin $\mathbf{S}$ points either in the direction of propagation $\mathbf{k}$ or opposite to it, which is called positive or negative helicity, see Fig. 2.3.

Figure 2.3: a) Positive or b) negative helicity: Spin $\mathbf{S}$ points in or opposite to the direction of propagation $\mathbf{k}/|\mathbf{k}|$.

In order to quantify the notion of a spin further, we have to consider the representation theory of rotations in the three-dimensional configuration space of the vector field $\mathbf{A}$, which corresponds to the space of coordinate vectors $\mathbf{x}$. A general rotation matrix turns out to have the form [21]

$$R_{jk}(\boldsymbol{\varphi}) = \frac{\varphi_i}{|\boldsymbol{\varphi}|}\,\epsilon_{ikj}\,\sin|\boldsymbol{\varphi}| + \frac{\varphi_j\varphi_k}{|\boldsymbol{\varphi}|^2}\,(1-\cos|\boldsymbol{\varphi}|) + \delta_{jk}\,\cos|\boldsymbol{\varphi}|\,. \tag{2.94}$$

We remark that the 3×3 matrix defined by (2.94) fulfills two properties, which are characteristic for describing a rotation around the axis $\boldsymbol{\varphi}$ with the angle $|\boldsymbol{\varphi}|$. On the one hand the rotation axis $\boldsymbol{\varphi}$ is an eigenvalue of the rotation matrix $R(\boldsymbol{\varphi})$ with eigenvalue 1:

$$R(\boldsymbol{\varphi})\,\boldsymbol{\varphi} = \boldsymbol{\varphi}\,. \tag{2.95}$$

On other hand the trace of the rotation matrix $R(\boldsymbol{\varphi})$ is related to the rotation angle $|\boldsymbol{\varphi}|$ via

$$\mathrm{Tr}\,R(\boldsymbol{\varphi}) = 1 + 2\cos|\boldsymbol{\varphi}|\,. \tag{2.96}$$

Restricting (2.94) to an infinitesimal rotation yields

$$R_{jk}(\boldsymbol{\varphi}) = \varphi_i\,\epsilon_{ikj}\,. \tag{2.97}$$

With this we obtain for the spin $\mathbf{S}$, which we identify with the generator $\mathbf{S} = (S_m)$ of rotations

$$(S_m)_{jk} = i\,\frac{\partial R_{jk}(\boldsymbol{\varphi})}{\partial\varphi_m}\bigg|_{\boldsymbol{\varphi}=\mathbf{0}}\,, \tag{2.98}$$

the components

$$(S_m)_{jk} = i\,\epsilon_{mkj}\,. \tag{2.99}$$

The resulting spin matrices read explicitly

$$S_1 = i\begin{pmatrix}0&0&0\\0&0&-1\\0&1&0\end{pmatrix}\,,\quad S_2 = i\begin{pmatrix}0&0&1\\0&0&0\\-1&0&0\end{pmatrix}\,,\quad S_3 = i\begin{pmatrix}0&-1&0\\1&0&0\\0&0&0\end{pmatrix} \tag{2.100}$$

and fulfill the commutation relations of the algebra of angular momenta:

$$[S_i, S_j]_- = i\,\epsilon_{ijk}S_k\,. \tag{2.101}$$

Conversely, the knowledge of the generators of rotations (2.100) allows to reconstruct the rotation matrix (2.94) on the basis of the Lie theorem by evaluating the matrix exponential function [21]

$$R(\boldsymbol{\varphi}) = \exp\Big\{ - i\boldsymbol{\varphi}\mathbf{S}\Big\}\,. \tag{2.102}$$

With the representation theory of rotations, the helicity operator is now defined by projecting the generator of rotations $\mathbf{S}$ upon the direction of propagation, which is defined by the wave vector $\mathbf{k}$:

$$\hat{h}(\mathbf{k}) = \frac{\mathbf{k}}{k}\,\mathbf{S}\,. \tag{2.103}$$

Inserting (2.100) into (2.102) yields the explicit form of the helicity operator:

$$\hat{h}(\mathbf{k}) = \frac{i}{k}\begin{pmatrix} 0 & -k_z & k_y \\ k_z & 0 & -k_x \\ -k_y & k_x & 0 \end{pmatrix}\,. \tag{2.104}$$

Now we introduce the polarization vectors $\boldsymbol{\epsilon}(\mathbf{k},\lambda)$ for plane waves, which propagate with the wave vector $\mathbf{k}$ and the helicity $\lambda = \pm 1$:

$$\mathbf{A}(\mathbf{x},t) = A\boldsymbol{\epsilon}(\mathbf{k},\lambda)e^{i(\mathbf{kx}-\omega_{\mathbf{k}}t)}\,. \tag{2.105}$$

Here the polarization vectors $\boldsymbol{\epsilon}(\mathbf{k},\lambda)$ represent the eigenvectors of the helicity operator (2.103) with the eigenvalues $\lambda = \pm 1$:

$$\hat{h}(\mathbf{k})\boldsymbol{\epsilon}(\mathbf{k},\lambda) = \lambda\boldsymbol{\epsilon}(\mathbf{k},\lambda)\,. \tag{2.106}$$

From (2.92) and (2.105) we read off the polarization vectors $\boldsymbol{\epsilon}(k\mathbf{e}_z,\lambda)$ for a propagation in z-direction:

$$\boldsymbol{\epsilon}(k\mathbf{e}_z,\lambda) = \frac{1}{\sqrt{2}}\begin{pmatrix} 1 \\ \lambda i \\ 0 \end{pmatrix}\,. \tag{2.107}$$

Indeed, the polarization vectors (2.107) fulfill due to (2.104) the eigenvalue problem

$$\hat{h}(k\mathbf{e}_z)\boldsymbol{\epsilon}(k\mathbf{e}_z,\lambda) = \lambda\boldsymbol{\epsilon}(k\mathbf{e}_z,\lambda)\,. \tag{2.108}$$

Now we construct the polarization vectors $\boldsymbol{\epsilon}(\mathbf{k},\lambda)$ with a general wave vector $\mathbf{k}$ by rotating the polarization vectors $\boldsymbol{\epsilon}(k\mathbf{e}_z,\lambda)$ in the same way as the original wave vector $k\mathbf{e}_z$. To this end we need the rotation matrix $R(\theta,\phi)$, which rotates the original wave vector $k\mathbf{e}_z$ to the general wave vector $\mathbf{k}$, where the latter is described in terms of spherical coordinates k, θ, and ϕ:

$$\mathbf{k} = k\begin{pmatrix} \sin\theta\cos\phi \\ \sin\theta\sin\phi \\ \cos\theta \end{pmatrix}\,. \tag{2.109}$$

Here the rotation matrix $R(\theta,\phi)$ is constructed such that first the rotation $R_y(\theta)$ around the y-axis with angle θ and then the rotation $R_z(\phi)$ around the z-axis with angle ϕ is applied:

$$R(\theta,\phi) = R_z(\phi)\, R_y(\theta)\,. \tag{2.110}$$

The individual rotation matrices follow from evaluating matrix exponential functions

$$R_z(\phi) \;=\; e^{-iL_3\phi} = \begin{pmatrix} \cos\phi & \sin\phi & 0 \\ -\sin\phi & \cos\phi & 0 \\ 0 & 0 & 1 \end{pmatrix}, \tag{2.111}$$

$$R_y(\theta) \;=\; e^{-iL_2\theta} = \begin{pmatrix} \cos\theta & 0 & \sin\theta \\ 0 & 1 & 0 \\ -\sin\theta & 0 & \cos\theta \end{pmatrix}, \tag{2.112}$$

where the respective generators stem from (2.100). As a result we obtain for the rotation (2.110)

$$R(\theta,\phi) = \begin{pmatrix} \cos\theta\cos\phi & -\sin\phi & \sin\theta\cos\phi \\ \cos\theta\sin\phi & \cos\phi & \sin\theta\sin\phi \\ -\sin\theta & 0 & \cos\theta \end{pmatrix}. \tag{2.113}$$

Indeed, the rotation matrix $R(\theta,\phi)$ maps the original wave vector $k\mathbf{e}_z$ to the general wave vector (2.109) as follows from the third column of (2.113):

$$R(\theta,\phi)k\mathbf{e}_z = \mathbf{k}\,. \tag{2.114}$$

Transforming correspondingly also the polarization vectors $\boldsymbol{\epsilon}(k\mathbf{e}_z,\lambda)$ from (2.107) with the rotation matrix $R(\theta,\phi)$, i.e.

$$\boldsymbol{\epsilon}(\mathbf{k},\lambda) = R(\theta,\phi)\boldsymbol{\epsilon}(k\mathbf{e}_z,\lambda)\,, \tag{2.115}$$

we obtain the explicit result

$$\boldsymbol{\epsilon}(\mathbf{k},\lambda) = \frac{1}{\sqrt{2}} \begin{pmatrix} \cos\theta\cos\phi - \lambda i\sin\phi \\ \cos\theta\sin\phi + \lambda i\cos\phi \\ -\sin\theta \end{pmatrix}. \tag{2.116}$$

Indeed, taking into account (2.104) and (2.109) one can show that the polarization vectors (2.116) fulfill the eigenvalue problem of the helicity operator (2.106). Furthermore, as expected, the polarization vectors (2.116) reduce for the special case $\theta = \phi = 0$ to the original polarization vectors (2.107).

2.10 Properties of Polarization Vectors

Due to the Coulomb gauge (2.16) the Fourier components $\hat{\mathbf{A}}(\mathbf{k})$ in the decomposition (2.82) must obey the transversality condition

$$\mathbf{k}\cdot\hat{\mathbf{A}}(\mathbf{k}) = 0\,. \tag{2.117}$$

This means that the Fourier operators $\hat{\mathbf{A}}(\mathbf{k})$ have two transversal dynamical degrees of freedom. Performing the ansatz

$$\hat{\mathbf{A}}(\mathbf{k}) = N_{\mathbf{k}} \sum_{\lambda=\pm 1} \boldsymbol{\epsilon}(\mathbf{k},\lambda)\hat{a}_{\mathbf{k},\lambda} \tag{2.118}$$

with some normalization constants $N_{\mathbf{k}}$ the transversality condition (2.117) is fulfilled provided that the polarization vectors $\boldsymbol{\epsilon}(\mathbf{k},\lambda)$ are perpendicular to the propagation direction, which is defined by the wave vector (2.109):

$$\mathbf{k}\cdot\boldsymbol{\epsilon}(\mathbf{k},\lambda) = 0\,. \tag{2.119}$$

Due to (2.109) it is straight-forward to show that the polarization vectors determined in (2.116) obey (2.119). As another property of the polarization vectors (2.116) we investigate whether they obey the orthonormality relations (2.84). Showing separately

$$\boldsymbol{\epsilon}^*(\mathbf{k},\lambda)\boldsymbol{\epsilon}(\mathbf{k},\lambda) = 1\,, \tag{2.120}$$

$$\boldsymbol{\epsilon}^*(\mathbf{k},\lambda)\boldsymbol{\epsilon}(\mathbf{k},-\lambda) = 0\,, \tag{2.121}$$

we arrive, indeed, due to $\lambda = \pm 1$ at the orthonormality relations

$$\boldsymbol{\epsilon}^*(\mathbf{k},\lambda)\boldsymbol{\epsilon}(\mathbf{k},\lambda') = \delta_{\lambda,\lambda'}\,. \tag{2.122}$$

Another property of the polarization vectors (2.116), which will turn out to be quite useful for later calculations, is their behaviour concerning the inversion $\mathbf{k}\to-\mathbf{k}$. Obviously, such an inversion is obtained in spherical coordinates (2.109) via

$$\phi\to\phi+\pi: \qquad \sin\phi\to-\sin\phi\,, \qquad \cos\phi\to-\cos\phi\,, \tag{2.123}$$

$$\theta\to\theta-\pi: \qquad \sin\theta\to\sin\theta\,, \qquad \cos\theta\to-\cos\theta\,. \tag{2.124}$$

With this we then conclude from (2.116

$$\boldsymbol{\epsilon}(-\mathbf{k},\lambda) = \frac{1}{\sqrt{2}}\begin{pmatrix}\cos\theta\cos\phi+\lambda i\sin\phi\\ \cos\theta\sin\phi-\lambda i\cos\phi\\ -\sin\theta\end{pmatrix}\,. \tag{2.125}$$

Thus, from (2.116) and (2.125) we read off

$$\boldsymbol{\epsilon}(-\mathbf{k},\lambda) = \boldsymbol{\epsilon}(\mathbf{k},-\lambda) = \boldsymbol{\epsilon}^*(\mathbf{k},\lambda)\,. \tag{2.126}$$

And, inserting the decomposition (2.118) into (2.82) by taking into account (2.126), we finally get for the field operator

$$\hat{\mathbf{A}}(\mathbf{x},t) = \sum_{\lambda=\pm 1}\int d^3k\, N_{\mathbf{k}}\left\{\boldsymbol{\epsilon}(\mathbf{k},\lambda)e^{i(\mathbf{kx}-\omega_{\mathbf{k}}t)}\hat{a}_{\mathbf{k},\lambda} + \boldsymbol{\epsilon}^*(\mathbf{k},\lambda)e^{-i(\mathbf{kx}-\omega_{\mathbf{k}}t)}\hat{a}^\dagger_{\mathbf{k},\lambda}\right\}. \tag{2.127}$$

Note that this plane wave decomposition fulfills, indeed, the Coulomb gauge (2.16) due to the transversality condition (2.119). In the following we aim at unraveling the physical interpretation of the Fourier operators $\hat{a}_{\mathbf{k},\lambda}$ and $\hat{a}^\dagger_{\mathbf{k},\lambda}$ in the plane wave decomposition (2.127). As this leads to straight-forward but quite lengthy calculations, we restrict ourselves in the subsequent two sections to present a concise summary of the corresponding derivations.

2.11 Fourier Operators

We start with noting the plane wave decomposition for the momentum field operator, which follows from (2.64) and (2.127):

$$\hat{\boldsymbol{\pi}}(\mathbf{x},t) = \sum_{\lambda=\pm 1} \int d^3k\, \epsilon_0\, N_{\mathbf{k}} \left\{ -i\omega_{\mathbf{k}} \boldsymbol{\epsilon}(\mathbf{k},\lambda) e^{i(\mathbf{kx}-\omega_{\mathbf{k}}t)} \hat{a}_{\mathbf{k},\lambda} + i\omega_{\mathbf{k}} \boldsymbol{\epsilon}^*(\mathbf{k},\lambda) e^{-i(\mathbf{kx}-\omega_{\mathbf{k}}t)} \hat{a}^\dagger_{\mathbf{k},\lambda} \right\}. \quad (2.128)$$

The plane wave decompositions (2.127) and (2.128) for both the field operator $\hat{\mathbf{A}}(\mathbf{x},t)$ and the momentum field operator $\hat{\boldsymbol{\pi}}(\mathbf{x},t)$ can now be solved for the Fourier operators $\hat{a}_{\mathbf{k},\lambda}$ and $\hat{a}^\dagger_{\mathbf{k},\lambda}$:

$$\hat{a}_{\mathbf{k},\lambda} = \frac{1}{2(2\pi)^3 N_{\mathbf{k}}} \int d^3x\, \boldsymbol{\epsilon}^*(\mathbf{k},\lambda) e^{-i(\mathbf{kx}-\omega_{\mathbf{k}}t)} \left\{ \hat{\mathbf{A}}(\mathbf{x},t) + i\, \frac{\hat{\boldsymbol{\pi}}(\mathbf{x},t)}{\epsilon_0 \omega_{\mathbf{k}}} \right\}, \quad (2.129)$$

$$\hat{a}^\dagger_{\mathbf{k},\lambda} = \frac{1}{2(2\pi)^3 N_{\mathbf{k}}} \int d^3x\, \boldsymbol{\epsilon}(\mathbf{k},\lambda) e^{i(\mathbf{kx}-\omega_{\mathbf{k}}t)} \left\{ \hat{\mathbf{A}}(\mathbf{x},t) - i\, \frac{\hat{\boldsymbol{\pi}}(\mathbf{x},t)}{\epsilon_0 \omega_{\mathbf{k}}} \right\}. \quad (2.130)$$

Here we have used the symmetry of the dispersion (2.76) and the orthonormality relation of the polarization vectors (2.122). The expressions (2.129) and (2.130) allows us to determine the commutator relations between the Fourier operators $\hat{a}_{\mathbf{k},\lambda}$ and $\hat{a}^\dagger_{\mathbf{k},\lambda}$ from the equal-time commutator relations (2.44), (2.45), and (2.58) for the field operator $\hat{\mathbf{A}}(\mathbf{x},t)$ and the momentum field operator $\hat{\boldsymbol{\pi}}(\mathbf{x},t)$:

$$\left[\hat{a}_{\mathbf{k},\lambda}, \hat{a}_{\mathbf{k}',\lambda'}\right]_- = 0\,, \quad (2.131)$$

$$\left[\hat{a}^\dagger_{\mathbf{k},\lambda}, \hat{a}^\dagger_{\mathbf{k}',\lambda'}\right]_- = 0\,, \quad (2.132)$$

$$\left[\hat{a}_{\mathbf{k},\lambda}, \hat{a}^\dagger_{\mathbf{k}',\lambda'}\right]_- = \frac{\hbar}{2(2\pi)^3 \epsilon_0 \omega_{\mathbf{k}} N_{\mathbf{k}}^2}\, \delta_{\lambda,\lambda'}\, \delta(\mathbf{k}-\mathbf{k}')\,. \quad (2.133)$$

In order to obtain this result we need again the symmetry of the dispersion (2.76) and the orthonormality relation of the polarization vectors (2.122), but additionally we also have to take into account the explicit form of the transversal delta function (2.57), the Gauß law, and the transversality condition (2.119). From (2.133) we read off that, fixing the yet undetermined normalization constant according to

$$N_{\mathbf{k}} = \sqrt{\frac{\hbar}{2(2\pi)^3 \epsilon_0 \omega_{\mathbf{k}}}}\,, \quad (2.134)$$

we end up with the bosonic canonical commutation relation

$$\left[\hat{a}_{\mathbf{k},\lambda}, \hat{a}^\dagger_{\mathbf{k}',\lambda'}\right]_- = \delta_{\lambda,\lambda'}\, \delta(\mathbf{k}-\mathbf{k}')\,. \quad (2.135)$$

This means that the Fourier operators $\hat{a}_{\mathbf{k},\lambda}$ and $\hat{a}^\dagger_{\mathbf{k},\lambda}$ can be interpreted as the annihilation and creation operators of bosonic particles, which are characterized by the wave vector $\mathbf{k}$ and the polarization λ. In order to determine the respective properties of these particles we investigate in the subsequent section their contribution to the energy of the electromagnetic field in second quantization.

2.12 Energy

Taking into account the normalization constant (2.134) in the plane wave decompositions (2.127) and (2.128) for both the field operator $\hat{\mathbf{A}}(\mathbf{x},t)$ and the momentum field operator $\hat{\boldsymbol{\pi}}(\mathbf{x},t)$ we get

$$\hat{\mathbf{A}}(\mathbf{x},t) = \sum_{\lambda=\pm1}\int d^3k \sqrt{\frac{\hbar}{2(2\pi)^3\epsilon_0\omega_{\mathbf{k}}}}\left\{\boldsymbol{\epsilon}(\mathbf{k},\lambda)e^{i(\mathbf{kx}-\omega_{\mathbf{k}}t)}\hat{a}_{\mathbf{k},\lambda}+\boldsymbol{\epsilon}^*(\mathbf{k},\lambda)e^{-i(\mathbf{kx}-\omega_{\mathbf{k}}t)}\hat{a}^\dagger_{\mathbf{k},\lambda}\right\}, \quad (2.136)$$

$$\hat{\boldsymbol{\pi}}(\mathbf{x},t) = \sum_{\lambda=\pm1}\int d^3k \sqrt{\frac{\hbar\omega_{\mathbf{k}}\epsilon_0}{2(2\pi)^3}}\left\{-i\boldsymbol{\epsilon}(\mathbf{k},\lambda)e^{i(\mathbf{kx}-\omega_{\mathbf{k}}t)}\hat{a}_{\mathbf{k},\lambda}+i\boldsymbol{\epsilon}^*(\mathbf{k},\lambda)e^{-i(\mathbf{kx}-\omega_{\mathbf{k}}t)}\hat{a}^\dagger_{\mathbf{k},\lambda}\right\}. \quad (2.137)$$

Inserting (2.136) and (2.137) in the expression for the Hamilton operator (2.59) and using the definition of the light velocity (2.5), the linear dispersion (2.73) together with its symmetry (2.76) as well as the orthonormality relation of the polarization vectors (2.122), we yield after a lengthy but straightforward calculation

$$\hat{H} = \frac{1}{2}\sum_{\lambda=\pm1}\int d^3k\,\hbar\omega_{\mathbf{k}}\left(\hat{a}^\dagger_{\mathbf{k},\lambda}\hat{a}_{\mathbf{k},\lambda}+\hat{a}_{\mathbf{k},\lambda}\hat{a}^\dagger_{\mathbf{k},\lambda}\right). \quad (2.138)$$

First of all we remark that (2.138) turns out to be time independent, although the field operator (2.136) and the momentum field operator (2.137) explicitly depend on time due to the Heisenberg picture. The resulting time independence of the second-quantized Hamilton operator (2.138) reflects the fact that the energy of the electromagnetic field is conserved. Furthermore, comparing (2.138) with the Hamilton operator (A.6) of a harmonic oscillator in the ladder operator formalism, we recognize that the second quantized electromagnetic field consists of independent harmonic oscillators, where each energy quantum $\hbar\omega_{\mathbf{k}}$ is doubly degenerate due to the polarization degree of freedom $\lambda=\pm1$. Defining the vacuum state according to

$$\hat{a}_{\mathbf{k},\lambda}|0\rangle = 0 \qquad \Longleftrightarrow \qquad \langle 0|\hat{a}^\dagger_{\mathbf{k},\lambda} = 0\,, \quad (2.139)$$

we find by taking into account the commutation relation (2.135) that the vacuum energy of the electrodynamic field is given by a sum of the zero-point energy of all independent harmonic oscillators

$$\langle 0|\hat{H}|0\rangle = \int d^3k\,\hbar\omega_{\mathbf{k}}\,\delta(\mathbf{0})\,, \quad (2.140)$$

which is divergent due to two reasons. On the one hand the factor $\delta(\mathbf{0})$ is divergent and on the other hand the wave vector integral diverges as well due to the linear dispersion (2.73). Therefore, using the commutator relation (2.135) we obtain for the renormalized Hamilton operator

$$:\hat{H}: = \hat{H} - \langle 0|\hat{H}|0\rangle \quad (2.141)$$

the normal ordered result

$$:\hat{H}: = \sum_{\lambda=\pm 1} \int d^3k \, \hbar\omega_{\mathbf{k}} \, \hat{n}_{\mathbf{k},\lambda} \, . \tag{2.142}$$

Here the occupation number operator

$$\hat{n}_{\mathbf{k},\lambda} = \hat{a}^{\dagger}_{\mathbf{k},\lambda} \hat{a}_{\mathbf{k},\lambda} \tag{2.143}$$

counts the number of photons with wave vector $\mathbf{k}$ and polarization λ once it is applied to a photon state.

2.13 Momentum

Due to a theorem, which is due to Emmy Noether, the momentum of the electromagnetic field is defined by [22]

$$\mathbf{P} = \int d^3x \, \frac{\mathbf{S}(\mathbf{x}, t)}{c^2} \tag{2.144}$$

with the Poynting vector

$$\mathbf{S}(\mathbf{x}, t) = \frac{1}{\mu_0} \, \mathbf{E}(\mathbf{x}, t) \times \mathbf{B}(\mathbf{x}, t) \, . \tag{2.145}$$

Taking into account (2.5), (2.10), and (2.26), the momentum (2.145) is expressed in terms of the vector potential and the canonically conjugated momentum field via

$$\mathbf{P} = \int d^3x \, \left[\boldsymbol{\nabla} \times \mathbf{A}(\mathbf{x}, t) \right] \times \boldsymbol{\pi}(\mathbf{x}, t) \, . \tag{2.146}$$

Thus, in second quantization, the momentum operator of the electromagnetic field reads

$$\hat{\mathbf{P}} = \int d^3x \left[\boldsymbol{\nabla} \times \hat{\mathbf{A}}(\mathbf{x}, t) \right] \times \hat{\boldsymbol{\pi}}(\mathbf{x}, t) \, . \tag{2.147}$$

The further evaluation is based on taking into account the plane wave decompositions (2.136) and (2.137) for both the field operator $\hat{\mathbf{A}}(\mathbf{x}, t)$ and the momentum field operator $\hat{\boldsymbol{\pi}}(\mathbf{x}, t)$. Furthermore, the symmetry of the dispersion relation (2.76), the vector identity

$$(\mathbf{a} \times \mathbf{b}) \times \mathbf{c} = (\mathbf{ac})\mathbf{b} - (\mathbf{bc})\mathbf{a} \, , \tag{2.148}$$

the transversality condition (2.119), the orthonormality relation (2.122), and (2.126) are needed. Subsequently, performing the substitution $\mathbf{k} \to -\mathbf{k}$ and applying (2.76), (2.131), (2.132), we get the expression

$$\hat{\mathbf{P}} = \sum_{\lambda=\pm 1} \int d^3k \, \frac{\hbar\mathbf{k}}{2} \left(\hat{a}^{\dagger}_{\mathbf{k},\lambda} \hat{a}_{\mathbf{k},\lambda} + \hat{a}_{\mathbf{k},\lambda} \hat{a}^{\dagger}_{\mathbf{k},\lambda} \right) \, . \tag{2.149}$$

Note that the vacuum state has a vanishing momentum

$$\langle 0|\hat{\mathbf{P}}|0\rangle = \int d^3k\, \hbar\mathbf{k}\, \delta(\mathbf{0}) = \mathbf{0} \tag{2.150}$$

due to the odd symmetry of the integrand. Thus, taking into account the commutator relation (2.135) we recognize that (2.149) coincides with the renormalized momentum operator

$$:\hat{\mathbf{P}}: = \hat{\mathbf{P}} - \langle 0|\hat{\mathbf{P}}|0\rangle \ , \tag{2.151}$$

which finally yields the normal ordered result

$$:\hat{\mathbf{P}}: = \sum_{\lambda=\pm 1} \int d^3k\, \hbar\mathbf{k}\, \hat{a}^\dagger_{\mathbf{k},\lambda}\hat{a}_{\mathbf{k},\lambda}\,. \tag{2.152}$$

2.14 Spin Angular Momentum

According to the Noether theorem the spin angular momentum of the electromagnetic is given by [22]

$$\mathbf{S} = \int d^3x\, \mathbf{A}(\mathbf{x},t) \times \boldsymbol{\pi}(\mathbf{x},t)\,. \tag{2.153}$$

Thus, the corresponding second quantized spin angular momentum operator reads

$$\hat{\mathbf{S}} = \int d^3x\, \hat{\mathbf{A}}(\mathbf{x},t) \times \hat{\boldsymbol{\pi}}(\mathbf{x},t)\,. \tag{2.154}$$

Inserting the plane wave decompositions (2.136) and (2.137) for both the field operator $\hat{\mathbf{A}}(\mathbf{x},t)$ and the momentum field operator $\hat{\boldsymbol{\pi}}(\mathbf{x},t)$ and performing the substitution $\mathbf{k} \to -\mathbf{k}$ then yields the intermediate result

$$\hat{\mathbf{S}} = \sum_{\lambda=\pm 1}\sum_{\lambda'=\pm 1} \int d^3k\, \frac{i\hbar}{2} \left[\boldsymbol{\epsilon}(\mathbf{k},\lambda) \times \boldsymbol{\epsilon}(\mathbf{k},\lambda')^* \hat{a}_{\mathbf{k},\lambda}\hat{a}^\dagger_{\mathbf{k},\lambda'} + \boldsymbol{\epsilon}(\mathbf{k},\lambda') \times \boldsymbol{\epsilon}(\mathbf{k},\lambda)^* \hat{a}^\dagger_{\mathbf{k},\lambda}\hat{a}_{\mathbf{k},\lambda'}\right] . \tag{2.155}$$

Now we evaluate the vector product between two polarization vectors. At first we obtain from (2.126)

$$\boldsymbol{\epsilon}(\mathbf{k},\lambda) \times \boldsymbol{\epsilon}(\mathbf{k},-\lambda)^* = \mathbf{0}\,, \tag{2.156}$$

whereas we get from (2.109) and (2.116)

$$\boldsymbol{\epsilon}(\mathbf{k},\lambda) \times \epsilon(\mathbf{k},\lambda) = -i\lambda\, \frac{\mathbf{k}}{k}\,. \tag{2.157}$$

Thus, both (2.156) and (2.157) can be summarized by

$$\boldsymbol{\epsilon}(\mathbf{k},\lambda) \times \boldsymbol{\epsilon}(\mathbf{k},\lambda')^* = -i\lambda\, \frac{\mathbf{k}}{k}\, \delta_{\lambda,\lambda'}\,. \tag{2.158}$$

With this the intermediate result (2.155) for the spin angular momentum operator of the electromagnetic field reduces to

$$\hat{\mathbf{S}} = \sum_{\lambda=\pm 1} \int d^3k \, \lambda \, \frac{\hbar}{2} \, \frac{\mathbf{k}}{k} \, \left(\hat{a}^\dagger_{\mathbf{k},\lambda} \hat{a}_{\mathbf{k},\lambda} + \hat{a}_{\mathbf{k},\lambda} \hat{a}^\dagger_{\mathbf{k},\lambda} \right) . \tag{2.159}$$

Thus, the vacuum state has a vanishing spin angular momentum

$$\langle 0 | \hat{\mathbf{S}} | 0 \rangle = \hbar \left(\sum_{\lambda=\pm 1} \lambda \right) \left(\int d^3k \, \frac{\mathbf{k}}{k} \right) \delta(\mathbf{0}) = \mathbf{0} \tag{2.160}$$

due to the odd symmetry in both the summand and the integrand. Using the commutator relation (2.135) we read off that (2.159) coincides with the renormalized spin angular momentum operator

$$:\hat{\mathbf{S}}: = \hat{\mathbf{S}} - \langle 0 | \hat{\mathbf{S}} | 0 \rangle \ , \tag{2.161}$$

leading to the normal ordered result

$$:\hat{\mathbf{S}}: = \sum_{\lambda=\pm 1} \int d^3k \, \lambda \hbar \, \frac{\mathbf{k}}{k} \, \hat{a}^\dagger_{\mathbf{k},\lambda} \hat{a}_{\mathbf{k},\lambda} \, . \tag{2.162}$$

We observe that the decompositions of the second quantized expressions for the energy (2.142), the momentum (2.152), and the spin angular momentum (2.162) of the electromagnetic field turn out to be time independent and, thus, represent conserved quantities. Together with the commutator relations (2.131), (2.132), and (2.135) we furthermore conclude that the Fourier operators $\hat{a}_{\mathbf{k},\lambda}$ and $\hat{a}^\dagger_{\mathbf{k},\lambda}$ represent the annihilation and creation operators of photons with the energy $\hbar\omega_{\mathbf{k}}$, the momentum $\hbar\mathbf{k}$, and the spin angular momentum $\lambda\hbar\mathbf{k}/k$, where the latter amounts to the helicity $\lambda\hbar$.

2.15 Fock Basis

Now we construct a basis of the underlying second quantized Hilbert space. To this end we take advantage of the fact that $\hat{a}_{\mathbf{k},\lambda}$, $\hat{a}^\dagger_{\mathbf{k},\lambda}$ denote the annihilation and creation operators for photons with wave vector $\mathbf{k}$ and helicity λ, which fulfill the bosonic commutation relations (2.131), (2.132), and (2.135). Thus, this second-quantized operator algebra is formally analogous to the ladder operator approach for a first-quantized harmonic oscillator, which is outlined in Appendix A. Based on this analogy we use (A.21) in order to obtain a state $|n_{\mathbf{k},\lambda}\rangle$ with a fixed number of $n_{\mathbf{k},\lambda}$ photons with wave vector $\mathbf{k}$ and helicity λ by applying $n_{\mathbf{k},\lambda}$ times the creation operator $\hat{a}^\dagger_{\mathbf{k},\lambda}$ to the vacuum state defined in (2.139):

$$|n_{\mathbf{k},\lambda}\rangle = \frac{1}{\sqrt{n_{\mathbf{k},\lambda}!}} \, \left(\hat{a}^\dagger_{\mathbf{k},\lambda} \right)^{n_{\mathbf{k},\lambda}} \, |0\rangle \ . \tag{2.163}$$

In principle, we could allow for all wave vectors $\mathbf{k}$ and helicities λ an arbitrary number of photons $n_{\mathbf{k},\lambda}$, yielding

$$|\{n_{\mathbf{k},\lambda}\}\rangle = \prod_{\mathbf{k},\lambda} |n_{\mathbf{k},\lambda}\rangle \ . \tag{2.164}$$

In analogy to (A.24) and (A.25) we then read off that these states $|\{n_{\mathbf{k},\lambda}\}\rangle$ are both orthonormal

$$\langle\{n_{\mathbf{k},\lambda}\}|\{n'_{\mathbf{k},\lambda}\}\rangle = \prod_{\mathbf{k},\lambda} \delta_{n_{\mathbf{k},\lambda},n'_{\mathbf{k},\lambda}} \tag{2.165}$$

and complete

$$\sum_{\lambda=\pm1} \int d^3k \sum_{n_{\mathbf{k},\lambda}=0}^{\infty} |\{n_{\mathbf{k},\lambda}\}\rangle \langle\{n_{\mathbf{k},\lambda}\}| = 1 \, . \tag{2.166}$$

Thus, the linear envelope of all possible number states (2.164) defines then the so-called Fock space, which is named after the Soviet physicist Vladimir Fock:

$$\mathcal{F} = \mathrm{Span}\left\{ |0\rangle \, , |1_{\mathbf{k},\lambda}\rangle \, , |1_{\mathbf{k},\lambda} 1_{\mathbf{k}',\lambda'}\rangle \, , |2_{\mathbf{k},\lambda}\rangle \, , \dots \right\} . \tag{2.167}$$

As we have continuous wave vectors $\mathbf{k}$, the Fock space contains innumerable many photon states.

2.16 Quantum Fluctuations of Electric Field

Here we restrict ourselves to investigate exemplarily the quantum fluctuations of the electric field. The corresponding considerations for the magnetic field follow in an analogous way. We start with reading off from (2.26) and (2.136) the explicit structure of the electric field operator:

$$\hat{\mathbf{E}}(\mathbf{x},t) = \sum_{\lambda=\pm1} \int d^3k \sqrt{\frac{\hbar\omega_{\mathbf{k}}}{2(2\pi)^3\epsilon_0}} \, i \left\{ \boldsymbol{\epsilon}(\mathbf{k},\lambda) e^{i(\mathbf{kx}-\omega_{\mathbf{k}}t)} \hat{a}_{\mathbf{k},\lambda} - \boldsymbol{\epsilon}^*(\mathbf{k},\lambda) e^{-i(\mathbf{kx}-\omega_{\mathbf{k}})t} \hat{a}^\dagger_{\mathbf{k},\lambda} \right\} . \tag{2.168}$$

Its vacuum expectation value turns out to vanish due to (2.139):

$$\langle 0|\hat{\mathbf{E}}(\mathbf{x},t)|0\rangle = \mathbf{0} \, . \tag{2.169}$$

Therefore, we investigate now the correlation function of the electric field operator for different spatio-temporal arguments:

$$\langle 0|\hat{E}_i(\mathbf{x},t)\hat{E}_{i'}(\mathbf{x}',t')|0\rangle = \sum_{\lambda=\pm1}\sum_{\lambda'=\pm1} \int d^3k \int d^3k' \, \frac{\hbar\sqrt{\omega_{\mathbf{k}}\omega_{\mathbf{k}'}}}{2(2\pi)^3\epsilon_0} \, i^2 \langle 0| \Big\{ \epsilon_i(\mathbf{k},\lambda) e^{i(\mathbf{kx}-\omega_{\mathbf{k}}t)} \hat{a}_{\mathbf{k},\lambda}$$
$$- \epsilon_i^*(\mathbf{k},\lambda) e^{-i(\mathbf{kx}-\omega_{\mathbf{k}})t} \hat{a}^\dagger_{\mathbf{k},\lambda} \Big\} \Big\{ \epsilon_{i'}(\mathbf{k}',\lambda') e^{i(\mathbf{k}'\mathbf{x}'-\omega_{\mathbf{k}'}t')} \hat{a}_{\mathbf{k}',\lambda'} - \epsilon^*_{i'}(\mathbf{k}',\lambda') e^{-i(\mathbf{k}'\mathbf{x}'-\omega_{\mathbf{k}'})t'} \hat{a}^\dagger_{\mathbf{k}',\lambda'} \Big\} |0\rangle \, . \tag{2.170}$$

From the four terms, which arise from multiplying out both brackets, only one is non-vanishing due to (2.139). Applying (2.135) we obtain

$$\langle 0|\hat{a}_{\mathbf{k},\lambda}\hat{a}^\dagger_{\mathbf{k}',\lambda'}|0\rangle = \langle 0| \left[\hat{a}_{\mathbf{k},\lambda}, \hat{a}^\dagger_{\mathbf{k}',\lambda'}\right]_- |0\rangle = \delta_{\lambda,\lambda'}\delta(\mathbf{k}-\mathbf{k}') \, . \tag{2.171}$$

With this the correlation function (2.170) reduces to

$$\langle 0|\hat{E}_i(\mathbf{x},t)\hat{E}_{i'}(\mathbf{x}',t')|0\rangle = \sum_{\lambda=\pm1}\int d^3k\,\frac{\hbar\omega_{\mathbf{k}}}{2(2\pi)^3\epsilon_0}\,e^{i[\mathbf{k}(\mathbf{x}-\mathbf{x}')-\omega_{\mathbf{k}}(t-t')]}\,\epsilon_i(\mathbf{k},\lambda)\epsilon^*_{i'}(\mathbf{k},\lambda)\,. \tag{2.172}$$

A contraction of the components of the correlation function (2.172) yields due to the dispersion (2.73) and the orthonormality relation (2.122):

$$\langle 0|\hat{\mathbf{E}}(\mathbf{x},t)\hat{\mathbf{E}}(\mathbf{x}',t')|0\rangle = \int d^3k\,\frac{\hbar c|\mathbf{k}|}{(2\pi)^3\epsilon_0}\,e^{i[\mathbf{k}(\mathbf{x}-\mathbf{x}')-|\mathbf{k}|c(t-t')]}\,. \tag{2.173}$$

Using spherical coordinates the integral goes over into

$$\langle 0|\hat{\mathbf{E}}(\mathbf{x},t)\hat{\mathbf{E}}(\mathbf{x}',t')|0\rangle = \frac{\hbar c}{(2\pi)^2\epsilon_0}\int_0^\infty dk\,k^3\int_0^\pi d\vartheta\,\sin\vartheta\,e^{i[k|\mathbf{x}-\mathbf{x}'|\cos\vartheta-kc(t-t')]}\,. \tag{2.174}$$

Evaluating the angular integral leads to

$$\langle 0|\hat{\mathbf{E}}(\mathbf{x},t)\hat{\mathbf{E}}(\mathbf{x}',t')|0\rangle = \frac{\hbar c}{4\pi^2 i\epsilon_0|\mathbf{x}-\mathbf{x}'|}\int_0^\infty dk\,k^2\left\{e^{-ik[c(t-t')-|\mathbf{x}-\mathbf{x}'|]}-e^{-ik[c(t-t')+|\mathbf{x}-\mathbf{x}'|]}\right\}. \tag{2.175}$$

The remaining integral can be solved with the help of the Gamma function [23, (8.310.1)]

$$\Gamma(x) = \int_0^\infty dt\,t^{x-1}\,e^{-t}\,,\qquad x>0\,. \tag{2.176}$$

Performing a partial integration we obtain the useful recursion formula

$$\Gamma(x+1) = x\,\Gamma(x)\,,\qquad x>0\,. \tag{2.177}$$

Thus, applying (2.177) recursively, we conclude that the Gamma function interpolates between the factorials:

$$n! = \Gamma(n+1)\,. \tag{2.178}$$

Now we perform the integration along the closed contour $\mathcal{C}=\mathcal{C}_1+\mathcal{C}_2+\mathcal{C}_3$ of a quarter circle with radius R according to Fig. 2.4 with the help of the residue theorem we get according to the residue theorem

$$\int_{\mathcal{C}_1} dz\,z^{x-1}\,e^{-z}+\int_{\mathcal{C}_2} dz\,z^{x-1}\,e^{-z}+\int_{\mathcal{C}_3} dz\,z^{x-1}\,e^{-z}=0\,, \tag{2.179}$$

as the integrand has no singularity within the integration contour $\mathcal{C}$. In the limit $R\to\infty$ the integral along $\mathcal{C}_2$ vanishes and with the parametrizations

$$\mathcal{C}_1: \qquad z(t) = t\,,\qquad t\in[0,\infty)\,, \tag{2.180}$$

$$\mathcal{C}_3: \qquad z(t) = it\,,\qquad t\in(\infty,0] \tag{2.181}$$

we read off from (2.176) and (2.179)

$$\int_0^\infty dt\,t^{x-1}\,e^{-t}+\int_\infty^0 dt\,i\,(it)^{x-1}\,e^{-it}=0 \qquad\Longrightarrow\qquad \Gamma(x)=i^x\int_0^\infty dt\,t^{x-1}\,e^{-it}\,. \tag{2.182}$$

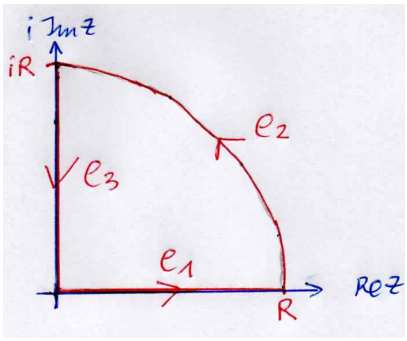

Figure 2.4: Closed contour $\mathcal{C} = \mathcal{C}_1 + \mathcal{C}_2 + \mathcal{C}_3$ of a quarter circle with radius R.

Performing subsequently the substitution $t(\tau) = a\tau$ with $a > 0$, then (2.182) reduces to

$$\int_0^\infty d\tau\, \tau^{x-1}\, e^{-ia\tau} = \frac{\Gamma(x)}{(ia)^x}\,, \qquad a > 0\,. \tag{2.183}$$

Instead we could also have performed the substitution $t(\tau) = a\tau$ with $a > 0$ in (2.176), yielding

$$\int_0^\infty d\tau\, \tau^{x-1}\, e^{-a\tau} = \frac{\Gamma(x)}{a^x}\,, \qquad a > 0\,. \tag{2.184}$$

Note that (2.184) is called the Schwinger trick, which is frequently used in statistical and quantum field theory in order to evaluate Feynman diagrams [24, 25, 26]. Furthermore, we recognize that (2.183) directly follows from (2.184) via an analytic continuation. Evaluating the remaining integral in (2.175) with (2.183) by identifying $x = 3$ and $a = c(t - t') \mp |\mathbf{x} - \mathbf{x}'|$, we obtain

$$\langle 0|\hat{\mathbf{E}}(\mathbf{x}, t)\hat{\mathbf{E}}(\mathbf{x}', t')|0\rangle = \frac{\hbar c}{2\pi^2\epsilon_0|\mathbf{x} - \mathbf{x}'|}\left\{\frac{1}{[c(t - t') - |\mathbf{x} - \mathbf{x}'|\,]^3} - \frac{1}{[c(t - t') + |\mathbf{x} - \mathbf{x}'|\,]^3}\right\}. \tag{2.185}$$

We mention that such a vacuum correlation function of the two electric field operators with different space-time coordinates can not be measured with an intensity measurement as this would necessarily involve the same space-time coordinates. Thus, a direct experimental proof of such a vacuum correlation function was missing for quite a long time. This was achieved only recently by using the electro-optic detection in a nonlinear crystal placed in a cryogenic environment [27]. To this end two probe pulses with different space-time coordinates sample the electric field of the propagating waves in the crystal with the repetition rate of the laser used. With this the vacuum field fluctuations, which couple from the environment into the detection crystal, are detected. They are found to be non-zero and their corresponding power spectrum is measured. The latter is well reproduced in simulations, which take the specific experimental set-up into account. The remaining difference between the simulations and the experimental results is attributed to a remaining uncertainty in the phase matching of the two waves.

Note that in Eq. (2.185) the limit $|\mathbf{x} - \mathbf{x}'| \to 0$ can be performed with the rule of de l'Hôpital or with a Taylor expansion, yielding

$$\langle 0|\hat{\mathbf{E}}(\mathbf{x}, t)\hat{\mathbf{E}}(\mathbf{x}, t')|0\rangle = \frac{3\hbar}{\pi^2\epsilon_0 c^3(t - t')^4}\,. \tag{2.186}$$

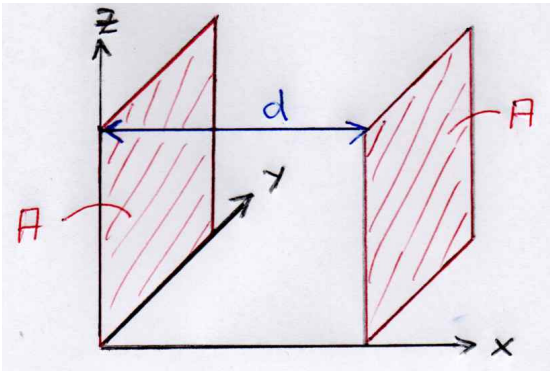

Figure 2.5: Set-up for Casimir effect: two plane-parallel metal plates of area A at distance d.

Thus, the correlation function for the same space points remains finite for different times $t \neq t'$. In the limit $t \to t'$, however, the correlation function diverges. This result is consistent with the previous observation that the energy of the electromagnetic field in the vacuum (2.140) turned out to be infinitely large. Despite of this divergency of the vacuum energy the quantum fluctuations are responsible for the Casimir effect, which is discussed in the subsequent section.

2.17 Casimir Effect

In quantum field theory, the Casimir effect corresponds to a physical force acting on the macroscopic boundaries of a confined space, which arises from the quantum fluctuations of the field. It is named after the Dutch physicist Hendrik Casimir, who predicted the effect for electromagnetic systems in 1948. In order to analyze the Casimir effect we consider two plane-parallel metal plates of a large area A at distance d. According to Fig. 2.5 we choose the coordinate system such that the metal plates are located at $x = 0$ and $x = d$.

2.17.1 Electromagnetic Modes

In order to find the electromagnetic modes for this configuration, we have to solve the Maxwell equations (2.1)–(2.4) in vacuum, i.e. in case of (2.23). But in addition we have also to fulfill the boundary conditions for the electromagnetic field at the metal plates. Applying at the interface of vacuum and metal plates the Gauß law to the homogeneous Maxwell equation (2.3) one obtains

$$\mathbf{e}_x \cdot \mathbf{B} = 0\,, \qquad \text{for } x = 0 \text{ and } x = d \tag{2.187}$$

and, correspondingly, the Stokes law together with (2.3) yields

$$\mathbf{e}_x \times \mathbf{E} = \mathbf{0}\,, \qquad \text{for } x = 0 \text{ and } x = d\,, \tag{2.188}$$

respectively. Solving this boundary value problem, the Maxwell theory admits two types of standing-wave solutions, which read with the transversal wave vector $\mathbf{k}_\perp = k_y \mathbf{e}_y + k_z \mathbf{e}_z$ as an abbreviation:

- Transversal electric (TE) modes, i.e. $\mathbf{e}_x \cdot \mathbf{E} = 0$:

$$\mathbf{E}(x,y,z,t) = N_{\mathrm{TE}}\, i\omega \sin(k_x x)\, \mathbf{e}_x \times \mathbf{k}_\perp\, e^{i(k_y y + k_z z - \omega t)}\,, \tag{2.189}$$

$$\mathbf{B}(x,y,z,t) = N_{\mathrm{TE}} \left[i k_\perp^2 \sin(k_x x) \mathbf{e}_x - k_x \cos(k_x x) \mathbf{k}_\perp \right] e^{i(k_y y + k_z z - \omega t)}\,. \tag{2.190}$$

  The boundary conditions (2.187) and (2.188) have the consequence that the x-component of the wave vector $\mathbf{k}$ has discrete values:

$$0 = \sin(k_x x)\Big|_{x=0} = \sin(k_x x)\Big|_{x=d} \qquad \Longrightarrow \qquad k_x = \frac{\pi}{d}\, n\,, \quad n = 1,2,3,\ldots\,. \tag{2.191}$$

  Note that the mode $n = 0$, i.e. $k_x = 0$, is not allowed as then both the electric field (2.189) and the magnetic induction (2.190) vanish.

- Transversal magnetic (TM) modes, i.e. $\mathbf{e}_x \cdot \mathbf{B} = 0$:

$$\mathbf{B}(x,y,z,t) = N_{\mathrm{TM}}\, \frac{\omega}{c^2} \cos(k_x x)\, \mathbf{e}_x \times \mathbf{k}_\perp\, e^{i(k_y y + k_z z - \omega t)}\,, \tag{2.192}$$

$$\mathbf{E}(x,y,z,t) = N_{\mathrm{TM}} \left[i k_x \sin(k_x x) \mathbf{k}_\perp - k_\perp^2 \cos(k_x x) \mathbf{e}_x \right] e^{i(k_y y + k_z z - \omega t)}\,. \tag{2.193}$$

  Here the boundary condition (2.187) is already fulfilled and (2.188) yields for the x-component of the wave vector $\mathbf{k}$:

$$0 = \sin(k_x x)\Big|_{x=0} = \sin(k_x x)\Big|_{x=d} \qquad \Longrightarrow \qquad k_x = \frac{\pi}{d}\, n\,, \quad n = 0,1,2,3,\ldots\,. \tag{2.194}$$

  We remark that now the mode with $n = 0$, i.e. $k_x = 0$, is allowed in case of $\mathbf{k}_\perp \neq \mathbf{0}$, as then both electric field (2.193) and magnetic induction (2.193) are non-vanishing and fulfill the Maxwell boundary value problem.

In addition, both for the transversal electric and the transversal magnetic modes (2.189), (2.190) and (2.192), (2.193) the frequency ω is determined by a linear dispersion (2.73) with the quantization conditions (2.191) and (2.194):

$$\omega_n = c \sqrt{\frac{\pi^2 n^2}{d^2} + \mathbf{k}_\perp^2}\,, \qquad \text{with} \quad \begin{cases} n = 1,2,3,\ldots \text{ (TE modes)} \\ n = 0,1,2,3,\ldots \text{ (TM modes)} \end{cases}\,. \tag{2.195}$$

Furthermore, we assume that the lengths L_y and L_z of the metal plates in y- and z-direction are much larger than d, so that the quantization of the transverse momenta becomes irrelevant. For instance, invoking periodic boundary conditions the allowed wave vector component k_y is restricted as follows:

$$e^{i k_y y}\big|_{y=0} = e^{i k_y y}\big|_{y=L_y} \qquad \Longrightarrow \qquad k_y = \frac{2\pi}{L_y}\, n_y\,, \qquad n_y \in \mathbb{Z}\,. \tag{2.196}$$

This means that changing the mode number in y-direction by one amounts to

$$1 = \Delta n_y = \frac{L_y}{2\pi}\, dk_y\,, \tag{2.197}$$

so summing over all modes corresponds to an integral:

$$\sum_{n_y=-\infty}^{\infty} 1 = L_y \int_{-\infty}^{\infty} \frac{dk_y}{2\pi}\,. \tag{2.198}$$

Thus, in the thermodynamic limit of an infinitely large L_y, L_z yields a nearly continuous set of states denoted by the transversal wave vectors $\mathbf{k}_\perp$ with the transverse density of states $A/(2\pi)^2$, where the area is given by $A = L_y L_z$. With this we obtain for the vacuum energy between the two metal plates in analogy to (2.140):

$$E_{\text{plates}}^{\text{inside}} = 2\sum_{n=0}^{\infty}\left(1 - \frac{1}{2}\,\delta_{n,0}\right) A \int \frac{d^2k_\perp}{(2\pi)^2}\,\frac{1}{2}\,\hbar c\,\sqrt{\frac{\pi^2 n^2}{d^2} + \mathbf{k}_\perp^2}\,. \tag{2.199}$$

Correspondingly, outside of two metal plates the wave vectors are not restricted at all, yielding for a length $L_x \gg d$ the vacuum energy

$$E_{\text{plates}}^{\text{outside}} = 2(L_x - d)A \int_{-\infty}^{\infty} \frac{dk_x}{2\pi} \int \frac{d^2k_\perp}{(2\pi)^2}\,\frac{1}{2}\,\hbar c\,\sqrt{k_x^2 + \mathbf{k}_\perp^2}\,. \tag{2.200}$$

In absence of the metal plates the total vacuum energy in the box with volume $L_x A$ would read

$$E_{\text{plates}}^{\text{no}} = 2L_x A \int_{-\infty}^{\infty} \frac{dk_x}{2\pi} \int \frac{d^2k_\perp}{(2\pi)^2}\,\frac{1}{2}\,\hbar c\,\sqrt{k_x^2 + \mathbf{k}_\perp^2}\,. \tag{2.201}$$

Note that in (2.200) as well as in (2.201) the prefactor two takes both transveral degrees of freedom of the electromagnetic field into account, which are energetically degenerate. Installing the metal plates, thus, leads to the following change of the vacuum energy:

$$E_{\text{C}} = E_{\text{plates}}^{\text{inside}} + E_{\text{plates}}^{\text{outside}} - E_{\text{plates}}^{\text{no}}\,, \tag{2.202}$$

which reduces with (2.199)–(2.201) to

$$E_{\text{C}} = \hbar c A \left(\sum_{n=0}^{\infty}{}' - \int_0^{\infty} dn\right) \int \frac{d^2k_\perp}{(2\pi)^2}\,\sqrt{\frac{\pi^2 n^2}{d^2} + \mathbf{k}_\perp^2}\,, \tag{2.203}$$

Here we have introduced the abbreviation

$$\sum_{n=0}^{\infty}{}' f_n = \sum_{n=0}^{\infty} f_n - \frac{1}{2}\,f_0\,, \tag{2.204}$$

which formally takes into account that the respected TE and TM modes are enumerated differently according to (2.195). Although both the sum and the integral in (2.203) is divergent for itself, their difference turns out to be finite.

2.17.2 Analytic Continuations

In order to evaluate (2.203) we have to tame the possible infinities by introducing some regularization procedure. Note that the finite result for the difference (2.203) does not depend upon the particular choice of the regularization procedure. Here we choose the method of dimensional regularization, which was invented by Gerard 't Hooft and Martinus Veltman in 1972, as it is quite popular in quantum and statistical field theory. Instead of considering the Casimir energy in $D = 3$ according to (2.203) one performs a calculation in an arbitrary dimension D

$$E_{\mathrm{C}} = \hbar c A \left(\sum_{n=0}^{\infty}{}' - \int_0^\infty dn \right) \int \frac{d^{D-1}k_\perp}{(2\pi)^{D-1}} \sqrt{\frac{\pi^2 n^2}{d^2} + \mathbf{k}_\perp^2} \tag{2.205}$$

and continues analytically its result to the physical dimension $D = 3$ at the end. At first, the major problem is how to perform in (2.205) the integral over the transversal wave vector $\mathbf{k}_\perp$. In order to investigate its superficial degree of divergence we introduce an ultraviolet cut-off Λ and approximate the integrand for large transversal wave vectors $\mathbf{k}_\perp$:

$$\int \frac{d^{D-1}k_\perp}{(2\pi)^{D-1}} \sqrt{\frac{\pi^2 n^2}{d^2} + \mathbf{k}_\perp^2} \sim \int_0^\Lambda dk_\perp \, k_\perp^{D-2} \cdot k_\perp \sim \Lambda^D \,. \tag{2.206}$$

Thus, at the physical dimension $D = 3$ the integral over the transversal wave vector $\mathbf{k}_\perp$ diverges, and the ultraviolet divergency vanishes for any dimension $D < 0$.

In view of performing the transversal wave vector $\mathbf{k}_\perp$ we might have the idea to apply the Schwinger trick (2.184) for $x = -1/2$ and $a = \pi^2 n^2/d^2 + \mathbf{k}_\perp^2$. However, at a first glance, this is not allowed as the integral definition of the Gamma function $\Gamma(x)$ in (2.176) is not defined for negative arguments, i.e. $x < 0$. But it turns out that the recursion formula (2.177) for the Gamma function $\Gamma(x)$ allows to analytically continue it piecewise. Thus, the values of $\Gamma(x)$ in the interval $-1 < x < 0$ follow due to (2.177) from the interval $0 < x < 1$ yielding, for instance

$$\Gamma\left(-\frac{1}{2}\right) = -2\sqrt{\pi} \tag{2.207}$$

as $\Gamma(1/2) = \sqrt{\pi}$ follows directly from the integral definition (2.176). In this way the Gamma function $\Gamma(x)$ can be defined for all real $x \neq 0, -1, -2, \ldots$ as depicted in Fig. 2.6. Having this analytic continuation of the Gamma function in mind, we can now apply the Schwinger trick (2.184) for $x = -1/2$ and $a = \pi^2 n^2/d^2 + \mathbf{k}_\perp^2$, yielding with (2.207)

$$\sqrt{\frac{\pi^2 n^2}{d^2} + k_y^2 + k_z^2} = \frac{1}{(\pi^2 n^2/d^2 + k_y^2 + k_z^2)^{-1/2}} = \frac{-1}{2\sqrt{\pi}} \int_0^\infty d\tau \, \tau^{-3/2} \, e^{-(\pi^2 n^2/d^2 + \mathbf{k}_\perp^2)\tau} \,. \tag{2.208}$$

Inserting (2.208) into (2.205) reveals the advantage of the Schwinger trick. Namely, due to having introduced the artificial Schwinger integral with respect to τ, the integral with respect to the transversal wave vector $\mathbf{k}_\perp$ turns out to be Gaussian

$$\int \frac{d^{D-1}k_\perp}{(2\pi)^{D-1}} \sqrt{\frac{\pi^2 n^2}{d^2} + \mathbf{k}_\perp^2} = \frac{-1}{2\sqrt{\pi}} \int_0^\infty d\tau \, \tau^{-3/2} \, e^{-\pi^2 n^2/d^2 \tau} \int \frac{d^{D-1}k_\perp}{(2\pi)^{D-1}} \, e^{-\mathbf{k}_\perp^2 \tau} \,, \tag{2.209}$$

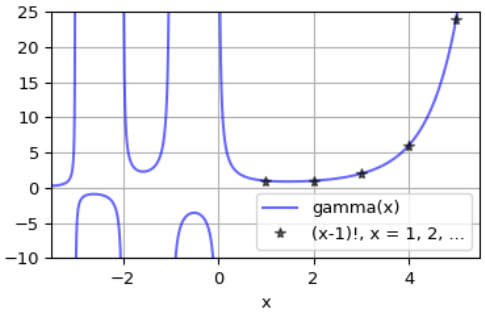

Figure 2.6: Gamma function $\Gamma(x)$ represents for $x > 0$ an interpolation between the factorials (2.178) and is analytically continued to $x < 0$ via the recursion formula (2.177).

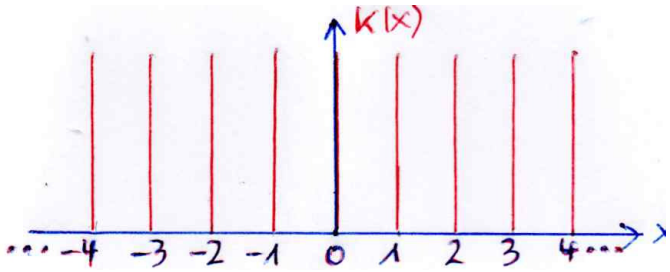

Figure 2.7: The Dirac comb (2.212) is an infinite series of Dirac delta functions with unity spacing.

which can straight-forwardly be evaluated:

$$\int \frac{d^{D-1}k_\perp}{(2\pi)^{D-1}}\, e^{-\mathbf{k}_\perp^2 \tau} = \frac{1}{(4\pi)^{(D-1)/2}}\, \tau^{(1-D)/2}\,. \tag{2.210}$$

Taking into account the side calculations (2.209) and (2.210), the Casimir (2.205) results in

$$E_{\rm C} = \frac{-\hbar c A}{2\sqrt{\pi}(4\pi)^{(D-1)/2}} \int_0^\infty d\tau\, \tau^{-D/2-1} \left(\sum_{n=0}^{\infty}{}' - \int_0^\infty dn \right) e^{-\pi^2 n^2 \tau/d^2}\,. \tag{2.211}$$

Here it remains to evaluate the difference between a sum and an integral. This can be achieved with the Poisson sum formula, which represents an intriguing tool for both quantum and statistical field theory.

2.17.3 Poisson Sum Formula

Let us consider the Dirac comb function

$$K(x) = \sum_{n=-\infty}^{\infty} \delta(x-n)\,, \tag{2.212}$$

which is periodic

$$K(x+k) = K(x)\,; \qquad k = 0, \pm 1, \pm 2, \ldots \tag{2.213}$$

and is illustrated in Fig. 2.7. Due to its periodicity the Dirac comb function (2.212) can be decomposed into a Fourier series

$$K(x) = \sum_{m=-\infty}^{\infty} K_m \, e^{-2\pi i m x} \,, \tag{2.214}$$

where the respective Fourier coefficients K_m follow from an integration over one period:

$$K_m = \int_{-1/2}^{+1/2} dx \, K(x) \, e^{2\pi i m x} \,. \tag{2.215}$$

Inserting (2.212) into (2.214) by taking into account (2.215) then leads to the distributional identity

$$\sum_{n=-\infty}^{\infty} \delta(x-n) = \sum_{m=-\infty}^{\infty} e^{-2\pi i m x} \,. \tag{2.216}$$

Multiplying (2.216) with some function $f(x)$ and integrating over the whole real axis finally yields the celebrated Poisson sum formula:

$$\sum_{n=-\infty}^{\infty} f(n) = \sum_{m=-\infty}^{\infty} \int_{-\infty}^{\infty} dx \, f(x) \, e^{-2\pi i m x} \,. \tag{2.217}$$

Thus, the Poisson sum formula (2.217) allows to calculate a given sum on the left-hand side by mapping it to another sum on the right-hand side, where the result of the summation is possibly known. In case that the function $f(x)$ is even, i.e. $f(-x) = f(x)$, Eq. (2.217) reduces with (2.204) to

$$\left(\sum_{n=0}^{\infty}{}' - \int_0^{\infty} dn \right) f(n) = \sum_{m=1}^{\infty} \mathrm{Re} \int_{-\infty}^{\infty} dx \, f(x) \, e^{-2\pi i m x} \,, \qquad f(-x) = f(x) \,. \tag{2.218}$$

Thus, in view of the Casimir energy (2.211) we specialize the Poisson sum formula (2.218) to the even function $f(x) = e^{-\pi^2 x^2 \tau / d^2}$, where the remaining Gaussian function is directly evaluated:

$$\left(\sum_{n=0}^{\infty}{}' - \int_0^{\infty} dn \right) e^{-\pi^2 n^2 \tau / d^2} = \sum_{m=1}^{\infty} \mathrm{Re} \int_{-\infty}^{\infty} dx \, e^{-\pi^2 x^2 \tau / d^2 - 2\pi i m x} = \frac{d}{\sqrt{\pi \tau}} \sum_{m=1}^{\infty} e^{-m^2 d^2 / \tau} \,. \tag{2.219}$$

Inserting (2.219) into (2.211) it is obvious to perform the substitution $u(\tau) = 1/\tau$

$$E_{\mathrm{C}} = \frac{-\hbar c A d}{2\pi (4\pi)^{(D-1)/2}} \sum_{m=1}^{\infty} \int_0^{\infty} du \, u^{(D-1)/2} \, e^{-m^2 d^2 u} \,, \tag{2.220}$$

as then the remaining integral with respect to u is again of the form of the form of the Schwinger trick (2.184) but this time with $x = (D+1)/2$ and $a = m^2 d^2$, yielding

$$E_{\mathrm{C}} = \frac{-\Gamma((D+1)/2) \zeta(D+1) \hbar c A}{2\pi (4\pi)^{(D-1)/2} d^D} \,, \tag{2.221}$$

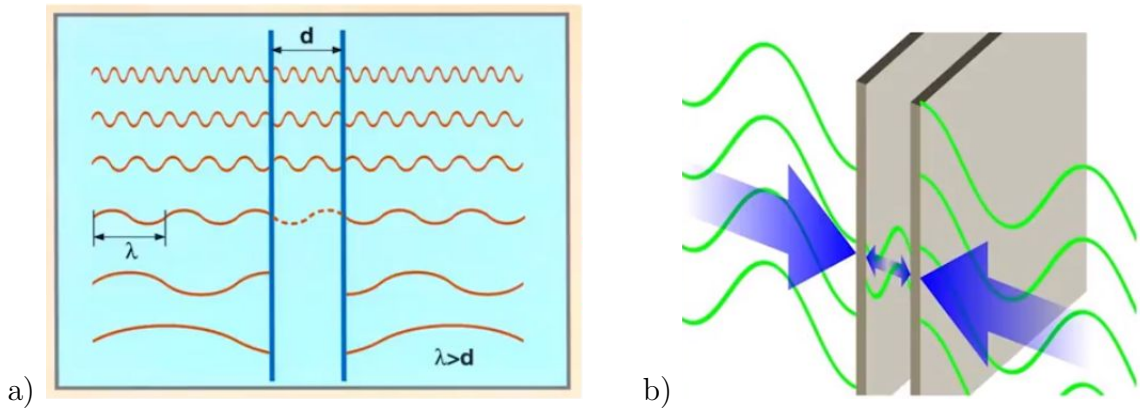

Figure 2.8: Heuristic explanation of Casimir effect: a) Mode density is larger outside of the plates than in between the plates, thus b) both plates are pressed together.

where we have introduced the Riemann zeta function

$$\zeta(z) = \sum_{n=1}^{\infty} \frac{1}{n^z} \,. \tag{2.222}$$

Thus, specializing in (2.221) the dimension D to the physical dimension $D = 3$ and using the value for the Riemann zeta function $\zeta(4)$ in (B.21), we get for the Casimir energy

$$E_{\mathrm{C}} = -\frac{\pi^2 \hbar c A}{720 d^3} \,. \tag{2.223}$$

2.17.4 Physical Discussion

First of all we read off from the negative sign that the vacuum fluctuations of the electromagnetic field lead to a lowering of the energy. This manifests itself in an attractive force between the two metal plates, which decreases with the inverse fourth power of the distance:

$$F_{\mathrm{C}} = -\frac{\partial E_{\mathrm{C}}}{\partial d} = -\frac{\pi^2 \hbar c A}{240 d^4} \,. \tag{2.224}$$

The attraction of the Casimir force can be understood on heuristic grounds as follows. According to Fig. 2.8a) there is a larger number of modes outside of the plates than in between the plates as the photons inside the plates have a wavelength, which is shorter than the distance between the plates. Thus, due to the larger density of states outside of the plates, both plates are pressed together, see Fig. 2.8b). Furthermore, apart from the geometrical quantities d and A the force (2.224) depends only on fundamental values of the Planck constant $\hbar$ and the speed of light c. At scales, which are smaller than $1\,\mu$m, this Casimir force turns out to be the dominant one between electrically neutral objects and is, thus, relevant for nanotechnology. For an area of $A = (1\,\mu\mathrm{m})^2$ the Casimir force amounts to the value $F_{\mathrm{C}} = 1.3\,\mathrm{pN}$, which is an order of magnitude being measurable with a force microscope. Experimentally it is hard to configure two parallel plates uniformly separated by distances less than a micron. Therefore,

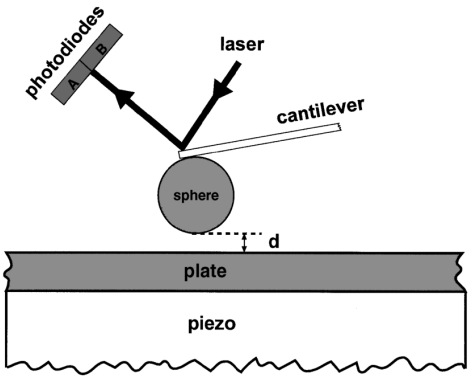

Figure 2.9: Schematic diagram of the experimental setup in Ref. [30]. Application of voltage to the piezo results in the movement of the plate towards the sphere.

it is advantageous in an experiment to replace one of the plates by a metal sphere of radius R with the condition $R \gg d$. For such a geometry the Casimir force reads instead of (2.224) [30]:

$$F_{\mathrm{C}} = -\frac{\pi^3 \hbar c R}{360 d^3} \,. \tag{2.225}$$

A high-precision measurement of such a Casimir force between a metallized sphere of diameter $196\,\mu$m and a flat plate was performed with an atomic force microscope, see Fig. 2.9. The force was measured for plate-sphere surface separations from 0.1 to $0.9\,\mu$m. The experimental results turned out to be consistent with present theoretical calculations including the finite conductivity, roughness, and temperature corrections.

An interesting application of the Casimir effect occurs when one searches for non-Newtonian gravity in the micrometre range [31]. Subtracting the respective contributions of the Casimir force from experimental data reveals a possible contribution from a so-called fifth force. Here a deviation from the Newtonian potential by an additional Yukawa potential is described by the parameters A and Λ in the phenomenological ansatz

$$\frac{1}{r} \qquad \Longrightarrow \qquad \frac{1 + A e^{-r/\Lambda}}{r} \,, \tag{2.226}$$

for which an upper bound can be determined. In order to obtain precise predictions one has to take into account several theoretical corrections. Usually a different geometry is considered as, for instance, two spheres. In addition to the vacuum fluctuations also thermal fluctuations occur in experiments, whose magnitude has to be estimated. Furthermore deviations occur provided that the two surfaces are not perfectly conducting. Also surface roughnesses are important to study. And in case of magnetic materials other boundary conditions might occur so that the Casimir force can become repulsive. Although the last decade of experiments has resulted in solid demonstrations of the Casimir force, the situation is not yet conclusive with respect to being able to discover new physics in the context of non-Newtonian gravity.

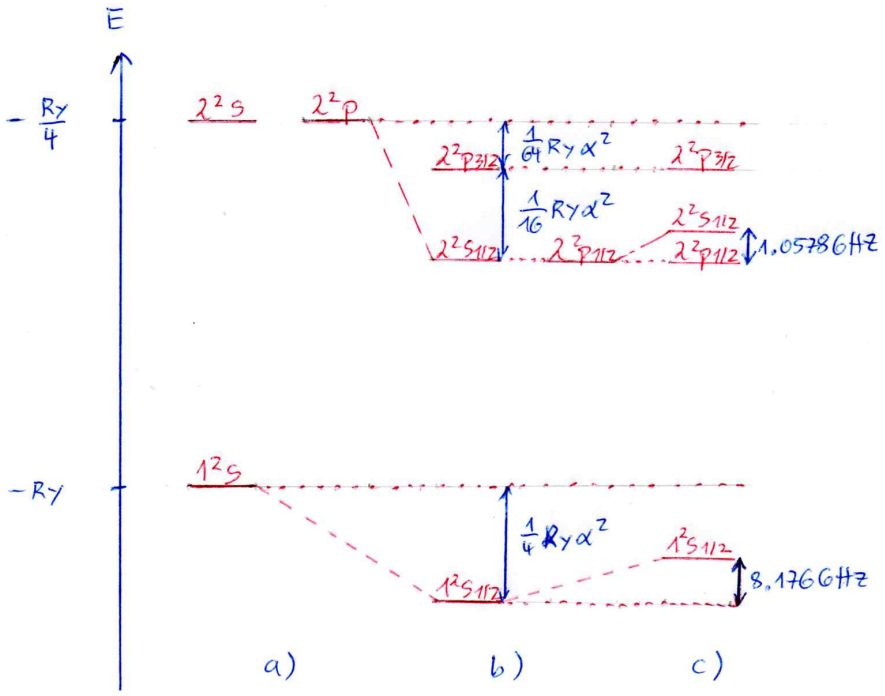

Figure 2.10: Not to scale sketch of hydrogen energy levels according to a) Bohr-Sommerfeld theory, b) Dirac theory, and c) quantum electrodynamics.

2.18 Lamb Shift

As discussed in the previous section the Casimir effect tells us that the presence of the two plane-parallel metal plates affects the vacuum fluctuations of the electromagnetic field. In contrast to that the Lamb shift, named after Willis Lamb, describes a difference in energy between two energy levels $2^2s_{1/2}$ and $2^2p_{1/2}$, which was not predicted by the Dirac equation, according to which these states should have the same energy. Subsequent to its discovery in 1947 it was explained by the interaction between vacuum energy fluctuations of the electromagnetic field and the hydrogen electron in these different orbitals. The importance of the Lamb shift is best illustrated by a statement of Freeman Dyson on the occasion of Lamb's 65th birthday: ,,Those years, when the Lamb shift was the central theme of physics, were golden years for all the physicists of my generation. You were the first to see that this tiny shift, so elusive and hard to measure, would clarify our thinking about particles and fields." The Lamb shift has since played a significant role through vacuum energy fluctuations in theoretical prediction in general and in the Hawking radiation from black holes in particular [32].

2.18.1 Energy Levels of Hydrogen Atom

We start with reviewing the development of atomic physics by the example how the energy levels of the hydrogen atom have become known more and more precisely.

In the Bohr-Schrödinger theory one treats the hydrogen atom within non-relativistic quantum mechanics without taking into account the spin of the electron. The resulting energy levels (C.12) are determined by the Rydberg energy (C.11)–(C.15) as the relevant energy scale and the principal quantum number n. Thus, they are degenerate with respect to the azimuthal quantum number $l = 0, 1, 2, \ldots, n-1$, the magnetic quantum number $m_l = -l, -l+1, \ldots, l-1, l$ and the spin quantum number $m_s = -1/2, 1/2$. Each atomic state is described by a term symbol of the form $n^{2s+1}L$, where $2s+1 = 2$ denotes the multiplicity with respect to the spin $s = 1/2$ and L abbreviates a letter $s, p, d, f, \ldots$ corresponding to $l = 0, 1, 2, 3, \ldots$. Thus, according to the Bohr-Schrödinger theory, the ground state of the hydrogen atom with the energy $E_1 = -\mathrm{Ry}$ is denoted by 1^2s, whereas the first excited states 2^2s and 2^2p are degenerate and have the energy $E_2 = -\mathrm{Ry}/4$, see Fig. 2.10a).

The Dirac theory treats the hydrogen atom within relativistic quantum mechanics, where the spin of the electron is taken into account. The energy states of the hydrogen atom can be calculated exactly within the Dirac theory and read:

$$E_{nj} = Mc^2 \sqrt{1 - \frac{\alpha^2}{n^2 + 2(n-j-1/2)\left[(j+1/2)^2 - \alpha^2\right] - j - 1/2}}\,. \tag{2.227}$$

Here (2.227) depends apart from the principal quantum number n also from the total angular momentum quantum number $j = l \pm 1/2$, which accounts for the spin-orbit coupling. Expanding (2.227) in powers of the Sommerfeld fine-structure constant α defined in (C.11) yields for the leading relativistic correction of the non-relativistic energy values (C.12) three different contributions. The first one stems from taking into account the relativistic energy-momentum dispersion, the second one from the spin-orbit coupling, and the third one is the Darwin term, which describes the Zitterbewegung of an electron in an s-shell around its position due its interaction with virtual electron-positron pairs. With all three contributions together one obtains

$$E_{nj} = -\mathrm{Ry}\,\frac{1}{n^2} + E_{nj}^{\mathrm{FS}} + \ldots\,. \tag{2.228}$$

Here the fine-structure energy

$$E_{nj}^{\mathrm{FS}} = -\frac{\mathrm{Ry}\alpha^2}{n^4}\,\left(\frac{n}{j+1/2} - \frac{3}{4}\right) \tag{2.229}$$

turns out to be always negative. Note that the relativistic energy reduction (2.229) was originally determined by Arnold Sommerfeld by discarding Bohr circles in favour of Kepler ellipses for the electron orbits with the proton being located at the focus. Is the electron nearer to the proton it moves faster and gets due to special relativity a larger mass, which implies according to (C.13) a lowering of the energy. As the fine-structure energy (2.229) depends on the total angular momentum quantum number j, the original term symbol $n^{2s+1}L$ for the atomic states is extended to the form $n^{2s+1}L_j$. As a consequence of the fine-structure (2.229) the ground state $1^2\mathrm{s}_{1/2}$ is just reduced by the energy $\mathrm{Ry}\alpha^2/4$. But the impact for the first excited state is more significant. Although the original degeneracy between the Bohr-Schrödinger atomic

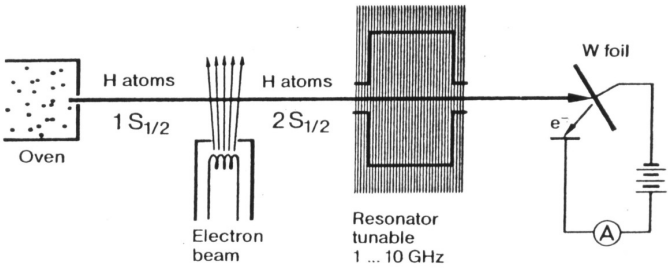

Figure 2.11: Experimental set-up from Lamb and Retherford for detecting the Lamb shift in the microwave range.

states 2^2s and 2^2p is lifted, a new degeneracy with respect to the total angular momentum quantum number j emerges. Now we have the energetically higher state $2^2\mathrm{p}_{3/2}$, which has just a fine-structure reduction of $\mathrm{Ry}\alpha^2/64$, whereas the two degenerate energy states $2^2\mathrm{s}_{1/2}$ and $2^2\mathrm{p}_{1/2}$ get the same fine-structure reduction $5\mathrm{Ry}\alpha^2/64$, see Fig. 2.10b).

A full quantum electrodynamic treatment takes into account that the electron of the hydrogen atom is interacting with the vacuum fluctuations of the electromagnetic field. As we will show shortly, this only affects in leading order only the s-states, where the electron has a non-vanishing probability to stay in the vicinity of the proton, and leads to a positive shift of the energy levels. For the ground state $1^2\mathrm{s}_{1/2}$ this amounts to an upwards shift of

$$\Delta E_{\mathrm{L}}(1^2\mathrm{s}_{1/2})/h = 8.17\,\mathrm{GHz}\,. \tag{2.230}$$

And for the two degenerate energy states $2^2\mathrm{s}_{1/2}$ and $2^2\mathrm{p}_{1/2}$ this has the consequence that the energy level $2^2\mathrm{p}_{1/2}$ is not affected, whereas $2^2\mathrm{s}_{1/2}$ acquires a Lamb shift of

$$\Delta E_{\mathrm{L}}(2^2\mathrm{s}_{1/2})/h = 1.0578\,\mathrm{GHz}\,, \tag{2.231}$$

which amounts to 1/10 of the fine-structure spacing $\mathrm{Ry}\alpha^2/16$ between the states $2^2\mathrm{p}_{1/2}$ and $2^2\mathrm{p}_{3/2}$, see Fig. 2.10c). Thus, we conclude, that the vacuum fluctuations of the electromagnetic field ultimately lift the degeneracy of the Dirac energy levels with respect to the total angular momentum quantum number j.

2.18.2 Detection in Microwave Range

In 1947 Willis Lamb and Robert Retherford carried out an experiment using microwave techniques to stimulate radio-frequency transitions between the $2^2\mathrm{s}_{1/2}$ and $2^2\mathrm{p}_{1/2}$ levels of hydrogen. The corresponding experimental set-up is sketched in Fig. 2.11. With an oven at 2 500 °C H_2-molecules thermally dissociate into H-atoms. The resulting beam of $1^2\mathrm{s}_{1/2}$ hydrogen atoms travels past an electron beam, which excites a smaller fraction of atoms to the metastable state $2^2\mathrm{s}_{1/2}$. Note that optical transitions from the $2^2\mathrm{s}_{1/2}$ to the $1^2\mathrm{s}_{1/2}$ state are forbidden due to the selection rule $\Delta l = \pm 1$, see Appendix F. The atoms then pass a microwave resonator, which is

tunable within the range of 1 and 10 GHz, see Fig. 1.1, and then hit a Wolfram plate. There the metastable $2^2s_{1/2}$-atoms release their excitation energy as they go over into the ground state $1^2s_{1/2}$ by liberating electrons from the metal plate. One then detects the number of electrons, which is a measure for the number of metastable $2^2s_{1/2}$ atoms. But those atoms, which are excited within the resonator from the $2^2s_{1/2}$ to the $2^2p_{3/2}$ level in the range of 10 000 MHz lead to a reduction of the electron current. Their number is detected due to an optical transition into the ground state $1^2s_{1/2}$. Additionally, Lamb and Retherford found in 1947 that the same effect, i.e. a reduction of the electron current, occurs when $2^2s_{1/2}$ atoms absorb microwaves at the frequency 1 000 MHz, which leads to a transition from the $2^2s_{1/2}$ to the $2^2p_{1/2}$ state, see Fig. 2.10. This showed impressively that even states with the same total angular momentum j are energetically different.

2.18.3 Qualitative Explanation

Let us qualitatively discuss the interaction of electrons with the vacuum of the light field. Due to the energy-time uncertainty the conservation of energy can briefly be violated, allowing the hydrogen electron to virtually absorb and emit photons, see Fig. 2.12. This leads to an atomic energy shift, which is infinitely large. Also a free electron can continuously absorb and emit photons, which leads likewise to an infinite decrease of its energy. But experimentally it turns out that the atoms have a finite energy. The basic idea for solving this ,,infinity problem" of the energy shift is therefore the following. One has to subtract from the infinitely large energy shift of the bound electrons the corresponding infinitely large energy shift of the free electrons in order to obtain an experimentally finite value. This process is called renormalization in physics. It also involves a renormalization of the electron mass. Within the realm of the renomalization theory of quantum electrodynamics one has worked out a procedure, which eliminates systematically all infinities of the theory. With this one can calculate, for instance, the Lamb shift and the Landé factor of the electron with an unprecedented precision. In this way one finds the highest agreement between theory and experiment in all natural sciences. This is best illustrated by a statement of Richard Feynman in the introduction of his book [35]: ,,To give you a feeling for the accuracy of these numbers, it comes out something like this: If you were to measure the distance from Los Angeles to New York to this accuracy, it would be exact to the thickness of a human hair."

2.18.4 Vacuum Fluctuations

In quantum electrodynamics one would have to determine the Lamb shift via a quantization of both the Dirac and the Maxwell field. But as the Lamb shift represents the leading quantum electrodynamical correction, the matter can still be treated non-relativistically. Thus, it is sufficient to take into account in perturbation theory the impact of the quantized light field upon the hydrogen atom described by the Schrödinger theory. This leads to a surprisingly simple

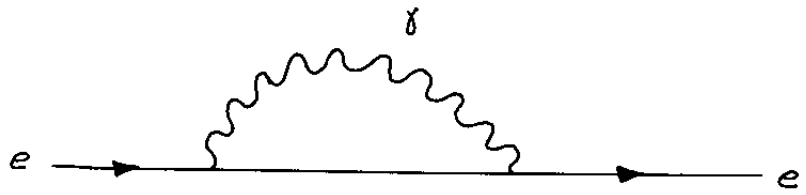

Figure 2.12: A moving electron can emit and absorb a virtual photon.

physical interpretation: The quantum mechanical zero-point fluctuations of the electromagnetic field act statistically upon the hydrogen electron, which effectively leads to a shift of its potential energy.

The starting point is the Coulomb potential for the electron in the hydrogen atom:

$$V(\mathbf{x}) = -\frac{e^2}{4\pi\epsilon_0|\mathbf{x}|}\,. \tag{2.232}$$

In case that the electron is elongated by some fluctuations of the electromagnetic field due to absorption and emissions of photons, one has to consider instead of (2.232) the potential $V(\mathbf{r}+\mathbf{s})$, where the inequality $|\mathbf{s}| \ll |\mathbf{r}|$ holds. Thus, applying a Taylor expansion is physically justified:

$$V(\mathbf{x}+\mathbf{s}) = V(\mathbf{x}) + \sum_{i=1}^{3} \frac{\partial V(\mathbf{x})}{\partial x_i}\, s_i + \frac{1}{2}\sum_{i=1}^{3}\sum_{j=1}^{3} \frac{\partial^2 V(\mathbf{x})}{\partial x_i \partial x_j}\, s_i s_j + \dots\,. \tag{2.233}$$

Denoting with $\langle\bullet\rangle$ the averaging over all fluctuations $\mathbf{s}$ we get

$$\langle V(\mathbf{x}+\mathbf{s})\rangle = V(\mathbf{x}) + \sum_{i=1}^{3} \frac{\partial V(\mathbf{x})}{\partial x_i}\, \langle s_i\rangle + \frac{1}{2}\sum_{i=1}^{3}\sum_{j=1}^{3} \frac{\partial^2 V(\mathbf{x})}{\partial x_i \partial x_j}\, \langle s_i s_j\rangle + \dots\,. \tag{2.234}$$

Due to the isotropy of the fluctuations we can assume

$$\langle s_i\rangle = 0\,, \qquad \langle s_i s_j\rangle = \frac{1}{3}\,\langle \mathbf{s}^2\rangle\,\delta_{ij}\,, \tag{2.235}$$

so (2.234) reduces on average in leading order to the following change in potential energy

$$\langle V(\mathbf{x}+\mathbf{s})\rangle - V(\mathbf{x}) = \frac{1}{6}\,\Delta V(\mathbf{x})\,\langle \mathbf{s}^2\rangle\,. \tag{2.236}$$

For the hydrogen atom this leads to the following energy shift of the atomic state in first order of perturbation theory:

$$\Delta E_{\mathrm{L}} = \int d^3x\, \psi^*_{nlm}(\mathbf{x}) \Big[\langle V(\mathbf{x}+\mathbf{s})\rangle - V(\mathbf{x})\Big] \psi_{nlm}(\mathbf{x})\,. \tag{2.237}$$

Inserting (2.232) and (2.236) into (2.237) and taking into account

$$\Delta\,\frac{1}{|\mathbf{x}|} = -4\pi\,\delta(\mathbf{x}) \tag{2.238}$$

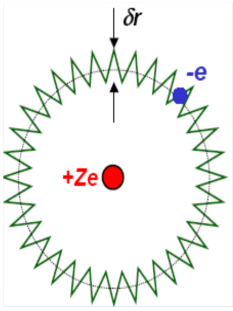

Figure 2.13: Zitterbewegung of an electron: The length scale δr corresponds in case of the Darwin term to the Compton wavelength λ_{C} due to the creation of electron-positron pairs, whereas the Lamb shift stems from the average of the squared displacement of the electron $\sqrt{\langle \mathbf{s}^2 \rangle}$, which is due to the absorption and emission of photons and occurs on a much smaller length scale, see Eqs. (2.268) and (2.269).

then yields

$$\Delta E_{\mathrm{L}} = \frac{e^2}{6\epsilon_0} \left|\psi_{nlm}(\mathbf{0})\right|^2 \langle \mathbf{s}^2 \rangle \,. \tag{2.239}$$

We read off from (2.239) that the Lamb shift occurs only for hydrogen wave functions, which are non-vanishing at the origin, i.e. for s-states, where the energy levels are increased. Note that the result (2.239) should not be confused with the Darwin term, which arises within the non-relativistic limit of the Dirac equation, see the remark on page 39. There the length scale $\sqrt{\langle \mathbf{s}^2 \rangle}$ of the Zitterbewegung of the electron can be interpreted by the Compton wave length $\lambda_{\mathrm{C}} = 2\pi\hbar/Mc$. Vacuum quantum fluctuations allow for the creation of electron-positron pairs during the lifetime $2\pi\hbar/Mc^2$, where the pairs travel the distance $\lambda_{\mathrm{C}} = 2\pi\hbar/Mc$. In contrast to that the Lamb shift (2.239) stems from the Zitterbewegung of the electron due to absorption and emission of virtual photons, which occurs on a much smaller length scale as we will see below, see Fig. 2.13.

As the probability density of the hydrogen electron in an s-state with principal quantum number n is given by

$$\left|\psi_{nlm}(\mathbf{0})\right|^2 = \frac{1}{\pi a_{\mathrm{B}}^3 n^3} \,, \tag{2.240}$$

where a_{B} denotes the Bohr radius (C.8), the Lamb shift (2.239) reduces to

$$\Delta E_{\mathrm{L},n} = \frac{e^2}{6\pi\epsilon_0 a_{\mathrm{B}}^3 n^3} \langle \mathbf{s}^2 \rangle \,. \tag{2.241}$$

Ignoring for the moment a possible dependence of $\langle \mathbf{s}^2 \rangle$ from the principal quantum number n, we expect that the Lamb shifts for $n = 1$ and $n = 2$ have the ratio $\Delta E_{\mathrm{L}}(1^2\mathrm{s}_{1/2})/\Delta E_{\mathrm{L}}(2^2\mathrm{s}_{1/2}) = 8$, which agrees quite well with the experimentally measured ratio 7.7 following from (2.230) and (2.231). In order to determine the Lamb shift from (2.241) it remains to determine the average of the squared displacement of the electron due to the absorption and emission of photons. In

the following we provide both a classical and a quantum mechanical calculation of $\langle \mathbf{s}^2 \rangle$ and show that both turn out to agree.

2.18.5 Classical Approach

At first we consider at first within a classical treatment the Newton equation

$$M\ddot{\mathbf{s}}_\omega(t) = -e\mathbf{E}_\omega(t) \tag{2.242}$$

for a periodic change of the electric field

$$\mathbf{E}_\omega(t) = \mathbf{E}_0(\omega)\, e^{i\omega t}\,. \tag{2.243}$$

The solution of (2.242) and (2.243) follows straight-forwardly

$$\mathbf{s}_\omega(t) = \mathbf{s}_0(\omega)\, e^{i\omega t}\,, \qquad \mathbf{s}_0(\omega) = \frac{e}{M\omega^2}\,\mathbf{E}_0(\omega)\,. \tag{2.244}$$

Interpreting the averaging over all fluctuations $\langle \bullet \rangle$ as a time average then yields for the average of the squared displacement of the electron

$$\langle \mathbf{s}^2 \rangle_\omega = \frac{\omega}{2\pi}\int_0^{2\pi/\omega} dt\, |\mathbf{s}_\omega^2(t)|^2 = \frac{e^2|\mathbf{E}_0(\omega)|^2}{M^2\omega^4}\,. \tag{2.245}$$

Now we have to determine the amplitude $\mathbf{E}_0(\omega)$ of the electric field. To this end we take into account that both electric and magnetic field equally contribute to the the zero-point energy of the electromagnetic field. Thus we obtain in the frequency interval between ω and $\omega + d\omega$ in volume V for the density of the electric field:

$$\frac{\epsilon_0}{2}\,|\mathbf{E}_0(\omega)|^2 = \frac{1}{2}\,\frac{\hbar\omega}{2}\,\rho(\omega)d\omega\,. \tag{2.246}$$

Here appears the mode density $\rho(\omega)$, which represents the number of electromagnetic modes per angular frequency ω and per volume V. Thus, the total number of modes is given on the one hand by

$$N_{\text{modes}} = V\int_0^\infty d\omega\,\rho(\omega)\,. \tag{2.247}$$

On the other hand the total number of modes also follows similar to (2.196)–(2.198) by integrating over all wave vectors and by taking into account the two transversal degrees of freedom

$$N_{\text{modes}} = 2V\int \frac{d^3k}{(2\pi)^3}\,. \tag{2.248}$$

Thus, introducing in the integrand of (2.248) the identity

$$1 = \int_0^\infty d\omega\,\delta\left(\omega - c|\mathbf{k}|\right)\,, \tag{2.249}$$

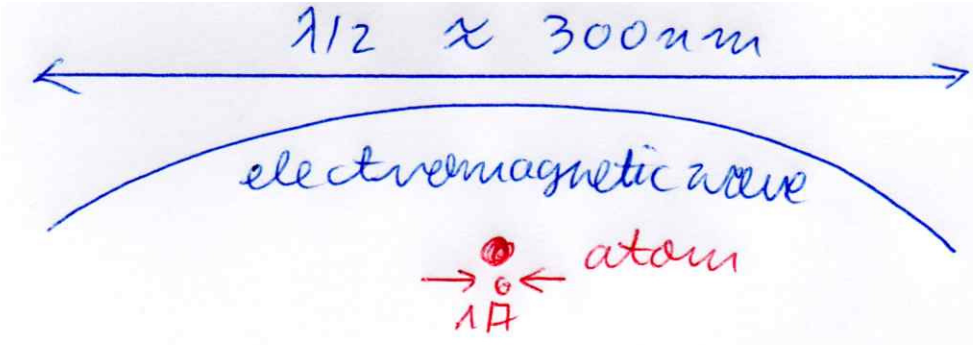

Figure 2.14: Comparison of length scales: electromagnetic wavelength versus extension of an atom.

where we use the linear dispersion (2.73), we obtain by comparison with (2.248) for the mode density

$$\rho(\omega) = 2 \int \frac{d^3k}{(2\pi)^3} \, \delta \left(\omega - c|\mathbf{k}| \right) \, . \tag{2.250}$$

Evaluating the integral yields due to the isotropy of the integrand

$$\rho(\omega) = \frac{\omega^2}{\pi^2 c^3} \, , \tag{2.251}$$

i.e. the mode density increases quadratically with the frequency ω. With this mode density the absolute square of the electric field amplitude $\mathbf{E}_0(\omega)$ in (2.246) reduces to

$$|\mathbf{E}_0(\omega)|^2 = \frac{\hbar \omega^3}{2\pi^2 \epsilon_0 c^3} \, d\omega \, . \tag{2.252}$$

Inserting (2.252) into (2.245) we have to integrate over all frequencies ω, yielding for the average of the squared displacement of the electron

$$\langle \mathbf{s}^2 \rangle = \int_0^\infty d\omega \, \langle \mathbf{s}^2 \rangle_\omega = \frac{\hbar e^2}{2\pi^2 \epsilon_0 M^2 c^3} \int_0^\infty d\omega \, \frac{1}{\omega} \, . \tag{2.253}$$

This integral has both an infrared and an ultraviolet divergency as it diverges both for the lower and the upper integration boundary.

2.18.6 Quantum Mechanical Approach

We show now that a quantum mechanical treatment of the electromagnetic field yields precisely the same divergent result (2.253). To this end we have to go back to the electric field operator (2.168). Here the absolute value of the wave vector $\mathbf{k}$, i.e. $|\mathbf{k}| = 2\pi/\lambda$ is determined by the wavelength λ. In the optical range, the wavelength varies between 400 nm and 700 nm according to Fig. 1.1. Thus, we obtain the following estimate for an atom with an extension in the range of an Angström, see Fig. 2.14:

$$|\mathbf{k} \cdot \mathbf{x}| \leq |\mathbf{k}| \cdot |\mathbf{x}| \approx \frac{2\pi}{600 \, \mathrm{nm}} \cdot 1 \mathrm{\AA} \approx 10^{-3} \ll 1 \, . \tag{2.254}$$

This means that the electric field operator (2.168) does not change over the extension of an atom and is, therefore, approximately homogeneous. This leads to the so-called *dipole approximation*, where we can approximately neglect the spatial dependence of the electric field operator (2.168) for spatial vectors $\mathbf{x}$ pointing at the atom and yield

$$\hat{\mathbf{E}}(t) = \sum_{\lambda=\pm1} \int d^3k \sqrt{\frac{\hbar\omega_{\mathbf{k}}}{2(2\pi)^3\epsilon_0}}\, i \left\{ \boldsymbol{\epsilon}(\mathbf{k},\lambda) e^{-i\omega_{\mathbf{k}}t} \hat{a}_{\mathbf{k},\lambda} - \boldsymbol{\epsilon}^*(\mathbf{k},\lambda) e^{i\omega_{\mathbf{k}}t} \hat{a}^\dagger_{\mathbf{k},\lambda} \right\} . \tag{2.255}$$

The corresponding Newton equation reads now instead of (2.242)

$$M\ddot{\hat{\mathbf{s}}}(t) = -e\hat{\mathbf{E}}(t) \,, \tag{2.256}$$

which has the solution

$$\hat{\mathbf{s}}(t) = \sum_{\lambda=\pm1} \int d^3k \, \frac{e}{M\omega_{\mathbf{k}}^2} \sqrt{\frac{\hbar\omega_{\mathbf{k}}}{2(2\pi)^3\epsilon_0}}\, i \left\{ \boldsymbol{\epsilon}(\mathbf{k},\lambda) e^{-i\omega_{\mathbf{k}}t} \hat{a}_{\mathbf{k},\lambda} - \boldsymbol{\epsilon}^*(\mathbf{k},\lambda) e^{i\omega_{\mathbf{k}}t} \hat{a}^\dagger_{\mathbf{k},\lambda} \right\} . \tag{2.257}$$

This operator-valued elongation (2.257) describes the Zitterbewegung of the electron, which is due to the vacuum fluctuations of the electromagnetic field. Therefore, the average over the squared elongation $\langle \mathbf{s}^2 \rangle$ needed for (2.239) is interpreted as the vacuum expectation values

$$\langle \mathbf{s}^2 \rangle = \left\langle 0 \left| \hat{\mathbf{s}}(t)^2 \right| 0 \right\rangle . \tag{2.258}$$

Inserting (2.257) into (2.258) we have to evaluate:

$$\begin{aligned} \langle \mathbf{s}^2 \rangle = \sum_{\lambda=\pm1} \sum_{\lambda'=\pm1} \int d^3k \int d^3k' \, \frac{-e^2}{M^2\omega_{\mathbf{k}}^2\omega_{\mathbf{k}'}^2} \sqrt{\frac{\hbar\omega_{\mathbf{k}}}{2(2\pi)^3\epsilon_0}} \sqrt{\frac{\hbar\omega_{\mathbf{k}'}}{2(2\pi)^3\epsilon_0}} \\ \times \left\langle 0 \left| \left\{ \boldsymbol{\epsilon}(\mathbf{k},\lambda) e^{-i\omega_{\mathbf{k}}t} \hat{a}_{\mathbf{k},\lambda} - \boldsymbol{\epsilon}^*(\mathbf{k},\lambda) e^{i\omega_{\mathbf{k}}t} \hat{a}^\dagger_{\mathbf{k},\lambda} \right\} \left\{ \boldsymbol{\epsilon}(\mathbf{k}',\lambda') e^{-i\omega_{\mathbf{k}'}t} \hat{a}_{\mathbf{k}',\lambda'} - \boldsymbol{\epsilon}^*(\mathbf{k}',\lambda') e^{i\omega_{\mathbf{k}'}t} \hat{a}^\dagger_{\mathbf{k}',\lambda'} \right\} \right| 0 \right\rangle . \end{aligned} \tag{2.259}$$

Multiplying out the brackets yields in total four terms, but among them is only one, which does not vanish due to (2.131), (2.132), and (2.135), and this one coincides with (2.171). With this we obtain

$$\langle \mathbf{s}^2 \rangle = \frac{e^2\hbar}{\epsilon_0 M^2} \int \frac{d^3k}{(2\pi)^3} \frac{1}{\omega_{\mathbf{k}}^3} \,, \tag{2.260}$$

which reduces due to the linear dispersion (2.73) finally to the previous classical result (2.253).

2.18.7 Infrared and Ultraviolet Cut-Off

In order to proceed further we identify the prefactor in (2.253) with the Compton wave length λ_{C} from (C.10) and the Sommerfeld fine-structure constant from (C.11). Furthermore, in order to regularize the divergent frequency integral (2.253), we introduce both an infrared and an ultraviolet cut-off $\omega_{\min}$ and $\omega_{\max}$. With this (2.253) reduces to

$$\langle \mathbf{s}^2 \rangle = \frac{\alpha\lambda_{\mathrm{C}}^2}{2\pi^3} \int_{\omega_{\min}}^{\omega_{\max}} d\omega \, \frac{1}{\omega} \,, \tag{2.261}$$

which can be straight-forwardly calculated:

$$\langle \mathbf{s}^2 \rangle = \frac{\alpha \lambda_{\mathrm{C}}^2}{2\pi^3} \ln \frac{\omega_{\max}}{\omega_{\min}} \,. \tag{2.262}$$

Thus, the averaged squared elongation turns out to depend on the choice of both cut-offs, which have now to be specified. The ultraviolet cut-off $\omega_{\max}$ can be physically reasonably fixed as follows. As we perform a non-relativistic calculation, we have to exclude relativistic effects. Therefore, we choose for the ultraviolet cut-off the frequency $\omega_{\max} = Mc^2/\hbar$, above which relativistic effects kick-in. In contrast to that the infrared cut-off $\omega_{\min}$ can not that clearly be defined and turns out to depend on the principal quantum number n. One possibility would be to choose for $\omega_{\min}$ the frequency of an electron at the Bohr radius. From the equality of the Coulomb force and the centrifugal force then follows

$$\frac{e^2}{4\pi\epsilon_0 a_n^2} = M\omega_{\min,n}^{(1)2} a_n \qquad \Longrightarrow \qquad \omega_{\min,n}^{(1)} = \frac{c\alpha}{a_{\mathrm{B}} n^3} \,, \tag{2.263}$$

where we have used the Sommerfeld fine-structure constant from (C.11) and the dependence of the Bohr radius a_n from the principal quantum number n according to (C.7). Another possibility would be to identify the infrared cut-off with the frequency of the photon on the Bohr radius, which yields

$$\omega_{\min,n}^{(2)} = \frac{2\pi c}{a_n} = \frac{2\pi c}{a_{\mathrm{B}} n^2} \,. \tag{2.264}$$

Taking into account the Compton wave length λ_{C} from (C.10) and the Sommerfeld fine-structure constant from (C.11) this yields for the ratios of the cut-offs

$$\frac{\omega_{\max}}{\omega_{\min,n}^{(1)}} = \frac{n^3}{\alpha^2} \,, \qquad \frac{\omega_{\max}}{\omega_{\min,n}^{(2)}} = \frac{n^2}{2\pi\alpha} \,. \tag{2.265}$$

The logarithms of their ratios yield for the principle quantum number $n = 1$ the values

$$\ln \frac{\omega_{\max}}{\omega_{\min,1}^{(1)}} = 9.8 \,, \qquad \ln \frac{\omega_{\max}}{\omega_{\min,1}^{(2)}} = 3.1 \,, \tag{2.266}$$

whereas we get for $n = 2$

$$\ln \frac{\omega_{\max}}{\omega_{\min,2}^{(1)}} = 11.9 \,, \qquad \ln \frac{\omega_{\max}}{\omega_{\min,2}^{(2)}} = 4.4 \,. \tag{2.267}$$

In both cases the estimates (2.266) and (2.267) differ by a factor of the order 3. With this the average displacement following from (2.262) turns out to be of the order of a few per cent of the Compton wave length:

$$\frac{\sqrt{\langle \mathbf{s}^2 \rangle_1}}{\lambda_{\mathrm{C}}} = \sqrt{\frac{\alpha}{2\pi^3} \ln \frac{\omega_{\max}}{\omega_{\min,1}}} = \begin{cases} 3.4\,\% \\ 1.9\,\% \end{cases} \,, \tag{2.268}$$

$$\frac{\sqrt{\langle \mathbf{s}^2 \rangle_2}}{\lambda_{\mathrm{C}}} = \sqrt{\frac{\alpha}{2\pi^3} \ln \frac{\omega_{\max}}{\omega_{\min,2}}} = \begin{cases} 3.7\,\% \\ 2.3\,\% \end{cases} \,. \tag{2.269}$$

Inserting the result (2.262) into the Lamb shift (2.241) and taking into account the atomic units from Appendix C we obtain

$$\Delta E_{\mathrm{L},n} = \frac{8}{3\pi n^3}\,\mathrm{Ry}\,\alpha^3\,\ln\frac{\omega_{\max}}{\omega_{\min,n}}\,, \tag{2.270}$$

which also depends on the choice of both cut-offs. Evaluating the Lamb shift (2.270) for $n = 1$ we find that $\Delta E_{\mathrm{L}}(1^2\mathrm{s}_{1/2})$ must be in the interval $[0.39, 1.3]\,\mathrm{GHz}$, which is, indeed fulfilled according to the measurement result (2.230). Furthermore, for $n = 2$ we factorize the Lamb shift (2.270) according to

$$\Delta E_{\mathrm{L},2} = \frac{1}{16}\,\mathrm{Ry}\,\alpha^2 \cdot F_2\,, \tag{2.271}$$

where the first factor denotes the $2^2\mathrm{s}_{1/2}$–$2^2\mathrm{p}_{3/2}$ fine structure splitting and the second factor yields

$$F_2 = \frac{16\alpha}{3\pi}\,\ln\frac{\omega_{\max}}{\omega_{\min,2}}\,, \tag{2.272}$$

which leads to the values

$$F_2^{(1)} = 0.15\,, \qquad F_2^{(2)} = 0.05 \tag{2.273}$$

for the two choices of the infrared cut-off. The experimental result $F_2 = 0.1$, which corresponds to (2.231), turns out to lie within the interval $[F_2^{(2)}, F_2^{(1)}] = [0.05, 0.15]$. In order to document the precision in the comparison of the full quantum electrodynamic theory and experiment we finally mention the following results for the Lamb shift of the hydrogen state $1^2\mathrm{s}_{1/2}$:

$$\text{experiment (1986)}: \qquad 1057845(9)\,\mathrm{kHz} \tag{2.274}$$

$$\text{QED theory (1984)}: \qquad 1057857(14)\,\mathrm{kHz} \tag{2.275}$$

Thus, quantum electrodynamics is extremely successful.

Chapter 3

Quantum States of Radiation Field

According to the previous chapter the quantized light field can be in different states. In the following we focus on a single mode of the electromagnetic field. This may be considered to be an oversimplification, but single-mode fields have become part of the experimental reality with the advent of high-quality optical cavities. These devices provide within the region between two well-reflecting mirrors an electromagnetic field, whose amplitude is much higher at some resonant frequencies. In this case the mode function is not a plane wave but a certain standing wave. In the transverse directions, one often has a Gaussian profile. Around a cavity resonance, it is an ubiquitous approximation to treat the full field as if it contained only a single mode. The inherent coupling to other modes can be modelled by taking into account a loss.

With these assumptions in mind the simplest quantum states of the single mode field are the so-called Fock states or number states, which correspond to the well-known stationary states of a harmonic oscillator. Another class are the coherent states, which are specific quantum states of the quantum harmonic oscillator, whose dynamics most closely resembles the oscillatory behavior of a classical harmonic oscillator. Furthermore, a squeezed state is a quantum state that is characterized by two non-commuting observables, where one of them has a standard deviation below and the other one above that of the ground state with the Heisenberg uncertainty being still valid. And, finally, being more general than the pure states mentioned so far, we also introduce a thermal state as an example for a mixed state. It appears in the realm of quantum statistics in the context of the Planck black-body radiation.

All these quantum states of a single radiation mode can be vividly represented in a pictorial way in phase space, which is spanned by two conjugate variables. Due to Heisenberg's uncertainty relation a quantum optical state can not be characterized by a single point in phase space. Therefore, we cannot attribute a probability to a point in phase space. Nevertheless, quasi-probability distributions exist and are useful in the quantum mechanical description of electromagnetic field states. Here we restrict ourselves in introducing as a particular example for such a quasi-probability distribution the Husimi function. To this end we determine the Husimi function for all the single mode quantum states introduced above.

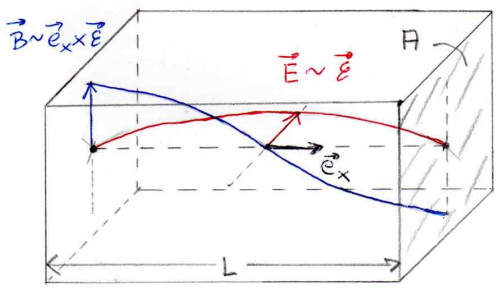

Figure 3.1: Ground-state transversal magnetic mode of a cavity: cavity axis, electric field (3.1), and magnetic induction (3.5) represent a legal system, with the magnetic induction lagging behind the electric field by a quarter period.

3.1 Single Cavity Mode

For the sake of simplicity we restrict ourselves in the following to one mode of the electromagnetic field. In vacuum this would mean that the electric field operator would just consist of one of the terms from (2.168), which is characterized by some wave vector $\mathbf{k}$ and some polarization λ. But in a cavity of length L the electric field operator is given instead in the Heisenberg picture by

$$\hat{\mathbf{E}}(\mathbf{x},t) = iE_0\,\boldsymbol{\epsilon}\left(\hat{a}\,e^{-i\omega t} - \hat{a}^\dagger\,e^{i\omega t}\right)\,\sin(k_x x)\,, \tag{3.1}$$

where x denotes the coordinate along the cavity axis and the transversal extension of the mode is assumed to be homogeneous in the yz-plane, see Fig. 3.1. Note that (3.1) follows both from the transversal electric mode (2.189) and the transversal magnetic mode (2.193) by identifying the normalization constants via

$$N_{\mathrm{TE}} = \frac{E_0}{\omega k_\perp}\,, \qquad N_{\mathrm{TM}} = \frac{E_0}{k_x k_\perp} \tag{3.2}$$

and by performing formally the limit $\mathbf{k}_\perp \to \mathbf{0}$. The resulting polarization vector $\boldsymbol{\epsilon}$ points perpendicular to the cavity axis, but in case of the transversal electric mode (2.189) it is given by

$$\boldsymbol{\epsilon} = \mathbf{e}_x \times \lim_{\mathbf{k}_\perp \to \mathbf{0}} \frac{\mathbf{k}_\perp}{k_\perp}\,, \tag{3.3}$$

whereas for the transversal magnetic mode (2.193) we yield

$$\boldsymbol{\epsilon} = \lim_{\mathbf{k}_\perp \to \mathbf{0}} \frac{\mathbf{k}_\perp}{k_\perp}\,. \tag{3.4}$$

In the same limiting procedure also the magnetic induction corresponding to (3.1) follows from the transversal electric mode (2.190) and the transversal magnetic mode (2.192), see Fig. 3.1:

$$\hat{\mathbf{B}}(\mathbf{x},t) = \frac{E_0}{c}\,\mathbf{e}_x \times \boldsymbol{\epsilon}\left(\hat{a}\,e^{-i\omega t} + \hat{a}^\dagger\,e^{i\omega t}\right)\,\cos(k_x x)\,. \tag{3.5}$$

In order to guarantee that the transversal component of (3.1) vanishes at the cavity mirrors positioned at $x = 0$ and $x = L$ as demanded by (2.188), the longitudinal component of the wave vector is fixed according to $k_x = m\pi/L$ with $m = 1, 2, 3, \ldots$. Furthermore, the linear dispersion (2.73) reduces here to $\omega = ck_x$. And the electric field amplitude E_0, which represents the electric field per photon in the cavity, corresponds to the prefactor in (2.168), where the term $2(2\pi)^3$ is substituted by the cavity volume $V = AL$, which is filled by the mode, see Fig. 3.1:

$$E_0 = \sqrt{\frac{\hbar\omega}{V\epsilon_0}}\,. \tag{3.6}$$

Indeed, with (3.1) and (3.5) the operators for the electric and magnetic field energy density in the cavity read

$$\frac{\epsilon_0}{2}\,\hat{\mathbf{E}}^2(\mathbf{x},t) = \frac{\epsilon_0}{2}\,E_0^2\sin^2(k_x x)\left(\hat{a}\hat{a}^\dagger + \hat{a}^\dagger\hat{a} - \hat{a}^2 e^{-2i\omega t} - \hat{a}^{\dagger\,2}e^{2i\omega t}\right)\,, \tag{3.7}$$

$$\frac{1}{2\mu_0}\,\hat{\mathbf{B}}^2(\mathbf{x},t) = \frac{E_0^2}{2\mu_0 c^2}\cos^2(k_x x)\left(\hat{a}\hat{a}^\dagger + \hat{a}^\dagger\hat{a} + \hat{a}^2 e^{-2i\omega t} + \hat{a}^{\dagger\,2}e^{2i\omega t}\right)\,, \tag{3.8}$$

so the Hamilton operator for the electromagnetic field

$$\hat{H} = A\int_0^L dx\,\left[\frac{\epsilon_0}{2}\,\hat{\mathbf{E}}^2(\mathbf{x},t) + \frac{1}{2\mu_0}\,\hat{\mathbf{B}}^2(\mathbf{x},t)\right] \tag{3.9}$$

is time-independent due to (2.5). Furthermore, taking into account (3.6), we get

$$\hat{H} = \frac{\hbar\omega}{2}\left(\hat{a}\hat{a}^\dagger + \hat{a}^\dagger\hat{a}\right)\,, \tag{3.10}$$

which corresponds to the Hamilton operator of a single harmonic oscillator. Here the operators $\hat{a}$ and $\hat{a}^\dagger$ fulfill the same algebra as the ladder operators of the harmonic oscillator discussed in Appendix A, i.e.

$$\left[\hat{a},\hat{a}\right]_- = \left[\hat{a}^\dagger,\hat{a}^\dagger\right]_- = 0\,, \qquad \left[\hat{a},\hat{a}^\dagger\right]_- = 1\,, \tag{3.11}$$

but here they describe the annihilation and the creation of a single photon. Applying (3.11) and using the photon number operator

$$\hat{n} = \hat{a}^\dagger\hat{a}\,, \tag{3.12}$$

the Hamilton operator (3.10) reduces to its standard form

$$\hat{H} = \hbar\omega\left(\hat{n} + \frac{1}{2}\right)\,. \tag{3.13}$$

The corresponding intensity per photon, i.e. the electromagnetic field energy passing through a certain area per unit time, follows then to be

$$I_0 = \frac{\hbar\omega c}{V}\,. \tag{3.14}$$

For a transverse mode size of $1\,\mu$m and a cavity length of 1 cm, we obtain for the ground mode $m = 1$ the intensity $I_0 = 0.3\,\mathrm{W/m^2}$. This is about a factor 10^{-4} smaller than the solar constant I_E =1.361 kW/m^2, which measures the mean solar electromagnetic radiation arriving on the surface of the earth.

3.2 Fock States of Single Mode

According to the second quantization of the electromagnetic field introduced in the previous chapter it is possible to define quantum states $|n\rangle$, where the quantum number $n = 0, 1, 2, \ldots$ represents the number of photons occupying that field mode. They are called Fock states, span an infinite-dimensional Hilbert space, and are defined by the eigenvalue problem of the photon number operator (3.12):

$$\hat{n}\,|n\rangle = n\,|n\rangle\ . \tag{3.15}$$

As the quantum states $|n\rangle$ have the properties

$$\hat{a}\,|n\rangle = \sqrt{n}\,|n-1\rangle\ , \tag{3.16}$$

$$\hat{a}^\dagger\,|n\rangle = \sqrt{n+1}\,|n+1\rangle\ , \tag{3.17}$$

they lead to the matrix elements

$$\langle n'|\,\hat{a}\,|n\rangle = \sqrt{n}\,\delta_{n',n-1}\,, \tag{3.18}$$

$$\langle n'|\,\hat{a}^\dagger\,|n\rangle = \sqrt{n+1}\,\delta_{n',n+1}\,, \tag{3.19}$$

which play an important role when one computes the probability amplitude that an atomic state absorbs or emits a photon. From all these relations it follows that the quantum states $|n\rangle$ can be obtained via

$$|n\rangle = \frac{\left(\hat{a}^\dagger\right)^n}{\sqrt{n!}}\,|0\rangle \tag{3.20}$$

with the vacuum state $|0\rangle$ obeying

$$\hat{a}\,|0\rangle = 0 \qquad \Longleftrightarrow \qquad \langle 0|\,\hat{a}^\dagger = 0\,. \tag{3.21}$$

Note that they fulfill both the orthonormality relation

$$\langle n|n'\rangle = \delta_{n,n'} \tag{3.22}$$

and the completeness relation

$$\sum_{n=0}^{\infty} |n\rangle\langle n| = 1\,. \tag{3.23}$$

Let us denote the expectation value with respect to such number states $|n\rangle$ according to

$$\langle \bullet \rangle_n = \langle n|\,\bullet\,|n\rangle\,. \tag{3.24}$$

Then the expectation value of the number operator (3.12) and its square with respect to the number states $|n\rangle$ turn out to be

$$\langle \hat{n} \rangle_n = \langle n|\,\hat{n}\,|n\rangle = n\,, \tag{3.25}$$

$$\langle \hat{n}^2 \rangle_n = \langle n|\,\hat{n}^2\,|n\rangle = n^2\,. \tag{3.26}$$

Thus, we conclude that the standard deviation vanishes:

$$\Delta n = \sqrt{\langle n^2 \rangle_n - \langle n \rangle_n^2} = 0 \,, \tag{3.27}$$

so the photon number is sharply defined. This is physically interesting insofar as the energy of the electromagnetic field is proportional to the photon number according to (3.13) and, thus, no energy fluctuations occur in these states. Concerning the electric field operator of a single cavity mode (3.1) we conclude that its expectation value with respect to any Fock state vanishes due to (3.21):

$$\langle \hat{\mathbf{E}}(\mathbf{x}, t) \rangle_n = \mathbf{0} \,. \tag{3.28}$$

But there are fluctuations around this average called ,,quantum noise", for which we get according to (3.7) and (3.21):

$$\langle \hat{\mathbf{E}}^2(\mathbf{x}, t) \rangle_n = E_0^2 (2n+1) \sin^2(k_x x) \,. \tag{3.29}$$

Thus, we conclude that the expectation values (3.28) and (3.29) differ considerably from what one would expect from a ,,classical" state, where the first moment of the electric field operator should be non-vanishing and its variance should be small or even zero. Therefore, in quantum optics, the number states $|n\rangle$ represent extremely ,,non-classical" states that are difficult to prepare experimentally [36].

3.3 Quadratures

In order to further characterize a quantum state of the electromagnetic field we introduce now a family of operators

$$\hat{x}_\theta = \frac{1}{\sqrt{2}} \left(\hat{a} e^{-i\theta} + \hat{a}^\dagger e^{i\theta} \right) \,, \tag{3.30}$$

which depend on a phase θ. They represent observables as they are hermitian:

$$\hat{x}_\theta^\dagger = \hat{x}_\theta \,. \tag{3.31}$$

Such operators (3.30) appear ubiquitously in quantum optics. For instance, we obtain from (3.1) and (3.5) that the dynamics of the electromagnetic field operators of a single cavity mode is characterized by

$$\hat{\mathbf{E}}(\mathbf{x}, t) = \sqrt{2} E_0 \, \boldsymbol{\epsilon} \, \hat{x}_{\omega t - \pi/2} \sin(k_x x) \sim \hat{x}_{\omega t - \pi/2} \,, \tag{3.32}$$

$$\hat{\mathbf{B}}(\mathbf{x}, t) = \frac{\sqrt{2} E_0}{c} \, \mathbf{e}_x \times \boldsymbol{\epsilon} \, \hat{x}_{\omega t} \cos(k_x x) \sim \hat{x}_{\omega t} \,. \tag{3.33}$$

We note that the latter proportionalities emphasize the photonic content of the amplitudes of the electric field and the magnetic induction (3.1) and (3.5), which is independent from

the respective polarization and the spatial profile. Furthermore, from (3.32), (3.33) we read off directly that the magnetic induction operator lags behind the electric field operator by a quarter period, see Fig. 3.1. Another application for the family of operators (3.30) occurs when we consider the position and the momentum operator of a harmonic oscillator of frequency ω in the Heisenberg picture. On the basis of Appendix A we obtain in dimensionless units $\hbar = 1 = M$:

$$\hat{x}(t) = \frac{1}{\sqrt{2}} \left(\hat{a} e^{-i\omega t} + \hat{a}^\dagger e^{i\omega t} \right) = \hat{x}_{\omega t} \,, \tag{3.34}$$

$$-\hat{p}(t) = \frac{1}{\sqrt{2}i} \left(\hat{a} e^{-i\omega t} - \hat{a}^\dagger e^{i\omega t} \right) = \hat{x}_{\omega t - \pi/2} \,. \tag{3.35}$$

Thus, a comparison of (3.32), (3.33) with (3.34), (3.35) yields the fundamental result

$$\hat{\mathbf{E}}(\mathbf{x}, t) \sim -\hat{p}(t) \,, \tag{3.36}$$

$$\hat{\mathbf{B}}(\mathbf{x}, t) \sim \hat{x}(t) \,, \tag{3.37}$$

i.e. the electric field (magnetic induction) operator corresponds to the negative momentum (position) operator of a harmonic oscillator. Note that (3.36) agrees formally with (2.26), (2.38). Later on the finding (3.36), (3.37) will be the key point for working out a phase space representation of the electromagnetic field, which is quite popular in quantum optics [14].

For the commutator of two family operators (3.30) with the phases θ and θ' we find

$$[\hat{x}_\theta, \hat{x}_{\theta'}]_- = \frac{1}{2} \left\{ e^{-i(\theta - \theta')} \left[\hat{a}, \hat{a}^\dagger \right]_- + e^{i(\theta - \theta')} \left[\hat{a}^\dagger, \hat{a} \right]_- \right\} = -i \sin(\theta - \theta') \,. \tag{3.38}$$

Thus, two family operators $\hat{x}_\theta$ and $\hat{x}_{\theta'}$ with the property $\theta - \theta' = -\pi/2$ are canonically conjugated:

$$\left[\hat{x}_\theta, \hat{x}_{\theta + \frac{\pi}{2}} \right]_- = i \,. \tag{3.39}$$

Such operators $\hat{x}_\theta$ and $\hat{x}_{\theta + \pi/2}$ are called quadratures. We read off from (3.36), (3.37) that position operator $\hat{x}(t) = \hat{x}_{\omega t}$ and momentum operator $\hat{p}(t) = \hat{x}_{\omega t + \pi/2}$ represent a prominent example for such quadratures.

Now we use the Heisenberg uncertainty, which is derived in Appendix D. To this end we apply (D.7) for two family operators $\hat{A} = \hat{x}_\theta$ and $\hat{B} = \hat{x}_{\theta'}$ by taking into account (3.38):

$$\langle \Delta \hat{x}_\theta^2 \rangle \, \langle \Delta \hat{x}_{\theta'}^2 \rangle \geq \frac{1}{4} \sin^2(\theta - \theta') \,. \tag{3.40}$$

Note that this result is independent of the state $|\psi\rangle$ with which we define the expectation value (D.1), thus it is generally valid. Furthermore, we remark that the largest possible uncertainty occurs for two quadratures with $\theta - \theta' = -\pi/2$, where (3.39) holds, which is valid, for instance, for position and momentum operator of a harmonic oscillator:

$$\langle \Delta \hat{x}_\theta^2 \rangle \, \langle \Delta \hat{x}_{\theta + \frac{\pi}{2}}^2 \rangle \geq \frac{1}{4} \,. \tag{3.41}$$

Now we specialize these expectation values for the Fock states of a mode defined in (3.24), i.e. we consider $|\psi\rangle = |n\rangle$. For the first moment we get

$$\langle \hat{x}_\theta \rangle_n = \frac{1}{\sqrt{2}} \, \langle n| \, \hat{a} e^{-i\theta} + \hat{a}^\dagger e^{i\theta} \, |n\rangle = 0 \,, \tag{3.42}$$

whereas the expectation value of the product of two family operators turns out to be

$$\langle \hat{x}_\theta \hat{x}_{\theta'} \rangle_n = \frac{1}{2} \left\{ e^{-i(\theta-\theta')} \, \langle n| \, \hat{a}\hat{a}^\dagger \, |n\rangle + e^{i(\theta-\theta')} \, \langle n| \, \hat{a}^\dagger \hat{a} \, |n\rangle \right\} = n \cos(\theta - \theta') + \frac{1}{2} \, e^{-i(\theta-\theta')} \,. \tag{3.43}$$

Thus, for the special case $\theta' = \theta$ Eq. (3.43) reduces to

$$\langle \hat{x}_\theta^2 \rangle_n = n + \frac{1}{2} \,, \tag{3.44}$$

so taking into account (3.42) we get the uncertainty

$$\langle \Delta \hat{x}_\theta^2 \rangle_n = n + \frac{1}{2} \,. \tag{3.45}$$

As the result (3.45) is independent of θ, it also holds for the uncertainties of both the position operator $\hat{x}(t) = \hat{x}_{\omega t}$ and the momentum operator $\hat{p}(t) = \hat{x}_{\omega t + \pi/2}$ of the harmonic oscillator. Thus, we conclude from (3.45)

$$\langle \Delta \hat{x}^2(t) \rangle_n \cdot \langle \Delta \hat{p}^2(t) \rangle_n = \left(n + \frac{1}{2} \right)^2 \,, \tag{3.46}$$

from which we read off the Heisenberg uncertainty relation (D.7) for position and momentum operator:

$$\langle \Delta \hat{x}^2(t) \rangle_n \cdot \langle \Delta \hat{p}^2(t) \rangle_n \geq \frac{1}{4} \,. \tag{3.47}$$

Note that the uncertainty becomes minimal for the vacuum fluctuations $n = 0$.

With these considerations we arrive at the following phase space representation for a Fock state with n photons. According to (3.25), (3.27) it is characterized by a fixed photon number, i.e. we have $\Delta n = 0$, and an arbitrary phase. Thus, a Fock state corresponds in phase space to a circle, which is centered around the origin due to (3.42) and has the radius $\sqrt{n + 1/2}$ due to (3.45), see Fig. 3.2.

3.4 Unitary Transformation

We now aim for introducing new photon states. To this end we consider a certain unitary transformation, which is characterized by

$$\hat{U}^\dagger \hat{U} = \hat{1} \qquad \Longleftrightarrow \qquad \hat{U}^\dagger = \hat{U}^{-1} \,, \tag{3.48}$$

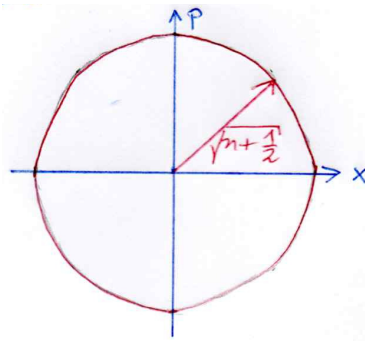

Figure 3.2: Representation of a Fock state $|n\rangle$ in phase space.

and apply it to a Fock state:

$$|n\rangle' = \hat{U}\,|n\rangle \qquad \Longleftrightarrow \qquad |n\rangle = \hat{U}^\dagger\,|n\rangle' \,. \tag{3.49}$$

We then define the unitary transformation for an operator $\hat{O}$ such that its expectation values remain unchanged

$$'\langle n|\hat{O}'|m\rangle' \;=\; \langle n|\,\hat{U}^\dagger\hat{O}'\hat{U}\,|m\rangle = \langle n|\,\hat{O}\,|m\rangle \;, \tag{3.50}$$

so we conclude

$$\hat{O} = \hat{U}^\dagger\hat{O}'\hat{U} \qquad \Longleftrightarrow \qquad \hat{O}' = \hat{U}\hat{O}\hat{U}^\dagger \,. \tag{3.51}$$

For instance, the transformation of the creation and annihilation operator reads

$$\hat{a}^{\dagger\prime} = \hat{U}\hat{a}^\dagger\hat{U}^\dagger \,, \qquad \hat{a}' = \hat{U}\hat{a}\hat{U}^\dagger \,. \tag{3.52}$$

With this we observe that the canonical commutator relations (3.11) remain unchanged:

$$[\hat{a}',\hat{a}']_- = \left[\hat{a}^{\dagger\prime},\hat{a}^{\dagger\prime}\right]_- = 0 \,, \qquad \left[\hat{a}',\hat{a}^{\dagger\prime}\right]_- = 1 \,. \tag{3.53}$$

Thus, also the transformed operators $\hat{a}^{\dagger\prime}, \hat{a}'$ represent creation and annihilation operators of the transformed Fock states as they fulfill analogous to (3.15)–(3.17)

$$\hat{n}'\,|n\rangle' \;=\; \sqrt{n}\,|n\rangle' \,, \tag{3.54}$$

$$\hat{a}^{\dagger\prime}\,|n\rangle' \;=\; \sqrt{n+1}\,|n+1\rangle' \,, \tag{3.55}$$

$$\hat{a}'\,|n\rangle' \;=\; \sqrt{n}\,|n-1\rangle' \,. \tag{3.56}$$

Here $\hat{n}' = \hat{a}^{\dagger\prime}\hat{a}'$ denotes the transformed particle number operator. Furthermore, also the transformed Fock states form a basis in the Hilbert space. For instance, the transformed ground state is defined according to

$$\hat{a}'\,|0\rangle' = 0 \qquad \langle 0|'\,\hat{a}^{\dagger\prime} = 0 \,. \tag{3.57}$$

Although the algebraic relations between the transformed states and operators are identical to the original ones, the properties of the transformed states $|n\rangle'$ can differ significantly from those of the original states $|n\rangle$. This depends, of course, on the particular choice of the unitary transformation $\hat{U}$. In the following we discuss in detail two prominent examples for such a unitary transformation in quantum optics, which lead to coherent and squeezed states, respectively.

3.5 Shifting Operator

Let us consider for some complex number $\alpha \in \mathbb{C}$ the transformation

$$\hat{D}(\alpha) = e^{\alpha\hat{a}^\dagger - \alpha^*\hat{a}}\,. \tag{3.58}$$

Then we conclude for its adjoint at first

$$\hat{D}^\dagger(\alpha) = e^{\alpha^*\hat{a} - \alpha\hat{a}^\dagger} = e^{-(\alpha\hat{a}^\dagger - \alpha^*\hat{a})} = \hat{D}(-\alpha)\,. \tag{3.59}$$

Due to the property

$$\hat{D}(\alpha)\hat{D}(-\alpha) = \hat{D}(0) = \hat{1} \tag{3.60}$$

we then have

$$\hat{D}^\dagger(\alpha) = D^{-1}(\alpha)\,, \tag{3.61}$$

so that the transformation (3.58) is, indeed, unitary.

Now we can reveal the properties of the transformed annihilation operator

$$\hat{a}'(\alpha) = \hat{D}(\alpha)\hat{a}\hat{D}^\dagger(\alpha)\,. \tag{3.62}$$

To this end we calculate the derivative

$$\begin{aligned}\frac{d\hat{a}'(\alpha t)}{dt} &= \hat{D}(\alpha t)\big\{\,\big(\alpha\hat{a}^\dagger - \alpha^*\hat{a}\big)\,\hat{a} - \hat{a}\,\big(\alpha\hat{a}^\dagger - \alpha^*\hat{a}\big)\,\big\}\hat{D}(-\alpha t)\\ &= \hat{D}(\alpha t)\,\big[\alpha\hat{a}^\dagger - \alpha^*\hat{a}, \hat{a}\big]_-\,\hat{D}(-\alpha t) = -\alpha\hat{D}(\alpha t)\hat{D}(-\alpha t) = -\alpha\,.\end{aligned} \tag{3.63}$$

Integrating (3.63) then yields

$$\hat{a}'(\alpha t) = \hat{c} - \alpha t \tag{3.64}$$

with the operator-valued integration constant $\hat{c}$. As we read off from (3.58) and (3.62) the initial condition $\hat{a}'(0) = \hat{a}$, we obtain from (3.64) $\hat{c} = \hat{a}$ and conclude

$$\hat{a}'(\alpha) = \hat{a} - \alpha\,. \tag{3.65}$$

This finding justifies to call (3.58) a ,,shifting operator". Let us denote the transformed vacuum state according to

$$|\alpha\rangle = |0\rangle' = \hat{D}(\alpha)\,|0\rangle\ , \tag{3.66}$$

which parametrically depends on α. Then it follows from (3.57) and (3.65):

$$\hat{a}'(\alpha)\,|\alpha\rangle = (\hat{a} - \alpha)\,|\alpha\rangle = 0 \qquad \Longrightarrow \qquad \hat{a}\,|\alpha\rangle = \alpha\,|\alpha\rangle\ . \tag{3.67}$$

Thus, the transformed vacuum state $|\alpha\rangle$ is an eigenstate of the annihilation operator. One calls it a coherent state or a Glauber state as the seminal pioneer of theoretical quantum optics and Nobel laureate Roy Glauber invented this new photon state in 1963.

3.6 Group Property

Let us consider the successive execution of two displacement operators:

$$\hat{D}(\alpha)\hat{D}(\beta) = e^{\alpha\hat{a}^\dagger - \alpha^*\hat{a}}\, e^{\beta\hat{a}^\dagger - \beta^*\hat{a}}\,. \tag{3.68}$$

In order to evaluate (3.68) we apply Baker-Campbell-Hausdorff formula [28, Appendix 2A]

$$e^{\hat{A}}\, e^{\hat{B}} = \exp\left\{\hat{A} + \hat{B} + \frac{1}{2}\left[\hat{A},\hat{B}\right]_- + \frac{1}{12}\left[\hat{A},\left[\hat{A},\hat{B}\right]_-\right]_- - \frac{1}{12}\left[\hat{B},\left[\hat{A},\hat{B}\right]_-\right]_- + \ldots\right\}\,. \tag{3.69}$$

To this end we identify the operators $\hat{A}$ and $\hat{B}$ via

$$\hat{A} = \alpha\hat{a}^\dagger - \alpha^*\hat{a}\,, \qquad \hat{B} = \beta\hat{a}^\dagger - \beta^*\hat{a}\,, \tag{3.70}$$

so their commutator turns out to be

$$\left[\hat{A},\hat{B}\right]_- = \alpha\beta^* - \alpha^*\beta = 2i\,\mathrm{Im}\,(\alpha\beta^*)\,. \tag{3.71}$$

From (3.68), (3.69), and (3.71) we then obtain

$$\hat{D}(\alpha)\hat{D}(\beta) = \hat{D}(\alpha+\beta)\, e^{i\,\mathrm{Im}\,(\alpha\beta^*)}\,. \tag{3.72}$$

This result is connected to group theory. In case that the phase factor vanishes, then the mapping $\alpha \to \hat{D}(\alpha)$ corresponds to a representation of the addition of complex numbers in the space of unitary transformations of the Hilbert space. In case that the phase factor does not vanish, then (3.72) defines a so-called projective representation.

3.7 Properties of Coherent States

Let us denote the expectation value with respect to a coherent state $|\alpha\rangle$ according to

$$\langle\bullet\rangle_\alpha = \langle\alpha|\,\bullet\,|\alpha\rangle\,. \tag{3.73}$$

Then we get the expectation value (3.73) for the family of operators (3.30) by taking into account (3.67):

$$\begin{aligned}\langle\hat{x}_\theta\rangle_\alpha &= \langle\alpha|\,\hat{x}_\theta\,|\alpha\rangle = \frac{1}{\sqrt{2}}\left\{\langle\alpha|\,\hat{a}\,|\alpha\rangle\, e^{-i\theta} + \langle\alpha|\,\hat{a}^\dagger\,|\alpha\rangle\, e^{i\theta}\right\} = \frac{1}{\sqrt{2}}\left\{\alpha e^{-i\theta} + \alpha^* e^{i\theta}\right\} \\ &= \sqrt{2}\,(\mathrm{Re}\,\alpha\,\cos\theta + \mathrm{Im}\,\alpha\,\sin\theta)\,. \end{aligned}\tag{3.74}$$

This can be physically interpreted in two ways. On the one hand, we yield that the averages of the electric field operator (3.32) and the magnetic induction operator (3.33) are non-zero

$$\langle\hat{\mathbf{E}}(\mathbf{x},t)\rangle_\alpha = 2E_0\,|\alpha|\,\boldsymbol{\epsilon}\,\sin(\omega t - \varphi)\sin(k_x x)\,, \tag{3.75}$$

$$\langle\hat{\mathbf{B}}(\mathbf{x},t)\rangle_\alpha = \frac{2E_0}{c}\,|\alpha|\,\mathbf{e}_x \times \boldsymbol{\epsilon}\,\cos(\omega t - \varphi)\cos(k_x x) \tag{3.76}$$

with the phase $\varphi = \arctan(\mathrm{Im}\,\alpha/\mathrm{Re}\,\alpha)$. In fact, (3.75) and (3.76) correspond to a classical standing wave in the cavity. Therefore, we conclude that coherent states are quite useful to represent laser fields. Furthermore, we read off from (3.75) and that (3.76) that the strength of the averaged electromagnetic field operators depend on both the electric field per photon E_0 from (3.6) and the absolute value of α. Computing the average photon number in a coherent state, we get due to (3.67)

$$\langle \hat{n} \rangle_\alpha = \langle \alpha | \hat{a}^\dagger \hat{a} | \alpha \rangle = \langle \hat{a}\alpha | \hat{a}\alpha \rangle = |\alpha|^2 \,. \tag{3.77}$$

Therefore, the average of the electric field operator (3.75) with respect to a coherent state turns out to be of the order $|\langle \mathbf{E}(\mathbf{x},t) \rangle_\alpha| \approx E_0 \sqrt{\langle \hat{n} \rangle_\alpha}$, i.e. it increases with the square root of the photon number $\langle \hat{n} \rangle_\alpha$.

On the other hand, we obtain for the expectation value of position and momentum operator (3.34) and (3.35) in the Heisenberg picture:

$$\begin{pmatrix} \langle \hat{x}(t) \rangle_\alpha \\ \langle \hat{p}(t) \rangle_\alpha \end{pmatrix} = \sqrt{2} \begin{pmatrix} \cos(\omega t) & \sin(\omega t) \\ -\sin(\omega t) & \cos(\omega t) \end{pmatrix} \begin{pmatrix} \mathrm{Re}\,\alpha \\ \mathrm{Im}\,\alpha \end{pmatrix} . \tag{3.78}$$

This means that real and imaginary part of the complex number α can be interpreted as the expectation value of the position and the momentum operator at time $t = 0$, respectively.

Correspondingly also the expectation value of two family operators $\hat{x}_\theta$ and $\hat{x}_{\theta'}$

$$\langle \hat{x}_\theta \hat{x}_{\theta'} \rangle_\alpha = \frac{1}{2} \langle \alpha | \, \hat{a}^2 e^{-i(\theta+\theta')} + \hat{a}^\dagger \hat{a} e^{-i(\theta'-\theta)} + \hat{a}\hat{a}^\dagger e^{-i(\theta-\theta')} + \hat{a}^{\dagger 2} e^{i(\theta+\theta')} \, | \alpha \rangle \tag{3.79}$$

is evaluated by using (3.67), yielding

$$\begin{aligned} \langle \hat{x}_\theta \hat{x}_{\theta'} \rangle_\alpha \;\; = \;\; & \frac{1}{2} e^{-i(\theta-\theta')} + 2 \left(\mathrm{Re}\,\alpha\right)^2 \cos\theta \cos\theta' + 2 \left(\mathrm{Im}\,\alpha\right)^2 \sin\theta \sin\theta' \\ & + 2\,\mathrm{Re}\,\alpha\,\mathrm{Im}\alpha \left(\sin\theta\cos\theta' + \cos\theta\sin\theta'\right) . \end{aligned} \tag{3.80}$$

Combining (3.74) and (3.80) we get

$$\langle \hat{x}_\theta \hat{x}_{\theta'} \rangle_\alpha = \frac{1}{2} e^{-i(\theta-\theta')} + \langle \hat{x}_\theta \rangle_\alpha \langle \hat{x}_{\theta'} \rangle_\alpha \,. \tag{3.81}$$

In the special case $\theta' = \theta$ Eq. (3.81) reduces to

$$\langle (\Delta \hat{x}_\theta)^2 \rangle_\alpha = \langle \hat{x}_\theta^2 \rangle_\alpha - \langle \hat{x}_\theta \rangle_\alpha^2 = \frac{1}{2} \,, \tag{3.82}$$

so the variance of a family operator (3.30) for coherent states does not depend on the angle θ.

We recall that the Heisenberg uncertainty relation (3.40) for two family operators $\hat{x}_\theta$ and $\hat{x}_{\theta'}$ holds for any expectation value and that the largest possible uncertainty occurs for two quadratures, which obey $\theta - \theta' = \pi/2$ according to (3.41). Thus, we conclude from (3.41) and (3.82) that coherent states have a minimal uncertainty irrespective of the choice of $\alpha \in \mathbb{C}$.

With this we finally arrive at a phase space representation for a coherent state $|\alpha\rangle$ as depicted in Fig. 3.3. From (3.78) we read off that the expectation values of position and momentum

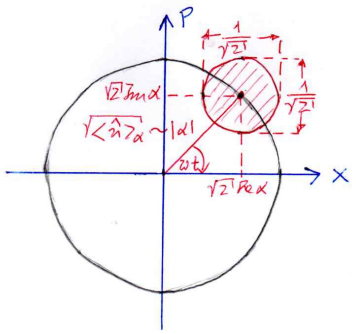

Figure 3.3: Representation of a coherent state $|\alpha\rangle$ in phase space.

operator rotate in phase space clockwise with frequency ω on a radius, whose size is determined by the photon number n via $|\alpha| = \sqrt{(\mathrm{Re}\,\alpha)^2 + (\mathrm{Im}\,\alpha)^2} = \sqrt{\langle\hat{n}\rangle_\alpha}$ according to (3.77). Furthermore, the coherent state has due to (3.82) at each time instant t both in position and momentum the minimal standard deviation $1/\sqrt{2}$.

3.8 Squeezing Operator

We have seen so far by several examples that the quantized electrodynamic field essentially differs from a classical field due to the unavoidable presence of quantum fluctuations. This raises the question whether it may be possible to reduce the quantum noise at least in one of the two field quadratures to realize a state that is even more classical. As one cannot beat the Heisenberg inequality, the reduced fluctuations in one quadrature have to be paid by an enhanced quantum noise in the other one.

In order to describe such a situation we consider in the following for some complex parameter $\xi \in \mathbb{C}$ the transformation

$$\hat{S}(\xi) = e^{\left(\xi^*\hat{a}^2 - \xi\hat{a}^{\dagger 2}\right)/2}\,. \tag{3.83}$$

In contrast to the shifting operator (3.58), where the argument of the exponential function contains the creation and annihilation operator linearly, the argument of the exponential function (3.83) depends quadratically on these operators. Analogous to the reasoning (3.59)–(3.61) we obtain that also the transformation (3.83) is unitary:

$$\hat{S}^\dagger(\xi) = \hat{S}(-\xi) = \hat{S}^{-1}(\xi)\,. \tag{3.84}$$

We are interested to determine the the properties of the transformed annihilation operator

$$\hat{a}'(\xi) = \hat{S}(\xi)\hat{a}\hat{S}^\dagger(\xi)\,. \tag{3.85}$$

Also here we proceed by calculating a derivative:

$$\begin{aligned}\frac{d\hat{a}'(\xi t)}{dt} &= \hat{S}(\xi t)\,\frac{1}{2}\left\{\left(\xi^*\hat{a}^2 - \xi\hat{a}^{\dagger 2}\right)\hat{a} - \hat{a}\left(\xi^*\hat{a}^2 - \xi\hat{a}^{\dagger 2}\right)\right\}\hat{S}(-\xi t) \qquad (3.86)\\ &= \hat{S}(\xi t)\,\frac{1}{2}\left[\left(\xi^*\hat{a}^2 - \xi\hat{a}^{\dagger 2}\right),\hat{a}\right]_-\hat{S}(-\xi t) = \hat{S}(\xi t)\,\frac{\xi}{2}\left[\hat{a},\hat{a}^{\dagger 2}\right]_-\hat{S}(-\xi t) = \xi\hat{S}(\xi t)\hat{a}^\dagger\hat{S}(-\xi t)\,.\end{aligned}$$

Thus, taking into account (3.85) we obtain from (3.86) the operator-valued ordinary differential equation

$$\frac{d\hat{a}'(\xi t)}{dt} = \xi \hat{a}^{\dagger\prime}(\xi t)\,. \tag{3.87}$$

In order to obtain a closed set of ordinary differential equations, also the transformed creation operator must be considered in a similar way. Performing the corresponding calculation leads to

$$\frac{d\hat{a}^{\dagger\prime}(\xi t)}{dt} = \xi^* \hat{a}'(\xi t)\,. \tag{3.88}$$

The coupled system (3.87) and (3.88) is now decoupled as follows:

$$\frac{d}{dt}\frac{d\hat{a}'(\xi t)}{dt} = \frac{d}{dt}\,\hat{a}^{\dagger\prime}(\xi t)\xi = |\xi|^2\,\hat{a}'(\xi t)\,. \tag{3.89}$$

The general solution of second-order differential equation (3.89) reads

$$\hat{a}'(\xi t) = \hat{c}_1\, e^{|\xi| t} + \hat{c}_2\, e^{-|\xi| t} \tag{3.90}$$

and depends on two operators $\hat{c}_1$ and $\hat{c}_2$. Inserting (3.90) in (3.87) leads to

$$\hat{a}^{\dagger\prime}(\xi t) = \frac{|\xi|}{\xi}\left(\hat{c}_1 e^{|\xi| t} - \hat{c}_2 e^{-|\xi| t}\right)\,. \tag{3.91}$$

With the help of (3.90) and (3.91) we now adjust the initial condition

$$\hat{a}'(\xi t)\Big|_{t=0} = \hat{c}_1 + \hat{c}_2 = \hat{a}\,, \tag{3.92}$$

$$\hat{a}^{\dagger\prime}(\xi t)\Big|_{t=0} = \frac{|\xi|}{\xi}\,(\hat{c}_1 - \hat{c}_2) = \hat{a}^\dagger\,. \tag{3.93}$$

In order to facilitate the analysis, we now perform a polar decomposition of the complex parameter ξ into its absolute value and its phase

$$\xi = |\xi|\, e^{i\varphi}\,. \tag{3.94}$$

With this the solution of (3.92) and (3.93) reads as follows:

$$\hat{c}_1 = \frac{1}{2}\left(\hat{a} + e^{i\varphi}\hat{a}^\dagger\right)\,, \tag{3.95}$$

$$\hat{c}_2 = \frac{1}{2}\left(\hat{a} - e^{i\varphi}\hat{a}^\dagger\right)\,. \tag{3.96}$$

Inserting (3.95) and (3.96) into (3.90) and (3.91), respectively, leads to:

$$\hat{a}'(\xi t) = \cosh(|\xi|\, t)\hat{a} + e^{i\varphi}\sinh(|\xi|\, t)\hat{a}^\dagger\,, \tag{3.97}$$

$$\hat{a}^{\dagger\prime}(\xi t) = \cosh(|\xi|\, t)\hat{a}^\dagger + e^{-i\varphi}\sinh(|\xi|\, t)\hat{a}\,. \tag{3.98}$$

Evaluating this result at $t = 1$ leads to the transformed creation and annihilation operator

$$\hat{a}'(\xi) = \mu\hat{a} + \nu\hat{a}^\dagger \,, \tag{3.99}$$

$$\hat{a}^{\dagger\prime}(\xi) = \mu\hat{a}^\dagger + \nu^*\hat{a} \,. \tag{3.100}$$

Here we have introduced the new parameters

$$\mu = \cosh|\xi| \,, \tag{3.101}$$

$$\nu = e^{i\varphi}\sinh|\xi| \,, \tag{3.102}$$

which fulfill the constraint

$$\mu^2 - |\nu|^2 = \cosh^2|\xi| - \sinh^2|\xi| = 1 \,. \tag{3.103}$$

Note that this constraint could be used, for instance, to eliminate the parameter μ. Furthermore, this constraint corresponds to the invariance of the standard commutator relation:

$$\left[\hat{a}'(\xi), \hat{a}^{\dagger\prime}(\xi)\right]_- = \mu^2\left[\hat{a}, \hat{a}^\dagger\right]_- + \nu\nu^*\left[\hat{a}^\dagger, \hat{a}\right]_- = \mu^2 - |\nu|^2 = 1 \,. \tag{3.104}$$

With these results we define now the squeezed states by applying the unitary transformation (3.83) upon the vacuum state:

$$|0\rangle' = \hat{S}(\xi)\,|0\rangle = |\xi\rangle \ . \tag{3.105}$$

Sometimes (3.105) is also called a squeezed vacuum.

3.9 Expectation Value of Squeezed States

At first we calculate the expectation value for the family of operators (3.30) with respect to a squeezed state:

$$\langle\hat{x}_\theta\rangle_\xi = \langle\xi|\,\hat{x}_\theta\,|\xi\rangle = \frac{1}{\sqrt{2}}\left\{\langle\xi|\,\hat{a}\,|\xi\rangle\, e^{-i\theta} + \langle\xi|\,\hat{a}^\dagger\,|\xi\rangle\, e^{i\theta}\right\} \ . \tag{3.106}$$

Here the adjoint state to (3.105) is defined by taking into account (3.84):

$${}'\langle 0| = \langle 0|\,\hat{S}^\dagger(\xi) = \langle\xi| = \langle 0|\,\hat{S}(-\xi) \,. \tag{3.107}$$

From (3.105)–(3.107) follows then

$$\langle\hat{x}_\theta\rangle_\xi = \frac{1}{\sqrt{2}}\,\langle 0|\,\hat{a}'(-\xi)e^{-i\theta} + \hat{a}^{\dagger\prime}(-\xi)e^{i\theta}\,|0\rangle \ . \tag{3.108}$$

A polar decomposition of $-\xi$ similar to (3.94)

$$-\xi = |\xi|\, e^{i(\varphi+\pi)} \tag{3.109}$$

then yields due to (3.101) and (3.102) the symmetry relations

$$\mu(-\xi) = \mu(\xi)\,, \tag{3.110}$$
$$\nu(-\xi) = -\nu(\xi)\,. \tag{3.111}$$

From (3.99), (3.100), (3.108), and (3.109) follows then

$$\langle\hat{x}_\theta\rangle_\xi = \frac{1}{\sqrt{2}}\langle 0|\left(\mu\hat{a} - \nu\hat{a}^\dagger\right)e^{-i\theta} + \left(\mu\hat{a}^\dagger - \nu^*\hat{a}\right)e^{i\theta}|0\rangle = 0\,. \tag{3.112}$$

The expectation value of the quadrature operator vanishes with respect to a squeezed state independent of θ. This means, in particular, that both the position and the momentum expectation values of squeezed states vanish also.

3.10 Variance of Squeezed States

For the expectation value of the product of two quadrature operators (3.30) we obtain with (3.105) and (3.107)

$$\langle\hat{x}_\theta\hat{x}_{\theta'}\rangle_\xi = \frac{1}{2}\langle 0|\,\hat{S}(-\xi)\left[\hat{a}^2e^{-i(\theta+\theta')} + \hat{a}^\dagger\hat{a}e^{i(\theta-\theta')} + \hat{a}\hat{a}^\dagger e^{i(\theta'-\theta)} + \hat{a}^{\dagger 2}e^{i(\theta+\theta')}\right]\hat{S}(\xi)\,|0\rangle\ . \tag{3.113}$$

Taking into account the action of the unitary transformation (3.83) according to (3.85), we get

$$\begin{aligned}\langle\hat{x}_\theta\hat{x}_{\theta'}\rangle_\xi &= \frac{1}{2}\langle 0|\,\hat{a}'(-\xi)^2e^{-i(\theta+\theta')} + \hat{a}^{\dagger\prime}(-\xi)\hat{a}'(-\xi)e^{i(\theta-\theta')}\\ &\quad +\hat{a}'(-\xi)\hat{a}^{\dagger\prime}(-\xi)e^{i(\theta'-\theta)} + \hat{a}^{\dagger\prime}(-\xi)^2e^{i(\theta+\theta')}\,|0\rangle\ .\end{aligned} \tag{3.114}$$

Thus, implementing (3.99) and (3.100) as well as the symmetry relations (3.110) and (3.111) yields

$$\langle\hat{x}_\theta\hat{x}_{\theta'}\rangle_\xi = \frac{1}{2}\langle 0|\,\hat{a}\hat{a}^\dagger[-\mu\nu e^{-i(\theta+\theta')} + |\nu|^2\,e^{i(\theta-\theta')} + \mu^2e^{-i(\theta-\theta')} - \mu\nu^*e^{i(\theta+\theta')}]\,|0\rangle\ . \tag{3.115}$$

With the side calculation

$$\langle 0|\,\hat{a}\hat{a}^\dagger\,|0\rangle = \langle 0|\left[\hat{a},\hat{a}^\dagger\right]_-|0\rangle = 1 \tag{3.116}$$

then follows for the variance (3.115)

$$\langle\hat{x}_\theta\hat{x}_{\theta'}\rangle_\xi = \frac{1}{2}\left[\mu^2e^{i(\theta'-\theta)} + |\nu|^2\,e^{i(\theta-\theta')} - \mu\nu e^{-i(\theta+\theta')} - \mu\nu^*e^{i(\theta+\theta')}\right]\,, \tag{3.117}$$

which factorizes according to

$$\langle\hat{x}_\theta\hat{x}_{\theta'}\rangle_\xi = \frac{1}{2}\left[\mu e^{-i\theta} - \nu^*e^{i\theta}\right]\left[\mu e^{i\theta'} - \nu e^{-i\theta'}\right]\,. \tag{3.118}$$

This result specialises for $\theta' = \theta$ to

$$\langle\hat{x}_\theta^2\rangle_\xi = \frac{1}{2}\left|\mu - \nu e^{-2i\theta}\right|^2\,. \tag{3.119}$$

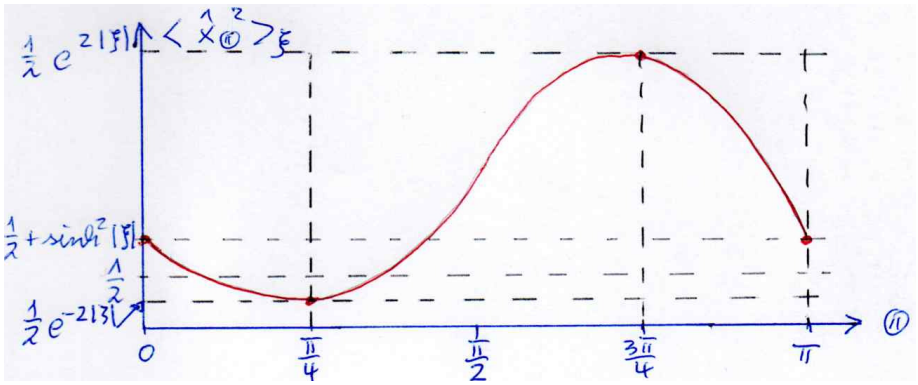

Figure 3.4: Angle dependence of expectation value (3.120) for $\varphi = \pi/2$ with minimum (maximum) at $\theta_{\min} = \pi/4$ ($\theta_{\max} = 3\pi/4$) according to (3.124) and (3.129) with $k = 0$.

Taking into account (3.101)–(3.103) this reduces to

$$\langle \hat{x}_\theta^2 \rangle_\xi = \frac{1}{2}\left[1 + 2\,|\nu|^2 - 2\,|\nu|\,\sqrt{1+|\nu|^2}\,\cos(2\theta - \varphi)\right]. \tag{3.120}$$

Thus, the expectation value $\langle \hat{x}_\theta^2 \rangle_\xi$, which coincides due to (3.112) with the variance $\langle (\Delta \hat{x}_\theta)^2 \rangle_\xi$ is π-periodic with respect to θ, see Fig. 3.4. For any fixed ξ the expectation value $\langle \hat{x}_\theta^2 \rangle_\xi$ depends sensitively on the chosen parameter θ. In the limit $\xi \to 0$, i.e. $|\nu| \downarrow 0$, this sensitivity disappears and we obtain the variance of the ground state

$$\lim_{\xi \to 0} \langle \hat{x}_\theta^2 \rangle_\xi = \frac{1}{2}\,. \tag{3.121}$$

Instead for $\xi \neq 0$ the variance can be larger or smaller than this minimal uncertainty.

A smaller uncertainty occurs provided that the inequality

$$\sqrt{\frac{1+|\nu|^2}{|\nu|^2}}\,\cos(2\theta - \varphi) > 1 \tag{3.122}$$

is fulfilled. The smallest possible uncertainty is present for

$$\cos(2\theta - \varphi) = 1\,, \tag{3.123}$$

which yields

$$\theta_{\min} = k\pi + \frac{\varphi}{2}\,, \qquad k \in \mathbb{Z}\,. \tag{3.124}$$

This minimal uncertainty follows from inserting (3.124) into (3.120)

$$\langle \hat{x}_{\theta_{\min}}^2 \rangle_\xi = \frac{1}{2}\left[1 + 2\,|\nu|^2 - 2\,|\nu|\,\sqrt{1+|\nu|^2}\,\right]. \tag{3.125}$$

Using (3.102) this finally reduces to

$$\langle \hat{x}_{\theta_{\min}}^2 \rangle_\xi = \frac{1}{2}\,e^{-2|\xi|}\,. \tag{3.126}$$

This means that the smallest possible uncertainty can be made exponentially small.

A larger uncertainty occurs for

$$\sqrt{\frac{1+|\nu|^2}{|\nu|^2}}\cos(2\theta-\varphi)<1\,. \tag{3.127}$$

The largest possible uncertainty is present provided

$$\cos(2\theta-\varphi)=-1\,, \tag{3.128}$$

which leads to

$$\theta_{\max}=\left(k+\frac{1}{2}\right)\pi+\frac{\varphi}{2}\,,\quad k\in\mathbb{Z}\,. \tag{3.129}$$

Inserting (3.129) into (3.120) this yields

$$\langle\hat{x}^2_{\theta_{\max}}\rangle_\xi=\frac{1}{2}\left[1+2\,|\nu|^2+2\,|\nu|\sqrt{1+|\nu|^2}\,\right]\,. \tag{3.130}$$

Taking into account (3.102) we conclude

$$\langle\hat{x}^2_{\theta_{\max}}\rangle_\xi=\frac{1}{2}\,e^{2|\xi|}\,. \tag{3.131}$$

Thus, the largest possible uncertainty can therefore be made exponentially large.

We note that the family operator with $\theta=\theta_{\max}$ in (3.129) and $\theta=\theta_{\min}$ in (3.124) are canonically conjugated to each other due to (3.38) and (3.39):

$$\theta_{\min}-\theta_{\max}=-\frac{\pi}{2}\,. \tag{3.132}$$

It now follows from (3.125) and (3.130) that squeezed states, like coherent states, have minimal uncertainty in accordance with the Heisenberg uncertainty principle (3.41):

$$\langle(\Delta\hat{x}_{\theta_{\max}})^2\rangle_\xi\;\langle(\Delta\hat{x}_{\theta_{\min}})^2\rangle_\xi=\frac{1}{4}\,. \tag{3.133}$$

The phase space representation for a squeezed state is more complicated as it basically amounts to an ellipse centered around the origin, whose semi-axes can be rotated. Before we can discuss this in more detail we have to define the density operator and work out its phase space representation in terms of a quasi-probability distribution.

3.11 Density Operator

In quantum mechanics, the state of a quantum system is represented by a state vector, denoted by $|\psi\rangle$. Provided that the state of a quantum system is only described by such a state vector $|\psi\rangle$, it is called a pure state. However, it is also possible for a quantum system to be in a

statistical ensemble of different state vectors. For example, there may be a 50 % probability that the state vector is $|\psi_1\rangle$ and a 50 % chance that the state vector is $|\psi_2\rangle$. This system would then be in a mixed state.

A generic example of pure and mixed states in quantum optics is provided by light polarization. Photons can have two helicities, corresponding to two orthogonal quantum states, $|R\rangle$ for right circular polarization and $|L\rangle$ for left circular polarization. A photon can also be in a superposition state, such as $(|R\rangle + |L\rangle)/\sqrt{2}$, which represents a vertical polarization or $|R\rangle - |L\rangle)/\sqrt{2}$, which denotes a horizontal polarization. More generally, it can be in any state $\alpha|R\rangle + \beta|L\rangle$ with the coefficients α and β fulfilling the normalization constraint $|\alpha|^2 + |\beta|^2 = 1$, corresponding to linear, circular, or elliptical polarization. If we pass $(|R\rangle + |L\rangle)/\sqrt{2}$ polarized light through a circular polarizer, which allows either only $|R\rangle$ polarized light, or only $|L\rangle$ polarized light, the intensity would be reduced by half in both cases. This may make it seem like half of the photons are in state $|R\rangle$ and the other half in state $|L\rangle$, but this is not correct: both $|R\rangle$ and $|L\rangle$ photons are partly absorbed by a vertical linear polarizer, but the $(|R\rangle + |L\rangle)/\sqrt{2}$ light will pass through that polarizer with no absorption whatsoever.

In quantum statistics, one describes a mixture of pure states with the help of the density operator $\hat{\rho}$, which was introduced by John von Neumann in 1927. In an axiomatic approach, the density operator is defined by the following axioms. The density operator $\hat{\rho}$ is a linear, hermitian operator according to axiom A1. Furthermore, axiom A2 prescribes that the density operator $\hat{\rho}$ is positive, i.e.

$$\langle\psi|\,\hat{\rho}\,|\psi\rangle \geq 0 \text{ for all } |\psi\rangle \qquad \Longleftrightarrow \qquad \text{all eigenvalues are positive}\,. \tag{3.134}$$

And, axiom A3 expresses the normalization of the density operator $\hat{\rho}$ via

$$\mathrm{Tr}\,(\hat{\rho}) = 1\,. \tag{3.135}$$

At first we conclude from axiom A1 that the density operator $\hat{\rho}$ obeys an eigenvalue problem

$$\hat{\rho}\,|\psi_i\rangle = p_i\,|\psi_i\rangle \tag{3.136}$$

with real eigenvalues

$$p_i = p_i^* \tag{3.137}$$

as well as the eigenstates $|\psi_i\rangle$ fulfill both the orthonormality

$$\langle\psi_i|\psi_j\rangle = \delta_{ij} \tag{3.138}$$

and the completeness

$$\sum_i |\psi_i\rangle\,\langle\psi_i| = 1\,. \tag{3.139}$$

Thus, the trace can be defined with the help of these eigenstates $|\psi_i\rangle$ as follows:

$$\mathrm{Tr}\,(\bullet) = \sum_i \langle\psi_i| \bullet |\psi_i\rangle \ . \tag{3.140}$$

And we read off that the density operator $\hat{\rho}$ has the representation

$$\hat{\rho} = \sum_i p_i \, |\psi_i\rangle \, \langle\psi_i| \ . \tag{3.141}$$

Furthermore, we deduce from axiom A2 and (3.134) that the eigenvalues p_i of the density operator are positive:

$$p_i = \langle\psi_i| \, \hat{\rho} \, |\psi_i\rangle \geq 0 \, . \tag{3.142}$$

And we conclude from axiom A3 due to (3.135), (3.140), and (3.141) that the sum over the eigenvalues yields unity:

$$\sum_i p_i = 1 \, . \tag{3.143}$$

In combination with (3.142) we then obtain the inequality

$$0 \leq p_i \leq 1 \, . \tag{3.144}$$

Thus, from (3.139) and (3.141) we get for the diagonal matrix elements of the density matrix

$$\langle\psi| \, \hat{\rho} \, |\psi\rangle = \sum_i p_i \, \langle\psi|\psi_i\rangle \, \langle\psi_i|\psi\rangle \leq \sum_i \langle\psi|\psi_i\rangle \, \langle\psi_i|\psi\rangle = \langle\psi|\psi\rangle = 1 \, . \tag{3.145}$$

This finding means that the diagonal matrix elements of the density operator can be interpreted as probabilities. An important application is to calculate the expectation value of an observable for a mixed state, which is defined by

$$\langle\hat{A}\rangle = \mathrm{Tr}\,(\hat{A}\hat{\rho}) \, . \tag{3.146}$$

Due to the orthonormality (3.138), the definition of the trace in (3.140), and the representation (3.141) this leads to

$$\langle\hat{A}\rangle = \sum_i \langle\psi_i| \, \hat{A}\hat{\rho} \, |\psi_i\rangle = \sum_i p_i \, \langle\psi_i| \, \hat{A} \, |\psi_i\rangle \ . \tag{3.147}$$

This means that the quantum mechanical expectation value $\langle\psi_i| \, \hat{A} \, |\psi_i\rangle$ in state i is weighted with the probability p_i in the mixture.

We now continue the axiomatic reasoning in view of the density operator $\hat{\rho}$ and specify when it is a pure state. A density operator $\hat{\rho}$ is pure provided that the idempotence property

$$\hat{\rho}^2 = \hat{\rho} \tag{3.148}$$

holds, i.e. provided that $\hat{\rho}$ represents a projector. Let us illustrate this definition by two examples. The first one deals with the density matrix

$$\hat{\rho} = |n\rangle \langle n| \tag{3.149}$$

corresponding to a pure Fock state. Due to the orthonormality (3.22) we conclude here that (3.148), indeed, holds:

$$\hat{\rho}^2 = |n\rangle \langle n|n\rangle \langle n| = |n\rangle \langle n| = \hat{\rho}\,. \tag{3.150}$$

In the second example we consider the density operator

$$\hat{\rho} = |\psi\rangle \langle \psi|\,, \qquad |\psi\rangle = \frac{1}{\sqrt{2}} \left(|0\rangle + |1\rangle\right) \tag{3.151}$$

and find that it also represents a pure state:

$$\hat{\rho}^2 = |\psi\rangle \langle \psi|\psi\rangle \langle \psi| = |\psi\rangle \langle \psi| = \hat{\rho}\,. \tag{3.152}$$

But note in this case

$$\hat{\rho}^2 = \frac{1}{2} \left(|0\rangle + |1\rangle\right) \left(\langle 0| + \langle 1|\right) \neq \frac{1}{2} \left(|0\rangle \langle 0| + |1\rangle \langle 1|\right)\,. \tag{3.153}$$

The notion of purity P for a density operator $\hat{\rho}$ can now be quantified as follows:

$$P(\hat{\rho}) = \mathrm{Tr}\left(\hat{\rho}^2\right). \tag{3.154}$$

In the eigenbasis of the density operator $\hat{\rho}$ we then obtain from the representation (3.141) by taking into account the orthonormality (3.138)

$$\hat{\rho}^2 = \sum_i \sum_j p_i p_j \, |\psi_i\rangle \langle \psi_i|\psi_j\rangle \langle \psi_j| = \sum_i p_i^2 \, |\psi_i\rangle \langle \psi_i|\,. \tag{3.155}$$

Thus, the purity (3.155) results to

$$P(\hat{\rho}) = \sum_i p_i^2 \tag{3.156}$$

and due to the inequality (3.144) and the normalization condition (3.143) we conclude

$$0 \leq P(\hat{\rho}) \leq 1\,. \tag{3.157}$$

Let us finalize the discussion of the purity by the following interpretation. From the normalization of the density operator (3.135) and the definition of the purity (3.154) we get

$$P(\hat{\rho}) = \mathrm{Tr}\left(\hat{\rho}^2 + 1 - \hat{\rho}\right) = 1 + \mathrm{Tr}\left(\hat{\rho}^2 - \hat{\rho}\right), \tag{3.158}$$

which implies

$$\hat{\rho}^2 = \hat{\rho} \qquad \Longleftrightarrow \qquad P(\hat{\rho}) = 1\,. \tag{3.159}$$

Indeed, from (3.148) and (3.158) follows (3.159) from left to right. Let us now, conversely, assume that the right-hand side of (3.159) holds. Due to (3.144) and (3.156) we must have exactly one j with $p_i = \delta_{ij}$, which yields (3.148) due to (3.141).

3.12 Husimi Function of Coherent State

There exist different quasi-probability distributions, which are commonly used in quantum mechanics to represent a quantum state such as light in the phase space formulation of quantum optics. The first one was introduced by Eugene Wigner in 1932 to study quantum corrections to classical statistical mechanics [37]. The goal was to link the wave function that appears in Schrödinger's equation to a quasi-probability distribution in phase space. Expectation values turn out to be accessible for observables in the Weyl order, where the corresponding operators are ordered in a totally symmetric way. An equivalent formulation was worked out by George Sudarshan and Roy Glauber in 1963, where the so-called Sudarshan-Glauber P-representation expresses observables in normal order and which is further elaborated in the exercises. In the present lecture notes, however, we will focus on the Husimi function, introduced by Kôdi Husimi in 1940. It represents a quasi-probability distribution, also called the Q-function, which allows to calculate expectation values for observables in the anti-normal order as we will see below. It is defined as the expectation value of the density operator $\hat{\rho}$ with respect to a coherent state as follows:

$$Q_{\hat{\rho}}(\alpha) = \frac{1}{\pi} \langle \alpha | \, \hat{\rho} \, | \alpha \rangle \ . \tag{3.160}$$

This phase space function indicates the probability that the coherent state $|\alpha\rangle$ is to be found in the density matrix $\hat{\rho}$. Note that the reason for the additional prefactor $1/\pi$ in the definition (3.160) is only revealed below.

In order to get a first insight into the Husimi function, we evaluate it for the case of a pure coherent state, i.e. the density operator $\hat{\rho}$ is assumed to be given by

$$\hat{\rho} = |\alpha_0\rangle \langle \alpha_0| \ . \tag{3.161}$$

Inserting (3.161) in (3.160) leads to

$$Q_{|\alpha_0\rangle\langle\alpha_0|}(\alpha) = \frac{1}{\pi} \, |\langle \alpha | \alpha_0 \rangle|^2 \ . \tag{3.162}$$

Thus, the evaluation of (3.162) necessitates to determine the overlap of two coherent states, which we accomplish with the following three steps:

- A useful special case of the Baker-Campbell-Hausdorff formula (3.69) reads

$$e^{\hat{A}+\hat{B}} = e^{\hat{A}} e^{\hat{B}} e^{-\left[\hat{A},\hat{B}\right]_-/2}, \qquad \text{if } \left[\hat{A},\hat{B}\right]_- \in \mathbb{C} \, . \tag{3.163}$$

  With the identifications

$$\hat{A} = \alpha \hat{a}^\dagger \, , \qquad \hat{B} = -\alpha^* \hat{a} \, , \qquad \left[\hat{A},\hat{B}\right]_- = |\alpha|^2 \left[\hat{a},\hat{a}^\dagger\right]_- = |\alpha|^2 \tag{3.164}$$

  we then obtain with (3.163) for the shift operator (3.58) its normal ordered form:

$$\hat{D}(\alpha) = e^{\alpha \hat{a}^\dagger} e^{-\alpha^* \hat{a}} \, e^{-|\alpha|^2/2} \, . \tag{3.165}$$

- Applying (3.165) to the vacuum state yields for a coherent state (3.66) the representation

$$|\alpha\rangle = \hat{D}(\alpha)\,|0\rangle = e^{-|\alpha|^2/2}\,e^{\alpha\hat{a}^\dagger}\,|0\rangle\ . \tag{3.166}$$

Note that we have used here the identity

$$e^{-\alpha^*\hat{a}}\,|0\rangle = |0\rangle\ , \tag{3.167}$$

which follows immediately from the property (3.21) that the annihilation operator $\hat{a}$ being applied to the vacuum state $|0\rangle$ vanishes. The adjoint of (3.166) results correspondingly in

$$\langle\alpha| = e^{-|\alpha|^2/2}\,\langle 0|\,e^{\alpha^*\hat{a}}\,. \tag{3.168}$$

With (3.166) and (3.168) we then get for the scalar product between two coherent states:

$$\langle\alpha|\alpha_0\rangle = e^{-\left(|\alpha|^2+|\alpha_0|^2\right)/2}\,\langle 0|\,e^{\alpha^*\hat{a}}\,e^{\alpha_0\hat{a}^\dagger}e^{-\alpha^*\hat{a}}\,|0\rangle\ , \tag{3.169}$$

where we have applied again (3.167).

- Performing a Taylor expansion we obtain

$$e^{\alpha^*\hat{a}}\left(e^{\alpha_0\hat{a}^\dagger}\right)e^{-\alpha^*\hat{a}} = \exp\left\{\alpha_0\,e^{\alpha^*\hat{a}}\,\hat{a}^\dagger\,e^{-\alpha^*\hat{a}}\right\}. \tag{3.170}$$

In order to evaluate this expression we define the operator-valued function

$$\hat{f}(t) = e^{t\alpha^*\hat{a}}\hat{a}^\dagger e^{-t\alpha^*\hat{a}} \tag{3.171}$$

and determine its derivative with respect to the parameter t:

$$\frac{d\hat{f}(t)}{dt} = e^{t\alpha^*\hat{a}}\alpha^*\left(\hat{a}\hat{a}^\dagger - \hat{a}^\dagger\hat{a}\right)e^{-t\alpha^*\hat{a}} = \alpha^*\,, \tag{3.172}$$

where the latter equality follows from the commutator relation (3.11). As (3.172) is a c-number, its integration can be straight-forwardly performed, yielding

$$\hat{f}(t) = \hat{c} + \alpha^* t\,. \tag{3.173}$$

As we read off from (3.171) the operator-valued initial condition $\hat{f}(0) = \hat{c} = \hat{a}^\dagger$ it follows from (3.171) and (3.173):

$$\hat{f}(1) = e^{\alpha^*\hat{a}}\hat{a}^\dagger e^{-\alpha^*\hat{a}} = \hat{a}^\dagger + \alpha^*\,. \tag{3.174}$$

Inserting (3.174) in (3.170) we get

$$e^{\alpha^*\hat{a}}\,e^{\alpha_0\hat{a}^\dagger}e^{-\alpha^*\hat{a}} = e^{\left(\hat{a}^\dagger+\alpha^*\right)\alpha_0}\,. \tag{3.175}$$

Substituting (3.175) into (3.169) finally leads to the scalar product between two coherent states:

$$\langle\alpha|\alpha_0\rangle = e^{-\left(|\alpha|^2+|\alpha_0|^2\right)/2}\, e^{\alpha^*\alpha_0}\,, \tag{3.176}$$

as the adjoint of (3.167) yields

$$\langle 0|\, e^{\alpha^*\hat{a}^\dagger} = \langle 0|\ . \tag{3.177}$$

This can algebraically be rewritten as

$$\langle\alpha|\alpha_0\rangle = e^{-\left(|\alpha|^2+|\alpha_0|^2-\alpha_0\alpha^*-\alpha_0^*\alpha\right)/2}\, e^{(\alpha^*\alpha_0-\alpha_0^*\alpha)/2} = e^{-|\alpha-\alpha_0|^2/2}\, e^{(\alpha^*\alpha_0-\alpha_0^*\alpha)/2}\,. \tag{3.178}$$

We read off that the coherent states are normalized in the sense of

$$\langle\alpha_0|\alpha_0\rangle = 1\,, \tag{3.179}$$

but not orthogonal

$$\langle\alpha|\alpha_0\rangle \neq 0\,, \qquad \text{for } \alpha \neq \alpha_0\,. \tag{3.180}$$

Note that this non-orthogonality is an immediate consequence of the fact that they are eigenstates of a non-hermitian operator according to (3.67). Thus, coherent states have mathematical features that are very different from those of a number state, for instance, two different coherent states are not orthonormal according to

$$\langle\alpha|\alpha_0\rangle \neq \delta(\alpha-\alpha_0)\,. \tag{3.181}$$

Substituting (3.178) into (3.162) shows that the Q-function of a coherent state turns out to be an isotropic Gaussian function:

$$Q_{|\alpha_0\rangle\langle\alpha_0|}(\alpha) = \frac{1}{\pi}\, e^{-|\alpha-\alpha_0|^2}\,. \tag{3.182}$$

Thus, depicting the lines of constant values of the Q-function (3.182) in the phase space spanned by both the real and imaginary part of α yields circles centered around α_0 as depicted in Fig. 3.5, which corresponds to the phase space representation of a coherent state in Fig. 3.3. Furthermore, we can explicitly show the normalization

$$\int d^2\alpha\, Q_{|\alpha_0\rangle\langle\alpha_0|}(\alpha) = 1\,, \tag{3.183}$$

where the two-dimensional integral is defined according to

$$\int d^2\alpha = \int_{-\infty}^{\infty} d\mathrm{Re}\,\alpha \int_{-\infty}^{\infty} d\mathrm{Im}\,\alpha\,. \tag{3.184}$$

Note that the prefactor $1/\pi$ in (3.182) is important in order to guarantee the normalization (3.183).

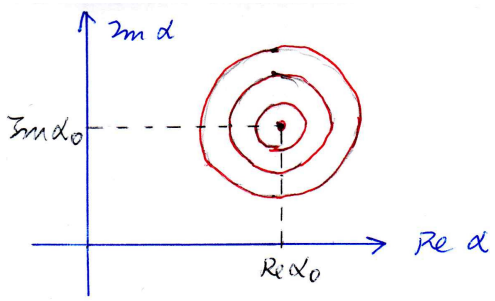

Figure 3.5: Phase space density (3.182) of the Q-function for a coherent state.

Furthermore, inserting (3.160) and (3.161) in the normalization (3.182) leads to

$$\langle\alpha_0|\left\{\int\frac{d^2\alpha}{\pi}\,|\alpha\rangle\langle\alpha|\right\}|\alpha_0\rangle = 1\,, \tag{3.185}$$

which suggests the identity

$$\int\frac{d^2\alpha}{\pi}\,|\alpha\rangle\langle\alpha| = 1\,. \tag{3.186}$$

This turns out to be, indeed, valid as is proven below and represents the overcompleteness of the coherent states.

3.13 Decomposition of Coherent State into Fock States

As the number states $|n\rangle$ represent a basis according to (3.23), a coherent state $|\alpha\rangle$ can be expanded with respect to it:

$$|\alpha\rangle = \sum_{n=0}^{\infty}|n\rangle\,\langle n|\alpha\rangle\ . \tag{3.187}$$

Due to (3.20) the matrix element in (3.187) is given by

$$\langle n|\alpha\rangle = \frac{1}{\sqrt{n!}}\,\langle 0|\,\hat{a}^n\,|\alpha\rangle\ . \tag{3.188}$$

Applying (3.58) and (3.67) in (3.188) leads to

$$\langle n|\alpha\rangle = \frac{\alpha^n}{\sqrt{n!}}\,\langle 0|\alpha\rangle = \frac{\alpha^n}{\sqrt{n!}}\,\langle 0|\,\hat{D}(\alpha)\,|0\rangle\ . \tag{3.189}$$

Substituting the normal ordered shifting operator (3.165) into (3.189) and taking into account the identities (3.167) and (3.177) then yields

$$\langle n|\alpha\rangle = \frac{\alpha^n}{\sqrt{n!}}\,e^{-|\alpha|^2/2}\,, \tag{3.190}$$

from which we can draw two insightful conclusions.

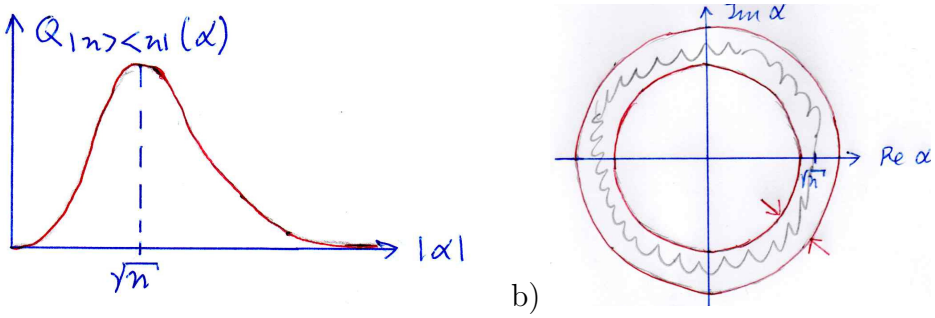

a) b)

Figure 3.6: Husimi function for a pure Fock state (3.191): a) Maximum occurs at $|\alpha_{\max}| = \sqrt{n}$; b) Contour plot in complex α-plane reveals a volcano shape.

On the one hand we read off from (3.190) the Husimi function (3.160) for a pure Fock state

$$Q_{|n\rangle\langle n|}(\alpha) = \frac{1}{\pi}\,|\langle n|\alpha\rangle|^2 = \frac{1}{\pi}\,\frac{|\alpha|^{2n}}{n!}\,e^{-|\alpha|^2}\,, \tag{3.191}$$

which turns out to be normalized. Indeed, due to the isotropy of (3.191) in phase space, we express the integration measure by polar coordinates

$$\alpha = \mathrm{Re}\,\alpha + i\mathrm{Im}\,\alpha = re^{i\varphi} \tag{3.192}$$

$$d^2\alpha = d\mathrm{Re}\,\alpha\, d\mathrm{Im}\,\alpha = rdrd\varphi\,, \tag{3.193}$$

so the normalization integral of (3.191) yields at first

$$\int d^2\alpha\, Q_{|n\rangle\langle n|}(\alpha) = \frac{2}{n!}\int_0^\infty dr\, r^{2n+1}\, e^{-r^2}\,. \tag{3.194}$$

Subsequently, the radial integral reduces due to the substitution $u(r) = r^2$ to the Gamma function (2.176), which interpolates for integers according to (2.178) between the factorials, thus we get

$$\int d^2\alpha\, Q_{|n\rangle\langle n|}(\alpha) = 1\,. \tag{3.195}$$

Furthermore, extremizing the Husimi function for a pure Fock state (3.191)

$$\left.\frac{\partial Q_{|n\rangle\langle n|}(\alpha)}{\partial|\alpha|}\right|_{\alpha=\alpha_0} = 0\,, \tag{3.196}$$

we obtain that the maximum occurs for $|\alpha_{\max}| = \sqrt{n}$, see Fig. 3.6a). As a consequence, the Husimi function (3.191) has in phase space a shape, which is reminiscent of a volcano as indicated in Fig. 3.6b).

On the other hand (3.190) implies that the probability of a coherent state $|\alpha\rangle$ having n photons is determined by a Poisson statistics:

$$p_n(\alpha) = \frac{|\alpha|^{2n}}{n!}\,e^{-|\alpha|^2}\,. \tag{3.197}$$

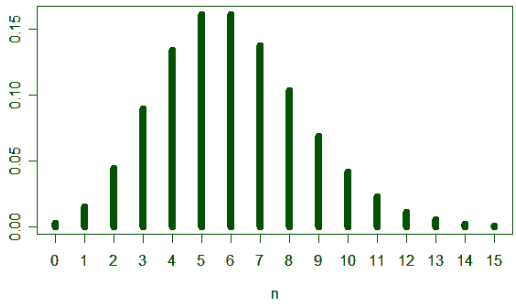

Figure 3.7: Poisson statistics (3.202) for finding n photons in a coherent state with having on average $\langle\hat{n}\rangle_\alpha = 6$ photons.

The normalisation of the Poisson statistics (3.197) follows straight-forwardly:

$$\sum_{n=0}^{\infty} p_n(\alpha) = e^{-|\alpha|^2} \sum_{n=0}^{\infty} \frac{\left(|\alpha|^2\right)^n}{n!} = e^{-|\alpha|^2} e^{|\alpha|^2} = 1\,. \tag{3.198}$$

For the average photon number we obtain in accordance with (3.77):

$$\begin{aligned} \langle\hat{n}\rangle_\alpha &= \sum_{n=0}^{\infty} n p_n(\alpha) = e^{-|\alpha|^2} \sum_{n=0}^{\infty} \frac{1}{n!}\, n \left(|\alpha|^2\right)^n = e^{-|\alpha|^2} \sum_{n=0}^{\infty} \frac{1}{(n)!}\, |\alpha|^2 \frac{\partial}{\partial|\alpha|^2} \left(|\alpha|^2\right)^n \\ &= e^{-|\alpha|^2}\, |\alpha|^2 \frac{\partial}{\partial|\alpha|^2} \sum_{n=0}^{\infty} \frac{1}{(n)!} \left(|\alpha|^2\right)^n = e^{-|\alpha|^2}\, |\alpha|^2 \frac{\partial}{\partial|\alpha|^2}\, e^{|\alpha|^2} = |\alpha|^2\,. \end{aligned} \tag{3.199}$$

Thus, the mean photon number $\langle\hat{n}\rangle_\alpha$ in a coherent state is determined by $|\alpha|^2$. Correspondingly we also calculate the second moment:

$$\begin{aligned} \langle\hat{n}^2\rangle_\alpha &= \sum_{n=0}^{\infty} n^2 p_n(\alpha) = e^{-|\alpha|^2} |\alpha|^2 \frac{\partial}{\partial|\alpha|^2}\, |\alpha|^2 \frac{\partial}{\partial|\alpha|^2}\, e^{|\alpha|^2} \\ &= e^{-|\alpha|^2} |\alpha|^2 \frac{\partial}{\partial|\alpha|^2} \left(|\alpha|^2 e^{|\alpha|^2}\right) = |\alpha|^2 + |\alpha|^4\,. \end{aligned} \tag{3.200}$$

We read off that variance and mean photon number turn out to coincide:

$$\langle(\Delta\hat{n})^2\rangle_\alpha = \langle\hat{n}^2\rangle_\alpha - \langle\hat{n}\rangle_\alpha^2 = |\alpha|^2\,. \tag{3.201}$$

This represents the characteristic property of a Poisson statistics. Inserting the finding (3.199) into the Poisson statistics (3.197), the photon number distribution can also be written in the form

$$p_n(\langle\hat{n}\rangle_\alpha) = \frac{\left(\langle\hat{n}\rangle_\alpha\right)^n}{n!}\, e^{-\langle\hat{n}\rangle_\alpha}\,, \tag{3.202}$$

which is depicted in Fig. 3.7. The Mandel Q-parameter was introduced in quantum optics by Leonard Mandel in 1979. It measures the departure of the occupation number distribution from Poissonian statistics:

$$Q = \frac{\langle(\Delta\hat{n})^2\rangle - \langle\hat{n}\rangle}{\langle\hat{n}\rangle} = \frac{\langle\hat{n}^2\rangle - \langle\hat{n}\rangle^2}{\langle\hat{n}\rangle} - 1\,. \tag{3.203}$$

Thus, for coherent states, which have a Poissonian photon-number statistics (3.197), we immediately obtain $Q = 0$. A positive value of Q occurs for a super-Poissonian photon statistics, where the variance is larger than the mean, i.e. the distribution is broader than a Poissonian:

$$Q \geq 0 \qquad \Longleftrightarrow \qquad \langle (\Delta\hat{n})^2 \rangle \geq \langle \hat{n} \rangle \; . \tag{3.204}$$

In contrast to that a negative value of Q corresponds to a state, whose variance of the photon number is less than the mean:

$$-1 \leq Q \leq 0 \qquad \Longleftrightarrow \qquad \langle (\Delta\hat{n})^2 \rangle \leq \langle \hat{n} \rangle \; . \tag{3.205}$$

The Mandel Q-parameter is a convenient way to characterize non-classical states with negative values (3.205) indicating a sub-Poissonian statistics, which have no classical analog. Their photon statistics is characterized by being narrower than a Poissonian.

From the above we now deduce that the coherent states are overcomplete along the following lines. Taking into account the completeness of the Fock states from (3.23) and the overlap (3.190) we obtain

$$\begin{aligned} \int d^2\alpha \, |\alpha\rangle \langle\alpha| &= \sum_{n=0}^{\infty} \sum_{m=0}^{\infty} |n\rangle \langle m| \int d^2\alpha \, \langle n|\alpha\rangle \langle\alpha|m\rangle \; . \\ &= \sum_{n=0}^{\infty} \sum_{m=0}^{\infty} |n\rangle \langle m| \int d^2\alpha \, \frac{\alpha^n}{\sqrt{n!}} \, e^{-|\alpha|^2/2} \, \frac{\alpha^{*m}}{\sqrt{m!}} \, e^{-|\alpha|^2/2} \, . \end{aligned} \tag{3.206}$$

Using the polar coordinate coordinates in phase space (3.192) and (3.193), the integral (3.206) yields

$$\int d^2\alpha \, |\alpha\rangle \langle\alpha| = \sum_{n=0}^{\infty} \sum_{m=0}^{\infty} \frac{|n\rangle \langle m|}{\sqrt{n!m!}} \int_0^{\infty} dr \, r^{n+m+1} \, e^{-r^2} \int_0^{2\pi} d\varphi \, e^{i(n-m)\varphi} \, . \tag{3.207}$$

The angle integral leads to the Kronecker symbol

$$\int_0^{2\pi} d\varphi \, e^{i(n-m)\varphi} = 2\pi \, \delta_{n,m} \tag{3.208}$$

and the radial integral reduces due to the substitution $u(r) = r^2$ to the Gamma function (2.176), which interpolates for integers according to (2.178) between the factorials, thus yielding

$$\int_0^{\infty} dr \, r^{2n+1} \, e^{-r^2} = \frac{n!}{2} \, . \tag{3.209}$$

As a result we obtain from (3.207)–(3.209) due to the completeness (3.23) of the Fock states

$$\int d^2\alpha \, |\alpha\rangle \langle\alpha| = \pi \sum_{n=0}^{\infty} |n\rangle \langle n| = \pi \, , \tag{3.210}$$

which coincides with the identity (3.186) suggested above. The deviation from 1 in (3.210) expresses the overcompleteness. This surprising finding can also be illustrated from a different

angle. To this end we work with coherent states, which are defined on a circle, i.e. $\alpha = re^{i\varphi}$, and obtain similar to (3.206):

$$|re^{i\varphi}\rangle = \sum_{n=0}^{\infty} |n\rangle \langle n|re^{i\varphi}\rangle = \sum_{n=0}^{\infty} |n\rangle \frac{r^n e^{in\varphi}}{\sqrt{n!}} e^{-r^2/2} . \tag{3.211}$$

Inverting (3.211) according to

$$|n\rangle = \frac{e^{r^2/2}}{r^n} \frac{\sqrt{n!}}{2\pi} \int_0^{2\pi} d\varphi \, e^{-in\varphi} |re^{i\varphi}\rangle \tag{3.212}$$

reveals that already one circle is enough to characterize all Fock states. This illustrates vividly that the complex plane of all coherent states contains more information than would be necessary for spanning the Fock space.

3.14 Properties of Husimi Function

Let us discuss now some generic properties of the Husimi function (3.160), which are not only valid for a pure state but also for a mixed state. At first, we consider the normalization of the density operator (3.135) and take into account the overcompleteness relation of the coherent states (3.186) in order to obtain the normalization of the Husimi function (3.160):

$$1 = \mathrm{Tr}\ (\hat{\rho}) = \int \frac{d^2\alpha}{\pi} \langle\alpha| \hat{\rho} |\alpha\rangle = \int d^2\alpha \, Q_{\hat{\rho}}(\alpha) . \tag{3.213}$$

This justifies a posteriori having evaluated the normalizations (3.183) and (3.195) for the particular Husimi functions (3.182) and (3.191). Furthermore, as the diagonal matrix elements of the density operator are positive according to (3.134), we read off from (3.160) that also the Husimi function is positive and, thus together with (3.213), allows for a probabilistic interpretation. This observation becomes even more conclusive by considering the expectation value (z156) of an anti-normally ordered operator product $\hat{a}^p \hat{a}^{\dagger q}$, where p, q denote some natural numbers. Using the completeness relation of the Fock states (3.23) as well as the overcompleteness relation of the coherent states (3.186) yields

$$\langle \hat{a}^p \hat{a}^{\dagger q} \rangle = \mathrm{Tr}\ \left(\hat{a}^p \hat{a}^{\dagger q} \hat{\rho} \right) = \sum_{n=0}^{\infty} \langle n| \hat{a}^p \hat{a}^{\dagger q} \hat{\rho} |n\rangle = \sum_{n=0}^{\infty} \int \frac{d^2\alpha}{\pi} \langle n| \hat{a}^p |\alpha\rangle \langle\alpha| \hat{a}^{\dagger q} \hat{\rho} |n\rangle . \tag{3.214}$$

Inserting the fundamental property of a coherent state (3.67), the completeness relation of the Fock states (3.23) and the definition of the Husimi function (3.160) yield:

$$\langle \hat{a}^p \hat{a}^{\dagger q} \rangle = \int \frac{d^2\alpha}{\pi} \alpha^p \alpha^{*q} \langle\alpha| \hat{\rho} \sum_{n=0}^{\infty} |n\rangle \langle n|\alpha\rangle = \int \frac{d^2\alpha}{\pi} \alpha^p \alpha^{*q} \langle\alpha| \hat{\rho} |\alpha\rangle = \int d^2\alpha \, Q_{\hat{\rho}}(\alpha) \alpha^p \alpha^{*q} . \tag{3.215}$$

This confirms the probability interpretation of the Husimi function.

3.15 Husimi Function of Squeezed State

Let us now specialize to the case that the density operator is defined by a pure squeezed state:

$$\hat{\rho} = |\xi\rangle \langle\xi| \ . \tag{3.216}$$

Inserting (3.216) into (3.160) leads to the corresponding Husimi function

$$Q_{|\xi\rangle\langle\xi|}(\alpha) = \frac{1}{\pi} |\langle\alpha|\xi\rangle|^2 \ . \tag{3.217}$$

We need now the following two steps for calculating (3.217):

- At first we consider the scalar product between a coherent state (3.66) and a squeezed state (3.105) and take (3.61) into account:

$$\langle\alpha|\xi\rangle = \langle\hat{D}(\alpha)0|\hat{S}(\xi)0\rangle = \langle 0|\hat{D}(-\alpha)\hat{S}(\xi)|0\rangle \ . \tag{3.218}$$

  Then we use from the literature the involved proof that the normal ordered form of the squeezing operator reads [38, (6.177)]

$$\hat{S}(\xi) = e^{-\nu\hat{a}^{\dagger 2}/2\mu} \left(\frac{1}{\mu}\right)^{\hat{n}+1/2} e^{\nu^*\hat{a}^2/2\mu} \, . \tag{3.219}$$

  Applying (3.219) to the vacuum state then yields straight-forwardly

$$\hat{S}(\xi)\,|0\rangle = \frac{1}{\sqrt{\mu}}\, e^{-\nu\hat{a}^{\dagger 2}/2\mu}\,|0\rangle \ . \tag{3.220}$$

  Subsequently we insert (3.168) and (3.220) in (3.218):

$$\langle\alpha|\xi\rangle = \frac{e^{-|\alpha|^2/2}}{\sqrt{\mu}}\,\langle 0|\, e^{\alpha^*\hat{a}} e^{-\nu\hat{a}^{\dagger 2}/2\mu}\,|0\rangle \ . \tag{3.221}$$

- Due to the identity (3.167) we obtain from (3.221):

$$\langle\alpha|\xi\rangle = \frac{e^{-|\alpha|^2/2}}{\sqrt{\mu}}\,\langle 0|\, e^{\alpha^*\hat{a}} e^{-\nu\hat{a}^{\dagger 2}/2\mu} e^{-\alpha^*\hat{a}}\,|0\rangle \ . \tag{3.222}$$

  A Taylor expansion of the exponential function then yields

$$e^{\alpha^*\hat{a}} \left(e^{-\nu\hat{a}^{\dagger 2}/2\mu}\right) e^{-\alpha^*\hat{a}} = \exp\left\{-\frac{\nu}{2\mu}\left(e^{\alpha^*\hat{a}}\hat{a}^\dagger e^{-\alpha^*\hat{a}}\right)^2\right\} \ . \tag{3.223}$$

  Applying the previous result (3.174) in (3.223) then leads to

$$e^{\alpha^*\hat{a}} e^{-\nu\hat{a}^{\dagger 2}/2\mu} e^{-\alpha^*\hat{a}} = \exp\left\{-\frac{\nu}{2\mu}\left(\hat{a}^\dagger + \alpha^*\right)^2\right\} \ . \tag{3.224}$$

  Substituting (3.224) into (3.222) and using (3.177) determines the scalar product between a squeezed and a coherent state:

$$\langle\alpha|\xi\rangle = \frac{e^{-|\alpha|^2/2}}{\sqrt{\mu}}\, e^{-\nu\alpha^{*2}/2\mu} \, . \tag{3.225}$$

From (3.217) and (3.225) we then obtain the Husimi function of the squeezed state:

$$Q_{|\xi\rangle\langle\xi|}(\alpha) = \frac{1}{\pi\mu}\,\exp\left\{-|\alpha|^2 - \frac{\nu\alpha^{*2} + \nu^*\alpha^2}{2\mu}\right\}. \tag{3.226}$$

The straight-forward algebraic manipulation

$$2\mathrm{Re}\left(\nu\alpha^{*2}\right) = 2|\nu|\Big\{\cos\varphi\left[(\mathrm{Re}\,\alpha)^2 - (\mathrm{Im}\,\alpha)^2\right] + 2\sin\varphi\,\mathrm{Re}\,\alpha\,\mathrm{Im}\,\alpha\Big\} \tag{3.227}$$

converts into (3.226) into

$$\begin{aligned} Q_{|\xi\rangle\langle\xi|}(\alpha) &= \frac{1}{\pi\mu}\,\exp\left\{-\left(1+\frac{|\nu|}{\mu}\,\cos\varphi\right)(\mathrm{Re}\,\alpha)^2 - \left(1-\frac{|\nu|}{\mu}\,\cos\varphi\right)(\mathrm{Im}\,\alpha)^2\right. \\ &\quad \left. -2\,\frac{|\nu|}{\mu}\,\sin\varphi\,\mathrm{Re}\,\alpha\,\mathrm{Im}\,\alpha\right\}. \end{aligned} \tag{3.228}$$

We examine now the form of this Q-function:

- At first we consider the special case $\varphi = 0$. In the exponent of (3.228) appears then an ellipse with semi-axes parallel to the $\mathrm{Re}\,\alpha$- and $\mathrm{Im}\,\alpha$-axes, whose values read with (3.101) and (3.102):

$$a = \sqrt{\frac{\mu}{\mu+|\nu|}} = \sqrt{\frac{\cosh|\xi|}{\cosh|\xi|+\sinh|\xi|}} = \frac{1}{\sqrt{2}}\,\sqrt{1+e^{-2|\xi|}} < 1\,, \tag{3.229}$$

$$b = \sqrt{\frac{\mu}{\mu-|\nu|}} = \sqrt{\frac{\cosh|\xi|}{\cosh|\xi|-\sinh|\xi|}} = \frac{1}{\sqrt{2}}\,\sqrt{e^{2|\xi|}+1} > 1\,. \tag{3.230}$$

- In case of the angle $\varphi \neq 0$, we carry out a rotation around an angle γ, which is still to be determined:

$$\begin{pmatrix} \mathrm{Re}\,\alpha \\ \mathrm{Im}\,\alpha \end{pmatrix} = \begin{pmatrix} \cos\gamma & -\sin\gamma \\ \sin\gamma & \cos\gamma \end{pmatrix} \begin{pmatrix} \mathrm{Re}\,\alpha' \\ \mathrm{Im}\,\alpha' \end{pmatrix}. \tag{3.231}$$

  Thus, inserting (3.231) into the generic quadratic form of (3.228)

$$A\,(\mathrm{Re}\,\alpha)^2 + B\,(\mathrm{Im}\,\alpha)^2 + C\,\mathrm{Re}\,\alpha\,\mathrm{Im}\,\alpha \tag{3.232}$$

  yields

$$\begin{aligned} &= A\,(\cos\gamma\,\mathrm{Re}\,\alpha' - \sin\gamma\,\mathrm{Im}\,\alpha')^2 + B\,(\sin\gamma\,\mathrm{Re}\,\alpha' + \cos\gamma\,\mathrm{Im}\,\alpha')^2 \\ &\quad + C\,(\cos\gamma\,\mathrm{Re}\,\alpha' - \sin\gamma\,\mathrm{Im}\,\alpha')\,(\sin\gamma\,\mathrm{Re}\,\alpha' + \cos\gamma\,\mathrm{Im}\,\alpha')\,. \end{aligned} \tag{3.233}$$

  Thus, we can now determine the rotation angle γ from the condition that the mixed terms $\mathrm{Re}\,\alpha'\,\mathrm{Im}\,\alpha'$ in (3.233) vanish:

$$-(A-B)2\sin\gamma\cos\gamma + C\left(\cos^2\gamma - \sin^2\gamma\right) = 0\,. \tag{3.234}$$

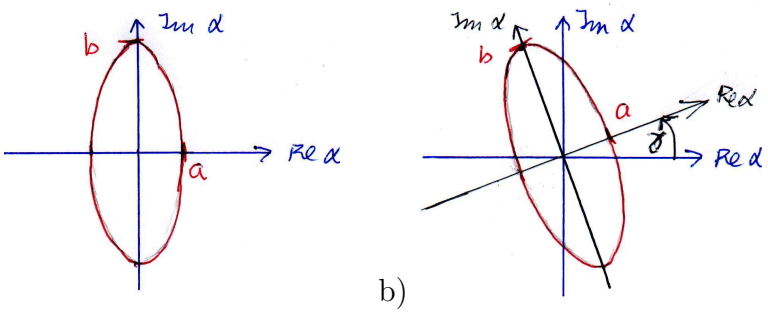

a) b)

Figure 3.8: Contour plot of Husimi function for a pure squeezed state (3.228): Semi-axes of ellipses (3.229), (3.230) are a) not rotated for $\varphi = 0$ and b) rotated by the angle (3.236) in case of $\varphi \neq 0$.

Due to trigonometric addition theorems we then obtain

$$(A - B)\sin(2\gamma) = C\cos(2\gamma) \qquad \Longrightarrow \qquad \tan(2\gamma) = \frac{C}{A - B}\,. \tag{3.235}$$

The explicit evaluation of (3.235) due to the identification of (3.228) with (3.232) yields:

$$\tan(2\gamma) = \frac{2\frac{|\nu|}{\mu}\sin\varphi}{\left(1 + \frac{|\nu|}{\mu}\cos\varphi\right) - \left(1 - \frac{|\nu|}{\mu}\cos\varphi\right)} = \tan\varphi \qquad \Longrightarrow \qquad \gamma = \frac{\varphi}{2}\,. \tag{3.236}$$

The prefactor of $(\mathrm{Re}\,\alpha')^2$ in (3.233) reads then with (3.236)

$$A\cos^2\gamma + B\sin^2\gamma + C\sin\gamma\cos\gamma = 1 + \frac{|\nu|}{\mu}\cos(\varphi - 2\gamma) = 1 + \frac{|\nu|}{\mu} = \frac{2}{1 + e^{-2|\xi|}} \tag{3.237}$$

and, correspondingly we obtain for the prefactor of $(\mathrm{Im}\alpha')^2$ in (3.233)

$$A\cos^2\gamma + B\sin^2\gamma + C\sin\gamma\cos\gamma = 1 - \frac{|\nu|}{\mu}\cos(\varphi - 2\gamma) = 1 - \frac{|\nu|}{\mu} = \frac{2}{1 + e^{2|\xi|}}\,, \tag{3.238}$$

so (3.237) and (3.238) lead to the semi-axes (3.229) and (3.230), respectively. With this we conclude that the complex parameter $\xi = |\xi|^{i\varphi}$ of a squeezed state allows for the following interpretation. The angle φ describes a rotation of the ellipse in the mathematical sense, while the amplitude $|\xi|$ defines the magnitude of the semi-axes of the ellipse.

The resulting contour plot of the Husimi function for a squeezed state is sketched in Fig. 3.8.

3.16 Decomposition of Squeezed State into Fock States

As the number states $|n\rangle$ represent a basis according to (3.23), a squeezed state $|\xi\rangle$ can be expanded with respect to it:

$$|\xi\rangle = \sum_{n=0}^{\infty} |n\rangle\,\langle n|\xi\rangle\,. \tag{3.239}$$

Instead of determining the amplitude $\langle n|\xi\rangle$ directly, we consider its generating function

$$f(t) = \sum_{n=0}^{\infty} \frac{t^n}{\sqrt{n!}} \langle n|\xi\rangle \ . \tag{3.240}$$

At first we get due to the definition of both Fock states (3.20) and and a squeezed state (3.105)

$$f(t) = \sum_{n=0}^{\infty} \frac{t^n}{\sqrt{n!}} \langle 0| \frac{\hat{a}^n}{\sqrt{n!}} |\xi\rangle = \langle 0| e^{t\hat{a}} \hat{S}(\xi) |0\rangle \ . \tag{3.241}$$

Inserting (3.220) in (3.241) and taking into account the identity (3.167) leads to

$$f(t) = \frac{1}{\sqrt{\mu}} \langle 0| e^{t\hat{a}} e^{-\nu\hat{a}^{\dagger 2}/2\mu} |0\rangle = \frac{1}{\sqrt{\mu}} \langle 0| e^{t\hat{a}} \left(e^{-\nu\hat{a}^{\dagger 2}/2\mu}\right) e^{-t\hat{a}} |0\rangle \ . \tag{3.242}$$

A Taylor expansion of the exponential function and an application of (3.174) then yields

$$f(t) = \frac{1}{\sqrt{\mu}} \langle 0| \exp\left\{-\frac{\nu}{2\mu}\left(e^{t\hat{a}}\hat{a}^{\dagger}e^{-t\hat{a}}\right)^2\right\} |0\rangle = \frac{1}{\sqrt{\mu}} \langle 0| e^{-\nu\left(\hat{a}^{\dagger}+t\right)^2/2\mu} |0\rangle \ . \tag{3.243}$$

As we can imagine that the annihilation operator $\hat{a}^{\dagger}$ is acting to the vacuum bra-state, it vanishes according to (3.177) and we finally get

$$f(t) = \frac{1}{\sqrt{\mu}} e^{-\nu t^2/2\mu} \, . \tag{3.244}$$

We now use the generating function of the Hermite polynomials [23, (8.957.1)]:

$$e^{-t^2+2tx} = \sum_{n=0}^{\infty} \frac{H_n(x)}{n!} t^n \, . \tag{3.245}$$

Substituting (3.245) into (3.244), a comparison with (3.240) gives

$$f(t) = \frac{1}{\sqrt{\mu}} \sum_{n=0}^{\infty} \frac{1}{n!} H_n(0) \left(\frac{\nu}{2\mu}\right)^{\frac{n}{2}} t^n = \sum_{n=0}^{\infty} \frac{t^n}{\sqrt{n!}} \langle n|\xi\rangle \ , \tag{3.246}$$

so we conclude

$$\langle n|\xi\rangle = \frac{1}{\sqrt{\mu n!}} H_n(0) \left(\frac{\nu}{2\mu}\right)^{\frac{n}{2}} \ . \tag{3.247}$$

Evaluating the generating function of the Hermite polynomials (3.245) for $x = 0$ involves the Hermite polynomials $H_n(0)$:

$$e^{-t^2} = \sum_{n=0}^{\infty} \frac{(-1)^n}{n!} t^{2n} = \sum_{n=0}^{\infty} \frac{H_n(0)}{n!} t^n \, . \tag{3.248}$$

Thus, we directly read off

$$H_{2n+1}(0) = 0 \, , \qquad n = 0, 1, 2, \dots \ , \tag{3.249}$$

i.e., due to (3.247), a squeezed state consists only of an even number of photons. This indicates that squeezed light is generated by some nonlinear process [39]. As a prominent example you analyse in the exercises the generation of squeezed light from parametric down conversion. It represents a nonlinear optical process that converts one photon of higher energy, namely a pump photon, into a pair of photons, namely a signal photon and an idler photon of lower energy.

Furthermore, we obtain from (3.248):

$$H_{2n}(0) = \frac{(2n)!}{n!}\,(-1)^n\,. \tag{3.250}$$

The finding (3.249) reduces (3.239) to

$$|\xi\rangle = \sum_{n=0}^{\infty} |2n\rangle\,\langle 2n|\xi\rangle \tag{3.251}$$

and the corresponding amplitudes result from (3.247) and (3.250) by taking into account (3.101) and (3.102):

$$\langle 2n|\xi\rangle = \frac{1}{\sqrt{\mu(2n)!}}\left(\frac{\nu}{2\mu}\right)^n H_{2n}(0) = \frac{1}{\sqrt{\cosh|\xi|}}\,\frac{\sqrt{(2n)!}}{n!}\left(-\frac{1}{2}\,e^{i\varphi}\tanh|\xi|\right)^n\,. \tag{3.252}$$

The probability of encountering $2n$ photons in a squeezed state amounts therefore to

$$p_{2n}(\xi) = |\langle 2n|\xi\rangle|^2 = \frac{(2n)!}{(n!)^2\cosh|\xi|}\left(\frac{1}{2}\tanh|\xi|\right)^{2n}\,. \tag{3.253}$$

Using the elementary Taylor expansion

$$\frac{1}{\sqrt{1-4x}} = \sum_{n=0}^{\infty}\frac{(2n!)}{(n!)^2}\,x^n \tag{3.254}$$

allows to check the normalisation of this probability distribution:

$$\sum_{n=0}^{\infty} p_{2n}(\xi) = \frac{1}{\cosh|\xi|\sqrt{1-\tanh^2|\xi|)}} = 1\,. \tag{3.255}$$

Let us calculate now the mean photon number, which amounts to evaluating the series

$$\langle\hat{n}\rangle_\xi = \sum_{n=0}^{\infty} 2n p_{2n}(\xi) = \frac{1}{\cosh|\xi|}\sum_{n=0}^{\infty}\frac{(2n)!}{(n!)^2}\,(2n)\left(\frac{1}{2}\tanh(|\xi|)\right)^{2n}\,. \tag{3.256}$$

To proceed further, we need the side calculation

$$\frac{\partial}{\partial|\xi|}\left(\tanh|\xi|\right)^{2n} = 2n\left(\tanh(|\xi|)\right)^{2n-1}\frac{1}{\cosh^2|\xi|}\,, \tag{3.257}$$

which leads to

$$2n\left(\tanh(|\xi|)\right)^{2n} = \tanh|\xi|\cosh^2|\xi|\,\frac{\partial}{\partial|\xi|}\left(\tanh|\xi|\right)^{2n}\,. \tag{3.258}$$

Applying (3.257) in (3.256) allows to evaluate the series, yielding

$$\langle \hat{n} \rangle_\xi = \frac{1}{\cosh|\xi|} \tanh|\xi| \cosh^2|\xi| \frac{\partial}{\partial|\xi|} \cosh|\xi| \,, \tag{3.259}$$

which reduces to the result

$$\langle \hat{n} \rangle_\xi = \sinh^2|\xi| \,. \tag{3.260}$$

Accordingly, the amplitude of the squeezing parameter $\xi = |\xi| e^{i\varphi}$ determines the mean photon number. In a similar way we proceed to determine also the second moment:

$$\begin{aligned} \langle \hat{n}^2 \rangle_\xi &= \sum_{n=0}^{\infty} (2n)^2 P_{2n} = \frac{1}{\cosh|\xi|} \tanh|\xi| \cosh^2(|\xi|) \frac{\partial}{\partial|\xi|} \tanh|\xi| \cosh^2|\xi| \frac{\partial}{\partial|\xi|} \cosh|\xi| \\ &= \sinh|\xi| \frac{\partial}{\partial|\xi|} \left(\sinh^2|\xi| \cosh|\xi| \right) = 2\sinh^2|\xi| \cosh^2|\xi| + \sinh^4|\xi| \,. \end{aligned} \tag{3.261}$$

Thus the variance amounts to

$$\langle (\Delta\hat{n})^2 \rangle_\xi = \langle \hat{n}^2 \rangle_\xi - \langle \hat{n} \rangle_\xi^2 = \frac{1}{2} \sinh^2(2|\xi|) \,. \tag{3.262}$$

Furthermore, combining (3.260) with (3.261) yields for the corresponding Mandel Q-parameter (3.203)

$$Q = \cosh(2|\xi|) \,, \tag{3.263}$$

which is positive and corresponds to a super-Poissonian photon statistics. Inserting the finding (3.260) into (3.253), the photon statistics for a single-mode squeezed state reads

$$p_{2n}(\xi) = \frac{(2n)! \left(\langle \hat{n} \rangle_\xi \right)^n}{4^n (n!)^2 \left(1 + \langle \hat{n} \rangle_\xi \right)^{n+1/2}} \,. \tag{3.264}$$

A typical distribution for such a squeezed vacuum is shown in Fig. 3.9a) and is, indeed, broader than a Poisson distribution with the same average photon number, see Fig. 3.7.

Note that squeezed coherent states represent an even more general class of photonic states. They are generated by applying successively a squeezing operator $\hat{S}(\xi)$ and a shifting operator $\hat{D}(\alpha)$ to the vacuum state:

$$|\alpha, \xi\rangle = |\hat{D}(\alpha)\hat{S}(\xi)|0\rangle \,. \tag{3.265}$$

Thus, the properties of squeezed coherent states (3.265) depend on both complex parameters $\alpha = |\alpha| e^{i\psi}$ and $\xi = |\xi| e^{i\varphi}$. In particular, tuning the respective phases ψ and φ has the consequence that squeezed coherent states have photon statistics, which can change between a super-Poissonian and a sub-Poissonian distribution as is depicted in Fig. 3.9b).

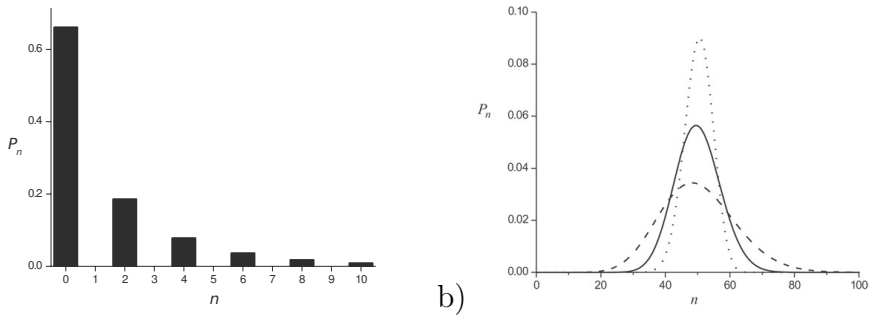

Figure 3.9: a) Histogram illustrating the photon number distribution for a squeezed vacuum state (3.264). b) Photon probability distributions (valid only at integers) for the coherent state with $|\alpha|^2 = 50$ (solid line) and the squeezed states for $|\alpha|^2 = 50, |\xi| = 0.5$ with the phase differences $\psi - \varphi/2 = 0$ (dotted line) and $\psi - \varphi/2 = \pi/2$ (dashed line). Taken from Ref. [6].

3.17 Thermal States

In statistical physics, Boltzmann studied stationary states in the canonical ensemble. The probability of finding a microstate with energy E in the canonical ensemble is given by the Boltzmann distribution:

$$p(E) \sim e^{-\beta E}\,, \tag{3.266}$$

where $\beta = 1/k_{\mathrm{B}}T$ denotes the reciprocal temperature. The application to a photon gas with the energies $E_n = \hbar\omega(n + 1/2)$ then results in

$$p(E_n) \sim e^{-\hbar\beta\omega(n+1/2)}\,. \tag{3.267}$$

As such a photon gas in the canonical ensemble represents a mixture of pure Fock states, it is adequately described in quantum statistics with a density operator $\hat{\rho}$ of the form

$$\hat{\rho}_T = \frac{1}{Z}\, e^{-\beta\hat{H}}\,, \tag{3.268}$$

where the Hamilton operator reads

$$\hat{H} = \hbar\omega\left(\hat{n} + \frac{1}{2}\right)\,. \tag{3.269}$$

The normalisation of the density operator (3.268) allows to determine the partition function Z:

$$\mathrm{Tr}\,(\hat{\rho}_T) = \frac{1}{Z}\,\mathrm{Tr}\left(e^{-\beta\hat{H}}\right) = 1 \qquad \Longrightarrow \qquad Z = \mathrm{Tr}\left(e^{-\beta\hat{H}}\right)\,. \tag{3.270}$$

The trace in (3.270) is straight-forwardly evaluated in the basis of the Fock states, as they diagonalize the Hamilton operator (3.269):

$$Z = \sum_{n=0}^{\infty} \langle n|\, e^{-\beta\hat{H}}\, |n\rangle = \sum_{n=0}^{\infty} e^{-\beta\hbar\omega(n+1/2)} = e^{-\hbar\beta\omega/2} \sum_{n=0}^{\infty} \left(e^{-\beta\hbar\omega}\right)^n\,. \tag{3.271}$$

The remaining series is geometric, so we end up with

$$Z = \frac{e^{-\hbar\beta\omega/2}}{1 - e^{-\hbar\beta\omega}} = \frac{1}{2\sinh(\hbar\beta\omega/2)} \,. \tag{3.272}$$

Inserting (3.272) into (3.268) leads with the completeness relation of Fock states (3.23) to the following representation of the density operator:

$$\hat{\rho}_T = \left(1 - e^{-\hbar\beta\omega}\right) e^{-\hbar\beta\omega\hat{n}} = \sum_{n=0}^{\infty} \left(1 - e^{-\hbar\beta\omega}\right) e^{-\hbar\beta\omega n} \left|n\right\rangle \left\langle n\right| \,. \tag{3.273}$$

This is of the general form (3.141) of a density operator, i.e.

$$\hat{\rho}_T = \sum_{n=0}^{\infty} p_n \left|n\right\rangle \left\langle n\right| \tag{3.274}$$

with the probabilities

$$0 \leq p_n = \frac{e^{-\hbar\beta\omega n}}{Z'} \leq 1 \,, \tag{3.275}$$

where we have introduced the new partition function:

$$Z' = \mathrm{Tr}\left(e^{-\beta\hbar\omega\hat{n}}\right) = \frac{1}{1 - e^{-\hbar\beta\omega}} \,. \tag{3.276}$$

The representation (3.274) of the thermal density operator $\hat{\rho}_T$ means that the quantum mechanical pure states $\left|n\right\rangle \left\langle n\right|$ are weighted therein with the classical probability p_n given by (3.275). Therefore it represents a mixed state. In order to quantify the degree of mixedness further, we have to determine the purity of the thermal state (3.154) and to show according to (3.159) that $P(\hat{\rho}_T)$ is, indeed, smaller than one. From (3.154) and (3.275) we obtain at first

$$P(\hat{\rho}_T) = \sum_{n=0}^{\infty} p_n^2 = \frac{1}{Z'^2} \sum_{n=0}^{\infty} e^{-2\hbar\beta\omega n} \,, \tag{3.277}$$

which also represents a geometric series:

$$P(\hat{\rho}_T) = \frac{\left(1 - e^{-\hbar\beta\omega}\right)^2}{1 - e^{-2\hbar\beta\omega}} = \tanh\left(\hbar\beta\omega/2\right) \,. \tag{3.278}$$

The dependence of the purity (3.278) on the dimensionless parameter $\hbar\beta\omega$ is depicted in Fig. 3.10a) . For small $\hbar\beta\omega$ we have hot temperatures, which represents the classical limit with a quite small purity, so the state is clearly mixed. In the opposite limit of large $\hbar\beta\omega$, where have nearly absolute zero temperature, we reach the quantum mechanical limit with purity of nearly one, which corresponds to a pure state.

Let us discuss these general considerations in more detail by considering some concrete numbers. For yellow light we have a wavelength of 500 nm, which amounts according to the linear dispersion (2.73) to the circular frequency $\omega = 2\pi c/\lambda = 2\pi \times 6 \cdot 10^{14}\, 1/\mathrm{s}$. At the temperature

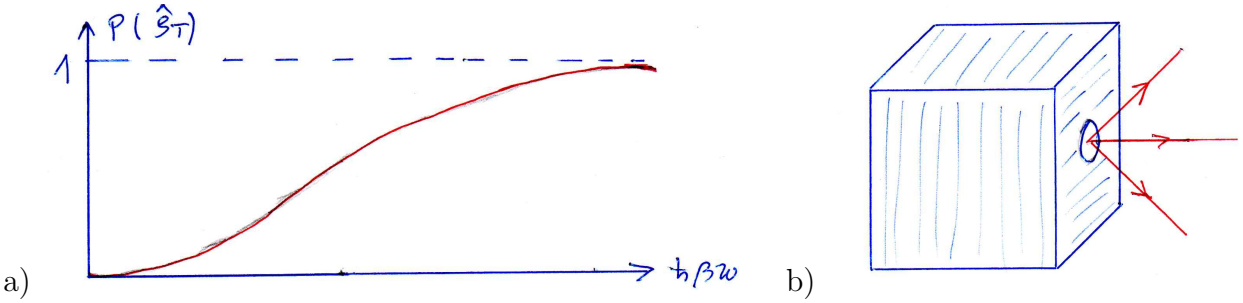

Figure 3.10: a) Purity of thermal light (3.278) as a function of dimensionless parameter $\hbar\beta\omega$. b) Sketch of a black body: thermal light emerges from a tiny hole in the walls.

$T = 300\,\mathrm{K}$ this then yields a dimensionless parameter $\hbar\beta\omega = \hbar\omega/k_\mathrm{B}T$ of about 95.6, which is much larger than one. Thus, thermal visible light can safely be treated quantum mechanically.

Thermal states occur in black-body radiation. Here, a black body can be modelled by considering a cavity in which the light field is in thermal equilibrium with its walls, see Fig. 3.10b). In this way, the light field is coupled to a heat bath with a fixed temperature and can be described in the canonical ensemble. The expectation value of the particle number operator results in the mean photon number in thermodynamic equilibrium. Evaluating the trace in the corresponding expression

$$\langle\hat{n}\rangle_T = \mathrm{Tr}\,(\hat{n}\hat{\rho}_T) \tag{3.279}$$

in the Fock basis yields due to (3.274) and (3.275):

$$\langle\hat{n}\rangle_T = \sum_{n=0}^{\infty}\langle n|\,\hat{n}\hat{\rho}_T\,|n\rangle = \sum_{n=0}^{\infty} n\,\frac{e^{-\hbar\beta\omega n}}{Z'} = \frac{1}{Z'}\left(-\frac{\partial}{\partial\hbar\beta\omega}\right)Z'\,. \tag{3.280}$$

Inserting the new partition function (3.276) we obtain

$$\langle\hat{n}\rangle_T = \left(1-e^{-\hbar\beta\omega}\right)\left(-\frac{\partial}{\partial\hbar\beta\omega}\right)\frac{1}{1-e^{-\hbar\beta\omega}} = \frac{1}{e^{\hbar\beta\omega}-1}\,, \tag{3.281}$$

which represents the seminal Bose-Einstein distribution. In the classical high-temperature limit we have

$$\langle\hat{n}\rangle_T \approx \frac{1}{\hbar\beta\omega}\,, \qquad \hbar\beta\omega \ll 1\,, \tag{3.282}$$

whereas the quantum mechanical low-temperature limit yields

$$\langle\hat{n}\rangle_T \approx e^{-\hbar\beta\omega}\,, \qquad \hbar\beta\omega \gg 1 \tag{3.283}$$

For yellow light, i.e. $\lambda = 500\,\mathrm{nm}$, and room temperature $T = 300\,\mathrm{K}$ we obtain the extremely small average photon number $\langle\hat{n}\rangle_T \approx e^{-95.6} \approx 3\cdot 10^{-42}$. At the temperature $T = 6\,000\,\mathrm{K}$, which corresponds to the temperature at the surface of the sun, we have instead $\hbar\beta\omega = 95.6\cdot 300/6\,000 = 4.78$, which yields already $\langle\hat{n}\rangle_T \approx e^{-4.78} = 0.008$. In general we record that the

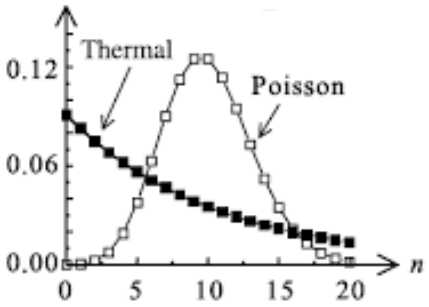

Figure 3.11: Comparison of a thermal distribution (3.286) and a Poisson distribution (3.202) with the same number of average photons $\langle \hat{n} \rangle_T = 10$.

mean photon occupation increases with increasing wavelength. At $T = 300\,\mathrm{K}$ the wavelengths $\lambda = 10 - 100\,\mu\mathrm{m}$ in the infrared amount to $\langle \hat{n} \rangle_T \approx 1$, but already for the wavelengths of microwaves $\lambda = 1\,\mathrm{mm} - 300\,\mathrm{mm}$ we get $\langle \hat{n} \rangle_T \gg 1$.

The Bose-Einstein distribution (3.281) allows to determine the average photon number $\langle \hat{n} \rangle_T$ for a given dimensionless parameter $\hbar\beta\omega$. But this relation can also be inverted

$$e^{-\hbar\beta\omega} = \frac{\langle \hat{n} \rangle_T}{1 + \langle \hat{n} \rangle_T}\,, \tag{3.284}$$

which allows, conversely, to determine the dimensionless parameter $\hbar\beta\omega$ from a given average photon number $\langle \hat{n} \rangle_T$. Inserting (3.284) into the probability of finding n photons in the thermal state, which follows from (3.274) and (3.275)

$$p_n = \left(1 - e^{-\hbar\beta\omega}\right) e^{-\hbar\omega\beta n}\,, \tag{3.285}$$

we get

$$p_n = \frac{\left(\langle \hat{n} \rangle_T\right)^n}{\left(1 + \langle \hat{n} \rangle_T\right)^{n+1}}\,. \tag{3.286}$$

Thus, we read off that p_n decreases monotonically with n and the largest possible probability occurs for the vacuum state $n = 0$. The dependence of the probabilities (3.286) from the photon number n is sketched in Fig. 3.11

Let us now determine also the second moment of the photon number for a thermal state:

$$\langle \hat{n}^2 \rangle_T = \mathrm{Tr}\,\left(\hat{n}^2 \hat{\rho}_T\right)\,. \tag{3.287}$$

The trace is evaluated in the Fock basis, yielding due to (3.274) and (3.275)

$$\langle \hat{n}^2 \rangle_T = \sum_{n=0}^{\infty} n^2\, \frac{e^{-\hbar\beta\omega n}}{Z'} = \frac{1}{Z'} \left(-\frac{\partial}{\partial \hbar\beta\omega}\right)^2 Z'\,. \tag{3.288}$$

With the new partition function (3.276) this reduces to

$$\langle \hat{n}^2 \rangle_T = \left(1 - e^{-\hbar\beta\omega}\right) \left(-\frac{\partial}{\partial \hbar\beta\omega}\right)^2 \frac{1}{1 - e^{-\hbar\beta\omega}}\,, \tag{3.289}$$

which, finally, results in

$$\langle \hat{n}^2 \rangle_T = \frac{e^{\hbar\beta\omega} + 1}{\left(e^{\hbar\beta\omega} - 1\right)^2} \,. \tag{3.290}$$

From (3.281) and (3.290) follows then the variance

$$\langle \Delta\hat{n}^2 \rangle_T = \langle \hat{n}^2 \rangle_T - \langle \hat{n} \rangle_T^2 = \frac{e^{\hbar\beta\omega}}{\left(e^{\hbar\beta\omega} - 1\right)^2} \,, \tag{3.291}$$

which reduces due to (3.284) to

$$\langle \Delta\hat{n}^2 \rangle_T = \langle \hat{n} \rangle_T^2 + \langle \hat{n} \rangle_T \,. \tag{3.292}$$

On the one hand we conclude from (3.292) that the black-body radiation is characterized by a Mandel Q-parameter (3.203), which coincides with the average of the photon number, i.e. $Q = \langle \hat{n} \rangle_T$ and is, thus, positive. Therefore, thermal light is a prominent example for a super-Poissonian photon statistics. This is illustrated in Fig. 3.11, where the thermal photon distribution is obviously broader than a Poissonian statistics with the same average number of photons. On the other hand we read off from (3.292) that the corresponding standard deviation amounts to

$$\sqrt{\langle \Delta\hat{n}^2 \rangle_T} = \sqrt{\langle \hat{n} \rangle_T^2 + \langle \hat{n} \rangle_T} = \begin{cases} \langle \hat{n} \rangle_T + 1/2 \,; & \langle \hat{n} \rangle_T \gg 1 \\ \sqrt{\langle \hat{n} \rangle_T} \,; & \langle \hat{n} \rangle_T \ll 1 \end{cases} \,, \tag{3.293}$$

so the relative standard deviation leads to

$$\frac{\sqrt{\langle \Delta\hat{n}^2 \rangle_T}}{\langle \hat{n} \rangle_T} \;=\; \begin{cases} 1 \,; & \langle \hat{n} \rangle_T \gg 1 \\ 1/\sqrt{\langle \hat{n} \rangle_T} \,; & \langle \hat{n} \rangle_T \ll 1 \end{cases} \,. \tag{3.294}$$

Here the conditions $\langle \hat{n} \rangle_T \gg 1$ and $\langle \hat{n} \rangle_T \ll 1$ correspond to the classical and the quantum limit, respectively.

Furthermore, we determine the first moment of the family of operators (3.30)

$$\langle \hat{x}_\theta \rangle_T = \mathrm{Tr}\, \left(\hat{x}_\theta \hat{\rho}_T \right) \,. \tag{3.295}$$

Inserting therein (3.30) as well as (3.274) and (3.275) yields

$$\langle \hat{x}_\theta \rangle_T = \sum_{n=0}^{\infty} \langle n | \, \frac{1}{\sqrt{2}} \left(\hat{a} e^{-i\theta} + \hat{a}^\dagger e^{i\theta} \right) | n \rangle \, p_n = 0 \,. \tag{3.296}$$

In the same way also the second moment is calculated

$$\langle \hat{x}_\theta^2 \rangle_T = \mathrm{Tr}\, (\hat{x}_\theta^2 \hat{\rho}_T) = \sum_{n=0}^{\infty} \langle n | \, \frac{1}{2} \left(\hat{a} e^{-\theta} + \hat{a}^\dagger e^{-i\theta} \right)^2 | n \rangle \, p_n = \sum_{n=0}^{\infty} \left(n + \frac{1}{2} \right) p_n = \langle \hat{n} \rangle_T + \frac{1}{2} \,, \tag{3.297}$$

yielding with the Bose-Einstein distribution (3.281)

$$\langle \hat{x}_\theta^2 \rangle_T = \frac{1}{2} \coth \hbar\beta\omega/2 \,. \tag{3.298}$$

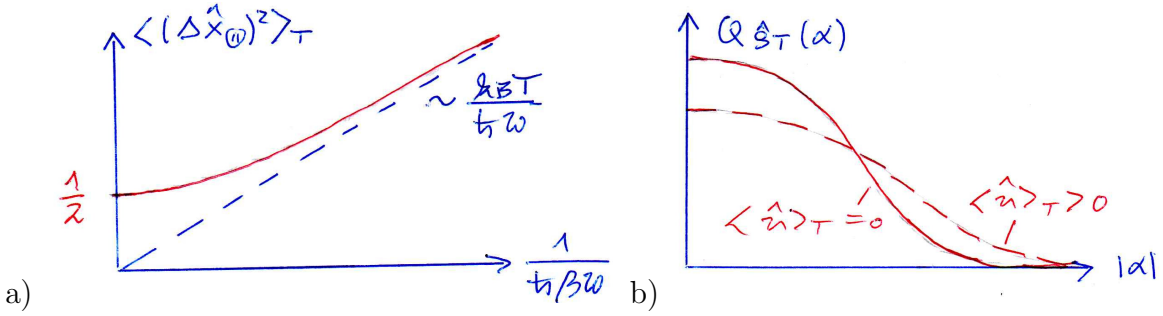

Figure 3.12: Properties of thermal light: a) Variance (3.298) as function of the dimensionless parameter $1/\hbar\beta\omega \sim T$; b) Husimi function (3.302) with $\langle\hat{n}\rangle_T = 0$ and $\langle\hat{n}\rangle_T > 0$.

Thus (3.298) represents the variance of thermal light, which is plotted in Fig. 3.12a) as a function of the dimensionless parameter $1/\hbar\beta\omega \sim T$. In the quantum mechanical limit of zero temperature the variance gets minimal, i.e. $\langle\hat{x}_\theta^2\rangle_T \to 1/2$ for $T \downarrow 0$, whereas in the classical limit of an infinitely large temperature the Dulong-Petit law occurs, i.e. $\langle\hat{x}_\theta^2\rangle_T \to k_\mathrm{B}T/\hbar\omega$ for $T \to \infty$.

Finally, we also calculate the Husimi function of the thermal state (3.274):

$$Q_{\hat{\rho}_T}(\alpha) = \frac{1}{\pi}\,\langle\alpha|\,\hat{\rho}_T\,|\alpha\rangle = \frac{1}{\pi}\sum_{n=0}^{\infty} p_n\,|\langle\alpha|n\rangle|^2\ . \tag{3.299}$$

With the matrix element (3.190) and the probabilities (3.275) this gives

$$Q_{\hat{\rho}_T}(\alpha) = \frac{1}{\pi}\sum_{n=0}^{\infty}\frac{e^{-\hbar\beta\omega n}}{Z'}\,\frac{|\alpha|^{2n}}{n!}\,e^{-|\alpha|^2} = \frac{e^{-|\alpha|^2}}{\pi Z'}\sum_{n=0}^{\infty}\frac{\left(|\alpha|^2\,e^{-\hbar\beta\omega}\right)^n}{n!}\,. \tag{3.300}$$

Evaluating the geometric series yields

$$Q_{\hat{\rho}_T}(\alpha) = \quad = \frac{1}{\pi}\left(1-e^{-\hbar\beta\omega}\right)\,\exp\Big\{-|\alpha|^2\left(1-e^{-\hbar\beta\omega}\right)\Big\}\,, \tag{3.301}$$

which gives due to (3.284)

$$Q_{\hat{\rho}_T}(\alpha) = \frac{1}{\pi}\,\frac{1}{1+\langle\hat{n}\rangle_T}\,\exp\Big\{-|\alpha|^2\,\frac{1}{1+\langle\hat{n}\rangle_T}\Big\}\,. \tag{3.302}$$

Thus, the thermal state looks like the vacuum state, which corresponds to $\langle\hat{n}\rangle_T = 0$, but is wider by the factor $\sqrt{1+\langle\hat{n}\rangle_T}$, see Fig. 3.12b).

We conclude this section with the radiation formula, whose derivation by Max Planck in 1900 marks the birth of quantum mechanics. It describes how much energy per volume and frequency is radiated by a black body, see Fig. 3.10. To this end we have to multiply the energy $\hbar\omega$ of one photon with both the mode density (2.251) and the Bose-Einstein distribution (3.281), yielding

$$U(\omega) = \hbar\omega\cdot\frac{\omega^2}{\pi^2c^3}\cdot\frac{1}{e^{\hbar\omega/k_\mathrm{B}T}-1} = \frac{\hbar\omega^3}{\pi^2c^3}\,\frac{1}{e^{\hbar\omega/k_\mathrm{B}T}-1}\,. \tag{3.303}$$

This Planck law of black-body radiation is sketched in Fig. 3.13. In the classical limit $\hbar\omega \ll k_\mathrm{B}T$

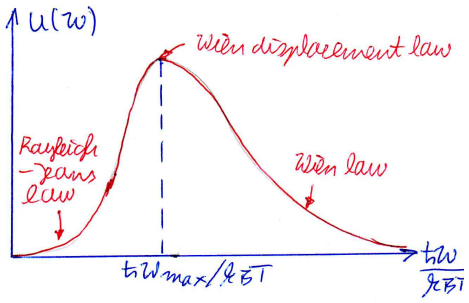

Figure 3.13: Planck law of black-body radiation (3.303) together with the classical Rayleigh-Jeans law (3.304) and the quantum mechanical Wien law (3.305).

one obtains the Rayleigh-Jeans law

$$U_{\mathrm{RJ}}(\omega) \approx \frac{\omega^2 k_{\mathrm{B}} T}{\pi^2 c^3} \,. \tag{3.304}$$

It does not contain anymore the Planck constant $\hbar$ and follows from multiplying the mode density (2.251) with the average energy $\hbar\omega$ of a harmonic oscillator according to the equipartition theorem of classical statistical mechanics. And in the quantum mechanical limit $\hbar\omega \gg k_{\mathrm{B}} T$ we obtain from (3.303) the Wien law

$$U_{\mathrm{W}}(\omega) \approx \frac{\hbar\omega^3}{\pi^2 c^3}\, e^{-\hbar\omega/k_{\mathrm{B}}T} \,. \tag{3.305}$$

It is obtained from multiplying the quantum mechanical energy $\hbar\omega$ with the mode density (2.251) and with a classical Boltzmann distribution.

Let us now investigate, where the maximal energy per volume occurs. This so-called Wien displacement law turns out to exist in two different formulations. Extremizing (3.303) with respect to the circular frequency ω yields for the dimensionless abbreviation $x = \hbar\omega/k_{\mathrm{B}}T$ the transcendental equation

$$e^x = \frac{1}{1 - x/3} \,, \tag{3.306}$$

which is solved by $x_1 \approx 2.8214393721$. Thus, in this case the Wien displacement law determines the frequency for maximal energy according to

$$\omega_{\max} = x_1 \frac{k_{\mathrm{B}} T}{\hbar} \qquad \Longrightarrow \qquad \nu_{\max} = \frac{\omega_{\max}}{2\pi} \approx 5.879 \cdot 10^{10}\,\mathrm{Hz}\,\frac{T}{\mathrm{K}} \,. \tag{3.307}$$

But, alternatively, we could also analyze the Planck law of black-body radiation (3.303) as a function of wavelength λ, for which holds

$$U(\lambda) = U(\omega) \left| \frac{d\omega}{d\lambda} \right| \,, \tag{3.308}$$

so that we have the same amount of energy per volume in the frequency interval $d\omega$ and in the wavelength interval $d\lambda$, respectively. Taking into account the linear dispersion (2.73) yields

$$\omega = \frac{2\pi c}{\lambda} \qquad \Longrightarrow \qquad \left| \frac{d\omega}{d\lambda} \right| = \frac{2\pi c}{\lambda^2} \tag{3.309}$$

and we get from (3.308)

$$U(\lambda) = \frac{16\pi^2\hbar c}{\lambda^5}\,\frac{1}{e^{2\pi\hbar c/k_{\mathrm{B}}T\lambda}-1}\,. \tag{3.310}$$

Extremizing now (3.310) with respect to the wavelength λ and introducing the dimensionless abbreviation $x = 2\pi\hbar c/k_{\mathrm{B}}T\lambda$, we end up with a transcendental equation different from (3.306)

$$e^x = \frac{1}{1-x/5}\,, \tag{3.311}$$

which has the solution $x_2 \approx 4.9651142317$. As a consequence, the wavelength for maximal energy leads to another form of the Wien displacement law:

$$\lambda_{\max} = \frac{2\pi\hbar c}{x_2 k_{\mathrm{B}}T} \qquad \Longrightarrow \qquad \lambda_{\max} \approx \frac{2\,898\,\mu\mathrm{m\,K}}{T}\,. \tag{3.312}$$

Note that (3.307) and (3.312) represent different positions for the maximal energy, as they do not fulfill the linear dispersion (3.309)

$$\omega_{\max} \neq \frac{2\pi c}{\lambda_{\max}} \tag{3.313}$$

due to the fact that the functions $U(\omega)$ and $U(\lambda)$ are related via the transformation law (3.308). But (3.307) and (3.312) have in common to describe how the frequency and the wavelength emitted most intensely by a black body shifts, i.e. is displaced, with the temperature, which is why they are called to be a *displacement law*. For instance, this law may be used to determine the temperature of bodies of stars by measuring the frequency or wavelength of their maximally emitted energy. Inserting the solar surface temperature of $T \approx 6\,000\,\mathrm{K}$ into the (3.312) we find $\lambda_{\max} \approx 480\,\mathrm{nm}$, which is approximately the wavelength of green light, whereas (3.307) yields a frequency corresponding to about 830 nm, which is in the near infrared being invisible for human beings.

The total average energy per volume follows then from integrating (3.303) over all frequencies:

$$U = \int_0^\infty d\omega\,\frac{\hbar\omega^3}{\pi^2c^3}\,\frac{1}{e^{\hbar\omega/k_{\mathrm{B}}T}-1}\,. \tag{3.314}$$

Introducing as a dimensionless integration variable $x = \hbar\omega/k_{\mathrm{B}}T$ then converts (3.314) to

$$U = \frac{k_{\mathrm{B}}^4T^4}{\pi^2\hbar^3c^3}\,I\,, \tag{3.315}$$

where the remaining integral reads

$$I = \int_0^\infty dx\,\frac{x^3}{e^x-1}\,. \tag{3.316}$$

According to Appendix B we obtain

$$I = \frac{\pi^4}{15}\,, \tag{3.317}$$

thus from (3.315) follows the Stefan-Boltzmann law:

$$U = \frac{\pi^2k_{\mathrm{B}}^4T^4}{15\hbar^3c^3}\,. \tag{3.318}$$

It states that the energy U per volume of a black body increases with the fourth power of its temperature T.

Chapter 4

Emission and Absorption of Light by Matter

This chapter focuses on the intricate interaction between light and matter and, thus, represents the main part of the whole quantum optics lecture. In Section 4.1 we start with outlining general aspects. To this end the individual atoms are modelled quantum mechanically, but we leave it open whether light is treated either classically or quantum mechanically. In particular, we revisit the dipole approximation, which was already introduced in Subsection 2.18.6, and show that it allows to simplify the light-matter interaction within the radiation gauge. As a result we recognize that the electromagnetic field interacts effectively only with the electric field via a coupling to the electric dipole moment of the matter.

Subsequently, the interaction of an atom with a classical and a quantum mechanical electric field is treated perturbatively in Sections 4.2 and 4.3, respectively. In the classical case we find that the probability for a transition does not depend upon whether the initial or the final atomic state is energetically higher or lower. This symmetry is then broken in the quantum mechanical case and, ultimately, leads to the three elementary processes for the interaction of light and matter, which were discovered by Albert Einstein in 1916 within his rederivation of the black-body radiation formula of Max Planck. Whereas absorption and induced emission happen to be identical as a consequence of an incident electromagnetic wave, the spontaneous emission can even occur randomly in the absence of any photons and, thus, is exclusively of quantum mechanical origin.

These perturbative results are only valid provided that the population transfer between the initial and the final state is small. Therefore, Sections 4.4 and 4.5 investigates the classical or quantum mechanical light-matter interaction exactly. But one simplifies the analysis by restricting oneself to light, which is approximately resonant to two atomic states, so that all other atomic states can safely be neglected. The classical case represents the Rabi model, which turns out to be formally equivalent to the interaction of a spin 1/2 with a magnetic field. Thus, the transition between the two atomic states is described by the optical Bloch equations,

whose solution we work out in detail. The corresponding quantum electrodynamic version of the Rabi model is known as the Jaynes-Cummings model whose dynamics turns out to be more intricate. For resonant light we find vacuum Rabi oscillations as well as the phenomenon of collapse and revival. And for non-resonant light the dynamics is accessible on the basis of the stationary states of the Jaynes-Cummings Hamiltonian, which are called dressed states. In the case that the light is highly non-resonant a direct atomic transition does not occur, but an effective dispersive interaction between a single atom a cavity field emerges. Finally, we discuss in Section 4.6 an experimental realization for the Jaynes-Cummings model, which is provided by a single Rydberg atom in a microwave cavity, and, thus, introduce the modern field cavity quantum electrodynamics.

4.1 Light-Matter Interaction

At first we consider a single electron, which is bound to the atomic nucleus by a static, radial-symmetric potential $V(r)$ with $r = |\mathbf{x}|$. In spatial representation the underlying Hamilton operator is given by

$$\hat{H}^{(0)}(\mathbf{x}) = \frac{1}{2M}\left(\frac{\hbar}{i}\boldsymbol{\nabla}\right)^2 + V(r)\,. \tag{4.1}$$

The time-independent Schrödinger equation

$$\hat{H}^{(0)}(\mathbf{x})\psi_n^{(0)}(\mathbf{x}) = E_n^{(0)}\psi_n^{(0)}(\mathbf{x}) \tag{4.2}$$

determines then for each discrete quantum number n both the energy eigenvalues $E_n^{(0)}$ and the stationary states $\psi_n^{(0)}(\mathbf{x})$. Here we assume that the latter are both orthonormal

$$\int d^3r\, \psi_m^{(0)*}(\mathbf{x})\psi_n^{(0)}(\mathbf{x}) = \delta_{m,n} \tag{4.3}$$

and complete

$$\sum_n \psi_n^{(0)*}(\mathbf{x})\psi_n^{(0)}(\mathbf{x}') = \delta(\mathbf{x}-\mathbf{x}')\,. \tag{4.4}$$

In the presence of an external vector potential $\mathbf{A}(\mathbf{x},t)$ and an external scalar potential $\varphi(\mathbf{x},t)$, the Hamilton operator (4.1) is extended via minimal coupling [21, Subsection 10.1.4] to

$$\hat{H}(\mathbf{x},t) = \frac{1}{2M}\left[\frac{\hbar}{i}\boldsymbol{\nabla} + e\mathbf{A}(\mathbf{x},t)\right]^2 + V(r) - e\varphi(\mathbf{x},t)\,. \tag{4.5}$$

Here we have used the International System of Units, which is abbreviated by SI from the French Système international d'unités, and the charge $q = -e$ of the electron, where $e > 0$ denotes the elementary charge. The corresponding electric and magnetic fields (2.10), (2.11)

are invariant under the gauge transformation (2.14), (2.15), where $\Lambda(\mathbf{x},t)$ denotes an arbitrary gauge function. In the presence of the external fields, the corresponding time-dependent Schrödinger equation must be solved:

$$i\hbar\,\frac{\partial\psi(\mathbf{x},t)}{\partial t} = \hat{H}(\mathbf{x},t)\psi(\mathbf{x},t)\,. \tag{4.6}$$

We now aim at simplifying the light-matter interaction. To this end we transform the wave function according to

$$\psi'(\mathbf{x},t) = \hat{U}(\mathbf{x},t)\psi(\mathbf{x},t) \qquad \Longleftrightarrow \qquad \psi(\mathbf{x},t) = \hat{U}^\dagger(\mathbf{x},t)\psi'(\mathbf{x},t) \tag{4.7}$$

with a unitary transformation

$$\hat{U}(\mathbf{x},t)\hat{U}^\dagger(\mathbf{x},t) = 1\,. \tag{4.8}$$

For the transformed wave function we then also obtain a time-dependent Schrödinger equation:

$$i\hbar\,\frac{\partial\psi'(\mathbf{x},t)}{\partial t} = i\hbar\frac{\partial\hat{U}(\mathbf{x},t)}{\partial t}\,\psi(\mathbf{x},t) + \hat{U}(\mathbf{x},t)\hat{H}(\mathbf{x},t)\psi(\mathbf{x},t) = \hat{H}'(\mathbf{x},t)\psi'(\mathbf{x},t)\,, \tag{4.9}$$

where the transformed Hamilton operator turns out to be

$$\hat{H}'(\mathbf{x},t) = \hat{U}(\mathbf{x},t)\hat{H}(\mathbf{x},t)\hat{U}^\dagger(\mathbf{x},t) + i\hbar\,\frac{\partial\hat{U}(\mathbf{x},t)}{\partial t}\,\hat{U}^\dagger(\mathbf{x},t)\,. \tag{4.10}$$

Let us now choose the special unitary transformation

$$\hat{U}(\mathbf{x},t) = e^{ie\Lambda(\mathbf{x},t)/\hbar}\,, \qquad \hat{U}^\dagger(\mathbf{x},t) = e^{-ie\Lambda(\mathbf{x},t)/\hbar}\,, \tag{4.11}$$

which has due to (4.8) the properties

$$i\hbar\,\frac{\partial\hat{U}(\mathbf{x},t)}{\partial t}\,\hat{U}^\dagger(\mathbf{x},t) = -e\,\frac{\partial\Lambda(\mathbf{x},t)}{\partial t}\,, \tag{4.12}$$

$$\hat{U}(\mathbf{x},t)\left[\frac{\hbar}{i}\,\boldsymbol{\nabla} + e\mathbf{A}(\mathbf{x},t)\right]\hat{U}^\dagger(\mathbf{x},t) = \frac{\hbar}{i}\,\boldsymbol{\nabla} + e\mathbf{A}(\mathbf{x},t) - e\boldsymbol{\nabla}\Lambda(\mathbf{x},t)\,. \tag{4.13}$$

Thus, with (4.12), (4.13) the transformed Hamiltonian operator (4.10) has the same form as the original Hamiltonian operator (4.5), but contains instead of the original potentials the gauge transformed potentials (2.14), (2.15):

$$\hat{H}'(\mathbf{x},t) = \frac{1}{2M}\left[\frac{\hbar}{i}\,\boldsymbol{\nabla} + e\mathbf{A}'(\mathbf{x},t)\right]^2 + V(r) - e\varphi'(\mathbf{x},t)\,. \tag{4.14}$$

Without loss of generality we now choose the radiation gauge, i.e. we assume that the scalar potential vanishes (2.24) and that the vector potential is transversal due to the Coulomb gauge (2.16). In this radiation gauge, the original Hamilton operator (4.5) reads explicitly

$$\hat{H}(\mathbf{x},t) = -\frac{\hbar^2}{2M}\,\Delta + \frac{e}{M}\,\mathbf{A}(\mathbf{x},t)\cdot\frac{\hbar}{i}\,\boldsymbol{\nabla} + \frac{e^2}{2M}\,\mathbf{A}^2(\mathbf{x},t) + V(r)\,, \tag{4.15}$$

while the transformed Hamilton operator (4.10) is given by

$$\hat{H}'(\mathbf{x},t) = \frac{1}{2M}\left[\frac{\hbar}{i}\boldsymbol{\nabla} + e\mathbf{A}(\mathbf{x},t) - e\boldsymbol{\nabla}\Lambda(\mathbf{x},t)\right]^2 + V(r) - e\,\frac{\partial\Lambda(\mathbf{x},t)}{\partial t}\,. \tag{4.16}$$

The light-matter interaction in the transformed Hamilton operator (4.16) can now be simplified as follows. Outside the atom there are no sources for the electromagnetic field, i.e. the vector potential satisfies the homogeneous wave equation in the radiation gauge (2.25), which has fundamental solutions in form of plane waves

$$\mathbf{A}(\mathbf{x},t) = \mathbf{A}_0\, e^{i(\mathbf{kx}-\omega t)} + \text{c.c.} \tag{4.17}$$

with the linear dispersion (2.73). In the optical range the estimate (2.254) holds, i.e. the vector potential does not change over the extension of an atom and is, therefore, approximately homogeneous, see Fig. 2.14. This leads to the so-called *dipole approximation*, where we can approximately neglect the spatial dependence of the vector potential $\mathbf{A}(\mathbf{x},t)$ for spatial vectors $\mathbf{x}$ pointing at the atomic electron:

$$\mathbf{A}(\mathbf{x},t) \approx \mathbf{A}(t)\,. \tag{4.18}$$

Furthermore, we choose as a gauge function $\Lambda(\mathbf{x},t) = \mathbf{x}\cdot\mathbf{A}(t)$, which has due to (2.11) and (2.24) the properties

$$\boldsymbol{\nabla}\Lambda(\mathbf{x},t) = \mathbf{A}(t)\,, \qquad \frac{\partial\Lambda(\mathbf{x},t)}{\partial t} = \mathbf{x}\cdot\frac{\partial\mathbf{A}(t)}{\partial t} = -\mathbf{x}\cdot\mathbf{E}(t)\,.$$

These considerations reduce the transformed Hamilton operator (4.16) to

$$\hat{H}'(\mathbf{x},t) = -\frac{\hbar^2}{2M}\,\Delta + V(r) + e\mathbf{x}\cdot\mathbf{E}(t)\,. \tag{4.19}$$

In contrast to the original Hamilton operator (4.5), there is now only one term instead of two that describes the light-matter interaction. With the definition of the electric dipole moment of the electron

$$\mathbf{d} = q\mathbf{x} = -e\mathbf{x} \tag{4.20}$$

we finally obtain in dipole approximation:

$$\hat{H}'(\mathbf{x},t) = \hat{H}^{(0)}(\mathbf{x}) - \mathbf{d}\cdot\mathbf{E}(t)\,. \tag{4.21}$$

The result (4.21) means that the electromagnetic field only interacts with the electric field via a coupling to the electric dipole moment of the matter. As we have not yet specified explicitly in this derivation of the light-matter interaction whether the electric field is to be treated classically or quantum mechanically, this result holds in both cases.

4.2 Interaction of Atom with Classical Field

We first consider a classical field

$$\mathbf{E}(t) = \mathbf{E}_0 \cos(\omega t) \tag{4.22}$$

with amplitude $\mathbf{E}_0$ and frequency ω that is suddenly switched on at time $t = 0$. We assume that the atom at time $t = 0$ is in the initial state $\psi_i^{(0)}(\mathbf{x})$, which fulfills the time-independent Schrödinger equation:

$$\hat{H}^{(0)}(\mathbf{x})\psi_i^{(0)}(\mathbf{x}) = E_i^{(0)}\psi_i^{(0)}(\mathbf{x})\,. \tag{4.23}$$

For times $t > 0$ we expand the wave function $\psi(\mathbf{x}, t)$ with respect to all stationary states $\psi_n^{(0)}(\mathbf{x})$ due to their completeness (4.4):

$$\psi(\mathbf{x}, t) = \sum_n c_n(t)\, e^{-iE_n^{(0)}t/\hbar}\, \psi_n^{(0)}(\mathbf{x})\,. \tag{4.24}$$

Here, the time-dependent expansion amplitudes $c_n(t)$ satisfy the normalisation condition

$$\sum_n |c_n(t)|^2 = 1\,. \tag{4.25}$$

Inserting this ansatz into the time-dependent Schrödinger equation

$$i\hbar\,\frac{\partial\psi(\mathbf{x}, t)}{\partial t} = \left[\hat{H}^{(0)}(\mathbf{x}) + \hat{H}^{(\mathrm{p})}(t)\right]\psi(\mathbf{x}, t)\,, \tag{4.26}$$

where the perturbative Hamilton operator

$$\hat{H}^{(\mathrm{p})}(t) = -\mathbf{d}\cdot\mathbf{E}(t) \tag{4.27}$$

follows from (4.19), yields

$$\sum_n i\hbar\,\frac{\partial c_n(t)}{\partial t}\, e^{-iE_n^{(0)}t/\hbar}\, \psi_n^{(0)}(\mathbf{x}) = \sum_n c_n(t)\, e^{-iE_n^{(0)}t/\hbar}\, H^{(\mathrm{p})}(t)\psi_n^{(0)}(\mathbf{x})\,. \tag{4.28}$$

Taking into account the orthonormality (4.3) of the stationary states $\psi_n^{(0)}(\mathbf{x})$ then leads to coupled first-order ordinary differential equations for the time-dependent expansion coefficients

$$i\hbar\,\frac{\partial c_n(t)}{\partial t} = \sum_m e^{i\omega_{nm}^{(0)}t}\, H_{nm}^{(\mathrm{p})}(t)c_m(t) \tag{4.29}$$

with the matrix elements

$$H_{nm}^{(\mathrm{p})}(t) = \int d^3x\, \psi_n^{(0)*}(\mathbf{x})\hat{H}^{(\mathrm{p})}(t)\psi_m^{(0)}(\mathbf{x}) \tag{4.30}$$

and the transition frequencies

$$\omega_{nm} = \frac{E_n^{(0)} - E_m^{(0)}}{\hbar}\,. \tag{4.31}$$

As an initial condition we require that only the initial state i is occupied:

$$c_i(0) = 1\,; \qquad c_n(t) = 0\,, \text{ for } n \neq i\,. \tag{4.32}$$

As time progresses, the state i becomes less occupied, while the occupation of a previously unoccupied state f increases. The probability for a transition of the atom from state i to state f at time $t > 0$ is given by

$$P_{i\to f}(t) = |c_f(t)|^2\,. \tag{4.33}$$

The coupled equations (4.29) can only be solved analytically exactly in exceptional cases. Therefore, numerical or analytical approximative solution methods are generically used. In the case of time-dependent perturbation theory, it is assumed that the amplitude of the electric field and, thus, the perturbative Hamilton operator $\hat{H}^{(\mathrm{p})}(t)$ is small. Expanding the time-dependent amplitudes perturbatively

$$c_n(t) = c_n^{(0)}(t) + c_n^{(1)}(t) + c_n^{(2)}(t) + \dots\,, \tag{4.34}$$

then yields up to second order

$$\frac{\partial c_n^{(0)}(t)}{\partial t} = 0\,, \tag{4.35}$$

$$\frac{\partial c_n^{(1)}(t)}{\partial t} = -\frac{i}{\hbar}\sum_m e^{i\omega_{nm}t} H_{nm}^{(\mathrm{p})}(t) c_m^{(0)}(t)\,, \tag{4.36}$$

$$\frac{\partial c_n^{(2)}(t)}{\partial t} = -\frac{i}{\hbar}\sum_m e^{i\omega_{nm}t} H_{nm}^{(\mathrm{p})}(t) c_m^{(1)}(t)\,, \tag{4.37}$$

which can be solved iteratively. In zeroth order we get

$$c_n^{(0)}(t) = c_n^{(0)}(0) = \delta_{ni}\,, \tag{4.38}$$

while the first order results in

$$c_n^{(1)}(t) = -\frac{i}{\hbar}\int_0^t dt' e^{i\omega_{ni}t'} H_{ni}^{(\mathrm{p})}(t')\,. \tag{4.39}$$

Correspondingly follows for the second order

$$c_n^{(2)}(t) = \left(-\frac{i}{\hbar}\right)^2 \int_0^t dt' \int_0^{t'} dt'' \sum_m e^{i\omega_{nm}t'} H_{nm}^{(\mathrm{p})}(t') e^{i\omega_{mi}t''} H_{mi}^{(\mathrm{p})}(t'')\,. \tag{4.40}$$

The total transition probability from the initial state i to the final state f is determined from these expansion coefficients as follows:

$$P_{i\to f}(t) = \left| c_f^{(0)}(t) + c_f^{(1)}(t) + c_f^{(2)}(t) + \dots \right|^2\,. \tag{4.41}$$

The electric dipole moment (4.20) and, thus, the perturbed Hamilton operator (4.27) have odd parity, so that the diagonal matrix elements (4.30) vanish:

$$H_{nn}^{(\mathrm{p})}(t) = 0\,. \tag{4.42}$$

Therefore, the first-order correction (4.39) for the initial state i vanishes

$$c_i^{(1)}(t) = -\frac{i}{\hbar}\int_0^t dt' H_{ii}^{(\mathrm{p})}(t') = 0 \tag{4.43}$$

and results in $c_i(t) = c_i^{(0)}(t) = 1$ up to the first order. For the final state f, on the other hand, we get

$$c_f^{(1)}(t) = -\frac{i}{\hbar}\int_0^t dt' e^{i\omega_{fi}t'} H_{fi}^{(\mathrm{p})}(t') \,. \tag{4.44}$$

With the electric field (4.22) and the perturbed Hamilton operator (4.27) follows then

$$c_f^{(1)}(t) = \frac{i}{2\hbar}\,\mathbf{d}_{fi}\cdot\mathbf{E}_0 \int_0^t dt' \left[e^{i(\omega_{fi}+\omega)t'} + e^{i(\omega_{fi}-\omega)t'}\right] , \tag{4.45}$$

where the evaluation of the elementary integral yields

$$c_f^{(1)}(t) = \frac{1}{2\hbar}\,\mathbf{d}_{fi}\cdot\mathbf{E}_0 \left[\frac{e^{i(\omega_{fi}+\omega)t}-1}{\omega_{fi}+\omega} + \frac{e^{i(\omega_{fi}-\omega)t}-1}{\omega_{fi}-\omega}\right] \tag{4.46}$$

with the matrix element for the electric dipole moment of the electron (4.20)

$$\mathbf{d}_{fi} = -e\int d^3x\, \psi_f^{(0)*}(\mathbf{x})\,\mathbf{x}\,\psi_i^{(0)}(\mathbf{x}) \,. \tag{4.47}$$

In the case $\omega_{fi} > 0$ the second term dominates, as it is resonant. Thus, one can neglect the first term, as it is anti-resonant. This yields the so-called *rotating wave approximation*, which is ubiquitous in quantum optics:

$$c_f^{(1)}(t) = \frac{1}{2\hbar}\,\mathbf{d}_{fi}\cdot\mathbf{E}_0\,\frac{e^{i(\omega_{fi}-\omega)t}-1}{\omega_{fi}-\omega} \,. \tag{4.48}$$

Due to the initial condition $c_f^{(0)}(t) = 0$ we conclude that $c_f(t) = c_f^{(1)}(t)$ holds up to the first order and that the transition probability (4.41) is given in lowest order according to

$$P_{i\to f}(t) = \left|c_f^{(1)}(t)\right|^2 = \frac{\left|\mathbf{d}_{fi}\cdot\mathbf{E}_0\right|^2}{\hbar^2}\,\frac{\sin^2(\Delta t/2)}{\Delta^2} \,. \tag{4.49}$$

Here the detuning Δ is defined by the difference between the frequency ω of the electromagnetic field and the atomic frequency ω_{fi} for the transition from the initial and to the final state

$$\Delta = \omega - \omega_{fi} \,. \tag{4.50}$$

In the case of $\Delta > 0$ ($\Delta < 0$) one speaks of blue (red) detuning, whereas $\Delta = 0$ denotes the resonance case, see Fig. 4.1. At first we analyze the time dependence of the transition probability $P_{i\to f}(t)$ in (4.49). For a non-vanishing detuning, i.e. $\Delta \neq 0$, its maximum occurs at

$$\underset{t}{\mathrm{Max}}\;\; P_{i\to f}(t) = P_{i\to f}\left(\frac{\pi}{\Delta}\right) = \frac{\left|\mathbf{d}_{fi}\cdot\mathbf{E}_0\right|^2}{\hbar^2\Delta^2} \,. \tag{4.51}$$

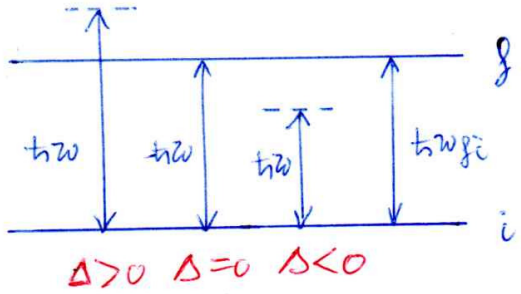

Figure 4.1: Definition of the detuning Δ between the light field frequency ω and the atomic transition frequency ω_{fi} according to (4.50).

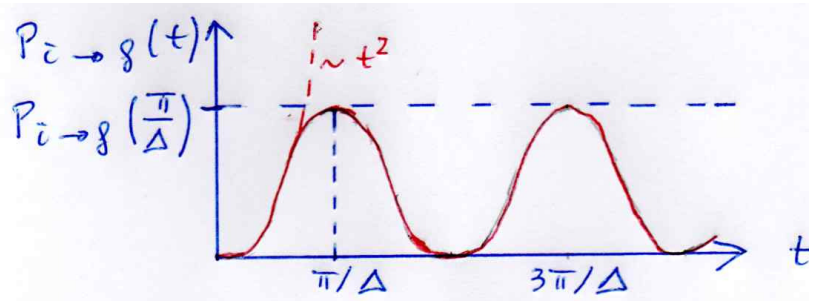

Figure 4.2: Time dependence of the transition probability (4.49).

In the resonance case $\Delta = 0$ we obtain instead that the transition probability (4.49) increases quadratically with time t:

$$P_{i\to f}(t) = \frac{|\mathbf{d}_{fi}\cdot\mathbf{E}_0|^2\, t^2}{4\hbar^2}\,, \tag{4.52}$$

see Fig. 4.2. However, in order that this perturbative treatment remains valid, we have to demand that $P_{i\to f}(t)$ must be small. In the non-resonant case $\Delta \neq 0$ this leads due to (4.51) to a minimal value for the absolute value of the detuning Δ, namely

$$\max_t\ P_{i\to f}(t) \ll 1 \qquad \Longrightarrow \qquad \frac{|\mathbf{d}_{fi}\cdot\mathbf{E}_0|}{\hbar} \ll |\Delta|\,, \tag{4.53}$$

while in the resonant case $\Delta = 0$ we read off from (4.52) that one is restricted to short times:

$$P_{i\to f}(t) \ll 1 \qquad \Longrightarrow \qquad t \ll \frac{2\hbar}{|\mathbf{d}_{fi}\cdot\mathbf{E}_0|}\,. \tag{4.54}$$

Considering the transition probability (4.49) as a function of the detuning Δ, we are reminded of a slit diffraction function, see Fig. 4.3. In particular, the transition probability $P_{i\to f}(t)$ has a sharp maximum at $\Delta = 0$ with a height proportional to t^2 and a width proportional to $1/t$. Thus, the area under the curve increases linearly with t:

$$\int_{-\infty}^{\infty} d\Delta\, \frac{\sin^2(\Delta t/2)}{\Delta^2} = \frac{t}{2}\int_{-\infty}^{\infty} dx\, \frac{\sin^2 x}{x^2} = \frac{\pi t}{2}\,. \tag{4.55}$$

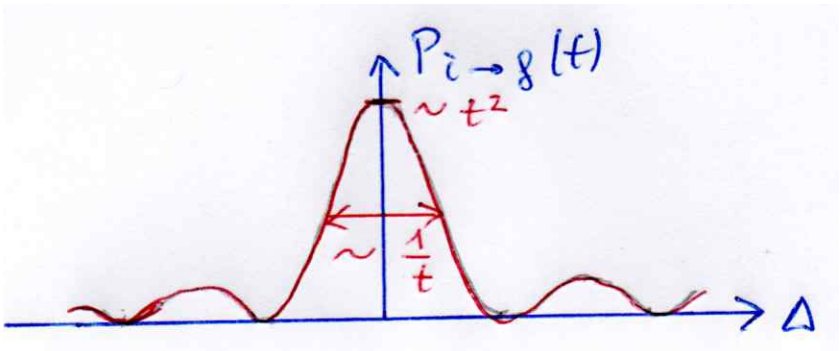

Figure 4.3: Dependence of the transition probability (4.49) as a function of the detuning Δ.

Here we applied the substitution $x(\Delta) = \Delta t/2$ and used the definite integral

$$\int_{-\infty}^{\infty} dx \, \frac{\sin^2 x}{x^2} = \pi \,, \tag{4.56}$$

which is derived in Appendix E. From Fig. 4.3 and (4.55) we then conclude the following representation of the delta function:

$$\lim_{t\to\infty} \frac{\sin^2(\Delta t/2)}{\Delta^2} = \frac{\pi t}{2}\, \delta(\Delta) \,. \tag{4.57}$$

Thus, taking into account the definition of the detuning in (4.50), the transition probability (4.49) converges in the long-time limit $t \to \infty$ towards a delta function:

$$P_{i\to f}(t) \to \frac{\pi t \, |\mathbf{d}_{fi} \cdot \mathbf{E}_0|^2}{2\hbar^2}\, \delta(\omega - \omega_{fi}) \,, \qquad t \to \infty \,. \tag{4.58}$$

This suggests to introduce in the long-time limit $t \to \infty$ a transition rate:

$$W_{i\to f} = \lim_{t\to\infty} \frac{P_{i\to f}(t)}{t} = \frac{\pi \, |\mathbf{d}_{fi} \cdot \mathbf{E}_0|^2}{2\hbar^2}\, \delta(\omega - \omega_{fi}) \,. \tag{4.59}$$

In practice, however, there will be several final states f, so that the respective transition rates have to be summed up, see Fig. 4.4:

$$W_{i\to[f]} = \frac{\pi}{2} \sum_{[f]} \frac{|\mathbf{d}_{fi} \cdot \mathbf{E}_0|^2}{\hbar^2}\, \delta(\omega - \omega_{fi}) \,. \tag{4.60}$$

This result is referred to in the literature as *Fermi's golden rule*. In practice, however, it can also be that the incoming light consists of different frequency components, so that the field amplitude $\mathbf{E}_0(\omega)$ becomes frequency dependent. In this case, we obtain for the transition rate

$$\frac{P_{i\to f}(t)}{t} = \frac{1}{\hbar^2} \int_{-\infty}^{\infty} d\omega \; |\mathbf{d}_{fi} \cdot \mathbf{E}_0(\omega)|^2 \; \frac{\sin^2[(\omega - \omega_{fi})t/2]}{(\omega - \omega_{fi})^2 t} \,. \tag{4.61}$$

Provided that $\mathbf{E}_0(\omega)$ is varying slowly, we obtain due to (4.57) in the limit $t \to \infty$ the transition rate

$$W_{i\to f} = \frac{\pi}{2\hbar^2} \, |\mathbf{d}_{fi} \cdot \mathbf{E}_0(\omega_{fi})|^2 \,. \tag{4.62}$$

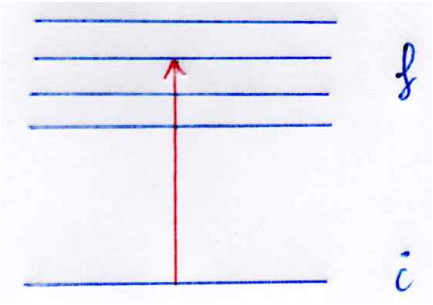

Figure 4.4: Summing the transition rates in (4.60) over all possible final states f.

4.3 Interaction of Atom with Quantised Field

For an atom interacting with a classical light field it does not matter whether the initial or the final state has a lower energy, i.e. the transition probabilities for an absorption or an emission of light coincide. But for the interaction of an atom with a quantised light field it turns out that the symmetry between absorption and emission of light is broken. In particular, an emission can occur even when no photons are present at all, i.e. in vacuum. This means that this so-called spontaneous emission is exclusively of quantum mechanical nature.

4.3.1 Einstein Elementary Processes

We start with considering the electric field strength (2.168) in second quantisation in vacuum, where we have continuous wave vectors $\mathbf{k}$. In a cavity with finite volume V, on the other hand, the wave vectors $\mathbf{k}$ are discrete. Thus, if we go over from the vacuum to a cavity with finite volume V, the following substitution rule applies:

$$\int d^3k \frac{1}{\sqrt{(2\pi)^3}} \qquad \Longrightarrow \qquad \sum_{\mathbf{k}} \frac{1}{\sqrt{V}} \,. \tag{4.63}$$

Furthermore, in the dipole approximation (4.18), the spatial dependence of the plane wave can be neglected as the wavelength is large in comparison with the atomic dimension, see Fig. 2.14. This reduces the quantised electric field strength (2.168) according to

$$\hat{\mathbf{E}}(t) = i \sum_{\lambda=\pm 1} \sum_{\mathbf{k}} \sqrt{\frac{\hbar\omega_{\mathbf{k}}}{2V\epsilon_0}} \left\{ \boldsymbol{\epsilon}(\mathbf{k},\lambda) e^{-i\omega_{\mathbf{k}} t} \hat{a}_{\mathbf{k},\lambda} - \boldsymbol{\epsilon}^*(\mathbf{k},\lambda) e^{i\omega_{\mathbf{k}} t} \hat{a}^\dagger_{\mathbf{k},\lambda} \right\} . \tag{4.64}$$

In the following, we limit ourselves for the sake of simplicity to a single mode and obtain

$$\hat{\mathbf{E}}(t) = i\boldsymbol{\epsilon}_0 \left(e^{-i\omega t} \hat{a} - e^{i\omega t} \hat{a}^\dagger \right) , \tag{4.65}$$

where the amplitude vector is given by

$$\boldsymbol{\epsilon}_0 = \sqrt{\frac{\hbar\omega}{2V\epsilon_0}}\, \boldsymbol{\epsilon} \,. \tag{4.66}$$

Note that we have omitted in this notation both the wave vector $\mathbf{k}$ and the polarization λ of the mode, which we consider. Furthermore, (4.65) represents the electric field strength operator in the Heisenberg picture. Accordingly, the interaction Hamiltonian (4.27) in the Schrödinger picture reads

$$\hat{H}^{(\mathrm{p})} = -i\mathbf{d}\cdot\boldsymbol{\epsilon}_0\,\left(\hat{a}-\hat{a}^\dagger\right)\,, \tag{4.67}$$

so it has no longer an explicit time dependence. The unperturbed Hamilton operator, however, is now composed of that of the atom $\hat{H}^{(0)}_{\mathrm{atom}}$ as in (4.1) and that of the light field

$$\hat{H}^{(0)}_{\mathrm{field}} = \hbar\omega\hat{a}^\dagger\hat{a}\,, \tag{4.68}$$

where the zero-point energy was omitted without loss of generality:

$$\hat{H}^{(0)} = \hat{H}^{(0)}_{\mathrm{atom}} + \hat{H}^{(0)}_{\mathrm{field}}\,. \tag{4.69}$$

The solutions of the unperturbed eigenvalue problem

$$\hat{H}^{(0)}\,|\psi^{(0)}\rangle = E^{(0)}\,|\psi^{(0)}\rangle \tag{4.70}$$

consist now of product states of atom and light

$$|\psi^{(0)}\rangle = |\psi^{(0)}_{\mathrm{atom}}\rangle\;|\psi^{(0)}_{\mathrm{field}}\rangle\;, \tag{4.71}$$

whereas the energy eigenvalues are correspondingly additive:

$$E^{(0)} = E^{(0)}_{\mathrm{atom}} + E^{(0)}_{\mathrm{field}}\,. \tag{4.72}$$

In particular, we are interested in the following unperturbed solutions. At first we characterize the initial state to consist of the atom being in some state a and n photons representing the field state:

$$|i^0\rangle = |a\rangle\,|n\rangle\;, \qquad\qquad E^{(0)}_i = E_a + n\hbar\omega\,. \tag{4.73}$$

Then we have two options for the final state, where the atom is in another state b. In case of $E_b > E_a$ and $E_b < E_a$ the process of a photon absorption and emission has occurred, so that the field state consists of $n-1$ and $n+1$ photons, respectively:

$$|f^{(0)}_1\rangle = |b\rangle\,|n-1\rangle\;, \qquad E^{(0)}_{f_1} = E_b + (n-1)\hbar\omega\,, \tag{4.74}$$

$$|f^{(0)}_2\rangle = |b\rangle\,|n+1\rangle\;, \qquad E^{(0)}_{f_2} = E_b + (n+1)\hbar\omega\,. \tag{4.75}$$

The perturbation theory of the previous section can now be applied as follows. The solution of the time-dependent Schrödinger equation

$$i\hbar\frac{\partial}{\partial t}\,|\psi(t)\rangle = \left[\hat{H}^{(0)} + \hat{H}^{(\mathrm{p})}\right]\,|\psi(t)\rangle \tag{4.76}$$

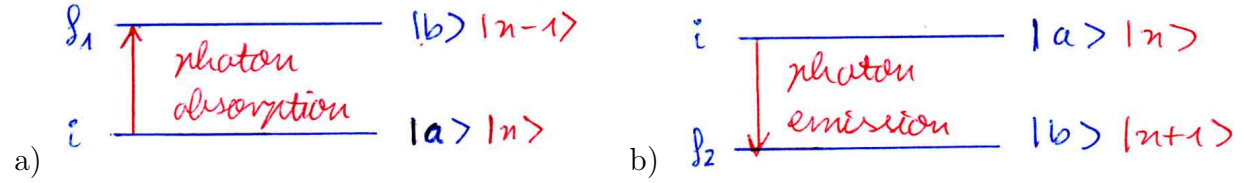

Figure 4.5: Elementary photon processes: a) Absorption of a photon for $\omega_{ba} > 0$ with $\omega = \omega_{ba}$. b) Emission of a photon for $\omega_{ba} = -|\omega_{ba}| < 0$ with $\omega = -\omega_{ba} = |\omega_{ba}|$.

reads

$$\begin{aligned} |\psi(t)\rangle &= c_i(t)\,|a\rangle\,|n\rangle\,e^{-i(E_a+n\hbar\omega)t/\hbar} \\ &\quad + c_{f_1}(t)\,|b\rangle\,|n-1\rangle\,e^{-i[E_b+(n-1)\hbar\omega]t/\hbar} + c_{f_2}(t)\,|b\rangle\,|n+1\rangle\,e^{-i[E_b+(n+1)\hbar\omega]t/\hbar}\,, \end{aligned} \tag{4.77}$$

where the initial condition $|\psi(0)\rangle = |a\rangle\,|n\rangle$ leads in zeroth order to the coefficients

$$c_i(0) = c_i^{(0)}(t) = 1\,, \qquad c_{f_1}(0) = c_{f_1}^{(0)}(t) = 0\,, \qquad c_{f_2}(0) = c_{f_2}^{(0)}(t) = 0\,. \tag{4.78}$$

In first order perturbation theory we then obtain for the transitions according to (4.44):

$$c_{f_1}^{(1)}(t) = -\frac{i}{\hbar}\int_0^t dt'\,e^{iE_{f_1 i}^{(0)}t'/\hbar}\,H_{f_1 i}^{(\mathrm{p})}(t')\,, \tag{4.79}$$

$$c_{f_2}^{(1)}(t) = -\frac{i}{\hbar}\int_0^t dt'\,e^{iE_{f_2 i}^{(0)}t'/\hbar}\,H_{f_2 i}^{(\mathrm{p})}(t')\,. \tag{4.80}$$

Here we obtain from (4.73)–(4.75) both the energy differences

$$E_{f_1 i}^{(0)} = E_{f_1}^{(0)} - E_i^{(0)} = [E_b + (n-1)\hbar\omega] - (E_a + n\hbar\omega) = E_b - E_a - \hbar\omega\,, \tag{4.81}$$

$$E_{f_2 i}^{(0)} = E_{f_2}^{(0)} - E_i^{(0)} = [E_b + (n+1)\hbar\omega] - (E_a + n\hbar\omega) = E_b - E_a + \hbar\omega \tag{4.82}$$

and the matrix elements of (4.67)

$$H_{f_1 i}^{(\mathrm{p})}(t) = \langle f_1^{(0)}|\hat{H}^{(\mathrm{p})}(t)|i\rangle = \langle b|\,\langle n-1|\,(-i)\mathbf{d}\cdot\boldsymbol{\epsilon}_0\left(\hat{a}-\hat{a}^\dagger\right)|a\rangle\,|n\rangle = -i\mathbf{d}_{ba}\cdot\boldsymbol{\epsilon}_0\sqrt{n}\,, \tag{4.83}$$

$$H_{f_2 i}^{(\mathrm{p})}(t) = \langle f_2^{(0)}|\hat{H}^{(\mathrm{p})}(t)|i\rangle = \langle b|\,\langle n+1|\,(-i)\mathbf{d}\cdot\boldsymbol{\epsilon}_0\left(\hat{a}-\hat{a}^\dagger\right)|a\rangle\,|n\rangle = i\mathbf{d}_{ba}\cdot\boldsymbol{\epsilon}_0\sqrt{n+1} \tag{4.84}$$

with the dipole matrix element

$$\mathbf{d}_{ba} = \langle b|\,\mathbf{d}\,|a\rangle\,. \tag{4.85}$$

Thus, (4.79) and (4.80) describe the absorption and the emission of a photon respectively, see Fig. 4.5. For large photon numbers n, the matrix elements of absorption (4.83) and emission (4.84) are equal. This corresponds to the classical limiting case of the previous section. But for small photon numbers n the matrix elements of absorption (4.83) and emission (4.84) are different. In the extreme case of the vacuum, when there are no photons at all, i.e. $n = 0$, even no absorption occurs but the so-called spontaneous emission is still present. Thus, in the factor $\sqrt{n+1}$ of the matrix element of emission (4.84) one distinguishes between the term n, which

describes the induced emission, and the term 1, which is due to the spontaneous emission. Note that the induced emission plays an important role, for example, for the LASER, which is an acronym for Light Amplification by Stimulated Emission of Radiation.

We consider now the probability amplitude for the atomic transition from $|a\rangle$ to $|b\rangle$, i.e. $c_f^{(1)}(t) = c_{f_1}^{(1)}(t) + c_{f_2}^{(1)}(t)$, and obtain from (4.79)–(4.84)

$$c_f^{(1)}(t) = -\frac{i}{\hbar} i\mathbf{d}_{ba} \cdot \boldsymbol{\epsilon}_0 \left[\sqrt{n+1} \int_0^t dt' \, e^{i(\omega_{ba}+\omega)t'} - \sqrt{n} \int_0^t dt' \, e^{i(\omega_{ba}-\omega)t'} \right] \tag{4.86}$$

with the corresponding atomic transition frequency

$$\omega_{ba} = \frac{E_b - E_a}{\hbar} \, . \tag{4.87}$$

An evaluation of the integrals yields:

$$c_f^{(1)}(t) = -\frac{i}{\hbar} \, \mathbf{d}_{ba} \cdot \boldsymbol{\epsilon}_0 \left[\sqrt{n+1} \, \frac{e^{i(\omega_{ba}+\omega)t} - 1}{\omega_{ba} + \omega} - \sqrt{n} \, \frac{e^{i(\omega_{ba}-\omega)t} - 1}{\omega_{ba} - \omega} \right] . \tag{4.88}$$

We observe that two resonances $\omega_{ba} \pm \omega = 0$ occur. The first term in (4.88) corresponds to the resonance $\omega_{ba} + \omega = 0$ and occurs for the emission, whereas the second term is resonant for $\omega_{ba} - \omega = 0$ and describes the absorption, see Fig. 4.5. Furthermore, we recognize for the case $\omega \approx \omega_{ba}$ that the absorption dominates and the emission can be neglected, whereas, conversely, for the case of $\omega \approx -\omega_{ba}$ the emission dominates and the absorption can be neglected.

The comparison with the classical result of the previous section for large photon numbers n shows the following useful correspondence. The classical amplitude $\mathbf{E}_0$ in (4.48) corresponds due to the rotating wave approximation and (4.88) in case of the absorption to the quantum mechanical expression

$$\mathbf{E}_{0,\text{abs.}} = 2i\sqrt{n}\boldsymbol{\epsilon}_0 \, , \tag{4.89}$$

whereas for the emission holds

$$\mathbf{E}_{0,\text{emis.}} = -2i\sqrt{n+1}\boldsymbol{\epsilon}_0 \, . \tag{4.90}$$

With this correspondence at hand Fermi's golden rule can directly be transferred to the quantized light field. For instance, for slowly varying amplitudes $\boldsymbol{\epsilon}_0(\omega)$ we obtain for the transition rates (4.62) of absorption and emission the ratio

$$\frac{W_{\text{abs.}}}{W_{\text{emis.}}} = \frac{|\mathbf{d}_{ba} \cdot \mathbf{E}_{0,\text{abs.}}|^2}{|\mathbf{d}_{ba} \cdot \mathbf{E}_{0,\text{emis.}}|^2} = \frac{n}{n+1} \, . \tag{4.91}$$

Thus we conclude that the emission rate is always larger than the absorption rate.

4.3.2 Derivation of Spontaneous Emission Rate

We derived in (4.59) in the long-time limit $t \to \infty$ the transition rate $W_{i\to f}$ for one field mode in form of Fermi's golden rule, which contains the classical electric field strength $\mathbf{E}_0$. According to (4.66) and (4.90) the amplitude of the quantized electric field in vacuum, where we have $n = 0$, corresponds to the classical electric field strength for spontaneous emission:

$$\mathbf{E}_{0,\text{spon.emis.}} = -2i\sqrt{\frac{\hbar\omega}{2V\epsilon_0}}\,\boldsymbol{\epsilon}\,. \tag{4.92}$$

Inserting (4.92) into (4.59) and summing over the degrees of freedom $\mathbf{k}$ and λ of the quantised light field, which have been omitted temporarily in order to simplify the notation, we obtain for the spontaneous emission rate

$$W_{\text{spon.emis.}} = \sum_{\mathbf{k}}\sum_{\lambda} \frac{\pi\omega_{\mathbf{k}}\left|\mathbf{d}_{fi}\cdot\boldsymbol{\epsilon}(\mathbf{k},\lambda)\right|^2}{V\hbar\epsilon_0}\,\delta(\omega_{\mathbf{k}}-\omega_{fi})\,. \tag{4.93}$$

In the continuum limit we take into account the substitution rule (4.63), so the sum over all wave vectors $\mathbf{k}$ in (4.93) becomes the integral

$$W_{\text{spon.emis.}} = \int \frac{d^3k}{(2\pi)^3}\sum_{\lambda} \frac{\pi\omega_{\mathbf{k}}\left|\mathbf{d}_{fi}\cdot\boldsymbol{\epsilon}(\mathbf{k},\lambda)\right|^2}{\hbar\epsilon_0}\,\delta(\omega_{\mathbf{k}}-\omega_{fi})\,. \tag{4.94}$$

Due to the linear dispersion (2.73) the three-dimensional integral can be calculated in spherical coordinates as follows:

$$W_{\text{spon.emis.}} = \sum_{\lambda}\int_0^\infty d\omega\,\frac{\omega^2}{8\pi^3c^3}\int_0^\pi d\vartheta\,\sin\vartheta\int_0^{2\pi}d\varphi\,\frac{\pi\omega\left|\mathbf{d}_{fi}\cdot\boldsymbol{\epsilon}(\mathbf{k},\lambda)\right|^2}{\hbar\epsilon_0}\,\delta(\omega-\omega_{fi})\,. \tag{4.95}$$

The frequency integral can be calculated exactly due to the delta function:

$$W_{\text{spon.emis.}} = \frac{\omega_{fi}^3}{8\pi^2\hbar\epsilon_0c^3}\int_0^\pi d\vartheta\,\sin\vartheta\int_0^{2\pi}d\varphi\sum_{\lambda}\left|\mathbf{d}_{fi}\cdot\boldsymbol{\epsilon}(\mathbf{k},\lambda)\right|^2\,. \tag{4.96}$$

The sum over all polarization degrees of freedom gives:

$$\sum_{\lambda}\left|\mathbf{d}_{fi}\cdot\boldsymbol{\epsilon}(\mathbf{k},\lambda)\right|^2 = (d_{fi})_k(d_{fi})_l\sum_{\lambda}\epsilon_k(\mathbf{k},\lambda)\epsilon_l^*(\mathbf{k},\lambda)\,. \tag{4.97}$$

As both polarization vectors $\boldsymbol{\epsilon}(\mathbf{k},\lambda)$ and the direction of propagation $\mathbf{k}/k$ represent a basis in the three-dimensional configuration space, we conclude from their completeness relation

$$\sum_{\lambda}\left|\mathbf{d}_{fi}\cdot\boldsymbol{\epsilon}(\mathbf{k},\lambda)\right|^2 = (d_{fi})_k(d_{fi})_l\left(\delta_{kl}-\frac{k_kk_l}{k^2}\right) = \mathbf{d}_{fi}^2-\frac{(\mathbf{d}_{fi}\cdot\mathbf{k})^2}{k^2}\,. \tag{4.98}$$

This result can also directly be obtained by using the explicit representation of the polarisation vectors from (2.116):

$$\begin{aligned}
&\sum_\lambda \epsilon_k(\mathbf{k},\lambda)\epsilon_l^*(\mathbf{k},\lambda) = \epsilon_k(\mathbf{k},+1)\epsilon_l^*(\mathbf{k},+1) + \epsilon_k(\mathbf{k},-1)\epsilon_l^*(\mathbf{k},-1) \\
&= \frac{1}{2}\begin{pmatrix} \cos\vartheta\cos\varphi + i\sin\varphi \\ \cos\vartheta\sin\varphi - i\cos\varphi \\ -\sin\vartheta \end{pmatrix} (\cos\vartheta\cos\varphi - i\sin\varphi\,,\, \cos\vartheta\sin\varphi + i\cos\varphi\,,\, -\sin\vartheta) + \text{c.c} \\
&= \begin{pmatrix} 1 & 0 & 0 \\ 0 & 1 & 0 \\ 0 & 0 & 0 \end{pmatrix} - \begin{pmatrix} \sin^2\vartheta\cos^2\varphi & \sin^2\vartheta\sin\varphi\cos\varphi & \sin\vartheta\cos\vartheta\cos\varphi \\ \sin^2\vartheta\sin\varphi\cos\varphi & \sin^2\vartheta\sin^2\varphi & \sin\vartheta\cos\vartheta\sin\varphi \\ \sin\vartheta\cos\vartheta\cos\varphi & \sin\vartheta\cos\vartheta\sin\varphi & \cos^2\vartheta \end{pmatrix} . \qquad (4.99)
\end{aligned}$$

Without loss of generality, we now assume that the electric dipole moment points in z-direction, i.e.

$$\mathbf{d}_{fi} = d_{fi}\mathbf{e}_z\,, \qquad (4.100)$$

so that (4.98) reduces to

$$\sum_\lambda |\mathbf{d}_{fi}\cdot\boldsymbol{\epsilon}(\mathbf{k},\lambda)|^2 = d_{fi}^2\left(1-\cos^2\vartheta\right) = d_{fi}^2\sin^2\vartheta\,. \qquad (4.101)$$

The remaining angular integrals lead to the following expression for the rate of spontaneous emission:

$$W_{\text{spon.emis.}} = \frac{\omega_{fi}^3 d_{fi}^2}{4\pi\hbar\epsilon_0 c^3}\int_0^\pi d\vartheta\,\sin^3\vartheta = \frac{\omega_{fi}^3 d_{fi}^2}{12\pi\hbar\epsilon_0 c^3}\Big[-2\cos\vartheta - \cos\vartheta\sin^2\vartheta\Big]_0^\pi = \frac{\omega_{fi}^3 d_{fi}^2}{3\pi\hbar\epsilon_0 c^3}\,. \qquad (4.102)$$

Thus it depends on the properties of the initial and the final atomic state via the cubic power of the atomic frequency ω_{fi} defined in (4.31) and the square of the electric dipole moment d_{fi}.

4.3.3 Calculation of Spontaneous Emission Rate

At first, we estimate the order of magnitude of this spontaneous emission rate. To this end we approximate the electric dipole moment according to $d_{fi} \sim e a_{\text{B}}$ with the Bohr radius a_{B}, which is introduced in (C.8), and the atomic frequency ω_{fi}, which is estimated to be of the order $\alpha^2 c/\lambda_{\text{C}}$ according to (C.16). With this and taking into account the Sommerfeld fine-structure constant (C.11) we get for the spontaneous emission rate (4.102):

$$W_{\text{spon.emis.}} \sim \frac{\alpha^4}{\lambda_{\text{C}}^2}\,\frac{e^2 a_{\text{B}}^2}{\hbar\epsilon_0 c}\,\omega_{fi} \sim \alpha^3\,\omega_{fi} \sim 10^{-6}\,\omega_{fi}\,. \qquad (4.103)$$

This means that the spontaneous emission rate is quite small in comparison with the resonance frequency ω_{fi}. Only after 10^6 orbits of the electron around the hydrogen atom does the spontaneous emission occur. The lifetime is therefore of the order

$$\tau \sim \frac{1}{W_{\text{spon.emis.}}} \sim \frac{10^6}{10^3\,\text{THz}} = \frac{10^6}{10^3\cdot 10^{12}}\,\text{s} = 10^{-9}\,\text{s} = 1\,\text{ns}\,. \qquad (4.104)$$

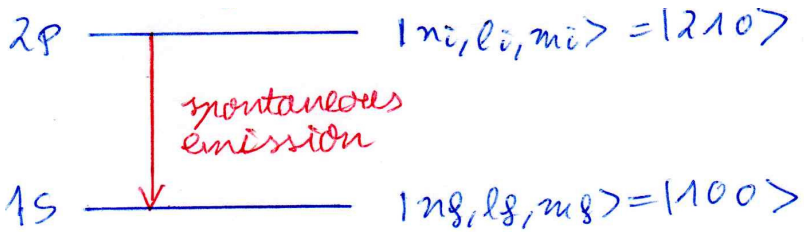

Figure 4.6: Spontaneous transition from the 2p to the 1s-state of the hydrogen atom in accordance with the selection rules (4.106).

Let us now look at a concrete example for a spontaneous emission process. For this purpose we recall the selection rules for electric dipole transitions in the hydrogen atom. They follow from the dipole matrix elements

$$\mathbf{d}_{fi} = e \int d^3x \, \psi^*_{n_f l_f m_f}(\mathbf{x}) \, \mathbf{x} \, \psi_{n_i l_i m_i}(\mathbf{x}) \,, \tag{4.105}$$

where $\psi_{nlm}(\mathbf{x})$ denote the wave function of the electron in the hydrogen atom in spherical coordinates with the main quantum number n, the angular quantum number l, and the magnetic quantum number m. In Appendix F we prove that the z-component of the dipole matrix elements (4.105) is different from zero only provided that the selection rules

$$\Delta l = l_f - l_i = \pm 1 \,, \qquad \Delta m = m_f - m_i = 0 \tag{4.106}$$

are fulfilled. As a concrete example for the selection rules (4.106) we determine the lifetime of the 2p-state with $m = 0$ in the hydrogen atom against the decay into the 1s-state as depicted in Fig. 4.6, where we have $\Delta l = -1$ and $\Delta m = 0$. Thus, the wave functions being involved in the transition have the explicit form [40, Tab. 9.1]

$$\psi_{210}(r, \vartheta, \varphi) = \frac{1}{8\sqrt{\pi a_{\mathrm{B}}^3}} \frac{r}{a_{\mathrm{B}}} \, e^{-r/2a_{\mathrm{B}}} \sqrt{2} \cos\vartheta \,, \tag{4.107}$$

$$\psi_{100}(r, \vartheta, \varphi) = \frac{1}{\sqrt{\pi a_{\mathrm{B}}^3}} \, e^{-r/a_{\mathrm{B}}} \,. \tag{4.108}$$

Taking into account the energy eigenvalues of the hydrogen atom (C.12), the corresponding frequency for this transition is given by

$$\omega_{fi} = \frac{E_{2\mathrm{p}} - E_{1\mathrm{s}}}{\hbar} = \frac{\mathrm{Ry}}{\hbar} \left(-\frac{1}{4} + 1 \right) = \frac{3\mathrm{Ry}}{4\hbar} = \frac{3Mc^2}{8\hbar} \, \alpha^2 \,, \tag{4.109}$$

where we have used (C.14) in the last step.

Now we calculate the dipole matrix element $\mathbf{d}_{fi} = e z_{fi} \mathbf{e}_z$ with the matrix element

$$z_{fi} = \int d^3x \, \psi^*_{100}(r, \vartheta, \varphi) \, z \, \psi_{210}(r, \vartheta, \varphi) \,. \tag{4.110}$$

Inserting therein the respective wave functions (4.107), (4.108) we get

$$z_{fi} = \int_0^\infty dr r^2 \int_0^\pi d\vartheta \, \sin\vartheta \int_0^{2\pi} d\varphi \, \frac{1}{8\sqrt{\pi a_{\mathrm{B}}^3}} \frac{r}{a_{\mathrm{B}}} \, e^{-r/2a_{\mathrm{B}}} \sqrt{2} \cos\vartheta \, r \cos\vartheta \, \frac{1}{\sqrt{\pi a_{\mathrm{B}}^3}} \, e^{-r/a_{\mathrm{B}}} \,. \tag{4.111}$$

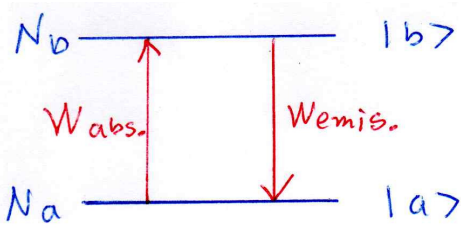

Figure 4.7: Emission and absorption processes between the states $|a\rangle\,, |b\rangle$ determine the number of atoms N_a, N_b according to the classical rate equations (4.115), (4.116).

Evaluating both the angular and the radial integrals yields

$$z_{fi} = 4\sqrt{2}\left(\frac{2}{3}\right)^5 a_{\mathrm{B}}\,. \tag{4.112}$$

Inserting (4.109) and $\mathbf{d}_{fi} = e z_{fi}\mathbf{e}_z$ with (4.112) into (4.102) yields the spontaneous emission rate for this specific decay:

$$W_{2\mathrm{p}\to 1\mathrm{S}} = 8\left(\frac{2}{3}\right)^8 \frac{c\alpha^4}{a_{\mathrm{B}}} = 5\cdot 10^9\,\frac{1}{\mathrm{s}}\,. \tag{4.113}$$

This means that the lifetime of the 2p-state compared to the spontaneous decay into the 1s-state amounts to 0.2 ns, which is compatible with the previous estimate of the order of magnitude in (4.104).

4.3.4 Planck Radiation Formula

With the obtained knowledge we are now in a position to rederive the back-body radiation formula of Max Planck in (3.303) from a different point of view. To this end we assume that the atoms in the walls of the black body, see Fig. 3.10b), interact resonantly with the quantised light field, i.e. the frequency ω of the light field coincides with the transition frequency (4.87):

$$\omega = \frac{E_b - E_a}{\hbar}\,. \tag{4.114}$$

Denoting with N_a, N_b the number of atoms in the states $|a\rangle\,, |b\rangle$ and representing the absorption and emission rates by $W_{\mathrm{abs.}}$ and $W_{\mathrm{emis.}}$, respectively, we can write down classical rate equations according to Fig. 4.7 as follows:

$$\frac{dN_a}{dt} = -W_{\mathrm{abs.}}N_a + W_{\mathrm{emis.}}N_b\,, \tag{4.115}$$

$$\frac{dN_b}{dt} = W_{\mathrm{abs.}}N_a - W_{\mathrm{emis.}}N_b\,. \tag{4.116}$$

Thus, the total number of atoms is conserved with time, i.e. an increase of the number of atoms in state $|a\rangle$ corresponds to a decrease of the number of atoms in state $|b\rangle$ and vice versa:

$$\frac{dN_a}{dt} = -\frac{dN_b}{dt}\,. \tag{4.117}$$

For the steady state then follows from (4.115) and (4.116):

$$\frac{dN_a}{dt} = \frac{dN_b}{dt} = 0 \qquad \Longrightarrow \qquad \frac{N_a}{N_b} = \frac{W_{\text{emis.}}}{W_{\text{abs.}}} \,. \tag{4.118}$$

In thermal equilibrium, the different occupations of the states N_a, N_b are given by a Boltzmann distribution according to $N_a \sim e^{-E_a/k_{\text{B}}T}$, $N_b \sim e^{-E_b/k_{\text{B}}T}$, so we have with the resonance condition (4.114)

$$\frac{N_a}{N_b} = e^{(E_b - E_a)/k_{\text{B}}T} = e^{\hbar\omega/k_{\text{B}}T} \,, \tag{4.119}$$

On the other hand, we have obtained in (4.91) the result that the ratio of absorption and emission rate is determined by the photon number n. Thus, combining the equations (4.91) and (4.119) yields the Bose-Einstein distribution (3.281) with n representing the average photon number:

$$n + 1 = n e^{\hbar\omega/k_{\text{B}}T} \qquad \Longrightarrow \qquad n = \frac{1}{e^{\hbar\omega/k_{\text{B}}T} - 1} \,. \tag{4.120}$$

We now compare this derivation with the corresponding one of Albert Einstein from 1916. Here, the spontaneous and induced emission as well as the absorption are considered as the elementary processes for the interaction of light and matter, which are characterized by corresponding rate coefficients A, B, and C. The rate equation for the occupation of $|a\rangle$ then reads

$$\frac{dN_a}{dt} = \left[A + BU(\omega)\right] N_b - CU(\omega) N_a \,, \tag{4.121}$$

where the energy density $U(\omega)$ in the cavity enhances both the induced emission rate and the absorption rate. Furthermore, due to the conservation of the total number of atoms (4.117), the rate equation for the occupation of $|b\rangle$ then follows as

$$\frac{dN_b}{dt} = -\left[A + BU(\omega)\right] N_b + CU(\omega) N_a \,. \tag{4.122}$$

The equilibrium is then characterized by

$$\left[A + BU(\omega)\right] N_b = CU(\omega) N_a \qquad \Longrightarrow \qquad \frac{N_a}{N_b} = \frac{A + BU(\omega)}{CU(\omega)} = e^{\hbar\omega/k_{\text{B}}T} \,, \tag{4.123}$$

where we have assumed again (4.119). Thus, the energy density is determined according to

$$A + BU(\omega) = CU(\omega) e^{\hbar\omega/k_{\text{B}}T} \qquad \Longrightarrow \qquad U(\omega) = \frac{A/B}{e^{\hbar\omega/k_{\text{B}}T} C/B - 1} \,. \tag{4.124}$$

A comparison of the energy density (4.124) with the Planck radiation formula (3.303) then yields the following conclusions:

- The induced emission rate $BU(\omega)$ and the absorption rate $CU(\omega)$ coincide, so the Einstein coefficients B and C are equal:

$$B = C \,. \tag{4.125}$$

- The ratio of the Einstein coefficients for spontaneous and induced emission is determined by

$$\frac{A}{B} = \frac{\hbar\omega^3}{\pi c^3}\,. \tag{4.126}$$

Thus, taking into account (3.303) and (4.126), the ratio of the spontaneous and the induced emission rates leads to

$$\frac{A}{BU(\omega)} = e^{\hbar\omega/k_{\mathrm{B}}T} - 1\,. \tag{4.127}$$

For the temperature $T = 6000\,\mathrm{K}$ at the surface of the sun the wavelengths 400 nm and 700 nm yield for the ratio (4.127) the values 400 and 30, respectively. Thus, in that case the spontaneous emission rate dominates the induced emission rate.

4.4 Rabi Model

In the perturbative treatment of the light-matter interaction one assumes that the occupation of the atomic initial state does not change and that the probability amplitude for the transition to another atomic state remains to be small. These assumptions are certainly justified as long as the amplitude of the light field is not too large. On the other hand, shining in a strong laser field with a frequency, that is resonant to an atomic transition, certainly leads to a large population transfer. In this case, one cannot apply perturbation theory. Instead, one limits oneself to two atomic states and treats their interaction with the light field exactly. In the case of a classical light field, one speaks of the Rabi model, since it was introduced by Isidor Isaac Rabi in the context of magnetic resonance.

4.4.1 Treatment of Rabi Model

We approximate an atom by a two-level system, which consists according to Fig. 4.8 of the ground state of energy E_g and an excited state of energy E_e, so that the atomic transition frequency is given by

$$\omega_0 = \frac{E_e - E_g}{\hbar}\,. \tag{4.128}$$

Provided that the atom is irradiated with a light field of the frequency ω, this leads to the detuning

$$\Delta = \omega - \omega_0\,. \tag{4.129}$$

The underlying Hamiltonian decomposes according to

$$\hat{H}(t) = \hat{H}^{(0)} + \hat{H}^{(p)}(t)\,. \tag{4.130}$$

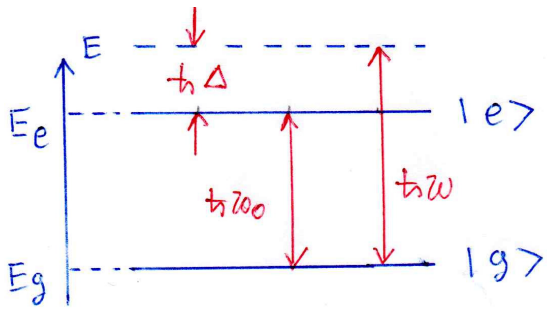

Figure 4.8: Sketch of Rabi model containing the two energies E_g, E_e as well as the atomic transition frequency (4.128), the light frequency ω, and the dentuning (4.129).

Here the Hamiltonian of the two-level system reads

$$\hat{H}^{(0)} = E_g \left|g\right\rangle \left\langle g\right| + E_e \left|e\right\rangle \left\langle e\right| \,, \tag{4.131}$$

where the states $|g\rangle$, $|e\rangle$ are supposed to be orthonormal:

$$\langle g|g\rangle = 1 = \langle e|e\rangle \,, \qquad \langle g|e\rangle = 0 = \langle e|g\rangle \,. \tag{4.132}$$

And the Hamiltonian, which describes the interaction of this two-level system with the light field, is given in dipole approximation due to (4.21) by

$$\hat{H}^{(p)}(t) = \hat{V}_0 \cos(\omega t) \,, \qquad \hat{V}_0 = -\hat{\mathbf{d}} \cdot \mathbf{E}_0 \,. \tag{4.133}$$

Accordingly, the time-dependent Schrödinger equation must be solved:

$$i\hbar \frac{\partial}{\partial t} \left|\psi(t)\right\rangle = \left[\hat{H}^{(0)} + \hat{H}^{(p)}(t)\right] \left|\psi(t)\right\rangle \,. \tag{4.134}$$

Since only two atomic levels are considered, the general ansatz for the wave function is of the form

$$\left|\psi(t)\right\rangle = c_g(t) e^{-iE_g t/\hbar} \left|g\right\rangle + c_e(t) e^{-iE_e t/\hbar} \left|e\right\rangle \,. \tag{4.135}$$

In case that the system is in the state $|g\rangle$ at time $t = 0$, the initial conditions read

$$c_g(0) = 1 \,, \qquad c_e(0) = 0 \,. \tag{4.136}$$

Inserting the ansatz (4.135) into the time-dependent Schrödinger equation (4.134) we obtain

$$\begin{aligned} & i\hbar \frac{\partial c_g(t)}{\partial t} \, e^{-iE_g t/\hbar} \left|g\right\rangle + i\hbar \frac{\partial c_e(t)}{\partial t} \, e^{-iE_e t/\hbar} \left|e\right\rangle \\ & = c_g(t) \hat{V}_0 \cos(\omega t) \, e^{-iE_g t/\hbar} \left|g\right\rangle + c_e(t) \hat{V}_0 \cos(\omega t) \, e^{-iE_e t/\hbar} \left|e\right\rangle \,. \end{aligned} \tag{4.137}$$

Multiplying with $\langle g|$ and $\langle e|$ projects (4.137) to the corresponding contributions of the ground and the excited state, respectively. As a result we obtain a closed system of two first-order differential equations, which determine the dynamics of the expansion coefficients $c_g(t)$, $c_g(t)$:

$$i\hbar \frac{\partial c_g(t)}{\partial t} = \cos(\omega t) \left[\left\langle g\right| \hat{V}_0 \left|g\right\rangle c_g(t) + \left\langle g\right| \hat{V}_0 \left|e\right\rangle e^{-i(E_e - E_g)t/\hbar} \, c_e(t)\right] \,, \tag{4.138}$$

$$i\hbar \frac{\partial c_e(t)}{\partial t} = \cos(\omega t) \left[\left\langle e\right| \hat{V}_0 \left|g\right\rangle e^{i(E_e - E_g)t/\hbar} \, c_g(t) + \left\langle e\right| \hat{V}_0 \left|e\right\rangle c_e(t)\right] \,. \tag{4.139}$$

For symmetry reasons the matrix elements of the interaction with the same states disappear

$$\langle g|\,\hat{V}_0\,|g\rangle = 0 = \langle e|\,\hat{V}_0\,|e\rangle\ , \tag{4.140}$$

and for the non-vanishing matrix elements we introduce for brevity the abbreviations

$$V_{0eg} = \langle e|\,\hat{V}_0\,|g\rangle\ , \qquad V_{0ge} = \langle g|\,\hat{V}_0\,|e\rangle\ . \tag{4.141}$$

Furthermore, we conclude from the hermiticity of the interaction (4.133), i.e. $\hat{V}_0 = \hat{V}_0^\dagger$:

$$V_{0ge} = \langle \hat{V}_0 e|g\rangle^* = \langle e|\,\hat{V}_0\,|g\rangle^* = V_{0eg}^*\,. \tag{4.142}$$

Taking also the transition frequency (4.128) into account, the system of differential equations, which has finally to be solved, reads:

$$i\hbar\,\frac{\partial c_g(t)}{\partial t} = V_{0eg}^*\,\cos(\omega t)\,e^{-i\omega_0 t}\,c_e(t)\,, \tag{4.143}$$

$$i\hbar\frac{\partial c_e(t)}{\partial t} = V_{0eg}\,\cos(\omega t)\,e^{i\omega_0 t}\,c_g(t)\,. \tag{4.144}$$

It can be straight-forwardly transformed into

$$\dot{c}_g(t) = -\frac{i}{2\hbar}\,V_{0eg}^*\left[e^{i(\omega-\omega_0)t} + e^{-i(\omega+\omega_0)t}\right]c_e(t)\,, \tag{4.145}$$

$$\dot{c}_e(t) = -\frac{i}{2\hbar}\,V_{0eg}\left[e^{i(\omega+\omega_0)t} + e^{-i(\omega-\omega_0)t}\right]c_g(t)\,. \tag{4.146}$$

In the vicinity of the resonance $\omega \approx \omega_0$ we recognize that there is, on the one hand, a slow time dependence due to the term $e^{\pm i(\omega-\omega_0)t}$ and, on the other hand, a fast time dependence due to the term $e^{\pm i(\omega+\omega_0)t}$. The latter is neglected within the framework of the rotating wave approximation, yielding:

$$\dot{c}_g(t) = -\frac{i}{2\hbar}\,V_{0eg}^*\,e^{i(\omega-\omega_0)t}\,c_e(t)\,, \tag{4.147}$$

$$\dot{c}_e(t) = -\frac{i}{2\hbar}\,V_{0eg}\,e^{-i(\omega-\omega_0)t}\,c_g(t)\,. \tag{4.148}$$

Now the expansion coefficient $c_g(t)$ is eliminated, resulting in a single differential equation of second order with constant coefficients for $c_e(t)$:

$$\ddot{c}_e(t) + i(\omega-\omega_0)\dot{c}_e(t) + \frac{|V_{0eg}|^2}{4\hbar^2}c_e(t) = 0\,. \tag{4.149}$$

The exponential solution ansatz $c_e(t) = e^{\lambda t}$ then leads to the characteristic equation

$$\lambda^2 + i\Delta\lambda + \frac{|V_{0eg}|^2}{4\hbar^2} = 0\,, \tag{4.150}$$

where we used the detuning defined in Eq. (4.129). This quadratic equation has the following two solutions for the characteristic exponents:

$$\lambda_\pm = \frac{i}{2}\left[-\Delta \pm \sqrt{\Delta^2 + \frac{|V_{0eg}|^2}{\hbar^2}}\ \right]\,. \tag{4.151}$$

Here the Rabi frequency

$$\Omega_{\rm R} = \sqrt{\Delta^2 + \frac{|V_{0eg}|^2}{\hbar^2}} \tag{4.152}$$

occurs in the difference of both characteristic exponents according to

$$\lambda_+ - \lambda_- = i\Omega_{\rm R}\,, \tag{4.153}$$

so that (4.151) reduces to

$$\lambda_\pm = \frac{i}{2}\left(-\Delta \pm \Omega_{\rm R}\right)\,. \tag{4.154}$$

The general solution for $c_e(t)$ follows now from a linear combination of the two fundamental solutions

$$c_e(t) = A_+\, e^{\lambda_+ t} + A_-\, e^{\lambda_- t}\,. \tag{4.155}$$

From $c_e(t)$ we then obtain $c_g(t)$ from (4.148) and (4.155) according to

$$c_g(t) = \frac{2i\hbar}{V_{0eg}}\, e^{i\Delta t}\, \dot{c}_e(t) = \frac{2i\hbar}{V_{0eg}}\, e^{i\Delta t}\left(\lambda_+ A_+\, e^{\lambda_+ t} + \lambda_- A_-\, e^{\lambda_- t}\right)\,. \tag{4.156}$$

Implementing the initial conditions (4.136) yields from (4.155) and (4.156)

$$c_g(0) \;=\; \frac{2i\hbar}{V_{0eg}}\,\left(\lambda_+ A_+ + \lambda_- A_-\right) = 1\,, \tag{4.157}$$

$$c_e(0) \;=\; A_+ + A_- = 0 \tag{4.158}$$

They represent a linear inhomogeneous system of equations for the yet unknown expansion coefficients A_+, A_-

$$\left(\begin{array}{cc} \dfrac{2i\hbar}{V_{0eg}}\,\lambda_+ & \dfrac{2i\hbar}{V_{0eg}}\,\lambda_- \\ 1 & 1 \end{array}\right)\left(\begin{array}{c} A_+ \\ A_- \end{array}\right) = \left(\begin{array}{c} 1 \\ 0 \end{array}\right)\,, \tag{4.159}$$

which has due to (4.153) the solution

$$\left(\begin{array}{c} A_+ \\ A_- \end{array}\right) = \frac{V_{0eg}}{2i\hbar(\lambda_+ - \lambda_-)}\left(\begin{array}{cc} 1 & -\dfrac{2i\hbar}{V_{0eg}}\,\lambda_- \\ -1 & \dfrac{2i\hbar}{V_{0eg}}\,\lambda_+ \end{array}\right)\left(\begin{array}{c} 1 \\ 0 \end{array}\right) = \frac{V_{0eg}}{2\hbar\Omega_{\rm R}}\left(\begin{array}{c} -1 \\ 1 \end{array}\right)\,. \tag{4.160}$$

Thus, the expansion coefficients are determined by

$$A_+ = -\frac{V_{0eg}}{2\hbar\Omega_{\rm R}}\,, \qquad A_- = \frac{V_{0eg}}{2\hbar\Omega_{\rm R}}\,. \tag{4.161}$$

Inserting (4.161) into (4.155) we yield for the amplitude $c_e(t)$

$$c_e(t) = i\,\frac{V_{0eg}}{\hbar\Omega_{\rm R}}\, e^{-i\Delta t/2}\,\sin\left(\frac{\Omega_{\rm R}}{2}t\right)\,. \tag{4.162}$$

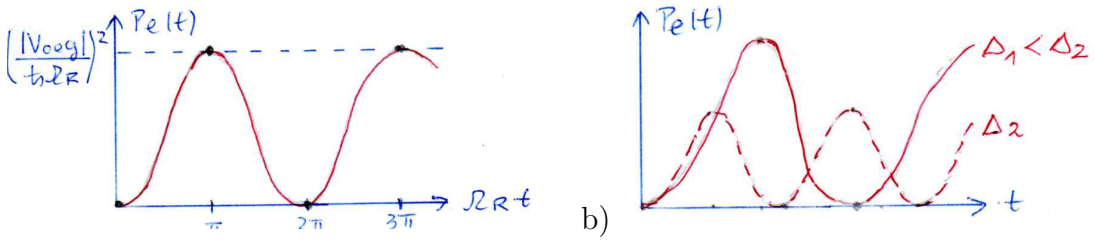

Figure 4.9: Probability (4.164) to find the atom in state $|e\rangle$: a) Oscillations occur with half the Rabi frequency (4.152); b) Decreasing the detuning Δ increases both the period and the amplitude of the Rabi oscillations.

With this we obtain for the amplitude $c_g(t)$ according to (4.156):

$$c_g(t) = e^{i\Delta t/2}\left[\cos\left(\frac{\Omega_\mathrm{R}}{2}t\right) - i\frac{\Delta}{\Omega_\mathrm{R}}\sin\left(\frac{\Omega_\mathrm{R}}{2}t\right)\right]. \tag{4.163}$$

The probability, that the atom is in state $|e\rangle$, is then given by

$$P_e(t) = |c_e(t)|^2 = \left(\frac{|V_{0eg}|}{\hbar\Omega_\mathrm{R}}\right)^2 \sin^2\left(\frac{\Omega_\mathrm{R}t}{2}\right) \tag{4.164}$$

and oscillates at half the Rabi frequency (4.152), see Fig. 4.9a). Furthermore, we can discuss the dependence of these Rabi oscillations on the detuning Δ. To this end we get for the amplitude of the Rabi oscillations from (4.164) by taking into account (4.152):

$$\left(\frac{|V_{0eg}|}{\hbar\Omega_\mathrm{R}}\right)^2 = \frac{1}{1+\left(\hbar\Delta/|V_{0eg}|\right)^2}. \tag{4.165}$$

Thus, for smaller detuning both the amplitude and the period of the Rabi oscillations becomes larger as is indicated in Fig. 4.9b).

In the resonance case, where the detuning disappears, i.e. $\Delta = 0$, we decompose the dipole matrix element into absolute value and phase according to

$$V_{0eg} = |V_{0eg}|\, e^{i\varphi_{0eg}}, \tag{4.166}$$

and read off from (4.162) and (4.163):

$$c_g(t) = \cos\left(\frac{|V_{0eg}|}{2\hbar}t\right), \qquad c_e(t) = ie^{i\varphi_{0eg}}\sin\left(\frac{|V_{0eg}|}{2\hbar}t\right). \tag{4.167}$$

Thus, after the time $t_\pi = \pi\hbar/|V_{0eg}|$ the atomic population is in the excited state:

$$c_g\left(t_\pi\right) = 0, \qquad c_e\left(t_\pi\right) = ie^{i\varphi_{0eg}}, \tag{4.168}$$

which corresponds to the probabilities

$$P_g(t_\pi) = |c_g(t_\pi)|^2 = 0, \qquad P_e(t_\pi) = |c_e(t_\pi)|^2 = 1. \tag{4.169}$$

In the context of nuclear magnetic resonance (NMR) this represents a π-pulse. On the other hand, considering the time $t_{\frac{\pi}{2}} = \pi\hbar/2\,|V_{0eg}|$, we obtain instead

$$c_g\left(t_{\frac{\pi}{2}}\right) = \frac{1}{\sqrt{2}}\,, \qquad c_e\left(t_{\frac{\pi}{2}}\right) = \frac{i}{\sqrt{2}}\,e^{i\varphi_{0eg}}\,, \tag{4.170}$$

which leads to the probabilities

$$P_g(t_{\frac{\pi}{2}}) = \left|c_g(t_{\frac{\pi}{2}})\right|^2 = \frac{1}{2}\,, \qquad P_e(t_{\frac{\pi}{2}}) = \left|c_e(t_{\frac{\pi}{2}})\right|^2 = \frac{1}{2}\,. \tag{4.171}$$

This means that the both states $|g\rangle$ and $|e\rangle$ are equally occupied:

$$|\psi(t_{\frac{\pi}{2}})\rangle = \frac{1}{\sqrt{2}}\Big(\,|g\rangle - ie^{i\varphi_{0eg}}\,|e\rangle\,\Big)\,, \tag{4.172}$$

and one then speaks of a $\pi/2$-pulse. Such π- and $\pi/2$-pulses are standard methods for manipulating spin states not only in NMR but are also applied in many atomic and ionic systems.

The non-perturbative treatment of the Rabi model goes over into the perturbative result of Section 4.2 in case of a weak light field, where we have

$$\frac{|V_{0eg}|}{\hbar} \ll \Delta\,. \tag{4.173}$$

Then we get from (4.152) approximately $\Omega_{\rm R} \approx \Delta$, so that the amplitudes (4.162) and (4.163) reduce to

$$c_g(t) \;\approx\; e^{i\Delta t/2}\left[\cos\left(\frac{\Delta t}{2}\right) - i\sin\left(\frac{\Delta t}{2}\right)\right] = 1\,, \tag{4.174}$$

$$c_e(t) \;\approx\; i\,\frac{V_{0eg}}{\hbar\Delta}\,e^{-i\Delta t/2}\,\sin\left(\frac{\Delta t}{2}\right)\,. \tag{4.175}$$

Thus, the expansion coefficients (4.174) and (4.175) agree with the previous results (4.43) and (4.48), where in the latter case the detuning (4.129) has to be taken into account. Indeed, the coefficient (4.175) is small because $|V_{0eg}|\,/\hbar$ is assumed to be small in comparison with the detuning Δ according to (4.173).

4.4.2 Translation of Rabi Model into Spin 1/2 System

As we consider the atomic system to be a two-level system, its two states $|g\rangle$ and $|e\rangle$ can be formally identified with a spin down and a spin up state as follows:

$$|g\rangle = \begin{pmatrix} 0 \\ 1 \end{pmatrix}\,, \qquad |e\rangle = \begin{pmatrix} 1 \\ 0 \end{pmatrix}\,. \tag{4.176}$$

Correspondingly, projecting the Hamilton operator $\hat{H}^{(0)}$ onto these two states, it can be represented by a 2×2-matrix $H^{(0)}$. To this end we take advantage of the fact that the unit matrix and the Pauli matrices together represent a basis in the space of complex-valued 2×2-matrices:

$$\sigma_0 = \begin{pmatrix} 1 & 0 \\ 0 & 1 \end{pmatrix}\,, \quad \sigma_1 = \begin{pmatrix} 0 & 1 \\ 1 & 0 \end{pmatrix}\,, \quad \sigma_2 = \begin{pmatrix} 0 & -i \\ i & 0 \end{pmatrix}\,, \quad \sigma_3 = \begin{pmatrix} 1 & 0 \\ 0 & -1 \end{pmatrix}\,. \tag{4.177}$$

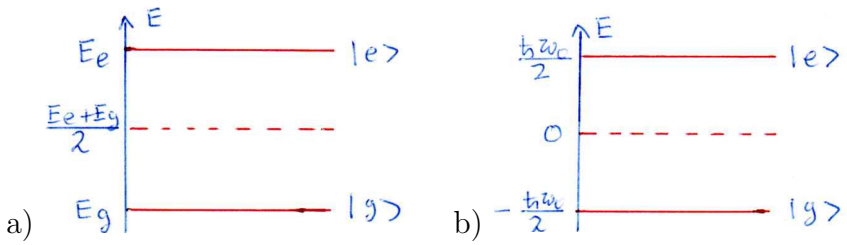

Figure 4.10: Unperturbed energy levels of the Rabi model a) before and b) after the shift of the zero-point energy according to (4.179) and (4.180).

At first we consider the unperturbed Hamiltonian of the Rabi model (4.131). The projection onto the two states $|g\rangle$ and $|e\rangle$ leads to the following 2×2-matrix:

$$H^{(0)} = \begin{pmatrix} H^{(0)}_{ee} & H^{(0)}_{eg} \\ H^{(0)}_{ge} & H^{(0)}_{gg} \end{pmatrix} = \begin{pmatrix} \langle e| \hat{H}^{(0)} |e\rangle & \langle e| \hat{H}^{(0)} |g\rangle \\ \langle g| \hat{H}^{(0)} |e\rangle & \langle g| \hat{H}^{(0)} |g\rangle \end{pmatrix} = \begin{pmatrix} E_e & 0 \\ 0 & E_g \end{pmatrix} . \tag{4.178}$$

It can be decomposed into the basis of 2×2-matrices (4.177) as follows

$$H^{(0)} = \frac{E_e + E_g}{2} \begin{pmatrix} 1 & 0 \\ 0 & 1 \end{pmatrix} + \frac{E_e - E_g}{2} \begin{pmatrix} 1 & 0 \\ 0 & -1 \end{pmatrix} = \frac{E_e + E_g}{2}\, \sigma_0 + \frac{\hbar\omega_0}{2}\, \sigma_3 \,, \tag{4.179}$$

where we used the atomic transition frequency (4.128). The first term in (4.179) corresponds to the energy in the middle between the two energy levels, see Fig. 4.10a). In the last section we have seen that this energy is physically irrelevant for the dynamics of the Rabi model. Therefore, we can also shift the energy scale by this value and identify the Hamiltonian (4.179) just with

$$H^{(0)} = \frac{\hbar\omega_0}{2}\, \sigma_3 \,, \tag{4.180}$$

as is sketched in Fig. 4.10b). Now we also project accordingly the interaction Hamiltonian (4.133) to these two states $|g\rangle$ and $|e\rangle$:

$$H^{(p)}(t) = \begin{pmatrix} H^{(p)}_{ee}(t) & H^{(p)}_{eg}(t) \\ H^{(p)}_{ge}(t) & H^{(p)}_{gg}(t) \end{pmatrix} = \begin{pmatrix} \langle e| \hat{V}_0 |e\rangle & \langle e| \hat{V}_0 |g\rangle \\ \langle g| \hat{V}_0 |e\rangle & \langle g| \hat{V}_0 |g\rangle \end{pmatrix} \cos(\omega t) \,. \tag{4.181}$$

Taking into account the matrix elements (4.140)–(4.142) reduces Eq. (4.181) to

$$H^{(p)}(t) = \begin{pmatrix} 0 & V_{0eg} \\ V^*_{0eg} & 0 \end{pmatrix} \cos(\omega t) \,. \tag{4.182}$$

This 2×2-matrix could be represented with the help of σ_1 and σ_2 matrices due to (4.177). But it turns out to be advantageous to introduce instead the raising and the lowering Pauli matrices

$$\sigma_+ = \frac{1}{2}\,(\sigma_1 + i\sigma_2) = \begin{pmatrix} 0 & 1 \\ 0 & 0 \end{pmatrix} , \tag{4.183}$$

$$\sigma_- = \frac{1}{2}\,(\sigma_1 - i\sigma_2) = \begin{pmatrix} 0 & 0 \\ 1 & 0 \end{pmatrix} , \tag{4.184}$$

which have the properties

$$\sigma_+ \begin{pmatrix} 1 \\ 0 \end{pmatrix} = \begin{pmatrix} 0 \\ 0 \end{pmatrix}, \qquad \sigma_+ \begin{pmatrix} 0 \\ 1 \end{pmatrix} = \begin{pmatrix} 1 \\ 0 \end{pmatrix}, \tag{4.185}$$

$$\sigma_- \begin{pmatrix} 1 \\ 0 \end{pmatrix} = \begin{pmatrix} 0 \\ 1 \end{pmatrix}, \qquad \sigma_- \begin{pmatrix} 0 \\ 1 \end{pmatrix} = \begin{pmatrix} 0 \\ 0 \end{pmatrix}. \tag{4.186}$$

With this the interaction (4.182) is described as follows:

$$H^{(p)}(t) = \left(V_{0eg}\,\sigma_+ + V_{0eg}^*\,\sigma_-\right)\frac{1}{2}\left(e^{i\omega t} + e^{-i\omega t}\right). \tag{4.187}$$

Now we consider the underlying time-dependent Schrödinger equation

$$i\hbar\frac{\partial}{\partial t}\,|\psi(t)\rangle = H(t)\,|\psi(t)\rangle \tag{4.188}$$

with the Hamiltonian

$$H(t) = H^{(0)} + H^{(p)}(t) = \begin{pmatrix} \dfrac{\hbar\omega_0}{2} & \dfrac{V_{0eg}}{2}\left(e^{i\omega t} + e^{-i\omega t}\right) \\ \dfrac{V_{0eg}^*}{2}\left(e^{i\omega t} + e^{-i\omega t}\right) & -\dfrac{\hbar\omega_0}{2} \end{pmatrix}. \tag{4.189}$$

In a first step we simplify this problem by transforming it into a system rotating with some frequency ω. To this end we introduce a general time-dependent unitary transformation:

$$|\tilde{\psi}(t)\rangle = S(t)\,|\psi(t)\rangle\,, \qquad |\psi(t)\rangle = S^\dagger(t)\,|\tilde{\psi}(t)\rangle\,, \qquad S^\dagger(t) = S^{-1}(t)\,, \tag{4.190}$$

so the transformed time-dependent Schrödinger equation then reads

$$i\hbar\,\frac{\partial}{\partial t}\,|\tilde{\psi}(t)\rangle = \tilde{H}(t)\,|\tilde{\psi}(t)\rangle \tag{4.191}$$

with the transformed Hamiltonian

$$\tilde{H}(t) = S(t)H(t)S^\dagger(t) + i\hbar\frac{\partial S(t)}{\partial t}S^\dagger(t)\,. \tag{4.192}$$

Let us specialise to the following time-dependent unitary transformation

$$S(t) = e^{i\sigma_3\omega t/2} = \begin{pmatrix} e^{i\omega t/2} & 0 \\ 0 & e^{-i\omega t/2} \end{pmatrix}, \qquad S^\dagger(t) = \begin{pmatrix} e^{-i\omega t/2} & 0 \\ 0 & e^{i\omega t/2} \end{pmatrix}, \tag{4.193}$$

which has the properties

$$i\hbar\,\frac{\partial S(t)}{\partial t} = \begin{pmatrix} -\dfrac{\hbar\omega}{2}\,e^{i\omega t/2} & 0 \\ 0 & \dfrac{\hbar\omega}{2}\,e^{-i\omega t/2} \end{pmatrix}, \qquad i\hbar\,\frac{\partial S(t)}{\partial t}\,S^\dagger(t) = \begin{pmatrix} -\dfrac{\hbar\omega}{2} & 0 \\ 0 & \dfrac{\hbar\omega}{2} \end{pmatrix} \tag{4.194}$$

as well as

$$S(t)H(t)S^\dagger(t) = \begin{pmatrix} \dfrac{\hbar\omega_0}{2} & \dfrac{V_{0eg}}{2}\left(1 + e^{2i\omega t}\right) \\ \dfrac{V_{0eg}^*}{2}\left(1 + e^{-2i\omega t}\right) & -\dfrac{\hbar\omega_0}{2} \end{pmatrix}. \tag{4.195}$$

Thus we obtain for the transformed Hamiltonian (4.192):

$$\tilde{H}(t) = \begin{pmatrix} \frac{\hbar}{2}(\omega_0 - \omega) & \frac{V_{0eg}}{2}(1 + e^{2i\omega t}) \\ \frac{V_{0eg}^*}{2}(1 + e^{-2i\omega t}) & -\frac{\hbar}{2}(\omega_0 - \omega) \end{pmatrix} . \tag{4.196}$$

Within the framework of the rotating wave approximation one neglects the rapidly oscillating terms and obtains with the detuning (4.129) the approximate time-independent Hamiltonian:

$$\tilde{H}(t) = -\frac{\hbar\Delta}{2}\,\sigma_3 + \frac{1}{2}\left(V_{0eg}\,\sigma_+ + V_{0eg}^*\,\sigma_-\right) . \tag{4.197}$$

Decomposing the dipole matrix element into absolute value and phase according to (4.166), a side calculation leads to

$$V_{0eg}\,\sigma_+ + V_{0eg}^*\,\sigma_- = |V_{0eg}|\left[\cos(\varphi_{0eg})\,\sigma_1 - \sin(\varphi_{0eg})\,\sigma_2\right] , \tag{4.198}$$

so the transformed Hamiltonian (4.197) results to

$$\tilde{H}(t) = \frac{|V_{0eg}|}{2}\cos(\varphi_{0eg})\,\sigma_1 - \frac{|V_{0eg}|}{2}\sin(\varphi_{0eg})\,\sigma_2 - \frac{\hbar\Delta}{2}\,\sigma_3 . \tag{4.199}$$

Taking into account the explicit form of the Pauli matrices (4.177) we finally get

$$\tilde{H}(t) = \boldsymbol{\omega}\cdot\frac{\hbar}{2}\,\boldsymbol{\sigma} \tag{4.200}$$

with the angular frequency vector

$$\boldsymbol{\omega} = \begin{pmatrix} \frac{|V_{0eg}|}{\hbar}\cos(\varphi_{0eg}) \\ -\frac{|V_{0eg}|}{\hbar}\sin(\varphi_{0eg}) \\ -\Delta \end{pmatrix} . \tag{4.201}$$

The transformed Hamiltonian (4.200) formally corresponds to the Zeeman interaction of the magnetic moment of a spin 1/2-particle with a magnetic field, which is proportional to the angular frequency vector (4.201).

4.4.3 Relation to Optical Bloch Equations

We now describe the state of the two-level atom or the effective spin 1/2-particle by a density matrix ρ, which is also represented by a 2×2-matrix. Here we exploit again the fact that the unity matrix σ_0 and the three Pauli-matrices σ_i in (4.177) form a basis in the space of complex valued 2×2-matrices by considering the decomposition of ρ in terms of the Bloch vector $\mathbf{s}$:

$$\rho = \frac{1}{2}\left(\sigma_0 + \mathbf{s}\,\boldsymbol{\sigma}\right) . \tag{4.202}$$

In component notation this decomposition reads

$$\rho = \frac{1}{2}\begin{pmatrix} 1+s_3 & s_1 - is_2 \\ s_1 + is_2 & 1-s_3 \end{pmatrix} . \tag{4.203}$$

As the normalization property

$$\mathrm{Tr}\,\rho = 1 \tag{4.204}$$

is fulfilled, ρ from (4.202) describes, indeed, a density matrix. Furthermore, the decomposition (4.202) suggests that we assign to each Bloch vector $\mathbf{s}$ a density matrix ρ and, vice versa, for each density matrix ρ a corresponding Bloch vector $\mathbf{s}$. In order to explore the latter case we calculate the expectation value of the Pauli matrices with respect to the density matrix.

$$\langle \boldsymbol{\sigma} \rangle = \mathrm{Tr}\,(\boldsymbol{\sigma}\rho)\,. \tag{4.205}$$

Although this can be evaluated by using the explicit representation of the 2×2 matrices in (4.177), we will use instead a more elegant approach, which takes both the commutator and the anticommutator relations of the Pauli matrices into account. Namely, based on their explicit representation (4.177), it can be shown that they represent a Clifford-Algebra

$$[\sigma_i, \sigma_j]_+ = \sigma_i\sigma_j + \sigma_j\sigma_i = 2\delta_{ij}\sigma_0 \tag{4.206}$$

and at the same time also a Lie algebra

$$[\sigma_i, \sigma_j]_- = \sigma_i\sigma_j - \sigma_j\sigma_i = 2i\epsilon_{ijk}\sigma_k\,. \tag{4.207}$$

Here ϵ_{klm} denotes the three-dimensional Levi-Cività tensor, which has the value $\epsilon_{123} = 1$ and is anti-symmetric with respect to two of its three indices:

$$\epsilon_{klm} = -\epsilon_{lkm} = -\epsilon_{mlk} = -\epsilon_{kml}\,. \tag{4.208}$$

Adding both relations (4.206) and (4.207) one obtains the useful result that the product of two Pauli matrices can be reduced to Pauli matrices according to the prescription

$$\sigma_i\sigma_j = \delta_{ij}\sigma_0 + i\epsilon_{ijk}\sigma_k\,. \tag{4.209}$$

Thus, we evaluate the expectation value of the Pauli matrices (4.205) with the density matrix (4.202) by taking into account (4.209) and obtain at first

$$\langle \sigma_i \rangle = \mathrm{Tr}\,(\sigma_i\rho) = \frac{1}{2}\,\mathrm{Tr}\,\left(\sigma_i\sigma_0 + s_j\sigma_i\sigma_j\right) = \frac{1}{2}\,\mathrm{Tr}\left[\sigma_i + \left(\delta_{ij}\sigma_0 + i\epsilon_{ijk}\sigma_k\right)s_j\right]. \tag{4.210}$$

Due to the trace properties

$$\mathrm{Tr}\,(\sigma_0) = 2\,, \qquad \mathrm{Tr}\,(\sigma_i) = 0 \tag{4.211}$$

following straight-forwardly from (4.177), this reduces to the result

$$\mathbf{s} = \langle \boldsymbol{\sigma} \rangle\ . \tag{4.212}$$

This means that the Bloch vector $\mathbf{s}$ can be interpreted as the expectation value of the vector of Pauli matrices $\boldsymbol{\sigma}$ for a given density matrix ρ.

Now we investigate how the property, that the density matrix ρ describes a pure state, affects the Bloch vector $\mathbf{s}$. To this end we consider the square of the density matrix (4.202)

$$\rho^2 = \frac{1}{4}\left(\sigma_0 + 2\mathbf{s}\boldsymbol{\sigma} + s_i s_j \sigma_i \sigma_j\right) \tag{4.213}$$

and simplify it by taking into account (4.209):

$$\rho^2 = \frac{1}{4}\left[\sigma_0 + 2\mathbf{s}\boldsymbol{\sigma} + s_i s_j \left(\delta_{ij}\sigma_0 + i\epsilon_{ijk}\sigma_k\right)\right] = \frac{1}{4}\left[\sigma_0\left(1+\mathbf{s}^2\right) + 2\mathbf{s}\boldsymbol{\sigma}\right] . \tag{4.214}$$

Evaluating the trace of (4.214) with the help of (4.211) then yields

$$\mathrm{Tr}\left(\rho^2\right) = \frac{1+\mathbf{s}^2}{2} . \tag{4.215}$$

In case that a pure state is present, i.e. the density matrix ρ fulfills the property (3.159), this corresponds to a Bloch vector $\mathbf{s}$ with the absolute value

$$|\mathbf{s}| = 1 . \tag{4.216}$$

The Bloch vector $\mathbf{s}$ is thus located on the surface of sphere with unit radius, which is called the Bloch sphere. As a first example let us consider the density matrix (4.203) describing the ground state

$$\rho = |g\rangle\langle g| = \begin{pmatrix} 0 \\ 1 \end{pmatrix}(0,1) = \begin{pmatrix} 0 & 0 \\ 0 & 1 \end{pmatrix} = \frac{1}{2}\begin{pmatrix} 1+s_3 & s_1 - is_2 \\ s_1 + is_2 & 1-s_3 \end{pmatrix} , \tag{4.217}$$

which corresponds to the Bloch vector

$$\mathbf{s}_g = \begin{pmatrix} 0 \\ 0 \\ -1 \end{pmatrix} . \tag{4.218}$$

In the second example we scrutinize the excited state, which reads in terms of the density matrix (4.203)

$$\rho = |e\rangle\langle e| = \begin{pmatrix} 1 \\ 0 \end{pmatrix}(1,0) = \begin{pmatrix} 1 & 0 \\ 0 & 0 \end{pmatrix} = \frac{1}{2}\begin{pmatrix} 1+s_3 & s_1 - is_2 \\ s_1 + is_2 & 1-s_3 \end{pmatrix} , \tag{4.219}$$

so its Bloch vector is given by

$$\mathbf{s}_e = \begin{pmatrix} 0 \\ 0 \\ 1 \end{pmatrix} . \tag{4.220}$$

Thus the pure state of an atom being in the ground (excited) state is represented on the Bloch sphere by its south (north) pole, see Fig. 4.11. Consequently for a mixed state, which is defined

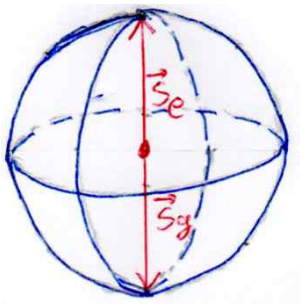

Figure 4.11: Ground and excited state of the two-level system correspond due to (4.218) and (4.220) to the south and the north pole on the Bloch sphere (4.216), respectively.

by a purity with $\mathrm{Tr}\,(\rho^2) < 1$, then follows $|\mathbf{s}| < 1$, i.e. the Bloch vector $\mathbf{s}$ lies within the Bloch sphere. For instance, the origin of the Bloch sphere

$$\mathbf{s} = \mathbf{0} \qquad \Longleftrightarrow \qquad \rho = \frac{1}{2}\,\sigma_0 \tag{4.221}$$

represents a maximally mixed state, since then the purity $\mathrm{Tr}\,(\rho^2) = \mathrm{Tr}\,(\sigma_0/4) = 1/2$ is minimal.

We now examine the temporal evolution of the Bloch vector, which is induced by the Hamiltonian (4.200). To this end one can optionally use either the Schrödinger or the Heisenberg picture, in which either the states or the operators are time dependent, while the expectation values coincide. For instance, the expectation value for the Pauli matrices in both pictures read

$$\mathbf{s}(t) = \mathrm{Tr}\,(\rho(t)\boldsymbol{\sigma}) = \mathrm{Tr}\,(\rho\boldsymbol{\sigma}(t))\,. \tag{4.222}$$

In the Heisenberg picture the dynamics of the expectation value is determined by the Heisenberg equation for the vector of Pauli matrices

$$i\hbar\,\frac{\partial}{\partial t}\,\boldsymbol{\sigma}(t) = \Big[\boldsymbol{\sigma}(t), \tilde{H}(t)\Big]_-\,. \tag{4.223}$$

Due to the equality of the expectation values in both pictures (4.222) we then conclude for the Schödinger picture that the dynamics of the expectation value follows from the evolution of the density matrix $\rho(t)$, which is governed by the von Neumann equation

$$i\hbar\,\frac{\partial}{\partial t}\,\rho(t) = \Big[\tilde{H}(t), \rho(t)\Big]_-\,. \tag{4.224}$$

Note that the right-hand sides of (4.223) and (4.224) differ by a minus sign. In the following we derive the equation of motion for the Bloch vector $\mathbf{s}(t)$ within the Schrödinger picture. For the von Neumann equation (4.224) of the density matrix (4.202) we obtain for the Hamiltonian (4.200):

$$i\hbar\,\frac{\partial}{\partial t}\,\rho(t) = \left[\frac{\hbar}{2}\,\omega_i\sigma_i, \frac{1}{2}\left\{\sigma_0 + s_j(t)\sigma_j\right\}\right]_- = \frac{\hbar}{4}\,\omega_i s_j(t)\,[\sigma_i, \sigma_j]_-\,. \tag{4.225}$$

Taking into account the Lie algebra of the Pauli matrices (4.207) then leads with (4.202) to

$$i\hbar\,\frac{\partial}{\partial t}\,\rho(t) = \frac{\hbar}{4}\,\omega_i s_j(t)\,2i\epsilon_{ijk}\sigma_k = \frac{i\hbar}{2}\,\epsilon_{ijk}\omega_i s_j(t)\sigma_k = \frac{i\hbar}{2}\,\dot{s}_k(t)\sigma_k\,. \tag{4.226}$$

With this we have derived the optical Bloch equations:

$$\frac{d\mathbf{s}(t)}{dt} = \boldsymbol{\omega} \times \mathbf{s}(t)\,. \tag{4.227}$$

They state that the Bloch vector $\mathbf{s}(t)$ precesses around the angular frequency vector $\boldsymbol{\omega}$ defined in (4.201) with a precession frequency, which is given by its absolute value

$$|\boldsymbol{\omega}| = \sqrt{\frac{|V_{0eg}|^2}{\hbar^2} + \Delta^2} = \Omega_{\mathrm{R}} \tag{4.228}$$

and turns out to coincide with the Rabi frequency (4.152). Due to the precession (4.227), the length of the Bloch vector $\mathbf{s}(t)$ is preserved during the dynamics:

$$\frac{d|\mathbf{s}(t)|^2}{dt} = 2\mathbf{s}(t) \cdot \frac{d\mathbf{s}(t)}{dt} = 2\mathbf{s}(t) \cdot [\boldsymbol{\omega} \times \mathbf{s}(t)] = 0\,. \tag{4.229}$$

This means that a pure state at the beginning $t = 0$, which obeys $|\mathbf{s}(0)| = 1$, remains a pure state for all times $t > 0$, i.e. $|\mathbf{s}(t)| = 1$ holds.

4.4.4 Solution of Optical Bloch Equations

In component notation the optical Bloch equations (4.227) turn out to represent a linear system of first-order differential equations

$$\frac{d\mathbf{s}(t)}{dt} = M\,\mathbf{s}(t)\,. \tag{4.230}$$

Its solution is based on determining the eigenvalues of the matrix M, which follow from the characteristic equation:

$$\det\left(M - \lambda I\right) = 0\,. \tag{4.231}$$

On the one hand, we note that the matrix

$$M = \begin{pmatrix} 0 & \Delta & -\dfrac{|V_{0eg}|}{\hbar}\,\sin(\varphi_{0eg}) \\ -\Delta & 0 & -\dfrac{|V_{0eg}|}{\hbar}\,\cos(\varphi_{0eg}) \\ \dfrac{|V_{0eg}|}{\hbar}\,\sin(\varphi_{0eg}) & \dfrac{|V_{0eg}|}{\hbar}\,\cos(\varphi_{0eg}) & 0 \end{pmatrix}. \tag{4.232}$$

is anti-symmetric, i.e. it holds $M^T = -M$. Due to the latter property we conclude for $D = 3$ dimensions

$$\det\left(M - \lambda I\right) = \det\left(M - \lambda I\right)^T = \det\left(M^T - \lambda I\right) = \det\left(-M - \lambda I\right) = -\det\left(M + \lambda I\right)\,, \tag{4.233}$$

so we deduce from the characteristic equation (4.231)

$$\det\left(M + \lambda I\right) = 0\,. \tag{4.234}$$

Due to (4.231) and (4.234) we read off that with λ also $-\lambda$ is an eigenvalue of the matrix M. On the other hand, the characteristic polynomial $\det(M-\lambda I)=0$ consists of real coefficients, so the eigenvalues are either real or conjugate complex to each other. However, real eigenvalues are not possible as then there would always be a solution which exponentionally increases with time and, thus, does not respect $|\mathbf{s}(t)|=1$. Therefore, since the characteristic equation (4.231) is a third-order polynomial, we finally obtain that we have two complex conjugate eigenvalues and one vanishing eigenvalue:

$$\lambda_1 = i\Omega\,, \qquad \lambda_2 = -i\Omega\,, \qquad \lambda_3 = 0\,. \tag{4.235}$$

In fact, the characteristic equation (4.231) reads explicitly

$$\lambda\left(\lambda^2+\Delta^2+\frac{|V_{0eg}|^2}{\hbar^2}\right)=0\,, \tag{4.236}$$

which has, indeed, a solution of the form (4.235)

$$\lambda_1 = i\Omega_\mathrm{R}\,, \qquad \lambda_2 = -i\Omega_\mathrm{R}\,, \qquad \lambda_3 = 0 \tag{4.237}$$

with the Rabi frequency (4.152).

At first we determine the eigenvector $\mathbf{s}_3$ to the eigenvalue λ_3, which leads to the homogeneous linear system of equations

$$\begin{pmatrix} 0 & \Delta & -\dfrac{|V_{0eg}|}{\hbar}\sin(\varphi_{0eg}) \\ -\Delta & 0 & -\dfrac{|V_{0eg}|}{\hbar}\cos(\varphi_{0eg}) \\ \dfrac{|V_{0eg}|}{\hbar}\sin(\varphi_{0eg}) & \dfrac{|V_{0eg}|}{\hbar}\cos(\varphi_{0eg}) & 0 \end{pmatrix} \begin{pmatrix} s_{31} \\ s_{32} \\ s_{33} \end{pmatrix} = \begin{pmatrix} 0 \\ 0 \\ 0 \end{pmatrix}. \tag{4.238}$$

Since the three equations are linear dependent, we can restrict ourselves to the first two equations without loss of generality:

$$\left.\begin{aligned} \Delta s_{32} - \frac{|V_{0eg}|}{\hbar}\sin(\varphi_{0eg})s_{33} = 0 \\ -\Delta s_{31} - \frac{|V_{0eg}|}{\hbar}\cos(\varphi_{0eg})s_{33} = 0 \end{aligned}\right\} \qquad \Longrightarrow \qquad \mathbf{s}_3 = N_3 \begin{pmatrix} \dfrac{|V_{0eg}|}{\hbar}\cos(\varphi_{0eg}) \\ -\dfrac{|V_{0eg}|}{\hbar}\sin(\varphi_{0eg}) \\ -\Delta \end{pmatrix}. \tag{4.239}$$

Demanding the normalization of the eigenvector yields with (4.152) and (4.201)

$$|\mathbf{s}_3| = N_3\,\Omega_\mathrm{R} = 1 \qquad \Longrightarrow \qquad N_3 = \frac{1}{\Omega_\mathrm{R}} \qquad \Longrightarrow \qquad \mathbf{s}_3 = \frac{\boldsymbol{\omega}}{\Omega_\mathrm{R}}\,. \tag{4.240}$$

Thus, the angular frequency vector $\boldsymbol{\omega}$ points in the direction of the eigenvector $\mathbf{s}_3$ of the eigenvalue $\lambda_3=0$. Since we have $\lambda_3=0$, the eigenvector $\mathbf{s}_3$ does not change in time during the

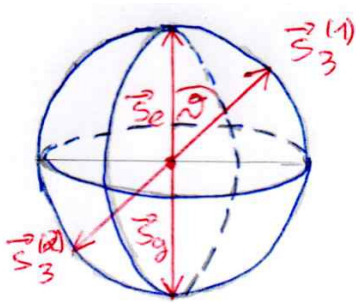

Figure 4.12: Illustration of the stationary states (4.241) of the optical Bloch equations (4.227) and the rotation angle (4.243).

precession of the Bloch vector $\mathbf{s}$, there are two stationary states on the Bloch sphere

$$\mathbf{s}_3^{(1)} = -\frac{\boldsymbol{\omega}}{\Omega_\mathrm{R}} = \begin{pmatrix} -\dfrac{|V_{0eg}|}{\hbar\Omega_\mathrm{R}}\cos(\varphi_{0eg}) \\ \dfrac{|V_{0eg}|}{\hbar\Omega_\mathrm{R}}\sin(\varphi_{0eg}) \\ \dfrac{\Delta}{\Omega_\mathrm{R}} \end{pmatrix}, \qquad \mathbf{s}_3^{(2)} = \frac{\boldsymbol{\omega}}{\Omega_\mathrm{R}} = \begin{pmatrix} \dfrac{|V_{0eg}|}{\hbar\Omega_\mathrm{R}}\cos(\varphi_{0eg}) \\ -\dfrac{|V_{0eg}|}{\hbar\Omega_\mathrm{R}}\sin(\varphi_{0eg}) \\ -\dfrac{\Delta}{\Omega_\mathrm{R}} \end{pmatrix}, \tag{4.241}$$

which are depicted in Fig. 4.12. In the limit $|V_{0eg}| \to 0$ these two points on the Bloch sphere reduce with (4.152) to

$$\mathbf{s}_3^{(1)} \to \mathbf{s}_e\,, \qquad \mathbf{s}_3^{(2)} \to \mathbf{s}_g\,. \tag{4.242}$$

The angle ϑ between the direction of $\mathbf{s}_e$ and $\mathbf{s}_3^{(1)}$ is determined by taking into account (4.152):

$$\mathbf{s}_e \cdot \mathbf{s}_3^{(1)} = \cos\vartheta = \frac{\Delta}{\Omega_\mathrm{R}} \qquad \Longrightarrow \qquad \tan\vartheta = \frac{\sqrt{1-\cos^2\vartheta}}{\cos\vartheta} = \frac{|V_{0eg}|}{\hbar\Delta}\,. \tag{4.243}$$

Now we calculate the state vectors corresponding to these stationary Bloch vectors. For a pure state, the following applies in general:

$$\begin{aligned} \rho &= |\psi\rangle\langle\psi| = \left(c_g|g\rangle + c_e|e\rangle\right)\left(c_g^*\langle g| + c_e^*\langle e|\right) = \begin{pmatrix} c_e c_e^* & c_g^* c_e \\ c_g c_e^* & c_g c_g^* \end{pmatrix} \\ &= \frac{1}{2}\begin{pmatrix} 1+s_3 & s_1 - is_2 \\ s_1 + is_2 & 1-s_3 \end{pmatrix}. \end{aligned} \tag{4.244}$$

Provided that the Bloch-vector $\mathbf{s}$ is given, then follows from the diagonal elements of (4.244)

$$|c_e|^2 = \frac{1}{2}(1+s_3)\,, \qquad |c_g|^2 = \frac{1}{2}(1-s_3)\,, \tag{4.245}$$

so the normalization holds

$$|c_e|^2 + |c_g|^2 = 1 \tag{4.246}$$

and we can conclude

$$c_e = \sqrt{\frac{1+s_3}{2}}\,e^{i\varphi_e}\,, \qquad c_g = \sqrt{\frac{1-s_3}{2}}\,e^{i\varphi_g}\,. \tag{4.247}$$

From the off-diagonal elements in (4.244) and from (4.247) we then obtain by taking into account (4.216):

$$c_g c_e^* = \frac{\sqrt{s_1^2+s_2^2}}{2}\, e^{i(\varphi_g-\varphi_e)} = \frac{s_1+is_2}{2} = \frac{\sqrt{s_1^2+s_2^2}}{2}\, e^{i\varphi_0}\,, \tag{4.248}$$

which finally reduces to

$$\varphi_0 = \arctan\left(\frac{s_2}{s_1}\right) = \varphi_g - \varphi_e\,. \tag{4.249}$$

For the first steady state (4.241) we read off from (4.245)

$$\left|c_e^{(1)}\right| = \sqrt{\frac{1}{2}\left(1+\frac{\Delta}{\Omega_\mathrm{R}}\right)}\,, \qquad \left|c_g^{(1)}\right| = \sqrt{\frac{1}{2}\left(1-\frac{\Delta}{\Omega_\mathrm{R}}\right)} \tag{4.250}$$

and we get from (4.249)

$$\varphi_g^{(1)} - \varphi_e^{(1)} = -\varphi_{0eg} + \pi \qquad \Longrightarrow \qquad \varphi_g^{(1)} = -\varphi_{0eg} + \pi\,, \quad \varphi_e^{(1)} = 0\,, \tag{4.251}$$

so the pure state results in

$$|\psi^{(1)}\rangle = c_e^{(1)}\,|e\rangle + c_g^{(1)}\,|g\rangle = \sqrt{\frac{1}{2}\left(1+\frac{\Delta}{\Omega_\mathrm{R}}\right)}\,|e\rangle - \sqrt{\frac{1}{2}\left(1-\frac{\Delta}{\Omega_\mathrm{R}}\right)}e^{-i\varphi_{0eg}}\,|g\rangle\ . \tag{4.252}$$

Correspondingly, the second steady state (4.241) yields with (4.245) and (4.249)

$$\left|c_e^{(2)}\right| = \sqrt{\frac{1}{2}\left(1-\frac{\Delta}{\Omega_\mathrm{R}}\right)}\,, \qquad \left|c_g^{(2)}\right| = \sqrt{\frac{1}{2}\left(1+\frac{\Delta}{\Omega_\mathrm{R}}\right)} \tag{4.253}$$

$$\varphi_g^{(2)} - \varphi_e^{(2)} = -\varphi_{0eg} \qquad \Longrightarrow \qquad \varphi_g^{(2)} = 0\,, \quad \varphi_e^{(2)} = \varphi_{0eg}\,, \tag{4.254}$$

which leads to

$$|\psi^{(2)}\rangle = c_e^{(2)}\,|e\rangle + c_g^{(2)}\,|g\rangle = \sqrt{\frac{1}{2}\left(1-\frac{\Delta}{\Omega_\mathrm{R}}\right)}e^{i\varphi_{0eg}}\,|e\rangle + \sqrt{\frac{1}{2}\left(1+\frac{\Delta}{\Omega_\mathrm{R}}\right)}\,|g\rangle\ . \tag{4.255}$$

Thus, in the limit $|V_{0eg}| \to 0$ we read from (4.252) and (4.253) in agreement with (4.242):

$$|\psi^{(1)}\rangle \to |e\rangle\ , \qquad |\psi^{(2)}\rangle \to |g\rangle\ . \tag{4.256}$$

Furthermore, (4.250) together with the normalization (4.246) suggests to introduce as an abbreviation the mixing angle θ via

$$\cos\theta = \sqrt{\frac{1}{2}\left(1+\frac{\Delta}{\Omega_\mathrm{R}}\right)}\,, \qquad \sin\theta = \sqrt{\frac{1}{2}\left(1-\frac{\Delta}{\Omega_\mathrm{R}}\right)}\,, \tag{4.257}$$

which satisfies the trigonometric Pythagoras $\sin^2\theta + \cos^2\theta = 1$, so we obtain

$$\tan(2\theta) = \frac{\sin(2\theta)}{\cos(2\theta)} = \frac{2\sin\theta\cos\theta}{\cos^2\theta - \sin^2\theta} = \frac{|V_{0eg}|}{\hbar\Delta}\,. \tag{4.258}$$

Thus, comparing (4.243) and (4.258) we yield $\theta = \vartheta/2$, i.e. a rotation in coordinate space with the angle ϑ corresponds in spin space to a rotation around the angle $\theta = \vartheta/2$. This observation is characteristic for a spin 1/2-system. For instance, performing a rotation in coordinate space yields for the Dirac field that the corresponding spinor is rotated with just half the angle [21, Section 9.3].

In addition, we read off from (4.252) and (4.255) that the stationary states $|e\rangle, |g\rangle$ for $|V_{0eg}| \to 0$ can be mapped into the stationary states $|\psi^{(1)}\rangle, |\psi^{(2)}\rangle$ for $V_{0eg} \neq 0$ by applying a linear transformation U, which contains the mixing angle θ.

$$\begin{pmatrix} |\psi^{(1)}\rangle \\ |\psi^{(2)}\rangle \end{pmatrix} = U \begin{pmatrix} |e\rangle \\ |g\rangle \end{pmatrix}, \qquad U = \begin{pmatrix} \cos\theta & \sin\theta\, e^{i\varphi_{0eg}} \\ -\sin\theta\, e^{-i\varphi_{0eg}} & \cos\theta \end{pmatrix}. \tag{4.259}$$

It turns out that this linear transformation is unitary:

$$U^\dagger U = \begin{pmatrix} \cos\theta & -\sin\theta\, e^{i\varphi_{0eg}} \\ \sin\theta\, e^{-i\varphi_{0eg}} & \cos\theta \end{pmatrix} \begin{pmatrix} \cos\theta & \sin\theta\, e^{i\varphi_{0eg}} \\ -\sin\theta\, e^{-i\varphi_{0eg}} & \cos\theta \end{pmatrix} = \begin{pmatrix} 1 & 0 \\ 0 & 1 \end{pmatrix}. \tag{4.260}$$

Now we determine the eigenvector $\mathbf{s}_1$ to $\lambda_1 = i\Omega_\mathrm{R}$:

$$\begin{pmatrix} -i\Omega_\mathrm{R} & \Delta & -\dfrac{|V_{0eg}|}{\hbar}\sin(\varphi_{0eg}) \\ -\Delta & -i\Omega_\mathrm{R} & -\dfrac{|V_{0eg}|}{\hbar}\cos(\varphi_{0eg}) \\ \dfrac{|V_{0eg}|}{\hbar}\sin(\varphi_{0eg}) & \dfrac{|V_{0eg}|}{\hbar}\cos(\varphi_{0eg}) & -i\Omega_\mathrm{R} \end{pmatrix} \begin{pmatrix} s_{11} \\ s_{12} \\ s_{13} \end{pmatrix} = \begin{pmatrix} 0 \\ 0 \\ 0 \end{pmatrix}. \tag{4.261}$$

From the first equation follows immediately

$$s_{11} = -i\frac{\Delta}{\Omega_\mathrm{R}}\, s_{12} + i\frac{|V_{0eg}|}{\hbar\Omega_\mathrm{R}}\, \sin(\varphi_{0eg}) s_{13}\,, \tag{4.262}$$

therefore we get from the second equation

$$-\Delta\left[-i\frac{\Delta}{\Omega_\mathrm{R}} s_{12} + i\frac{|V_{0eg}|}{\hbar\Omega_\mathrm{R}}\sin(\varphi_{0eg}) s_{13}\right] - i\Omega_\mathrm{R} s_{12} - \frac{|V_{0eg}|}{\hbar}\cos(\varphi_{0eg}) s_{13} = 0\,, \tag{4.263}$$

which reduces to

$$s_{12} = i\frac{\hbar\Omega_\mathrm{R}}{|V_{0eg}|}\left[\cos(\varphi_{0eg}) + i\frac{\Delta}{\Omega_\mathrm{R}}\sin(\varphi_{0eg})\right] s_{13}\,. \tag{4.264}$$

Choosing the third component according to

$$s_{13} = N_1\,\frac{|V_{0eg}|}{\hbar} \tag{4.265}$$

then fixes immediately the other components:

$$s_{12} = N_1\left[i\Omega_\mathrm{R}\cos(\varphi_{0eg}) - \Delta\sin(\varphi_{0eg})\right], \qquad s_{11} = N_1\left[\Delta\cos(\varphi_{0eg}) + i\Omega_\mathrm{R}\sin(\varphi_{0eg})\right]. \tag{4.266}$$

Thus the eigenvector $\mathbf{s}_1$ to the eigenvalue $\lambda_1 = i\Omega_\mathrm{R}$ is given by

$$\mathbf{s}_1 = N_1 \begin{pmatrix} \Delta\cos(\varphi_{0eg}) + i\Omega_\mathrm{R}\sin(\varphi_{0eg}) \\ -\Delta\sin(\varphi_{0eg}) + i\Omega_\mathrm{R}\cos(\varphi_{0eg}) \\ |V_{0eg}|/\hbar \end{pmatrix}, \tag{4.267}$$

where the normalization constant is fixed by

$$\mathbf{s}_1^* \cdot \mathbf{s}_1 = 1 \qquad \Longrightarrow \qquad N_1 = \frac{1}{\sqrt{2}\Omega_\mathrm{R}}. \tag{4.268}$$

The complex conjugate then yields the eigenvector $\mathbf{s}_2$ corresponding to the eigenvalue $\lambda_2 = -i\Omega_\mathrm{R}$:

$$\mathbf{s}_2 = \mathbf{s}_1^* = \frac{1}{\sqrt{2}\Omega_\mathrm{R}} \begin{pmatrix} \Delta\cos(\varphi_{0eg}) - i\Omega_\mathrm{R}\sin(\varphi_{0eg}) \\ -\Delta\sin(\varphi_{0eg}) - i\Omega_\mathrm{R}\cos(\varphi_{0eg}) \\ |V_{0eg}|/\hbar \end{pmatrix}. \tag{4.269}$$

In fact, the three eigenvectors $\mathbf{s}_1$, $\mathbf{s}_2$, $\mathbf{s}_3$ are orthogonal to each other:

$$\mathbf{s}_1^* \cdot \mathbf{s}_3 = 0\,, \qquad \mathbf{s}_2^* \cdot \mathbf{s}_3 = 0\,, \qquad \mathbf{s}_1^* \cdot \mathbf{s}_2 = 0\,. \tag{4.270}$$

The general solution for the dynamics of the Bloch vector is then a superposition of all three fundamental solutions:

$$\mathbf{s}(t) = A_1\mathbf{s}_1 e^{\lambda_1 t} + A_2\mathbf{s}_2 e^{\lambda_2 t} + A_3\mathbf{s}_3 e^{\lambda_3 t}\,. \tag{4.271}$$

Inserting the concrete form of both the eigenvalues and the eigenvectors then yields

$$\begin{aligned} \mathbf{s}(t) \;=\; & \frac{A_1}{\sqrt{2}\Omega_\mathrm{R}} \begin{pmatrix} \Delta\cos(\varphi_{0eg}) + i\Omega_\mathrm{R}\sin(\varphi_{0eg}) \\ -\Delta\sin(\varphi_{0eg}) + i\Omega_\mathrm{R}\cos(\varphi_{0eg}) \\ |V_{0eg}|/\hbar \end{pmatrix} e^{i\Omega_\mathrm{R}t} \\ & + \frac{A_2}{\sqrt{2}\Omega_\mathrm{R}} \begin{pmatrix} \Delta\cos(\varphi_{0eg}) - i\Omega_\mathrm{R}\sin(\varphi_{0eg}) \\ -\Delta\sin(\varphi_{0eg}) - i\Omega_\mathrm{R}\cos(\varphi_{0eg}) \\ |V_{0eg}|/\hbar \end{pmatrix} e^{-i\Omega_\mathrm{R}t} + \frac{A_3}{\Omega_\mathrm{R}} \begin{pmatrix} \frac{|V_{0eg}|}{\hbar}\cos(\varphi_{0eg}) \\ -\frac{|V_{0eg}|}{\hbar}\sin(\varphi_{0eg}) \\ -\Delta \end{pmatrix}. \end{aligned} \tag{4.272}$$

As the Bloch vector is reel, i.e. $\mathbf{s}^*(t) = \mathbf{s}(t)$, we conclude that

$$A_2 = A_1^* \tag{4.273}$$

must hold. The initial condition to be in the ground state

$$\mathbf{s}(0) = \begin{pmatrix} 0 \\ 0 \\ -1 \end{pmatrix} \tag{4.274}$$

implies additionally

$$A_2 = A_1 \,. \tag{4.275}$$

Combining (4.272)–(4.275) we get for the unknown coefficients

$$\begin{pmatrix} \sqrt{2}\Delta & |V_{0eg}|/\hbar \\ \sqrt{2}\,|V_{0eg}|/\hbar & -\Delta \end{pmatrix} \begin{pmatrix} A_1 \\ A_3 \end{pmatrix} = \begin{pmatrix} 0 \\ -\Omega_{\mathrm{R}} \end{pmatrix} , \tag{4.276}$$

which leads to the following solution:

$$\begin{pmatrix} A_1 \\ A_3 \end{pmatrix} = -\frac{1}{\sqrt{2}\Omega_{\mathrm{R}}^2} \begin{pmatrix} -\Delta & -\dfrac{|V_{0eg}|}{\hbar} \\ -\sqrt{2}\,\dfrac{|V_{0eg}|}{\hbar} & \sqrt{2}\Delta \end{pmatrix} \begin{pmatrix} 0 \\ -\Omega_{\mathrm{R}} \end{pmatrix} = \begin{pmatrix} -\dfrac{|V_{0eg}|}{\sqrt{2}\hbar\Omega_{\mathrm{R}}} \\ \dfrac{\Delta}{\Omega_{\mathrm{R}}} \end{pmatrix} . \tag{4.277}$$

Thus, inserting (4.273) together with (4.277) into (4.272) yields for the dynamics of the individual components Bloch vector the result

$$s_1(t) = \frac{\Delta\,|V_{0eg}|}{\hbar\Omega_{\mathrm{R}}^2}\,\cos(\varphi_{0eg})\,[1-\cos(\Omega_{\mathrm{R}}t)] + \frac{|V_{0eg}|}{\hbar\Omega_{\mathrm{R}}}\,\sin(\varphi_{0eg})\sin(\Omega_{\mathrm{R}}t)\,, \tag{4.278}$$

$$s_2(t) = -\frac{\Delta\,|V_{0eg}|}{\hbar\Omega_{\mathrm{R}}^2}\sin(\varphi_{0eg})\,[1-\cos(\Omega_{\mathrm{R}}t)] + \frac{|V_{0eg}|}{\hbar\Omega_{\mathrm{R}}}\,\cos(\varphi_{0eg})\sin(\Omega_{\mathrm{R}}t)\,, \tag{4.279}$$

$$s_3(t) = -\frac{\Delta^2}{\Omega_{\mathrm{R}}^2} - \frac{|V_{0eg}|^2}{(\hbar\Omega_{\mathrm{R}})^2}\,\cos(\Omega_{\mathrm{R}}t)\,. \tag{4.280}$$

In order to check this finding we compare it with the corresponding dynamics found for the Rabi model in subsection 4.4.1. To this end we have to consider how the Rabi model was mapped onto the spin 1/2-model via the following steps:

- At first we have to take into account that the energy was shifted by going over from (4.179) to (4.180). To this we go back to (4.135) and rewrite $E_g = (E_e + E_g)/2 - \hbar\omega_0/2$ as well as $E_e = (E_e + E_g)/2 + \hbar\omega_0/2$, yielding

$$|\psi(t)\rangle = e^{-i(E_e+E_g)t/2\hbar}\Big[c_g(t)e^{-i\omega_0 t/2}\,|g\rangle + c_e(t)e^{i\omega_0 t/2}\,|e\rangle\Big]\,. \tag{4.281}$$

- Afterwards the unitary transformation (4.190) and (4.193) is performed, which leads with the detuning (4.129) to

$$|\tilde{\psi}(t)\rangle = e^{-i(E_e+E_g)t/2\hbar}\Big[\tilde{c}_g(t)\,|g\rangle + \tilde{c}_e(t)\,|e\rangle\Big]\,, \tag{4.282}$$

  where the respective transformed coefficients read

$$\tilde{c}_g(t) = c_g(t)e^{i\Delta t/2}\,|g\rangle\ , \qquad \tilde{c}_e(t) = c_e(t)e^{-i\Delta t/2}\,|e\rangle\ . \tag{4.283}$$

- Inserting the solution of the Rabi model (4.162) and (4.163) in (4.283) then yields for the transformed coefficients

$$\tilde{c}_e(t) = -i\frac{|V_{0eg}|}{\hbar\Omega_{\rm R}}e^{i\varphi_{0eg}}\,\sin\left(\frac{\Omega_{\rm R}t}{2}\right), \tag{4.284}$$

$$\tilde{c}_g(t) = \cos\left(\frac{\Omega_{\rm R}t}{2}\right) - i\frac{\Delta}{\Omega_{\rm R}}\,\sin\left(\frac{\Omega_{\rm R}t}{2}\right). \tag{4.285}$$

- The density matrix corresponding to the pure state (4.281) turns out to not depend on the physically irrelevant energy scale $E_g = (E_e + E_g)/2$:

$$\tilde{\rho}(t) = |\tilde{\psi}(t)\rangle\,\langle\tilde{\psi}(t)| = \begin{pmatrix} |\tilde{c}_e(t)|^2 & \tilde{c}_e(t)\tilde{c}_g^*(t) \\ \tilde{c}_e^*(t)\tilde{c}_g(t) & |\tilde{c}_g(t)|^2 \end{pmatrix}. \tag{4.286}$$

  On the other hand the density matrix must also be of the generic form (4.203):

$$\tilde{\rho}(t) = \frac{1}{2}\begin{pmatrix} 1+s_3(t) & s_1(t)-is_2(t) \\ s_1(t)+is_2(t) & 1-s_3(t) \end{pmatrix}. \tag{4.287}$$

Combining (4.284)–(4.287) a straight-forward algebraic calculation then shows with taking into account the Rabi frequency (4.152) that the components of the Bloch vector $\mathbf{s}(t)$ coincide, indeed, with the Bloch vector (4.278)–(4.280).

4.5 Jaynes-Cummings Model

We now treat the quantum electrodynamic version of the Rabi model, i.e. we study a two-level system, which is coupled to a quantised electromagnetic field. For this purpose we assume for the sake of simplicity that we can restrict ourselves to a single mode of the electromagnetic field. This seems to be an unrealistic model, since a free atom interacts with all field modes, as we saw in the treatment of spontaneous emission. On the other hand, it is possible to construct environments for an atom through cavities in such a way that the density of states of the electromagnetic field deviates significantly from the one of free space. Thus, microwaves or optical cavities are able to select only single modes or multiple modes with large frequency separations. In such cases, it is therefore quite appropriate to consider the interaction of a two-level system with a single light mode.

4.5.1 Derivation of Model Hamiltonian

The starting point of the description is thus a Hamilton operator, which consists of three parts:

$$\hat{H} = \hat{H}^{(0)}_{\rm field} + \hat{H}^{(0)}_{\rm atom} + \hat{H}^{(p)}. \tag{4.288}$$

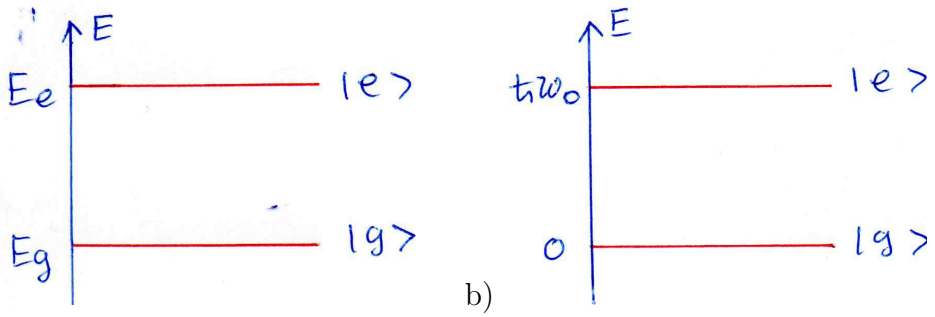

Figure 4.13: Unperturbed atomic energy levels a) before and b) after the shift of the zero-point energy by the ground-state energy E_g according to (4.293).

In the Hamiltonian of the electromagnetic field we neglect the vacuum energy, so it is given by

$$\hat{H}^{(0)}_{\text{field}} = \hbar\omega \hat{a}^\dagger \hat{a}\,, \tag{4.289}$$

and the Hamiltonian of the two-level system reads

$$\hat{H}^{(0)}_{\text{atom}} = E_g \left|g\right\rangle \left\langle g\right| + E_e \left|e\right\rangle \left\langle e\right| . \tag{4.290}$$

Formally, the two atomic states $|g\rangle$ and $|e\rangle$ can be identified with a spin down and a spin up state according to (4.176). Thus, the Hamiltonian of the two-level system can be represented by a 2×2-matrix:

$$\hat{H}^{(0)}_{\text{atom}} = \begin{pmatrix} E_e & 0 \\ 0 & E_g \end{pmatrix} , \tag{4.291}$$

which is equivalent to

$$\hat{H}^{(0)}_{\text{atom}} = E_g \begin{pmatrix} 1 & 0 \\ 0 & 1 \end{pmatrix} + (E_e - E_g) \begin{pmatrix} 1 & 0 \\ 0 & 0 \end{pmatrix} . \tag{4.292}$$

Shifting the energy zero point by the ground-state energy E_g, as depicted in Fig. 4.13, then leads to

$$\hat{H}^{(0)\prime}_{\text{atom}} = \hat{H}^{(0)}_{\text{atom}} - E_g \begin{pmatrix} 1 & 0 \\ 0 & 1 \end{pmatrix} = \hbar\omega_0 \begin{pmatrix} 1 & 0 \\ 0 & 0 \end{pmatrix} , \tag{4.293}$$

where we have introduced the atomic transition frequency (4.128). We now exploit the fact that the unit matrix and the Pauli-matrices (4.177) form a basis in the space of complex-valued 2×2-matrices: To this end we consider the raising and lowering Pauli matrices (4.183) which have the properties (4.185). With this we obtain

$$\sigma_+\sigma_- = \begin{pmatrix} 0 & 1 \\ 0 & 0 \end{pmatrix} \begin{pmatrix} 0 & 0 \\ 1 & 0 \end{pmatrix} = \begin{pmatrix} 1 & 0 \\ 0 & 0 \end{pmatrix} , \tag{4.294}$$

so the Hamiltonian of the two-level system (4.293) reduces to

$$\hat{H}^{(0)}_{\text{atom}} = \hbar\omega_0 \sigma_+\sigma_- \tag{4.295}$$

From (4.66) and (4.67) we know that the interaction of the two-level system with an electromagnetic mode is given in the Schrödinger picture by

$$\hat{H}^{(p)} = -i\sqrt{\frac{\hbar\omega}{2V\epsilon_0}}\,\mathbf{d}\cdot\mathbf{e}\,\left(\hat{a}-\hat{a}^\dagger\right)\,, \tag{4.296}$$

so the projection of the electric dipole moment $\mathbf{d}$ in the direction of the polarisation vector $\mathbf{e}$ occurs. Now we translate this interaction operator into the spin language and project it onto both the ground state $|g\rangle$ and the excited state $|e\rangle$:

$$\begin{pmatrix} H_{ee}^{(p)} & H_{eg}^{(p)} \\ H_{ge}^{(p)} & H_{gg}^{(p)} \end{pmatrix} = \begin{pmatrix} \langle e|\,\hat{H}^{(p)}\,|e\rangle & \langle e|\,\hat{H}^{(p)}\,|g\rangle \\ \langle g|\,\hat{H}^{(p)}\,|e\rangle & \langle g|\,\hat{H}^{(p)}\,|g\rangle \end{pmatrix} = -i\sqrt{\frac{\hbar\omega}{2V\epsilon_0}}\begin{pmatrix} 0 & d_{eg} \\ d_{eg}^* & 0 \end{pmatrix}\left(\hat{a}-\hat{a}^\dagger\right)\,,$$

where we used the dipole matrix element

$$d_{eg} = \langle e|\,\mathbf{d}\cdot\mathbf{e}\,|g\rangle \tag{4.297}$$

as an abbreviation. Thus, the raising and lowering Pauli matrices (4.183) occur also in (4.297):

$$\hat{H}^{(p)} = -i\sqrt{\frac{\hbar\omega}{2V\epsilon_0}}\left(d_{eg}\sigma_+ + d_{eg}^*\sigma_-\right)\left(\hat{a}-\hat{a}^\dagger\right)\,. \tag{4.298}$$

Multiplying out the two brackets yields in total four interaction terms:

$$\hat{H}^{(p)} = -i\sqrt{\frac{\hbar\omega}{2V\epsilon_0}}\left(d_{eg}\sigma_+\hat{a} - d_{eg}\sigma_+\hat{a}^\dagger + d_{eg}^*\sigma_-\hat{a} - d_{eg}^*\sigma_-\hat{a}^\dagger\right)\,. \tag{4.299}$$

Now we switch from the Schrödinger to the Heisenberg picture and discuss the resulting time dependence of the respective operators. To this end we consider the Heisenberg equations for the dynamics without interaction:

$$i\hbar\frac{\partial\hat{a}}{\partial t} = \left[\hat{a},\hat{H}_{\rm field}^{(0)}\right]_- = \hbar\omega\left[\hat{a},\hat{a}^\dagger\hat{a}\right]_- = \hbar\omega\hat{a}\,, \tag{4.300}$$

$$i\hbar\frac{\partial\sigma_+}{\partial t} = \left[\sigma_+,\hat{H}_{\rm atom}^{(0)}\right]_- = \hbar\omega_0\left[\sigma_+,\sigma_+\sigma_-\right]_- = -\hbar\omega_0\sigma_+\,. \tag{4.301}$$

From (4.300) we conclude for the dynamics of the field operators

$$\hat{a}(t) = \hat{a}(0)e^{i\omega t}\,, \qquad \hat{a}^\dagger(t) = \hat{a}^\dagger(0)e^{-i\omega t}\,, \tag{4.302}$$

and, correspondingly, we read off from (4.301) for the dynamics of the spin matrices

$$\sigma_+(t) = \sigma_+(0)e^{-i\omega_0 t}\,, \qquad \sigma_-(t) = \sigma_-(0)e^{i\omega_0 t}\,. \tag{4.303}$$

This gives qualitatively the following time dependencies for the four interaction terms of (4.299) in the Heisenberg picture:

$$\hat{H}^{(p)}(t) \sim e^{-i\omega_0 t}e^{i\omega t} - e^{-i\omega_0 t}e^{-i\omega t} + e^{i\omega_0 t}e^{i\omega t} - e^{i\omega_0 t}e^{-i\omega t}\,. \tag{4.304}$$

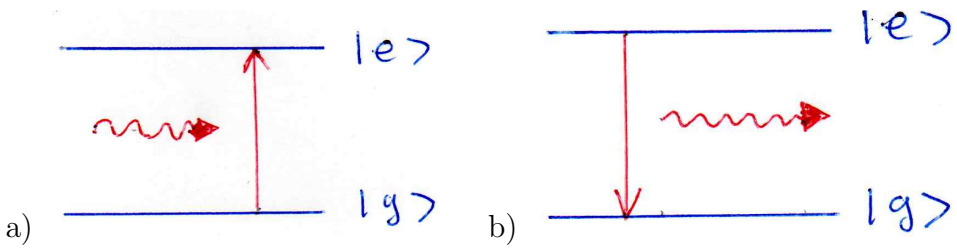

Figure 4.14: Illustration of the elementary interaction processes (4.307) between atomic two-level system and cavity mode in the Jaynes-Cummings model: a) Absorption of photon and excitation of two-level system as well as b) relaxation of two-level system and emission of photon.

In the context of the rotating wave approximation, both the second and the third term can be neglected because they oscillate rapidly, yielding approximately

$$\hat{H}^{(p)} = -i\sqrt{\frac{\hbar\omega}{2V\epsilon_0}}\left(d_{eg}\sigma_+\hat{a} - d_{eg}^*\sigma_-\hat{a}^\dagger\right) \tag{4.305}$$

With this we are able to introduce a complex quantity g, which characterises the strength of the light-matter interaction and has the physical dimension of a frequency:

$$\hbar g = -i\sqrt{\frac{\hbar\omega}{2V\epsilon_0}}\, d_{eg}\,, \qquad \hbar g^* = i\sqrt{\frac{\hbar\omega}{2V\epsilon_0}}\, d_{eg}^*\,. \tag{4.306}$$

Thus, the interaction operator (4.305) is then given by

$$\hat{H}^{(p)} = \hbar g\sigma_+\hat{a} + \hbar g^*\sigma_-\hat{a}^\dagger\,. \tag{4.307}$$

Here the first term means that the absorption of a photon yields a transition of the atom from the ground to the excited state, whereas correspondingly the second term describes an atomic transition from the excited to the ground state giving rise to the emission of a photon, see Fig. 4.14. As a result we obtain the model suggested by Edwin Jaynes und Fred Cummings in 1963, which is described by the Hamilton operator [41, 42]

$$\hat{H}_{\rm JC} = \hbar\omega\hat{a}^\dagger\hat{a} + \hbar\omega_0\sigma_+\sigma_- + \hbar g\sigma_+\hat{a} + \hbar g^*\sigma_-\hat{a}^\dagger\,. \tag{4.308}$$

In the following we investigate the properties of this model analytically. It should be noted that the Jaynes-Cummings model can also be solved exactly without the rotating wave approximation used here [43, 44].

4.5.2 Eigenvalue Problem of Model Hamiltonian

First of all, let us characterise the underlying Hilbert space. It is spanned by the basis states

$$\{|g\rangle\,|N\rangle\,, |e\rangle\,|N\rangle\}\,, \qquad N = 0, 1, \ldots\,. \tag{4.309}$$

This means that the two-level system is either in the ground or in the excited state and that a certain number of photons N is stored in the electromagnetic mode. These basis states are already eigenstates of the non-interacting Jaynes-Cummings Hamiltonian:

$$\left(\hbar\omega\hat{a}^\dagger\hat{a} + \hbar\omega_0\sigma_+\sigma_-\right)|g\rangle\,|N\rangle = \hbar\omega N\,|g\rangle\,|N\rangle\;, \tag{4.310}$$

$$\left(\hbar\omega\hat{a}^\dagger\hat{a} + \hbar\omega_0\sigma_+\sigma_-\right)|e\rangle\,|N\rangle = (\hbar\omega N + \hbar\omega_0)\,|e\rangle\,|N\rangle\;. \tag{4.311}$$

This observation raises the question how the basis states (4.309) are affected by the interaction operator (4.307). The observation

$$\hbar g\sigma_+\hat{a}\,|g\rangle\,|N\rangle = \hbar g\sqrt{N}\,|e\rangle\,|N-1\rangle\;,\; \hbar g^*\sigma_-\hat{a}^\dagger\,|e\rangle\,|N-1\rangle = \hbar g^*\sqrt{N}\,|g\rangle\,|N\rangle \tag{4.312}$$

suggests that the two-dimensional subspace, which is spanned by $|g\rangle\,|N\rangle$ and $|e\rangle\,|N-1\rangle$, could possibly be an eigenspace of the Jaynes-Cummings Hamilton operator (4.308). In order to explore this further let us consider the operator

$$\hat{N} = \hat{a}^\dagger\hat{a} + |e\rangle\langle e| = \hat{a}^\dagger\hat{a} + \sigma_+\sigma_-\,, \tag{4.313}$$

which measures the number of polaritons, i.e. the number of excitations at which the two-level system and the light field are coupled together. The operator (4.313) has the property to be already diagonal with respect to the basis states $|g\rangle\,|N\rangle$ and $|e\rangle\,|N-1\rangle$ of each two-dimensional subspace:

$$\hat{N}\,|g\rangle\,|N\rangle = N\,|g\rangle\,|N\rangle\;, \qquad \hat{N}\,|e\rangle\,|N-1\rangle = N\,|e\rangle\,|N-1\rangle\;. \tag{4.314}$$

Furthermore, we can explicitly show that the polariton number operator (4.313) commutes with the Jaynes-Cummings Hamiltonian (4.308):

$$\begin{aligned}\left[\hat{N}, \hat{H}_{\rm JC}\right]_- &= \left[\hat{a}^\dagger\hat{a} + \sigma_+\sigma_-, \cancel{\hbar\omega\hat{a}^\dagger\hat{a}} + \cancel{\hbar\omega_0\sigma_+\sigma_-} + \hbar g\sigma_+\hat{a} + \hbar g^*\sigma_-\hat{a}^\dagger\right]_- \\ &= \hbar g\left(\left[\hat{a}^\dagger\hat{a}, \hat{a}\right]_-\sigma_+ + \left[\sigma_+\sigma_-, \sigma_+\right]_-\hat{a}\right) + \hbar g^*\left(\left[\hat{a}^\dagger\hat{a}, \hat{a}^\dagger\right]_-\sigma_- + \left[\sigma_+\sigma_-, \sigma_-\right]_-\hat{a}^\dagger\right) \\ &= \hbar g\left(-\hat{a}\sigma_+ + \sigma_+\hat{a}\right) + \hbar g^*\left(\hat{a}^\dagger\sigma_- - \hat{a}^\dagger\sigma_-\right) = 0\,. \end{aligned} \tag{4.315}$$

This means that $\hat{N}$ and $\hat{H}_{\rm JC}$ have a common set of eigenstates. They can be characterised by the quantum number N of the polariton number operator $\hat{N}$. In the special case $N = 0$ the following applies:

$$\hat{H}_{\rm JC}\,|g, 0\rangle = 0\,. \tag{4.316}$$

On the other hand in case of $N = 1, 2, 3, \ldots$ there is a two-dimensional subspace that is spanned by the states $|g, N\rangle$ and $|e, N-1\rangle$. Therefore, the Jaynes-Cummings Hamiltonian is diagonalised in this two-dimensional subspace. Let us consider the matrix elements of the Jaynes-Cummings Hamiltonian (4.308) in the two-dimensional subspace

$$H_{\rm JC}^{(N)} = \begin{pmatrix} \langle e, N-1|\,\hat{H}_{\rm JC}\,|e, N-1\rangle & \langle e, N-1|\,\hat{H}_{\rm JC}\,|g, N\rangle \\ \langle g, N|\,\hat{H}_{\rm JC}\,|e, N-1\rangle & \langle g, N|\,\hat{H}_{\rm JC}\,|g, N\rangle \end{pmatrix}, \tag{4.317}$$

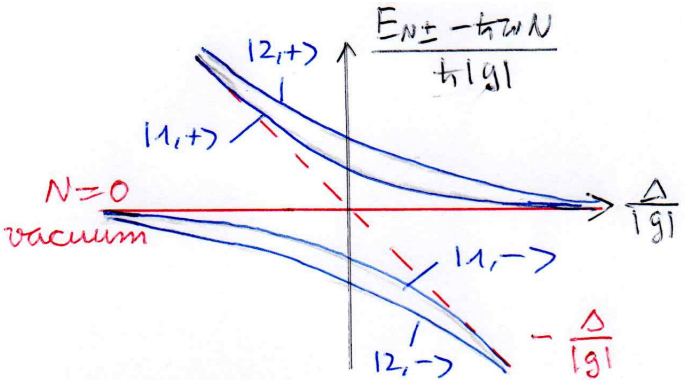

Figure 4.15: Polariton branches (4.323) of the Jaynes-Cummings model as a function of the detuning Δ.

which reduce to

$$H_{\rm JC}^{(N)} = \begin{pmatrix} \hbar\omega(N-1)+\hbar\omega_0 & \hbar g\sqrt{N} \\ \hbar g^*\sqrt{N} & \hbar\omega N \end{pmatrix} . \tag{4.318}$$

For the eigenvalues of the 2×2-matrix

$$\text{Det}\left(H_{\rm JC}^{(N)} - E\right) = \begin{vmatrix} \hbar\omega(N-1)+\hbar\omega_0 - E & \hbar g\sqrt{N} \\ \hbar g^*\sqrt{N} & \hbar\omega N - E \end{vmatrix} = 0 \tag{4.319}$$

we get with the detuning (4.129) the quadratic equation

$$E^2 - (2\hbar\omega N - \hbar\Delta)\, E + \hbar\omega N\,(\hbar\omega N - \hbar\Delta) - \hbar^2\,|g|^2\, N = 0\,. \tag{4.320}$$

Its solution yields

$$E_{N\pm} = \hbar\omega N - \frac{\hbar\Delta}{2} \pm \frac{\hbar}{2} R_N(\Delta)\,, \tag{4.321}$$

where we have introduced the generalized Rabi frequency

$$R_N(\Delta) = \sqrt{\Delta^2 + 4\,|g|^2\, N}\,. \tag{4.322}$$

Thus, there exist two energy eigenvalues for each polariton number N, namely the upper polariton branch E_{N+} and the lower polariton branch E_{N-}. In view of a suitable graphical representation we rewrite (4.321) as follows:

$$\frac{E_{N\pm} - \hbar\omega N}{\hbar\,|g|} = -\frac{\Delta}{2\,|g|} \pm \sqrt{\left(\frac{\Delta}{2\,|g|}\right)^2 + N}\,. \tag{4.323}$$

In Fig. 4.15 we depict that the polariton energies (4.323) as a function of the detuning Δ represent hyperbolas that asymptotically approach the red lines. We observe that no energetic degeneracy occurs and that we have a non-linear dependence on the polariton number N due to generalised Rabi frequency (4.322). Therefore, the Jaynes-Cummings model has a much more complicated dynamics than the Rabi model, as we will now reveal step by step.

4.5.3 Vacuum Rabi Oscillations

We first consider the special case of resonance $\omega = \omega_0$, where the detuning vanishes, i.e. we have $\Delta = 0$. The Jaynes-Cumming-Hamiltonian (4.308) then reduces with the polariton operator (4.313) to:

$$\hat{H}_{\mathrm{JC}} = \hbar\omega\hat{N} + \hbar g\sigma_+\hat{a} + \hbar g^*\sigma_-\hat{a}^\dagger \,. \tag{4.324}$$

In the following we determine the solution of the corresponding time-dependent Schrödinger equation

$$i\hbar\frac{\partial}{\partial t}\,|\psi(t)\rangle = \hat{H}_{\mathrm{JC}}\,|\psi(t)\rangle \tag{4.325}$$

for the initial state

$$|\psi(0)\rangle = |i\rangle = |e, N\rangle \;; \qquad N = 0, 1, 2, \ldots \,. \tag{4.326}$$

Due to the Jaynes-Cummings Hamiltonian (4.324), this initial state $|i\rangle$ is only coupled to the final state

$$|f\rangle = |g, N+1\rangle \,. \tag{4.327}$$

Therefore, we perform the solution ansatz

$$|\psi(t)\rangle = c_i(t)\,|i\rangle + c_f(t)\,|f\rangle \;, \tag{4.328}$$

so that the initial condition (4.327) translates into

$$c_i(0) = 1\,, \qquad c_f(0) = 0\,. \tag{4.329}$$

Inserting the solution ansatz (4.328) into the time-dependent Schrödinger equation (4.325), we get at first

$$i\hbar\dot{c}_i(t)\,|i\rangle + i\hbar\dot{c}_f(t)\,|f\rangle = \hat{H}_{\mathrm{JC}}\Big[c_i(t)\,|i\rangle + c_f(t)\,|f\rangle\Big]\,. \tag{4.330}$$

Projecting (4.330) to the initial state $|i\rangle$ then leads to

$$i\hbar\dot{c}_i(t) = c_i(t)\,\langle i|\,\hat{H}_{\mathrm{JC}}\,|i\rangle + c_f(t)\,\langle i|\,\hat{H}_{\mathrm{JC}}\,|f\rangle \;, \tag{4.331}$$

which reduces to

$$i\hbar\dot{c}_i(t) = \hbar\omega\,(N+1)\,c_i(t) + \hbar g\sqrt{N+1}\,c_f(t)\,. \tag{4.332}$$

Correspondingly the projection of (4.330) to the final state $|f\rangle$ results to

$$i\hbar\dot{c}_f(t) = c_i(t)\,\langle f|\,\hat{H}_{\mathrm{JC}}\,|i\rangle + c_f(t)\,\langle f|\,\hat{H}_{\mathrm{JC}}\,|f\rangle \;, \tag{4.333}$$

yielding

$$i\hbar\dot{c}_f(t) = \hbar g^* \sqrt{N+1}\, c_i(t) + \hbar\omega\,(N+1)\, c_f(t)\,. \tag{4.334}$$

Due to the assumed resonance $\omega = \omega_0$ both differential equations (4.332) and (4.334) are simplified by transforming into a co-rotating coordinate system:

$$c_i(t) = \tilde{c}_i(t) e^{-i\omega(N+1)t}\,, \qquad c_f(t) = \tilde{c}_f(t) e^{-i\omega(N+1)t}\,. \tag{4.335}$$

The transformed coefficients then satisfy the following two differential equations:

$$\dot{\tilde{c}}_i(t) = -ig\sqrt{N+1}\,\tilde{c}_f(t)\,, \tag{4.336}$$

$$\dot{\tilde{c}}_f(t) = -ig^*\sqrt{N+1}\,\tilde{c}_i(t)\,. \tag{4.337}$$

Eliminating $\tilde{c}_f(t)$ leads to a second-order differential equation for $\tilde{c}_i(t)$, which corresponds to a harmonic oscillator:

$$\ddot{\tilde{c}}_i(t) = -ig\sqrt{N+1}\,\dot{\tilde{c}}_f(t) = -\,|g|^2\,(N+1)\;\tilde{c}_i(t)\,. \tag{4.338}$$

The general solution of (4.338) reads

$$\tilde{c}_i(t) = A\cos\left(|g|\sqrt{N+1}t\right) + B\sin\left(|g|\sqrt{N+1}t\right)\,, \tag{4.339}$$

so we obtain for $\tilde{c}_f(t)$ the result

$$\tilde{c}_f(t) = \frac{i\dot{\tilde{c}}_i(t)}{g\sqrt{N+1}} = \frac{i\,|g|}{g}\left[-A\sin\left(|g|\sqrt{N+1}t\right) + B\cos\left(|g|\sqrt{N+1}t\right)\right]\,. \tag{4.340}$$

Incorporating the initial condition (4.329) leads to

$$\left.\begin{aligned}\tilde{c}_i(0) &= A = 1\\ \tilde{c}_f(0) &= i\sqrt{\frac{g^*}{g}}B = 0\end{aligned}\right\} \quad\Longrightarrow\quad \begin{cases}\tilde{c}_i(t) = \cos\left(|g|\sqrt{N+1}t\right)\\ \tilde{c}_f(t) = -i\sqrt{\dfrac{g^*}{g}}\sin\left(|g|\sqrt{N+1}t\right)\end{cases}\,. \tag{4.341}$$

With this the probability of being in the initial or final state results in

$$P_i(t) = |c_i(t)|^2 = |\tilde{c}_i(t)|^2 = \cos^2\left(|g|\sqrt{N+1}t\right) = \frac{1}{2}\left[1+\cos\left(2\,|g|\sqrt{N+1}t\right)\right]\,, \tag{4.342}$$

$$P_f(t) = |c_f(t)|^2 = |\tilde{c}_f(t)|^2 = \sin^2\left(|g|\sqrt{N+1}t\right) = \frac{1}{2}\left[1-\sin\left(2\,|g|\sqrt{N+1}t\right)\right]\,. \tag{4.343}$$

This means that the probabilities (4.342) and (4.343) oscillate in the same way as in the Rabi model according to (4.164), see Fig. 4.16. But in the Jaynes-Cummings case the quantum electrodynamic Rabi frequency reads

$$\Omega_{\mathrm{R}}(N) = 2\,|g|\sqrt{N+1}\,, \tag{4.344}$$

which depends nonlinearily on the photon number N. This means that Rabi oscillations even occur in the vacuum, which is characterised by having no photon at all, i.e. $N = 0$. In contrast

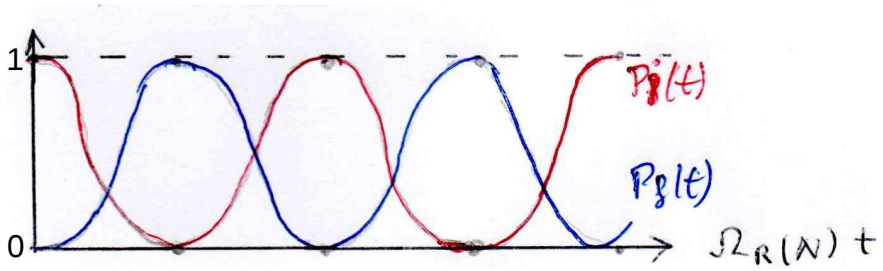

Figure 4.16: Probabilities to be in the excited state (4.342) or in the ground state (4.343) oscillate with the quantum electrodynamic Rabi frequency (4.344).

to that oscillations in the Rabi model only exist according to (4.164) provided that the electric field and, thus, the matrix dipole moment is different from zero. The vacuum Rabi oscillations in the Jaynes-Cummings model have therefore no classical counterpart. Physically, they can be explained by the fact that the atom spontaneously emits a photon, see Fig. 4.14b) and then reabsorbs it again, see Fig. 4.14a), which is a reversible process. Such effects can be observed in atoms in a cavity, where the lifetime of a photon is long enough.

4.5.4 Collapse and Revival

Actually, it is astonishing that a non-classical Fock state as an initial condition of the Jaynes-Cummings dynamics leads to an oscillation that corresponds to that of the classical Rabi model. In contrast to that one would rather expect that a coherent state as an initial condition would lead to a classical Rabi oscillation of the Jaynes-Cummings model. In the following we will see that this intuition fails and that a coherent state as an initial condition leads instead to a surprisingly complex Jaynes-Cummings dynamics.

To this end we solve again the time-dependent Schrödinger equation (4.325) for the Jaynes-Cummings Hamiltonian without detuning (4.324). The most general solution is described by the following ansatz:

$$|\psi(t)\rangle = \sum_{n=0}^{\infty} \Big[c_{gn}(t)\,|g\rangle + c_{en}(t)\,|e\rangle \Big]\,|n\rangle \ . \tag{4.345}$$

Inserting this ansatz into the time-dependent Schrödinger equation (4.325) with the Jaynes-Cummings Hamiltonian (4.308) leads to:

$$\begin{aligned} i\hbar \sum_{n=0}^{\infty} \Big[\dot{c}_{gn}(t)\,|g\rangle + \dot{c}_{en}(t)\,|e\rangle \Big]\,|n\rangle &= \hbar\omega \sum_{n=0}^{\infty} \Big[n c_{gn}(t)\,|g\rangle + (n+1)\,c_{en}(t)\,|e\rangle \Big]\,|n\rangle \\ +\hbar g \sum_{n=0}^{\infty} \sqrt{n} c_{gn}(t)\,|e\rangle\,|n-1\rangle + \hbar g^* \sum_{n=0}^{\infty} \sqrt{n+1} c_{en}(t)\,|g\rangle\,|n+1\rangle \ . \end{aligned} \tag{4.346}$$

Here we perform in the last two terms the resummations $n' = n-1$ and $n' = n+1$, respectively, so that they turn out to be of the same form as the rest of the terms. This makes it possible

to project (4.346) onto the states $|g\rangle|n\rangle$ and $|e\rangle|n\rangle$:

$$i\hbar\dot{c}_{gn}(t) = \hbar\omega n c_{gn}(t) + \hbar g^*\sqrt{n}c_{en-1}(t)\,, \tag{4.347}$$

$$i\hbar\dot{c}_{en}(t) = \hbar\omega\,(n+1)\,c_{en}(t) + \hbar g\sqrt{n+1}c_{gn+1}(t)\,. \tag{4.348}$$

As expected from the general structure of the Jaynes-Cummings Hamiltonian, we obtain for $c_{gn}(t)$ and $c_{en-1}(t)$ a closed system of differential equations:

$$\dot{c}_{gn}(t) = -i\omega n c_{gn}(t) - ig^*\sqrt{n}c_{en-1}(t)\,, \tag{4.349}$$

$$\dot{c}_{en-1}(t) = -i\omega n c_{en-1}(t) - ig\sqrt{n}c_{gn}(t)\,. \tag{4.350}$$

Since the detuning is assumed to disappear, also this system of differential equations simplifies considerably when we transform into a corresponding co-rotating system according to

$$c_{gn}(t) = \tilde{c}_{gn}(t)e^{-i\omega nt}\,, \qquad c_{en-1}(t) = \tilde{c}_{en-1}(t)e^{-i\omega nt}\,. \tag{4.351}$$

With this (4.349) and (4.350) are converted into

$$\dot{\tilde{c}}_{gn}(t) = -ig^*\sqrt{n}\tilde{c}_{en-1}(t)\,, \tag{4.352}$$

$$\dot{\tilde{c}}_{en-1}(t) = -ig\sqrt{n}\tilde{c}_{gn}(t)\,. \tag{4.353}$$

Eliminating $\tilde{c}_{en-1}(t)$ we obtain a second-order differential equation for $\tilde{c}_{gn}(t)$:

$$\ddot{\tilde{c}}_{gn}(t) = -ig^*\sqrt{n}\dot{\tilde{c}}_{en-1}(t) = -\,|g|^2\,n\tilde{c}_{gn}(t)\,. \tag{4.354}$$

This represents the differential equation of a harmonic oscillator, which has the general solution:

$$\tilde{c}_{gn}(t) = A_n\cos\left(|g|\,\sqrt{n}t\right) + B_n\sin\left(|g|\,\sqrt{n}t\right)\,. \tag{4.355}$$

The corresponding general solution for $\tilde{c}_{en-1}(t)$ then reads

$$\tilde{c}_{en-1}(t) = \frac{i}{g^*\sqrt{n}}\dot{\tilde{c}}_{gn}(t) = i\sqrt{\frac{g}{g^*}}\left[-A_n\sin\left(|g|\,\sqrt{n}t\right) + B_n\cos\left(|g|\,\sqrt{n}t\right)\right]\,. \tag{4.356}$$

Let us consider as the initial state $|\psi(0)\rangle$ the most general possible pure state, which consists of the atomic state

$$|\psi_{\text{atom}}\rangle = c_g\,|g\rangle + c_e\,|e\rangle \tag{4.357}$$

and the field state

$$|\psi_{\text{field}}\rangle = \sum_{n=0}^{\infty} c_n\,|n\rangle \tag{4.358}$$

via the factorization

$$|\psi(0)\rangle = |\psi_{\text{atom}}\rangle\;|\psi_{\text{field}}\rangle\,. \tag{4.359}$$

This has the following consequences for the initial values of the coefficients $c_{gn}(t)$ and $c_{en}(t)$:

$$c_{gn}(0) = \tilde{c}_{gn}(0) = A_n = c_g c_n \,, \tag{4.360}$$

$$c_{en}(0) = \tilde{c}_{en}(0) = i\sqrt{\frac{g}{g^*}} B_{n+1} = c_e c_n \,, \tag{4.361}$$

where we conclude from (4.361)

$$B_n = -i\sqrt{\frac{g^*}{g}}\, c_e c_{n-1} \,. \tag{4.362}$$

With the coefficients A_n and B_n determined according to (4.360) and (4.362), the solution of the initial value problem follows from (4.355) and (4.356):

$$\begin{aligned} |\psi(t)\rangle = \sum_{n=0}^{\infty} \Bigg\{ & e^{-i\omega(n+1)t} \left[c_e c_n \cos\left(|g|\sqrt{n+1}t\right) - i\sqrt{\frac{g}{g^*}} c_g c_{n+1} \sin\left(|g|\sqrt{n+1}t\right) \right] |e\rangle \\ & + e^{-i\omega n t} \left[c_g c_n \cos\left(|g|\sqrt{n}t\right) - i\sqrt{\frac{g^*}{g}} c_e c_{n-1} \sin\left(|g|\sqrt{n}t\right) \right] |g\rangle \Bigg\} |n\rangle \,. \end{aligned} \tag{4.363}$$

Thus, we read off from (4.363) that an initial pure product state of light and matter (4.359) becomes a mixed state of light and matter due to the Jaynes-Cummings dynamics.

In the following we restrict ourselves to the special case $c_e = 1$, $c_g = 0$ and obtain

$$|\psi(t)\rangle = |\psi_e(t)\rangle\,|e\rangle + |\psi_g(t)\rangle\,|g\rangle \tag{4.364}$$

with the atomic wave functions

$$|\psi_e(t)\rangle = \sum_{n=0}^{\infty} e^{-i\omega(n+1)t} c_n \cos\left(|g|\sqrt{n+1}t\right) |n\rangle \,, \tag{4.365}$$

$$|\psi_g(t)\rangle = -i\sqrt{\frac{g^*}{g}} \sum_{n=0}^{\infty} e^{-i\omega(n+1)t} c_n \sin\left(|g|\sqrt{n+1}t\right) |n+1\rangle \,. \tag{4.366}$$

As a crosscheck, we note that the subsequent specialisation $c_n = \delta_{n,N}$ leads, indeed, to the vacuum Rabi oscillations (4.335) and (4.341) discussed in the previous section. But without this further specialisation we obtain a quite complicated dynamics. For the probabilities of being in the excited state and in the ground state, respectively, we get

$$P_e(t) = \langle\psi_e(t)|\psi_e(t)\rangle = \sum_{n=0}^{\infty} |c_n|^2 \cos^2\left(\sqrt{n+1}\,|g|\,t\right) \,, \tag{4.367}$$

$$P_g(t) = \langle\psi_g(t)|\psi_g(t)\rangle = \sum_{n=0}^{\infty} |c_n|^2 \sin^2\left(\sqrt{n+1}\,|g|\,t\right) \,, \tag{4.368}$$

so that the atomic occupation inversion results in

$$W(t) = P_e(t) - P_g(t) = \sum_{n=0}^{\infty} |c_n|^2 \cos\left(2\sqrt{n+1}\,|g|\,t\right) \,. \tag{4.369}$$

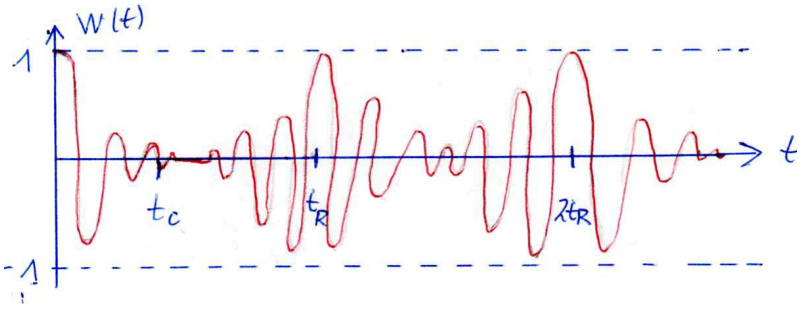

Figure 4.17: Collapse and revival dynamics of the atomic occupation inversion (4.371) sketched for an average photon number $\langle \hat{n} \rangle_\alpha = 5$. Collapse time t_c and revival time t_r are determined below in (4.386) and in (4.391), respectively.

As a concrete example, we now consider as an initial state the most classical of all quantum states of light, namely a coherent state $|\alpha\rangle$, which is Poissonian distributed with respect to the Fock states according to (3.190), see Fig. 3.7:

$$c_n = \frac{\alpha^n}{\sqrt{n!}} e^{-|\alpha|^2/2}, \qquad P_n = |c_n|^2 = \frac{|\alpha|^{2n}}{n!} e^{-|\alpha|^2}. \tag{4.370}$$

In fact, we have checked in (3.198) that the Poisson distribution (4.370) is normalised. Furthermore, the average photon number led in (3.199) to the result $\langle \hat{n} \rangle_\alpha = |\alpha|^2$, so that the Poisson distribution (4.370) can also be rewritten according to (3.202). With this we obtain for the atomic occupation inversion (4.369)

$$W(t) = e^{-\langle \hat{n} \rangle_\alpha} \sum_{n=0}^{\infty} \frac{\langle \hat{n} \rangle_\alpha^n}{n!} \cos\left(2\sqrt{n+1}\,|g|\,t\right). \tag{4.371}$$

We read off that the fully quantised dynamics represents a superposition of Rabi oscillations with the quantum electrodynamic Rabi frequencies (4.344) and, thus, differs strongly from a classical Rabi oscillation as is illustrated in Fig. 4.17:

- At the beginning, the Rabi oscillations seem to be damped, which is called a *collapse*. This was already noticed early on in the analysis of the Jaynes-Cummings model.
- Only a few years later, after the computer programs ran longer, it was discovered that after a certain rest period the Rabi oscillations begin again, which represents a *revival*.
- At even later times, one finds a sequence of collapses and revivals, with the revivals becoming less pronounced as time progresses.

Let us at first roughly estimate the *collapse time*. To this end we note that the dominant contribution in the series comes from that summand n, which coincides with the average photon number $\langle \hat{n} \rangle_\alpha$. The corresponding quantum electrodynamic Rabi frequency (4.344) is:

$$\Omega_R(\langle \hat{n} \rangle_\alpha) = 2\,|g|\,\sqrt{\langle \hat{n} \rangle_\alpha + 1} \approx 2\,|g|\,\sqrt{\langle \hat{n} \rangle_\alpha}. \tag{4.372}$$

The physical origin for the collapse is a dephasing due to a superposition of Rabi oscillations, which occur in the interval $[\langle\hat{n}\rangle_\alpha - \Delta n, \langle\hat{n}\rangle_\alpha + \Delta n]$ with the frequency uncertainty

$$\Delta\Omega_{\mathrm{R}} = \Omega_{\mathrm{R}}\left(\langle\hat{n}\rangle_\alpha + \Delta n\right) - \Omega_{\mathrm{R}}\left(\langle\hat{n}\rangle_\alpha - \Delta n\right) . \tag{4.373}$$

In case of a large average photon number, i.e. $\langle\hat{n}\rangle_\alpha \gg 1$, we conclude from (4.372)

$$\Omega_{\mathrm{R}}\left(\langle\hat{n}\rangle_\alpha \pm \Delta n\right) = 2\,|g|\,\sqrt{\langle\hat{n}\rangle_\alpha}\sqrt{1 + \frac{1 \pm \Delta n}{\langle\hat{n}\rangle_\alpha}} \approx 2\,|g|\,\sqrt{\langle\hat{n}\rangle_\alpha}\left(1 + \frac{1 \pm \Delta n}{2\,\langle\hat{n}\rangle_\alpha}\right) , \tag{4.374}$$

so that the frequency uncertainty (4.373) amounts to

$$\Delta\Omega_{\mathrm{R}} = 2\,|g|\,\frac{\Delta n}{\sqrt{\langle\hat{n}\rangle_\alpha}} . \tag{4.375}$$

As a coherent state has the property $\Delta n = \sqrt{\langle\hat{n}\rangle_\alpha}$ according to (3.201), the frequency uncertainty (4.375) reduces to

$$\Delta\Omega_{\mathrm{R}} = 2\,|g| . \tag{4.376}$$

The collapse time can then be crudely estimated from the uncertainty relation between time and frequency:

$$t_{\mathrm{c}} \cdot \Delta\Omega_{\mathrm{R}} \approx 1 \qquad \Longrightarrow \qquad t_{\mathrm{c}} = \frac{1}{2\,|g|} . \tag{4.377}$$

Thus, the collapse time in case of $\langle\hat{n}\rangle_\alpha \gg 1$ turns out to be independent of the mean photon number $\langle\hat{n}\rangle_\alpha$ and is only given by the light-matter interaction strength g.

Now we aim at determining the collapse time more precisely. Here we are guided by the idea that all summands n contribute in the immediate vicinity of $\langle\hat{n}\rangle_\alpha$, so that $n - \langle\hat{n}\rangle_\alpha$ can be regarded as a small quantity. This allows us to approximate the quantum electrodynamic Rabi frequencies (4.344) involved as follows:

$$\begin{aligned}
\Omega_{\mathrm{R}}(n) &= 2\,|g|\,\sqrt{n+1} = 2\,|g|\,\sqrt{\langle\hat{n}\rangle_\alpha + 1 + (n - \langle\hat{n}\rangle_\alpha)} = 2\,|g|\,\sqrt{\langle\hat{n}\rangle_\alpha + 1}\sqrt{1 + \frac{n - \langle\hat{n}\rangle_\alpha}{\langle\hat{n}\rangle_\alpha + 1}} \\
&\approx 2\,|g|\,\sqrt{\langle\hat{n}\rangle_\alpha + 1}\left[1 + \frac{n - \langle\hat{n}\rangle_\alpha}{2\,(\langle\hat{n}\rangle_\alpha + 1)}\right] = 2\,|g|\,\sqrt{\langle\hat{n}\rangle_\alpha + 1} + |g|\,\frac{n - \langle\hat{n}\rangle_\alpha}{\sqrt{\langle\hat{n}\rangle_\alpha + 1}} .
\end{aligned} \tag{4.378}$$

In this approximation, the atomic occupation inversion (4.371) is given by

$$W(t) = e^{-\langle\hat{n}\rangle_\alpha}\sum_{n=0}^{\infty}\frac{\langle\hat{n}\rangle_\alpha^n}{2n!}\left[\exp\left(\frac{i\,|g|\,tn}{\sqrt{\langle\hat{n}\rangle_\alpha + 1}} + 2i\,|g|\,\sqrt{\langle\hat{n}\rangle_\alpha + 1}t - \frac{i\,|g|\,\langle\hat{n}\rangle_\alpha\,t}{\sqrt{\langle\hat{n}\rangle_\alpha + 1}}\right) + \text{h.c.}\right] . \tag{4.379}$$

Now the series can be evaluated explicitly

$$\sum_{n=0}^{\infty}\frac{1}{n!}\left[\langle\hat{n}\rangle_\alpha \exp\left(\pm\frac{i\,|g|\,t}{\sqrt{\langle\hat{n}\rangle_\alpha + 1}}\right)\right]^n = \exp\left[\langle\hat{n}\rangle_\alpha \exp\left(\pm\frac{i\,|g|\,t}{\sqrt{\langle\hat{n}\rangle_\alpha + 1}}\right)\right] . \tag{4.380}$$

Inserting (4.380) into the atomic occupation inversion (4.379) we obtain

$$W(t) = \frac{1}{2}\left\{\exp\left[i\left(2\left|g\right|\sqrt{\left\langle\hat{n}\right\rangle_\alpha + 1} - \frac{\left|g\right|\left\langle\hat{n}\right\rangle_\alpha}{\sqrt{\left\langle\hat{n}\right\rangle_\alpha + 1}}\right)t + \left\langle\hat{n}\right\rangle_\alpha\left(e^{\frac{i\left|g\right|t}{\sqrt{\left\langle\hat{n}\right\rangle_\alpha+1}}} - 1\right)\right] + \text{h.c.}\right\} . \quad (4.381)$$

With the help of the Euler formula

$$e^{i\frac{\left|g\right|t}{\sqrt{\left\langle\hat{n}\right\rangle_\alpha+1}}} = \cos\left(\frac{\left|g\right|t}{\sqrt{\left\langle\hat{n}\right\rangle_\alpha + 1}}\right) + i\sin\left(\frac{\left|g\right|t}{\sqrt{\left\langle\hat{n}\right\rangle_\alpha + 1}}\right) \quad (4.382)$$

this leads directly to the final result

$$\begin{aligned} W(t) &= \cos\left[\left(2\left|g\right|\sqrt{\left\langle\hat{n}\right\rangle_\alpha + 1} - \frac{\left|g\right|\left\langle\hat{n}\right\rangle_\alpha}{\sqrt{\left\langle\hat{n}\right\rangle_\alpha + 1}}\right)t + \left\langle\hat{n}\right\rangle_\alpha \sin\left(\frac{\left|g\right|t}{\sqrt{\left\langle\hat{n}\right\rangle_\alpha + 1}}\right)\right] \\ &\quad \times \exp\left\{-\left\langle\hat{n}\right\rangle_\alpha\left[1 - \cos\left(\frac{\left|g\right|t}{\sqrt{\left\langle\hat{n}\right\rangle_\alpha + 1}}\right)\right]\right\} . \end{aligned} \quad (4.383)$$

Now we analyze (4.383) in view of the collapse, which occurs for small times t. Therefore, we assume that the inequality

$$\frac{\left|g\right|t}{\sqrt{\left\langle\hat{n}\right\rangle_\alpha + 1}} \ll 1 \quad (4.384)$$

is fulfilled, so that the atomic occupation inversion (4.383) reduces to

$$W(t) \approx \cos\left(2\left|g\right|\sqrt{\left\langle\hat{n}\right\rangle_\alpha + 1}\, t\right) \exp\left[-\frac{\left\langle\hat{n}\right\rangle_\alpha \left|g\right|^2 t^2}{2\left(\left\langle\hat{n}\right\rangle_\alpha + 1\right)}\right] . \quad (4.385)$$

Here, the first factor describes, indeed, a classical Rabi oscillation with the quantum electrodynamic Rabi frequency (4.372), which comes from the mean photon number $\left\langle\hat{n}\right\rangle_\alpha$. The second factor, however, represents a Gaussian envelope from which the collapse time can be read off:

$$t_{\text{c}} = \frac{1}{\left|g\right|}\sqrt{\frac{2\left(\left\langle\hat{n}\right\rangle_\alpha + 1\right)}{\left\langle\hat{n}\right\rangle_\alpha}} . \quad (4.386)$$

At first we note that the obtained collapse time (4.386) does, indeed, satisfy the approximation of small times demanded in (4.384). Namely it holds

$$\frac{\left|g\right|t_{\text{c}}}{\sqrt{\left\langle\hat{n}\right\rangle_\alpha + 1}} = \sqrt{\frac{2}{\left\langle\hat{n}\right\rangle_\alpha}} \ll 1 \quad (4.387)$$

provided that the mean photon number $\left\langle\hat{n}\right\rangle_\alpha$ is large enough, i.e. $\left\langle\hat{n}\right\rangle_\alpha \gg 1$ is fulfilled. Furthermore, we conclude in this limit $\left\langle\hat{n}\right\rangle_\alpha \gg 1$ that the collapse time (4.386) is approximately independent of $\left\langle\hat{n}\right\rangle_\alpha$:

$$t_{\text{c}} \approx \frac{\sqrt{2}}{\left|g\right|} . \quad (4.388)$$

This result agrees with that of the above rough estimate (4.377) except for the numerical factor.

Let us now roughly estimate the *revival time*. To this end we recall that the atomic occupation inversion (4.371) is a superposition of Rabi oscillations with the quantum electrodynamic Rabi frequencies (4.344). In case that two neighbouring terms have the phase $(2k+1)\,\pi$ or $2k\pi$ with $k \in \mathbb{N}$, then the largest possible destructive or constructive interference occurs. Thus, a revival occurs provided that

$$\left[\Omega_{\mathrm{R}}\left(\langle\hat{n}\rangle_{\alpha}+1\right)-\Omega_{\mathrm{R}}\left(\langle\hat{n}\rangle_{\alpha}\right)\right]t_{\mathrm{r}}=2k\pi \tag{4.389}$$

is fulfilled, since the summand with $n=\langle\hat{n}\rangle_{\alpha}$ makes the dominant contribution. Using (4.374) with $\Delta n=1$ or $\Delta n=0$ we deduce from (4.389)

$$\frac{|g|\,t_{\mathrm{r}}}{\sqrt{\langle\hat{n}\rangle_{\alpha}}}=2k\pi \qquad \Longrightarrow \qquad t_{\mathrm{r}}=\frac{\sqrt{\langle\hat{n}\rangle_{\alpha}}}{|g|}\,2k\pi\,. \tag{4.390}$$

In the case of $\langle\hat{n}\rangle_{\alpha}=5$, this leads to the revival time $t_{\mathrm{r}}=2\pi\sqrt{5}/\,|g|\approx 14/\,|g|$, see Fig. 4.17.

Subsequently, we also calculate the revival time more precisely. To this end we go back to the previous result (4.383) and directly apply the approximation of a large mean photon number, i.e. $\langle\hat{n}\rangle_{\alpha}\gg 1$. The first factor in (4.383) describes then the dominant fast oscillating Rabi oscillation with the frequency (4.372). The second factor, however, represents the envelope, which leads for small times to the result (4.386) for the collapse time. For large times, however, the envelope is periodic and the maximum amplitude occurs at

$$\frac{|g|\,t_{\mathrm{r}}}{\sqrt{\langle\hat{n}\rangle_{\alpha}+1}}=2k\pi \qquad \Longrightarrow \qquad t_{\mathrm{r}}=\frac{\sqrt{\langle\hat{n}\rangle_{\alpha}+1}}{|g|}\,2k\pi\,. \tag{4.391}$$

In case of $\langle\hat{n}\rangle_{\alpha}\gg 1$ this is consistent with the above rough estimate (4.390). Furthermore, provided one knows that the photon statistics leading to Jaynes-Cumming collapse and revival dynamics stems from a coherent state, measuring collapse and revival time (4.386) and (4.391) allows to reconstruct both the mean photon number according to

$$\langle\hat{n}\rangle_{\alpha}=2\left(\frac{t_{\mathrm{c}}}{t_{\mathrm{r}}}\right)^{2} \tag{4.392}$$

and the light-matter interaction strength via

$$|g|=\frac{\sqrt{2t_{\mathrm{c}}^{2}+t_{r}^{2}}}{t_{\mathrm{r}}^{2}}\,. \tag{4.393}$$

In this context we mention that Ref. [45] analyzes the collapse-revival dynamics (4.371) of the atomic occupation inversion in the Jaynes-Cummings model in more detail on the basis of the Poisson sum formula (2.217) introduced in Subsection 2.17.3. On the one hand it becomes possible to determine the collapse and the revivals for a general photon distribution by approximately evaluating the involved integrals in case of a slowly varying photon distribution. This approach is illustrated by dealing with the examples of both a coherent and a squeezed photon distribution. On the other hand this also allows to reconstruct the underlying photon statistics of the quantized field by measuring the atomic collapse of a single revival.

4.5.5 Dressed States

There are many methods available for determining the dynamics of the Jaynes-Cummings model. So far we have directly solved the underlying Schrödinger equation for some initial wave function of both the two-level atom and the electromagnetic mode. By doing so, we have restricted ourselves to a vanishing detuning in order to reduce the complexity of the calculation. Now, however, we work out another important approach to unravel the dynamics of the Jaynes-Cummings, which is based on the stationary states of its Hamiltonian. For reasons, which become clear shortly, these eigenstates are called *dressed states*. And for this dressed states approach we do not demand a vanishing detuning but we consider the more general case of a finite detuning and go back to the Jaynes-Cummings Hamiltonian (4.308). In Subsection 4.5.2 we have seen that the underlying Hilbert space is spanned by the basis states (4.309) and that it decomposes into the ground state $|g,0\rangle$ and an infinite set of two-dimensional subspaces

$$\{|g,N\rangle\,,|e,N-1\rangle\}\;,\qquad N=1,2,\ldots\;. \tag{4.394}$$

Each one of these two-dimensional subspaces is spanned by the states

$$|\psi_{1N}\rangle=|e,N-1\rangle\;,\qquad |\psi_{2N}\rangle=|g,N\rangle\;, \tag{4.395}$$

which are orthonormal

$$\langle\psi_{iN}|\psi_{jN}\rangle=\delta_{ij}\,. \tag{4.396}$$

Projecting the Jaynes-Cummings Hamiltonian (4.308) into such a two-dimensional subspace leads according to (4.318) to a 2×2-matrix:

$$\Big(H^{(N)}_{\mathrm{JC},ij}\Big)=\Big(\langle\psi_{iN}|\,\hat{H}_{\mathrm{JC}}\,|\psi_{jN}\rangle\Big)=\begin{pmatrix}\hbar\omega N-\hbar\Delta & \hbar g\sqrt{N}\\ \hbar g^*\sqrt{N} & \hbar\omega N\end{pmatrix}. \tag{4.397}$$

In Subsection 4.5.2 we have determined its energy eigenvalues (4.321), which depend via the generalized Rabi frequencies (4.322) on the detuning (4.129). But now we determine the corresponding eigenstates:

$$\Big(H^{(N)}_{\mathrm{JC},ij}-\delta_{ij}E_{N\pm}\Big)\begin{pmatrix}c_1^{N,\pm}\\ c_2^{N,\pm}\end{pmatrix}=\begin{pmatrix}0\\0\end{pmatrix}. \tag{4.398}$$

Thus, we have to solve the following set of linear homogeneous equations:

$$\begin{pmatrix}-\dfrac{\hbar}{2}\,\Delta\mp\dfrac{\hbar}{2}\,R_N(\Delta) & \hbar g\sqrt{N}\\ \hbar g^*\sqrt{N} & \dfrac{\hbar}{2}\,\Delta\mp\dfrac{\hbar}{2}\,R_N(\Delta)\end{pmatrix}\begin{pmatrix}c_1^{N,\pm}\\ c_2^{N,\pm}\end{pmatrix}=\begin{pmatrix}0\\0\end{pmatrix}. \tag{4.399}$$

As both equations are linear dependent, we can restrict ourselves to one of them without loss of generality. For the upper polariton branch, which corresponds to the case "+", we take the first one from (4.399)

$$-\frac{\hbar}{2}\Big[\Delta+R_N(\Delta)\Big]c_1^{N,+}+\hbar g\sqrt{N}c_2^{N,+}=0\quad\Longrightarrow\quad\begin{cases}c_1^{N,+}=2g\sqrt{N}c^{N,+}\\ c_2^{N,+}=\Big[R_N(\Delta)+\Delta\Big]c^{N,+}\end{cases}. \tag{4.400}$$

The normalisation condition yields:

$$\left|c_1^{N,+}\right|^2 + \left|c_2^{N,+}\right|^2 = 1 \quad \Longrightarrow \quad c^{N,+} = \frac{e^{i\varphi^{N,+}}}{\sqrt{2R_N(\Delta)\left[R_N(\Delta)+\Delta\right]}}\,. \tag{4.401}$$

With this the eigenstate for the upper polariton branch finally reads with the generalized Rabi frequency (4.322) and $g = |g|\,e^{i\varphi_g}$

$$c_1^{N,+} = \frac{2g\sqrt{N}e^{i\varphi^{N,+}}}{\sqrt{2R_N(\Delta)\left[R_N(\Delta)+\Delta\right]}} = \sqrt{\frac{R_N(\Delta)-\Delta}{2R_N(\Delta)}}\,e^{i\left(\varphi^{N,+}+\varphi_g\right)}\,, \tag{4.402}$$

$$c_2^{N,+} = \sqrt{\frac{R_N(\Delta)+\Delta}{2R_N(\Delta)}}\,e^{i\varphi^{N,+}}\,. \tag{4.403}$$

For the lower polariton branch, which is characterized by the case "-", however, we take the second equation from (4.399)

$$\hbar g^*\sqrt{N}c_1^{N,-} + \frac{\hbar}{2}\left[\Delta + R_N(\Delta)\right]c_2^{N,-} = 0 \quad \Longrightarrow \quad \begin{cases} c_1^{N,-} = \left[R_N(\Delta)+\Delta\right]c^{N,-} \\ c_2^{N,-} = -2g^*\sqrt{N}c^{N,-} \end{cases}\,. \tag{4.404}$$

The subsequent normalisation yields the normalisation constant

$$\left|c_1^{N,-}\right|^2 + \left|c_2^{N,-}\right|^2 = 1 \quad \Longrightarrow \quad c^{N,-} = \frac{e^{i\varphi^{N,-}}}{\sqrt{2R_N(\Delta)\left[R_N(\Delta)+\Delta\right]}}\,. \tag{4.405}$$

Thus, the eigenstate for the lower polariton branch reads

$$c_1^{N,-} = \sqrt{\frac{R_N(\Delta)+\Delta}{2R_N(\Delta)}}\,e^{i\varphi^{N,-}}\,, \tag{4.406}$$

$$c_2^{N,-} = \frac{-2g^*\sqrt{N}e^{i\varphi^{N,-}}}{\sqrt{2R_N(\Delta)\left[R_N(\Delta)+\Delta\right]}} = -\sqrt{\frac{R_N(\Delta)-\Delta}{2R_N(\Delta)}}\,e^{i\left(\varphi^{N,-}-\varphi_g\right)}\,. \tag{4.407}$$

Indeed, both eigenstates are orthogonal

$$c_1^{N,+*}c_1^{N,-} + c_2^{N,+*}c_2^{N,-} = 0\,. \tag{4.408}$$

Thus, the coefficients $c_i^{N,\pm}$ define a linear transformation with the matrix

$$U(\Delta,g) = \begin{pmatrix} \sqrt{\dfrac{R_N(\Delta)-\Delta}{2R_N(\Delta)}}\,e^{i\left(\varphi_g+\varphi^{N,+}\right)} & \sqrt{\dfrac{R_N(\Delta)+\Delta}{2R_N(\Delta)}}\,e^{i\varphi^{N,+}} \\ \sqrt{\dfrac{R_N(\Delta)+\Delta}{2R_N(\Delta)}}\,e^{i\varphi^{N,-}} & -\sqrt{\dfrac{R_N(\Delta)-\Delta}{2R_N(\Delta)}}\,e^{i\left(-\varphi_g+\varphi^{N,-}\right)} \end{pmatrix}\,, \tag{4.409}$$

which maps the bare states $|\psi_{iN}\rangle$ defined in (4.395) to the dressed states $|N,\pm\rangle$:

$$\begin{pmatrix} |N,+\rangle \\ |N,-\rangle \end{pmatrix} = U(\Delta,g)\begin{pmatrix} |\psi_{1N}\rangle \\ |\psi_{2N}\rangle \end{pmatrix}\,. \tag{4.410}$$

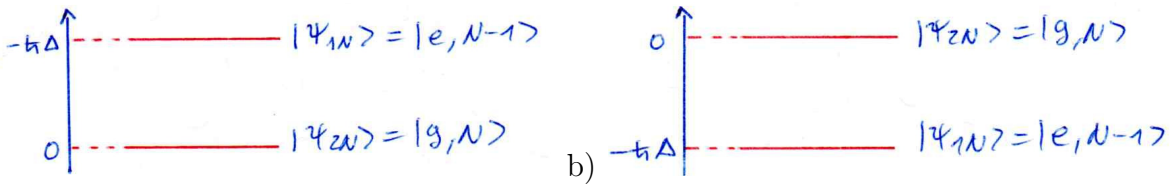

Figure 4.18: The relative position of the bare energy levels corresponding to the bare states defined in (4.395) depends on the sign of the detuning: a) $\Delta < 0$ and b) $\Delta > 0$.

Now we still have to fix the phases $\varphi^{N,\pm}$ from the normalisation constants (4.401) and (4.405). To this end we note that the relative position of the bare energy levels depends on the sign of the detuning Δ as is sketched in Fig. 4.18. Furthermore, we specialize the transformation matrix (4.409) for vanishing coupling, i.e. $g = 0$, so that the generalized Rabi frequencies (4.322) reduce to $R_N(\Delta) = |\Delta|$:

$$U(\Delta, g = 0) = \begin{pmatrix} \sqrt{\dfrac{|\Delta| - \Delta}{2\,|\Delta|}}\, e^{i\left(\varphi_g + \varphi^{N,+}\right)} & \sqrt{\dfrac{|\Delta| + \Delta}{2\,|\Delta|}}\, e^{i\varphi^{N,+}} \\ \sqrt{\dfrac{|\Delta| + \Delta}{2\,|\Delta|}}\, e^{i\varphi^{N,-}} & -\sqrt{\dfrac{|\Delta| - \Delta}{2\,|\Delta|}}\, e^{i\left(\varphi_g - \varphi^{N,-}\right)} \end{pmatrix} . \tag{4.411}$$

In the case $\Delta < 0$, i.e. $\Delta = -|\Delta|$, the matrix $U(\Delta, g = 0)$ coincides with the identity matrix provided that the phase $\varphi^{N,\pm}$ are fixed according to

$$\varphi^{N,+} = -\varphi_g\,, \qquad \varphi^{N,-} = \varphi_g + \pi \tag{4.412}$$

With this the transformation matrix (4.409) turns out to the manifestly unitary form

$$U(\Delta, g) = \begin{pmatrix} \cos\left(\frac{\phi_N}{2}\right) & \sin\left(\frac{\phi_N}{2}\right) e^{-i\varphi_g} \\ -\sin\left(\frac{\phi_N}{2}\right) e^{i\varphi_g} & \cos\left(\frac{\phi_N}{2}\right) \end{pmatrix} \tag{4.413}$$

due to the identification

$$\cos\left(\frac{\phi_N}{2}\right) = \sqrt{\frac{R_N(\Delta) - \Delta}{2R_N(\Delta)}}\,, \qquad \sin\left(\frac{\phi_N}{2}\right) = \sqrt{\frac{R_N(\Delta) + \Delta}{2R_N(\Delta)}}\,. \tag{4.414}$$

Indeed, the trigonometric Pythagoras is fulfilled

$$\cos^2\left(\frac{\phi_N}{2}\right) + \sin^2\left(\frac{\phi_N}{2}\right) = 1\,. \tag{4.415}$$

Furthermore, the angle ϕ_N is determined via

$$\tan(\phi_N) = \frac{\sin(\phi_N)}{\cos(\phi_N)} = \frac{2\sin\left(\frac{\phi_N}{2}\right)\cos\left(\frac{\phi_N}{2}\right)}{\cos^2\left(\frac{\phi_N}{2}\right) - \sin\left(\frac{\phi_N}{2}\right)} = \frac{2\,|g|\,N}{-\Delta} \quad \Longrightarrow \quad \phi_N = \arctan\left(\frac{2\,|g|\,N}{-\Delta}\right). \tag{4.416}$$

Thus, the dressed states, which are also called the Jaynes-Cummings doublet, coincide for vanishing coupling $g = 0$ with the bare states. Conversely, the bare states at $g = 0$ split into

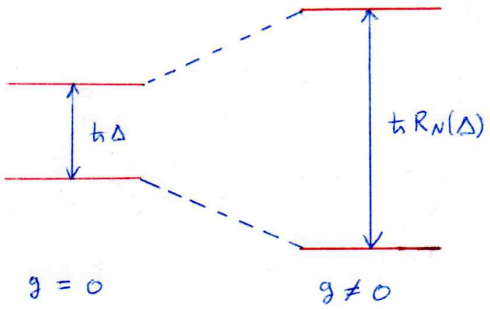

Figure 4.19: The interaction between light and matter changes the bare states $|\psi_{iN}\rangle$ at $g = 0$ into the dressed states $|N, \pm\rangle$ at $g \neq 0$.

the dressed states at $g \neq 0$, see Fig. 4.19. This is a kind of Stark shift, which is often called the AC or dynamic Stark shift.

Note that in the limit of an exact resonance, where the detuning Δ vanishes, the bare states (4.395) are degenerate, but the splitting of the dressed states remains due to (4.321) and amounts to $R_N(\Delta = 0) = 2|g|N$. In this limit $\Delta = 0$ the angle (4.416) is given by $\phi_N = \pi/2$ and the unitary matrix (4.413) turns out to be independent of the absolute value of the coupling $|g|$:

$$U(\Delta = 0, g) = \frac{1}{\sqrt{2}} \begin{pmatrix} 1 & e^{-i\varphi_g} \\ -e^{i\varphi_g} & 1 \end{pmatrix} . \tag{4.417}$$

The concept of the dressed states turns out to be quite useful for determining the dynamics of the Jaynes-Cummings model even for non-vanishing detuning, i.e. $\Delta \neq 0$. In order to explore this notion in detail, we assume the initial condition that the two-level atom is in the excited state and allow any configuration of the electromagnetic field mode. Taking into account the bare states (4.395) we thus have

$$|\psi(0)\rangle = |e\rangle \sum_{N=0}^{\infty} c_N |N\rangle = \sum_{N'=1}^{\infty} c_{N'-1} |e, N' - 1\rangle = \sum_{N=1}^{\infty} c_{N-1} |\psi_{1N}\rangle . \tag{4.418}$$

Inverting relation (4.410) between the bare and the dressed states yields due to the unitarity of the matrix $U(\Delta, g)$

$$\begin{pmatrix} |\psi_{1N}\rangle \\ |\psi_{2N}\rangle \end{pmatrix} = U^{\dagger}(\Delta, g) \begin{pmatrix} |N, +\rangle \\ |N, -\rangle \end{pmatrix} , \tag{4.419}$$

so we get with (4.413) in particular

$$|\psi_{1N}\rangle = \cos\left(\frac{\phi_N}{2}\right) |N, +\rangle - \sin\left(\frac{\phi_N}{2}\right) e^{-i\varphi_g} |N, -\rangle \tag{4.420}$$

and the initial condition (4.418) reads finally

$$|\psi(0)\rangle = \sum_{N=1}^{\infty} c_{N-1} \left[\cos\left(\frac{\phi_N}{2}\right) |N, +\rangle - \sin\left(\frac{\phi_N}{2}\right) e^{-i\varphi_g} |N, -\rangle\right] . \tag{4.421}$$

The time evolution of the state is determined by applying the Jaynes-Cummings time evolution operator to this initial state:

$$|\psi(t)\rangle = e^{-i\hat{H}_{\mathrm{JC}}t/\hbar}\,|\psi(0)\rangle\ . \tag{4.422}$$

Here we can use the fact that the dressed states $|N,\pm\rangle$ are by construction eigenstates of the Jaynes-Cummings Hamiltonian:

$$e^{-i\hat{H}_{\mathrm{JC}}t/\hbar}\,|N,\pm\rangle = e^{-iE_{N,\pm}t/\hbar}\,|N,\pm\rangle\ . \tag{4.423}$$

Thus, combining (4.421)–(4.423) the time-dependent state reads

$$|\psi(t)\rangle = \sum_{N=1}^{\infty} c_{N-1}\left[\cos\left(\frac{\phi_N}{2}\right)e^{-iE_{N,+}t/\hbar}\,|N,+\rangle - \sin\left(\frac{\phi_N}{2}\right)e^{-i\varphi_g}\,e^{-iE_{N,-}t/\hbar}\,|N,-\rangle\right]\ . \tag{4.424}$$

Now we insert therein the relation between the bare and the dressed states, which follows from (4.410) and (4.413)

$$|N,+\rangle = \cos\left(\frac{\phi_N}{2}\right)|\psi_{1N}\rangle + \sin\left(\frac{\phi_N}{2}\right)e^{-i\varphi_g}\,|\psi_{2N}\rangle\ , \tag{4.425}$$

$$|N,-\rangle = -\sin\left(\frac{\phi_N}{2}\right)e^{i\varphi_g}\,|\psi_{1N}\rangle + \cos\left(\frac{\phi_N}{2}\right)|\psi_{2N}\rangle\ , \tag{4.426}$$

and obtain with this

$$\begin{aligned}|\psi(t)\rangle = \sum_{N=1}^{\infty} c_{N-1}\Bigg\{ &\cos\left(\frac{\phi_N}{2}\right)e^{-iE_{N,+}t/\hbar}\left[\cos\left(\frac{\phi_N}{2}\right)|\psi_{1N}\rangle + \sin\left(\frac{\phi_N}{2}\right)e^{-i\varphi_g}\,|\psi_{2N}\rangle\right]\\ &-\sin\left(\frac{\phi_N}{2}\right)e^{-i\varphi_g}e^{-iE_{N,-}t/\hbar}\left[-\sin\left(\frac{\phi_N}{2}\right)e^{i\varphi_g}\,|\psi_{1N}\rangle + \cos\left(\frac{\phi_N}{2}\right)|\psi_{2N}\rangle\right]\Bigg\}\ .\end{aligned} \tag{4.427}$$

Taking into account the energy eigenvalues (4.321) then gives

$$\begin{aligned}|\psi(t)\rangle = \sum_{N=1}^{\infty} c_{N-1}e^{-i(\omega N+\Delta/2)t}\Bigg\{ &\left[\cos^2\left(\frac{\phi_N}{2}\right)e^{-iR_N(\Delta)t/2} + \sin^2\left(\frac{\phi_N}{2}\right)e^{iR_N(\Delta)t/2}\right]|\psi_{1N}\rangle\\ &+\sin\left(\frac{\phi_N}{2}\right)\cos\left(\frac{\phi_N}{2}\right)e^{-i\varphi_g}\left[e^{-iR_N(\Delta)t/2} - e^{iR_N(\Delta)t/2}\right]|\psi_{2N}\rangle\Bigg\}\ .\end{aligned} \tag{4.428}$$

Applying the Euler formula leads to

$$\begin{aligned}|\psi(t)\rangle = \sum_{N=1}^{\infty} c_{N-1}e^{-i(\omega N+\Delta/2)t}\Bigg\{ &\Bigg[\left(\cos^2\left(\frac{\phi_N}{2}\right) + \sin^2\left(\frac{\phi_N}{2}\right)\right)\cos\left(\frac{R_N(\Delta)}{2}t\right)\\ &-i\left(\cos^2\left(\frac{\phi_N}{2}\right) - \sin^2\left(\frac{\phi_N}{2}\right)\right)\sin\left(\frac{R_N(\Delta)}{2}t\right)\Bigg]|\psi_{1N}\rangle\\ &-2i\sin\left(\frac{\phi_N}{2}\right)\cos\left(\frac{\phi_N}{2}\right)e^{-i\varphi_g}\sin\left(\frac{R_N(\Delta)}{2}t\right)|\psi_{2N}\rangle\Bigg\}\ .\end{aligned} \tag{4.429}$$

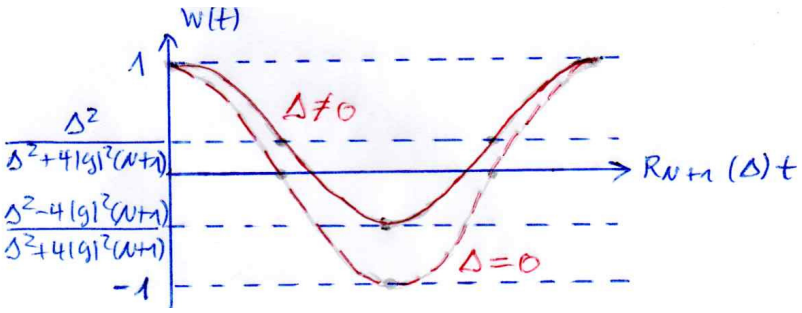

Figure 4.20: Vacuum Rabi oscillation with generalized Rabi frequency (4.322) for vanishing and non-vanishing detuning Δ.

Using the generalized Rabi frequencies (4.322) and the definition (4.416) of the angle ϕ_N trigonometric identities yield in case of $\Delta < 0$:

$$\cos^2\left(\frac{\phi_N}{2}\right) - \sin^2\left(\frac{\phi_N}{2}\right) = \cos(\phi_N) = \frac{1}{\sqrt{1+\tan^2(\phi_N)}} = \frac{1}{\sqrt{1+\frac{4|g|^2N}{\Delta^2}}} = \frac{-\Delta}{R_N(\Delta)}\,, \quad (4.430)$$

$$2\sin\left(\frac{\phi_N}{2}\right)\cos\left(\frac{\phi_N}{2}\right) = \sin(\phi_N) = \frac{\tan(\phi_N)}{\sqrt{1+\tan^2(\phi_N)}} = \frac{2\,|g|\,\sqrt{N}}{R_N(\Delta)}\,, \quad (4.431)$$

which implies:

$$|\psi(t)\rangle = \sum_{N=0}^{\infty} c_N e^{-i[\omega(N+1)+\Delta/2]t}\left\{\left[\cos\left(\frac{R_{N+1}(\Delta)}{2}t\right) + i\frac{\Delta}{R_{N+1}(\Delta)}\sin\left(\frac{R_{N+1}(\Delta)}{2}t\right)\right]|e,N\rangle \right.$$
$$\left. -i\frac{2g^*\sqrt{N+1}}{R_{N+1}(\Delta)}\sin\left(\frac{R_{N+1}(\Delta)}{2}t\right)|g,N+1\rangle\right\}. \quad (4.432)$$

This result is of the generic form (4.364) with

$$|\psi_e(t)\rangle = \sum_{N=0}^{\infty} c_N e^{-i[\omega(N+1)+\Delta/2]t}\left[\cos\left(\frac{R_{N+1}(\Delta)t}{2}\right) + i\frac{\Delta}{R_{N+1}(\Delta)}\sin\left(\frac{R_{N+1}(\Delta)t}{2}\right)\right]|N\rangle\,,$$
$$|\psi_g(t)\rangle = \sum_{N=0}^{\infty} c_N e^{-i[\omega(N+1)+\Delta/2]t}\,\frac{-i2g^*\sqrt{N+1}}{R_{N+1}(\Delta)}\sin\left(\frac{R_{N+1}(\Delta)t}{2}\right)|N+1\rangle\,. \quad (4.433)$$

Thus, the atomic population inversion $W(t) = \langle\psi_e(t)|\psi_e(t)\rangle - \langle\psi_g(t)|\psi_g(t)\rangle$ yields with the generalized Rabi frequency (4.322)

$$W(t) = \sum_{N=0}^{\infty}|c_N|^2\,\frac{\Delta^2+4\,|g|^2\,(N+1)\cos\left(\sqrt{\Delta^2+4\,|g|^2\,(N+1)}t\right)}{\Delta^2+4\,|g|^2\,(N+1)}\,. \quad (4.434)$$

For vanishing detuning $\Delta = 0$ we observe that Eq. (4.434) recovers the previous result (4.371). Furthermore, in the limit of large detuning, i.e. $\Delta \to \infty$, we obtain for the atomic population inversion (4.434) the result $W(t) \to 1$, i.e. the system remains in the excited atomic state irrespective of the photonic distribution. Finally, we mention the interesting special case to

consider an initial Fock state, which corresponds to restricting (4.434) to one term and leads to a vacuum Rabi oscillation with the generalized Rabi frequency $R_{n+1}(\Delta)$ defined in (4.322), see Fig. 4.20. We recognize that for increasing detuning Δ the vacuum Rabi oscillation occurs with a larger frequency and a smaller amplitude.

4.5.6 Density-Matrix Approach

So far we have always assumed that, initially, the field and the atom are in a pure state. In general, however, one or both subsystems may initially be in a mixed state. Then, it becomes mandatory to determine the dynamics of the Jaynes-Cummings system from the point of view of the density matrix. To this end we start with the underlying Hamiltonian at resonance $\omega = \omega_0$, i.e. $\Delta = 0$, given in (4.324) and decompose it according to

$$\hat{H}_{\mathrm{JC}} = \hat{H}_{\mathrm{JC}}^{(0)} + \hat{H}_{\mathrm{JC}}^{(p)} \,, \tag{4.435}$$

into the unperturbed term

$$\hat{H}_{\mathrm{JC}}^{(0)} = \hbar\omega \left(\hat{a}^\dagger \hat{a} + \sigma_+ \sigma_- \right) \tag{4.436}$$

and the perturbation

$$\hat{H}_{\mathrm{JC}}^{(p)} = \hbar g \sigma_+ \hat{a} + \hbar g^* \sigma_- \hat{a}^\dagger \,. \tag{4.437}$$

In the following we use this decomposition (4.435)–(4.437) of the resonant Jaynes-Cummings Hamiltonian and calculate the corresponding dynamics of the density matrix perturbatively. But instead of truncating the perturbation series at any finite order we will show that it is possible to sum it up to infinite order and, thus, to obtain the Jaynes-Cummings dynamics exactly.

At first we deduce the evolution equation for the density matrix

$$\hat{\rho}(t) = |\psi(t)\rangle \langle\psi(t)| \tag{4.438}$$

of a pure state. Combining the Schrödinger equation and its adjoint

$$i\hbar \frac{\partial}{\partial t} |\psi(t)\rangle = \hat{H} |\psi(t)\rangle \,, \qquad -i\hbar \frac{\partial}{\partial t} \langle\psi(t)| = \langle\psi(t)| \hat{H} \tag{4.439}$$

we straight-forwardly obtain

$$i\hbar \frac{\partial}{\partial t} \hat{\rho}(t) = \left[\hat{H}, \hat{\rho}(t) \right]_- \,. \tag{4.440}$$

This von-Neumann equation describes the evolution of the density matrix also when not a pure but a mixed state is considered. As the Schrödinger equation and its adjoint (4.439) are formally solved with the time evolution operator

$$|\psi(t)\rangle = e^{-i\hat{H}t/\hbar} |\psi(0)\rangle \tag{4.441}$$

and its adjoint

$$\langle\psi(t)| = \langle\psi(0)|\, e^{i\hat{H}t/\hbar}\,, \tag{4.442}$$

the evolution of the density matrix $\hat{\rho}(t) = |\psi(t)\rangle\langle\psi(t)|$ of a pure state reads

$$\hat{\rho}(t) = e^{-i\hat{H}t/\hbar}\hat{\rho}(0)e^{i\hat{H}t/\hbar} \tag{4.443}$$

with the initial condition $\hat{\rho}(0) = |\psi(0)\rangle\langle\psi(0)|$. A differentiation with respect to time shows that (4.443) solves, indeed, the von-Neumann equation (4.440) also for a mixed state.

In the second step we work out how to proceed in perturbation theory within the Dirac interaction picture. The starting point is that the Hamiltonian decomposes like in (4.435) according to

$$\hat{H} = \hat{H}^{(0)} + \hat{H}^{(p)}\,. \tag{4.444}$$

Schrödinger and Heisenberg picture are then defined by a time-dependent state vector $|\psi(t)\rangle$ and a time-independent state vector $|\psi(0)\rangle$, respectively, which are related via (4.441). This implies a corresponding relation for their respective operators, where conversely the operator in the Schrödinger picture $\hat{O}_{\rm S}$ is time-independent and its counterpart $\hat{O}_{\rm H}(t)$ in the Heisenberg picture gets time dependent. To this end we use the fact that the expectation values in both pictures coincide

$$\langle\psi(t)|\,\hat{O}_{\rm S}\,|\psi(t)\rangle = \langle\psi(0)|\,e^{i\hat{H}t/\hbar}\hat{O}_{\rm S}e^{-i\hat{H}t/\hbar}\,|\psi(0)\rangle = \langle\psi(0)|\,\hat{O}_{\rm H}(t)\,|\psi(0)\rangle\ , \tag{4.445}$$

so the operators transform via

$$\hat{O}_{\rm H}(t) = e^{i\hat{H}t/\hbar}\,\hat{O}_{\rm S}\,e^{-i\hat{H}t/\hbar}\,. \tag{4.446}$$

Now we introduce the Dirac interaction picture by transforming the operators not with the full Hamiltonian $\hat{H}$ but only with the unperturbed one $\hat{H}^{(0)}$:

$$\hat{O}_{\rm D}(t) = e^{i\hat{H}^{(0)}t/\hbar}\,\hat{O}_{\rm S}\,e^{-i\hat{H}^{(0)}t/\hbar}\,. \tag{4.447}$$

As also the expectation values in the Schrödinger and the Dirac interaction have to coincide

$$\langle\psi_{\rm D}(t)|\,\hat{O}_{\rm D}(t)\,|\psi_{\rm D}(t)\rangle = \langle\psi_{\rm D}(t)|\,e^{i\hat{H}^{(0)}t/\hbar}\,\hat{O}_{\rm S}\,e^{-i\hat{H}^{(0)}t/\hbar}\,|\psi_{\rm D}(t)\rangle = \langle\psi(t)|\,\hat{O}_{\rm S}\,|\psi(t)\rangle\ , \tag{4.448}$$

this leads to the following transformation of the state vector:

$$|\psi(t)\rangle = e^{-i\hat{H}^{(0)}t/\hbar}\,|\psi_{\rm D}(t)\rangle\ , \qquad |\psi_{\rm D}(t)\rangle = e^{i\hat{H}^{(0)}t/\hbar}\,|\psi(t)\rangle\ . \tag{4.449}$$

Thus the evolution equation for the state vector in the interaction picture reads

$$i\hbar\frac{\partial}{\partial t}\,|\psi_{\rm D}(t)\rangle = e^{i\hat{H}^{(0)}t/\hbar}\,\hat{H}^{(p)}\,|\psi(t)\rangle = \hat{H}^{(p)}_{\rm D}(t)\,|\psi_{\rm D}(t)\rangle\ . \tag{4.450}$$

From (4.449) and (4.450) we conclude that the perturbed Hamiltonian in the Dirac interaction picture is defined like in (4.447)

$$\hat{H}_{\mathrm{D}}^{(p)}(t) = e^{i\hat{H}^{(0)}t/\hbar}\,\hat{H}^{(p)}\,e^{-i\hat{H}^{(0)}t/\hbar} \tag{4.451}$$

and, therefore, carries in general an explicit time dependence. Solving formally (4.450) yields the time evolution of the state vector in the Dirac interaction picture

$$|\psi_{\mathrm{D}}(t)\rangle = \hat{U}_{\mathrm{D}}(t)\,|\psi_{\mathrm{D}}(0)\rangle \tag{4.452}$$

with the time evolution operator $\hat{U}_{\mathrm{D}}(t)$ and the initial state is given by the corresponding one in the Schrödinge picture due to (4.448):

$$|\psi_{\mathrm{D}}(0)\rangle = |\psi(0)\rangle\ . \tag{4.453}$$

In order that (4.452) solves (4.450), the time evolution operator $\hat{U}_{\mathrm{D}}(t)$ must fulfill the initial value problem

$$i\hbar\frac{\partial}{\partial t}\hat{U}_{\mathrm{D}}(t) = \hat{H}_{\mathrm{D}}^{(p)}(t)\hat{U}_{\mathrm{D}}(t)\,, \qquad \hat{U}_{\mathrm{D}}(0) = 1\,. \tag{4.454}$$

The dynamics of the density matrix in the Dirac interaction picture is given for a pure state due to (4.452) by

$$\hat{\rho}_{\mathrm{D}}(t) = |\psi_{\mathrm{D}}(t)\rangle\,\langle\psi_{\mathrm{D}}(t)| = \hat{U}_{\mathrm{D}}(t)\,|\psi(0)\rangle\,\langle\psi(0)|\,\hat{U}_{\mathrm{D}}^{\dagger}(t) = \hat{U}_{\mathrm{D}}(t)\hat{\rho}(0)\hat{U}_{\mathrm{D}}^{\dagger}(t)\,. \tag{4.455}$$

But (4.455) turns out to hold also for a mixed state.

Thirdly, we specialise these general relations to the resonant Jaynes-Cummings model (4.435)–(4.437). To this end we start with determining the time dependence of the respective operators in the Dirac interaction picture:

- The time evolution of the photon annihilation operator in the Dirac interaction picture follows from (4.436) and (4.447):

$$\hat{a}_{\mathrm{D}}(t) = e^{i\hat{H}_{\mathrm{JC}}^{(0)}t/\hbar}\,\hat{a}\,e^{-i\hat{H}_{\mathrm{JC}}^{(0)}t/\hbar} = e^{i\omega\hat{a}^{\dagger}\hat{a}t}\hat{a}e^{-i\omega\hat{a}^{\dagger}\hat{a}t}\,. \tag{4.456}$$

  In order to simplify (4.456) we determine the corresponding equation of motion:

$$i\hbar\frac{\partial}{\partial t}\hat{a}_{\mathrm{D}}(t) = \hbar\omega e^{i\omega\hat{a}^{\dagger}\hat{a}t}\left[\hat{a},\hat{a}^{\dagger}\hat{a}\right]_{-}e^{-i\omega\hat{a}^{\dagger}\hat{a}t} = \hbar\omega e^{i\omega\hat{a}^{\dagger}\hat{a}t}\hat{a}e^{-i\omega\hat{a}^{\dagger}\hat{a}t} = \hbar\omega\hat{a}_{\mathrm{D}}(t)\,. \tag{4.457}$$

  Thus, integrating (4.457) yields

$$\hat{a}_{\mathrm{D}}(t) = e^{-i\omega t}\hat{a} \qquad \Longrightarrow \qquad \hat{a}_{\mathrm{D}}^{\dagger}(t) = e^{i\omega t}\hat{a}^{\dagger}\,, \tag{4.458}$$

  so that $\hat{a}_{\mathrm{D}}(t)$ and $\hat{a}_{\mathrm{D}}^{\dagger}(t)$ turn out to fulfill the bosonic equal-time commutation relations:

$$\left[\hat{a}_{\mathrm{D}}(t),\hat{a}_{\mathrm{D}}(t)\right]_{-} = \left[\hat{a}_{\mathrm{D}}^{\dagger}(t),\hat{a}_{\mathrm{D}}^{\dagger}(t)\right]_{-} = 0\,, \qquad \left[\hat{a}_{\mathrm{D}}(t),\hat{a}_{\mathrm{D}}^{\dagger}(t)\right]_{-} = 1\,. \tag{4.459}$$

  This means that also in the Dirac interaction picture $\hat{a}_{\mathrm{D}}(t)$ and $\hat{a}_{\mathrm{D}}^{\dagger}(t)$ represent an annihilation and creation operator for a photon, respectively.

- In the same way we obtain also the dynamics of the raising operator of the Pauli matrix in the Dirac interaction picture from (4.436) and (4.447):

$$\sigma_{+\mathrm{D}}(t) = e^{i\hat{H}^{(0)}_{\mathrm{JC}}t/\hbar}\,\sigma_+\,e^{-i\hat{H}^{(0)}_{\mathrm{JC}}t/\hbar} = e^{i\omega\sigma_+\sigma_-t}\sigma_+e^{-i\omega\sigma_+\sigma_-t}\,. \tag{4.460}$$

Again we simplify by differentiating (4.460) with respect to time, yielding due to (4.301):

$$i\hbar\frac{\partial}{\partial t}\sigma_{+\mathrm{D}}(t) = \hbar\omega e^{i\omega\sigma_+\sigma_-t}\,[\sigma_+,\sigma_+\sigma_-]_-\,e^{-i\omega\sigma_+\sigma_-t} = -\hbar\omega e^{i\omega\sigma_+\sigma_-t}\sigma_+e^{-i\omega\sigma_+\sigma_-t} = -\hbar\omega\sigma_{+\mathrm{D}}(t)\,. \tag{4.461}$$

Thus, integrating (4.461) we conclude

$$\sigma_{+\mathrm{D}}(t) = e^{i\omega t}\sigma_+ \qquad\Longrightarrow\qquad \sigma_{-\mathrm{D}}(t) = e^{-i\omega t}\sigma_-\,. \tag{4.462}$$

With this we can now calculate the perturbed Hamiltonian (4.437) in the interaction picture (4.451) as follows:

$$\hat{H}^{(p)}_{\mathrm{DJC}}(t) = e^{i\hat{H}^{(0)}_{\mathrm{JC}}t/\hbar}\left(\hbar g\sigma_+\hat{a} + \hbar g^*\sigma_-\hat{a}^\dagger\right)e^{-i\hat{H}^{(0)}_{\mathrm{JC}}t/\hbar} = \hbar g\sigma_{+\mathrm{D}}(t)\hat{a}_{\mathrm{D}}(t) + \hbar g^*\sigma_{-\mathrm{D}}(t)\hat{a}^\dagger_{\mathrm{D}}(t)\,. \tag{4.463}$$

Inserting (4.458) and (4.462) in (4.463) leads to

$$\hat{H}^{(p)}_{\mathrm{DJC}}(t) = \hbar g e^{i\omega t}\sigma_+e^{-i\omega t}\hat{a} + \hbar g^*e^{-i\omega t}\sigma_-e^{i\omega t}\hat{a}^\dagger = \hbar g\sigma_+\hat{a} + \hbar g^*\sigma_-\hat{a}^\dagger = \hat{H}^{(p)}_{\mathrm{JC}}\,. \tag{4.464}$$

Thus, due to the assumed resonance, the perturbed Hamiltonian in the Dirac interaction picture turns out to be time independent. As a consequence, the initial value problem (4.454) for the time evolution operator in the Dirac interaction picture reduces to

$$i\hbar\frac{\partial}{\partial t}\hat{U}_{\mathrm{D}}(t) = \hat{H}^{(p)}_{\mathrm{JC}}\hat{U}_{\mathrm{D}}(t)\,, \qquad \hat{U}_{\mathrm{D}}(0) = 1\,, \tag{4.465}$$

which is solved by

$$\hat{U}_{\mathrm{D}}(t) = e^{-i\hat{H}^{(p)}_{\mathrm{JC}}t/\hbar} = e^{-i\left(g\sigma_+\hat{a}+g^*\sigma_-\hat{a}^\dagger\right)t}\,. \tag{4.466}$$

Thus it remains to evaluate an exponential function

$$\hat{U}_{\mathrm{D}}(t) = e^{-i\hat{O}t} \tag{4.467}$$

involving the operator

$$\hat{O} = g\sigma_+\hat{a} + g^*\hat{a}^\dagger = \begin{pmatrix} 0 & g\hat{a} \\ g^*\hat{a}^\dagger & 0 \end{pmatrix}. \tag{4.468}$$

via its Taylor series. To this end we decompose the latter into even and odd powers of the operator $\hat{O}$ according to

$$\hat{U}_{\mathrm{D}}(t) = \sigma_0 + \sum_{n=1}^{\infty}\frac{(-it)^{2n}}{(2n)!}\hat{O}^{2n} + \sum_{n=0}^{\infty}\frac{(-it)^{2n+1}}{(2n+1)!}\hat{O}^{2n+1}\,. \tag{4.469}$$

The first powers of the operator (4.468) yield

$$\hat{O}^2 = |g|^2 \begin{pmatrix} \hat{a}\hat{a}^\dagger & 0 \\ 0 & \hat{a}^\dagger\hat{a} \end{pmatrix}, \tag{4.470}$$

$$\hat{O}^3 = \hat{O}^2\hat{O} = |g|^2 \begin{pmatrix} 0 & g\hat{a}\hat{a}^\dagger\hat{a} \\ g^*\hat{a}^\dagger\hat{a}\hat{a}^\dagger & 0 \end{pmatrix}, \tag{4.471}$$

$$\hat{O}^4 = \hat{O}^2\hat{O}^2 = |g|^4 \begin{pmatrix} \left(\hat{a}\hat{a}^\dagger\right)^2 & 0 \\ 0 & \left(\hat{a}^\dagger\hat{a}\right)^2 \end{pmatrix}. \tag{4.472}$$

From (4.470) and (4.472) we read off via complete induction that the even powers of $\hat{O}$ result in

$$\hat{O}^{2n} = |g|^{2n} \begin{pmatrix} \left(\hat{a}\hat{a}^\dagger\right)^n & 0 \\ 0 & \left(\hat{a}^\dagger\hat{a}\right)^n \end{pmatrix}, \tag{4.473}$$

whereas the odd powers follow from (4.468) and (4.471)

$$\hat{O}^{2n+1} = |g|^{2n} \begin{pmatrix} 0 & g\hat{a}\left(\hat{a}^\dagger\hat{a}\right)^n \\ g^*\hat{a}^\dagger\left(\hat{a}\hat{a}^\dagger\right)^n & 0 \end{pmatrix}. \tag{4.474}$$

Inserting (4.473) and (4.474) in (4.469) we get in total

$$\hat{U}_{\mathrm{D}}(t) = \begin{pmatrix} 1 + \sum\limits_{n=1}^{\infty} \dfrac{(-1)^n \left(|g|\, t\sqrt{\hat{a}\hat{a}^\dagger}\right)^{2n}}{(2n)!} & -itg\hat{a} \sum\limits_{n=0}^{\infty} \dfrac{(-1)^n \left(|g|\, t\sqrt{\hat{a}^\dagger\hat{a}}\right)^{2n}}{(2n+1)!} \\ -itg^*\hat{a}^\dagger \sum\limits_{n=0}^{\infty} \dfrac{(-1)^n \left(|g|\, t\sqrt{\hat{a}\hat{a}^\dagger}\right)^{2n}}{(2n+1)!} & 1 + \sum\limits_{n=1}^{\infty} \dfrac{(-1)^n \left(|g|\, t\sqrt{\hat{a}^\dagger\hat{a}}\right)^{2n}}{(2n)!} \end{pmatrix}, \tag{4.475}$$

so we recover the Taylor series of trigonometric functions:

$$\cos x = \sum_{n=0}^{\infty} \frac{(-1)^n x^{2n}}{(2n)!}, \qquad \frac{\sin x}{x} = \sum_{n=0}^{\infty} \frac{(-1)^n x^{2n}}{(2n+1)!}. \tag{4.476}$$

Thus, the resulting time evolution operator in the interaction picture is of the form

$$\hat{U}_{\mathrm{D}}(t) = \begin{pmatrix} \hat{c}(t) & \hat{s}'(t) \\ \hat{s}(t) & \hat{c}'(t) \end{pmatrix} \tag{4.477}$$

with the respective operator-valued entries

$$\hat{c}(t) = \cos\left(|g|\, t\sqrt{\hat{a}\hat{a}^\dagger}\right), \qquad \hat{c}'(t) = \cos\left(|g|\, t\sqrt{\hat{a}^\dagger\hat{a}}\right), \tag{4.478}$$

$$\hat{s}(t) = -i\sqrt{\frac{g^*}{g}}\,\hat{a}^\dagger \frac{\sin\left(|g|\, t\sqrt{\hat{a}\hat{a}^\dagger}\right)}{\sqrt{\hat{a}\hat{a}^\dagger}}, \qquad \hat{s}'(t) = -i\sqrt{\frac{g}{g^*}}\,\hat{a} \frac{\sin\left(|g|\, t\sqrt{\hat{a}^\dagger\hat{a}}\right)}{\sqrt{\hat{a}^\dagger\hat{a}}}. \tag{4.479}$$

The adjoint of the time evolution operator in the Dirac interaction picture (4.477) then reads

$$\hat{U}_{\mathrm{D}}^\dagger(t) = \begin{pmatrix} \hat{c}(t) & -\hat{s}'(t) \\ -\hat{s}(t) & \hat{c}'(t) \end{pmatrix}. \tag{4.480}$$

The time evolution of the density matrix in the interaction picture (4.455) results due to (4.477)–(4.480) in

$$\hat{\rho}_{\mathrm{D}}(t) = \begin{pmatrix} \hat{c}(t) & \hat{s}'(t) \\ \hat{s}(t) & \hat{c}'(t) \end{pmatrix} \hat{\rho}(0) \begin{pmatrix} \hat{c}(t) & -\hat{s}'(t) \\ -\hat{s}(t) & \hat{c}'(t) \end{pmatrix} \tag{4.481}$$

irrespective of the particular choice of the initial density matrix $\hat{\rho}(0)$. Let us assume that the initial density matrix factorizes according to

$$\hat{\rho}(0) = \hat{\rho}_{\mathrm{A}} \otimes \hat{\rho}_{\mathrm{F}} \tag{4.482}$$

and that both the atomic and the field part represent a mixed state. In case of the two-level system the states

$$|\psi_{\mathrm{A}}\rangle = c_e |e\rangle + c_g |g\rangle \ , \qquad \langle\psi_{\mathrm{A}}| = \langle e| c_e^* + \langle g| c_g^* \tag{4.483}$$

lead to the density matrix

$$\hat{\rho}_{\mathrm{A}} = |\psi_{\mathrm{A}}\rangle \langle\psi_{\mathrm{A}}| = c_e c_e^* |e\rangle \langle e| + c_g c_e^* |g\rangle \langle e| + c_e c_g^* |e\rangle \langle g| + c_g c_g^* |g\rangle \langle g| \ . \tag{4.484}$$

In the spin 1/2-notation for the two-level system this amounts to

$$|e\rangle \langle e| = \begin{pmatrix} 1 \\ 0 \end{pmatrix} (1,0) = \begin{pmatrix} 1 & 0 \\ 0 & 0 \end{pmatrix} , \qquad |g\rangle \langle g| = \begin{pmatrix} 0 \\ 1 \end{pmatrix} (0,1) = \begin{pmatrix} 0 & 0 \\ 0 & 1 \end{pmatrix} \tag{4.485}$$

$$|g\rangle \langle e| = \begin{pmatrix} 0 \\ 1 \end{pmatrix} (1,0) = \begin{pmatrix} 0 & 0 \\ 1 & 0 \end{pmatrix} , \qquad |e\rangle \langle g| = \begin{pmatrix} 1 \\ 0 \end{pmatrix} (0,1) = \begin{pmatrix} 0 & 1 \\ 0 & 0 \end{pmatrix} \tag{4.486}$$

resulting in the 2×2 matrix

$$\hat{\rho}_{\mathrm{A}} = \begin{pmatrix} c_e c_e^* & c_e c_g^* \\ c_g c_e^* & c_g c_g^* \end{pmatrix} . \tag{4.487}$$

Correspondingly we characterize the field by the states

$$|\psi_{\mathrm{F}}\rangle = \sum_{n=0}^{\infty} c_n |n\rangle \ , \qquad \langle\psi_{\mathrm{F}}| = \sum_{n=0}^{\infty} c_n^* \langle n| \ , \tag{4.488}$$

so that its density matrix results in

$$\hat{\rho}_{\mathrm{F}} = |\psi_{\mathrm{F}}\rangle \langle\psi_{\mathrm{F}}| = \sum_{n_1=0}^{\infty} \sum_{n_2=0}^{\infty} c_{n_1} c_{n_2}^* |n_1\rangle \langle n_2| \ . \tag{4.489}$$

Inserting (4.482), (4.484), and (4.489) into (4.481) has now the following consequence:

$$\begin{aligned} \hat{\rho}_{\mathrm{D}}(t) &= \begin{pmatrix} \hat{c}(t) & \hat{s}'(t) \\ \hat{s}(t) & \hat{c}'(t) \end{pmatrix} \hat{\rho}_{\mathrm{F}} \begin{pmatrix} c_e c_e^* & c_e c_g^* \\ c_g c_e^* & c_g c_g^* \end{pmatrix} \begin{pmatrix} \hat{c}(t) & -\hat{s}'(t) \\ -\hat{s}(t) & \hat{c}'(t) \end{pmatrix} \\ &= \begin{pmatrix} \hat{c}(t) & \hat{s}'(t) \\ \hat{s}(t) & \hat{c}'(t) \end{pmatrix} \hat{\rho}_{\mathrm{F}} \begin{pmatrix} c_e c_e^* \hat{c}(t) - c_e c_g^* \hat{s}(t) & -c_e c_e^* \hat{s}'(t) + c_e c_g^* \hat{c}'(t) \\ c_g c_e^* \hat{c}(t) - c_g c_g^* \hat{s}(t) & -c_g c_e^* \hat{s}'(t) + c_g c_g^* \hat{c}'(t) \end{pmatrix} . \end{aligned} \tag{4.490}$$

A trace over all Fock states of the field yields the atomic reduced density matrix:

$$\hat{\rho}_{\mathrm{DA}}(t) = \mathrm{Tr}_{\mathrm{F}}\left[\hat{\rho}_{\mathrm{D}}(t)\right] = \sum_{n=0}^{\infty} \langle n|\, \hat{\rho}_{\mathrm{D}}(t)\, |n\rangle = \begin{pmatrix} \rho_{ee}^{\mathrm{DA}}(t) & \rho_{eg}^{\mathrm{DA}}(t) \\ \rho_{ge}^{\mathrm{DA}}(t) & \rho_{gg}^{\mathrm{DA}}(t) \end{pmatrix} \tag{4.491}$$

with the respective components

$$\rho_{ij}^{\mathrm{DA}}(t) = \langle i|\, \hat{\rho}_{\mathrm{DA}}(t)\, |j\rangle \;; \qquad i = g, e\,. \tag{4.492}$$

Due to the normalisation of the reduced density matrix we conclude

$$\mathrm{Tr}_{\mathrm{A}}\left[\hat{\rho}_{\mathrm{DA}}(t)\right] = \rho_{ee}^{\mathrm{DA}}(t) + \rho_{gg}^{\mathrm{DA}}(t) = 1 \qquad \Longrightarrow \qquad \rho_{gg}^{\mathrm{DA}}(t) = 1 - \rho_{ee}^{\mathrm{DA}}(t)\,. \tag{4.493}$$

Thus, the atomic population inversion results from

$$W(t) = \rho_{ee}^{\mathrm{DA}}(t) - \rho_{gg}^{\mathrm{DA}}(t) = 2\rho_{ee}^{\mathrm{DA}}(t) - 1\,. \tag{4.494}$$

In order to determine $W(t)$, we only have to calculate $\rho_{ee}^{\mathrm{DA}}(t)$, which follows due to (4.490) from

$$\hat{\rho}_{ee}^{\mathrm{D}}(t) = c_e c_e^* \hat{c}(t)\hat{\rho}_F \hat{c}(t) - c_e c_g^* \hat{c}(t)\hat{\rho}_F \hat{s}(t) + c_g c_e^* \hat{s}'(t)\hat{\rho}_F \hat{c}(t) - c_g c_g^* \hat{s}'(t)\hat{\rho}_F \hat{s}(t) \tag{4.495}$$

via tracing out the Fock states of the field. At first we consider the case $c_e = 1$, $c_g = 0$, which yields

$$\rho_{ee}^{\mathrm{DA}}(t) = \mathrm{Tr}_{\mathrm{F}}\left[\hat{\rho}_{ee}^{\mathrm{D}}(t)\right] = \sum_{n=0}^{\infty} \langle n|\, \hat{c}(t)\hat{\rho}_{\mathrm{F}}\hat{c}(t)\, |n\rangle\;. \tag{4.496}$$

Taking into account (4.489) we get

$$\rho_{ee}^{\mathrm{DA}}(t) = \sum_{n=0}^{\infty}\sum_{n_1=0}^{\infty}\sum_{n_2=0}^{\infty} c_{n_1} c_{n_2}^*\, \langle n|\, \hat{c}(t)\, |n_1\rangle\, \langle n_2|\, \hat{c}(t)\, |n\rangle\;, \tag{4.497}$$

where the matrix elements follow from (4.478)

$$\langle n|\, \hat{c}(t)\, |n_1\rangle = \delta_{n,n_1} \cos\left(|g|\, t\sqrt{n_1+1}\,\right)\;, \tag{4.498}$$

finally leading to

$$W(t) = 2\sum_{n=0}^{\infty} |c_n|^2 \cos^2\left(|g|\, t\sqrt{n+1}\,\right) - 1 = \sum_{n=0}^{\infty} |c_n|^2 \left[2\cos^2\left(|g|\, t\sqrt{n+1}\,\right) - 1\right]\;. \tag{4.499}$$

This reproduces the previous result (4.371), which reveals vacuum Rabi oscillations as well as the collapse and revival dynamics as discussed in Subsections 4.5.3 and 4.5.4, respectively. In the second case $c_e = 0$, $c_g = 1$ we get instead

$$\rho_{ee}^{\mathrm{DA}}(t) = \mathrm{Tr}_{\mathrm{F}}\left[\hat{\rho}_{ee}^{\mathrm{D}}(t)\right] = -\sum_{n=0}^{\infty} \langle n|\, \hat{s}'(t)\hat{\rho}_{\mathrm{F}}\hat{s}(t)\, |n\rangle\;, \tag{4.500}$$

so using (4.489) we obtain

$$\rho_{ee}^{\mathrm{DA}}(t) = -\sum_{n=0}^{\infty}\sum_{n_1=0}^{\infty}\sum_{n_2=0}^{\infty} \langle n|\,\hat{s}'(t)\,|n_1\rangle\,\langle n_2|\,\hat{s}(t)\,|n\rangle\,c_{n_1}c_{n_2}^{*}\,. \tag{4.501}$$

Due to the matrix elements following from (4.479)

$$\langle n|\,\hat{s}'(t)\,|n_1\rangle = -i\sqrt{\frac{g}{g^*}}\,\delta_{n,n_1-1}\sin\left(|g|\,t\sqrt{n_1}\,\right)\,, \tag{4.502}$$

$$\langle n_2|\,\hat{s}(t)\,|n\rangle = -i\sqrt{\frac{g^*}{g}}\,\delta_{n_2,n+1}\sin\left(|g|\,t\sqrt{n+1}\right) \tag{4.503}$$

this leads to

$$\rho_{ee}^{\mathrm{DA}}(t) = \sum_{n=0}^{\infty} c_{n+1}c_{n+1}^{*}\sin^2\left(|g|\,t\sqrt{n+1}\right) = \sum_{n=0}^{\infty}|c_n|^2\sin^2\left(|g|\,t\sqrt{n}\,\right)\,. \tag{4.504}$$

The resulting atomic population inversion

$$W(t) = \sum_{n=0}^{\infty}|c_n|^2\left[2\sin^2\left(|g|\,t\sqrt{n}\,\right)-1\right] = -\sum_{n=0}^{\infty}|c_n|^2\cos\left(2\,|g|\,t\sqrt{n}\,\right) \tag{4.505}$$

does not reveal a vacuum Rabi oscillation. Thus, a necessary condition for a vacuum Rabi oscillation is $c_e \neq 0$. This conclusion is supported by the physical explanation of the vacuum Rabi oscillation at the end of Subsection 4.5.3. Nameley, this intriguing quantum phenomenon can only occur once the atom is able to spontaneously emit a photon, which implies $c_e \neq 0$.

4.5.7 Large Detuning: Dispersive Interaction

So far we have discussed the Jaynes-Cummings model for a vanishing or a small detuning (4.129). Now we deal with such a large detuning that a direct atomic transition does not occur as is discussed below Eq. (4.434). Instead we find here that, nevertheless, an effective *dispersive interaction* between a single atom and a cavity field does occur, i.e. the bare states remain to be energy eigenstates but are shifted energetically. In order to obtain this result we use again perturbative methods, but in case of a large detuning we do not manage to sum up the perturbative series to infinite order, so we have to truncate it at a finite order.

Thus we consider in the following the full Jaynes-Cummings Hamiltonian (4.308), which also decomposes according to (4.435). But here the unperturbed part reads

$$\hat{H}_{\mathrm{JC}}^{(0)} = \hbar\omega\hat{a}^{\dagger}\hat{a} + \hbar\omega_0\sigma_{+}\sigma_{-} \tag{4.506}$$

and the perturbed part is again given by (4.437). In the previous subsection we have determined the time-dependent photon operators and Pauli matrices in the Dirac interaction picture. Whereas the result (4.458) for the photon annihilation and creation operators remains to be

valid also here, we have to change the time dependence for the raising and lowering Pauli matrices in (4.462) by subsituting ω by ω_0 due to (4.506). Using this the perturbed part of the Jaynes-Cummings Hamiltonian (4.437) reads in the Dirac interaction picture

$$\hat{H}^{(p)}_{\mathrm{JC}}(t) = \hbar g \sigma_{+\mathrm{D}}(t)\hat{a}_{\mathrm{D}}(t) + \hbar g^* \sigma_{-\mathrm{D}}(t)\hat{a}^\dagger_{\mathrm{D}}(t) = \hbar g e^{-i\Delta t}\sigma_+ \hat{a} + \hbar g^* e^{i\Delta t}\sigma_- \hat{a}^\dagger \,. \tag{4.507}$$

Thus, a non-vanishing detuning implies an explicit time dependence of $\hat{H}^{(p)}_{\mathrm{DJC}}(t)$. In that case the time evolution operator in the Dirac interaction picture solving the initial value problem (4.454) reads [21, Section 10.6]

$$\hat{U}_{\mathrm{D}}(t) = \hat{T}\left\{\exp\left[-\frac{i}{\hbar}\int_0^t dt' \hat{H}^{(p)}_{\mathrm{DJC}}(t')\right]\right\}, \tag{4.508}$$

where the symbol $\hat{T}$ denotes the time-ordering operator. Given two time-dependent bosonic operators $\hat{A}(t)$ and $\hat{B}(t')$, their time-ordered product reads

$$\hat{T}\left[\hat{A}(t)\,\hat{B}(t')\right] = \Theta(t-t')\,\hat{A}(t)\,\hat{B}(t') + \Theta(t'-t)\,\hat{B}(t')\,\hat{A}(t)\,, \tag{4.509}$$

where we have used the Heaviside function

$$\Theta(t) = \begin{cases} 1\,; & t > 0 \\ 0\,; & t < 0 \end{cases} \,. \tag{4.510}$$

A Taylor expansion of the exponential function in (4.508) yields up to second order the following perturbative expansion:

$$\hat{U}_{\mathrm{D}}(t) = 1 + \frac{-i}{\hbar}\int_0^t dt' \hat{H}^{(p)}_{\mathrm{DJC}}(t') + \frac{1}{2}\left(\frac{-i}{\hbar}\right)^2 \int_0^t dt' \int_0^t dt''\, \hat{T}\left[\hat{H}^{(p)}_{\mathrm{DJC}}(t')\hat{H}^{(p)}_{\mathrm{DJC}}(t'')\right] + \ldots \,. \tag{4.511}$$

Due to the definition of the time-ordering operator (4.509) the time evolution operator (4.511) reduces to

$$\begin{aligned} \hat{U}_{\mathrm{D}}(t) &= 1 - \frac{i}{\hbar}\int_0^t dt' \hat{H}^{(p)}_{\mathrm{DJC}}(t') \\ &- \frac{1}{2\hbar^2}\left\{\int_0^t dt' \int_0^{t'} dt'' \left[\hat{H}^{(p)}_{\mathrm{DJC}}(t')\hat{H}^{(p)}_{\mathrm{DJC}}(t'')\right] + \int_0^t dt' \int_{t'}^t dt'' \left[\hat{H}^{(p)}_{\mathrm{DJC}}(t'')\hat{H}^{(p)}_{\mathrm{DJC}}(t')\right]\right\} + \ldots \,. \end{aligned} \tag{4.512}$$

The last term can be rewritten as follows:

$$\int_0^t dt' \int_{t'}^t dt'' \hat{H}^{(p)}_{\mathrm{DJC}}(t'')\hat{H}^{(p)}_{\mathrm{DJC}}(t') = \int_0^t dt'' \int_0^{t''} dt' \hat{H}^{(p)}_{\mathrm{DJC}}(t'')\hat{H}^{(p)}_{\mathrm{DJC}}(t') \,. \tag{4.513}$$

Here we use the fact that the upper triangle in Fig. 4.21 can be integrated in two ways. Either we first integrate over t'' and then over t' or, conversely, first over t' and then over t''. Exchanging both integration variables at the right-hand side of (4.513) we conclude that the two integrals in the second line of (4.512) turn out to coincide, yielding

$$\hat{U}_{\mathrm{D}}(t) = 1 - \frac{i}{\hbar}\int_0^t dt' \hat{H}^{(p)}_{\mathrm{DJC}}(t')\left[1 - \frac{i}{\hbar}\int_0^{t'} dt'' \hat{H}^{(p)}_{\mathrm{DJC}}(t'')\right] + \ldots \,. \tag{4.514}$$

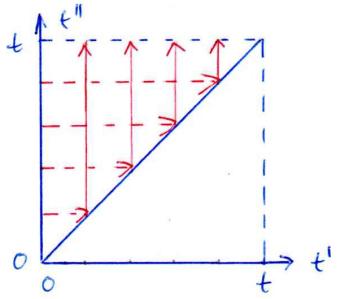

Figure 4.21: The upper triangle can be integrated in two ways, where the red solid (dashed) line corresponds to the integration on the left- (right-)hand side of Eq. (4.513).

The inner time integral in (4.514) can now be performed explicitly by taking into account (4.507), yielding

$$\int_0^{t'} dt'' \hat{H}_{\mathrm{DJC}}^{(p)}(t'') = \hbar g \frac{e^{-i\Delta t'}-1}{-i\Delta}\sigma_+\hat{a} + \hbar g^* \frac{e^{i\Delta t'}-1}{i\Delta}\sigma_-\hat{a}^\dagger\,. \tag{4.515}$$

Inserting (4.515) into (4.514) the time evolution operator has the following intermediate form:

$$\hat{U}_{\mathrm{D}}(t) = 1 + \int_0^t dt' \left\{ -ige^{-i\Delta t'}\sigma_+\hat{a} - ig^* e^{i\Delta t'}\sigma_-\hat{a}^\dagger + \frac{i\,|g|^2}{\Delta}\left[\left(1-e^{-i\Delta t'}\right)\sigma_-\sigma_+\hat{a}^\dagger\hat{a}\right.\right. \tag{4.516}$$
$$\left.\left. - \left(1-e^{i\Delta t'}\right)\sigma_+\sigma_-\hat{a}\hat{a}^\dagger\right] - \frac{ig^2}{\Delta}\left(e^{-2i\Delta t'}-e^{-i\Delta t'}\right)\sigma_+^2\hat{a}^2 + \frac{ig^{*2}}{\Delta}\left(e^{2i\Delta t'}-e^{i\Delta t'}\right)\sigma_-^2\hat{a}^{\dagger 2}\right\} + \ldots\,.$$

In the limit of a large detuning Δ we argue that the exponential functions $e^{\pm i\Delta t'}$ and $e^{\pm 2i\Delta t'}$ in the first and second perturbative order are oscillating so fast that their time integrals vanish approximately:

$$\int_0^t dt'\, e^{\pm i\Delta t'} \approx 0\,, \qquad \int_0^t dt'\, e^{\pm 2i\Delta t'} \approx 0\,. \tag{4.517}$$

Thus, we see that the rotating wave approximation is not only applicable for a fast oscillating external classical electric field but can also be applied for a time-independent quantum system, once a transformation in a co-rotating reference frame leads to fast oscillating terms. With the rotating wave approximation (4.517) the time evolution operator (4.516) reads

$$\hat{U}_{\mathrm{D}}(t) \approx 1 - it\frac{|g|^2}{\Delta}\left(\sigma_+\sigma_-\hat{a}\hat{a}^\dagger - \sigma_-\sigma_+\hat{a}^\dagger\hat{a}\right) + \ldots\,. \tag{4.518}$$

For large detuning Δ the dynamics in the interaction picture described by (4.518) can even further be approximated by identifying it with the time evolution operator of a time-independent Hamiltonian

$$\hat{U}_{\mathrm{D}}(t) \approx e^{-i\hat{H}_{\mathrm{eff}}t/\hbar}\,, \tag{4.519}$$

where we have introduced

$$\hat{H}_{\mathrm{eff}} = \hbar\frac{|g|^2}{\Delta}\left(\sigma_+\sigma_-\hat{a}\hat{a}^\dagger - \sigma_-\sigma_+\hat{a}^\dagger\hat{a}\right)\,. \tag{4.520}$$

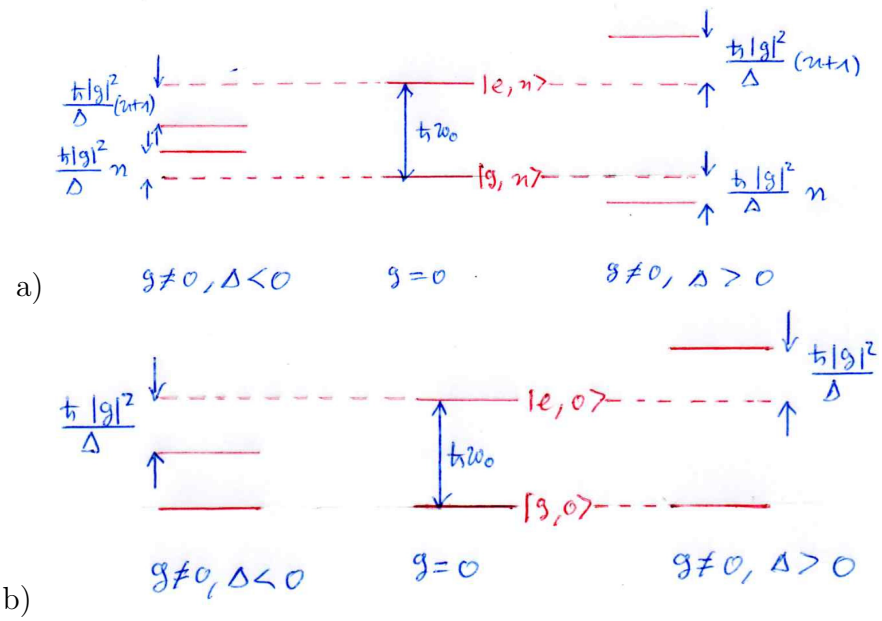

Figure 4.22: Shift of bare energy levels for large detuning according to (4.521): a) in the presence and b) in the absence of photons in the cavity.

Due to the commutation relation of the photonic operators (3.11) the effective Hamiltonian (4.520) can be rewritten as

$$\hat{H}_{\text{eff}} = \hbar\chi \left(\sigma_+\sigma_- + \sigma_3 \hat{a}^\dagger \hat{a}\right) , \tag{4.521}$$

where we have introduced the abbreviation

$$\chi = \frac{|g|^2}{\Delta} \tag{4.522}$$

and have used the following identity among the Pauli matrices (4.177), (4.183), and (4.184)

$$\sigma_3 = \sigma_+\sigma_- - \sigma_-\sigma_+ = \begin{pmatrix} 1 & 0 \\ 0 & -1 \end{pmatrix} . \tag{4.523}$$

Thus, the energy levels $|e\rangle$ and $|g\rangle$ are so far out of resonance with the quantized electric field that there are no direct transitions between them. Therefore, the bare states are not coupled to dressed states and they turn out to be also eigenstates of the effective Hamiltonian (4.521):

$$\hat{H}_{\text{eff}}|e,n\rangle = \hbar\chi(n+1)|e,n\rangle , \tag{4.524}$$

$$\hat{H}_{\text{eff}}|g,n\rangle = -\hbar\chi n|g,n\rangle . \tag{4.525}$$

Only a dispersive interaction occurs in the sense that the bare energy levels are just shifted as described by (4.524), (4.525) and illustrated in Fig. 4.22a). Note that term $\hbar\chi\sigma_+\sigma_-$ in (4.521) induces an energy shift of the bare excited atomic state, which is even present in the absence of photons in the cavity, see Fig. 4.22b). As it depends quadratically on the light-matter interaction strength g due to (4.522), it represents a kind of cavity-induced atomic Kerr effect

raising or lowering the energy of the bare excited atomic state depending on the sign of the detuning Δ.

Now we investigate exemplarily, which consequences the effective Hamiltonian (4.521) has upon the dynamics of particular states. Let us consider first the case, where the light field is initially in a Fock state, so that applying (4.524) and (4.525) yields

$$e^{-i\hat{H}_{\rm eff}t/\hbar}\,|g,n\rangle \;=\; e^{i\chi nt}\,|g,n\rangle\;, \tag{4.526}$$

$$e^{-i\hat{H}_{\rm eff}t/\hbar}\,|e,n\rangle \;=\; e^{-i\chi(n+1)t}\,|e,n\rangle\;. \tag{4.527}$$

Evidently nothing interesting happens, irrespective of having the two-level atom in the ground or in the excited state, only unmeasurable phase factors emerge. But this changes drastically in the case, where the light field is initially in a coherent state. In the case that the atom is in the ground state the effective Hamiltonian (4.521) yields

$$e^{-i\hat{H}_{\rm eff}t}\,|g,\alpha\rangle = |g\rangle\,e^{i\chi\hat{a}^\dagger\hat{a}t}\,|\alpha\rangle\;. \tag{4.528}$$

In order to evaluate this further, we have to remember that a coherent state consists according to (3.187) and (3.190) of a Poisson distribution of Fock states:

$$|\alpha\rangle = \sum_{n=0}^{\infty}\frac{\alpha^n}{\sqrt{n!}}\,e^{-|\alpha|^2/2}\,|n\rangle\;. \tag{4.529}$$

Combining (4.528) and (4.529) we get

$$e^{i\chi\hat{a}^\dagger\hat{a}t}\,|\alpha\rangle = \sum_{n=0}^{\infty}\frac{\left(\alpha e^{i\chi t}\right)^n}{\sqrt{n!}}\,e^{-\left|\alpha e^{i\chi t}\right|^2/2}\,|n\rangle = |\alpha e^{i\chi t}\rangle\;, \tag{4.530}$$

so that we obtain finally

$$e^{-i\hat{H}_{\rm eff}t/\hbar}\,|g,\alpha\rangle = |g,\alpha e^{i\chi t}\rangle\;. \tag{4.531}$$

Correspondingly we have in the case that the atom is in the excited state

$$e^{-i\hat{H}_{\rm eff}t/\hbar}\,|e,\alpha\rangle = e^{-i\chi\sigma_+\sigma_-t}\,|e\rangle\,e^{-i\chi\hat{a}^\dagger\hat{a}t}\,|\alpha\rangle = e^{-i\chi t}\,|e,\alpha e^{-i\chi t}\rangle\;. \tag{4.532}$$

We notice that the coherent-state amplitude is rotated in phase space by an angle χt, but that the rotation direction depends on the state of the two-level atom. This can be best illustrated by the Husimi function (3.160), which is given for a coherent state by the isotropic Gauß function (3.182). Thus, provided that the two-level atom is in the ground state (excited state), the coherent state amplitude rotates in the mathematical positive (negative) sense in phase space. Let us suppose now that the initially prepared state factorizes into an atomic state and a coherent state according to

$$|\psi(0)\rangle = |\psi_{\rm A}\rangle\,|\alpha\rangle\;, \tag{4.533}$$

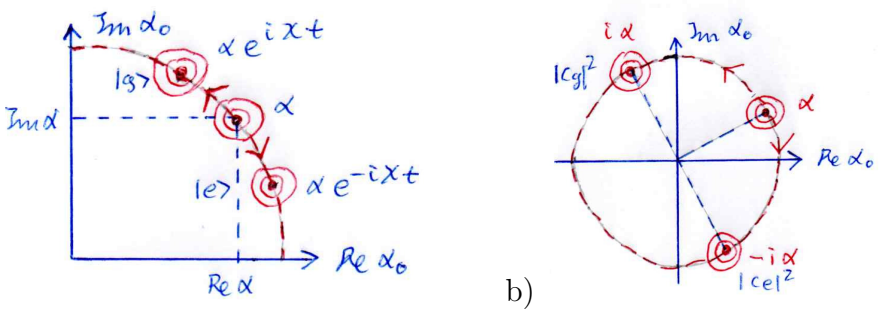

Figure 4.23: Phase space representation of a photonic reduced density matrix revealing entanglement between light and matter: Two coherent states according to a) (4.539) at time t and b) (4.542) at time $t_0 = \pi/2\chi$.

where the former is in a superposition of the ground and the excited state:

$$|\psi_{\rm A}\rangle = c_g\,|g\rangle + c_e\,|e\rangle\ . \tag{4.534}$$

Then we obtain the following dynamics

$$|\psi(t)\rangle = e^{-i\hat{H}_{\rm eff}t/\hbar}\,|\psi(0)\rangle = c_g\,|g,\alpha e^{i\chi t}\rangle + c_e e^{-i\chi t}\,|e,\alpha e^{-i\chi t}\rangle\ , \tag{4.535}$$

which reveals in general entanglement between the atom and the field. In order to determine the corresponding Husimi function, we have to calculate first the density matrix (4.438) and then to trace out the atomic degrees of freedom. The resulting photonic reduced density matrix

$$\hat{\rho}_{\rm F}(t) = {\rm Tr}_{\rm A}\left[\hat{\rho}(t)\right] = \langle g|\,\hat{\rho}(t)\,|g\rangle + \langle e|\,\hat{\rho}(t)\,|e\rangle \tag{4.536}$$

corresponding to (4.535) then reads:

$$\hat{\rho}_{\rm F}(t) = |c_g|^2\,|\alpha e^{i\chi t}\rangle\,\langle\alpha e^{i\chi t}| + |c_e|^2\,|\alpha e^{-i\chi t}\rangle\,\langle\alpha e^{-i\chi t}|\ . \tag{4.537}$$

From this we read off the corresponding Husimi function

$$Q_{\hat{\rho}_{\rm F}(t)}(\alpha_0) = \frac{1}{\pi}\,\langle\alpha_0|\,\hat{\rho}_{\rm F}(t)\,|\alpha_0\rangle = \frac{1}{\pi}\left[|c_g|^2\left|\langle\alpha_0|\alpha e^{i\chi t}\rangle\right|^2 + |c_e|^2\left|\langle\alpha_0|\alpha e^{-i\chi t}\rangle\right|^2\right]\ , \tag{4.538}$$

which simplifies due to the scalar product between two coherent states given in (3.169) according to

$$Q_{\hat{\rho}_{\rm F}(t)}(\alpha_0) = \frac{1}{\pi}\left[|c_g|^2\,e^{-\left|\alpha_0-\alpha e^{i\chi t}\right|^2} + |c_e|^2\,e^{-\left|\alpha_0-\alpha e^{-i\chi t}\right|^2}\right]\ . \tag{4.539}$$

Let us illustrate the result (4.539) in phase space. Whereas initially the Husimi function represents a Gauß function located at α due to

$$Q_{\hat{\rho}_{\rm F}(0)}(\alpha_0) = \frac{1}{\pi}\,e^{-|\alpha_0-\alpha|^2}\ , \tag{4.540}$$

for times $t > 0$ it splits into two Gauß functions centered around $\alpha e^{\pm i\chi t}$, see Fig. 4.23a). Thereby the centers of all Gauß functions lie on a circle of radius α, which is given by the initial mean

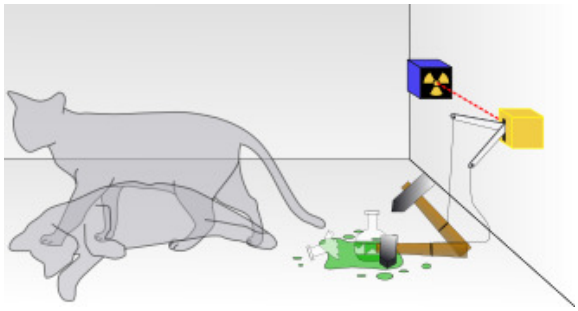

Figure 4.24: The though experiment of Schrödinger consists of a cat, a flask of poison, and a radioactive source, which are all placed in a sealed box. If an internal monitor as, for instance, a Geiger counter detects radioactivity in form of the decay of a single atom, the flask is broken, releasing the poison, which kills the cat.

photon number due to (3.199). But the Gauß function for the ground and the excited state is rotated with the angle χt and $-\chi t$, respectively. Note that initial atomic amplitudes c_g and c_e determine the time-independent weights $|c_g|^2$ and $|c_e|^2$ for the corresponding Gauß functions. The most extreme situation occurs at time $t_0 = \pi/2\chi$ due to

$$e^{\pm i\chi t_0} = e^{\pm i\pi/2} = \pm i\,, \tag{4.541}$$

so we get

$$Q_{\hat{\rho}_{\mathrm{F}}(t_0)}(\alpha_0) = \frac{1}{\pi}\left[|c_g|^2\, e^{-|\alpha_0 - i\alpha|^2} + |c_e|^2\, e^{-|\alpha_0 + i\alpha|^2}\right]. \tag{4.542}$$

Thus, in this phase space picture we have two coherent states, which are maximally separated by 180°, see Fig. 4.23b). Provided that $|\alpha| \gg 1$ holds, i.e. the mean photon number is large enough according to (3.199), there is essentially no overlap between both coherent states and they are said to be macroscopically distinguishable. Therefore, this entangled state of light and matter represents an example for a Schrödinger cat being in an entanglement between life and death and a non-decayed or decayed radioactive microscopic atom:

$$|\psi(t)\rangle = c_g\,|\text{atom not decayed}\rangle\,|\text{cat alive}\rangle + c_e\,|\text{atom decayed}\rangle\,|\text{cat dead}\rangle\,. \tag{4.543}$$

Note that Schrödinger's cat is a thought experiment in quantum mechanics, which was devised by Erwin Schödinger in 1935 in order to illustrate the paradox of quantum superposition. Due to the Copenhagen interpretation of quantum mechanics the thought experiment implies that a hypothetical cat may be considered simultaneously both alive and dead as a result of its fate being linked to a random atomic event that may or may not occur, see Fig. 4.24. When one looks in the box, one sees that the cat is either alive or dead, but one never observes the cat to be both alive and dead. This poses the question of when exactly quantum superposition ends and reality resolves into one possibility or the other.

4.6 Cavity Quantum Electrodynamics

Now we discuss a particular experimental realization of quantum optical phenomena, which are due to the interaction of an effective two-level atom with a quantized electrodynamic field mode in a cavity. Thus, we deal with an experiment in the realm of cavity quantum electrodynamics (cavity QED) [46]. Although strictly speaking this experiment is not optical as it works with microwaves, it realizes nevertheless the Jaynes-Cummings model. To this end we focus on a single Rydberg atom in a microwave cavity, where photons live long enough. In order to quantify the latter statement one uses in quantum optics the quality factor or Q factor, which is a dimensionless parameter describing how underdamped a resonator is. It is defined as the ratio of the resonator frequency ω and the bandwidth $\Delta\omega$, i.e. we have $Q = \omega/\Delta\omega$. A resonator with a high quality factor Q has low damping, thus the photon lifetime is larger.

4.6.1 Rydberg Atoms

A Rydberg atom is an alkali atom, where the single valence electron is excited to a state of very high principal quantum number n. An example is provided by a rubidium atom with the valence electron being in an excited state n of the order of 50 or higher. The electronic binding energy of a Rydberg atom is given by

$$E_{nl} = -\frac{\mathrm{Ry}}{(n-\delta_l)^2} \tag{4.544}$$

with the Rydberg energy (C.13)–(C.15) and the angular momentum quantum number $l = 0, 1, \ldots, n-1$. Here the quantum defect δ_l describes the deviation of the binding energy from a purely hydrogenic situation and depends on the angular momentum quantum number l. For small l it turns out that δ_l is of the order of unity, but for larger l the quantum defect δ_l is quite small. In order to describe a Rydberg atom, whose binding energy resembles most closely that of a hydrogen atom, one has to choose the largest possible angular quantum number $l = n-1$ with the magnetic quantum number $m = -(n-1), \ldots, n-1$. Note that states with the maximal magnetic quantum number $|m| = n-1$ are known as circular Rydberg states as they describe in the classical limit an electron in a circular orbit. Cavity QED relies on using such circular Rydberg states. There are various properties of circular Rydberg states, which make them suitable candidates for cavity QED experiments:

(1) They represent a close approximation of a two-level system. The one-electron dipole transition of a circular Rydberg state is restricted to involve another circular Rydberg state. The reason is that the dipole moment selection rules $\Delta l = \pm 1$, $\Delta m = 0, \pm 1$ favour the transition from $n, l = n-1$, $|m| = n-1$ to $n-1$, $l = n-2$, $|m| = n-2$, see also Appendix F.

(2) The dipole moments of the allowed transitions are large, so the coupling of circular Rydberg states to a single-mode cavity field can be quite large. Indeed, the dipole moment

between two circular Rydberg atom states n and $n' = n - 1$ scales like

$$d = \langle n| \hat{d} |n-1\rangle \sim e a_n \,, \tag{4.545}$$

where the classical radius of the Rydberg atom scales a_n like (C.7) with the Bohr radius a_B:

(3) Circular Rydberg states have a quite large lifetime. To this end we remind that the rate of spontaneous emission, whose reciprocal value defines the lifetime, is given according to (4.102) by

$$\Gamma = \frac{d^2 \omega_0^3}{3\pi\epsilon_0 \hbar c^3} \,. \tag{4.546}$$

Here ω_0 denotes the frequency of the radiation emitted in a transition. As the quantum defect δ_l is negligibly small for a circular Rydberg state, we obtain from (4.544) for $n - n' = 1$:

$$\omega_0 = \frac{E_{nl} - E_{n'l'}}{\hbar} \approx \frac{\mathrm{Ry}}{\hbar} \left[\frac{1}{(n-1)^2} - \frac{1}{n^2} \right] \approx \frac{\mathrm{Ry}}{\hbar} \left[\frac{1}{n^2} \left(1 + \frac{2}{n} \right) - \frac{1}{n^2} \right] = \frac{2\mathrm{Ry}}{\hbar} \frac{1}{n^3} \,. \tag{4.547}$$

Thus, inserting (4.545), (4.547), and (C.7) into the rate of spontaneous emission (4.546), it scales like

$$\Gamma \sim \left(n^2\right)^2 \left(n^{-3}\right)^3 \Gamma_0 = n^{-5} \Gamma_0 \tag{4.548}$$

with the rate $\Gamma_0 \approx 10^9\, 1/\mathrm{s}$ following from (4.104). This means that the spontaneous lifetime of about $\tau_0 = 1/\Gamma_0 = 10^{-9}\,\mathrm{s}$ is scaled for a circular Rydberg state of $n = 50$ to the value $\tau = 1/\Gamma = n^5 \tau_0 \approx 0.1\,\mathrm{s}$. Note that for $n = 50$ the transition frequency amounts to $\nu_0 = \omega_0/2\pi \sim 36\,\mathrm{GHz}$, which corresponds to the wavelength $\lambda_0 = c/\nu_0 \sim 8\,\mathrm{mm}$ and, thus, represents microwave radiation. This wavelength sets the scale for the distance of the two mirrors in the cavity to support a standing microwave field.

(4) Atomic state detection is possible due to selective ionization by applied electric fields. In a Rydberg atom the valence electron is typically far away from the hydrogenic cave due to (C.7). As a consequence its binding energy is relatively small, so the valence electron can easily be ionized by an external applied field. As the Coulomb law implies due to (C.7)

$$E = \frac{e}{4\pi\epsilon_0 a_n^2} = \frac{E_0}{n^4} \,, \qquad E_0 = \frac{e}{4\pi\epsilon_0 a_\mathrm{B}^2} \,, \tag{4.549}$$

the ionization rate $I(n)$ goes like n^{-4}. Then the ionization rates of two adjacent circular Rydberg states $n - n' = 1$ differ by

$$I(n-1) - I(n) \sim \frac{1}{(n-1)^4} - \frac{1}{n^4} \approx \frac{1}{n^4} \left(1 + \frac{4}{n} \right) - \frac{1}{n^4} = \frac{4}{n} \,. \tag{4.550}$$

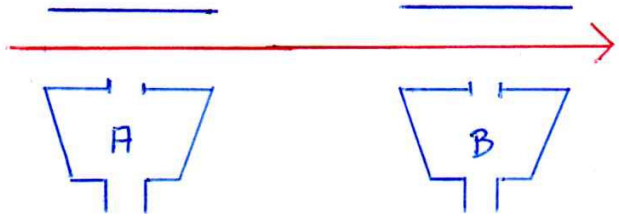

Figure 4.25: Experimental atomic state detection via field ionization: The red arrow indicates the flight direction of Rydberg atoms, which are ionized by an electric field gradient. In this way the detectors A and B detect circular Rydberg atoms with $n = 50$ and $n = 49$ corresponding to the excited state $|e\rangle$ and the ground state $|g\rangle$, respectively.

On the one hand this is a quite small difference for $n = 50$ compared with low-lying states of about $n = 5$. On the other hand it is still large enough for state-selective measurements to be performed by field ionization via the experimental set-up shown in Fig. 4.25. The atoms encounter first detector A, which has a smaller electric field to detect the atom with principal quantum number n corresponding to the excited state, and then detector B with a larger electric field to be sensitive for the principal quantum number $n - 1$ representing the ground state. Obviously, the detection of the field-ionized electron in one of the detectors constitutes the selective atomic-state detection.

4.6.2 Experimental Realization of Jaynes-Cummings Model

The experimental realization of the Jaynes-Cummings model was pioneered by Gerd Rempe at the Max-Planck Institute for Quantum Optics in Munich [48] and by Serge Haroche at the Ecole Normale Superieur in Paris [49] together with their respective research groups. A typical set up for a cavity QED experiment is shown in Fig. 4.26. The electric field stems from a source S of classical microwaves, a so-called klystron, is then transported via a waveguide W, and finally yields a coherent state in a cavity C. The latter consists of two curved mirrors separated by about 30 mm and has a high Q factor of about 10^8 in order to allow for a long enough lifetime for the photons of the cavity field. The Rydberg atoms stem from an oven O and are then prepared in the apparatus P in the excited state, velocity selected, and then directed into the cavity C. The selective ionization detectors A and B, see also Fig. 4.25, yield the statistics for the atomic population inversion as a function of the interaction time, which itself is controlled by the initial velocity selection.

Due to the temperature of the cavity walls of about 1 K there are on average about 0.7 microwave photons in the cavity. If one sends ground state atoms through the cavity, they absorb photons and, thus, reduce the average microwave photons to roughly 0.1. This represents an effective cooling mechanism.

The storage time for circular Rydberg atoms in a microwave cavity is determined by their veloc-

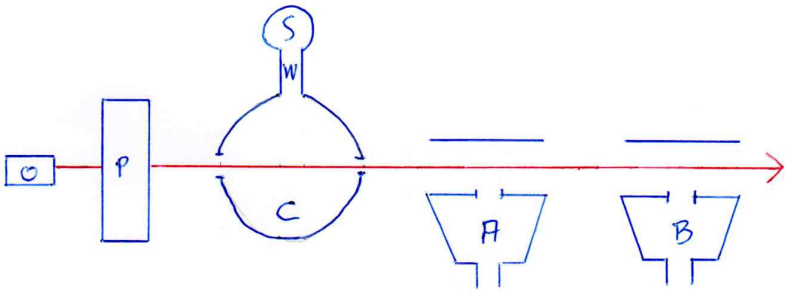

Figure 4.26: Experimental set-up for realizing the Jaynes-Cummings model consists of microwave source S, waveguide W, cavity C, oven O, state preparation P and detectors A, B.

ity and amounts to about 1 ms. This is shorter than the atomic decay time due to spontaneous emission, which amounts to about 0.1 s as we have estimated below (4.548). But it is larger than the atom-field interaction time, which is about few μs for the speed of atoms injected in the cavity.

Let us briefly mention some results of the experiment in the Haroche group from Fig. 2 of Ref. [49], where the dynamics of the transfer rate from the excited to the ground state shows clearly several oscillations. A more detailed analysis of the data reveals that the signal exhibits discrete Fourier components at frequencies proportional to the square root of successive integers. This provides direct evidence of field quantization in the cavity. For coherent fields of increasing mean photon number, a collapse followed by a revival is evident. This represents the collapse and revival dynamics of the Jaynes-Cummings model, which was discussed in Subsection 4.5.4.

Note that the collapse and revival dynamics of the Jaynes-Cummings model is realisable experimentally with different platforms [9]. For instance, apart from a cavity QED set-up also the centre-of-mass motion of trapped ions [50] can be used. Furthermore, a collapse and revival dynamics of different physical origin was also observed for matter waves by dealing with a Bose-Einstein condensate confined by a three-dimensional optical lattice, where each potential well can be prepared in a coherent superposition of different atom number states, with constant relative phases between neighbouring lattice sites [51].

Chapter 5

Quantum Mechanical Equations of Light Field and Atoms

In the previous part of the lecture, we treated only the light field in second quantization, in order to have access to describe an ensemble of photons. In contrast to that for the matter we only considered one atom and approximated it to a two-level system, which could still be dealt with in first quantization. But in order to be able to describe a laser, which consists of many laser-active atoms, we have to switch gears and consider an ensemble of atoms, which needs then also to be described within the realm of second quantization. Thus, we deal here with a bosonic second quantization for the light field and, due to the description of the electrons in the atoms, with a fermionic quantization for the matter. With this framework we derive the corresponding equations of motion of the photon and the electron operators for a closed system, so that both losses and pumping are not taken into account. To this end we consider the second quantized operators of light field and matter in the Heisenberg picture. In particular, we treat the interaction between light and matter within the dipole approximation and apply, subsequently, the two-level approximation for the atoms and the rotating wave approximation. The resulting model Hamiltonian turns out to be a sum of Jaynes-Cummings Hamiltonians with respect to different field mode and atomic degrees of freedom.

5.1 Quantization of Light Field

In Chapter 2 we worked out in detail the quantization of the electromagnetic field. In order to simplify the description we have chosen the radiation gauge. This means that the scalar potential vanishes, i.e. $\varphi(\mathbf{x}, t) = 0$, and that the vector potential fulfills the Coulomb gauge, i.e. $\operatorname{div} \mathbf{A}(\mathbf{x}, t) = 0$. Although the radiation gauge is not manifestly Lorentz invariant, it has the advantage that the remaining two degrees of freedom of the Maxwell field are the transversal ones. The second quantization of the Maxwell field in vacuum determines the operators of both the vector potential and the electric field according to (2.136) and (2.168), respectively. Going

over from the vacuum to a cavity with finite volume V, the substitution rule (4.63) applies and yields in the Heisenberg picture for the field operator

$$\hat{\mathbf{A}}(\mathbf{x},t) = \sum_{\lambda=\pm1}\sum_{\mathbf{k}}\sqrt{\frac{\hbar}{2V\epsilon_0\omega_{\mathbf{k}}}}\left\{\boldsymbol{\epsilon}(\mathbf{k},\lambda)e^{i\mathbf{kx}}\hat{b}_{\mathbf{k},\lambda}(t)+\boldsymbol{\epsilon}^*(\mathbf{k},\lambda)e^{-i\mathbf{kx}}\hat{b}^\dagger_{\mathbf{k},\lambda}(t)\right\} \tag{5.1}$$

and correspondingly for the operator of the electric field

$$\hat{\mathbf{E}}(\mathbf{x},t) = i\sum_{\lambda=\pm1}\sum_{\mathbf{k}}\sqrt{\frac{\hbar\omega_{\mathbf{k}}}{2V\epsilon_0}}\left\{\boldsymbol{\epsilon}(\mathbf{k},\lambda)e^{i\mathbf{kx}}\hat{b}_{\mathbf{k},\lambda}(t)-\boldsymbol{\epsilon}^*(\mathbf{k},\lambda)e^{-i\mathbf{kx}}\hat{b}^\dagger_{\mathbf{k},\lambda}(t)\right\}. \tag{5.2}$$

Here we have assumed for simplicity that the cavity of volume V has a box shape so that its mode functions are just given by plane waves. In view of the laser, however, we need instead a more generic notation, which is valid in principle for any cavity shape. To this end we use from now on instead of plane waves general cavity basis functions $\mathbf{u}_{\boldsymbol{\lambda}}(\mathbf{x})$ for the transversal electrodynamic degrees of freedom. Here we have summarized all quantum numbers into the vector $\boldsymbol{\lambda}$ and we assume the following orthonormality relations to hold:

$$\int d^3x\, u^*_{\boldsymbol{\lambda}}(\mathbf{x})\, u_{\boldsymbol{\lambda}'}(\mathbf{x}) = \delta_{\boldsymbol{\lambda},\boldsymbol{\lambda}'}\,. \tag{5.3}$$

Indeed, the cavity with box shape is included in this more generic notation by identifying the vector of quantum numbers with both the wave vector and the helicity, i.e. $\boldsymbol{\lambda}=\{\mathbf{k},\lambda\}$, as well as the basis functions with the plane waves according to

$$\mathbf{u}_{\boldsymbol{\lambda}}(\mathbf{x}) = \frac{1}{\sqrt{V}}\,\boldsymbol{\epsilon}(\mathbf{k},\lambda)e^{i\mathbf{kx}}\,, \tag{5.4}$$

which fulfills (5.3). Thus, the decompositions (5.1) and (5.2) for the vector potential and the electric field operator, respectively, go over into

$$\hat{\mathbf{A}}(\mathbf{x},t) = \sum_{\boldsymbol{\lambda}}\sqrt{\frac{\hbar}{2\epsilon_0\omega_{\boldsymbol{\lambda}}}}\left\{\mathbf{u}_{\boldsymbol{\lambda}}(\mathbf{x})\hat{b}_{\boldsymbol{\lambda}}(t)+\mathbf{u}^*_{\boldsymbol{\lambda}}(\mathbf{x})\hat{b}^\dagger_{\boldsymbol{\lambda}}(t)\right\}, \tag{5.5}$$

$$\hat{\mathbf{E}}(\mathbf{x},t) = i\sum_{\boldsymbol{\lambda}}\sqrt{\frac{\hbar\omega_{\boldsymbol{\lambda}}}{2\epsilon_0}}\left\{\mathbf{u}_{\boldsymbol{\lambda}}(\mathbf{x})\hat{b}_{\boldsymbol{\lambda}}(t)-\mathbf{u}^*_{\boldsymbol{\lambda}}(\mathbf{x})\hat{b}^\dagger_{\boldsymbol{\lambda}}(t)\right\}, \tag{5.6}$$

where $\omega_{\boldsymbol{\lambda}}$ denotes the resulting dispersion of the electromagnetic field in the cavity. The operators $\hat{b}_{\boldsymbol{\lambda}}(t)\,,\,\hat{b}^\dagger_{\boldsymbol{\lambda}}(t)$ represent annihilation and creation operators for photons in the quantum state $\boldsymbol{\lambda}$ and obey the bosonic equal-time commutation relations

$$\left[\hat{b}_{\boldsymbol{\lambda}}(t)\,,\,\hat{b}_{\boldsymbol{\lambda}'}(t)\right]_- = \left[\hat{b}^\dagger_{\boldsymbol{\lambda}}(t)\,,\,\hat{b}^\dagger_{\boldsymbol{\lambda}'}(t)\right]_- = 0\,,\qquad \left[\hat{b}_{\boldsymbol{\lambda}}(t)\,,\,\hat{b}^\dagger_{\boldsymbol{\lambda}'}(t)\right]_- = \delta_{\boldsymbol{\lambda},\boldsymbol{\lambda}'}\,. \tag{5.7}$$

Determining with the more general decompositions (5.5) and (5.6) the second-quantized Hamilton operator of the electromagnetic field according to similar steps as in Section 2.12 finally yields

$$\hat{H}_{\text{field}} = \sum_{\boldsymbol{\lambda}}\hbar\omega_{\boldsymbol{\lambda}}\hat{b}^\dagger_{\boldsymbol{\lambda}}(t)\hat{b}_{\boldsymbol{\lambda}}(t)\,. \tag{5.8}$$

5.2 Quantization of Electron Field

Within the second quantization also the first quantized electronic wave functions $\psi(\mathbf{x},t)$, $\psi^*(\mathbf{x},t)$ become operators $\hat{\psi}(\mathbf{x},t)$, $\hat{\psi}^\dagger(\mathbf{x},t)$, which obey the fermionic equal-time anti-commutation relations

$$\Big[\hat{\psi}(\mathbf{x},t)\,,\,\hat{\psi}(\mathbf{x}',t)\Big]_+ = \Big[\hat{\psi}^\dagger(\mathbf{x},t)\,,\,\hat{\psi}^\dagger(\mathbf{x}',t)\Big]_+ = 0\,, \qquad \Big[\hat{\psi}(\mathbf{x},t)\,,\,\hat{\psi}^\dagger(\mathbf{x}',t)\Big]_+ = \delta(\mathbf{x}-\mathbf{x}')\,. \quad (5.9)$$

For instance, the second equal-time anti-commutation relation in (5.9) includes the Pauli principle that two fermions can not be at the same space point:

$$\hat{\psi}^{\dagger\,2}(\mathbf{x},t) = 0\,. \quad (5.10)$$

Provided that the interaction between the electrons can be neglected, this second-quantized Hamiltonian is given by

$$\hat{H}_{\rm el} = \int d^3x\,\hat{\psi}^\dagger(\mathbf{x},t)\left\{-\frac{\hbar^2}{2M}\,\Delta + V(\mathbf{x})\right\}\hat{\psi}(\mathbf{x},t)\,. \quad (5.11)$$

Note that we applied here the *sandwich principle* for performing the transition from first to second quantization. Namely, in case of an observable the second-quantized operator follows from the corresponding first-quantized operator by multiplying it with $\hat{\psi}^\dagger(\mathbf{x},t)$ from the left as well as $\hat{\psi}(\mathbf{x},t)$ from the right and then performing the spatial integral. Let us choose as an appropriate basis the eigenfunctions of the first-quantized Hamiltonian

$$\left\{-\frac{\hbar^2}{2M}\,\Delta + V(\mathbf{x})\right\}\psi_{\mathbf{n}}(\mathbf{x}) = E_{\mathbf{n}}\psi_{\mathbf{n}}(\mathbf{x})\,, \quad (5.12)$$

which fulfill the orthonormality relation

$$\int d^3x\,\psi^*_{\mathbf{n}}(\mathbf{x})\psi_{\mathbf{n}'}(\mathbf{x}) = \delta_{\mathbf{n},\mathbf{n}'} \quad (5.13)$$

and the completeness relation

$$\sum_{\mathbf{n}}\psi^*_{\mathbf{n}}(\mathbf{x})\psi_{\mathbf{n}}(\mathbf{x}') = \delta(\mathbf{x}-\mathbf{x}')\,. \quad (5.14)$$

Then the electronic field operators can be expanded in the Heisenberg picture into this basis

$$\hat{\psi}(\mathbf{x},t) = \sum_{\mathbf{n}}\psi_{\mathbf{n}}(\mathbf{x})\hat{a}_{\mathbf{n}}(t) \qquad \Longleftrightarrow \qquad \hat{a}_{\mathbf{n}}(t) = \int d^3x\,\psi^*_{\mathbf{n}}(\mathbf{x})\hat{\psi}(\mathbf{x},t)\,, \quad (5.15)$$

$$\hat{\psi}^\dagger(\mathbf{x},t) = \sum_{\mathbf{n}}\psi^*_{\mathbf{n}}(\mathbf{x})\hat{a}^\dagger_{\mathbf{n}}(t) \qquad \Longleftrightarrow \qquad \hat{a}^\dagger_{\mathbf{n}}(t) = \int d^3x\,\psi_{\mathbf{n}}(\mathbf{x})\hat{\psi}^\dagger(\mathbf{x},t)\,. \quad (5.16)$$

Using (5.15) and (5.16) we deduce from the fermionic equal-time anti-commutation relations (5.9) that also the expansion operators $\hat{a}_{\mathbf{n}}(t)$, $\hat{a}^\dagger_{\mathbf{n}}(t)$ fulfill fermionic equal-time anti-commutation relations:

$$[\hat{a}_{\mathbf{n}}(t)\,,\,\hat{a}_{\mathbf{n}'}(t)]_+ = \Big[\hat{a}^\dagger_{\mathbf{n}}(t)\,,\,\hat{a}^\dagger_{\mathbf{n}'}(t)\Big]_+ = 0\,, \qquad \Big[\hat{a}_{\mathbf{n}}(t)\,,\,\hat{a}^\dagger_{\mathbf{n}'}(t)\Big]_+ = \delta_{\mathbf{n},\mathbf{n}'}\,. \quad (5.17)$$

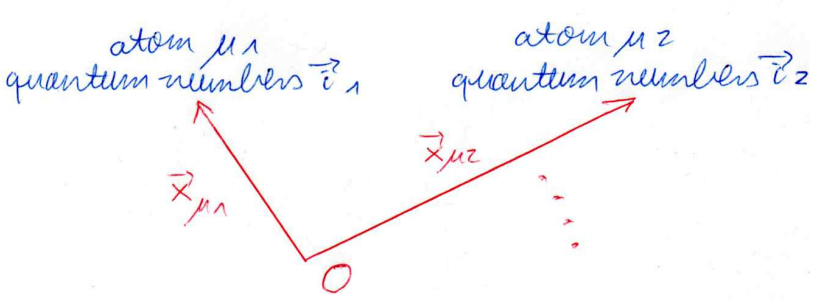

Figure 5.1: Schematic illustration of identical atoms indexed with μ at different positions $\mathbf{x}_\mu$ and their quantum numbers $\mathbf{i}$.

Thus, we conclude that the expansion operators $\hat{a}_\mathbf{n}(t)$, $\hat{a}^\dagger_\mathbf{n}(t)$ represent operators annihilating or creating an electron in state $\mathbf{n}$. For instance, the second equal-time anti-commutation relation in (5.17) corresponds to the Pauli principle that two fermions can not occupy one and the same quantum state:

$$\hat{a}^{\dagger\,2}_\mathbf{n} = 0\,. \tag{5.18}$$

Furthermore, we obtain from (5.12), (5.13) and (5.15), (5.16) that the second-quantized electronic Hamiltonian (5.11) goes over into

$$\hat{H}_\mathrm{el} = \sum_\mathbf{n} E_\mathbf{n} \hat{a}^\dagger_\mathbf{n}(t)\hat{a}_\mathbf{n}(t)\,. \tag{5.19}$$

With this description we may refer not only to electrons of one atom but also to electrons of other atoms. In the following we will assume that we have N identical atoms at positions $\mathbf{x}_{\mu_1}\,\mathbf{x}_{\mu_2}, \ldots$. Thus, we decompose the quantum numbers $\mathbf{n}$ into the quantum numbers $\mathbf{i}$ within each atom and the position index μ: $\mathbf{n} = \{\mathbf{i}, \mu\}$, see Fig. 5.1. Provided that the atoms are far enough away from each other it is justified to assume that the electronic wave functions of the different atoms do not overlap. This means that the electrons belonging to different atoms are considered to be distinguishable. Thus the orthonormality relation (5.13) reads now

$$\int d^3x\, \psi^*_{\mathbf{i},\mu}(\mathbf{x})\psi_{\mathbf{i}',\mu'}(\mathbf{x}) = \delta_{\mathbf{i},\mathbf{i}'}\delta_{\mu,\mu'} \tag{5.20}$$

and the completeness relation (5.14) goes over into

$$\sum_\mathbf{i}\sum_\mu \psi^*_{\mathbf{i},\mu}(\mathbf{x})\psi_{\mathbf{i},\mu}(\mathbf{x}') = \delta(\mathbf{x}-\mathbf{x}')\,. \tag{5.21}$$

Correspondingly, the decomposition of the electron field operators has the form

$$\hat{\psi}(\mathbf{x},t) = \sum_\mathbf{i}\sum_\mu \psi_{\mathbf{i},\mu}(\mathbf{x})\hat{a}_{\mathbf{i},\mu}(t)\,, \qquad \hat{\psi}^\dagger(\mathbf{x},t) = \sum_\mathbf{i}\sum_\mu \psi^*_{\mathbf{i},\mu}(\mathbf{x})\hat{a}^\dagger_{\mathbf{i},\mu}(t) \tag{5.22}$$

with the equal-time anti-commutator relations

$$\Big[\hat{a}_{\mathbf{i},\mu}(t)\,,\,\hat{a}_{\mathbf{i}',\mu'}(t)\Big]_+ = \Big[\hat{a}^\dagger_{\mathbf{i},\mu}(t)\,,\,\hat{a}^\dagger_{\mathbf{i}',\mu'}(t)\Big]_+ = 0\,, \qquad \Big[\hat{a}_{\mathbf{i},\mu}(t)\,,\,\hat{a}^\dagger_{\mathbf{i}',\mu'}(t)\Big]_+ = \delta_{\mathbf{i},\mathbf{i}'}\,\delta_{\mu,\mu'}\,. \tag{5.23}$$

Furthermore, the second-quantized electronic Hamiltonian (5.19) reduces to

$$\hat{H}_{\rm el} = \sum_{\mathbf{i}} \sum_{\mu} E_{\mathbf{i}}\, \hat{a}^{\dagger}_{\mathbf{i},\mu}(t)\, \hat{a}_{\mathbf{i},\mu}(t)\,, \tag{5.24}$$

where the energies $E_{\mathbf{i}}$ do not depend on the atom index μ, as we assume to have identical atoms,

5.3 Interaction Between Radiation and Electron Field

In Section 4.1 the interaction of light and matter was described such that the atom was dealt with in first quantization. In dipole approximation this led to

$$\hat{H}_{\rm int} = -\,\mathbf{d}\,\cdot\,\hat{\mathbf{E}}(\mathbf{x},t) \tag{5.25}$$

with the electric dipole moment of the electron (4.20). Thus, applying the sandwich principle to the first-quantized interaction Hamiltonian corresponding (5.25) yields its second-quantized counterpart:

$$\hat{H}_{\rm int} = -\int d^3x\, \hat{\psi}^{\dagger}(\mathbf{x},t)\, \mathbf{d}\,\cdot\,\hat{\mathbf{E}}(\mathbf{x},t)\hat{\psi}(\mathbf{x},t)\,. \tag{5.26}$$

Inserting the respective expansions (5.6), (5.22) for all second quantized field operators yields

$$\hat{H}_{\rm int} = -i \sum_{\boldsymbol{\lambda}} \sum_{\mathbf{i},\mathbf{i}'} \sum_{\mu,\mu'} \sqrt{\frac{\hbar\omega_{\boldsymbol{\lambda}}}{2\epsilon_0}}\, \hat{a}^{\dagger}_{\mathbf{i},\mu}(t) \left\{ I_{\mathbf{i},\mu,\boldsymbol{\lambda},\mathbf{i}',\mu'} \hat{b}_{\boldsymbol{\lambda}}(t) - J_{\mathbf{i},\mu,\boldsymbol{\lambda},\mathbf{i}',\mu'} \hat{b}^{\dagger}_{\boldsymbol{\lambda}}(t) \right\} \hat{a}_{\mathbf{i}',\mu'}(t)\,, \tag{5.27}$$

where we have introduced the two matrix elements

$$I_{\mathbf{i},\mu,\boldsymbol{\lambda},\mathbf{i}',\mu'} = \int d^3x\, \psi^{*}_{\mathbf{i},\mu}(\mathbf{x}) \mathbf{d}\cdot\mathbf{u}_{\boldsymbol{\lambda}}(\mathbf{x}) \psi_{\mathbf{i}',\mu'}(\mathbf{x})\,, \tag{5.28}$$

$$J_{\mathbf{i},\mu,\boldsymbol{\lambda},\mathbf{i}',\mu'} = \int d^3x\, \psi^{*}_{\mathbf{i},\mu}(\mathbf{x})\, \mathbf{d}\cdot\mathbf{u}^{*}_{\boldsymbol{\lambda}}(\mathbf{x})\, \psi_{\mathbf{i}',\mu'}(\mathbf{x})\,. \tag{5.29}$$

The first matrix element (5.28) vanishes for different atoms as the corresponding electronic wave functions are assumed to not overlap:

$$I_{\mathbf{i},\mu,\boldsymbol{\lambda},\mathbf{i}',\mu'} = \delta_{\mu,\mu'} \int d^3x\, \psi^{*}_{\mathbf{i},\mu}(\mathbf{x}) \mathbf{u}_{\boldsymbol{\lambda}}(\mathbf{x}) \cdot \mathbf{d} \psi_{\mathbf{i}',\mu}(\mathbf{x})\,. \tag{5.30}$$

As the electronic wave function $\psi_{\mathbf{i}',\mu}(\mathbf{x})$ is localized around the nucleus at space point $\mathbf{x}_{\mu}$, we can apply the dipole approximation discussed in Subsection 2.18.6. This means that we can approximate the slowly varying cavity mode function $\mathbf{u}_{\boldsymbol{\lambda}}(\mathbf{x})$ in the integral (5.30) by $\mathbf{u}_{\boldsymbol{\lambda}}(\mathbf{x}_{\mu})$ and put it in front of the integral, yielding

$$I_{\mathbf{i},\mu,\boldsymbol{\lambda},\mathbf{i}',\mu'} = \delta_{\mu,\mu'}\, \mathbf{u}_{\boldsymbol{\lambda}}(\mathbf{x}_{\mu}) \cdot \mathbf{d}_{\mathbf{i},\mathbf{i}'}\,. \tag{5.31}$$

Here the dipole matrix elements

$$\mathbf{d}_{\mathbf{i},\mathbf{i}'} = \int d^3x\, \psi^*_{\mathbf{i},\mu}(\mathbf{x})\, \mathbf{d}\, \psi_{\mathbf{i}',\mu}(\mathbf{x}) \tag{5.32}$$

no longer depend on the atom index μ as we assume to have identical atoms. Taking (5.31) into account the second matrix element (5.29) follows from the first matrix element (5.28) and we get

$$J_{\mathbf{i},\mu,\boldsymbol{\lambda},\mathbf{i}',\mu'} = \left\{ \int d^3x\, \psi^*_{\mathbf{i}',\mu'}(\mathbf{x})\, \mathbf{d}\cdot\mathbf{u}_{\boldsymbol{\lambda}}(\mathbf{x})\psi_{\mathbf{i},\mu}(\mathbf{x}) \right\}^* = I^*_{\mathbf{i}',\mu',\boldsymbol{\lambda},\mathbf{i},\mu} = \delta_{\mu,\mu'}\mathbf{u}^*_{\boldsymbol{\lambda}}(\mathbf{x}_\mu)\mathbf{d}^*_{\mathbf{i}',\mathbf{i}}\,. \tag{5.33}$$

Due to the hermiticity of the dipole matrix elements (5.32) we have

$$\mathbf{d}^*_{\mathbf{i}',\mathbf{i}} = \mathbf{d}_{\mathbf{i},\mathbf{i}'}\,, \tag{5.34}$$

so (5.33) reduces to

$$J_{\mathbf{i},\mu,\boldsymbol{\lambda},\mathbf{i}',\mu'}\delta_{\mu,\mu'}\, \mathbf{u}^*_{\boldsymbol{\lambda}}(\mathbf{x}_\mu)\mathbf{d}_{\mathbf{i},\mathbf{i}'}\,. \tag{5.35}$$

Inserting the results (5.31) and (5.35) for both matrix elements in the interaction Hamiltonian (5.27) leads finally to

$$\hat{H}_{\rm int} = \sum_{\boldsymbol{\lambda}}\sum_{\mathbf{i}}\sum_{\mathbf{i}'}\sum_{\mu}(-i)\sqrt{\frac{\hbar\omega_{\boldsymbol{\lambda}}}{2\epsilon_0}}\,\mathbf{d}_{\mathbf{i},\mathbf{i}'}\left\{\mathbf{u}_{\boldsymbol{\lambda}}(\mathbf{x}_\mu)\,\hat{b}_{\boldsymbol{\lambda}}(t) - \mathbf{u}^*_{\boldsymbol{\lambda}}(\mathbf{x}_\mu)\,\hat{b}^\dagger_{\boldsymbol{\lambda}}(t)\right\}\hat{a}^\dagger_{\mathbf{i},\mu}(t)\,\hat{a}_{\mathbf{i}',\mu}(t)\,. \tag{5.36}$$

5.4 Equations of Motion in Heisenberg Picture

The previous considerations finally yield the following Hamiltonian for the second-quantized description of light and matter:

$$\hat{H} = \hat{H}_{\rm field} + \hat{H}_{\rm el} + \hat{H}_{\rm int}\,. \tag{5.37}$$

The dynamics of any operator $\hat{O}(t)$ in the Heisenberg picture follows from its Heisenberg equation

$$\frac{\partial}{\partial t}\,\hat{O}(t) = \frac{i}{\hbar}\left[\hat{H},\hat{O}(t)\right]_-\,. \tag{5.38}$$

Let us start with determining the Heisenberg equation for the photonic creation operator:

$$\frac{\partial}{\partial t}\,\hat{b}^\dagger_{\boldsymbol{\lambda}}(t) = \frac{i}{\hbar}\left[\hat{H},\hat{b}^\dagger_{\boldsymbol{\lambda}}(t)\right]_- = \frac{i}{\hbar}\left[\hat{H}_{\rm field}+\hat{H}_{\rm int},\hat{b}^\dagger_{\boldsymbol{\lambda}}(t)\right]_-\,. \tag{5.39}$$

Inserting (5.8) and (5.36) into (5.39) we have to evaluate

$$\begin{aligned}\frac{\partial}{\partial t}\,\hat{b}^\dagger_{\boldsymbol{\lambda}}(t) &= \frac{i}{\hbar}\sum_{\boldsymbol{\lambda}'}\hbar\omega_{\boldsymbol{\lambda}'}\left[\hat{b}^\dagger_{\boldsymbol{\lambda}'}(t)\hat{b}_{\boldsymbol{\lambda}'}(t),\hat{b}^\dagger_{\boldsymbol{\lambda}}(t)\right]_- + \frac{i}{\hbar}\sum_{\boldsymbol{\lambda}'}\sum_{\mathbf{i}}\sum_{\mathbf{i}'}\sum_{\mu} \\ &\quad\times(-i)\sqrt{\frac{\hbar\omega_{\boldsymbol{\lambda}'}}{2\epsilon_0}}\,\mathbf{d}_{\mathbf{i},\mathbf{i}'}\left[\mathbf{u}_{\boldsymbol{\lambda}'}(\mathbf{x}_\mu)\,\hat{b}_{\boldsymbol{\lambda}'}(t) - \mathbf{u}^*_{\boldsymbol{\lambda}'}(\mathbf{x}_\mu)\,\hat{b}^\dagger_{\boldsymbol{\lambda}'}(t),\hat{b}^\dagger_{\boldsymbol{\lambda}}(t)\right]_-\hat{a}^\dagger_{\mathbf{i},\mu}(t)\,\hat{a}_{\mathbf{i}',\mu}(t)\,.\end{aligned} \tag{5.40}$$

Applying the ABC-rule for commutators (2.61) and the bosonic equal-time commutation relations (5.7) the Heisenberg equation (5.40) reduces to

$$\frac{\partial}{\partial t}\,\hat{b}^\dagger_{\boldsymbol{\lambda}}(t) = i\omega_{\boldsymbol{\lambda}}\hat{b}^\dagger_{\boldsymbol{\lambda}}(t) + \sqrt{\frac{\omega_{\boldsymbol{\lambda}}}{2\hbar\epsilon_0}}\sum_{\mathbf{i}}\sum_{\mathbf{i}'}\sum_{\mu}\mathbf{d}_{\mathbf{i},\mathbf{i}'}\cdot\mathbf{u}_{\boldsymbol{\lambda}}(\mathbf{x}_\mu)\,\hat{a}^\dagger_{\mathbf{i},\mu}(t)\,\hat{a}_{\mathbf{i}',\mu}(t)\,. \tag{5.41}$$

In order to obtain a closed set of equations, we have now also to determine the dynamics of the bilinear operators $\hat{a}^\dagger_{\mathbf{i},\mu}(t)\,\hat{a}_{\mathbf{i}',\mu}(t)$. Their corresponding Heisenberg equations read

$$\frac{\partial}{\partial t}\,\hat{a}^\dagger_{\mathbf{i},\mu}(t)\,\hat{a}_{\mathbf{i}',\mu}(t) = \frac{i}{\hbar}\left[\hat{H},\hat{a}^\dagger_{\mathbf{i},\mu}(t)\,\hat{a}_{\mathbf{i}',\mu}(t)\right]_- = \frac{i}{\hbar}\left[\hat{H}_{\rm el}+\hat{H}_{\rm int},\hat{a}^\dagger_{\mathbf{i},\mu}(t)\,\hat{a}_{\mathbf{i}',\mu}(t)\right]_-\,. \tag{5.42}$$

Thus we have to evaluate:

$$\frac{\partial}{\partial t}\,\hat{a}^\dagger_{\mathbf{i}\mu}(t)\,\hat{a}_{\mathbf{i}'\mu}(t) = \frac{i}{\hbar}\sum_{\mathbf{j}}\sum_{\mu'}E_{\mathbf{j}}\left[\hat{a}^\dagger_{\mathbf{j}\mu'}(t)\,\hat{a}_{\mathbf{j}\mu'}(t),\hat{a}^\dagger_{\mathbf{i}\mu}(t)\,\hat{a}_{\mathbf{i}'\mu}(t)\right]_- + \frac{i}{\hbar}\sum_{\boldsymbol{\lambda}}\sum_{\mathbf{j}}\sum_{\mathbf{j}'}\sum_{\mu'} \tag{5.43}$$
$$\times(-i)\sqrt{\frac{\hbar\omega_{\boldsymbol{\lambda}}}{2\epsilon_0}}\,\mathbf{d}_{\mathbf{j},\mathbf{j}'}\left\{\mathbf{u}_{\boldsymbol{\lambda}}(\mathbf{x}_{\mu'})\,\hat{b}_{\boldsymbol{\lambda}}(t) - \mathbf{u}^*_{\boldsymbol{\lambda}}(\mathbf{x}_{\mu'})\,\hat{b}^\dagger_{\boldsymbol{\lambda}}(t)\right\}\left[\hat{a}^\dagger_{\mathbf{j}\mu'}(t)\,\hat{a}_{\mathbf{j}'\mu'}(t),\hat{a}^\dagger_{\mathbf{i}\mu}(t)\,\hat{a}_{\mathbf{i}'\mu}(t)\right]_-\,.$$

Note that the first commutator in (5.43) is a special case of the second commutator. In order to evaluate the second commutator, we apply first the ABC rule for commutators (2.61)

$$\left[\hat{a}^\dagger_{\mathbf{j}\mu'}\hat{a}_{\mathbf{j}'\mu'},\hat{a}^\dagger_{\mathbf{i}\mu}\hat{a}_{\mathbf{i}'\mu}\right]_- = \hat{a}^\dagger_{\mathbf{j}\mu'}\left[\hat{a}_{\mathbf{j}'\mu'},\hat{a}^\dagger_{\mathbf{i}\mu}\hat{a}_{\mathbf{i}'\mu}\right]_- + \left[\hat{a}^\dagger_{\mathbf{j}\mu'},\hat{a}^\dagger_{\mathbf{i}\mu}\hat{a}_{\mathbf{i}'\mu}\right]_-\hat{a}_{\mathbf{j}'\mu'}\,. \tag{5.44}$$

Then we use the ABC rule for anti-commutators

$$\left[\hat{A}\hat{B},\hat{C}\right]_- = \hat{A}\left[\hat{B},\hat{C}\right]_+ - \left[\hat{A},\hat{C}\right]_+\hat{B}\,, \tag{5.45}$$

so that we finally obtain with the fermionic equal-time anti-commutator relations (5.23)

$$\left[\hat{a}^\dagger_{\mathbf{j}\mu'}\hat{a}_{\mathbf{j}'\mu'},\hat{a}^\dagger_{\mathbf{i}\mu}\hat{a}_{\mathbf{i}'\mu}\right]_- = \delta_{\mu\mu'}\left(\delta_{\mathbf{i}\mathbf{j}'}\hat{a}^\dagger_{\mathbf{j}\mu}\hat{a}_{\mathbf{i}'\mu} - \delta_{\mathbf{i}'\mathbf{j}}\hat{a}^\dagger_{\mathbf{i}\mu}\hat{a}_{\mathbf{j}'\mu}\right)\,. \tag{5.46}$$

Inserting (5.46) in the Heisenberg equation (5.43) yields

$$\frac{\partial}{\partial t}\hat{a}^\dagger_{\mathbf{i}\mu}(t)\hat{a}_{\mathbf{i}'\mu}(t) = \frac{i}{\hbar}\sum_{\mathbf{j}}E_{\mathbf{j}}\left[\delta_{\mathbf{i}\mathbf{j}}\hat{a}^\dagger_{\mathbf{j}\mu}(t)\hat{a}_{\mathbf{i}'\mu}(t) - \delta_{\mathbf{i}'\mathbf{j}}\hat{a}^\dagger_{\mathbf{i}\mu}(t)\hat{a}_{\mathbf{j}\mu}(t)\right] \tag{5.47}$$
$$+\frac{i}{\hbar}\sum_{\boldsymbol{\lambda}}(-i)\sqrt{\frac{\hbar\omega_{\boldsymbol{\lambda}}}{2\epsilon_0}}\left[\mathbf{u}_{\boldsymbol{\lambda}}(\mathbf{x}_\mu)\hat{b}_{\boldsymbol{\lambda}}(t) - \mathbf{u}^*_{\boldsymbol{\lambda}}(\mathbf{x}_\mu)\hat{b}^\dagger_{\boldsymbol{\lambda}}(t)\right]\sum_{\mathbf{j}\mathbf{j}'}\mathbf{d}_{\mathbf{j}\mathbf{j}'}\left[\delta_{\mathbf{j}\mathbf{j}'}\hat{a}^\dagger_{\mathbf{j}\mu}(t)\hat{a}_{\mathbf{j}\mu}(t) - \delta_{\mathbf{j}'\mathbf{j}}\hat{a}^\dagger_{\mathbf{j}\mu}(t)\hat{a}_{\mathbf{j}'\mu}(t)\right]\,.$$

Introducing the atomic transition frequencies

$$\Omega_{\mathbf{i}\mathbf{i}'} = \frac{E_{\mathbf{i}}-E_{\mathbf{i}'}}{\hbar} \tag{5.48}$$

the Heisenberg equation (5.47) finally reads

$$\frac{\partial}{\partial t}\,\hat{a}^\dagger_{\mathbf{j}\mu}(t)\hat{a}_{\mathbf{j}'\mu}(t) = i\Omega_{\mathbf{i}\mathbf{i}'}\hat{a}^\dagger_{\mathbf{i}\mu}(t)\hat{a}_{\mathbf{i}'\mu}(t) \tag{5.49}$$
$$+\sum_{\boldsymbol{\lambda}}\sqrt{\frac{\omega_{\boldsymbol{\lambda}}}{2\hbar\epsilon_0}}\left[\mathbf{u}_{\boldsymbol{\lambda}}(\mathbf{x}_\mu)\hat{b}_{\boldsymbol{\lambda}}(t) - \mathbf{u}^*_{\lambda}(\mathbf{x})\hat{b}^\dagger_{\lambda}(t)\right]\sum_{\mathbf{j}}\left[\mathbf{d}_{\mathbf{j}\mathbf{i}}\hat{a}^\dagger_{\mathbf{j}\mu}(t)\hat{a}_{\mathbf{i}'\mu}(t) - \mathbf{d}_{\mathbf{i}'\mathbf{j}}\hat{a}^\dagger_{\mathbf{i}\mu}(t)\hat{a}_{\mathbf{j}\mu}(t)\right]\,.$$

5.5 Two-Level Approximation

Now we approximate each atom by a two-level system. This means that the indices **i**, **i**', **j** can only assume the values 1 and 2. Furthermore, due to parity, we assume that the dipole matrix elements (5.32) simplify, i.e. the diagonal ones vanish

$$\mathbf{d}_{11} = \mathbf{d}_{22} = \mathbf{0} \tag{5.50}$$

and the non-diagonal ones fulfill due to the hermiticity (5.34)

$$\mathbf{d}_{21} = \mathbf{d}_{12}^* \,. \tag{5.51}$$

With this the Heisenberg equation for the photonic creation operator (5.41) reduces to

$$\frac{\partial}{\partial t}\,\hat{b}_{\boldsymbol{\lambda}}^\dagger(t) = i\omega_{\boldsymbol{\lambda}}\hat{b}_{\boldsymbol{\lambda}}^\dagger(t) + \sqrt{\frac{\omega_{\boldsymbol{\lambda}}}{2\hbar\epsilon_0}}\sum_\mu \mathbf{u}_{\boldsymbol{\lambda}}(\mathbf{x}_\mu)\left[\mathbf{d}_{12}\hat{a}_{1\mu}^\dagger(t)\hat{a}_{2\mu}(t) + \mathbf{d}_{21}\hat{a}_{2\mu}^\dagger(t)\hat{a}_{1\mu}(t)\right] . \tag{5.52}$$

In order to obtain a physical interpretation, let us calculate the second-quantized polarization operator

$$\hat{\mathbf{P}}(t) = \int d^3x\, \hat{\psi}^\dagger(\mathbf{x},t)\; \mathbf{d}\; \hat{\psi}(\mathbf{x},t)\,, \tag{5.53}$$

where again the sandwich principle was used. Inserting the expansions for the electronic field operators (5.22) yields

$$\hat{\mathbf{P}}(t) = \sum_{\mathbf{i}}\sum_{\mu}\sum_{\mathbf{i}'}\sum_{\mu'} \hat{a}_{\mathbf{i}\mu}^\dagger(t)\hat{a}_{\mathbf{i}'\mu'}(t)\int d^3x\, \psi_{\mathbf{i}\mu}^*(\mathbf{x})\; \mathbf{d}\; \psi_{\mathbf{i}'\mu'}(\mathbf{x})\,, \tag{5.54}$$

which straight-forwardly reduces with the help of dipole matrix elements (5.32) to

$$\hat{\mathbf{P}}(t) = \sum_{\mathbf{i}}\sum_{\mu}\sum_{\mathbf{i}'} \mathbf{d}_{\mathbf{i}\mathbf{i}'}\hat{a}_{\mathbf{i}\mu}^\dagger(t)\hat{a}_{\mathbf{i}'\mu}(t)\,. \tag{5.55}$$

Thus, modeling the atom by a two-level system, the second-quantized polarization operator decomposes according to

$$\hat{\mathbf{P}}(t) = \sum_\mu \hat{\mathbf{P}}_\mu(t)\,, \tag{5.56}$$

where the respective atomic contributions are given by

$$\hat{\mathbf{P}}_\mu(t) = \mathbf{d}_{12}\hat{a}_{1\mu}^\dagger(t)\hat{a}_{2\mu}(t) + \mathbf{d}_{21}\hat{a}_{2\mu}^\dagger(t)\hat{a}_{1\mu}(t)\,. \tag{5.57}$$

From (5.52) and (5.57) we read off that the dynamics of the photonic creation operator $\hat{b}_{\boldsymbol{\lambda}}^\dagger(t)$ is driven by the atomic polarization operator $\hat{\mathbf{P}}_\mu(t)$ according to

$$\frac{\partial}{\partial t}\,\hat{b}_{\boldsymbol{\lambda}}^\dagger(t) = i\omega_{\boldsymbol{\lambda}}\hat{b}_{\boldsymbol{\lambda}}^\dagger(t) + \sqrt{\frac{\omega_{\boldsymbol{\lambda}}}{2\hbar\epsilon_0}}\sum_\mu \mathbf{u}_{\boldsymbol{\lambda}}(\mathbf{x}_\mu)\hat{\mathbf{P}}_\mu(t)\,. \tag{5.58}$$

Let us now consider separately the dynamics of both operator contributions defining the atomic polarization operator (5.57) by specializing (5.49) correspondingly:

$$\frac{\partial}{\partial t}\,\hat{a}^{\dagger}_{1\mu}(t)\hat{a}_{2\mu}(t) = i\Omega_{12}\hat{a}^{\dagger}_{1\mu}(t)\hat{a}_{2\mu}(t) + \sum_{\boldsymbol{\lambda}}\sqrt{\frac{\omega_{\boldsymbol{\lambda}}}{2\hbar\epsilon_0}}\left[\mathbf{u}_{\boldsymbol{\lambda}}(\mathbf{x}_\mu)\hat{b}_{\boldsymbol{\lambda}}(t) - \mathbf{u}^{*}_{\boldsymbol{\lambda}}(\mathbf{x}_\mu)\hat{b}^{\dagger}_{\boldsymbol{\lambda}}(t)\right]\mathbf{d}_{21}\hat{d}_\mu(t)\,, \quad (5.59)$$

$$\frac{\partial}{\partial t}\,\hat{a}^{\dagger}_{2\mu}(t)\hat{a}^{\dagger}_{1\mu}(t) = i\Omega_{21}\hat{a}^{\dagger}_{2\mu}(t)\hat{a}^{\dagger}_{1\mu}(t) + \sum_{\boldsymbol{\lambda}}\sqrt{\frac{\omega_{\boldsymbol{\lambda}}}{2\hbar\epsilon_0}}\left[\mathbf{u}_{\boldsymbol{\lambda}}(\mathbf{x}_\mu)\hat{b}_{\boldsymbol{\lambda}}(t) - \mathbf{u}^{*}_{\boldsymbol{\lambda}}(\mathbf{x}_\mu)\hat{b}^{\dagger}_{\boldsymbol{\lambda}}(t)\right]\mathbf{d}_{12}\hat{d}_\mu(t)\,. \quad (5.60)$$

Here we have introduced as a further abbreviation the atomic inversion operator

$$\hat{d}_\mu(t) = \hat{a}^{\dagger}_{2\mu}(t)\hat{a}_{2\mu}(t) - \hat{a}^{\dagger}_{1\mu}(t)\hat{a}_{1\mu}(t)\,. \quad (5.61)$$

Also the dynamics of both operator contributions in (5.61) follows from specializing (5.49). Taking into account the atomic polarization (5.57) yields

$$\begin{aligned}\frac{\partial}{\partial t}\,\hat{a}^{\dagger}_{2\mu}(t)\hat{a}_{2\mu}(t) &= \sum_{\boldsymbol{\lambda}}\sqrt{\frac{\omega_{\boldsymbol{\lambda}}}{2\hbar\epsilon_0}}\left[\mathbf{u}_{\boldsymbol{\lambda}}(\mathbf{x}_\mu)\hat{b}_{\boldsymbol{\lambda}}(t) - \mathbf{u}^{*}_{\boldsymbol{\lambda}}(\mathbf{x}_\mu)\hat{b}^{\dagger}_{\boldsymbol{\lambda}}(t)\right] \\ &\quad\times\left[\mathbf{d}_{12}\hat{a}^{\dagger}_{1\mu}(t)\hat{a}_{2\mu}(t) - \mathbf{d}_{21}\hat{a}^{\dagger}_{2\mu}(t)\hat{a}_{1\mu}(t)\right]\,, \quad (5.62)\\ \frac{\partial}{\partial t}\,\hat{a}^{\dagger}_{1\mu}(t)\hat{a}_{1\mu}(t) &= -\sum_{\boldsymbol{\lambda}}\sqrt{\frac{\omega_{\boldsymbol{\lambda}}}{2\hbar\epsilon_0}}\left[\mathbf{u}_{\boldsymbol{\lambda}}(\mathbf{x}_\mu)\hat{b}_{\boldsymbol{\lambda}}(t) - \mathbf{u}^{*}_{\boldsymbol{\lambda}}(\mathbf{x}_\mu)\hat{b}^{\dagger}_{\boldsymbol{\lambda}}(t)\right] \\ &\quad\times\left[\mathbf{d}_{21}\hat{a}^{\dagger}_{2\mu}(t)\hat{a}_{1\mu}(t) - \mathbf{d}_{12}\hat{a}^{\dagger}_{1\mu}(t)\hat{a}_{2\mu}(t)\right]\,. \quad (5.63)\end{aligned}$$

From (5.62) and (5.63) we deduce for the dynamics of the atomic inversion operator (5.61)

$$\frac{\partial}{\partial t}\,\hat{d}_\mu(t) = 2\sum_{\boldsymbol{\lambda}}\sqrt{\frac{\omega_{\boldsymbol{\lambda}}}{2\hbar\epsilon_0}}\left[\mathbf{u}_{\boldsymbol{\lambda}}(\mathbf{x}_\mu)\hat{b}_{\boldsymbol{\lambda}}(t) - \mathbf{u}^{*}_{\boldsymbol{\lambda}}(\mathbf{x}_\mu)\hat{b}^{\dagger}_{\boldsymbol{\lambda}}(t)\right]\left[\mathbf{d}_{12}\hat{a}^{\dagger}_{1\mu}(t)\hat{a}_{2\mu}(t) - \mathbf{d}_{21}\hat{a}^{\dagger}_{2\mu}(t)\hat{a}_{1\mu}(t)\right]. \quad (5.64)$$

Thus we have obtained a closed set of equations for the operators of the light field and the atoms in the Heisenberg picture.

5.6 Rotating Wave Approximation

Let us now investigate more carefully the dynamics of the involved operators. To this end we focus upon the case, where the interaction between light and matter vanishes, which formally corresponds to a vanishing electric dipole moment matrix element, i.e. $\mathbf{d}_{12} = \mathbf{0}$. The dynamics of the photon operators (5.58) is then determined according to

$$\hat{b}^{\dagger}_{\boldsymbol{\lambda}}(t) \sim e^{i\omega_{\boldsymbol{\lambda}}t}\,, \qquad \hat{b}_{\boldsymbol{\lambda}}(t) \sim e^{-i\omega_{\boldsymbol{\lambda}}t}\,, \quad (5.65)$$

both contributions of the atomic polarization operator (5.57) evolve in (5.62) and (5.63) via

$$\hat{a}^{\dagger}_{1\mu}(t)\hat{a}_{2\mu}(t) \sim e^{-i\Omega t}\,, \qquad \hat{a}^{\dagger}_{2\mu}(t)\hat{a}_{1\mu}(t) \sim e^{i\Omega t} \quad (5.66)$$

with the atomic transition frequency being defined in case of $E_2 > E_1$ as

$$\Omega = \frac{E_2 - E_1}{\hbar}\,, \tag{5.67}$$

and for the atomic inversion operator (5.61) we get from (5.62) and (5.63)

$$\hat{a}^\dagger_{1\mu}(t)\hat{a}_{1\mu}(t) \;\sim\; 1\,, \qquad \hat{a}^\dagger_{2\mu}(t)\hat{a}_{2\mu}(t) \sim 1\,, \qquad \hat{d}_\mu(t) \sim 1\,. \tag{5.68}$$

Thus, in the equation (5.52) for $\hat{b}^\dagger_{\boldsymbol{\lambda}}(t)$ the term $\hat{a}^\dagger_{2\mu}\hat{a}_{1\mu}(t)$ but not the term $\hat{a}^\dagger_{1\mu}\hat{a}_{2\mu}(t)$ has approximately the same time dependence as $\hat{b}^\dagger_{\boldsymbol{\lambda}}(t)$. Within the rotating wave approximation we can therefore neglect the term $\hat{a}^\dagger_{1\mu}\hat{a}_{2\mu}(t)$ and obtain from (5.41):

$$\frac{\partial}{\partial t}\,\hat{b}^\dagger_{\boldsymbol{\lambda}}(t) = i\omega_{\boldsymbol{\lambda}}\hat{b}^\dagger_{\boldsymbol{\lambda}}(t) + \sqrt{\frac{\omega_{\boldsymbol{\lambda}}}{2\hbar\epsilon_0}}\sum_{\boldsymbol{\lambda}} \mathbf{u}_{\boldsymbol{\lambda}}(\mathbf{x}_\mu)\mathbf{d}_{21}\hat{a}^\dagger_{2\mu}(t)\hat{a}_{1\mu}(t)\,. \tag{5.69}$$

Here we can define a coupling constant, which characterizes the strength of the dipole interaction between the $\boldsymbol{\lambda}$th resonator mode and the μ th atom:

$$g_{\boldsymbol{\lambda},\mu} = -i\sqrt{\frac{\omega_{\boldsymbol{\lambda}}}{2\hbar\epsilon_0}}\,\mathbf{u}_{\boldsymbol{\lambda}}(\mathbf{x}_\mu)\cdot\mathbf{d}_{21}\,. \tag{5.70}$$

Furthermore we introduce the atomic polarisation amplitude operator

$$\hat{\alpha}_\mu(t) = \hat{a}^\dagger_{1\mu}(t)\hat{a}_{2\mu}(t)\,. \tag{5.71}$$

With this the dynamics of the photonic creation operator (5.69) reads concisely

$$\frac{\partial}{\partial t}\,\hat{b}^\dagger_{\boldsymbol{\lambda}}(t) = i\omega_{\boldsymbol{\lambda}}\hat{b}^\dagger_{\boldsymbol{\lambda}}(t) + i\sum_\mu g_{\boldsymbol{\lambda},\mu}\hat{\alpha}^\dagger_\mu(t) \tag{5.72}$$

and, correspondingly, we get for the photonic annihilation operator

$$\frac{\partial}{\partial t}\,\hat{b}_{\boldsymbol{\lambda}}(t) = -i\omega_{\boldsymbol{\lambda}}\hat{b}_{\boldsymbol{\lambda}}(t) - i\sum_\mu g^*_{\boldsymbol{\lambda},\mu}\hat{\alpha}_\mu(t)\,. \tag{5.73}$$

Similarly, in the equation (5.59) for the atomic polarisation amplitude operator (5.71) the term $\hat{b}_{\boldsymbol{\lambda}}(t)$ but not the term $\hat{b}^\dagger_{\boldsymbol{\lambda}}(t)$ has approximately the same time dependence as $\hat{\alpha}_\mu(t)$. Within the rotating wave approximation we can thus neglect the term $\hat{b}^\dagger_{\boldsymbol{\lambda}}(t)$ and obtain from (5.59) by taking into account (5.70)

$$\frac{\partial}{\partial t}\,\hat{\alpha}_\mu(t) = -i\Omega\hat{\alpha}_\mu(t) + i\sum_{\boldsymbol{\lambda}} g_{\boldsymbol{\lambda},\mu}\hat{b}_{\boldsymbol{\lambda}}(t)\hat{d}_\mu(t)\,. \tag{5.74}$$

Correspondingly the evolution of the adjoint atomic polarisation amplitude operator $\hat{\alpha}^\dagger_\mu(t)$ follows from

$$\frac{\partial}{\partial t}\,\hat{\alpha}^\dagger_\mu(t) = i\Omega\hat{\alpha}_\mu(t) - i\sum_{\boldsymbol{\lambda}} g^*_{\boldsymbol{\lambda},\mu}\hat{b}^\dagger_{\boldsymbol{\lambda}}(t)\hat{d}_\mu(t)\,. \tag{5.75}$$

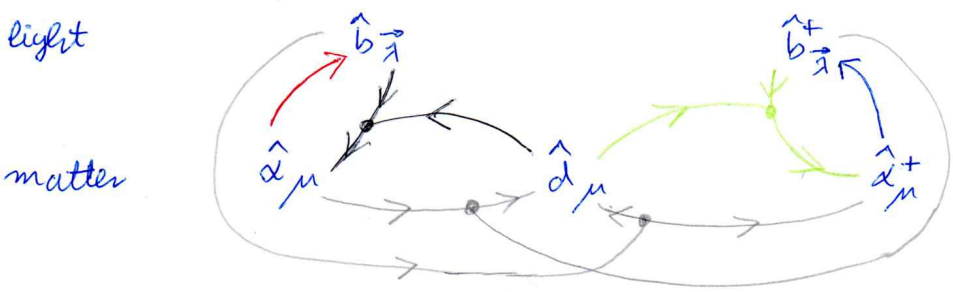

Figure 5.2: Closed system of differential equations for the operators of light and matter in the Heisenberg picture. Color coding: (5.72) in blue, (5.73) in red, (5.74) in black, (5.75) in green, and (5.76) in grey.

Finally, the equation (5.64) for the atomic inversion operator (5.61) consists of four terms, where only $\hat{b}_{\boldsymbol{\lambda}}(t)\hat{\alpha}^\dagger_\mu(t)$ and $\hat{b}^\dagger_{\boldsymbol{\lambda}}(t)\hat{\alpha}_\mu(t)$ have approximately the same time dependence as $\hat{d}_\mu(t)$. Thus, together with (5.70), we end up with

$$\frac{\partial}{\partial t}\,\hat{d}_\mu(t) = 2i\sum_{\boldsymbol{\lambda}}\left[g^*_{\boldsymbol{\lambda},\mu}\hat{b}^\dagger_{\boldsymbol{\lambda}}(t)\hat{\alpha}_\mu(t) - g_{\boldsymbol{\lambda},\mu}\hat{\alpha}^\dagger_\mu(t)\hat{b}_{\boldsymbol{\lambda}}(t)\right]. \tag{5.76}$$

We conclude that the rotating wave approximation led us to the last five equations, which represent a closed system of nonlinear differential equations determining the operators of both the light field and the atoms. Such a self-consistent interdependence between the relevant degrees of freedom as illustrated in Fig. 5.2 is exemplary for a *circular causality*, which is omnipresent in physics, natural sciences, and even beyond [52, Chapter 11]. In contrast to that one can characterize the working principle of mathematics with a linear causality as generically lemmas and theorems are directly proven on the basis of certain definitions and assumptions.

At this point the question arises whether those five equations constitute Heisenberg equations, which follow straight-forwardly from a corresponding Hamiltonian. To this end we have to express the original Hamiltonian of light and matter (5.37) in terms of the operators $\hat{b}_\lambda(t)$, $\hat{b}^\dagger_\lambda(t)$, $\hat{\alpha}_\mu(t)$, $\hat{\alpha}^\dagger_\mu(t)$, $\hat{d}_\mu(t)$ and apply the atomic two-level as well as the rotating wave approximation. Whereas the field Hamiltonian (5.8) has already the correct form, the electronic Hamiltonian (5.24) depends on the occupation number operators $\hat{a}^\dagger_{1\,\mu}(t)\hat{a}_{1\,\mu}(t)$ and $\hat{a}^\dagger_{2\,\mu}(t)\hat{a}_{2\,\mu}(t)$:

$$H_{\mathrm{el}} = \sum_\mu \left[E_1\hat{a}^\dagger_{1\,\mu}(t)\hat{a}_{1\,\mu}(t) + E_2\hat{a}^\dagger_{2\,\mu}(t)\hat{a}_{2\,\mu}(t)\right]. \tag{5.77}$$

Provided that each atomic two-level system μ describes just one electron, we conclude that the occupation number operators $\hat{a}^\dagger_{1\,\mu}(t)\hat{a}_{1\,\mu}(t)$ and $\hat{a}^\dagger_{2\,\mu}(t)\hat{a}_{2\,\mu}(t)$ fulfill the two equations (5.61) and

$$\hat{a}^\dagger_{2\,\mu}(t)\hat{a}_{2\,\mu}(t) + \hat{a}^\dagger_{1\,\mu}(t)\hat{a}_{1\,\mu}(t) = 1\,. \tag{5.78}$$

Thus, both occupation number operators can be expressed in terms of the respective atomic inversion operator (5.61) according to

$$\hat{a}^\dagger_{1\mu}(t)\hat{a}_{1\mu}(t) = \frac{1}{2}\left[1 - \hat{d}_\mu(t)\right], \qquad \hat{a}^\dagger_{2\mu}(t)\hat{a}_{2\mu}(t) = \frac{1}{2}\left[1 + \hat{d}_\mu(t)\right]. \tag{5.79}$$

With this the electronic Hamiltonian (5.77) reads due to (5.79)

$$\hat{H}_{\rm el} = \sum_{\mu} \left[\frac{E_1 + E_2}{2} + \frac{\hbar\Omega}{2}\, \hat{d}_\mu(t) \right] , \tag{5.80}$$

where the constant can be dropped in view of calculating the Heisenberg equations. Correspondingly, the atomic two-level approximation together with (5.50) and (5.51) reduces the interaction Hamiltonian (5.36) to

$$\hat{H}_{\rm int} = \sum_{\boldsymbol{\lambda}} \sum_{\mu} (-i) \sqrt{\frac{\hbar\omega_{\boldsymbol{\lambda}}}{2\epsilon_0}} \left[\mathbf{u}_{\boldsymbol{\lambda}}(\mathbf{x}_\mu) \hat{b}_{\boldsymbol{\lambda}}(t) - \mathbf{u}^*_{\boldsymbol{\lambda}}(\mathbf{x}_\mu) \hat{b}^\dagger_{\boldsymbol{\lambda}}(t) \right] \left[\mathbf{d}_{12} \hat{\alpha}_\mu(t) + \mathbf{d}_{21} \hat{\alpha}^\dagger_\mu(t) \right] . \tag{5.81}$$

Thus, the subsequent rotation-wave approximation eliminates the two non-resonant terms $\hat{b}_\lambda(t)\hat{\alpha}_\mu(t)$ and $\hat{b}^\dagger_\mu(t)\hat{\alpha}^\dagger_\mu(t)$:

$$\hat{H}_{\rm int} = \sum_{\boldsymbol{\lambda}} \sum_{\mu} (-i) \sqrt{\frac{\hbar\omega_{\boldsymbol{\lambda}}}{2\epsilon_0}} \left[\mathbf{u}_{\boldsymbol{\lambda}}(\mathbf{x}_\mu) \cdot \mathbf{d}_{21} \hat{b}_{\boldsymbol{\lambda}}(t) \hat{\alpha}^\dagger_\mu(t) - \mathbf{u}^*_{\boldsymbol{\lambda}}(\mathbf{x}_\mu) \cdot \mathbf{d}_{12} \hat{b}^\dagger_{\boldsymbol{\lambda}}(t) \hat{\alpha}_\mu(t) \right] . \tag{5.82}$$

Introducing the coupling constant (5.70) between the $\boldsymbol{\lambda}$th electromagnetic mode and the μth atom finally leads to

$$\hat{H}_{\rm int} = \sum_{\boldsymbol{\lambda}} \sum_{\mu} \left[\hbar g_{\boldsymbol{\lambda}\mu} \hat{b}_{\boldsymbol{\lambda}}(t) \hat{\alpha}^\dagger_\mu(t) + \hbar g^*_{\boldsymbol{\lambda}\mu} \hat{b}^\dagger_{\boldsymbol{\lambda}}(t) \hat{\alpha}_\mu(t) \right] . \tag{5.83}$$

Taking into account (5.8), (5.80), and (5.83) the resulting Hamiltonian of light and matter (5.37) reads

$$\hat{H} = \sum_{\boldsymbol{\lambda}} \hbar\omega_{\boldsymbol{\lambda}} \hat{b}^\dagger_{\boldsymbol{\lambda}}(t) \hat{b}_{\boldsymbol{\lambda}}(t) + \sum_{\mu} \frac{\hbar\Omega}{2}\, \hat{d}_\mu(t) + \sum_{\boldsymbol{\lambda}} \sum_{\mu} \left[\hbar g_{\boldsymbol{\lambda}\mu} \hat{b}_{\boldsymbol{\lambda}}(t) \hat{\alpha}^\dagger_\mu(t) + \hbar g^*_{\boldsymbol{\lambda}\mu} \hat{b}^\dagger_{\boldsymbol{\lambda}}(t) \hat{\alpha}_\mu(t) \right] . \tag{5.84}$$

Indeed, it turns out that the Heisenberg equations corresponding (5.84) lead to the closed set of differential equations (5.72)–(5.76). But to this end one has to take into account the respective equal-time commutation relations between the atomic operators $\hat{\alpha}_\mu(t)$, $\hat{\alpha}^\dagger_\mu(t)$, $\hat{d}_\mu(t)$, which follow from the fermionic anti-commutation relations (5.17) and the definitions (5.61) and (5.71):

$$\left[\hat{\alpha}_\mu(t), \hat{\alpha}_{\mu'}(t) \right]_- = 0 , \quad \left[\hat{\alpha}^\dagger_\mu(t), \hat{\alpha}^\dagger_{\mu'}(t) \right]_- = 0 , \quad \left[\hat{\alpha}^\dagger_\mu(t), \hat{\alpha}_{\mu'}(t) \right]_- = \delta_{\mu\mu'} \hat{d}_\mu(t) , \tag{5.85}$$

$$\left[\hat{\alpha}^\dagger_\mu(t), \hat{d}_{\mu'}(t) \right]_- = -2\delta_{\mu\mu'} \hat{\alpha}^\dagger_\mu(t) , \quad \left[\hat{\alpha}_\mu(t), \hat{d}_{\mu'}(t) \right]_- = 2\delta_{\mu\mu'} \hat{\alpha}_\mu(t) , \quad \left[\hat{d}_\mu(t), \hat{d}_{\mu'}(t) \right]_- = 0 . \tag{5.86}$$

5.7 Analogy with Jaynes-Cummings Interpretation

In case that each two-level atom just contains one electron, we conclude from applying the anti-commutation relation (5.23)

$$\hat{a}^\dagger_{\mathbf{i}\mu} \hat{a}_{\mathbf{j}\mu} \hat{a}^\dagger_{\mathbf{k}\mu} \hat{a}_{\mathbf{l}\mu} = \hat{a}^\dagger_{\mathbf{i}\mu} \left[\delta_{\mathbf{ik}} - \hat{a}^\dagger_{\mathbf{k}\mu} \hat{a}_{\mathbf{j}\mu} \right] \hat{a}_{\mathbf{l}\mu} = \delta_{\mathbf{ik}} \hat{a}^\dagger_{\mathbf{i}\mu} \hat{a}_{\mathbf{l}\mu} , \tag{5.87}$$

as the successive application of two creation or two annihilation operators at one atom μ has to vanish. Thus, for each two-level atom μ we have then the following additional anti-commutation relations between the atomic operators $\hat{\alpha}_\mu$, $\hat{\alpha}_\mu^\dagger$, $\hat{d}_\mu$ defined in (5.61) and (5.71):

$$\hat{\alpha}_\mu^2 = \hat{a}_{1\mu}^\dagger \hat{a}_{2\mu} \hat{a}_{1\mu}^\dagger \hat{a}_{2\mu} = \delta_{12} \hat{a}_{1\mu}^\dagger \hat{a}_{2\mu} = 0 \qquad \Longrightarrow \qquad \left[\hat{\alpha}_\mu, \hat{\alpha}_\mu\right]_+ = 0\,, \tag{5.88}$$

$$\hat{\alpha}_\mu^{\dagger\,2} = \hat{a}_{2\mu}^\dagger \hat{a}_{1\mu} \hat{a}_{2\mu}^\dagger \hat{a}_{1\mu} = \delta_{12} \hat{a}_{2\mu}^\dagger \hat{a}_{1\mu} = 0 \qquad \Longrightarrow \qquad \left[\hat{\alpha}_\mu^\dagger, \hat{\alpha}_\mu^\dagger\right]_+ = 0\,, \tag{5.89}$$

$$\left[\hat{\alpha}_\mu, \hat{\alpha}_\mu^\dagger\right]_+ = \hat{a}_{1\mu}^\dagger \hat{a}_{2\mu} \hat{a}_{2\mu}^\dagger \hat{a}_{1\mu} + \hat{a}_{2\mu}^\dagger \hat{a}_{1\mu} \hat{a}_{1\mu}^\dagger \hat{a}_{2\mu} = \hat{a}_{1\mu}^\dagger \hat{a}_{1\mu} + \hat{a}_{2\mu}^\dagger \hat{a}_{2\mu} = 1\,, \tag{5.90}$$

$$\begin{aligned}\left[\hat{\alpha}_\mu, \hat{d}_\mu\right]_+ &= \left[\hat{a}_{1\mu}^\dagger \hat{a}_{2\mu}, \hat{a}_{2\mu}^\dagger \hat{a}_{2\mu} - \hat{a}_{1\mu}^\dagger \hat{a}_{1\mu}\right]_+ = \hat{a}_{1\mu}^\dagger \hat{a}_{2\mu} \hat{a}_{2\mu}^\dagger \hat{a}_{2\mu} + \hat{a}_{1\mu}^\dagger \hat{a}_{2\mu} \hat{a}_{1\mu}^\dagger \hat{a}_{2\mu} \\ &\quad - \hat{a}_{1\mu}^\dagger \hat{a}_{2\mu} \hat{a}_{1\mu}^\dagger \hat{a}_{1\mu} - \hat{a}_{1\mu}^\dagger \hat{a}_{1\mu} \hat{a}_{1\mu}^\dagger \hat{a}_{1\mu} = \hat{a}_{1\mu}^\dagger \hat{a}_{2\mu} - \hat{a}_{1\mu}^\dagger \hat{a}_{2\mu} = 0\,,\end{aligned} \tag{5.91}$$

$$\begin{aligned}\left[\hat{\alpha}_\mu^\dagger, \hat{d}_\mu\right]_+ &= \left[\hat{a}_{2\mu}^\dagger \hat{a}_{1\mu}, \hat{a}_{2\mu}^\dagger \hat{a}_{2\mu} - \hat{a}_{1\mu}^\dagger \hat{a}_{1\mu}\right]_+ = \hat{a}_{2\mu}^\dagger \hat{a}_{1\mu} \hat{a}_{2\mu}^\dagger \hat{a}_{2\mu} + \hat{a}_{2\mu}^\dagger \hat{a}_{2\mu} \hat{a}_{2\mu}^\dagger \hat{a}_{1\mu} \\ &\quad - \hat{a}_{2\mu}^\dagger \hat{a}_{1\mu} \hat{a}_{1\mu}^\dagger \hat{a}_{1\mu} - \hat{a}_{1\mu}^\dagger \hat{a}_{1\mu} \hat{a}_{2\mu}^\dagger \hat{a}_{1\mu} = \hat{a}_{2\mu}^\dagger \hat{a}_{1\mu} - \hat{a}_{2\mu}^\dagger \hat{a}_{1\mu} = 0\,,\end{aligned} \tag{5.92}$$

as well as

$$\begin{aligned}\hat{d}_\mu^2 &= \left(\hat{a}_{2\mu}^\dagger \hat{a}_{2\mu} - \hat{a}_{1\mu}^\dagger \hat{a}_{1\mu}\right)\left(\hat{a}_{2\mu}^\dagger \hat{a}_{2\mu} - \hat{a}_{1\mu}^\dagger \hat{a}_{1\mu}\right) = \hat{a}_{2\mu}^\dagger \hat{a}_{2\mu} \hat{a}_{1\mu}^\dagger \hat{a}_{1\mu} + \hat{a}_{1\mu}^\dagger \hat{a}_{1\mu} \hat{a}_{1\mu}^\dagger \hat{a}_{1\mu} - \hat{a}_{1\mu}^\dagger \hat{a}_{1\mu} \hat{a}_{2\mu}^\dagger \hat{a}_{2\mu} \\ &\quad - \hat{a}_{2\mu}^\dagger \hat{a}_{2\mu} \hat{a}_{1\mu}^\dagger \hat{a}_{1\mu} = \hat{a}_{2\mu}^\dagger \hat{a}_{2\mu} + \hat{a}_{1\mu}^\dagger \hat{a}_{1\mu} = 1 \qquad \Longrightarrow \qquad \left[\hat{d}_\mu, \hat{d}_\mu\right]_+ = 2\,.\end{aligned} \tag{5.93}$$

All those commutator and anti-commutator relations (5.85), (5.86) and (5.87)–(5.93) imply that a single electron in a two-level system is formally equivalent to a single spin-1/2. Due to the above assumption $E_2 > E_1$ the indices 1 and 2 correspond to the ground and the excited state of the two-level system, which could be identified with the spin down and the spin up of the spin-1/2 system, respectively. This leads inevitably to the following identifications for the corresponding operators:

$$\sigma_{+\mu} = \sigma_{x\mu} + i\sigma_{y\mu} \qquad \Longleftrightarrow \qquad \hat{\alpha}_\mu^\dagger = \hat{a}_{2\mu}^\dagger \hat{a}_{1\mu}\,, \tag{5.94}$$

$$\sigma_{-\mu} = \sigma_{x\mu} - i\sigma_{y\mu} \qquad \Longleftrightarrow \qquad \hat{\alpha}_\mu = \hat{a}_{1\mu}^\dagger \hat{a}_{2\mu}\,, \tag{5.95}$$

$$\sigma_{z\mu} \qquad \Longleftrightarrow \qquad \hat{d}_\mu = \hat{a}_{2\mu}^\dagger \hat{a}_{2\mu} - \hat{a}_{1\mu}^\dagger \hat{a}_{1\mu}\,. \tag{5.96}$$

Indeed, the non-trivial commutators from (5.85), (5.86) go over into

$$\left[\sigma_{+\mu}, \sigma_{-\mu}\right]_- = \sigma_{z\mu}\,, \qquad \left[\sigma_{+\mu}, \sigma_{z\mu}\right]_- = -2\sigma_{+\mu}\,, \qquad \left[\sigma_{-\mu}, \sigma_{z\mu}\right]_- = 2\sigma_{-\mu}\,, \tag{5.97}$$

which is equivalent to the Lie algebra (4.207) of Pauli matrices. In the same way the anti-commutators (5.88)–(5.93) are converted to

$$\sigma_{+\mu}^2 = \sigma_{-\mu}^2 = 0\,, \quad \left[\sigma_{+\mu}, \sigma_{-\mu}\right]_+ = 1\,, \quad \left[\sigma_{+\mu}, \sigma_{z\mu}\right]_+ = \left[\sigma_{-\mu}, \sigma_{z\mu}\right]_+ = 0\,, \quad \sigma_{z\mu}^2 = 1\,, \tag{5.98}$$

which corresponds to the Clifford algebra (4.206) of Pauli matrices. Note that (5.97) and (5.98) could also directly be deduced from the corresponding matrix representation

$$\sigma_{+\mu} = \begin{pmatrix} 0 & 1 \\ 0 & 0 \end{pmatrix}_\mu\,, \qquad \sigma_{-\mu} = \begin{pmatrix} 0 & 0 \\ 1 & 0 \end{pmatrix}_\mu\,, \qquad \sigma_{z\mu} = \begin{pmatrix} 1 & 0 \\ 0 & -1 \end{pmatrix}_\mu\,. \tag{5.99}$$

Due to this formal equivalence the Hamiltonian for light and matter with rotated wave approximation (5.84) can also be cast in the form

$$\hat{H} = \sum_{\boldsymbol{\lambda}} \hbar\omega_{\boldsymbol{\lambda}} \hat{b}^\dagger_{\boldsymbol{\lambda}}(t)\hat{b}_{\boldsymbol{\lambda}}(t) + \sum_{\mu} \frac{\hbar\Omega}{2}\,\sigma_{z\mu}(t) + \sum_{\boldsymbol{\lambda}}\sum_{\mu} \left[\hbar g_{\boldsymbol{\lambda}\mu}\hat{b}_{\boldsymbol{\lambda}}(t)\sigma_{+\mu}(t) + \hbar g^*_{\boldsymbol{\lambda}\mu}\hat{b}^\dagger_{\boldsymbol{\lambda}}(t)\sigma_{-\mu}(t)\right] . \quad (5.100)$$

Thus, this Hamiltonian corresponds to a sum of Jaynes-Cummings Hamiltonians (4.308). Finally, for the sake of completeness, we also write down the closed set of Heisenberg equations of light and matter (5.72)–(5.76) in the spin 1/2 notation:

$$\frac{\partial}{\partial t}\,\hat{b}^\dagger_{\boldsymbol{\lambda}}(t) = i\omega_{\boldsymbol{\lambda}}\hat{b}^\dagger_{\boldsymbol{\lambda}}(t) + i\sum_{\mu} g_{\boldsymbol{\lambda}\mu}\sigma_{+\mu}(t)\,, \quad (5.101)$$

$$\frac{\partial}{\partial t}\,\hat{b}_{\boldsymbol{\lambda}}(t) = -i\omega_{\boldsymbol{\lambda}}\hat{b}_{\boldsymbol{\lambda}}(t) - i\sum_{\mu} g^*_{\boldsymbol{\lambda}\mu}\sigma_{-\mu}(t)\,, \quad (5.102)$$

$$\frac{\partial}{\partial t}\,\sigma_{-\mu}(t) = -i\Omega\sigma_{-\mu}(t) + i\sum_{\boldsymbol{\lambda}} g_{\boldsymbol{\lambda}\mu}\hat{b}_{\boldsymbol{\lambda}}(t)\sigma_{z\mu}(t)\,, \quad (5.103)$$

$$\frac{\partial}{\partial t}\,\sigma_{+\mu}(t) = i\Omega\sigma_{+\mu}(t) + i\sum_{\boldsymbol{\lambda}} g^*_{\boldsymbol{\lambda}\mu}\hat{b}_{\boldsymbol{\lambda}}(t)^\dagger\sigma_{z\mu}(t)\,, \quad (5.104)$$

$$\frac{\partial}{\partial t}\,\sigma_{z\mu}(t) = 2i\sum_{\boldsymbol{\lambda}} \left[g^*_{\boldsymbol{\lambda}\mu}\hat{b}^\dagger_{\boldsymbol{\lambda}}(t)\sigma_{-\mu}(t) - g_{\boldsymbol{\lambda}\mu}\hat{b}_{\boldsymbol{\lambda}}(t)\sigma_{+\mu}(t)\right] . \quad (5.105)$$

Chapter 6

Quantum Mechanical Equations of Light Field and Atoms with Baths

In the laser the cavity modes and the electrons in the atoms do not only interact with one another as described in Chapter 5, but also with their respective surroundings. For instance, the cavity field is coupled to mirrors and scattering centers, whereas the electrons are pumped or interact with lattice vibrations or suffer from atomic collisions leading to non-radiative atomic transitions All these external sources acting on the electromagnetic field and the electrons are called heat baths or reservoirs. In general, the heat baths are large systems compared to the subsystems of the laser. Therefore, one can assume that these heat baths are kept at their individual temperatures, which may differ from each other appreciably. For instance, the temperature of the pump source is much higher than that of the lattice vibrations. A heat bath has simultaneously two effects on the Heisenberg equations of the second quantized operators describing light and matter. On the one hand they lead to damping or pumping terms in the respective operator-valued equations of motion. However, such a damping or pumping alone would have the effect that the canonical equal-time commutator and anti-commutator relations between the second-quantized operators would decrease or increase with time. Therefore, a heat bath also has the second effect of giving rise to operator-valued stochastic forces, which are tuned in such a way that the canonical commutator or anti-commutator relations between the second-quantized operators are preserved during the dynamics upon a bath average. The aim of this chapter is now to derive those so-called quantum Langevin equations for the second-quantized operators of light and matter and to check those quantum mechanical consistency relations upon a bath average.

6.1 Heat Bath For Light Field

In principle, each cavity mode of the electromagnetic field is coupled to an individual heat bath. Therefore, we drop the cavity mode index $\boldsymbol{\lambda}$ for the time being and restrict the following

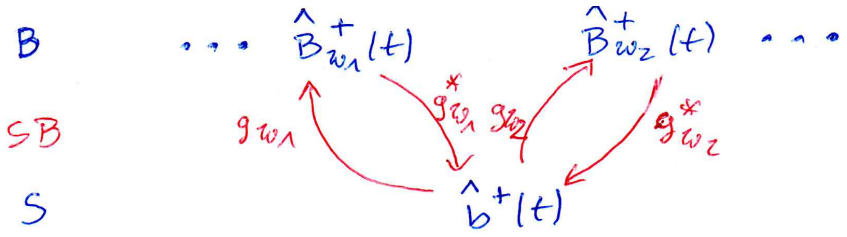

Figure 6.1: Illustration for the coupling of a photon operator to a bath of harmonic oscillators at frequencies ω, where the bilinear interaction is characterized by complex strengths g_ω.

consideration without loss of generality to a system which consists of one single cavity mode of frequency ω_0:

$$\hat{H}_{\rm S} = \hbar\omega_0 \hat{b}^\dagger(t)\hat{b}(t)\,. \tag{6.1}$$

The heat bath itself is modelled by an infinite number of harmonic oscillators

$$\hat{H}_{\rm B} = \sum_\omega \hbar\omega \hat{B}^\dagger_\omega(t)\hat{B}_\omega(t)\,, \tag{6.2}$$

where the bath operators $\hat{B}^\dagger_\omega$, $\hat{B}_\omega$ fulfill the usual equal-time bosonic commutator relations:

$$\left[\hat{B}_\omega(t), \hat{B}_{\omega'}(t)\right]_- = \left[\hat{B}^\dagger_\omega(t), \hat{B}^\dagger_{\omega'}(t)\right]_- = 0\,, \qquad \left[\hat{B}_\omega(t), \hat{B}^\dagger_{\omega'}(t)\right]_- = \delta_{\omega\,\omega'}\,. \tag{6.3}$$

The interaction between the system and the bath is now assumed to be bilinear in the system and the bath operators:

$$\hat{H}_{\rm SB} = \hat{b}^\dagger(t)\sum_\omega \hbar g_\omega \hat{B}_\omega(t) + \sum_\omega \hbar g^*_\omega \hat{B}^\dagger_\omega(t)\hat{b}(t)\,. \tag{6.4}$$

Thus, the annihilation (creation) of a bath quantum of energy $\hbar\omega$ occurs simultaneously with the creation (annihilation) of a photon of energy $\hbar\omega_0$ and g_ω denotes the corresponding complex-valued interaction strength at frequency ω. This system-bath model is illustrated in Fig. 6.1 and is described by the total Hamiltonian

$$\hat{H} = \hat{H}_{\rm S} + \hat{H}_{\rm B} + \hat{H}_{\rm SB} \tag{6.5}$$

determining the Heisenberg equation of any operator. On the one hand the evolution equation for the light field operator turns out to be

$$\frac{\partial}{\partial t}\hat{b}^\dagger(t) = \frac{i}{\hbar}\left[\hat{H}, \hat{b}^\dagger(t)\right]_- = i\omega_0 \hat{b}^\dagger(t) + i\sum_\omega g^*_\omega \hat{B}^\dagger_\omega(t) \tag{6.6}$$

and the dynamics of the bath operators follows from

$$\frac{\partial}{\partial t}\hat{B}^\dagger_\omega(t) = \frac{i}{\hbar}\left[\hat{H}, \hat{B}^\dagger_\omega(t)\right]_- = i\omega \hat{B}^\dagger_\omega(t) + ig_\omega \hat{b}^\dagger(t)\,. \tag{6.7}$$

The latter represents an inhomogeneous linear differential equation of first order determining $\hat{B}^\dagger_\omega(t)$, which can be solved with standard procedures as follows. At first, the homogeneous differential equation is solved with

$$\hat{B}^\dagger_{\omega,\mathrm{hom}}(t) = \hat{B}^\dagger_\omega(t_0) e^{i\omega(t-t_0)} \,. \tag{6.8}$$

Then a particular solution is obtained with the method of varying constants

$$\hat{B}^\dagger_{\omega,\mathrm{part}}(t) = \hat{C}(t) e^{i\omega(t-t_0)} \,. \tag{6.9}$$

Inserting the ansatz (6.9) in the inhomogeneous differential equation (6.7) yields a differential equation for the function $\hat{C}(t)$:

$$\frac{\partial \hat{C}(t)}{\partial t} = i g_\omega \hat{b}^\dagger(t) e^{-i\omega(t-t_0)} \,, \tag{6.10}$$

which can straight-forwardly be integrated

$$\hat{C}(t) = i g_\omega \int_{t_0}^{t} d\tau \, \hat{b}^\dagger(\tau) e^{-i\omega(\tau-t_0)} \,. \tag{6.11}$$

Adding now homogeneous and particular solution (6.8) and (6.9) with (6.11) yields the general solution for the dynamics of the bath operators:

$$\hat{B}^\dagger_\omega(t) = \hat{B}^\dagger_\omega(t_0) e^{i\omega(t-t_0)} + i g_\omega \int_{t_0}^{t} d\tau \, \hat{b}^\dagger(\tau) e^{i\omega(t-\tau)} \,. \tag{6.12}$$

Inserting this general solution for $\hat{B}^\dagger_\omega(t)$ into the evolution equation (6.6) for the photon creation operator $\hat{b}^\dagger(t)$ yields

$$\frac{\partial}{\partial t} \hat{b}^\dagger(t) = i\omega_0 \hat{b}^\dagger(t) + \hat{F}^\dagger(t) + \hat{\Gamma}^\dagger(t) \,. \tag{6.13}$$

The term from which the damping will emerge reads

$$\hat{F}^\dagger(t) = -\sum_\omega |g_\omega|^2 \int_{t_0}^{t} d\tau \, \hat{b}^\dagger(\tau) e^{i\omega(t-\tau)} \,. \tag{6.14}$$

Now we allow for both positive and negative frequencies and perform the limit of having a continuum of bath degrees of freedom, so that the sum over the frequencies leads to an integral. Furthermore, we assume that the constant g_ω, which describes the coupling between the system operator $\hat{b}^\dagger$ and the bath operator $\hat{B}^\dagger_\omega$, does not depend on the frequency ω, see Fig. 6.2. With this we get

$$\hat{F}^\dagger(t) = -|g|^2 \int_{t_0}^{t} d\tau \, \hat{b}^\dagger(\tau) \int_{-\infty}^{\infty} d\omega \, e^{i\omega(t-\tau)} \tag{6.15}$$

and the frequency integral yields a delta function

$$\hat{F}^\dagger(t) = -2\pi |g|^2 \int_{t_0}^{t} d\tau \, \hat{b}^\dagger(\tau) \delta(t-\tau) \,. \tag{6.16}$$

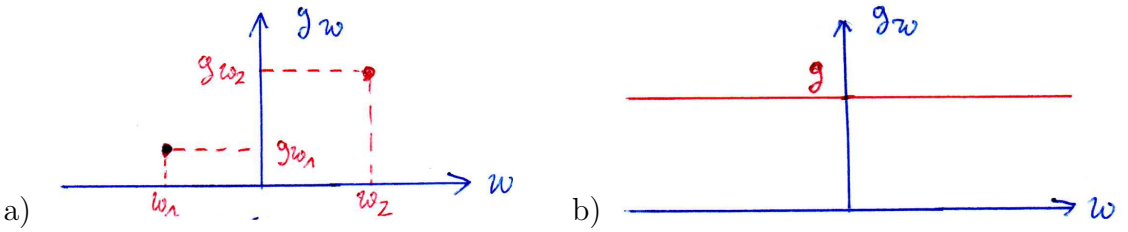

Figure 6.2: Strength of interaction g_ω between photon operator and bath operators at different frequencies ω: a) Discrete and b) continuum case.

For the evaluation of the integral it must be noted that the delta function has the property

$$\int_0^t d\tau\, \delta(t-\tau) = \frac{1}{2}\,. \tag{6.17}$$

Thus, finally we yield the damping term

$$\hat{F}^\dagger(t) = -\kappa \hat{b}^\dagger(t) \tag{6.18}$$

with the damping constant

$$\kappa = \pi\,|g|^2\,. \tag{6.19}$$

This damping describes photon losses, which are due to semi-transparent cavity mirrors or an interaction with scattering centers. Correspondingly the last term in the evolution equation (6.13) for $\hat{b}^\dagger(t)$ reads

$$\hat{\Gamma}^\dagger(t) = i\sum_\omega g_\omega^* \hat{B}_\omega^\dagger(t_0) e^{i\omega(t-t_0)}\,. \tag{6.20}$$

This represents an operator-valued fluctuating force. The reason is that the effect of the operator $\hat{B}_\omega^\dagger(t_0)$ at the initial time t_0 is not known precisely. If we assume that the heat bath is initially at equilibrium with some temperature T, it is described by the thermal density matrix

$$\hat{\rho}_{\rm B} = \frac{1}{Z_{\rm B}}\, e^{-\beta \hat{H}_{\rm B}} \tag{6.21}$$

with the bath Hamiltonian (6.2) and the partition function

$$Z_{\rm B} = {\rm Tr}_{\rm B}\, e^{-\beta \hat{H}_{\rm B}}\,. \tag{6.22}$$

Any thermal average over the heat bath is then defined by

$$\langle \bullet \rangle_{\rm B} = {\rm Tr}_{\rm B}\,(\hat{\rho}_{\rm B}\,\bullet)\,. \tag{6.23}$$

With this we obtain immediately from (6.20)–(6.23) that the heat bath average over the fluctuating field operator vanishes

$$\langle \hat{\Gamma}^\dagger(t)\rangle_{\rm B} = 0\,, \qquad \langle \hat{\Gamma}(t)\rangle_{\rm B} = 0 \tag{6.24}$$

due to the property

$$\langle \hat{B}^\dagger_\omega(t_0)\rangle_{\rm B} = 0\,, \qquad \langle \hat{B}_\omega(t_0)\rangle_{\rm B} = 0\,. \tag{6.25}$$

Correspondingly the correlation functions of the fluctuating field operators yield

$$\langle \hat{\Gamma}^\dagger(t)\hat{\Gamma}(t')\rangle_{\rm B} = \sum_\omega |g_\omega|^2\, e^{i\omega(t-t')}\overline{n}_\omega(T)\,, \tag{6.26}$$

$$\langle \hat{\Gamma}(t)\hat{\Gamma}^\dagger(t')\rangle_{\rm B} = \sum_\omega |g_\omega|^2\, e^{-i\omega(t-t')}\left[1+\overline{n}_\omega(T)\right]\,, \tag{6.27}$$

which is independent of the initial time t_0 due to the property

$$\langle \hat{B}^\dagger_\omega(t_0)\hat{B}_{\omega'}(t_0)\rangle_{\rm B} = \delta_{\omega,\omega'}\overline{n}_\omega(T)\,, \tag{6.28}$$

$$\langle \hat{B}_\omega(t_0)\hat{B}^\dagger_{\omega'}(t_0)\rangle_{\rm B} = \delta_{\omega,\omega'}\left[1+\overline{n}_\omega(T)\right]\,. \tag{6.29}$$

Here $\overline{n}_\omega(T)$ denotes the occupation number of the bath mode corresponding to the frequency ω of the heat bath at temperature T. Also in (6.26) and (6.27) we allow the coupling constant to the bath g_ω to be independent on the frequency ω, so that performing the limit of having a continuum of bath degrees of freedom converts the sums over the frequencies to integrals:

$$\langle \hat{\Gamma}^\dagger(t)\hat{\Gamma}(t')\rangle_{\rm B} = |g|^2\int_{-\infty}^{\infty} d\omega\, e^{i\omega(t-t')}\overline{n}_\omega(T)\,, \tag{6.30}$$

$$\langle \hat{\Gamma}(t)\hat{\Gamma}^\dagger(t')\rangle_{\rm B} = |g|^2\int_{-\infty}^{\infty} d\omega\, e^{-i\omega(t-t')}\left[1+\overline{n}_\omega(T)\right]\,. \tag{6.31}$$

As the thermal occupation $\overline{n}_\omega(T)$ of the bath mode is supposed to vary slowly around the frequency ω_0 of the photonic harmonic oscillator, it can be approximated by $\overline{n}_{\omega_0}(T)$, so by taking into account the damping constant (6.19) we get:

$$\langle \hat{\Gamma}^\dagger(t)\hat{\Gamma}(t')\rangle_{\rm B} = 2\kappa\overline{n}_{\omega_0}(T)\delta(t-t')\,, \tag{6.32}$$

$$\langle \hat{\Gamma}(t)\hat{\Gamma}^\dagger(t')\rangle_{\rm B} = 2\kappa\left[1+\overline{n}_{\omega_0}(T)\right]\delta(t-t')\,. \tag{6.33}$$

We read off from the delta function in time that the heat bath has a very short memory, which is called a *Markov property*. As the Fourier transform in time would lead to a constant in frequency space, such a noise is called to be *white*. Furthermore, the strength of both correlations (6.32) and (6.33) are proportional to the damping constant κ and is, thus, intimately connected with the dissipation. This represents an illustrative example of the seminal *fluctuation-dissipation theorem* that the strength of fluctuations is determined by the strength of the dissipation. In view of later purposes, we also obtain from (6.32), (6.33) for the bath average over the commutator of the operator-valued fluctuating force

$$\left\langle \left[\hat{\Gamma}(t),\hat{\Gamma}^\dagger(t')\right]_- \right\rangle_{\rm B} = 2\kappa\delta(t-t')\,. \tag{6.34}$$

Now we show explicitly how the fluctuating field operators restore quantum mechanical consistency. To this end we solve the evolution equation (6.13) for $\hat{b}^\dagger(t)$, which reduces due to (6.18) to

$$\frac{\partial}{\partial t}\,\hat{b}^\dagger(t) = (i\omega_0-\kappa)\,\hat{b}^\dagger(t) + \hat{\Gamma}^\dagger(t)\,, \tag{6.35}$$

and obtain

$$\hat{b}^\dagger(t) = \hat{b}^\dagger(0) e^{(i\omega_0 - \kappa)t} + \int_0^t d\tau\, \hat{\Gamma}^\dagger(\tau) e^{(i\omega_0-\kappa)(t-\tau)}\,. \tag{6.36}$$

Correspondingly the dynamics of $\hat{b}(t)$ is given by

$$\hat{b}(t) = \hat{b}(0) e^{(-i\omega_0 - \kappa)t} + \int_0^t d\tau\, \hat{\Gamma}(\tau) e^{(-i\omega_0-\kappa)(t-\tau)}\,. \tag{6.37}$$

With this we can calculate how the equal-time commutator of $\hat{b}(t)$ and $\hat{b}^\dagger(t)$ changes with time. Within the heat bath average we find due to (6.24)

$$\begin{aligned} \left\langle \left[\hat{b}(t), \hat{b}^\dagger(t)\right]_- \right\rangle_{\rm B} &= \left[\hat{b}(0), \hat{b}^\dagger(0)\right]_- e^{-2\kappa t} \\ &\quad + \int_0^t d\tau \int_0^t d\tau' \left\langle \left[\hat{\Gamma}(\tau), \hat{\Gamma}^\dagger(\tau')\right]_- \right\rangle_{\rm B} e^{(i\omega_0-\kappa)(t-\tau')} e^{(-i\omega_0-\kappa)(t-\tau)}\,. \end{aligned} \tag{6.38}$$

With the initial canonical bosonic commutator

$$\left[\hat{b}(0), \hat{b}^\dagger(0)\right]_- = 1 \tag{6.39}$$

and the heat bath average of the commutator of fluctuating field operators (6.34) this reduces to

$$\left\langle \left[\hat{b}(t), \hat{b}^\dagger(t)\right]_- \right\rangle_{\rm B} = e^{-2\kappa t} + 2\kappa e^{-2\kappa t} \int_0^t d\tau\, e^{2\kappa\tau}\,. \tag{6.40}$$

Evaluating the remaining elementary integral

$$\int_0^t d\tau\, e^{2\kappa\tau} = \frac{e^{2\kappa t} - 1}{2\kappa} \tag{6.41}$$

we obtain the intriguing result that the equal-time commutator relation is preserved with respect to the heat bath average for all times:

$$\left\langle \left[\hat{b}(t), \hat{b}^\dagger(t)\right]_- \right\rangle_{\rm B} = 1\,. \tag{6.42}$$

In a similar way we can also determine from (6.36) and (6.37) the heat bath average of the photon number operator:

$$\langle \hat{b}^\dagger(t)\hat{b}(t)\rangle_{\rm B} = \hat{b}^\dagger(0)\hat{b}(0) e^{-2\kappa t} + \int_0^t d\tau \int_0^t d\tau'\, \langle \hat{\Gamma}^\dagger(\tau)\hat{\Gamma}(\tau')\rangle_{\rm B}\, e^{(i\omega_0-\kappa)(t-\tau')} e^{(-i\omega-\kappa)(t-\tau)}\,. \tag{6.43}$$

Due to the above correlation function of the fluctuating field operators (6.32) this reduces to

$$\langle \hat{b}^\dagger(t)\hat{b}(t)\rangle_{\rm B} = \hat{b}^\dagger(0)\hat{b}(0) e^{-2\kappa t} + 2\kappa \overline{n}_{\omega_0}(T) e^{-2\kappa t} \int_0^t d\tau\, e^{2\kappa\tau}\,. \tag{6.44}$$

Taking into account the elementary integral (6.41) this finally yields for the time evolution of the heat bath average of the photon number operator

$$\langle \hat{b}^\dagger(t)\hat{b}(t)\rangle_{\mathrm{B}} = \overline{n}_{\omega_0}(T) + \left[\hat{b}^\dagger(0)\hat{b}(0) - \overline{n}_{\omega_0}(T)\right] e^{-2\kappa t}\,. \tag{6.45}$$

Thus, this heat bath average evolves exponentially starting from the operator-valued initial value

$$\lim_{t\to 0} \langle \hat{b}^\dagger(t)\hat{b}(t)\rangle_{\mathrm{B}} = \hat{b}^\dagger(0)\hat{b}(0) \tag{6.46}$$

to its long-time limit

$$\lim_{t\to \infty} \langle \hat{b}^\dagger(t)\hat{b}(t)\rangle_{\mathrm{B}} = \overline{n}_{\omega_0}(T)\,, \tag{6.47}$$

which is just a c-number and corresponds to the occupation number of the bath mode corresponding to the cavity mode frequency ω_0 of the heat bath at temperature T. Furthermore, we observe from (6.46) together with (6.24), (6.36), and (6.37)

$$\langle \hat{b}^\dagger(t)\hat{b}(t)\rangle_{\mathrm{B}} - \langle \hat{b}^\dagger(t)\rangle_{\mathrm{B}} \langle \hat{b}(t)\rangle_{\mathrm{B}} = \overline{n}_{\omega_0}(T)\left(1 - e^{-2\kappa t}\right)\,. \tag{6.48}$$

Thus, the variance of the photon number operator with respect to the heat bath average increases monotonously from the initial value zero to the the occupation number $\overline{n}_{\omega_0}(T)$ of the bath mode.

6.2 Heat Bath For Electron Field: Deterministic Part

In an analogous way we now treat also the heat bath for the electron field. As the respective atoms are assumed to be distinguishable, we restrict ourselves to the heat bath of one single atom, so we can drop the atom index μ. The starting point is again a total Hamiltonian $\hat{H}$ of the form (6.5). But this time the system Hamiltonian consists of non-interacting electrons with dispersion $E_{\mathbf{i}}$:

$$\hat{H}_{\mathrm{S}} = \sum_{\mathbf{i}} E_{\mathbf{i}} \hat{a}^\dagger_{\mathbf{i}} \hat{a}_{\mathbf{i}}\,. \tag{6.49}$$

Each operator $\hat{a}^\dagger_{\mathbf{i}}\hat{a}_{\mathbf{j}}$ of the electron field is coupled to its own bath operator $\hat{B}_{\mathbf{ij}\omega}$ according to

$$\hat{H}_{\mathrm{SB}} = \sum_{\mathbf{i},\mathbf{j}} \hat{a}^\dagger_{\mathbf{i}}\hat{a}_{\mathbf{j}}\hbar \sum_{\omega} g_{\mathbf{ij}\omega}\hat{B}_{\mathbf{ij}\omega} + \sum_{\mathbf{i},\mathbf{j}} \hbar \sum_{\omega} g^*_{\mathbf{ij}\omega}\hat{B}^\dagger_{\mathbf{ij}\omega}\hat{a}^\dagger_{\mathbf{j}}\hat{a}_{\mathbf{i}}\,, \tag{6.50}$$

where $g_{\mathbf{ij}\omega}$ denotes the respective coupling strength. And the bath Hamiltonian is again modelled by harmonic oscillators

$$\hat{H}_{\mathrm{B}} = \sum_{\mathbf{i},\mathbf{j}} \sum_{\omega} \hbar\omega \hat{B}^\dagger_{\mathbf{ij}\omega}\hat{B}_{\mathbf{ij}\omega}\,. \tag{6.51}$$

Note that also the bath operators $\hat{B}^\dagger_{\mathbf{ij}\omega}$, $\hat{B}_{\mathbf{ij}\omega}$ for the operators $\hat{a}^\dagger_{\mathbf{i}}\hat{a}_{\mathbf{j}}$ of the electron field fulfill the usual equal-time bosonic commutator relations:

$$\left[\hat{B}_{\mathbf{ij}\omega}(t),\hat{B}_{\mathbf{i'j'}\omega'}(t)\right]_- = \left[\hat{B}^\dagger_{\mathbf{ij}\omega}(t),\hat{B}^\dagger_{\mathbf{i'j'}\omega'}(t)\right]_- = 0\,, \quad \left[\hat{B}_{\mathbf{ij}\omega}(t),\hat{B}^\dagger_{\mathbf{i'j'}\omega'}(t)\right]_- = \delta_{\mathbf{i},\mathbf{i'}}\delta_{\mathbf{j},\mathbf{j'}}\delta_{\omega\,\omega'}\,. \tag{6.52}$$

At first we determine the Heisenberg equations for the operators $\hat{a}^\dagger_{\mathbf{i}}\hat{a}_{\mathbf{j}}$:

$$\begin{aligned}\frac{\partial}{\partial t}\,\hat{a}^\dagger_{\mathbf{i}}\hat{a}_{\mathbf{j}} &= \frac{i}{\hbar}\left[\hat{H},\hat{a}^\dagger_{\mathbf{i}}\hat{a}_{\mathbf{j}}\right]_- = \frac{i}{\hbar}\sum_{\mathbf{i'}} E_{\mathbf{i'}}\left[\hat{a}^\dagger_{\mathbf{i'}}\hat{a}_{\mathbf{i'}},\hat{a}^\dagger_{\mathbf{i}}\hat{a}_{\mathbf{j}}\right]_- \\ &+\frac{i}{\hbar}\sum_{\mathbf{i'},\mathbf{j'}}\left[\hat{a}^\dagger_{\mathbf{i'}}\hat{a}_{\mathbf{j'}},\hat{a}^\dagger_{\mathbf{i}}\hat{a}_{\mathbf{j}}\right]_-\hbar\sum_\omega g_{\mathbf{i'j'}\omega}\hat{B}_{\mathbf{i'j'}\omega} + \frac{i}{\hbar}\sum_{\mathbf{i'},\mathbf{j'}}\hbar\sum_\omega g^*_{\mathbf{i'j'}\omega}\hat{B}^\dagger_{\mathbf{i'j'}\omega}\left[\hat{a}^\dagger_{\mathbf{j'}}\hat{a}_{\mathbf{i'}},\hat{a}^\dagger_{\mathbf{i}}\hat{a}_{\mathbf{j}}\right]_-\,.\end{aligned} \tag{6.53}$$

Applying the above derived commutator relation (5.46) yields together with the atomic transition frequencies (5.48)

$$\begin{aligned}\frac{\partial}{\partial t}\,\hat{a}^\dagger_{\mathbf{i}}\hat{a}_{\mathbf{j}} &= i\Omega_{\mathbf{ij}}\hat{a}^\dagger_{\mathbf{i}}\hat{a}_{\mathbf{j}} + i\sum_{\mathbf{i'}}\hat{a}^\dagger_{\mathbf{i'}}\hat{a}_{\mathbf{j}}\sum_\omega g_{\mathbf{i'i}\omega}\hat{B}_{\mathbf{i'i}\omega} - i\sum_{\mathbf{j'}}\hat{a}^\dagger_{\mathbf{i}}\hat{a}_{\mathbf{j'}}\sum_\omega g_{\mathbf{jj'}\omega}\hat{B}_{\mathbf{jj'}\omega} \\ &+i\sum_{\mathbf{j'}}\sum_\omega g^*_{\mathbf{ij'}\omega}\hat{B}^\dagger_{\mathbf{ij'}\omega}\hat{a}^\dagger_{\mathbf{j'}}\hat{a}_{\mathbf{j}} - i\sum_{\mathbf{i'}}\sum_\omega g^*_{\mathbf{i'}j\omega}\hat{B}^\dagger_{\mathbf{i'}j\omega}\hat{a}^\dagger_{\mathbf{i}}\hat{a}_{\mathbf{i'}}\,.\end{aligned} \tag{6.54}$$

And the Heisenberg equations for the bath operators yield

$$\frac{\partial}{\partial t}\,\hat{B}^\dagger_{\mathbf{ij}\omega} = \frac{i}{\hbar}\left[\hat{H},\hat{B}^\dagger_{\mathbf{ij}\omega}\right]_- = i\omega\hat{B}^\dagger_{\mathbf{ij}\omega} + ig_{\mathbf{ij}\omega}\hat{a}^\dagger_{\mathbf{i}}\hat{a}_{\mathbf{j}}\,. \tag{6.55}$$

The solution of this inhomogeneous linear differential equation of first order reads

$$\hat{B}^\dagger_{\mathbf{ij}\omega}(t) = \hat{B}^\dagger_{\mathbf{ij}\omega}(t_0)e^{i\omega(t-t_0)} + ig_{\mathbf{ij}\omega}\int_{t_0}^t d\tau\,\hat{a}^\dagger_{\mathbf{i}}(\tau)\hat{a}_{\mathbf{j}}(\tau)e^{i\omega(t-\tau)} \tag{6.56}$$

with the correspondingly adjoint dynamics

$$\hat{B}_{\mathbf{ij}\omega}(t) = \hat{B}_{\mathbf{ij}\omega}(t_0)e^{-i\omega(t-t_0)} - ig^*_{\mathbf{ij}\omega}\int_{t_0}^t d\tau\,\hat{a}^\dagger_{\mathbf{j}}(\tau)\hat{a}_{\mathbf{i}}(\tau)e^{-i\omega(t-\tau)}\,. \tag{6.57}$$

Inserting the dynamics of the bath operators (6.56) and (6.57) back into the Heisenberg equations for the electron field (6.54) yields

$$\begin{aligned}\frac{\partial}{\partial t}\,\hat{a}^\dagger_{\mathbf{i}}(t)\hat{a}_{\mathbf{j}}(t) &= i\Omega_{\mathbf{ij}}\hat{a}^\dagger_{\mathbf{i}}(t)\hat{a}_{\mathbf{j}}(t) + i\sum_{\mathbf{i'}}\hat{a}^\dagger_{\mathbf{i'}}(t)\hat{a}_{\mathbf{j}}(t)\sum_\omega g_{\mathbf{i'}i\omega}(-i)g^*_{\mathbf{i'}i\omega}\int_{t_0}^t d\tau\,\hat{a}^\dagger_{\mathbf{i}}(\tau)\hat{a}_{\mathbf{i'}}(\tau)e^{-i\omega(t-\tau)} \\ &-i\sum_{\mathbf{i'}}\hat{a}^\dagger_{\mathbf{i}}\hat{a}_{\mathbf{i'}}\sum_\omega g_{\mathbf{ji'}\omega}(-i)g^*_{\mathbf{ji'}\omega}\int_{t_0}^t d\tau\,\hat{a}^\dagger_{\mathbf{i'}}(\tau)\hat{a}_{\mathbf{j}}(\tau)e^{-i\omega(t-\tau)} \\ &+i\sum_{\mathbf{i'}}\sum_\omega g^*_{\mathbf{ii'}\omega}ig_{\mathbf{ii'}\omega}\int_{t_0}^t d\tau\,\hat{a}^\dagger_{\mathbf{i}}(\tau)\hat{a}_{\mathbf{i'}}(\tau)e^{i\omega(t-\tau)}\hat{a}^\dagger_{\mathbf{i'}}(t)\hat{a}_{\mathbf{j}}(t) \\ &-i\sum_{\mathbf{i'}}\sum_\omega g^*_{\mathbf{i'}j\omega}ig_{\mathbf{i'}j\omega}\int_{t_0}^t d\tau\,\hat{a}^\dagger_{\mathbf{i'}}(\tau)\hat{a}_{\mathbf{j}}(\tau)e^{i\omega(t-\tau)}\hat{a}^\dagger_{\mathbf{i}}(t)\hat{a}_{\mathbf{i'}}(t) + \hat{\Gamma}_{\mathbf{ij}}(t)\,.\end{aligned} \tag{6.58}$$

Here the fluctuating field operators read

$$\hat{\Gamma}_{\mathbf{ij}}(t) = i\sum_{\mathbf{i}'} \hat{a}^\dagger_{\mathbf{i}'}(t)\hat{a}_{\mathbf{j}}(t)\sum_{\omega} g_{\mathbf{i}'\mathbf{i}\omega}\hat{B}_{\mathbf{i}'\mathbf{i}\omega}(t_0)e^{-i\omega(t-t_0)} - i\sum_{\mathbf{i}'} \hat{a}^\dagger_{\mathbf{i}}(t)\hat{a}_{\mathbf{i}'}(t)\sum_{\omega} g_{\mathbf{j}\mathbf{i}'\omega}\hat{B}_{\mathbf{j}\mathbf{i}'\omega}(t_0)e^{-i\omega(t-t_0)}$$
$$+i\sum_{\mathbf{i}'}\sum_{\omega} g^*_{\mathbf{i}\mathbf{i}'\omega}\hat{B}^\dagger_{\mathbf{i}\mathbf{i}'\omega}(t_0)e^{i\omega(t-t_0)}\hat{a}^\dagger_{\mathbf{i}'}(t)\hat{a}_{\mathbf{j}}(t) - i\sum_{\mathbf{i}'}\sum_{\omega} g^*_{\mathbf{i}'\mathbf{j}\omega}\hat{B}^\dagger_{\mathbf{i}'\mathbf{j}\omega}(t_0)e^{i\omega(t-t_0)}\hat{a}^\dagger_{\mathbf{i}}(t)\hat{a}_{\mathbf{i}'}(t)\,. \tag{6.59}$$

The discussion of their correlations is relegated to the subsequent section. Here we focus on identifying the respective deterministic terms in the Heisenberg equations (6.58) of the electronic operators. To this end we assume for the electron field bath that the coupling strengths $g_{\mathbf{ij}\omega}$ do not depend on the frequency ω and perform the limit of continuously many bath degrees of freedom similar to the photon bath case illustrated in Fig. 6.2. The resulting frequency integral leads to a delta function in time, which can be directly evaluated. With this the Heisenberg equations (6.58) reduce to

$$\frac{\partial}{\partial t}\,\hat{a}^\dagger_{\mathbf{i}}\hat{a}_{\mathbf{j}} = i\Omega_{\mathbf{ij}}\hat{a}^\dagger_{\mathbf{i}}\hat{a}_{\mathbf{j}} + \frac{1}{2}\sum_{\mathbf{i}'}\Big[\left(\gamma_{\mathbf{i}'\mathbf{i}}+\gamma_{\mathbf{i}'\mathbf{j}}\right)\hat{a}^\dagger_{\mathbf{i}'}\hat{a}_{\mathbf{j}}\hat{a}^\dagger_{\mathbf{i}}\hat{a}_{\mathbf{i}'} - \left(\gamma_{\mathbf{j}\mathbf{i}'}+\gamma_{\mathbf{i}\mathbf{i}'}\right)\hat{a}^\dagger_{\mathbf{i}}\hat{a}_{\mathbf{i}'}\hat{a}^\dagger_{\mathbf{i}'}\hat{a}_{\mathbf{j}}\Big] + \hat{\Gamma}_{\mathbf{ij}}\,, \tag{6.60}$$

where we have introduced the damping constants

$$\gamma_{\mathbf{ij}} = 2\pi\left|g_{\mathbf{ij}}\right|^2\,. \tag{6.61}$$

As we restrict ourselves to the description of one electron, the product of four electronic operators is further simplified according to (5.87). The evolution equation (4.138) thus simplifies to

$$\frac{\partial}{\partial t}\,\hat{a}^\dagger_{\mathbf{i}}\hat{a}_{\mathbf{j}} = i\Omega_{\mathbf{ij}}\hat{a}^\dagger_{\mathbf{i}}\hat{a}_{\mathbf{j}} + \frac{1}{2}\sum_{\mathbf{i}'}\Big[\left(\gamma_{\mathbf{i}'\mathbf{i}}+\gamma_{\mathbf{i}'\mathbf{j}}\right)\delta_{\mathbf{ij}}\hat{a}^\dagger_{\mathbf{i}'}\hat{a}_{\mathbf{i}'} - \left(\gamma_{\mathbf{j}\mathbf{i}'}+\gamma_{\mathbf{i}\mathbf{i}'}\right)\hat{a}^\dagger_{\mathbf{i}}\hat{a}_{\mathbf{j}}\Big] + \hat{\Gamma}_{\mathbf{ij}}\,. \tag{6.62}$$

We distinguish now two cases where the quantum numbers $\mathbf{i}$ and $\mathbf{j}$ are different and coincide, respectively:

$$\mathbf{i}\neq\mathbf{j}: \qquad \frac{\partial}{\partial t}\,\hat{a}^\dagger_{\mathbf{i}}\hat{a}_{\mathbf{j}} = \left(i\Omega_{\mathbf{ij}} - \sum_{\mathbf{i}'}\frac{\gamma_{\mathbf{j}\mathbf{i}'}+\gamma_{\mathbf{i}\mathbf{i}'}}{2}\right)\hat{a}^\dagger_{\mathbf{i}}\hat{a}_{\mathbf{j}} + \hat{\Gamma}_{\mathbf{ij}}\,, \tag{6.63}$$

$$\mathbf{i}=\mathbf{j}: \qquad \frac{\partial}{\partial t}\,\hat{a}^\dagger_{\mathbf{i}}\hat{a}_{\mathbf{i}} = \sum_{\mathbf{i}'}\gamma_{\mathbf{i}'\mathbf{i}}\hat{a}^\dagger_{\mathbf{i}'}\hat{a}_{\mathbf{i}'} - \sum_{\mathbf{i}'}\gamma_{\mathbf{i}\mathbf{i}'}\hat{a}^\dagger_{\mathbf{i}}\hat{a}_{\mathbf{i}} + \hat{\Gamma}_{\mathbf{ii}}\,. \tag{6.64}$$

Now we approximate each atom by a two-level system, so the indices $\mathbf{i}$, $\mathbf{j}$ can only assume the values 1 and 2. In case of identifying $\mathbf{i}$, $\mathbf{j}$ with 1, 2 and 2, 1, respectively, we obtain from (6.63) the dynamics of the atomic polarisation amplitude operator (5.71):

$$\frac{\partial}{\partial t}\,\hat{\alpha} = \left(-i\Omega-\gamma_\perp\right)\hat{\alpha} + \hat{\Gamma}_\alpha \tag{6.65}$$

and its adjoint

$$\frac{\partial}{\partial t}\,\hat{\alpha}^\dagger = \left(i\Omega-\gamma_\perp\right)\hat{\alpha}^\dagger + \hat{\Gamma}^\dagger_\alpha\,, \tag{6.66}$$

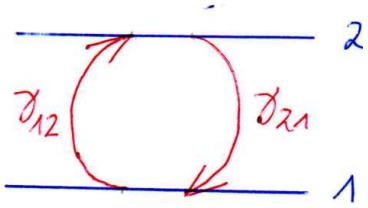

Figure 6.3: Schematic illustration of gains and losses for the occupations of both atomic levels: Rates γ_{12} and γ_{21} describe pumping processes and non-radiative atomic transitions, respectively.

which have the fluctuating operator

$$\hat{\Gamma}_\alpha = \hat{\Gamma}_{12}\,, \tag{6.67}$$
$$\hat{\Gamma}^\dagger_\alpha = \hat{\Gamma}^\dagger_{12}\,. \tag{6.68}$$

Here the transversal relaxation parameter

$$\gamma_\perp = \frac{1}{2}\left(\gamma_{11} + \gamma_{12} + \gamma_{21} + \gamma_{22}\right) \tag{6.69}$$

characterizes the line width of the frequency Ω in the two-level atom, which is caused by the decay of atomic dipole moments. Correspondingly, in case of identifying **i**=**j** with 1 and 2 leads in (6.64) to the dynamics of the population of the respective levels:

$$\frac{\partial}{\partial t}\,\hat{a}^\dagger_1\hat{a}_1 = \gamma_{21}\hat{a}^\dagger_2\hat{a}_2 - \gamma_{12}\hat{a}^\dagger_1\hat{a}_1 + \hat{\Gamma}_{11}\,, \tag{6.70}$$
$$\frac{\partial}{\partial t}\,\hat{a}^\dagger_2\hat{a}_2 = -\gamma_{21}\hat{a}^\dagger_2\hat{a}_2 + \gamma_{12}\hat{a}^\dagger_1\hat{a}_1 + \hat{\Gamma}_{22}\,. \tag{6.71}$$

The deterministic part describes gains and losses for the respective occupations as sketched in Fig. 6.3. The rate γ_{12} quantifies the pumping process, which can either be achieved with a separate light source or, as in case of the He-Ne laser, by a scattering of the two-level systems of Ne atoms with excited He atoms. The rate γ_{21} describes non-radiative atomic transitions which are due to interactions of the laser-active atom with the solid-state matrix. Thus, the resulting dynamics for the atomic population inversion operator (5.61) yields

$$\frac{\partial}{\partial t}\,\hat{d} = (\gamma_{12} - \gamma_{21}) - (\gamma_{12} + \gamma_{21})\,\hat{d} + \hat{\Gamma}_d\,, \tag{6.72}$$

with the fluctuating operator

$$\hat{\Gamma}_d = \hat{\Gamma}_{22} - \hat{\Gamma}_{11}\,. \tag{6.73}$$

Introducing the unsaturated population inversion

$$d_0 = \frac{\gamma_{12} - \gamma_{21}}{\gamma_{12} + \gamma_{21}} \tag{6.74}$$

and the longitudinal relaxation parameter

$$\gamma_{\parallel} = \gamma_{12} + \gamma_{21} \tag{6.75}$$

the dynamics of the population inversion operator (6.72) is finally of the form

$$\frac{\partial}{\partial t}\,\hat{d} = \gamma_{\parallel}\left(d_0 - \hat{d}\right) + \hat{\Gamma}_d\,. \tag{6.76}$$

Note that d_0 represents the population inversion in equilibrium, which adjusts itself in the absence of any interaction with the light field under the mutual impact of pumping and incoherent decay processes described by γ_{12} and γ_{21}, respectively, see Fig. 6.3. And $\gamma_{\parallel}$ denotes the relaxation time for the population inversion to reach equilibrium.

6.3 Heat Bath for Electron Field: Stochastic Part

In this section we determine the correlation functions of the fluctuating field operators for the electron field. To this end we assume that also the bath operators $\hat{B}_{\mathbf{ij}\omega}(t_0), \hat{B}^{\dagger}_{\mathbf{ij}\omega}(t_0)$ at the initial time t_0 are distributed according to the equilibrium density matrix (6.21) with the bath Hamiltonian (6.51). Thus, the thermal average (6.23) of the bath operators vanishes:

$$\langle \hat{B}_{\mathbf{ij}\omega}\rangle_{\mathrm{B}} = 0\,, \qquad \langle \hat{B}^{\dagger}_{\mathbf{ij}\omega}\rangle_{\mathrm{B}} = 0\,. \tag{6.77}$$

So far, the bath of the electron field has the same properties as the bath of the photon field. But the first essential difference is now that the energies of the bath operators of the electron field are supposed to be much larger than the photon field and the room temperature. Therefore, we conclude that the bath modes are approximately not occupied:

$$\langle \hat{B}^{\dagger}_{\mathbf{ij}\omega}(t_0)\hat{B}_{\mathbf{i'j'}\omega'}(t_0)\rangle_{\mathrm{B}} = \delta_{\mathbf{ii'}}\delta_{\mathbf{jj'}}\delta_{\omega\omega'}\overline{n}_{\mathbf{ij}\omega}(T) \approx 0\,. \tag{6.78}$$

In view of the calculation of the correlation functions of the fluctuating field operators for the electron field this has the consequence that only terms contribute which contain an expression of the form

$$\langle \hat{B}_{\mathbf{ij}\omega}(t_0)\hat{B}^{\dagger}_{\mathbf{i'j'}\omega'}(t_0)\rangle_{\mathrm{B}} = \delta_{\mathbf{ii'}}\delta_{\mathbf{jj'}}\delta_{\omega\omega'}\left[1 + \overline{n}_{\mathbf{ij}\omega}(T)\right] \approx \delta_{\mathbf{ii}}\delta_{\mathbf{jj'}}\delta_{\omega\omega'}\,. \tag{6.79}$$

But there is also a second qualitative difference between the bath of the electron field and the photon field. In case of the photon field the fluctuating field operators describe an *additive noise*. This means that $\hat{\Gamma}(t)$, $\hat{\Gamma}^{\dagger}(t)$ do not depend on the photon operators $\hat{b}(t)$, $\hat{b}^{\dagger}(t)$ as can be seen from (6.20) and its adjoint. In contrast to that the fluctuating field operators of the electron field describe multiplicative noise as $\hat{\Gamma}_{\mathbf{ij}}(t)$ depends explicitly on the electronic operators $\hat{a}^{\dagger}_{\mathbf{i}}(t), \hat{a}_{\mathbf{j}}(t)$ according to (6.59). This makes the evaluation for the fluctuating field operators more complicated for the case of the electronic field. But we use a time scale argument in order to determine the correlation functions at least approximately. Whereas the fluctuations

of the bath operators occur on a very short time scale, the response of the electronic degree of freedom is quite slow. This suggests to factorize the bath average as follows:

$$\langle \text{electron operators} \cdot \text{bath operators} \rangle_{\mathrm{B}} \approx \langle \text{electron operators} \rangle_{\mathrm{B}} \cdot \langle \text{bath operators} \rangle_{\mathrm{B}} \,. \quad (6.80)$$

Taking into account (6.59) and (6.77) we conclude from (6.80) that the bath average of the fluctuating field operators vanishes

$$\langle \hat{\Gamma}_{\mathbf{ij}}(t) \rangle_{\mathrm{B}} = 0 \,. \quad (6.81)$$

Subsequently we calculate the correlation function of the fluctuating field operators:

$$\langle \hat{\Gamma}_{\mathbf{ij}}(t) \hat{\Gamma}_{\mathbf{i'j'}}(t') \rangle_{\mathrm{B}} \quad (6.82)$$

Inserting therein (6.59) we obtain in total 16 terms from which only four terms survive due to (6.78). Applying for each of them the factorization approximation (6.80), this yields

$$\begin{aligned}
&\sum_{\mathbf{kk'}} \sum_{\omega\omega'} \Big[\langle \hat{a}^\dagger_{\mathbf{k}}(t) \hat{a}_{\mathbf{j}}(t) \hat{a}^\dagger_{\mathbf{i'}}(t') \hat{a}_{\mathbf{j'}}(t') \rangle_{\mathrm{B}} \, g_{\mathbf{ki}\omega} g^*_{\mathbf{k'j'}\omega'} \, \langle \hat{B}_{\mathbf{ki}\omega}(t_0) \hat{B}^\dagger_{\mathbf{k'j'}\omega'}(t_0) \rangle_{\mathrm{B}} \, e^{-i\omega(t-t_0)} e^{i\omega'(t'-t_0)} \\
&+ \langle \hat{a}^\dagger_{\mathbf{i}}(t) \hat{a}_{\mathbf{k}}(t) \hat{a}^\dagger_{\mathbf{k'}}(t') \hat{a}_{\mathbf{j'}}(t') \rangle_{\mathrm{B}} \, g_{\mathbf{jk}\omega} g^*_{\mathbf{i'k'}\omega'} \, \langle \hat{B}_{\mathbf{jk}\omega}(t_0) \hat{B}^\dagger_{\mathbf{i'k'}\omega'}(t_0) \rangle_{\mathrm{B}} \, e^{-i\omega(t-t_0)} e^{i\omega'(t'-t_0)} \\
&- \langle \hat{a}^\dagger_{\mathbf{k}}(t) \hat{a}_{\mathbf{j}}(t) \hat{a}^\dagger_{\mathbf{k'}}(t') \hat{a}_{\mathbf{j'}}(t') \rangle_{\mathrm{B}} \, g_{\mathbf{ki}\omega} g^*_{\mathbf{i'k'}\omega'} \, \langle \hat{B}_{\mathbf{ki}\omega}(t_0) \hat{B}^\dagger_{\mathbf{i'k'}\omega'}(t_0) \rangle_{\mathrm{B}} \, e^{-i\omega(t-t_0)} e^{i\omega'(t'-t_0)} \\
&- \langle \hat{a}^\dagger_{\mathbf{i}}(t) \hat{a}_{\mathbf{k}}(t) \hat{a}^\dagger_{\mathbf{i'}}(t') \hat{a}_{\mathbf{k'}}(t') \rangle_{\mathrm{B}} \, g_{\mathbf{jk}\omega} g^*_{\mathbf{k'j'}\omega'} \, \langle \hat{B}_{\mathbf{jk}\omega}(t_0) \hat{B}^\dagger_{\mathbf{k'j'}\omega'}(t_0) \rangle_{\mathrm{B}} \, e^{-i\omega(t-t_0)} e^{i\omega'(t'-t_0)} \Big] \,. \quad (6.83)
\end{aligned}$$

Inserting the thermal average for the bath operators (6.79) reduces the correlation function (6.83) to

$$\begin{aligned}
&\sum_{\mathbf{k}} \sum_{\omega} \Big[\langle \hat{a}^\dagger_{\mathbf{k}}(t) \hat{a}_{\mathbf{j}}(t) \hat{a}^\dagger_{\mathbf{i'}}(t') \hat{a}_{\mathbf{k}}(t') \rangle_{\mathrm{B}} \, \delta_{\mathbf{ij'}} \, |g_{\mathbf{ki}\omega}|^2 + \langle \hat{a}^\dagger_{\mathbf{i}}(t) \hat{a}_{\mathbf{k}}(t) \hat{a}^\dagger_{\mathbf{k}}(t') \hat{a}_{\mathbf{j'}}(t') \rangle_{\mathrm{B}} \, \delta_{\mathbf{i'j}} \, |g_{\mathbf{jk}\omega}|^2 \Big] \, e^{-i\omega(t-t')} \\
&- \sum_{\omega} \Big[\langle \hat{a}^\dagger_{\mathbf{i'}}(t) \hat{a}_{\mathbf{j}}(t) \hat{a}^\dagger_{\mathbf{i}}(t') \hat{a}_{\mathbf{j'}}(t') \rangle_{\mathrm{B}} \, |g_{\mathbf{i'i}\omega}|^2 + \langle \hat{a}^\dagger_{\mathbf{i}}(t) \hat{a}_{\mathbf{j'}}(t) \hat{a}^\dagger_{\mathbf{i'}}(t') \hat{a}_{\mathbf{j}}(t') \rangle_{\mathrm{B}} \, \left| g_{\mathbf{jj'}\omega} \right|^2 \Big] \, e^{-i\omega(t-t')} \,. \quad (6.84)
\end{aligned}$$

Assuming as usual that the coupling strengths $g_{\mathbf{ij}\omega}$ do not depend on ω and allowing positive as well as negative frequencies yields in the thermodynamic limit that the correlation functions are proportional to the delta function:

$$\langle \hat{\Gamma}_{\mathbf{ij}}(t) \hat{\Gamma}_{\mathbf{i'j'}}(t') \rangle_{\mathrm{B}} = \hat{\Gamma}_{\mathbf{iji'j'}} \delta(t-t') \,. \quad (6.85)$$

Thus, the fluctuating field operators of the electron field do not have any memory, which is called the Markov property. With the definition (6.61) of the electronic damping constants we obtain for the operator-valued weight in (6.85):

$$\begin{aligned}
\hat{\Gamma}_{\mathbf{iji'j'}} \;=\; & \sum_{\mathbf{k}} \Big[\gamma_{\mathbf{ki}} \delta_{\mathbf{ij'}} \, \langle \hat{a}^\dagger_{\mathbf{k}} \hat{a}_{\mathbf{j}} \hat{a}^\dagger_{\mathbf{i'}} \hat{a}_{\mathbf{k}} \rangle_{\mathrm{B}} + \gamma_{\mathbf{jk}} \delta_{\mathbf{i'j}} \, \langle \hat{a}^\dagger_{\mathbf{i}} \hat{a}_{\mathbf{k}} \hat{a}^\dagger_{\mathbf{k}} \hat{a}_{\mathbf{j'}} \rangle_{\mathrm{B}} \Big] \\
& - \gamma_{\mathbf{i'i}} \, \langle \hat{a}^\dagger_{\mathbf{i'}} \hat{a}_{\mathbf{j}} \hat{a}^\dagger_{\mathbf{i}} \hat{a}_{\mathbf{j'}} \rangle_{\mathrm{B}} - \gamma_{\mathbf{jj'}} \, \langle \hat{a}^\dagger_{\mathbf{i}} \hat{a}_{\mathbf{j'}} \hat{a}^\dagger_{\mathbf{i'}} \hat{a}_{\mathbf{j}} \rangle_{\mathrm{B}} \,. \quad (6.86)
\end{aligned}$$

Provided that the electronic operators just describe one electron, the product of four operators reduce to two operators according to (5.87), which simplifies (6.86) to

$$\hat{\Gamma}_{\mathbf{iji'j'}} = \sum_{\mathbf{k}} \left(\gamma_{\mathbf{ki}} \delta_{\mathbf{ij'}} \langle \hat{a}^\dagger_{\mathbf{k}} \hat{a}_{\mathbf{k}} \rangle_{\mathrm{B}} + \gamma_{\mathbf{jk}} \langle \hat{a}^\dagger_{\mathbf{i}} \hat{a}_{\mathbf{j'}} \rangle_{\mathrm{B}} \right) \delta_{\mathbf{i'j}} - \gamma_{\mathbf{i'i}} \delta_{\mathbf{ij}} \langle \hat{a}^\dagger_{\mathbf{i'}} \hat{a}_{\mathbf{j'}} \rangle_{\mathrm{B}} - \gamma_{\mathbf{jj'}} \delta_{\mathbf{i'j'}} \langle \hat{a}^\dagger_{\mathbf{i}} \hat{a}_{\mathbf{j}} \rangle_{\mathrm{B}} \,. \tag{6.87}$$

Special cases of (6.87) read

$$\hat{\Gamma}_{\mathbf{iii'i'}} = \sum_{\mathbf{k}} \left(\gamma_{\mathbf{ki}} \langle \hat{a}^\dagger_{\mathbf{k}} \hat{a}_{\mathbf{k}} \rangle_{\mathrm{B}} + \gamma_{\mathbf{ik}} \langle \hat{a}^\dagger_{\mathbf{i}} \hat{a}_{\mathbf{i'}} \rangle_{\mathrm{B}} \right) \delta_{\mathbf{ii'}} - \gamma_{\mathbf{i'i}} \langle \hat{a}^\dagger_{\mathbf{i'}} \hat{a}_{\mathbf{i'}} \rangle_{B} - \gamma_{\mathbf{ii'}} \langle \hat{a}^\dagger_{\mathbf{i}} \hat{a}_{\mathbf{i}} \rangle_{\mathrm{B}} \,, \tag{6.88}$$

$$\hat{\Gamma}_{\mathbf{ii'ii'}} = 0\,, \qquad \mathbf{i} \neq \mathbf{i'}\,, \tag{6.89}$$

$$\hat{\Gamma}_{\mathbf{ii'i'i}} = \sum_{\mathbf{k}} \left(\gamma_{\mathbf{ki}} \langle \hat{a}^\dagger_{\mathbf{k}} \hat{a}_{\mathbf{k}} \rangle_{\mathrm{B}} + \gamma_{\mathbf{i'k}} \langle \hat{a}^\dagger_{\mathbf{i}} \hat{a}_{\mathbf{i}} \rangle_{\mathrm{B}} \right) \,, \qquad \mathbf{i} \neq \mathbf{i'}\,. \tag{6.90}$$

Note that (6.88)–(6.90) coincide with [8, (IV.5.29)–(IV.5.31)]. Now we implement the two-level approximation, so that the indices $\mathbf{i}$, $\mathbf{i'}$ can only assume the values 1 and 2. With this we read off on the one hand from (6.88)

$$\hat{\Gamma}_{1111} = \hat{\Gamma}_{2222} = \gamma_{21} \langle \hat{a}^\dagger_2 \hat{a}_2 \rangle_{\mathrm{B}} + \gamma_{12} \langle \hat{a}^\dagger_1 \hat{a}_1 \rangle_{\mathrm{B}} = -\hat{\Gamma}_{1122} = -\hat{\Gamma}_{2211}\,. \tag{6.91}$$

Thus, we conclude for the correlation amplitude of the fluctuation operator of the population inversion operator (6.73) due to (6.85)

$$\langle \hat{\Gamma}_d(t) \hat{\Gamma}_d(t') \rangle_{\mathrm{B}} = \left(\hat{\Gamma}_{2222} + \hat{\Gamma}_{1111} - \hat{\Gamma}_{1122} - \hat{\Gamma}_{2211} \right) \delta(t - t') \tag{6.92}$$

with the amplitude following from (6.91):

$$\hat{\Gamma}_{2222} + \hat{\Gamma}_{1111} - \hat{\Gamma}_{1122} - \hat{\Gamma}_{2211} = 4 \left(\gamma_{21} \langle \hat{a}^\dagger_2 \hat{a}_2 \rangle_{\mathrm{B}} + \gamma_{12} \langle \hat{a}^\dagger_1 \hat{a}_1 \rangle_{\mathrm{B}} \right) \,. \tag{6.93}$$

Provided that each atomic two-level system describes just one electron both occupation number operators $\hat{a}^\dagger_1 \hat{a}_1$, $\hat{a}^\dagger_2 \hat{a}_2$ can be expressed in terms of the respective atomic inversion operator $\hat{d}$ according to (5.79). Taking into account the longitudinal relaxation parameter (6.75) and the unsaturated population inversion (6.74) we get for the amplitude (6.93)

$$\hat{\Gamma}_{2222} + \hat{\Gamma}_{1111} - \hat{\Gamma}_{1122} - \hat{\Gamma}_{2211} = 2\gamma_{\parallel} \left(1 - d_0 \langle \hat{d} \rangle_{\mathrm{B}} \right) \,. \tag{6.94}$$

On the other hand we obtain for the correlation of the fluctuation operator of the atomic polarisation amplitude operator (6.67), (6.68) from (6.90)

$$\langle \hat{\Gamma}_\alpha(t) \hat{\Gamma}^\dagger_\alpha(t') \rangle_{\mathrm{B}} = \hat{\Gamma}_{1221} \delta(t - t')\,, \tag{6.95}$$

$$\langle \hat{\Gamma}^\dagger_\alpha(t) \hat{\Gamma}_\alpha(t') \rangle_{\mathrm{B}} = \hat{\Gamma}_{2112} \delta(t - t')\,, \tag{6.96}$$

where the respective amplitudes are given by

$$\hat{\Gamma}_{1221} = \gamma_{11} \langle \hat{a}^\dagger_1 \hat{a}_1 \rangle_{\mathrm{B}} + \gamma_{21} \langle \hat{a}^\dagger_2 \hat{a}_2 \rangle_{\mathrm{B}} + \gamma_{21} \langle \hat{a}^\dagger_1 \hat{a}_1 \rangle_{\mathrm{B}} + \gamma_{22} \langle \hat{a}^\dagger_1 \hat{a}_1 \rangle_{\mathrm{B}} \,, \tag{6.97}$$

$$\hat{\Gamma}_{2112} = \gamma_{12} \langle \hat{a}^\dagger_1 \hat{a}_1 \rangle_{\mathrm{B}} + \gamma_{22} \langle \hat{a}^\dagger_2 \hat{a}_2 \rangle_{\mathrm{B}} + \gamma_{11} \langle \hat{a}^\dagger_2 \hat{a}_2 \rangle_{\mathrm{B}} + \gamma_{12} \langle \hat{a}^\dagger_2 \hat{a}_2 \rangle_{\mathrm{B}} \,. \tag{6.98}$$

Introducing again the atomic inversion operator $\hat{d}$ according to (5.79) and using (6.69), (6.74), and (6.75) yields

$$\hat{\Gamma}_{1221} = \gamma_\perp \left(1 - \langle \hat{d} \rangle_{\rm B}\right) - \frac{\gamma_\parallel}{2} \left(d_0 - \langle \hat{d} \rangle_{\rm B}\right) , \tag{6.99}$$

$$\hat{\Gamma}_{2112} = \gamma_\perp \left(1 + \langle \hat{d} \rangle_{\rm B}\right) + \frac{\gamma_\parallel}{2} \left(d_0 - \langle \hat{d} \rangle_{\rm B}\right) . \tag{6.100}$$

In addition we read off from (6.87)

$$\hat{\Gamma}_{1211} = -\gamma_{21} \langle \hat{a}_1^\dagger \hat{a}_2 \rangle_{\rm B} = -\hat{\Gamma}_{1222} , \qquad \hat{\Gamma}_{2111} = \gamma_{12} \langle \hat{a}_2^\dagger \hat{a}_1 \rangle_{\rm B} = -\hat{\Gamma}_{2122} . \tag{6.101}$$

From the definitions (6.75), (6.74) we straight-forwardly obtain the relations

$$\left.\begin{aligned} \gamma_\parallel d_0 &= \gamma_{12} - \gamma_{21} \\ \gamma_\parallel &= \gamma_{12} + \gamma_{21} \end{aligned}\right\} \qquad \Longleftrightarrow \qquad \begin{cases} \gamma_{12} = \gamma_\parallel \left(1 + d_0\right)/2 \\ \gamma_{21} = \gamma_\parallel \left(1 - d_0\right)/2 \end{cases} , \tag{6.102}$$

which thus yields due to (6.67), (6.68, and (6.73) the correlations

$$\langle \hat{\Gamma}_\alpha(t) \hat{\Gamma}_d(t') \rangle_{\rm B} = \left(\hat{\Gamma}_{1222} - \hat{\Gamma}_{1211}\right) \delta(t - t') , \tag{6.103}$$

$$\langle \hat{\Gamma}_\alpha^\dagger(t) \hat{\Gamma}_d(t') \rangle_{\rm B} = \left(\hat{\Gamma}_{2122} - \hat{\Gamma}_{2111}\right) \delta(t - t') \tag{6.104}$$

with the amplitudes

$$\hat{\Gamma}_{1222} - \hat{\Gamma}_{1211} = 2\gamma_{21} \langle \hat{a}_1^\dagger \hat{a}_1 \rangle_{\rm B} = \gamma_\parallel \left(1 - d_0\right) \langle \hat{\alpha} \rangle_{\rm B} , \tag{6.105}$$

$$\hat{\Gamma}_{2122} - \hat{\Gamma}_{2111} = -2\gamma_{12} \langle \hat{a}_1^\dagger \hat{a}_1 \rangle_{\rm B} = -\gamma_\parallel \left(1 + d_0\right) \langle \hat{\alpha}^\dagger \rangle_{\rm B} . \tag{6.106}$$

Correspondingly we also read off

$$\hat{\Gamma}_{1112} = \gamma_{12} \langle \hat{a}_1^\dagger \hat{a}_2 \rangle_B = -\hat{\Gamma}_{2212} , \qquad \hat{\Gamma}_{1121} = -\gamma_{21} \langle \hat{a}_2^\dagger \hat{a}_1 \rangle_B = -\hat{\Gamma}_{2221} , \tag{6.107}$$

so we also deduce the correlations

$$\langle \hat{\Gamma}_d(t) \hat{\Gamma}_\alpha(t') \rangle_{\rm B} = \left(\hat{\Gamma}_{2212} - \hat{\Gamma}_{1112}\right) \delta(t - t') , \tag{6.108}$$

$$\langle \hat{\Gamma}_d(t) \hat{\Gamma}_\alpha^\dagger(t') \rangle_{\rm B} = \left(\hat{\Gamma}_{2221} - \hat{\Gamma}_{1121}\right) \delta(t - t') . \tag{6.109}$$

with the amplitudes

$$\hat{\Gamma}_{2212} - \hat{\Gamma}_{1112} = -\gamma_\parallel \left(1 + d_0\right) \langle \hat{\alpha} \rangle_{\rm B} , \tag{6.110}$$

$$\hat{\Gamma}_{2221} - \hat{\Gamma}_{1121} = \gamma_\parallel \left(1 - d_0\right) \langle \hat{\alpha}^\dagger \rangle_{\rm B} . \tag{6.111}$$

Thus, the correlation functions obey the symmetry relations

$$\langle \hat{\Gamma}_d(t) \hat{\Gamma}_\alpha(t') \rangle_{\rm B} = \left\langle \left[\hat{\Gamma}_\alpha^\dagger(t) \hat{\Gamma}_d(t')\right]^\dagger \right\rangle_{\rm B} , \qquad \langle \hat{\Gamma}_d(t) \hat{\Gamma}_\alpha^\dagger(t') \rangle_{\rm B} = \left\langle \left[\hat{\Gamma}_\alpha(t) \hat{\Gamma}_d(t')\right]^\dagger \right\rangle_{\rm B} . \tag{6.112}$$

We conclude this section with the observation that also for the electron field the strength of fluctuations is determined by the strength of the deterministic forces describing dissipation and pumping, so that the fluctuation-dissipation theorem is also valid here.

6.4 Heat Bath for Electron Field: Consistency

Now we show explicitly that the fluctuating operators, whose properties were determined in the previous section, restore quantum mechanical consistency. To this end we formally solve at first the quantum Langevin equations of the electron field operators (6.65), (6.66), and (6.76):

$$\hat{\alpha}^\dagger(t) = \hat{\alpha}^\dagger(0)e^{(i\Omega-\gamma_\perp)t} + \int_0^t d\tau\, \hat{\Gamma}^\dagger_\alpha(\tau)e^{(i\Omega-\gamma_\perp)(t-\tau)}\,, \tag{6.113}$$

$$\hat{\alpha}(t) = \hat{\alpha}(0)e^{(-i\Omega-\gamma_\perp)t} + \int_0^t d\tau\, \hat{\Gamma}_\alpha(\tau)e^{(-i\Omega-\gamma_\perp)(t-\tau)}\,, \tag{6.114}$$

$$\hat{d}(t) = d_0 + \left[\hat{d}(0) - d_0\right] e^{-\gamma_\parallel t} + \int_0^t d\tau\, \hat{\Gamma}_d(\tau)e^{-\gamma_\parallel(t-\tau)}\,. \tag{6.115}$$

Here the respective Langevin forces have according to the previous section the following seven non-trivial correlation functions with respect to the bath average:

$$\langle\hat{\Gamma}^\dagger_\alpha(t)\rangle_{\rm B} = \langle\hat{\Gamma}_\alpha(t)\rangle_{\rm B} = \langle\hat{\Gamma}_d(t)\rangle_{\rm B} = 0\,, \tag{6.116}$$

$$\langle\hat{\Gamma}^\dagger_\alpha(t)\hat{\Gamma}_\alpha(t')\rangle_{\rm B} = \left\{\gamma_\perp\left[1+\langle\hat{d}(t)\rangle_{\rm B}\right] + \frac{\gamma_\parallel}{2}\left[d_0 - \langle\hat{d}(t)\rangle_{\rm B}\right]\right\}\delta(t-t')\,, \tag{6.117}$$

$$\langle\hat{\Gamma}_\alpha(t)\hat{\Gamma}^\dagger_\alpha(t')\rangle_{\rm B} = \left\{\gamma_\perp\left[1-\langle\hat{d}(t)\rangle_{\rm B}\right] - \frac{\gamma_\parallel}{2}\left[d_0 - \langle\hat{d}(t)\rangle_{\rm B}\right]\right\}\delta(t-t')\,, \tag{6.118}$$

$$\langle\hat{\Gamma}_d(t)\hat{\Gamma}_d(t')\rangle_{\rm B} = 2\gamma_\parallel\left[1 - d_0\,\langle\hat{d}(t)\rangle_B\right]\delta(t-t')\,, \tag{6.119}$$

$$\langle\hat{\Gamma}_\alpha(t)\hat{\Gamma}_d(t')\rangle_{\rm B} = \left\langle\left[\hat{\Gamma}_d(t)\hat{\Gamma}^\dagger_\alpha(t')\right]^\dagger\right\rangle_{\rm B} = \gamma_\parallel(1-d_0)\,\langle\hat{\alpha}(t)\rangle_{\rm B}\,\delta(t-t')\,, \tag{6.120}$$

$$\langle\hat{\Gamma}_d(t)\hat{\Gamma}_\alpha(t')\rangle_{\rm B} = \left\langle\left[\hat{\Gamma}^\dagger_\alpha(t)\hat{\Gamma}_d(t')\right]^\dagger\right\rangle_{\rm B} = -\gamma_\parallel(1+d_0)\,\langle\hat{\alpha}(t)\rangle_{\rm B}\,\delta(t-t')\,. \tag{6.121}$$

Now we have to check whether all commutator and anti-commutator relations listed in (5.85), (5.86) and (5.87)–(5.93) remain valid with respect to the thermal average. To this end we focus on the five non-vanishing commutator and anti-commutator relations and start with obtaining from (6.113), (6.114) by applying (6.116) and (6.117)

$$\begin{aligned}\langle\hat{\alpha}^\dagger(t)\hat{\alpha}(t)\rangle_{\rm B} &= \hat{\alpha}^\dagger(0)\hat{\alpha}(0)e^{-2\gamma_\perp t} \\ &\quad + e^{-2\gamma_\perp t}\int_0^t d\tau\left\{\gamma_\perp\left[1+\langle\hat{d}(\tau)\rangle_{\rm B}\right] + \frac{1}{2}\gamma_\parallel\left[d_0 - \langle\hat{d}(\tau)\rangle_{\rm B}\right]\right\}e^{2\gamma_\perp\tau}\end{aligned} \tag{6.122}$$

and, correspondingly, by applying (6.116) and (6.118)

$$\begin{aligned}\langle\hat{\alpha}(t)\hat{\alpha}^\dagger(t)\rangle_{\rm B} &= \hat{\alpha}(0)\hat{\alpha}^\dagger(0)e^{-2\gamma_\perp t} \\ &\quad + e^{-2\gamma_\perp t}\int_0^t d\tau\left\{\gamma_\perp\left[1-\langle\hat{d}(\tau)\rangle_{\rm B}\right] - \frac{1}{2}\gamma_\parallel\left[d_0 - \langle\hat{d}(\tau)\rangle_{\rm B}\right]\right\}e^{2\gamma_\perp\tau}\,.\end{aligned} \tag{6.123}$$

Thus, from combining (6.122) and (6.123) we directly read off the consistency for the anti-commutator

$$\left\langle\left[\hat{\alpha}^\dagger(t),\hat{\alpha}(t)\right]_+\right\rangle_{\rm B} = \left[\hat{\alpha}^\dagger(0),\hat{\alpha}(0)\right]_+ e^{-2\gamma_\perp t} + 2\gamma_\perp e^{-2\gamma_\perp t}\int_0^t d\tau\, e^{2\gamma_\perp\tau} \tag{6.124}$$

by taking into account (5.90) at the initial time $t = 0$ and the elementary integral (6.41):

$$\left\langle \left[\hat{\alpha}^\dagger(t), \hat{\alpha}(t)\right]_+ \right\rangle_{\rm B} = 1\,. \tag{6.125}$$

The investigation of the corresponding commutator is more involved as we yield from (6.122) and (6.123) at first

$$\begin{aligned}\left\langle \left[\hat{\alpha}^\dagger(t), \hat{\alpha}(t)\right]_- \right\rangle_{\rm B} &= \left[\hat{\alpha}^\dagger(0), \hat{\alpha}(0)\right]_- e^{-2\gamma_\perp t} \\ &+e^{-2\gamma_\perp t}\int_0^t d\tau \left\{2\gamma_\perp \langle \hat{d}(\tau)\rangle_{\rm B} + \gamma_\parallel \left[d_0 - \langle \hat{d}(\tau)\rangle_{\rm B}\right]\right\} e^{2\gamma_\perp \tau}\,. \end{aligned}\tag{6.126}$$

Inserting therein the solution of the population inversion operator (6.115) together with (6.116) we get

$$\begin{aligned}&\left\langle \left[\hat{\alpha}^\dagger(t), \hat{\alpha}(t)\right]_- \right\rangle_{\rm B} = \left[\hat{\alpha}^\dagger(0), \hat{\alpha}(0)\right]_- e^{-2\gamma_\perp t} \\ &+e^{-2\gamma_\perp t}\left\{2\gamma_\perp d_0 \int_0^t d\tau\, e^{2\gamma_\perp \tau} + \left(2\gamma_\perp - \gamma_\parallel\right)\left[\hat{d}(0) - d_0\right]\int_0^t d\tau\, e^{\left(2\gamma_\perp - \gamma_\parallel\right)\tau}\right\}\,, \end{aligned}\tag{6.127}$$

so that the remaining elementary integrals are of the type (6.41) and yield with (6.115) and (6.116), indeed, that the commutator (5.85) holds at time t provided that it is fulfilled at the initial time $t = 0$:

$$\left\langle \left[\hat{\alpha}^\dagger(t), \hat{\alpha}(t)\right]_- \right\rangle_{\rm B} = \langle \hat{d}(t)\rangle_{\rm B}\,. \tag{6.128}$$

In the same way we proceed for the bath average of the square of the population inversion operator (6.115), which reads due to (6.116)

$$\begin{aligned}\langle \hat{d}^2(t)\rangle_{\rm B} &= d_0^2 + \left[\hat{d}(0) - d_0\right]^2 e^{-2\gamma_\parallel t} + 2d_0\left[\hat{d}(0) - d_0\right] e^{-\gamma_\parallel t} \\ &+2\gamma_\parallel e^{-2\gamma_\parallel t}\int_0^t d\tau \left[1 - d_0\langle \hat{d}(\tau)\rangle_{\rm B}\right] e^{2\gamma_\parallel \tau}\,. \end{aligned}\tag{6.129}$$

Taking into account (6.115) and (6.116) the second line of (6.129) yields the integral

$$2\gamma_\parallel e^{-2\gamma_\parallel t}\left\{\left(1 - d_0^2\right)\int_0^t d\tau\, e^{2\gamma_\parallel \tau} - d_0\left[\hat{d}(0) - d_0\right]\int_0^t d\tau\, e^{\gamma_\parallel \tau}\right\}\,, \tag{6.130}$$

whose evaluation with the help of (6.41) yields

$$\left(1 - d_0^2\right)\left(1 - e^{-2\gamma_\parallel t}\right) - 2d_0\left[\hat{d}(0) - d_0\right]\left(e^{-\gamma_\parallel t} - e^{-2\gamma_\parallel t}\right)\,. \tag{6.131}$$

Thus, substituting the second line of (6.129) by (6.131) we finally end up with

$$\langle \hat{d}^2(t)\rangle_B = 1 + \left[\hat{d}^2(0) - 1\right] e^{-2\gamma_\parallel t}\,, \tag{6.132}$$

so that (5.93) is valid at time t provided it is valid at the initial time $t = 0$. Subsequently we deduce from (6.114) and (6.115) together with (6.116), (6.120), and (6.121)

$$\begin{aligned}\langle \hat{\alpha}(t)\hat{d}(t)\rangle_{\rm B} &= \hat{\alpha}(0)e^{(-i\Omega - \gamma_\perp)t}\left\{d_0 + \left[\hat{d}(0) - d_0\right] e^{-\gamma_\parallel t}\right\} \\ &+\gamma_\parallel\left(1 - d_0\right) e^{\left(-i\Omega - \gamma_\perp - \gamma_\parallel\right)t}\int_0^t d\tau\, \langle \hat{\alpha}(\tau)\rangle_{\rm B}\, e^{\left(i\Omega + \gamma_\perp + \gamma_\parallel\right)\tau} \end{aligned}\tag{6.133}$$

and also

$$\langle \hat{d}(t)\hat{\alpha}(t)\rangle_{\rm B} = \left\{ d_0 + \left[\hat{d}(0) - d_0\right] e^{-\gamma_\parallel t} \right\} \hat{\alpha}(0) e^{(-i\Omega-\gamma_\perp)t} - \gamma_\parallel (1+d_0)\, e^{\left(-i\Omega-\gamma_\perp-\gamma_\parallel\right)t} \int_0^t d\tau \, \langle \hat{\alpha}(\tau)\rangle_{\rm B}\, e^{\left(i\Omega+\gamma_\perp+\gamma_\parallel\right)\tau} . \quad (6.134)$$

Thus, inserting therein (6.114) and (6.116) and taking into account the elementary integral (6.41) yields for the commutator

$$\left\langle \left[\hat{\alpha}(t), \hat{d}(t)\right]_- \right\rangle_{\rm B} = \left[\hat{\alpha}(0), \hat{d}(0)\right]_- e^{\left(-i\Omega-\gamma_\perp-\gamma_\parallel\right)t} + 2\hat{\alpha}(0)\left(e^{\gamma_\parallel t} - 1\right) e^{\left(-i\Omega-\gamma_\perp-\gamma_\parallel\right)t} . \quad (6.135)$$

Provided that the commutator (5.86) is valid at the initial time $t = 0$ it remains to be valid at any time t due to (6.114) and (6.116):

$$\left[\hat{\alpha}(0), \hat{d}(0)\right]_- = 2\hat{\alpha}(0) \qquad \Longrightarrow \qquad \left\langle \left[\hat{\alpha}(t), \hat{d}(t)\right]_- \right\rangle_{\rm B} = 2\,\langle \hat{\alpha}(t)\rangle_{\rm B} . \quad (6.136)$$

Correspondingly we obtain also the adjoint of Eq. (6.136):

$$\left[\hat{\alpha}^\dagger(0), \hat{d}(0)\right]_- = -2\hat{\alpha}(0) \qquad \Longrightarrow \qquad \left\langle \left[\hat{\alpha}^\dagger(t), \hat{d}(t)\right]_- \right\rangle_{\rm B} = -2\left\langle \hat{\alpha}^\dagger(t)\right\rangle_{\rm B} . \quad (6.137)$$

Chapter 7

Semiclassical Laser Equations

At the beginning we review the quantum Langevin equations for the laser, which are too complicated to solve exactly. Therefore, we perform a series of approximations in order to be able to study at least roughly some laser properties. In a first step we determine the expectation values for all system observables, yielding the seminal microscopic semiclassical laser equations. Afterwards, we specialize to the homogeneous single-mode laser, which leads to a qualitative understanding of the laser dynamics in form of three macroscopic equations. Within the third step we adiabatically eliminate the polarization from the description, which reduces the three macroscopic equations to two rate equations. For the latter we then perform a linear stability analysis in order to determine both the laser threshold and the frequency of the laser. And, finally, in the fifth step we work out a nonlinear analysis in the immediate vicinity of the laser threshold, which allows to derive the underlying order parameter equation for the nonequilibrium phase transition from the incoherent lamp light to the coherent laser light.

7.1 Quantum Langevin Equations of Laser

We start with summarizing all the results of the preceding two chapters concerning both the coherent and the incoherent interaction of light and matter. Thus, we list the coupled equations for the light and the matter field operators, which represent quantum Lange quations and, thus, consist of both a deterministic and a stochastic part:

$$\frac{\partial}{\partial t}\,\hat{b}^\dagger_{\boldsymbol{\lambda}}(t) = (i\omega_{\boldsymbol{\lambda}} - \kappa)\,\hat{b}^\dagger_{\boldsymbol{\lambda}}(t) + i\sum_\mu g_{\boldsymbol{\lambda}\mu}\hat{\alpha}^\dagger_\mu(t) + \hat{\Gamma}^\dagger_{b\boldsymbol{\lambda}}(t)\,, \tag{7.1}$$

$$\frac{\partial}{\partial t}\,\hat{b}_{\boldsymbol{\lambda}}(t) = (-i\omega_{\boldsymbol{\lambda}} - \kappa)\,\hat{b}_{\boldsymbol{\lambda}}(t) - i\sum_\mu g^*_{\boldsymbol{\lambda}\mu}\hat{\alpha}_\mu(t) + \hat{\Gamma}_{b\boldsymbol{\lambda}}(t)\,, \tag{7.2}$$

$$\frac{\partial}{\partial t}\,\hat{\alpha}^\dagger_\mu(t) = (i\Omega - \gamma_\perp)\,\hat{\alpha}^\dagger_\mu(t) - i\sum_{\boldsymbol{\lambda}} g^*_{\boldsymbol{\lambda}\mu}\hat{d}^\dagger_\mu(t)\hat{b}^\dagger_{\boldsymbol{\lambda}}(t) + \hat{\Gamma}^\dagger_{\alpha\mu}(t)\,, \tag{7.3}$$

$$\frac{\partial}{\partial t}\,\hat{\alpha}_\mu(t) = (-i\Omega-\gamma_\perp)\,\hat{\alpha}_\mu(t) + i\sum_{\boldsymbol{\lambda}} g_{\boldsymbol{\lambda}\mu}\hat{d}_\mu(t)\hat{b}_{\boldsymbol{\lambda}}(t) + \hat{\Gamma}_{\alpha\mu}(t)\,, \tag{7.4}$$

$$\frac{\partial}{\partial t}\,\hat{d}_\mu(t) = \gamma_\parallel\Big[d_0-\hat{d}_\mu(t)\Big] + 2i\sum_{\boldsymbol{\lambda}}\Big[g^*_{\boldsymbol{\lambda}\mu}\hat{b}^\dagger_{\boldsymbol{\lambda}}(t)\hat{\alpha}_\mu(t) - g_{\boldsymbol{\lambda}\mu}\hat{\alpha}^\dagger_\mu(t)\hat{b}_{\boldsymbol{\lambda}}(t)\Big] + \hat{\Gamma}_{d\mu}(t)\,. \tag{7.5}$$

Here the bath expectation values of all Langevin operators vanish:

$$\langle\hat{\Gamma}^\dagger_{b\boldsymbol{\lambda}}(t)\rangle_{\rm B} = \langle\hat{\Gamma}_{b\boldsymbol{\lambda}}(t)\rangle_{\rm B} = \langle\hat{\Gamma}^\dagger_{\alpha\mu}(t)\rangle_{\rm B} = \langle\hat{\Gamma}_{\alpha\mu}(t)\rangle_{\rm B} = \langle\hat{\Gamma}_{d\mu}(t)\rangle_{\rm B} = 0\,. \tag{7.6}$$

The correlation functions of the Langevin field operators read

$$\langle\hat{\Gamma}_{b\boldsymbol{\lambda}}(t)\hat{\Gamma}_{b\boldsymbol{\lambda}'}(t')\rangle_{\rm B} = \langle\hat{\Gamma}^\dagger_{b\boldsymbol{\lambda}}(t)\hat{\Gamma}^\dagger_{b\boldsymbol{\lambda}'}(t')\rangle_{\rm B} = 0\,, \tag{7.7}$$

$$\langle\hat{\Gamma}^\dagger_{b\boldsymbol{\lambda}}(t)\hat{\Gamma}_{b\boldsymbol{\lambda}'}(t')\rangle_{\rm B} = 2\kappa\,\overline{n}_{\omega_0}(T)\delta_{\boldsymbol{\lambda}\boldsymbol{\lambda}'}\delta(t-t')\,, \tag{7.8}$$

$$\langle\hat{\Gamma}_{b\boldsymbol{\lambda}}(t)\hat{\Gamma}^\dagger_{b\boldsymbol{\lambda}'}(t')\rangle_{\rm B} = 2\kappa\big[\overline{n}_{\omega_0}(T)+1\big]\delta_{\boldsymbol{\lambda}\boldsymbol{\lambda}'}\delta(t-t')\,. \tag{7.9}$$

Here the Kronecker symbol $\delta_{\boldsymbol{\lambda}\boldsymbol{\lambda}'}$ describes the independence of the respective cavity modes. Furthermore, all correlation functions of the Langevin matter operators are given by

$$\langle\hat{\Gamma}_{d\mu}(t)\hat{\Gamma}_{d\mu'}(t')\rangle_{\rm B} = 2\gamma_\parallel\Big[1-d_0\,\langle\hat{d}_\mu(t)\rangle_{\rm B}\Big]\,\delta_{\mu\mu'}\delta(t-t')\,, \tag{7.10}$$

$$\langle\hat{\Gamma}_{\alpha\mu}(t)\hat{\Gamma}^\dagger_{\alpha\mu'}(t')\rangle_{\rm B} = \left\{\gamma_\perp\Big[1-\langle\hat{d}_\mu(t)\rangle_{\rm B}\Big] - \frac{1}{2}\gamma_\parallel\Big[d_0-\langle\hat{d}_\mu(t)\rangle_{\rm B}\Big]\right\}\delta_{\mu\mu'}\delta(t-t')\,, \tag{7.11}$$

$$\langle\hat{\Gamma}^\dagger_{\alpha\mu}(t)\hat{\Gamma}_{\alpha\mu'}(t')\rangle_{\rm B} = \left\{\gamma_\perp\Big[1+\langle\hat{d}_\mu(t)\rangle_{\rm B}\Big] + \frac{1}{2}\gamma_\parallel\Big[d_0-\langle\hat{d}_\mu(t)\rangle_{\rm B}\Big]\right\}\delta_{\mu\mu'}\delta(t-t')\,, \tag{7.12}$$

$$\langle\hat{\Gamma}_{\alpha\mu}(t)\hat{\Gamma}_{\alpha\mu'}(t')\rangle_{\rm B} = \langle\hat{\Gamma}^\dagger_{\alpha\mu}(t)\hat{\Gamma}^\dagger_{\alpha\mu'}(t')\rangle_{\rm B} = 0\,, \tag{7.13}$$

$$\langle\hat{\Gamma}_{\alpha\mu}(t)\hat{\Gamma}_{d\mu'}(t')\rangle_{\rm B} = \langle\hat{\Gamma}_{d\mu}(t)\hat{\Gamma}_{\alpha\mu'}(t')\rangle_{\rm B} = \gamma_\parallel\,(1-d_0)\,\langle\hat{\alpha}_\mu(t)\rangle_{\rm B}\,\delta_{\mu\mu'}\delta(t-t')\,, \tag{7.14}$$

$$\langle\hat{\Gamma}^\dagger_{\alpha\mu}(t)\hat{\Gamma}_{d\mu'}(t')\rangle_{\rm B} = \langle\hat{\Gamma}_{d\mu}(t)\hat{\Gamma}^\dagger_{\alpha\mu'}(t')\rangle_{\rm B} = -\gamma_\parallel\,(1+d_0)\,\langle\hat{\alpha}^\dagger_\mu(t)\rangle_{\rm B}\,\delta_{\mu\mu'}\delta(t-t')\,. \tag{7.15}$$

On the one hand, the Kronecker symbol $\delta_{\mu\mu'}$ reflects the distinguishability of the respective laser active atoms and, on the other hand, the delta function $\delta(t-t')$ represents the Markow property, i.e. the short memory of the Langevin operators.

7.2 Expectation Values

Performing the bath average upon the quantum Langevin equations of the laser (7.1)–(7.5), we observe at first that the Langevin operators drop out due to (7.6). Secondly, we use again the time scale hierarchy that the matter degrees of freedom vary much faster than the field degrees of freedom, yielding the factorization approximation (6.80). This leads to the following coupled

evolution equations for the bath expectation values of field and matter operators:

$$\frac{\partial}{\partial t}\left\langle \hat{b}^\dagger_{\boldsymbol{\lambda}}(t)\right\rangle_{\mathrm{B}} = (i\omega_{\boldsymbol{\lambda}} - \kappa)\left\langle \hat{b}^\dagger_{\boldsymbol{\lambda}}(t)\right\rangle_{\mathrm{B}} + i\sum_\mu g_{\boldsymbol{\lambda}\mu}\left\langle \hat{\alpha}^\dagger_\mu(t)\right\rangle_{\mathrm{B}} , \tag{7.16}$$

$$\frac{\partial}{\partial t}\left\langle \hat{b}_{\boldsymbol{\lambda}}(t)\right\rangle_{\mathrm{B}} = (-i\omega_{\boldsymbol{\lambda}} - \kappa)\left\langle \hat{b}_{\boldsymbol{\lambda}}(t)\right\rangle_{\mathrm{B}} - i\sum_\mu g^*_{\boldsymbol{\lambda}\mu}\left\langle \hat{\alpha}_\mu(t)\right\rangle_{\mathrm{B}} , \tag{7.17}$$

$$\frac{\partial}{\partial t}\left\langle \hat{\alpha}^\dagger_\mu(t)\right\rangle_{\mathrm{B}} = (i\Omega - \gamma_\perp)\left\langle \hat{\alpha}^\dagger_\mu(t)\right\rangle_{\mathrm{B}} - i\sum_{\boldsymbol{\lambda}} g^*_{\boldsymbol{\lambda}\mu}\left\langle \hat{d}_\mu(t)\right\rangle_{\mathrm{B}}\left\langle \hat{b}^\dagger_{\boldsymbol{\lambda}}(t)\right\rangle_{\mathrm{B}} , \tag{7.18}$$

$$\frac{\partial}{\partial t}\left\langle \hat{\alpha}_\mu(t)\right\rangle_{\mathrm{B}} = (-i\Omega - \gamma_\perp)\left\langle \hat{\alpha}_\mu(t)\right\rangle_{\mathrm{B}} + i\sum_{\boldsymbol{\lambda}} g_{\boldsymbol{\lambda}\mu}\left\langle \hat{d}_\mu(t)\right\rangle_{\mathrm{B}}\left\langle \hat{b}_{\boldsymbol{\lambda}}(t)\right\rangle_{\mathrm{B}} , \tag{7.19}$$

$$\frac{\partial}{\partial t}\left\langle \hat{d}_\mu(t)\right\rangle_{\mathrm{B}} = \gamma_\parallel\left[d_0 - \left\langle \hat{d}_\mu(t)\right\rangle_{\mathrm{B}}\right] + 2i\sum_{\boldsymbol{\lambda}}\left[g^*_{\boldsymbol{\lambda}\mu}\left\langle \hat{b}^\dagger_{\boldsymbol{\lambda}}(t)\right\rangle_{\mathrm{B}}\left\langle \hat{\alpha}_\mu(t)\right\rangle_{\mathrm{B}} - g_{\boldsymbol{\lambda}\mu}\left\langle \hat{\alpha}^\dagger_\mu(t)\right\rangle_{\mathrm{B}}\left\langle \hat{b}_{\boldsymbol{\lambda}}(t)\right\rangle_{\mathrm{B}}\right] . \tag{7.20}$$

Note that the bath expectation value of each operator has, in general, still an operator character concerning the system observable. However, in order to simplify the following discussion further, we eliminate also this operator character by restricting ourselves to the expectation values of those operators with respect to the degrees of freedom of the system:

$$b_{\boldsymbol{\lambda}}(t) = \left\langle\left\langle \hat{b}_{\boldsymbol{\lambda}}(t)\right\rangle_{\mathrm{B}}\right\rangle_{\mathrm{S}} , \qquad b^*_{\boldsymbol{\lambda}}(t) = \left\langle\left\langle \hat{b}^\dagger_{\boldsymbol{\lambda}}(t)\right\rangle_{\mathrm{B}}\right\rangle_{\mathrm{S}} , \tag{7.21}$$

$$\alpha_\mu(t) = \left\langle\left\langle \hat{\alpha}_\mu(t)\right\rangle_{\mathrm{B}}\right\rangle_{\mathrm{S}} , \qquad \alpha^*_\mu(t) = \left\langle\left\langle \hat{\alpha}^\dagger_\mu(t)\right\rangle_{\mathrm{B}}\right\rangle_{\mathrm{S}} , \qquad d_\mu(t) = \left\langle\left\langle \hat{d}_\mu(t)\right\rangle_{\mathrm{B}}\right\rangle_{\mathrm{S}} . \tag{7.22}$$

Also for the system expectation value we take advantage of the time scale hierarchy that light quantites vary on a time scale, which is much slower than the one of the matter quantities, and assume a corresponding factorization property:

$$\left\langle \text{light operators} \cdot \text{matter operators}\right\rangle_{\mathrm{S}} \approx \left\langle \text{light operators}\right\rangle_{\mathrm{S}} \cdot \left\langle \text{matter operators}\right\rangle_{\mathrm{S}} . \tag{7.23}$$

With this we obtain the field equations from (7.16) and (7.17):

$$\frac{\partial}{\partial t} b^*_{\boldsymbol{\lambda}}(t) = (i\omega_{\boldsymbol{\lambda}} - \kappa)\, b^*_{\boldsymbol{\lambda}}(t) + i\sum_\mu g_{\boldsymbol{\lambda}\mu}\alpha^*_\mu(t) , \tag{7.24}$$

$$\frac{\partial}{\partial t} b_{\boldsymbol{\lambda}}(t) = (-i\omega_{\boldsymbol{\lambda}} - \kappa)\, b_{\boldsymbol{\lambda}}(t) - i\sum_\mu g^*_{\boldsymbol{\lambda}\mu}\alpha_\mu(t) . \tag{7.25}$$

The first term describes the oscillation and the damping of a resonator mode in absence of any light-matter interaction. The second term takes into account that the dipole moments of all laser active atoms represent the source for the dynamics of a resonator mode. The second set of evolution equations concerns the matter degrees of freedom. According to (7.18) and (7.19) the atomic dipole moment changes via

$$\frac{\partial}{\partial t} \alpha^*_\mu(t) = (i\Omega - \gamma_\perp)\, \alpha^*_\mu(t) - i\sum_{\boldsymbol{\lambda}} g^*_{\boldsymbol{\lambda}\mu} d_\mu(t) b^*_{\boldsymbol{\lambda}}(t) , \tag{7.26}$$

$$\frac{\partial}{\partial t} \alpha_\mu(t) = (-i\Omega - \gamma_\perp)\, \alpha_\mu(t) + i\sum_{\boldsymbol{\lambda}} g_{\boldsymbol{\lambda}\mu} b_{\boldsymbol{\lambda}}(t) d_\mu(t) . \tag{7.27}$$

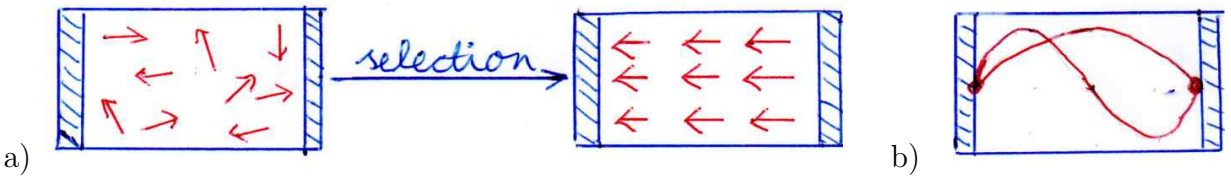

Figure 7.1: Two mode selection schemes: a) Selection of near axial modes with long lifetime and b) selection with respect to wavelength according to (7.29).

Here the first term denotes in absence of any light field the transition frequency of the two-level atom and its damping, where the latter is caused by the interaction of the atom with its environment. The second term accounts for the fact that any population inversion in presence of a light field yields an atomic polarization. Finally, the atomic population imbalance is governed by

$$\frac{\partial}{\partial t}\, d_\mu(t) = \gamma_\parallel \big[d_0 - d_\mu(t)\big] + 2i \sum_{\boldsymbol{\lambda}} \left[g^*_{\boldsymbol{\lambda}\mu} b^*_{\boldsymbol{\lambda}}(t)\alpha_\mu(t) - g_{\boldsymbol{\lambda}\mu}\alpha^*_\mu(t) b_{\boldsymbol{\lambda}}(t)\right] . \tag{7.28}$$

The first term describes the relaxation toward an equilibrium population imbalance, which is set by the competing effects of pumping and losses. The second term deals with the fact that a polarization in presence of a light field drives the population imbalance. Note that the semiclassical equations (7.24)–(7.28) also directly follow from describing the light-matter interaction within the Maxwell-Schrödinger theory.

7.3 Homogeneous Single-Mode Laser

In order to realistically describe the laser in the framework of the semiclassical laser theory one has to take into account approximately 10^3 resonator modes and 10^{18} laser active atoms. Because of the nonlinearity of the semiclassical equations this leads to such a complexity that it is not possible to obtain any analytic solution.

But for a more qualitative understanding of the laser it is sufficient to extract from the semiclassical laser equations a simple but physically reasonable model. To this end we perform the following physical approximations:

- So far we have already concentrated the description on a homogeneous laser as we always considered all laser active atoms to be equal. In principle, it could occur, for instance, that both the transition frequency Ω and the damping constant $\gamma_\perp$ vary from atom to atom, which would necessitate that they get an additional μ-index.

- From now on we restrict ourselves to the case that only one single field mode becomes dominant in the resonator. In principle, two mode selection schemes by the mirrors are feasible:

– Due to the arrangement of the mirrors only light, which is emitted very close to the axis, remains in the resonator long enough. This represents a mode selection with respect to the lifetime, see Fig. 7.1a).

– Because of interference effects only such axial modes can survive in the resonator, which vanish at both mirrors. According to Fig. 7.1b) this yields a mode selection with respect to the wavelength via

$$k_n = \frac{2\pi}{\lambda_n} = n\,\frac{\pi}{L} \qquad \Longrightarrow \qquad \lambda_n = \frac{2L}{n}\,, \qquad n \in \mathbb{N}\,. \tag{7.29}$$

- As a consequence of both previous assumptions the coupling constant $g_{\boldsymbol{\lambda}\mu}$ between the resonator mode $\boldsymbol{\lambda}$ and the laser active atom μ does no longer depend in the indices $\boldsymbol{\lambda}, \mu$:

$$g_{\boldsymbol{\lambda}\mu} = g\,. \tag{7.30}$$

With these physical approximations the semiclassical laser equations (7.24)–(7.28) reduce to

$$\dot{b}(t) = (-i\omega - \kappa)\, b(t) - ig^* \sum_\mu \alpha_\mu(t)\,, \tag{7.31}$$

$$\dot{\alpha}_\mu(t) = (-i\Omega - \gamma_\perp)\, \alpha_\mu(t) + igd_\mu(t)b(t)\,, \tag{7.32}$$

$$\dot{d}_\mu(t) = \gamma_\parallel \big[d_0 - d_\mu(t)\big] + 2i\big[g^* b^*(t)\alpha_\mu(t) - g\alpha_\mu^*(t)b(t)\big]\,. \tag{7.33}$$

Due to the assumed homogeneity of the laser we can now introduce macroscopic matter variables by summing over all respective microscopic matter variables. To this end we define the polarization

$$P(t) = \sum_\mu \alpha_\mu(t)\,, \tag{7.34}$$

the saturated population inversion

$$D(t) = \sum_\mu d_\mu(t) \tag{7.35}$$

and the unsaturated population inversion

$$D_0 = N d_0\,, \tag{7.36}$$

where the number of laser active atoms is denoted by

$$N = \sum_\mu 1\,. \tag{7.37}$$

With these definitions and identifying the field mode $b(t)$ with the electric field $E(t)$ we obtain from the microscopic semiclassical laser equations (7.31)–(7.33) the following macroscopic equations for the homogeneous single-mode laser:

$$\dot{E}(t) = (-i\omega - \kappa)\, E(t) - ig^* P(t)\,, \tag{7.38}$$

$$\dot{P}(t) = (-i\Omega - \gamma_\perp)\, P(t) + igD(t)E(t)\,, \tag{7.39}$$

$$\dot{D}(t) = \gamma_\parallel \big[D_0 - D(t)\big] + 2i\big[g^* E^*(t)P(t) - gP^*(t)E(t)\big]\,. \tag{7.40}$$

Note that we treat here the general off-resonant case that the resonator frequency ω and the transition frequency Ω of the laser active two-level atoms do not coincide.

7.4 Derivation of Rate Equations

We start with the observation that the evolution equations (7.38)–(7.40) have the following global $U(1)$-symmetry involving both the light and the matter degrees of freedom:

$$\begin{aligned} E(t) \to E(t)e^{-i\varphi}\,, \quad E^*(t) \to E^*(t)e^{i\varphi}\,, \\ P(t) \to P(t)e^{-i\varphi}\,, \quad P^*(t) \to P^*(t)e^{i\varphi}\,, \quad D(t) \to D(t)\,. \end{aligned} \tag{7.41}$$

It could happen that this global $U(1)$-symmetry is dynamically broken. In order to take into account this possibility we transform the respective variables into a co-rotating frame

$$\begin{aligned} E(t) \to \tilde{E}(t)e^{-i\tilde{\omega}t}\,, \quad E^*(t) \to \tilde{E}^*(t)e^{i\tilde{\omega}t}\,, \\ P(t) \to \tilde{P}(t)e^{-i\tilde{\omega}t}\,, \quad P^*(t) \to \tilde{P}^*(t)e^{i\tilde{\omega}t}\,, \quad D(t) \to \tilde{D}(t)\,. \end{aligned} \tag{7.42}$$

Here the frequency $\tilde{\omega}$ of the co-rotating frame corresponds to the laser frequency, which is currently not known but will be specified below. The ansatz (7.42) converts (7.38)–(7.40) into

$$\dot{E}(t) = \big[-i\,(\omega-\tilde{\omega})-\kappa\big]E(t) - ig^*P(t)\,, \tag{7.43}$$

$$\dot{P}(t) = \big[-i\,(\Omega-\tilde{\omega})-\gamma_\perp\big]P(t) + igD(t)E(t)\,, \tag{7.44}$$

$$\dot{D}(t) = \gamma_\parallel\big[D_0 - D(t)\big] + 2i\big[g^*E^*(t)P(t) - gP^*(t)E(t)\big]\,, \tag{7.45}$$

where we left out the tilde at all quantities for the sake of simplicity. We remark that in the resonant case the laser frequency $\tilde{\omega}$ can be chosen to coincide with $\omega = \Omega$ and, thus, the macrosopic laser equations (7.43)–(7.45) turn out to be formally equivalent to differential equations, which were set up in 1963 by the meteorologist Edward Lorenz as a simplified mathematical model for atmospheric convection [53].

The typical time scales of the electric field $E(t)$, the polarization $P(t)$, and the population inversion $D(t)$ are approximately determined by the time scales associated to the respective damping constants:

$$\kappa = \frac{1}{\tau_E}\,, \qquad \gamma_\perp = \frac{1}{\tau_P}\,, \qquad \gamma_\parallel = \frac{1}{\tau_D}\,. \tag{7.46}$$

In case of a homogeneous single-mode laser the typical time scales are of the order

$$\tau_E = 10^{-6}\,\mathrm{s}\,, \qquad \tau_P = 10^{-12}\,\mathrm{s}\,, \qquad \tau_D = 10^{-10}\,\mathrm{s}\,. \tag{7.47}$$

In a first approximation it is, therefore, justified to assume for so-called class A lasers [54, page 14], as for instance a dye laser or a semiconductor laser, the following time-scale hierarchy

$$\tau_P \ll \tau_E\,,\, \tau_D\,. \tag{7.48}$$

Thus, the polarization $P(t)$ is regarded as a fast decreasing quantity, whereas both the electric field $E(t)$ and the inversion $D(t)$ are the slowly varying quantities. This time-scale hierarchy

allows an adiabatic elimination of the polarization $P(t)$, i.e. its time derivate in (7.44) can be neglected:

$$\dot{P}(t) = \big[-i\,(\Omega - \tilde{\omega}) - \gamma_\perp \big] P(t) + igD(t)E(t) \approx 0\,. \tag{7.49}$$

Solving (7.49) for the polarization yields

$$P(t) = \frac{ig}{i\,(\Omega - \tilde{\omega}) + \gamma_\perp}\, D(t)E(t)\,. \tag{7.50}$$

Inserting the approximative result (7.50) for the polarization $P(t)$ into the evolution equations (7.43) and (7.45) for the electric field $E(t)$ and the population inversion $D(t)$ yields

$$\dot{E}(t) = \big[-i\,(\omega - \tilde{\omega}) - \kappa \big] E(t) + \frac{|g|^2}{i\,(\Omega - \tilde{\omega}) + \gamma_\perp}\, D(t)E(t)\,, \tag{7.51}$$

$$\dot{D}(t) = \gamma_\parallel \big[D_0 - D(t) \big] - 2\,|g|^2\, \frac{2\gamma_\perp}{(\Omega - \tilde{\omega})^2 + \gamma_\perp^2}\, |E(t)|^2\, D(t)\,. \tag{7.52}$$

Equation (7.52) suggests to introduce the photon number

$$n(t) = |E(t)|^2\,, \tag{7.53}$$

which is a measure for the intensity of the electric field $E(t)$. Thus, the evolution equation for the population inversion (7.52) is of the form

$$\dot{D}(t) = \gamma_\parallel \big[D_0 - D(t) \big] - 2Wn(t)D(t) \tag{7.54}$$

with the Einstein coefficient

$$W = |g|^2\, \frac{2\gamma_\perp}{(\Omega - \tilde{\omega})^2 + \gamma_\perp^2}\,. \tag{7.55}$$

Furthermore, decomposing the electric field into both its amplitude taking into account (7.53) and its phase according to

$$E(t) = \sqrt{n(t)}\, e^{i\varphi(t)} \tag{7.56}$$

we obtain from the real part of (7.51) and (7.55) an equation of motion for the photon number

$$\dot{n}(t) = -2\kappa n(t) + Wn(t)D(t)\,, \tag{7.57}$$

whereas the imaginary part gives the corresponding equation of motion for the phase

$$\dot{\varphi}(t) = \tilde{\omega} - \omega + (\tilde{\omega} - \Omega)\, \frac{W}{2\gamma_\perp}\, D(t)\,. \tag{7.58}$$

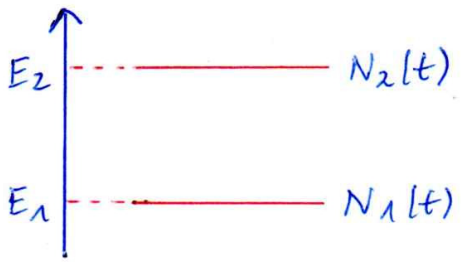

Figure 7.2: Laser active atoms modelled as two-level systems of energies E_1, E_2 and occupation numbers $N_1(t)$, $N_2(t)$.

7.5 Phenomenological Laser Theory

We argue now that the rate equations (7.54) and (7.57) for the population inversion $D(t)$ and the photon number $n(t)$ derived above within the realm of the semiclassical laser theory also follow from a phenomenological theory for the homogeneous single-mode laser. The underlying assumptions are the following:

- For the electric field is supposed that only one field mode survives in the cavity. Whereas in a full quantum mechanical treatment one introduces a photon number $n(t)$, whose possible values are positive integers, the phenomenological theory assumes that the photon number $n(t)$ can take any positive real value.
- The laser active atoms are modelled as two-level systems, see Fig. 7.2, so that the number $N_1(t)$, $N_2(t)$ of atoms occupying the states E_1, E_2 are assumed to take positive real numbers.

The field equation summarizes gains and losses for the photon number $n(t)$. By neglecting the spontaneous emission one obtains

$$\dot{n}(t) = -2\kappa n(t) + W_{21} N_2(t) n(t) - W_{12} N_1(t) n(t)\,, \tag{7.59}$$

where κ describes resonator losses, W_{21} stands for the induced emission, and W_{12} represents the absorption. Here the Einstein coefficients W_{12}, W_{21} characterize the strength of the coherent interaction between light and matter. Within the proper quantum mechanical treatment of Subsection 4.3.1 and within the phenomenological theory of Einstein for rederiving the Planck radiation formula in Subsection 4.3.4 we derived that both Einstein coefficients coincide:

$$W = W_{12} = W_{21}\,. \tag{7.60}$$

With this the evolution equation (7.59) for the photon number $n(t)$ reduces to (7.57), where we have introduced the population inversion as the difference of the occupation numbers in the higher and the lower level:

$$D(t) = N_2(t) - N_1(t)\,. \tag{7.61}$$

In order to obtain a closed system of equations it becomes necessary to regard also the evolution of the population inversion. To this end one has to take into account the gains and losses for the respective occupation numbers $N_1(t)$, $N_2(t)$:

$$\dot{N}_2(t) = \gamma_{12}N_1(t) - \gamma_{21}N_2(t) + W_{12}N_1(t)n(t) - W_{21}N_2(t)n(t)\,, \tag{7.62}$$

$$\dot{N}_1(t) = -\gamma_{12}N_1(t) + \gamma_{21}N_2(t) - W_{12}N_1(t)n(t) + W_{21}N_2(t)n(t)\,. \tag{7.63}$$

Here γ_{12} describes the pumping process and γ_{21} the non-radiative transitions, which are due to interactions of the laser active atoms with the surrounding solid-state matrix, see also Fig. 6.3. The last two terms take absorption and induced emission processes into account. As a result of these respective gains and losses for the occupation numbers $N_1(t)$, $N_2(t)$ the total number of laser active atoms is conserved:

$$N_1(t) + N_2(t) = N\,. \tag{7.64}$$

Correspondingly, the evolution equation for the population inversion (7.61) results due to (7.60) in

$$\dot{D}(t) = 2\gamma_{12}N_1(t) - 2\gamma_{21}N_2(t) - 2Wn(t)D(t)\,. \tag{7.65}$$

Eliminating N_1, N_2 via N, D from (7.61) and (7.65) yields

$$N_2(t) = \frac{1}{2}\big[N + D(t)\big]\,, \qquad N_1(t) = \frac{1}{2}\big[N - D(t)\big]\,, \tag{7.66}$$

and one gets then from (7.65)

$$\dot{D}(t) = (\gamma_{12} - \gamma_{21})\,N - (\gamma_{12} + \gamma_{21})\,D(t) - 2Wn(t)D(t)\,. \tag{7.67}$$

Introducing the unsaturated population inversion (7.36) together with (6.74) and the longitudinal relaxation parameter (6.75) thus finally converts the evolution equation of the population inversion (7.65) to the form (7.54). We conclude that the unsaturated inversion D_0 is the stationary solution of the population inversion provided that no interaction between light and matter would be present, i.e. $W = 0$. In order to guarantee that D_0 is positive, the pumping parameter γ_{12} has to be larger than the parameter γ_{21} describing the non-radiative transitions.

Note that without a net pumping, i.e. $D_0 = 0$, the rate equations (7.54) and (7.57) of the phenomenological laser theory have the form of the Lotka-Volterra model, which was originally designed to explain temporal oscillations of fish populations. To this end one has to identify the photon number $n(t)$ with the number of predator fishes and the population inversion $D(t)$ with the number of prey fishes [53].

As the semiclassical laser equations allow to derive the rate equations (7.54) and (7.57), we conclude that they already contain the induced emission and absorption as the elementary coherent interaction processes of light and matter. Consequently, we can read off from (7.55) how the corresponding Einstein coefficient (7.60) depends on the respective microscopic parameters.

But note that the frequency $\tilde{\omega}$ of the co-rotating frame has not yet been determined and does not explicitly appear in the rate equations.

The rate equations of the phenomenological laser theory (7.54) and (7.57) represent a set of first-order differential equations for the photon number $n(t)$ and the population inversion $D(t)$, which self-consistently depend on each other in the sense of circular causality as discussed on page 177. As it is not possible to solve them analytically, we perform further approximations in such a way that one can extract at least the most important information of the dynamics. In particular, the performed analysis aims at obtaining an approximate solution, which reflects that circular causality. To this end perform successively first a linear stability analysis and afterwards a nonlinear analysis.

7.6 Linear Stability Analysis

The rate equations of the phenomenological laser theory read due to (7.54) and (7.57):

$$\dot{n}(t) = F_1(n(t), D(t)) = -2\kappa n(t) + W n(t) D(t)\,, \tag{7.68}$$

$$\dot{D}(t) = F_2(n(t), D(t)) = \gamma_\parallel \left[D_0 - D(t)\right] - 2W n(t) D(t)\,. \tag{7.69}$$

They possess two stationary solutions, where the first one corresponds to the lamp light

$$n_1^0 = 0\,, \qquad D_1^0 = D_0\,, \tag{7.70}$$

whereas the second one deals with the laser light

$$n_2^0 = \frac{\gamma_\parallel}{4\kappa}\left(D_0 - \frac{2\kappa}{W}\right)\,, \qquad D_2^0 = \frac{2\kappa}{W}\,, \qquad D_0 \geq D_{0,\text{crit.}}\,. \tag{7.71}$$

Here the critical value of the unsaturated population inversion turns out to be given by the resonator damping in absence of any matter κ and the Einstein coefficient W:

$$D_{0,\text{crit.}} = \frac{2\kappa}{W}\,. \tag{7.72}$$

In order to perform a linear stability analysis around both stationary solutions one needs the Jacobian

$$\mathcal{L}(n, D) = \begin{pmatrix} \dfrac{\partial F_1(n,D)}{\partial n} & \dfrac{\partial F_1(n,D)}{\partial D} \\ \dfrac{\partial F_2(n,D)}{\partial n} & \dfrac{\partial F_2(n,D)}{\partial D} \end{pmatrix} = \begin{pmatrix} -2\kappa + WD & Wn \\ -2WD & -\gamma_\parallel - 2Wn \end{pmatrix}\,. \tag{7.73}$$

The linear stability analysis of the first stationary solution (7.70) yields from (7.73) the Jacobian

$$\mathcal{L} = \mathcal{L}(n_1^0, D_1^0) = \begin{pmatrix} -2\kappa + WD_0 & 0 \\ -2WD_0 & -\gamma_\parallel \end{pmatrix}\,, \tag{7.74}$$

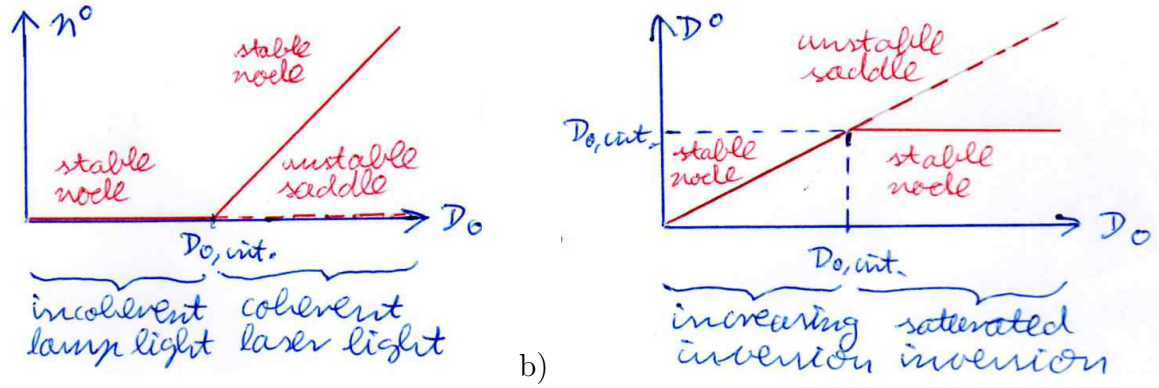

Figure 7.3: Bifurcation diagram of the rate equations (7.54) and (7.57): Increasing the unsaturated population inversion D_0 as the control parameter changes a) the photon number and b) the population inversion. Stability (instabilitiy) corresponds to a solid (dashed) line.

which has the eigenvalues

$$\lambda_{11} = -2\kappa + WD_0\,, \qquad \lambda_{12} = -\gamma_\parallel\,. \tag{7.75}$$

Increasing the control parameter of the unsaturated population inversion (7.36) by increasing the pumping, the stability of the first stationary solution changes as is generic for dynamical systems [53, 55]. For a smaller value of D_0 the first stationary solution (7.70) is a stable *node* due to

$$D_0 < D_{0,\text{crit.}} = \frac{2\kappa}{W}: \qquad \lambda_{11}(D_0) < 0\,, \qquad \lambda_{12}(D_0) < 0\,, \tag{7.76}$$

but for a larger value of D_0 it becomes an unstable *saddle* because of

$$D_0 > D_{0,\text{crit.}} = \frac{2\kappa}{W}: \qquad \lambda_{11}(D_0) > 0\,, \qquad \lambda_{12}(D_0) < 0\,. \tag{7.77}$$

Thus, provided that the pumping reaches the critical unsaturated population inversion $D_0 = D_{0,\text{crit.}}$, two effects occur simultaneously, namely the first stationary solution (7.70) becomes unstable and the second stationary solution (7.71) starts to exist. The linear stability analysis of the second stationary solution (7.71) yields from (7.73) the Jacobian

$$\mathcal{L} = \mathcal{L}(n_2^0, D_2^0) = \begin{pmatrix} 0 & \dfrac{\gamma_\parallel W}{4\kappa}\left(D_0 - \dfrac{2\kappa}{W}\right) \\ -4\kappa & -\dfrac{\gamma_\parallel W}{2\kappa} D_0 \end{pmatrix}, \tag{7.78}$$

which has the eigenvalues

$$\lambda_{2\pm} = -\frac{\gamma_\parallel W D_0}{4\kappa} \pm \sqrt{\left(\frac{\gamma_\parallel W D_0}{4\kappa}\right)^2 - \gamma_\parallel D\left(D_0 - \frac{2\kappa}{W}\right)} < 0\,, \qquad D_0 > D_{0,\text{crit.}}\,. \tag{7.79}$$

Thus, whenever the second stationary solution exists, it represents a stable node. The results of the linear stability analysis are summarized in the *bifurcation diagram* of Fig. 7.3, which shows

how the stationary solutions of both the photon number n and the saturated population inversion D change with increasing the control parameter of the unsaturated population inversion D_0.

As the second stationary solution (7.71) corresponds to coherent laser light, we can now answer the question, which frequency $\tilde{\omega}$ the laser light has. To this end we go back to the evolution equation of the phase (7.58) and demand stationarity:

$$0 = \tilde{\omega} - \omega + (\tilde{\omega} - \Omega)\,\frac{W}{2\gamma_\perp} D \qquad \Longrightarrow \qquad \tilde{\omega} = \frac{\omega + \Omega DW/2\gamma_\perp}{1 + DW/2\gamma_\perp}\,. \tag{7.80}$$

Inserting the stationary population imbalance D from (7.71) into (7.80) yields for the laser frequency the result

$$\tilde{\omega} = \frac{\gamma_\perp \omega + \kappa\Omega}{\gamma_\perp + \kappa}\,. \tag{7.81}$$

It represents a law of levels, where the laser frequency $\tilde{\omega}$ lies between the cavity mode frequency ω and the atomic transition frequency Ω. Which of the latter two frequencies dominates depends on the respective weights in form of the damping constant κ of the cavity mode and the line width $\gamma_\perp$ of the atomic transition. For instance, provided that κ is larger than $\gamma_\perp$ the cavity mode has such a short lifetime that the atomic transition survives and, thus, the laser mode frequency $\tilde{\omega}$ coincides approximately with the atomic transition frequency Ω and vice versa. A special case occurs for the resonance $\omega = \Omega$, when cavity mode frequency and atomic transition frequency coincide, so the laser frequency (7.81) reduces to

$$\tilde{\omega} = \omega = \Omega\,. \tag{7.82}$$

Furthermore, inserting the obtained laser frequency (7.81) in the Einstein coefficient (7.55) yields

$$W = \frac{2\,|g|^2}{\gamma_\perp}\,\frac{(\kappa + \gamma_\perp)^2}{(\omega - \Omega)^2 + (\kappa + \gamma_\perp)^2}\,. \tag{7.83}$$

Thus, the largest Einstein coefficient (7.83) for varying detuning $\Delta = \omega - \Omega$ occurs in the resonant case (7.81), where we get

$$W = \frac{2\,|g|^2}{\gamma_\perp}\,, \tag{7.84}$$

which is independent of both frequencies ω and Ω.

7.7 Adiabatic Elimination

From the linear stability analysis of the rate equations in the previous section we deduce that the dynamical behavior of the laser changes qualitatively provided that the control parameter

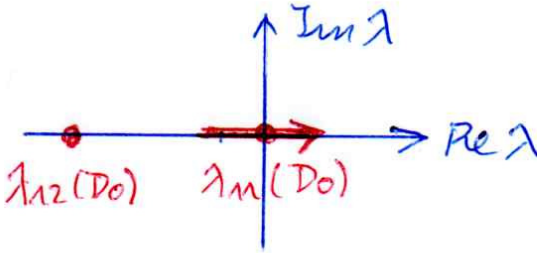

Figure 7.4: Eigenvalues of the first stationary solution (7.75) in the complex plane in the vicinity of the critical control parameter value (7.85).

D_0 reaches the critical value $D_{0,\text{crit.}}$. This motivates in the following to perform a subsequent nonlinear analysis of the equations, which is valid in the neighborhood of this critical control parameter value:

$$D_0 \approx D_{0,\text{crit.}} = \frac{2\kappa}{W} \,. \tag{7.85}$$

In this region of the control parameter the eigenvalues of the first stationary solution (7.75) obey the inequality

$$|\lambda_{11}(D_0)| \ll |\lambda_{12}(D_0)| \tag{7.86}$$

as is illustrated in Fig. 7.4. Each eigenvalue (7.75) generates a typical time scale

$$\tau_n = \frac{1}{|\lambda_{11}(D_0)|} \,, \qquad \tau_D = \frac{1}{|\lambda_{12}(D_0)|} \,. \tag{7.87}$$

Therefore, the inequality of the eigenvalues (7.86) is equivalent to a hierachy of the time scales (7.87):

$$\tau_n \gg \tau_D \,. \tag{7.88}$$

This means that the photon number $n(t)$ as the unstable mode is a slowly varying quantity. Depending on the value of the control parameter D_0 the photon number $n(t)$ slowly decreases, does not change, or slowly increases as is depicted in Fig. 7.5a). Contrary to that the population inversion $D(t)$ as the stable mode is a fast evolving quantity. Therefore, the inversion $D(t)$ quasi instantaneously tends to an equilibrium value

$$D_{\text{eq.}}(t) = D_{\text{eq.}}(n(t)) \,, \tag{7.89}$$

which is presribed by the slowly varying quantity, i.e. the photon number $n(t)$. Note that such an equilibrium (7.89) is known in the theory of dynamical systems as a *center manifold*. In order to obtain the equilibrium value (7.89) one applies the approximation of an adiabatic elimination of the fast decreasing quantity, i.e. the population inversion:

$$\dot{D}_{\text{eq.}}(t) = \gamma_\parallel \big[D_0 - D_{\text{eq.}}(t)\big] - 2W D_{\text{eq.}}(t) n(t) \approx 0 \,. \tag{7.90}$$

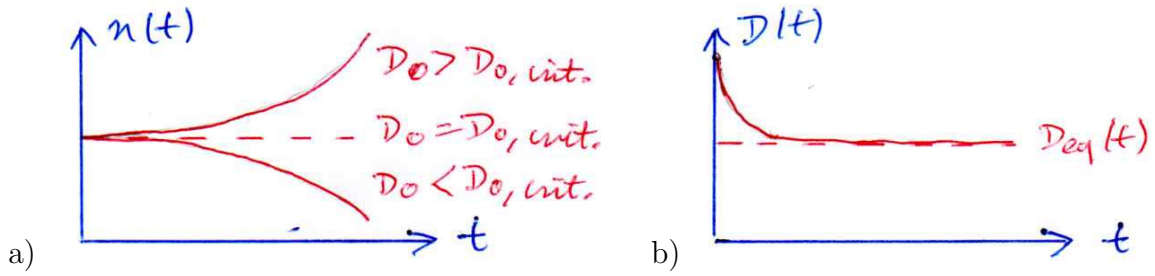

Figure 7.5: a) Photon number $n(t)$ and b) population inversion $D(t)$ change on a slow and a fast time scale, respectively, in the vicinity of the critical control parameter value (7.85).

Solving (7.90) for the saturated population inversion in equilibrium $D_{\text{eq.}}(t)$ yields the quasi-stationary result

$$D_{\text{eq.}}(t) = \frac{D_0}{1 + 2Wn(t)/\gamma_{\|}}\,, \tag{7.91}$$

which is smaller than the unsaturated population inversion D_0 being prescribed by the pumping mechanism as is illustrated by Fig. 7.5b). Near the instability, when the photon number $n(t)$ is smaller, this relation can be further approximated by

$$D_{\text{eq.}}(t) = D_0 - \frac{2WD_0}{\gamma_{\|}} n(t) + \mathcal{O}\left(n(t)^2\right)\,. \tag{7.92}$$

In the language of the self-organization theory *synergetics* one says that the photon number $n(t)$ has *enslaved* the population inversion $D_{\text{eq.}}(t)$ via (7.91) or (7.92) [53]. This has the consequence that the population inversion $D(t)$ no longer represents an independent dynamical variable, so that the two-dimensional system effectively reduces to a one-dimensional one. Indeed, inserting the relation between the population inversion $D_{\text{eq.}}(t)$ and the photon number $n(t)$ in the original ordinary differential equation of the photon number $n(t)$, one results in

$$\dot{n}(t) = \left(-2\kappa + WD_0\right) n(t) - \frac{2W^2 D_0}{\gamma_{\|}}\, n(t)^2 + \mathcal{O}\left(n(t)^2\right)\,. \tag{7.93}$$

This is the *order parameter* equation, which correctly describes the activity of the laser near its threshold. Within the theory of dynamical systems it is classified as the normal form of a *transcritical bifurcation*.

The order parameter equation can be compared with the evolution equation of a classical particle in a conservative potential under the influence of friction:

$$m\ddot{x}(t) = -\alpha\dot{x}(t) - \frac{\partial V\left(x(t)\right)}{\partial x(t)}\,. \tag{7.94}$$

In the overdamped case it is allowed to neglet the inertial force. By choosing an appropriate time scale according to $t' = \alpha t$ and $x'(t') = x\left(t'/\alpha\right)$ we obtain

$$\frac{dx'(t')}{dt'} = -\frac{\partial V\left(x'(t')\right)}{\partial x'(t')}\,. \tag{7.95}$$

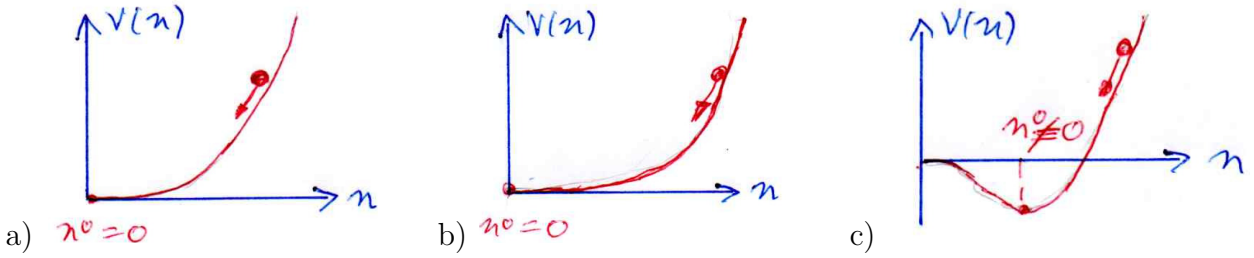

Figure 7.6: Shape of the potential (7.97) changes with the control parameter of the unsaturated population inversion D_0: a) $D_0 < D_{0,\text{crit.}}$, b) $D_0 = D_{0,\text{crit.}}$, and c) $D_0 > D_{0,\text{crit.}}$.

This result shows that the order parameter equation (7.93) can be interpreted as the overdamped mation of a particle in a conservative potential. Indeed, the order parameter equation (7.93) can be reformulated as

$$\dot{n}(t) = -\frac{\partial V(n(t))}{\partial n(t)} \tag{7.96}$$

by introducing the conservative potential

$$V(n) = \frac{1}{2}\left(2\kappa - WD_0\right) n^2 + \frac{2W^2 D_0}{3\gamma_\parallel} n^3 + \mathcal{O}(n^4)\,. \tag{7.97}$$

The dependence of the potential shape on the control parameter D_0 is illustrated in Fig. 7.6. The extrema of the potential correspond to the stationary solution of the order parameter equation (7.93). In case of $D_0 < D_{0,\text{crit.}}$ the equilibrium value of the photon number vanishes, which corresponds to lamp light, see Fig. 7.6a):

$$n_1^0 = 0\,. \tag{7.98}$$

At the critical point $D_0 = D_{0,\text{crit.}}$ it takes longer to reach the equilibrium (7.98) as the potential becomes flatter there, see Fig. 7.6b). This is a generic phenomenon of phase transitions known in the literature as *critical slowing down*. But in case of $D_0 > D_{0,\text{crit.}}$ the photon number acquires a positive value

$$n_2^0 = \frac{\gamma_\parallel}{2WD_0}\left(D_0 - \frac{2\kappa}{W}\right) \approx \frac{\gamma_\parallel}{4\kappa}\left(D_0 - \frac{2\kappa}{W}\right)\,, \tag{7.99}$$

which characterizes the laser light, see Fig. 7.6c). In this way one recovers the results of the linear stability analysis in the previous section from the nonlinear analysis. But in addition it is possible to integrate the order parameter equation (7.93) analytically by applying the method of separating variables. Thus, one obtains an approximation for the time evolution of the photon number $n(t)$ and the inversion $D(t)$ which is valid near the instability (7.85).

Chapter 8

Quantum Theory of Laser

The semiclassical laser theory allows to describe many properties of the laser, which ultimately originate from the induced emission and the absorption as elementary processes of the light-matter interaction. For instance, we found both wthin a linear stability analysis and a nonlinear analysis that there exists a critical pumping threshold above which the laser activity sets in, but below which no light exists. The latter finding is insofar unsatisfactorialy as the semiclassical laser theory does not cover the description of usual lamp light, which is based on the spontaneous emission and which is, thus, only accessible within a full quantum mechanical treatment. This means that, apart from the damping of the respective physical quantities, also their fluctuations have to be taken into account systematically. With this it is then possible to analyze in detail the fluctuation properties of the both the lamp and the laser light as well as the peculiar coherence properties of the laser light.

To this end we set up in a first step the quantum Langevin equations for the homogeneous single-mode laser and perform systematically an adiabatic elimination of the matter operators at zero temperature up to leading order in the light-matter interaction strength. With this we obtain a redual quantum Langevin equation for the photon operator, which contains apart from deterministic terms also an additive noise term, whose strength represents the spontaneous emission from all excited atoms. Subsequently we analyze the solution of the quantum Langevin equation in the immediate vicinity of the classical stationary solutions found within the linear stability analysis in the previous chapter. In this way we derive both for the lamp and the laser light the seminal Schawlow-Townes limit, i.e. the minimal spectral linewidth of a laser, which can not be undershot.

8.1 Homogeneous Single-Mode Laser

Let us start with the basic equations for the quantum theory of the homogeneous single-mode laser. In order to simplify the following discussion we assume now to be at resonance, i.e. the cavity mode frequency ω coincides with the atomic transition frequency Ω. With this we obtain

from (7.2), (7.4), and (7.5):

$$\frac{\partial}{\partial t}\,\hat{b}(t) = (-i\omega-\kappa)\,\hat{b}(t) - ig^*\sum_\mu \hat{\alpha}_\mu(t) + \hat{\Gamma}_b(t)\,, \tag{8.1}$$

$$\frac{\partial}{\partial t}\,\hat{\alpha}_\mu(t) = (-i\omega-\gamma_\perp)\,\hat{\alpha}_\mu(t) + ig\hat{d}_\mu(t)\hat{b}(t) + \hat{\Gamma}_{\alpha_\mu}(t)\,, \tag{8.2}$$

$$\frac{\partial}{\partial t}\,\hat{d}_\mu(t) = \gamma_\parallel\left[d_0-\hat{d}_\mu(t)\right] + 2i\left[g^*\hat{b}^\dagger(t)\hat{\alpha}_\mu(t) - g\hat{\alpha}^\dagger_\mu(t)\hat{b}(t)\right] + \hat{\Gamma}_{d_\mu}(t)\,. \tag{8.3}$$

Here the bath expectation values of the respective Langevin operators are defined in (7.6)–(7.15). They reveal the Markow property, i.e. a short memory of the Langevin operators, which turns out to be crucial in the following as it allows to work out an approximative solution for the quantum Langevin equation of the laser. Namely, the structural similiarity between those quantum mechanical equations and the previous semiclassical laser equations (7.31)–(7.33) motivates us to work out an adiabatic elimination solution strategy along similar lines as in the previous chapter. To this end we start with the transformation into a co-rotating frame:

$$\begin{aligned}\hat{b}(t) = \hat{\tilde{b}}(t)e^{-i\omega t}\,,\;\; \hat{b}^\dagger(t) = \hat{\tilde{b}}^\dagger(t)e^{i\omega t}\,,\\ \hat{\alpha}_\mu(t) = \hat{\tilde{\alpha}}_\mu(t)e^{-i\omega t}\,,\;\; \hat{\alpha}^\dagger_\mu(t) = \hat{\tilde{\alpha}}^\dagger_\mu(t)e^{i\omega t}\,,\;\; \hat{d}_\mu(t) = \hat{\tilde{d}}_\mu(t)\,,\end{aligned} \tag{8.4}$$

which also necessitates a corresponding transformation of the Langevin operators:

$$\hat{\Gamma}_b(t) = \hat{\tilde{\Gamma}}_b(t)e^{-i\omega t}\,, \qquad \hat{\Gamma}_{\alpha_\mu}(t) = \hat{\tilde{\Gamma}}_{\alpha_\mu}(t)e^{-i\omega t}\,, \qquad \hat{\Gamma}_{d_\mu}(t) = \hat{\tilde{\Gamma}}_{d_\mu}(t)\,. \tag{8.5}$$

Inserting (8.4) and (8.5) in (8.1)–(8.3) as well as omitting the tilde for all quantities we end up with

$$\frac{\partial}{\partial t}\,\hat{b}(t) = -\kappa\hat{b}(t) - ig^*\sum_\mu \hat{\alpha}_\mu(t) + \hat{\Gamma}_b(t)\,, \tag{8.6}$$

$$\frac{\partial}{\partial t}\,\hat{\alpha}_\mu(t) = -\gamma_\perp\hat{\alpha}_\mu(t) + ig\hat{d}_\mu(t)\hat{b}(t) + \hat{\Gamma}_{\alpha_\mu}(t)\,, \tag{8.7}$$

$$\frac{\partial}{\partial t}\,\hat{d}_\mu(t) = \gamma_\parallel\left[d_0-\hat{d}_\mu(t)\right] + 2i\left[g^*\hat{b}^\dagger(t)\hat{\alpha}_\mu(t) - g\hat{\alpha}^\dagger_\mu(t)\hat{b}(t)\right] + \hat{\Gamma}_{d_\mu}(t)\,. \tag{8.8}$$

Note that the transformation of the Langevin operators (8.5) does not affect the bath expectation values (7.6)–(7.15) due to the assume resonance. In this co-rotating frame the damping constants κ, $\gamma_\perp$, and $\gamma_\parallel$ determine the time scales upon which the respective quantities vary. Due to (7.46) and (7.47) the inequality of the damping constants

$$\kappa \ll \gamma_\perp\,,\,\gamma_\parallel \tag{8.9}$$

implies a time scale hierarchy. Whereas the field operator $\hat{b}(t)$ varies slowly, the matter operators $\hat{\alpha}_\mu(t)$, $\hat{d}_\mu(t)$ vary fast. This motivates to perform an adiabatic elimination of the matter operators $\hat{\alpha}_\mu(t)$, $\hat{d}_\mu(t)$ as follows. The adiabatic elimination of $\hat{\alpha}_\mu(t)$

$$\frac{\partial}{\partial t}\,\hat{\alpha}_\mu(t) \approx 0 \tag{8.10}$$

yields with (8.7):

$$\hat{\alpha}_\mu(t) = i\,\frac{g}{\gamma_\perp}\,\hat{d}_\mu(t)\hat{b}(t) + \frac{1}{\gamma_\perp}\,\hat{\Gamma}_{\alpha_\mu}(t)\,. \tag{8.11}$$

Inserting (8.11) into (8.8) yields together with an adiabatic elimination of $\hat{d}_\mu(t)$:

$$\begin{aligned}\frac{\partial}{\partial t}\,\hat{d}_\mu(t) &= \gamma_\parallel\left[d_0 - \hat{d}_\mu(t)\right] - \frac{4|g|^2}{\gamma_\perp}\,\hat{b}^\dagger(t)\hat{b}(t)\hat{d}_\mu(t) + \hat{\Gamma}_{d_\mu}(t) \\ &\quad + \frac{2i}{\gamma_\perp}\,\left[g^*\hat{b}^\dagger(t)\hat{\Gamma}_{\alpha_\mu}(t) - g\hat{\Gamma}^\dagger_{\alpha_\mu}(t)\hat{b}(t)\right] \approx 0\,. \end{aligned}\tag{8.12}$$

In the vicinity of the laser threshold the photon number operator

$$\hat{n}(t) = \hat{b}^\dagger(t)\hat{b}(t) \tag{8.13}$$

is small, thus we conclude from (8.12)

$$\hat{d}_\mu(t) \approx d_0\left[1 - \frac{4|g|^2}{\gamma_\perp\gamma_\parallel}\,\hat{b}^\dagger(t)\hat{b}(t)\right] + \text{fluctuating terms}\,. \tag{8.14}$$

Now we have to insert (8.14) in (8.11) and, subsequently (8.11) in (8.6) in order to obtain a resulting evolution equation for the field mode operator $\hat{b}(t)$. By doing so, we observe that the fluctuating terms, which have not been further specified in (8.14), would lead to noise terms for the field mode operator $\hat{b}(t)$, which are of quadratic or higher order in the light-matter interaction strength g. As we restrict ourselves here to noise terms in (8.6), which are at most of first order in g, we neglect the unspecified noise terms in (8.14). Note that the noise terms in (8.14) would lead to multiplicative noise in (8.6), so their neglection simplifies considerably the subsequent analysis. With this the adiabatic elimination of the matter operators $\hat{\alpha}_\mu(t)$ yields at first

$$\frac{\partial}{\partial t}\,\hat{b}(t) = -\kappa\hat{b}(t) - ig^*\sum_\mu\left\{\frac{igd_0}{\gamma_\perp}\left[1 - \frac{4|g|^2}{\gamma_\perp\gamma_\parallel}\,\hat{b}^\dagger(t)\hat{b}(t)\right]\hat{b}(t) + \frac{1}{\gamma_\perp}\,\hat{\Gamma}_{\alpha_\mu}(t)\right\} + \hat{\Gamma}_b(t)\,. \tag{8.15}$$

Using the unsaturated population inversion (7.36) with the atom number (7.37) as well as the Einstein coefficient (7.84), the final quantum Langevin equation for the field mode operator $\hat{b}(t)$ reads:

$$\frac{\partial}{\partial t}\,\hat{b}(t) = \left(-\kappa + \frac{WD_0}{2}\right)\hat{b}(t) - \frac{W^2D_0}{\gamma_\parallel}\,\hat{b}^\dagger(t)\hat{b}^2(t) + \hat{\Gamma}_{\text{tot}}(t)\,. \tag{8.16}$$

Provided that the cavity mode is occupied with a large number of photons, the second quantized photon operators could be substituted by c-numbers according to

$$\hat{b}(t) \approx \sqrt{n(t)}\,, \qquad \hat{b}^\dagger(t) \approx \sqrt{n(t)}\,, \tag{8.17}$$

so the deterministic part of the quantum Langevin equation (8.16) turns out to be equivalent to the order parameter equation for the photon number $n(t)$ derived in the previous chapter in Eq. (7.93). Furthermore, we note that the resulting Langevin operator in (8.16) is given by

$$\hat{\Gamma}_{\text{tot}}(t) = \hat{\Gamma}_b(t) - i\frac{g^*}{\gamma_\perp}\,\sum_\mu\hat{\Gamma}_{\alpha_\mu}(t)\,. \tag{8.18}$$

Its bath expectation values follow from those of the Langevin operators $\hat{\Gamma}_b(t)$ and $\hat{\Gamma}_{\alpha_\mu}(t)$, which are defined in (7.6)–(7.12). The trivial bath expectation values read

$$\left\langle \hat{\Gamma}_{\rm tot}(t) \right\rangle_{\rm B} = \left\langle \hat{\Gamma}^\dagger_{\rm tot}(t) \right\rangle_{\rm B} = \left\langle \hat{\Gamma}_{\rm tot}(t)\hat{\Gamma}_{\rm tot}(t') \right\rangle_{\rm B} = \left\langle \hat{\Gamma}^\dagger_{\rm tot}(t)\hat{\Gamma}^\dagger_{\rm tot}(t') \right\rangle_{\rm B} = 0\,. \tag{8.19}$$

and the non-trivial bath average yields at first

$$\left\langle \hat{\Gamma}^\dagger_{\rm tot}(t)\hat{\Gamma}_{\rm tot}(t') \right\rangle_{\rm B} = \left\langle \hat{\Gamma}^\dagger_b(t)\hat{\Gamma}_b(t') \right\rangle_{\rm B} + \frac{|g|^2}{\gamma_\perp^2} \sum_\mu \sum_{\mu'} \left\langle \hat{\Gamma}^\dagger_{\alpha_\mu}(t)\hat{\Gamma}_{\alpha_{\mu'}}(t') \right\rangle_{\rm B}\,. \tag{8.20}$$

Inserting (7.9) and (7.12) we get again a correlation function with Markov property

$$\left\langle \hat{\Gamma}^\dagger_{\rm tot}(t)\hat{\Gamma}_{\rm tot}(t') \right\rangle_{\rm B} = \hat{Q}\delta(t-t') \tag{8.21}$$

with the operator-valued amplitude

$$\hat{Q} = 2\kappa\,\overline{n}_\omega(T) + \frac{|g|^2}{\gamma_\perp^2} \sum_\mu \left\{ \gamma_\perp \left[1 + \langle \hat{d}_\mu(t) \rangle_{\rm B} \right] + \frac{1}{2}\gamma_\parallel \left[d_0 - \langle \hat{d}_\mu(t) \rangle_{\rm B} \right] \right\}\,. \tag{8.22}$$

The latter involves the bath average of the atomic population inversion, which follows from (8.14) and depends on the thermal average of the photon number operator (8.13) via

$$\langle \hat{d}_\mu(t) \rangle_{\rm B} = d_0 \left[1 - \frac{4|g|^2}{\gamma_\perp\gamma_\parallel}\, \langle \hat{n}(t) \rangle_{\rm B} \right] \tag{8.23}$$

as the bath average of each Langevin operator vanishes according to (7.6). Furthermore, performing the sum over all atoms in (8.22) with the help of (7.36) and (8.23), e.g.

$$\sum_\mu \langle \hat{d}_\mu(t) \rangle_{\rm B} = D_0 \left[1 - \frac{4|g|^2}{\gamma_\perp\gamma_\parallel}\, \langle \hat{n}(t) \rangle_{\rm B} \right]\,, \tag{8.24}$$

as well as taking into account (7.37) the operator-valued amplitude (8.22) yields

$$\hat{Q} = 2\kappa\,\overline{n}_\omega(T) + \frac{|g|^2}{\gamma_\perp}(N + D_0) + \frac{2|g|^4(\gamma_\parallel - 2\gamma_\perp)}{\gamma_\perp^3\gamma_\parallel}\, D_0\, \langle \hat{n}(t) \rangle_{\rm B}\,. \tag{8.25}$$

As already mentioned above, concerning the noise we restrict ourselves to the leading order in the light-matter interaction strength g, which is of quadratic order, so the last term in (8.25) can be dropped. Again this has the consequence that the more complicated multiplicative noise term is neglected, which simplifies the further considerations. Provided that the temperature T is small enough, we can neglect in addition also the thermal contribution and the operator-valued amplitude (8.25) reduces to the c-number

$$\hat{Q} = \frac{|g|^2}{\gamma_\perp}(N + D_0)\,. \tag{8.26}$$

Thus, under these assumptions the noise term in the quantum Langevin equation (8.16) turns out to be additive due to (8.21) and (8.26). However, the question arises how the c-number noise

strength (8.26) can be physically interpreted. To this end we recognize that (8.26) represents the product of two factors. The first is identified to be the Einstein coefficient W defined for vanishing detuning in (7.84), whereas the second one is recognized to coincide with the number of excited atoms N_2 due to combining (7.61) and (7.64), so we conclude

$$\hat{Q} = W N_2 \,. \tag{8.27}$$

Therefore we arrive at the physical interpretation that the c-number noise strength (8.27) corresponds to the spontaneous emission rate of all excited atoms.

8.2 Schawlow-Townes Limit

Let us analyze now the residual quantum Langevin equation of the photon operator (8.16). In order to simplify the discussion we focus here upon the case that we are below the threshold with a small number of photons, so that the nonlinear term is negligible. In that case the nonlinear Langevin equation (8.16) reduces to a linear one

$$\frac{\partial}{\partial t}\,\hat{b}(t) = -\tilde{\kappa}\hat{b}(t) + \hat{\Gamma}_{\rm tot}(t)\,, \tag{8.28}$$

where we have introduced the abbreviation

$$\tilde{\kappa} = \kappa - \frac{W D_0}{2}\,. \tag{8.29}$$

As the damping constant κ desribes the losses of the electric field due to resonator losses without light-matter interaction, one is tempted to interpret (8.29) as the effective damping constant in case that the light-matter interaction is taken into account. This would mean then that increasing the control parameter D_0 would correspond to a reduced laser linewidth. In order to justify this interpretation we determine

for both lamp and laser light. Here we follow the physical notion to analyze the fluctuations of the photon operators around the stationary solutions of the previous chapter. To this end we perform the ansatz

$$\hat{b}(t) = \sqrt{n^0} + \delta\hat{b}(t)\,, \tag{8.30}$$

where we have for lamp light according to

Appendix A

Harmonic Oscillator

The harmonic oscillator represents a standard quantum mechanical model with which it is possible to describe quite successfully, for instance, collective oscillations in molecules or in solids. The Hamilton operator of a one-dimensional harmonic oscillator with mass M and frequency ω reads

$$\hat{H} = \frac{\hat{p}^2}{2M} + \frac{M}{2}\,\omega^2 \hat{x}^2\,, \tag{A.1}$$

where one demands non-trivial commutation relations between the coordinate operator $\hat{q}$ and the momentum operator $\hat{p}$:

$$\big[\hat{x},\hat{x}\big]_- = \big[\hat{p},\hat{p}\big]_- = 0\,, \qquad \big[\hat{p},\hat{x}\big]_- = \frac{\hbar}{i}\,. \tag{A.2}$$

The problem is now to solve the eigenvalue problem of the Hamilton operator

$$\hat{H}|\alpha\rangle = E_\alpha|\alpha\rangle\,, \tag{A.3}$$

i.e. to determine how the energy eigenvalues E_α and the energy eigenfunctions $|\alpha\rangle$ depend on the quantum number α. Usually this representation-free eigenvalue problem (A.3) is transformed into the coordinate representation, so it amounts to solve the corresponding Schrödinger equation by taking into account the appropriate Dirichlet boundary condition. In the following, however, we proceed differently by solving the representation-free eigenvalue problem (A.3) directly by taking into account the commutator relations (A.2).

At first, the two hermitian operators $\hat{x}$ and $\hat{p}$ are transformed into two new operators $\hat{a}^\dagger$ and $\hat{a}$, which are adjoint with respect to each other:

$$\hat{a}^\dagger = \sqrt{\frac{M\omega}{2\hbar}}\,\left(\hat{x} - \frac{i}{M\omega}\,\hat{p}\right)\,, \qquad \hat{a} = \sqrt{\frac{M\omega}{2\hbar}}\,\left(\hat{x} + \frac{i}{M\omega}\,\hat{p}\right)\,. \tag{A.4}$$

The inverse transformation reads correspondingly

$$\hat{x} = \sqrt{\frac{\hbar}{2M\omega}}\,\left(\hat{a}^\dagger + \hat{a}\right)\,, \qquad \hat{p} = \sqrt{\frac{\hbar M\omega}{2}}\,i\,\left(\hat{a}^\dagger - \hat{a}\right)\,. \tag{A.5}$$

Here the physical dimension of the coordinate operator $\hat{x}$ is provided by the oscillator length $\sqrt{\hbar/(2M\omega)}$, whereas the corresponding one $\sqrt{\hbar M\omega/2}$ of the momentum operator $\hat{p}$ is related to the oscillator length via the Heisenberg uncertainty relation. Inserting (A.5) into (A.1), the Hamilton operator of the harmonic oscillator can be expressed in terms of the new operators $\hat{a}^\dagger$ and $\hat{a}$, yielding

$$\hat{H} = \frac{\hbar\omega}{2}\left(\hat{a}^\dagger\hat{a} + \hat{a}\hat{a}^\dagger\right). \tag{A.6}$$

Furthermore, the transformation (A.4) allows to deduce from (A.2) the commutation relations between the new operators $\hat{a}^\dagger$ and $\hat{a}$:

$$\left[\hat{a},\hat{a}\right]_- = \left[\hat{a}^\dagger,\hat{a}^\dagger\right]_- = 0\,, \qquad \left[\hat{a},\hat{a}^\dagger\right]_- = 1\,. \tag{A.7}$$

Using (A.7) the Hamilton operator of the harmonic oscillator (A.6) reduces to

$$\hat{H} = \hbar\omega\left(\hat{n} + \frac{1}{2}\right), \tag{A.8}$$

where the zero-point energy $\hbar\omega/2$ and the operator

$$\hat{n} = \hat{a}^\dagger\hat{a} \tag{A.9}$$

appear. Applying the ABC-rule for commutators (2.61) we obtain the commutation relations for the operator (A.9):

$$\left[\hat{n},\hat{a}^\dagger\right]_- = \hat{a}^\dagger\,, \tag{A.10}$$

$$\left[\hat{n},\hat{a}\right]_- = -\hat{a}\,. \tag{A.11}$$

Let us now consider the eigenvalue problem of the operator (A.9):

$$\hat{n}|\lambda\rangle = \lambda|\lambda\rangle \tag{A.12}$$

As the operator (A.9) is hermitian, its eigenvalues λ must be real. Furthermore, the commutation relations (A.10) and (A.11) allow to investigate which consequences occur once the operators $\hat{a}^\dagger$ and $\hat{a}$ are applied to the eigenfunctions $|\lambda\rangle$. On the one hand we read off from (A.10) and (A.12)

$$\hat{n}\hat{a}^\dagger|\lambda\rangle = \left(\hat{a}^\dagger\hat{n} + \hat{a}^\dagger\right)|\lambda\rangle = (\lambda+1)\hat{a}^\dagger|\lambda\rangle \qquad \Longrightarrow \qquad \hat{a}^\dagger|\lambda\rangle \sim |\lambda+1\rangle\,, \tag{A.13}$$

on the other hand we conclude from (A.11) and (A.12)

$$\hat{n}\hat{a}|\lambda\rangle = \left(\hat{a}\hat{n} - \hat{a}\right) = (\lambda-1)\hat{a}|\lambda\rangle \qquad \Longrightarrow \qquad \hat{a}|\lambda\rangle \sim |\lambda-1\rangle\,. \tag{A.14}$$

Thus, the operators $\hat{a}^\dagger$ and $\hat{a}$ can be considered as ladder operators, which allow to climb up or down the ladder of eigenfunctions $|\lambda\rangle$. Applying the raising (lowering) ladder operator $\hat{a}^\dagger$ ($\hat{a}$) to $|\lambda\rangle$ yields an eigenfunction corresponding to an eigenvalue which is increased (decreased) by one, see Fig. A.1

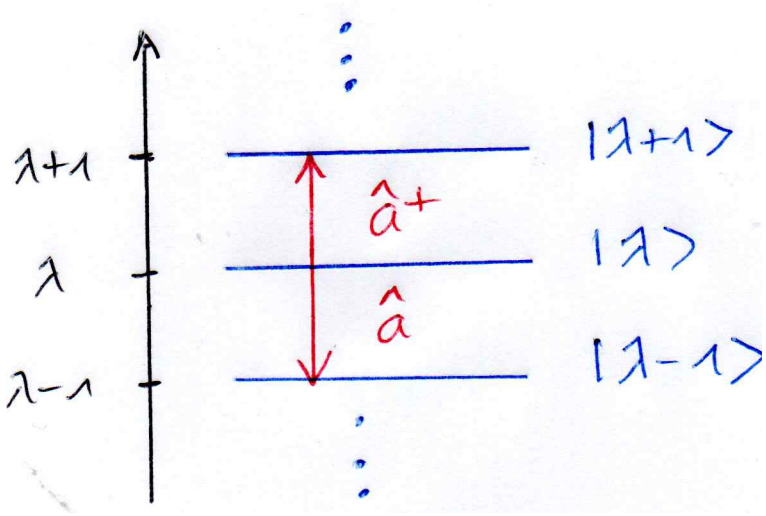

Figure A.1: Raising (lowering) operator $\hat{a}^\dagger$ ($\hat{a}$) increases (decreases) the quantum number λ of the harmonic oscillator by one.

Furthermore, one can show that the eigenvalues λ of the operator $\hat{n}$ are always positive by taking into account (A.9) and (A.12) and by assuming without loss of generality that the eigenfunctions $|\lambda\rangle$ are normalized:

$$0 \leq \langle \hat{a}\lambda | \hat{a}\lambda \rangle = \langle \lambda | \hat{a}^\dagger \hat{a} | \lambda \rangle = \langle \lambda | \hat{n} | \lambda \rangle = \lambda \langle \lambda | \lambda \rangle = \lambda \,. \tag{A.15}$$

From (A.14) and (A.15) we conclude that the eigenvalues λ are given by positive integer number including zero:

$$\lambda = n = 0, 1, 2, \ldots \,. \tag{A.16}$$

If there were a positive, non-integer eigenvalue λ, one could apply iteratively the lowering ladder operator $\hat{a}$ and reduce in this way the eigenvalue due to (A.14) until it would become negative. But this would then contradict the inequality (A.15). Thus, due to this contradiction proof, there must be a ground state $|0\rangle$ with the property

$$\hat{a}|0\rangle = 0 \qquad \Longleftrightarrow \qquad \langle 0 | \hat{a}^\dagger = 0 \,. \tag{A.17}$$

Based on this we construct now eigenfunctions $|n\rangle$, which are normalized

$$\langle n | n \rangle = 1 \,. \tag{A.18}$$

At first, we deduce from (A.7), (A.9), (A.12), (A.16), and (A.18):

$$\langle \hat{a}^\dagger n | \hat{a}^\dagger n \rangle = \langle n | \hat{a}\hat{a}^\dagger | n \rangle = \langle n | \big(\hat{a}^\dagger \hat{a} + 1 \big) | n \rangle = \langle n | \big(\hat{n} + 1 \big) | n \rangle = n + 1 \,. \tag{A.19}$$

From (A.13), (A.16), (A.18), and (A.19) follows a rule how applying the raising ladder operator $\hat{a}^\dagger$ upon the normalized eigenfunction $|n\rangle$ yields the next normalized eigenfunction $|n+1\rangle$:

$$\hat{a}^\dagger |n\rangle = C_n |n+1\rangle \quad \Longrightarrow \quad C_n^2 \langle n+1 | n+1 \rangle = n + 1 \quad \Longrightarrow \quad \hat{a}^\dagger |n\rangle = \sqrt{n+1}\, |n+1\rangle \,. \tag{A.20}$$

And then iterating (A.20) yields a prescription how the eigenfunctions $|n\rangle$ can be constructed from the ground state $|0\rangle$ defined by (A.17):

$$|n\rangle = \frac{1}{\sqrt{n}}\,\hat{a}^\dagger|n-1\rangle = \frac{1}{\sqrt{n(n-1)}}\left(\hat{a}^2\right)^2|n-2\rangle = \ldots \quad \Longrightarrow \quad |n\rangle = \frac{1}{\sqrt{n!}}\left(\hat{a}^\dagger\right)^n|0\rangle\,. \tag{A.21}$$

Apart from being normalized according to (A.18), two different eigenfunctions $|n\rangle$ and $|n'\rangle$ are orthogonal:

$$\langle n|n'\rangle = 0\,, \qquad n \neq n'\,. \tag{A.22}$$

Indeed, we have due to the eigenvalue problem (A.12) with (A.16) and the hermiticity of the operator (A.9)

$$n\langle n|n'\rangle = \langle \hat{n}n|n'\rangle = \langle n|\hat{n}n'\rangle = n'\langle n|n'\rangle\,, \tag{A.23}$$

which implies (A.22). Thus, (A.18) and (A.22) can be summarized by the orthonormality relation

$$\langle n|n'\rangle = \delta_{n,n'}\,. \tag{A.24}$$

Furthermore, the eigenfunctions (A.21) represent a basis for the Hilbert space of the quantum mechanical harmonic oscillator, so they fulfill the completeness relation

$$\sum_{n=0}^{\infty} |n\rangle\langle n| = 1\,. \tag{A.25}$$

For the sake of completeness we also determine the action of the lowering ladder operator $\hat{a}$ upon the eigenfunction $|n\rangle$. At first we obtain from (A.12) with (A.16) and (A.18)

$$\langle \hat{a}n|\hat{a}n\rangle = \langle n|\hat{a}^\dagger\hat{a}|n\rangle = \langle n|\hat{n}|n\rangle = n\,. \tag{A.26}$$

Thus, we conclude from (A.14) and (A.26)

$$\hat{a}|n\rangle = D_n|n-1\rangle \quad \Longrightarrow \quad D_n^2\langle n-1|n-1\rangle = n \quad \Longrightarrow \quad \hat{a}|n\rangle = \sqrt{n}\,|n-1\rangle\,. \tag{A.27}$$

Finally, we read off from (A.8), (A.9), (A.12), and (A.16) the energy eigenvalues of the harmonic oscillator

$$E_n = \hbar\omega\left(n + \frac{1}{2}\right)\,. \tag{A.28}$$

Appendix B

Values of Riemann Zeta Function

Here we consider the generating function

$$I(k) = \int_0^\infty dx \, \frac{\sin(kx)}{e^x - 1} \, . \tag{B.1}$$

A Taylor expansion of the sine-function in the numerator yields

$$I(k) = \sum_{n=0}^{\infty} \frac{(-1)^n}{(2n+1)!} \, k^{2n+1} \, I_n \, , \tag{B.2}$$

so the integrals

$$I_n = \int_0^\infty dx \, \frac{x^{2n+1}}{e^x - 1} \tag{B.3}$$

follow from the knowledge of the generating function via

$$I_n = \, (-1)^n \, \frac{\partial^{2n+1}}{\partial k^{2n+1}} \, I(k) \Big|_{k=0} \, . \tag{B.4}$$

Furthermore, from the geometric series follows a useful series representation for the Bose-Einstein function

$$\frac{1}{e^x - 1} = \sum_{m=1}^{\infty} e^{-mx} \tag{B.5}$$

and taking into account the Schwinger trick (2.184) we obtain from (B.3)

$$I_n = (2n+1)! \, \zeta(2n+2) \tag{B.6}$$

with the Riemann zeta (2.222). Thus, together with (B.4) we recognize

$$\zeta(2n+2) = \, \frac{(-1)^n}{(2n+1)!} \, \frac{\partial^{2n+1}}{\partial k^{2n+1}} \, I(k) \Big|_{k=0} \, , \qquad n \in \mathbb{N}_0 \, , \tag{B.7}$$

i.e. the Riemann zeta function for even integers follows from the generating function (B.1).

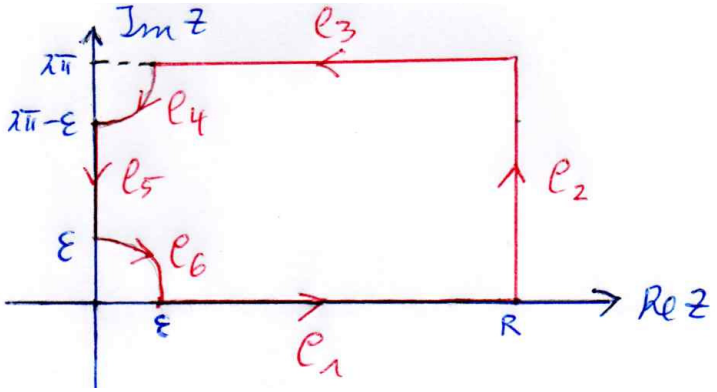

Figure B.1: The Dirac comb (2.212) is an infinite series of Dirac delta functions with unity spacing.

In order to calculate the generating function (B.1) we proceed as follows. At first we write $\sin(kx)$ as the imaginary part of e^{ikx}, so we can restate (B.1) as

$$I(k) = \lim_{\epsilon \downarrow 0} \mathrm{Im} \int_\epsilon^\infty dx \, \frac{e^{ikx}}{e^x - 1} \,. \tag{B.8}$$

In order to evaluate the integral we consider the following contour integral in the complex plane:

$$\oint_{\mathcal{C}(\epsilon,R)} dz \, \frac{e^{ikz}}{e^z - 1} \,. \tag{B.9}$$

Here $\mathcal{C}(\epsilon, R)$ denotes the contour from ϵ to R, then to $R + 2\pi i$, then to $\epsilon + 2\pi i$, then we go to the point $2\pi i - \epsilon i$ avoiding the pole at $2\pi i$ by taking a clockwise quarter circle with radius ϵ and center $2\pi i$. From there we go to ϵi, and finally we return to ϵ, avoiding the pole at zero by taking a clockwise quarter circle with radius ϵ and center zero, see Fig. B.1. Because there are no poles in the integration contour we conclude from the residue theorem

$$\oint_{\mathcal{C}(\epsilon,R)} dz \, \frac{e^{ikz}}{e^z - 1} = 0 \tag{B.10}$$

for any $R > \epsilon$. In the limit $R \to \infty$ the integral along $\mathcal{C}_2$ vanishes, and the integrals over $\mathcal{C}_1$ and $\mathcal{C}_3$ yield together:

$$\lim_{R\to\infty} \left(\int_{\mathcal{C}_1} dz \, \frac{e^{ikz}}{e^z - 1} + \int_{\mathcal{C}_3} dz \, \frac{e^{ikz}}{e^z - 1} \right) = \left(1 - e^{-2\pi k}\right) \int_\epsilon^\infty dx \, \frac{e^{ikx}}{e^x - 1} \,. \tag{B.11}$$

Correspondingly, we get for the integral over $\mathcal{C}_5$:

$$\int_{\mathcal{C}_5} dz \, \frac{e^{ikz}}{e^z - 1} = -i \int_\epsilon^{2\pi-\epsilon} dy \, \frac{e^{-ky}}{e^{iy} - 1} \,. \tag{B.12}$$

And, finally, for the integrals over $\mathcal{C}_4$ and $\mathcal{C}_6$ we use the fact that the integrations over clockwise quarter circles around simple poles are given by $-i\pi/2$ times the residues at the poles:

$$\int_{\mathcal{C}_4} dz \, \frac{e^{ikz}}{e^z - 1} = -i\frac{\pi}{2} \operatorname*{Res}_{z=2\pi i} \frac{e^{ikz}}{e^z - 1} = -i\frac{\pi}{2} \, e^{-2\pi k} \,, \tag{B.13}$$

$$\int_{\mathcal{C}_6} dz \, \frac{e^{ikz}}{e^z - 1} = -i\frac{\pi}{2} \operatorname*{Res}_{z=0} \frac{e^{ikz}}{e^z - 1} = -i\frac{\pi}{2} \,. \tag{B.14}$$

We remember that the residue of a function $f(z)$ at z_0 is defined as an anti-clockwise integral along a circle $\mathcal{C}$ around z_0, i.e.

$$\operatorname*{Res}_{z=z_0} f(z) = \frac{1}{2\pi i} \int_{\mathcal{C}} dz\, f(z)\,, \tag{B.15}$$

which is practically evaluated in case of $f(z)$ having a simple pole at z_0 according to

$$\operatorname*{Res}_{z=z_0} f(z) = \lim_{z\to z_0} (z - z_0)\, f(z)\,. \tag{B.16}$$

Thus, we conclude from (B.8)–(B.14):

$$\left(1 - e^{-2\pi k}\right) \int_{\epsilon}^{\infty} dx\, \frac{e^{ikx}}{e^x - 1} - \frac{1}{2} \int_{\epsilon}^{2\pi-\epsilon} dy\, e^{-ky} - \frac{\pi}{2}\, \left(1 + e^{-2\pi k}\right) = 0\,. \tag{B.17}$$

In the limit $\epsilon \downarrow 0$ we then finally get for the generating function (B.8):

$$I(k) = -\frac{1}{2k} + \frac{\pi}{2}\, \coth(\pi k)\,. \tag{B.18}$$

Using the Taylor expansion of the hyperbolic function

$$\coth x = \frac{1}{x} + \frac{1}{3}\, x - \frac{1}{45}\, x^3 + \ldots\,, \tag{B.19}$$

we obtain from (B.7) the special values of the Riemann zeta function for even integers:

$$\zeta(2) = \frac{\pi^2}{6}\,, \tag{B.20}$$

$$\zeta(4) = \frac{\pi^4}{90}\,. \tag{B.21}$$

Appendix C

Atomic Units

The Bohr-Sommerfeld model for the hydrogen atom assumes that the electron is held in a circular orbit of radius a by electrostatic attraction from the nucleus. The centripetal force is equal to the Coulomb force, e.g.

$$\frac{Mv^2}{a} = \frac{e^2}{4\pi\epsilon_0 a^2}\,, \tag{C.1}$$

where M and e denote the mass and the charge of the electron, respectively. This equation determines the velocity v of the electron at any radius a:

$$v = \sqrt{\frac{e^2}{4\pi\epsilon_0 Ma}}\,. \tag{C.2}$$

The total energy E of the electron

$$E = \frac{1}{2}\,Mv^2 - \frac{e^2}{4\pi\epsilon_0 a} \tag{C.3}$$

reduces due to (C.2) for any radius a to

$$E = -\frac{e^2}{8\pi\epsilon_0 a}\,. \tag{C.4}$$

Thus, the total energy (C.4) is half the potential energy, i.e. it is negative and inversely proportional to a. This means that it takes energy to pull the orbiting electron away from the proton. For infinite values of a the energy is zero, corresponding to a motionless electron infinitely far from the proton.

According to the Bohr-Sommerfeld condition the angular momentum of the electron

$$L = Mva \tag{C.5}$$

is not arbitrary but quantised via

$$L = n\hbar \tag{C.6}$$

with the principal quantum number $n \in \mathbb{N}$. Inserting (C.2) into (C.5) yields with (C.6) that the radius of the circular orbit is not arbitrary but takes the quantized values

$$a_n = a_{\mathrm{B}} n^2 \,. \tag{C.7}$$

Here the Bohr radius represents the characteristic length scale of the hydrogen atom, which is given by

$$a_{\mathrm{B}} = \frac{4\pi\epsilon_0 \hbar^2}{M e^2} \tag{C.8}$$

with the value

$$a_{\mathrm{B}} = 0.5\,\mathring{A} = 5 \cdot 10^{-11}\ \mathrm{m}\,. \tag{C.9}$$

Another important length scale is the Compton wavelength of the electron:

$$\lambda_{\mathrm{C}} = \frac{2\pi\hbar}{Mc}\,. \tag{C.10}$$

The ratio of the two length scales (C.8) and (C.10) yields the Sommerfeld fine-structure constant, which represents the smallness parameter of quantum electrodynamics:

$$\alpha = \frac{\lambda_{\mathrm{C}}}{2\pi a_{\mathrm{B}}} = \frac{e^2}{4\pi\hbar\epsilon_0 c} \approx \frac{1}{137}\,. \tag{C.11}$$

Furthermore, inserting (C.7) into (C.1) we get for the energy of the electron in the hydrogen atom a result, which also follows from Schrödinger theory, i.e. a non-relativistic quantum theory without spin:

$$E_n = -\mathrm{Ry}\,\frac{1}{n^2}\,, \qquad n \in \mathbb{N}\,. \tag{C.12}$$

Here the Rydberg energy represents the energy scale

$$\mathrm{Ry} = \frac{M e^4}{32\pi^2 \epsilon_0^2 \hbar^2}\,, \tag{C.13}$$

which can be re-expressed in terms of the rest energy Mc^2 and the Sommerfeld fine-structure constant (C.11):

$$\mathrm{Ry} = \frac{1}{2}\, Mc^2 \alpha^2\,. \tag{C.14}$$

With the rest energy Mc^2 of the electron being $0.511\,\mathrm{MeV}$, this yields for the Rydberg energy (C.14) the value

$$\mathrm{Ry} = \frac{0.511\,\mathrm{MeV}}{2(137)^2} = 13.6\,\mathrm{eV}\,. \tag{C.15}$$

Any atomic frequency is then of the order

$$\omega_{fi} \sim \frac{E(a_0)}{\hbar} \sim \alpha^2\,\frac{Mc^2}{\hbar} \sim \alpha^2\,\frac{c}{\lambda_{\mathrm{C}}}\,. \tag{C.16}$$

Appendix D

Heisenberg Uncertainty Relation

Here we recall the Heisenberg uncertainty principle, which is of fundamental importance for quantum mechanics. Defining the expectation value of an operator $\hat{O}$ with respect to some state $|\psi\rangle$ as follows

$$\langle \hat{O} \rangle = \langle \psi | \hat{O} | \psi \rangle \,, \tag{D.1}$$

we consider the variances of two hermitian operators $\hat{A}$ and $\hat{B}$:

$$\langle (\Delta \hat{A})^2 \rangle = \langle \hat{A}^2 \rangle - \langle \hat{A} \rangle^2 = \langle (\hat{A} - \langle \hat{A} \rangle)^2 \rangle \,, \tag{D.2}$$

$$\langle (\Delta \hat{B})^2 \rangle = \langle \hat{B}^2 \rangle - \langle \hat{B} \rangle^2 = \langle (\hat{B} - \langle \hat{B} \rangle)^2 \rangle \,. \tag{D.3}$$

The product of both variances then yields at first

$$\begin{aligned} &\langle (\Delta \hat{A})^2 \rangle \cdot \langle (\Delta \hat{B})^2 \rangle = \langle (\hat{A} - \langle \hat{A} \rangle)^2 \rangle \cdot \langle (\hat{B} - \langle \hat{B} \rangle)^2 \rangle \\ &= \langle (\hat{A} - \langle \hat{A} \rangle)\psi | (\hat{A} - \langle \hat{A} \rangle)\psi \rangle \cdot \langle (\hat{B} - \langle \hat{B} \rangle)\psi | (\hat{B} - \langle \hat{B} \rangle)\psi \rangle \,. \end{aligned} \tag{D.4}$$

Applying the Schwarz inequality we obtain the following lower bound:

$$\langle (\Delta \hat{A})^2 \rangle \cdot \langle (\Delta \hat{B})^2 \rangle \geq \left| \langle (\hat{A} - \langle \hat{A} \rangle)\psi | (\hat{B} - \langle \hat{B} \rangle)\psi \rangle \right|^2 \,. \tag{D.5}$$

The right-hand side represents the absolute square of some complex number $z \in \mathbb{C}$ for which the following general inequality holds:

$$|z|^2 \geq |\mathrm{Im}\ z|^2 = \left| \frac{z - z^*}{2i} \right|^2 \,. \tag{D.6}$$

With this follows the downward estimate

$$\langle (\Delta \hat{A})^2 \rangle \cdot \langle (\Delta \hat{B})^2 \rangle \geq \frac{1}{4} \left| \langle [\hat{A}, \hat{B}]_- \rangle \right|^2 \,, \tag{D.7}$$

which represents the Heisenberg uncertainty for any pair of hermitian operators $\hat{A}$ and $\hat{B}$.

Appendix E

Useful Integrals

Here we deal with two integrals, which appear occasionally in theoretical physics.

E.1 First Integral

At first we determine the integral

$$\int_{-\infty}^{\infty} dx\, \frac{\sin x}{x}\,, \tag{E.1}$$

where the integrand is known as the sinc-function. To this end we consider the family of auxiliary integrals

$$I(a) = \int_0^{\infty} dx\, \frac{\sin x}{x}\, e^{-ax}\,, \qquad a > 0\,, \tag{E.2}$$

which vanish in the limit that the family parameter a tends to infinity:

$$I(\infty) = 0\,. \tag{E.3}$$

The partial derivative of (E.2) with respect to a then yields the elementary integral

$$\frac{\partial I(a)}{\partial a} = -\int_0^{\infty} dx\, \sin x\, e^{-ax}\,, \tag{E.4}$$

which is straight-forwardly calculated, for instance, as follows:

$$\frac{\partial I(a)}{\partial a} = -\mathrm{Im} \int_0^{\infty} dx\, e^{-(a-i)x} = -\mathrm{Im}\, \frac{1}{a-i} = -\mathrm{Im}\, \frac{a+i}{a^2+1} = -\frac{1}{a^2+1}\,. \tag{E.5}$$

Integrating (E.5) with respect to a and implementing (E.3) we get $b = \pi/2$ and with this

$$I(a) = \frac{\pi}{2} - \arctan a\,. \tag{E.6}$$

Thus, due to (E.2), evaluating (E.6) at $a = 0$ leads to the wanted integral (E.1):

$$\int_{-\infty}^{\infty} dx\, \frac{\sin x}{x} = 2\, I(0) = \pi\,. \tag{E.7}$$

E.2 Second Integral

Now we deal with the integral, which appears in (4.55):

$$\int_{-\infty}^{\infty} dx \, \frac{\sin^2 x}{x^2} \,, \tag{E.8}$$

where the integrand is the square of the sinc-function, which occurs, for instance, also at the slit diffraction. Again we proceed by considering a family of integrals

$$J(b) = \int_{-\infty}^{\infty} dx \, \frac{\sin^2(bx)}{x^2} \,, \tag{E.9}$$

which fulfill the property

$$J(0) = 0 \,. \tag{E.10}$$

Performing here the derivative with respect to the family parameter b yields

$$\frac{\partial J(b)}{\partial b} = \int_{-\infty}^{\infty} dx \, \frac{\sin(2bx)}{x} \,, \tag{E.11}$$

which reduces with the substitution $z(x) = 2bx$ to the integral (E.7). Thus, we obtain a result, which turns out to be independent of b:

$$\frac{\partial J(b)}{\partial b} = \pi \,. \tag{E.12}$$

Integrating (E.12) with respect to b and taking into account (E.10) we finally obtain

$$\int_{-\infty}^{\infty} dx \, \frac{\sin^2 x}{x^2} = J(1) = \pi \,. \tag{E.13}$$

Appendix F

Selection Rules

In this Appendix we calculate the selection rules (4.106) for electric dipole transitions in the hydrogen atom. To this end we have to investigate for which quantum numbers the dipole matrix elements (4.105) do not vanish. To this end we have to take into account the wave functions of the electron in the hydrogen atom, which are given in spherical coordinates by [40, Sect. 9.2]

$$\psi_{nlm}(r,\vartheta,\varphi) = R_{nl}(r)Y_{lm}(\vartheta,\varphi)\,. \tag{F.1}$$

It turns out that the selection rules are not affected by the radial wave function $R_{nl}(r)$, only the angular dependences are decisive, which are determined by the spherical harmonics

$$Y_{lm}(\vartheta,\varphi) = N_{lm}P_l^{(m)}(\cos\vartheta)e^{im\varphi}\,. \tag{F.2}$$

Here the associated Legendre polynomials

$$P_l^{(m)}(x) = (-1)^m(1-x^2)^{m/2}\frac{\partial^m}{\partial x^m}P_l(x) \tag{F.3}$$

depend on the Legendre polynomials

$$P_l(x) = \frac{1}{2^l l!}\,\frac{d^l}{dx^l}\,(x^2-1)^l\,. \tag{F.4}$$

The spherical harmonics (F.2) are normalised according to

$$\int_0^\pi d\vartheta\,\sin\vartheta\int_0^{2\pi} d\varphi\,Y_{lm}^*(\vartheta,\varphi)Y_{l'm'}(\vartheta,\varphi) = \delta_{ll'}\delta_{mm'}\,, \tag{F.5}$$

which determines the normalisation constants to be

$$N_{lm} = \sqrt{\frac{2l+1}{4\pi}\,\frac{(l-m)!}{(l+m)!}}\,. \tag{F.6}$$

Now we investigate the matrix element (4.105), which is responsible for the spontaneous emission rate. Due to the assumption (4.100) it reduces to

$$z_{fi} = \int d^3x\,\psi^*_{n_f l_f m_f}(\mathbf{x})\,z\,\psi_{n_i l_i m_i}(\mathbf{x})\,. \tag{F.7}$$

Evaluating (F.7) in spherical coordinates, this matrix element factorises according to

$$z_{fi} = I_r \cdot I_{\vartheta,\varphi} \tag{F.8}$$

into the radial component

$$I_r = \int_0^\infty dr\, r^3\, R_{n_f l_f}(r) R_{n_i l_i}(r) \tag{F.9}$$

and the angular component

$$I_{\vartheta,\varphi} = \int_0^\pi d\vartheta\, \sin\vartheta \int_0^{2\pi} d\varphi\, Y^*_{l_f m_f}(\vartheta,\varphi)\, \cos\vartheta\, Y_{l_i m_i}(\vartheta,\varphi)\,. \tag{F.10}$$

Inserting (F.2) into (F.10) yields

$$I_{\vartheta,\varphi} = \int_0^\pi d\vartheta\, \sin\vartheta \int_0^{2\pi} d\varphi\, N_{l_f m_f} P_{l_f}^{(m_f)}(\cos\vartheta) e^{-i m_f \varphi} \cos\vartheta N_{l_i m_i} P_{l_i}^{(m_i)}(\cos\vartheta) e^{i m_i \varphi}\,. \tag{F.11}$$

Note that the associated Legendre polynomials satisfy the following recurrence relation [23, (8.733.2)]

$$x P_l^{(m)}(x) = \frac{l+1-m}{2l+1} P_{l+1}^{(m)}(x) + \frac{l+m}{2l+1} P_{l-1}^{(m)}(x)\,. \tag{F.12}$$

Therefore we obtain for the angular integral (F.11)

$$\begin{aligned} I_{\vartheta,\varphi} &= \int_0^\pi d\vartheta\, \sin\vartheta \int_0^{2\pi} d\varphi\, N_{l_f m_f} P_{l_f}^{(m_f)}(\cos\vartheta) e^{-i m_f \varphi} e^{i m_i \varphi} \qquad (F.13)\\ &\times \left\{ \frac{l_i+1-m_i}{2l_i+1} \frac{N_{l_i m_i}}{N_{l_i+1 m_i}} N_{l_i+1 m_i} P_{l_i+1}^{(m_i)}(\cos\vartheta) + \frac{l_i+m_i}{2l_i+1} \frac{N_{l_i m_i}}{N_{l_i-1 m_i}} N_{l_i-1 m_i} P_{l_i-1}^{(m_i)}(\cos\vartheta) \right\}. \end{aligned}$$

Taking into account the normalization constants (F.6), we yield the side calculation

$$\frac{l_{i+1}-m_i}{2l_{l+i}} \frac{N_{l_i m_i}}{N_{l_i+1 m_i}} = \sqrt{\frac{l_i+1+m_i}{(2l_i+1)(2l_i+3)(l_i+1-m_i)}}\,, \tag{F.14}$$

$$\frac{l_i+m_i}{2l_i+1} \frac{N_{l_i m_i}}{N_{l_i-1 m_i}} = \sqrt{\frac{l_i-m_i}{(2l_i+1)(2l_i-1)(l_i+m_i)}}\,. \tag{F.15}$$

With this the angular integral (F.13) goes over into

$$\begin{aligned} I_{\vartheta,\varphi} &= \int_0^\pi d\vartheta\, \sin(\vartheta) \int_0^{2\pi} d\varphi\, Y^*_{l_f m_f}(\vartheta,\varphi) \left\{ \sqrt{\frac{l_i+1+m_i}{(2l_i+1)(2l_i+3)(l_{i+1}-m_i)}}\, Y_{l_{i+1} m_i}(\vartheta,\varphi) \right. \\ &\left. + \sqrt{\frac{l_i-m_i}{(2l_i+1)(2l_i-1)(l_i+m_i)}}\, Y_{l_{i-1} m_i}(\vartheta,\varphi) \right\}, \end{aligned} \tag{F.16}$$

so that the orthonormality of the spherical harmonics (F.5) leads to

$$I_{\vartheta,\varphi} = \left\{ \sqrt{\frac{l_i+1-m_i}{(2l_i+1)(2l_i+3)(l_i+1-m_i)}}\, \delta_{l_f, l_{i+1}} + \sqrt{\frac{l_i-m_i}{(2l_i+1)(2l_i-1)(l_i+m_i)}}\, \delta_{l_f, l_{i-1}} \right\} \delta_{m_f, m_i} \tag{F.17}$$

From (F.17) we read off the selection rules for the z-component of the dipole matrix element in form of (4.106).

Appendix G

Lie Algebra Methods

G.1 Lie Algebra

A Lie algebra is a vector space $\mathcal{G}$ equipped with an inner product, called Lie bracket, which maps the vector space into itself:

$$\begin{aligned} \mathcal{G} \times \mathcal{G} &\rightarrow \mathcal{G}\,, \\ \left(\hat{A}, \hat{B}\right) &\rightarrow \left[\hat{A}, \hat{B}\right]\,. \end{aligned} \tag{G.1}$$

Such a Lie bracket has to fulfill the following properties. It is bilinear in both arguments, i.e.

$$\left[a\hat{A} + b\hat{B}, \hat{C}\right] = a\left[\hat{A}, \hat{C}\right] + b\left[\hat{B}, \hat{C}\right]\,, \tag{G.2}$$

$$\left[\hat{A}, b\hat{B} + c\hat{C}\right] = b\left[\hat{A}, \hat{B}\right] + c\left[\hat{A}, \hat{C}\right]\,, \tag{G.3}$$

respects the alternativity

$$\left[\hat{A}, \hat{A}\right] = 0\,, \tag{G.4}$$

and obeys the Jacobi identity

$$\left[\hat{A}, \left[\hat{B}, \hat{C}\right]\right] + \left[\hat{B}, \left[\hat{C}, \hat{A}\right]\right] + \left[\hat{C}, \left[\hat{A}, \hat{B}\right]\right] = 0\,. \tag{G.5}$$

In case of quantum mechanics the Lie bracket is obviously realized by the commutator

$$\left[\hat{A}, \hat{B}\right]_- = \hat{A}\hat{B} - \hat{B}\hat{A}\,. \tag{G.6}$$

From the closedness of the Lie algebra (G.56) follows that the commutator of any two operators $\hat{O}_i, \hat{O}_j$ in the vector space $\mathcal{G}$ must be an operator $\left[\hat{O}_i, \hat{O}_j\right]_-$ within this vector space $\mathcal{G}$. In case of a finite-dimensional vector space $\mathcal{G}$ there must be a basis of linear independent operators $\hat{O}_1, \hat{O}_2, \ldots, \hat{O}_N$ so that also the operators $\left[\hat{O}_i, \hat{O}_j\right]_-$ can be expanded with respect to them:

$$\left[\hat{O}_i, \hat{O}_j\right]_- = \sum_{k=1}^{N} c_{ijk}\hat{O}_k\,. \tag{G.7}$$

The basis operators $\hat{O}_1, \hat{O}_2, \ldots, \hat{O}_N$ are called generators and the expansion coefficients c_{ijk} are known as the structure constants of the Lie algebra. Note that the anti-commutativity of the commutator (G.6)

$$\left[\hat{O}_i, \hat{O}_j\right]_- = -\left[\hat{O}_j, \hat{O}_i\right]_- \tag{G.8}$$

and the Jacobi identity (G.5) imply the following constraints for the structure constants:

$$c_{ijk} = -c_{jik}\,, \tag{G.9}$$

$$c_{ijk} + c_{jki} + c_{kij} = 0\,. \tag{G.10}$$

G.2 Similarity Transformation

Let $\hat{S}$ be an invertible operator, so there exists its inverse $\hat{S}^{-1}$ with the property

$$\hat{S}\hat{S}^{-1} = \hat{S}^{-1}\hat{S} = 1\,. \tag{G.11}$$

Then such an invertible operator defines for any operator $\hat{A}$ of the Lie algebra $\mathcal{G}$ a so-called similarity transformation:

$$\hat{A} \to \hat{S}\hat{A}\hat{S}^{-1}\,. \tag{G.12}$$

For instance, the similarity transformed generators

$$\hat{O}_i \to \hat{S}\hat{O}_i\hat{S}^{-1}\,; \qquad i = 1, 2, \ldots, N \tag{G.13}$$

have the property that they have the same structure constants c_{ijk} of the Lie algebra as definied via (G.7):

$$\left[\hat{S}\hat{O}_i\hat{S}^{-1}, \hat{S}\hat{O}_j\hat{S}^{-1}\right]_- = \sum_{k=1}^{N} c_{ijk}\hat{S}\hat{O}_k\hat{S}^{-1}\,. \tag{G.14}$$

Thus, instead of considering the set of operators $\hat{O}_1, \hat{O}_2, \ldots, \hat{O}_N$ as the generators of the underlying Lie algebra, one could also view $\hat{S}\hat{O}_1\hat{S}^{-1}, \hat{S}\hat{O}_2\hat{S}^{-1}, \ldots, \hat{S}\hat{O}_N\hat{S}^{-1}$ as the generators. Furthermore, let $f(z)$ be any analytic function with a Taylor series

$$f(z) = \sum_{k=0}^{\infty} f_k z^k\,. \tag{G.15}$$

Then the similarity transformation of the operator-valued function $f(\hat{A})$ can be pulled inside the function by inserting multiple identities (G.11):

$$\hat{S}f(\hat{A})\hat{S}^{-1} = \sum_{k=0}^{\infty} f_k \hat{S}\hat{A}^k\hat{S}^{-1} = \sum_{k=0}^{\infty} f_k \left(\hat{S}\hat{A}\hat{S}^{-1}\right)^k = f\left(\hat{S}\hat{A}\hat{S}^{-1}\right)\,. \tag{G.16}$$

In particular, in quantum optics we are often interested in a similarity transformation of the form

$$\hat{O}_i(t) = e^{t\hat{Z}} \hat{O}_i e^{-t\hat{Z}} \,, \tag{G.17}$$

where t denotes a parameter, $\hat{O}_i$ represents a generator, and $\hat{Z}$ is an arbitrary element of the Lie algebra, so that it can be expanded with respect to the generators:

$$\hat{Z} = \sum_{i=1}^{N} z_i \hat{O}_i \,. \tag{G.18}$$

The similarity transformation (G.17) can be evaluated as follows. At first, we differentiate the transformation with respect to the parameter t, which yields

$$\frac{d\hat{O}_i(t)}{dt} = e^{t\hat{Z}} \hat{Z} \hat{O}_i e^{-t\hat{Z}} - e^{t\hat{Z}} \hat{O}_i \hat{Z} e^{-t\hat{Z}} = e^{t\hat{Z}} \left[\hat{Z}, \hat{O}_i\right]_- e^{-t\hat{Z}} \,. \tag{G.19}$$

Inserting (G.18) therein allows to evaluate the commutators via the structure constants according to (G.7), so we get

$$\frac{d\hat{O}_i(t)}{dt} = e^{t\hat{Z}} \sum_{j=1}^{N} z_j \left[\hat{O}_j, \hat{O}_i\right]_- e^{-t\hat{Z}} = \sum_{j=1}^{N} \sum_{k=1}^{N} z_j c_{jik} e^{t\hat{Z}} \hat{O}_k e^{-t\hat{Z}} \,. \tag{G.20}$$

Thus, the similarity transformation (G.17) follows from solving an operator-valued set of coupled first-order linear differential equations:

$$\frac{d\hat{O}_i(t)}{dt} = \sum_{j=1}^{N} \sum_{k=1}^{N} z_j c_{jik} \hat{O}_k(t) \,. \tag{G.21}$$

The corresponding initial conditions can directly be read off from (G.17):

$$\hat{O}_i(0) = \hat{O}_i \,; \qquad i = 1, 2, \ldots, N \,. \tag{G.22}$$

G.3 Disentangling an Exponential

Lie algebra methods can also be used to disentangle an exponential of operators into products:

$$e^{t\hat{Z}} = e^{f_1(t)\hat{O}_1} e^{f_2(t)\hat{O}_2} \cdots e^{f_N(t)\hat{O}_N} \,. \tag{G.23}$$

Here $\hat{Z}$ is again an arbitrary element of the Lie algebra with (G.18). The aim is now to find the unknown functions $f_1(t), f_2(t), \ldots, f_N(t)$. To this end we follow the same strategy as in the previous section and differentiate (G.23) with respect to the parameter t. Multiplying in addition from the right with the inverse of (G.23) yields

$$\frac{de^{t\hat{Z}}}{dt} e^{-t\hat{Z}} = \hat{Z} = \frac{d}{dt} \left(e^{f_1(t)\hat{O}_1} e^{f_2(t)\hat{O}_2} \cdots e^{f_N(t)\hat{O}_N}\right) e^{-f_N(t)\hat{O}_N} \cdots e^{-f_2(t)\hat{O}_2} e^{-f_1(t)\hat{O}_1} \,. \tag{G.24}$$

Together with (G.18) this reduces to

$$\sum_{i=1}^{N} z_i \hat{O}_i = \dot{f}_1(t)\hat{O}_1 + \dot{f}_2(t) e^{f_1(t)\hat{O}_1}\hat{O}_2 e^{-f_1(t)\hat{O}_1} + \dot{f}_3(t) e^{f_1(t)\hat{O}_1} e^{f_2(t)\hat{O}_2}\hat{O}_3 e^{-f_2(t)\hat{O}_2} e^{-f_1(t)\hat{O}_1}$$
$$+ \ldots + \dot{f}_N(t) e^{f_1(t)\hat{O}_1} e^{f_2(t)\hat{O}_2} \cdots e^{f_{N-1}(t)\hat{O}_{N-1}}\hat{O}_N e^{-f_{N-1}(t)\hat{O}_{N-1}} \cdots e^{-f_2(t)\hat{O}_2} e^{-f_1(t)\hat{O}_1} . \quad \text{(G.25)}$$

Here each similarity transformation $\hat{S}\hat{O}_i\hat{S}^{-1}$ on the right-hand side must be evaluated by using the techniques of the previous section. With this the right-hand side becomes a linear combination of the generators $\hat{O}_i$. Comparing the respective coefficients on both sides of this operator-valued equation yields a set of coupled first-order linear differential equations for the functions $f_1(t), f_2(t), \ldots, f_N(t)$. The corresponding initial conditions follow from (G.23) and read

$$f_i(0) = 0 ; \qquad i = 1, 2, \ldots, N . \quad \text{(G.26)}$$

G.4 Heisenberg-Weyl Algebra h_4

A prominent example for a Lie algebra is the four-dimensional Heisenberg-Weyl algebra h_4, whose generators consists apart from the identity operator 1 of three operators occuring for a harmonic oscillator, namely the raising (lowering) ladder operator $\hat{a}^\dagger$ ($\hat{a}$) and the number operator $\hat{n} = \hat{a}^\dagger\hat{a}$. From the respective non-trivial commutators (A.7), (A.10), and (A.11) one can immediately read off all non-vanishing structure constants:

$$c_{\hat{a}\hat{a}^\dagger 1} = 1 , \qquad c_{\hat{a}^\dagger\hat{a}1} = -1 , \quad \text{(G.27)}$$
$$c_{\hat{n}\hat{a}^\dagger\hat{a}^\dagger} = 1 , \qquad c_{\hat{a}^\dagger\hat{n}\hat{a}^\dagger} = -1 , \quad \text{(G.28)}$$
$$c_{\hat{n}\hat{a}\hat{a}} = -1 , \qquad c_{\hat{a}\hat{n}\hat{a}} = 1 . \quad \text{(G.29)}$$

G.4.1 Similarity Transformation

Let us consider for some complex number α the operator

$$\hat{Z} = \alpha\hat{a}^\dagger - \alpha^*\hat{a} \quad \text{(G.30)}$$

and the corresponding similarity-transformed annihiliation operator

$$\hat{a}(t) = e^{t\hat{Z}}\hat{a}e^{-t\hat{Z}} . \quad \text{(G.31)}$$

From (G.20) and the non-trivial commutators (G.27)–(G.29) we read off that (G.31) satisfies the differential equation

$$\frac{d\hat{a}(t)}{dt} = \alpha c_{\hat{a}^\dagger\hat{a}1} e^{t\hat{Z}} e^{-t\hat{Z}} = -\alpha . \quad \text{(G.32)}$$

It is solved by

$$\hat{a}(t) = \hat{c} - t\alpha\,, \tag{G.33}$$

where the operator-valued integration constant $\hat{c}$ is determined by the initial condition following from (G.31):

$$\hat{a}(0) = \hat{c} = \hat{a}\,. \tag{G.34}$$

Thus, the similarity-transformed annihiliation operator (G.31) reads

$$\hat{a}(t) = \hat{a} - t\alpha\,, \tag{G.35}$$

Specializing for $t = 1$ we find that the similarity transformation for the coherent displacement operator

$$\hat{D}(\alpha) = e^{\hat{Z}} = e^{\alpha\hat{a}^\dagger - \alpha^*\hat{a}} \tag{G.36}$$

is given by

$$\hat{D}(\alpha)\hat{a}\hat{D}^\dagger(\alpha) = \hat{a} - \alpha \tag{G.37}$$

as (G.36) represents a unitary transformation:

$$\hat{D}^\dagger(\alpha) = \hat{D}^{-1}(\alpha)\,. \tag{G.38}$$

G.4.2 Disentangling an Exponential

Let us aim now for disentangling the operator $e^{t\hat{Z}}$ with $\hat{Z}$ given in (G.30) as follows:

$$e^{t\alpha\hat{a}^\dagger - t\alpha^*\hat{a}} = e^{f_1(t)\hat{a}^\dagger} e^{f_2(t)\hat{n}} e^{f_3(t)\hat{a}} e^{f_4(t)}\,. \tag{G.39}$$

Applying the general disentangling rule (G.25) to the case (G.39) yields

$$\begin{aligned} \alpha\hat{a}^\dagger - \alpha^*\hat{a} \;=\; & \dot{f}_1(t)\hat{a}^\dagger + \dot{f}_2(t)e^{f_1(t)\hat{a}^\dagger}\hat{n}e^{-f_1(t)\hat{a}^\dagger} + \dot{f}_3(t)e^{f_1(t)\hat{a}^\dagger}e^{f_2(t)\hat{n}}\hat{a}e^{-f_2(t)\hat{n}}e^{-f_1(t)\hat{a}^\dagger} \\ & + \dot{f}_4(t)e^{f_1(t)\hat{a}^\dagger}e^{f_2(t)\hat{n}}e^{f_3(t)\hat{a}}e^{-f_3(t)\hat{a}}e^{-f_2(t)\hat{n}}e^{-f_1(t)\hat{a}^\dagger}\,. \end{aligned} \tag{G.40}$$

Here the occuring similarity transformations have to be evaluated one after the other in an iterative way:

$$e^{f_1(t)\hat{a}^\dagger}\hat{n}e^{-f_1(t)\hat{a}^\dagger} = \hat{a}^\dagger e^{f_1(t)\hat{a}^\dagger}\hat{a}e^{-f_1(t)\hat{a}^\dagger} = \hat{n} - \hat{a}^\dagger f_1(t)\,, \tag{G.41}$$

$$e^{f_1(t)\hat{a}^\dagger}e^{f_2(t)\hat{n}}\hat{a}e^{-f_2(t)\hat{n}}e^{-f_1(t)\hat{a}^\dagger} = e^{-f_2(t)}e^{f_1(t)\hat{a}^\dagger}\hat{a}e^{-f_1(t)\hat{a}^\dagger} = e^{-f_2(t)}\left[\hat{a} - f_1(t)\right]\,, \tag{G.42}$$

$$e^{f_1(t)\hat{a}^\dagger}e^{f_2(t)\hat{n}}e^{f_3(t)\hat{a}}e^{-f_3(t)\hat{a}}e^{-f_2(t)\hat{n}}e^{-f_1(t)\hat{a}^\dagger} = 1\,. \tag{G.43}$$

Note that we have used in (G.41) and (G.42) similarity transformations, which can be evaluated along the lines of Section G.2:

$$e^{s\hat{a}^\dagger}\hat{a}e^{-s\hat{a}^\dagger} \;=\; \hat{a} - s\,, \tag{G.44}$$

$$e^{s\hat{n}}\hat{a}e^{-s\hat{n}} \;=\; e^{-s}\hat{a}\,. \tag{G.45}$$

Thus, inserting (G.41)–(G.43) into (G.40) leads to the following set of differential equations:

$$\begin{aligned} \alpha &= \dot{f}_1(t) - \dot{f}_2(t) f_1(t)\,, && \text{(G.46)} \\ 0 &= \dot{f}_2(t)\,, && \text{(G.47)} \\ -\alpha^* &= \dot{f}_3(t) e^{-f_2(t)}\,, && \text{(G.48)} \\ 0 &= -\dot{f}_3(t) f_1(t) + \dot{f}_4(t)\,. && \text{(G.49)} \end{aligned}$$

They have to be solved by taking into the initial conditions, which directly follow from (G.39):

$$f_1(0) = f_2(0) = f_3(0) = f_4(0) = 0\,. \tag{G.50}$$

The solution reads

$$f_1(t) = \alpha t\,, \qquad f_2(t) = 0\,, \qquad f_3(t) = -\alpha^* t\,, \qquad f_4(t) = -\frac{t^2 \left|\alpha\right|^2}{2}\,, \tag{G.51}$$

so the disentangling formula (G.39) reduces for $t = 1$ to the following result for the displacement operator (G.36):

$$\hat{D}(\alpha) = e^{\alpha \hat{a}^\dagger} e^{-\alpha^* \hat{a}} e^{-|\alpha|^2/2}\,. \tag{G.52}$$

Note that (G.52) represents the displacement operator $\hat{D}$ in normal ordering as the operators are arranged in such a way that the creation (annihilation) operators are positioned to the left (right). The corresponding antinormally ordered product form can be found by inserting a unity factor:

$$\hat{D}(\alpha) = \left(e^{\alpha \hat{a}^\dagger} e^{-\alpha^* \hat{a}} e^{-\alpha \hat{a}^\dagger} \right) e^{\alpha \hat{a}^\dagger} e^{-|\alpha|^2/2}\,. \tag{G.53}$$

The term within the round brackets is recognized to be a similarity transformation of the operator-valued exponential function $e^{-\alpha^* \hat{a}}$. It is evaluated according to (G.16) by pulling the similarity transformation inside the exponential function

$$\hat{D}(\alpha) = \exp\left[e^{\alpha \hat{a}^\dagger} \left(-\alpha^* \hat{a}\right) e^{-\alpha \hat{a}^\dagger} \right] e^{\alpha \hat{a}^\dagger} e^{-|\alpha|^2/2} \tag{G.54}$$

and by using (G.44), yielding

$$\hat{D}(\alpha) = e^{-\alpha^* \hat{a}} e^{\alpha \hat{a}^\dagger} e^{|\alpha|^2/2}\,. \tag{G.55}$$

G.5 Lie Algebra $su(1,1)$

The Lie algebra $su(1,1)$ is three-dimensional and the generators $\hat{K}_1, \hat{K}_2, \hat{K}_3$ are defined by the commutation relations

$$\left[\hat{K}_1, \hat{K}_2\right]_- = -i\hat{K}_3\,, \qquad \left[\hat{K}_2, \hat{K}_3\right]_- = i\hat{K}_1\,, \qquad \left[\hat{K}_3, \hat{K}_1\right]_- = i\hat{K}_2\,. \tag{G.56}$$

We recognize that they differ in one minus sign from the corresponding commutation relations of the three-dimensional Lie algebra $su(2)$, which is better known as the angular momentum algebra, where the generators $\hat{L}_1, \hat{L}_2, \hat{L}_3$ obey

$$\left[\hat{L}_1, \hat{L}_2\right]_- = i\hat{L}_3\,, \qquad \left[\hat{L}_2, \hat{L}_3\right]_- = i\hat{L}_1\,, \qquad \left[\hat{L}_3, \hat{L}_1\right]_- = i\hat{L}_2\,. \tag{G.57}$$

Note that for the Lie algebra $su(2)$ one can choose as a different basis $\hat{L}_\pm = \hat{L}_1 \pm i\hat{L}_2$ and $\hat{L}_3$, in which case the commutation relations (G.57) turn into

$$\left[\hat{L}_+, \hat{L}_-\right]_- = 2\hat{L}_3\,, \qquad \left[\hat{L}_3, \hat{L}_\pm\right]_- = \pm\hat{L}_\pm\,. \tag{G.58}$$

Correspondingly one can also consider $\hat{K}_\pm = \hat{K}_1 \pm i\hat{K}_2$ and $\hat{K}_3$ as the generators of the Lie algebra $su(1,1)$, which converts (G.56) into

$$\left[\hat{K}_+, \hat{K}_-\right]_- = -2\hat{K}_3\,, \qquad \left[\hat{K}_3, \hat{K}_\pm\right]_- = \pm\hat{K}_\pm\,. \tag{G.59}$$

Thus, also the commutation relations (G.58) and (G.59) differ by one minus sign. Using the raising (lowering) ladder operator $\hat{a}^\dagger$ ($\hat{a}$) and the number operator $\hat{n} = \hat{a}^\dagger\hat{a}$ of the harmonic oscillator one can construct a representation of the Lie algebra $su(1,1)$ as follows:

$$\hat{K}_+ = \frac{\hat{a}^{\dagger 2}}{2}\,, \qquad \hat{K}_- = \frac{\hat{a}^2}{2}\,, \qquad \hat{K}_3 = \frac{1}{2}\left(\hat{n} + \frac{1}{2}\right)\,. \tag{G.60}$$

Indeed, from the respective non-trivial commutators (A.7), (A.10), and (A.11) we deduce that (G.59) is fulfilled.

G.5.1 Similarity Transformation

Here we consider the similarity transformation of the annihilation operator $\hat{a}$

$$\hat{a}(\theta) = e^{tZ}\hat{a}e^{-tZ} \tag{G.61}$$

with the operator

$$\hat{Z} = \xi^*\frac{\hat{a}^2}{2} - \xi\frac{\hat{a}^{\dagger 2}}{2}\,. \tag{G.62}$$

Taking the derivative

G.5.2 Disentangling an Exponential

In order to obtain the squeezing operator in normal ordering, we make the ansatz

$$e^{t\hat{Z}} = e^{f_+(t)\hat{a}^{\dagger 2}/2}e^{f_3(t)(\hat{n}+1/2)/2}e^{f_-(t)\hat{a}^2/2} \tag{G.63}$$

with the operator (G.62). Rewriting (G.63) in terms of the generators (G.60) of the Lie algebra $su(1,1)$, this disentangling of the exponential reads

$$e^{t(\xi^*\hat{K}_- - \xi\hat{K}_+)} = e^{f_+(t)\hat{K}_+} e^{f_3(t)K_3} e^{f_-(t)\hat{K}_-} \,. \tag{G.64}$$

Applying the general disentangling rule (G.25) to the case (G.64) yields at first

$$\begin{aligned} \xi^*\hat{K}_- - \xi\hat{K}_+ &= \dot{f}_+(t)\hat{K}_+ + \dot{f}_3(t) e^{f_+(t)\hat{K}_+}\hat{K}_3 e^{-f_+(t)\hat{K}_+} \\ &\quad + \dot{f}_-(t) e^{f_+(t)\hat{K}_+} e^{f_3(t)\hat{K}_3}\hat{K}_- e^{-f_3(t)\hat{K}_3} e^{-f_1(t)\hat{K}_+} \,. \end{aligned} \tag{G.65}$$

Here the respective similarity transformations have to be evaluated one after the other in an iterative way following Section G.2:

$$e^{s\hat{K}_+}\hat{K}_3 e^{-s\hat{K}_+} = \hat{K}_3 - s\hat{K}_+ \,, \tag{G.66}$$

$$e^{s\hat{K}_3}\hat{K}_- e^{-s\hat{K}_3} = e^{-s}\hat{K}_- \,, \tag{G.67}$$

$$e^{s\hat{K}_+}\hat{K}_- e^{-s\hat{K}_+} = \hat{K}_- - 2s\hat{K}_3 + s^2\hat{K}_+ \,. \tag{G.68}$$

Thus, inserting (G.66)–(G.68) into (G.65) leads to the following set of differential equations:

$$\xi^* = \dot{f}_-(t) e^{-f_3(t)} \,, \tag{G.69}$$

$$0 = \dot{f}_3(t) - 2f_+(t)\dot{f}_-(t) e^{-f_3(t)} \,, \tag{G.70}$$

$$-\xi = \dot{f}_+(t) - f_+(t)\dot{f}_3(t) + \dot{f}_-(t) f_+^2(t) e^{-f_3(t)} \,. \tag{G.71}$$

They have to be solved by taking into account the initial conditions, which follow straightforwardly from (G.63):

$$f_+(0) = f_3(0) = f_-(0) = 0 \,. \tag{G.72}$$

Combining (G.69)–(G.71) leads to the Ricatti differential equation:

$$\dot{f}_+(t) - \xi^* f_+^2(t) = -\xi \,. \tag{G.73}$$

With the polar decompositions $\xi = |\xi| e^{i\varphi}$, $\xi^* = |\xi| e^{-i\varphi}$, and the solution ansatz

$$f_+(t) = c\, e^{i\varphi} \frac{\dot{u}(t)}{u(t)} \tag{G.74}$$

the nonlinear Ricatti differential equation (G.73) reduces to the linear differential equation

$$\ddot{u}(t) - |\xi|^2 u(t) = 0 \tag{G.75}$$

provided one chooses the constant c to be fixed by $c = -1/|\xi|$. Solving (G.75) by taking into account the initial condition (G.72) yields due to (G.74)

$$f_+(t) = -e^{i\varphi} \tanh\left(|\xi| t\right) \,. \tag{G.76}$$

Correspondingly we then obtain from (G.69)–(G.72) also the other functions:

$$f_3(t) = -2\ln\left[\cosh\left(|\xi|t\right)\right] , \tag{G.77}$$

$$f_-(t) = e^{-i\varphi}\tanh\left(|\xi|t\right) . \tag{G.78}$$

Substituting the results (G.76)–(G.78) back into Eqs. (G.62), (G.63) and specializing to $t = 1$, we find that the disentangled exponential reads

$$e^{\left(\xi^*\hat{a}^2 - \xi\hat{a}^{\dagger 2}\right)/2} = e^{-e^{i\varphi}\tanh|\xi|\hat{a}^{\dagger 2}/2}\left(\frac{1}{\cosh|\xi|}\right)^{\hat{n}+1/2} e^{e^{-i\varphi}\tanh|\xi|\hat{a}^2/2} . \tag{G.79}$$

Bibliography

[1] M. Born and E. Wolf, *Principles of Optics: Electromagnetic Theory of Propagation, Interference and Diffraction of Light*, 7th Edition (Cambridge University Press, Cambridge, 1999)

[2] H. J. Carmichael, *Statistical Methods in Quantum Optics 1 - Master Equations and Fokker-Planck Equations* (Springer, Berlin, 1999)

[3] H. J. Carmichael, *Statistical Methods in Quantum Optics 2 - Non-Classical Fields* (Springer, Berlin, 2008)

[4] C. Cohen-Tannoudji, J. Dupont-Roc, and G. Grynberg, *Atom Photon Interactions* (Wiley, Weinheim, 2010)

[5] C. Gardiner and P. Zoller, *Quantum Noise* (Springer, Berlin, 2004)

[6] C. Gerry and P. Knight, *Introductory Quantum Optics* (Cambridge University Press, Cambridge, 2004)

[7] G. Grynberg, A. Aspect, C. Fabre, and C. Cohen-Tannoudji, *Introduction to Quantum Optics: From the Semi-Classical Approach to Quantized Light* (Cambridge University Press, Cambridge, 2010)

[8] H. Haken, *Laser Theory*, Vol. XXV/2c of Encyclopedia of Physics (Springer, Berlin, 1970)

[9] S. Haroche, J.-M. Raimond, *Exploring the quantum: atoms, cavities, and photons* (Oxford Universit Press, Oxford, 2006)

[10] J. R. Klauder and E. C. G. Sudarshan, *Fundamentals of quantum optics* (Benjamin, New York, 1968)

[11] R. Loudon, *The Quantum Theory of Light* (Oxford University Press, Oxford, 2000)

[12] L. Mandel and E. Wolf, *Optical Coherence and Quantum Optics* (Cambridge University Press, Cambridge, 1995)

[13] M. Sargent, M. O. Scully, and W. E. Lamb, *Laser Physics* (Perseus, New York, 1978)

[14] W. P. Schleich, *Quantum Optics in Phase Space* (Wiley, Weinheim, 2001)

[15] M. O. Scully and M. Zubairy, *Quantum Optics* (Cambridge University Press, Cambridge, 1998)

[16] D. A. Steck, *Quantum and Atom Optics*, `http://steck.us/teaching`, 2020

[17] D. F. Walls and G. J. Milburn, *Quantum Optics* (Springer, Berlin, 1994)

[18] J. Klaers, J. Schmitt, F. Vewinger, and M. Weitz, *Bose-Einstein condensation of photons in an optical microcavity*, Nature **468**, 545 (2010)

[19] J. Anglin, *Particles of Light*, Nature **468**, 517 (2010)

[20] H. Genz, *Nothingness – The Science of Empty Space* (Perseus, New York, 1999)

[21] A. Pelster, *Quantum Field Theory*, Lecture Notes at TU Kaiserslautern in Winter Term 2020/2021, `http://www-user.rhrk.uni-kl.de/~apelster/Manuscripts/qft.pdf`

[22] W. Greiner and J. Reinhardt, *Field Quantization* (Springer, Berlin, 2008)

[23] I.S. Gradshteyn and I.M. Ryzhik, *Table of Integrals, Series, and Products*, 7th ed. (Elsevier, New York, 2007)

[24] J. Zinn-Justin, *Quantum Field Theory and Critical Phenomena*, Fourth Edition (Oxford University Press, Oxford, 2002)

[25] H. Kleinert and V. Schulte-Frohlinde, *Critical Properties of* Φ^4*-Theories* (World Scientific, Singapore, 2001)

[26] H. Kleinert, *Particles and Quantum Fields* (World Scientific, Singapore, 2016)

[27] I.-C. Benea-Chelmus, F. F. Settembrini, G. Scalari, and J. Faist, *Electric field correlation measurements on the electromagnetic vacuum state*, Nature **568**, 202 (2019)

[28] H. Kleinert, *Path Integrals in Quantum Mechanics, Statistics, Polymer Physics, and Financial Markets*, 5th Edition (World Scientific, Singapore, 2009)

[29] A. Pelster, *Bose-Einstein Condensation* (in German), Lecture Notes at University Duisburg-Essen in Summer Term 2004,
`http://www-user.rhrk.uni-kl.de/~apelster/Manuscripts/bec.pdf`

[30] U. Mohideen and A. Roy, *Precision Measurement of the Casimir Force from 0.1 to 0.9* μm, Phys. Rev. Lett. **81**, 4549 (1998)

[31] R. Onofrio, *Casimir forces and non-Newtonian gravitation*, New J. Phys. **8**, 237 (2006)

[32] M. Scully, A. Sokolov, and A. Svidzinsky, *Virtual Photons: From the Lamb Shift to Black Holes*, Opt. Phot. News **29**, 34 (2018)

[33] H. Haken and H. C. Wolf, *The Physics of Atoms and Quanta – Introduction to Experiments and Theory*, 7th Edition (Springer, Berlin, 2005)

[34] W. Demtröder, *Atoms, Molecules and Photons – An Introduction to Atomic, Molecular- and Quantum Physics*, 3rd Edition (Springer, Berlin, 2018)

[35] R. P. Feynman, *The Strange Theory of Light and Matter* (Princeton University Press, Princeton, 1985)

[36] B. T. H. Varcoe1, S. Brattke, and H. Walther, *The creation and detection of arbitrary photon number states using cavity QED*, New J. Phys. **6**, 97 (2004)

[37] E. Wigner, *On the Quantum Correction For Thermodynamic Equilibrium*, Phys. Rev. **40**, 749 (1932)

[38] S. Y. Buhmann, *Theoretical Quantum Optics*, Lecture Notes at Albert-Ludwigs University Freiburg (2017)

[39] U. L. Andersen, T. Gehring, C. Marquardt, and G. Leuchs, *30 years of squeezed light generation*, Phys. Scr. **91**, 053001 (2016)

[40] W. Greiner, Quantum Mechanics – An Introduction, Fourth Edition (Springer, Berlin, 2000)

[41] B. W. Shore and P. L. Knight, *The Jaynes-Cummings Model*, J. Mod. Opt. **40**, 1195 (1993)

[42] A. D. Greentree1, J. Koch, and J. Larson, *Fifty years of JaynesCummings physics*, J. Phys. B: At. Mol. Opt. Phys.**46**, 220201 (2013)

[43] I. D. Feranchuk, L. I. Komarov, and A. P. Ulyanenkov, *Two-level system in a one-mode quantum field: numerical solution on the basis of the operator method*, J. Phys. A: Math. Gen. **29**, 4035 (1996)

[44] Q.-H. Chen, T. Liu, Y.-Y. Zhang, and K.-L. Wang, *Exact solutions to the Jaynes-Cummings model without the rotating-wave approximation* Europhys. Lett. **96**, 14003 (2011)

[45] M. Fleischhauer and W. P. Schleich, *Revivals made simple: Poisson summation formula as a key to the revivals in the Jaynes-Cummings model*, Phys. Rev. A **47**, 4258 (1993)

[46] H. Walther, B. T. H. Varcoe, B.-G. Englert, and T. Becker, *Cavity quantum electrodynamics*, Rep. Prog. Phys. **69**, 1325 (2006)

[47] M. P. A. Jones, L. G. Marcassa, and J. P. Shaffer, *Special Issue on Rydberg atom physics*, J. Phys. B: At. Mol. Opt. Phys. **50**, 060202 (2017)

[48] G. Rempe, H. Walther, and N. Klein, *Observation of quantum collapse and revival in a one-atom maser*, Phys. Rev. Lett. **58**, 353 (1987)

[49] M. Brune, F. Schmidt-Kaler, A. Maali, J. Dreyer, E. Hagley, J. M. Raimond, and S. Haroche, *Quantum Rabi Oscillation: A Direct Test of Field Quantization in a Cavity*, Phys. Rev. Lett. **76**, 1800 (1996)

[50] J. I. Cirac, R. Blatt, A. S. Parkins, and P. Zoller, *Quantum collapse and revival in the motion of a single trapped ion*, Phys. Rev. A **49**, 1202 (1994)

[51] M. Greiner, O. Mandel, T. W. Hänsch, and I. Bloch, *Collapse and revival of the matter wave field of a BoseEinstein condensate*, Nature **419**, 51 (2002)

[52] H. Haken and J. Portugali, *Synergetic Cities: Information, Steady State and Phase Transition: Implications to Urban Scaling, Smart Cities and Planning* (Springer, Berlin, 2021)

[53] H. Haken, *Synergetics: An Introduction Nonequilibrium Phase Transitions and Self-Organization in Physics, Chemistry and Biology*, 2nd enlarged edition (Springer, Berlin, 1978)

[54] C. O. Weiss and R. Vilaseca, *Dynamics of Lasers* (VCH Publishing, Weinheim, 1991)

[55] H. G. Schuster, *Deterministic Chaos*, Second Revised Edition (VCH Publishing, Weinheim, 1998)